

Diverticular disease of the colon: New perspectives in symptom development and treatment

Antonio Colecchia, Lorenza Sandri, Simona Capodicasa, Amanda Vestito, Giuseppe Mazzella, Tommaso Staniscia, Enrico Roda, Davide Festi

Antonio Colecchia, Lorenza Sandri, Giuseppe Mazzella, Enrico Roda, Davide Festi, Department of Internal Medicine and Gastroenterology, University of Bologna, Italy

Simona Capodicasa, Amanda Vestito, Tommaso Staniscia, Department of Medicine and Aging, University G. d'Annunzio, Chieti, Italy

Correspondence to: Davide Festi, M.D., Department of Internal Medicine and Gastroenterology, Policlinico S. Orsola-Malpighi, Via Massarenti 9, 40100 Bologna, Italy. festi@med.unibo.it

Telephone: +39-051-6364123 **Fax:** +39-051-63641223

Received: 2003-02-25 **Accepted:** 2003-03-15

Abstract

Diverticular disease of the colon is a common disease worldwide. Although the disease is asymptomatic in about 70-80 % of patients, it represents, at least in Western countries, one of the most important gastrointestinal diseases in terms of direct and indirect health costs. Pathogenesis of the disease is still unknown. However, it is the result of complex interactions between colonic structure, intestinal motility, diet and genetic factors. Whilst efficacious preventive strategies remain to be identified, fibre supplementation in the diet is recommended. Why symptoms develop is still unclear. Results of recent experimental studies on irritable bowel syndrome speculated that low grade inflammation of colonic mucosa, induced by changes in bacterial microflora, could affect the enteric nervous system, which is crucial for normal gut function, thus favouring symptom development. This hypothesis could be extrapolated also for diverticular disease, since bacterial overgrowth is present, at least in a subgroup of patients. These perspectives on symptom development are reviewed and new therapeutic approaches are hypothesized.

Colecchia A, Sandri L, Capodicasa S, Vestito A, Mazzella G, Staniscia T, Roda E, Festi D. Diverticular disease of the colon: New perspectives in symptom development and treatment. *World J Gastroenterol* 2003; 9(7): 1385-1389
<http://www.wjgnet.com/1007-9327/9/1385.asp>

INTRODUCTION

Diverticular disease (DD) of the colon is very common especially in the elderly^[1]. Although DD is present worldwide, a higher incidence has been reported in developed countries, compared to underdeveloped countries^[2]. DD has important socioeconomic implications on the health system, due not only to its worldwide distribution, but also to the lack of knowledge concerning its natural history and the risk factors involved in development of symptoms. As a consequence, it is difficult to define efficacious preventive strategies.

According to a recent report by the American Gastroenterological Association on the burden of digestive diseases in the United States^[3], DD represents, in terms of direct and indirect costs, the 5th most important gastrointestinal disease,

with a mortality-rate of 2.5 per 100 000 per year.

DD is a manifestation of an acquired deformity of the colon wall and is characterized by the development of pseudo-diverticula, i.e., protrusions of the mucosa and submucosa through the muscular wall. These protrusions occur in weak areas of the wall where blood vessels penetrate due to the high pressure inside the colon^[4].

No uniform definition of DD exists as yet. However, according to a recent Consensus Development Conference^[5], colonic DD can be defined as a condition involving primarily the sigmoid region of the colon. This condition may be either asymptomatic, and is referred to as "diverticulosis", or associated with symptoms, and termed "diverticular disease", which may, in turn, be either complicated or non-complicated. The term diverticulitis is used to indicate inflammation of the bowel wall.

A brief review is made herein of the epidemiology, pathogenesis and treatment of DD, and in accordance with recent experimental results, some hypotheses on pathogenesis of symptom development are advanced, which may be usefully taken into consideration in defining more effective preventive strategies.

EPIDEMIOLOGY

Epidemiological studies have demonstrated that the prevalence rates differ considerably from one country to another. Indeed, the disease is very common in Western developed countries, with a much higher frequency (30-40 %) than that in Eastern and developing countries (1-4 %)^[2, 6-8].

Furthermore, in Western countries, about 90 % of the patients have diverticula in the sigmoid segment, while in Asian populations the caecum and the right colon are most frequently involved^[9-12].

Recent studies, however, indicate an increase in the prevalence rate of DD also in Eastern populations, possibly due to increasing globalization and the fact that lifestyle has become increasingly similar in various parts of the world^[11-13].

No definitive data have emerged, so far, on the prevalence rate of DD, mainly because the majority of patients are asymptomatic, and are hence difficult to identify. The most important risk factor appears to be aging, the prevalence rate increases with age and varies from <10 % in subjects <40 years old to an estimated 50-66 % in patients >85 years^[1, 14, 15].

Some studies have reported a slightly higher frequency in females, however, no sex-related predominance has been demonstrated^[16, 17].

PATHOGENESIS

The pathogenetic mechanisms of DD are still poorly understood, however it is generally recognized that these are probably related to complex interactions between colon structure, intestinal motility, diet as well as genetic features^[18].

DD has been correlated with "a low residue diet"^[2], and furthermore, the prevalence of diverticulosis is higher with a reduced dietary intake of raw fibres^[19] and lower in vegetarians^[20]. These data are supported by studies both in

animals^[21, 22] and humans^[23-28]. However, although the fibre deficiency hypothesis has been widely quoted, conflicting evidence and much controversy still exist^[29, 30]. The exact mechanism involved remains to be defined, even if prolonged colonic transit time and decreased stool volume in subjects on a low residue diet, seem to induce an increase in intraluminal pressure, which in turn, predisposes to diverticular herniation^[31, 32]. Furthermore, the lower faecal bile acid output in patients with DD suggests a pathogenetic role of these compounds which stimulate colon motor activity and as a result reduce colonic transit time^[33]. Albeit, these hypotheses have not been confirmed by controlled clinical studies comparing healthy subjects with DD patients^[1].

As far as colonic structure is concerned, early surgical and autopsy studies demonstrated an association between muscular hypertrophy of the colon and presence of DD^[34, 35], thus suggesting that increased muscle bulk plays a role in enhancing intraluminal pressure.

Furthermore, electron microscopy evidence of a two-fold increase in elastin content in the taenia coli^[36] suggests a further pathogenetic mechanism. The elastin content in the taenia results in contraction and bunching of the circular muscle, giving the appearance of a hypertrophic muscle with narrowing of the bowel lumen.

The increased prevalence of DD with aging could be due to a progressive, age-related accumulation of elastin in the taenia coli^[36, 37]. In fact, in the elderly, the bowel wall is invariably increased in thickness with reduced elasticity^[1] and thus, intraluminal pressure increases and, according to Laplace's law, formation of diverticula is more likely.

The tendency to elastin accumulation in the taenia coli could be resulted from a low residue diet that extends the bowel intermittently and incompletely, thus favouring prolin (an elastin precursor) uptake^[1].

Whilst several pathogenetic hypotheses have been advanced to explain the development of colon diverticula, the fact remains that the pathologic aspects of the disease are resulted from lifelong exposure to a low residue diet and a complex interaction between colonic structure, intestinal motility and genetic factors^[18].

CLINICAL ASPECTS OF DIVERTICULAR DISEASE

Clinical classification

Current classifications of DD are based on localization, distribution, symptoms, clinical presentation and pathology^[1, 5, 38-40]. Two different types of classification have been proposed: a clinical classification and the Hinchey classification^[41], which is used to describe the stages of perforated DD. For the purposes of the present article, the clinical classification is taken into consideration here (Table 1).

Table 1 Classification of diverticular diseases of the colon

Clinical classification (modified from ref. 5)

- Symptomatic uncomplicated disease
- Recurrent symptomatic disease
- Complicated disease (haemorrhage, abscess, phlegmon, perforation, purulent and faecal peritonitis, stricture, fistula, small-bowel obstruction due to post-inflammatory adhesions)

Modified Hinchey classification (modified from refs. 41, 71)

- Stage I: pericolic abscess
- Stage IIa: distant abscess amenable to percutaneous drainage
- Stage IIb: complex abscess associated with/without fistula
- Stage III: generalized purulent peritonitis
- Stage IV: faecal peritonitis

However, the hallmark of painful DD is abdominal pain in the absence of any indications of inflammation. Pain is usually colicky, but may also be steady. It is exacerbated by eating, and is typically relieved by flatus or bowel movements. Associated symptoms vary considerably: diarrhoea, constipation, flatulence, heartburn, nausea and vomiting, palpable abdominal mass, abdominal distension^[1, 5, 38].

Natural history

The natural history of DD remains to be elucidated and the few prospective studies carried out so far^[9, 42-44] indicate that 80-85 % of patients with DD remain asymptomatic. Of the 15-20 % of patients presenting abdominal pain, approximately 75 % have a painful DD whilst the remainder have diverticulitis, as well as complications of diverticulitis and haemorrhage^[1]. Furthermore, about 1-2 % will require hospitalisation and 0.5 % will require surgery^[1, 45, 46]. Unfortunately, due to the lack of prospective studies, factors predicting the development of symptoms remain to be identified. However, it has been suggested^[47] that evaluation of the colonic motility index (pressure amplitude exceeding 120 mmHg), together with a brief history of left lower quadrant pain, a short segment of involved colon and a relatively younger age (about 50 years), may be useful in recognizing a group of patients at risk of developing symptoms.

Moreover, investigations^[48, 49] have suggested that lack of physical activity is independently associated with an increased risk of symptomatic DD, while smoking, caffeine and alcohol intake are not associated with a substantially increased risk of asymptomatic disease. Furthermore, a significant inverse association has been found between insoluble dietary fibre intake (especially fruit and vegetables, e.g. cellulose fibre) and the risk of subsequently developing symptomatic DD^[24]. In contrast, a study on the efficacy of fibre supplementation in symptomatic patients with DD did not lead to an improvement in symptoms^[50].

Since few data exist on risk factors, preventive measures for the development of diverticula are only speculative, and can be aimed only at preventing development of symptoms. Despite controversial data, fibre supplementation is recommended^[1, 38].

Symptom development

The causes of symptom development, in some patients, are still unclear. Since it has been observed that DD patients who have a history of diverticulitis have more episodes of recurrent abdominal pain and impaired bowel function^[6, 51, 52], a possible role of previous episodes of intestinal inflammation may be hypothesised. This finding is not unlike that which has been recently demonstrated in other gastrointestinal diseases such as infectious enteritis and inflammatory bowel disease^[53, 54] and, as also speculated^[55] in irritable bowel syndrome (IBS). In these patients, the presence of a chronic, low-grade intestinal inflammation would induce a sensory-motor dysfunction, leading to symptom development and/or persistence^[53-56].

Changes in intestinal microflora could be one of the putative mechanisms responsible for low grade inflammation, at least in IBS^[55]. In patients with DD, bacterial overgrowth may be present^[57]. This bacterial overgrowth aided by the faecal stasis inside the diverticula, could contribute to chronic low-grade inflammation which sensitises both intrinsic primary efferent and extrinsic primary afferent neurons. These alterations could lead to smooth muscle hypertrophy, and increased sensitivity to abdominal distension^[56, 58], and finally, to symptom development. This hypothesis is based mainly on experimental studies, investigation in man, being limited at present. However, an increased level of the neuropeptide substance P, which may be related to impaired visceral sensation, has been

demonstrated in patients with DD with abdominal pain but without inflammation^[59]. This finding is not unlike that observed by Di Sebastiano *et al*^[60] who documented a role of neuroproliferation within the appendix, associated with an increased concentration of substance P and vasoactive intestinal polypeptide, in the pathophysiology of right iliac fossa pain in the absence of inflammation. Moreover, in patients with diverticulitis, abnormal nerves with axonal sprouting have been observed^[61], suggesting previous injury. These findings would appear to be compatible with post-inflammatory neural and muscle dysfunction, probably induced also by intestinal bacterial overgrowth, which would contribute to symptom development.

Further studies, both experimental and in man, are obviously needed to confirm the pathogenetic role (which is summarized in Figure 1) of intestinal infection and low grade inflammation, in the development of symptoms in patients with DD.

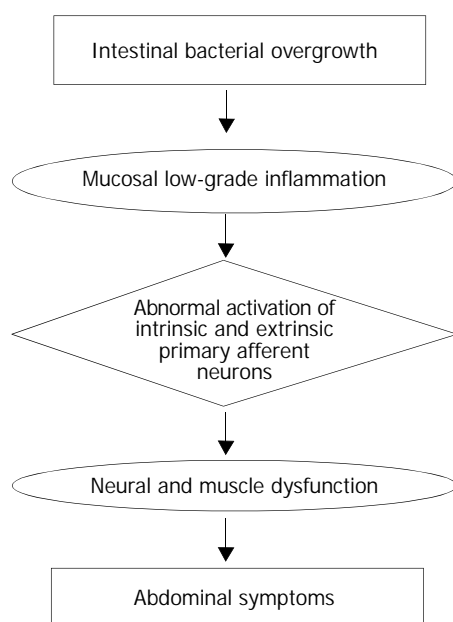


Figure 1 Diverticular disease: putative role of intestinal bacterial overgrowth in symptom development. Altered intestinal microflora could contribute to chronic low-grade inflammation (supported by both immunocytes and mast cells) which abnormally sensitised both intrinsic primary efferent and extrinsic primary afferent neurons. This condition could lead to neural and muscle dysfunction (i.e. altered intestinal motility and visceral sensitivity) and, finally, to symptom development.

Non-surgical treatment

There is a general consensus that conservative treatment is indicated in cases with newly onset uncomplicated diverticulitis^[5, 38, 62, 63]. The rationale for this strategy is that about 50-70 % of patients treated for a first episode of acute diverticulitis will recover and have no further clinical problems.

Furthermore, only about 20 % of these patients will develop symptoms whilst those with recurrent symptoms have a 60 % risk of developing disease complications^[5, 44].

In patients with uncomplicated diverticulosis, a diet with abundant fruit and vegetables is recommended since it seems that this protective effect reduces symptom development and prevents major complications as demonstrated in uncontrolled studies. Nevertheless, recent guidelines^[38] advise the use of a high fibre diet, which should be prescribed also for the well-known potential health benefits.

Anticholinergic and antispasmodic agents may be effective in some cases of uncomplicated DD. However, their use remains to be confirmed by controlled studies.

Although the role of antibiotics in uncomplicated DD is still debated^[38], recent clinical studies^[64-66] have demonstrated that cyclic administration of rifaximin (Normix®, Alfa Wassermann S.p.A., Alanno Scalo, Chieti, Italy) (a broad-spectrum poorly absorbable antibiotic) is more effective in reducing symptoms than fibre supplementation alone (Table 2).

Latella *et al*^[66] performed a large, multicentre, prospective, randomized study, enrolling 968 outpatients with symptomatic diverticulosis. Among them, 595 patients received fibre supplement (glucomannan 4 g/day) plus rifaximin 400 mg bid for 7 days, per month, and 373 patients received glucomannan alone. After 12 months, a significant reduction in the occurrence rate of symptoms was documented in the group treated with rifaximin and fibre. 56.5 % of the patients were asymptomatic as compared to 29.2 % of the fibre group. Moreover, the incidence of major complications was lower in the rifaximin plus fibre group vs the group treated with fibre alone. The mechanism of rifaximin in reducing the frequency of symptoms and the rate of complications of DD is only speculative. It has been suggested that rifaximin reduces the metabolic activity of intestinal bacterial flora, the degradation of dietary fibres, and the production of gas. The latter effect is important since an increased production of intestinal gas and of gas-related symptoms such as pain and bloating have recently been documented, in patients with IBS^[67]. Furthermore, treatment with non-absorbable antibiotics was shown to reduce symptoms frequency and intensity in these patients. Similar results were obtained by others^[68] who documented an association between small intestinal overgrowth and functional intestinal disorders. Moreover, eradication of bacterial overgrowth seems to be related to a reduction in intestinal symptoms.

In conclusion, if low grade mucosal inflammation is confirmed in DD patients, and if such inflammation is provoked and maintained by changes in bacterial microflora as in IBD (change IBD with IBS), then these impairments likely play a role in the pathogenesis and symptom development of both diseases, and thus, new preventive approaches could be identified. According to this hypothesis, cyclic administrations of antibiotics, and in particular of non-absorbable antibiotics such as rifaximin, could reverse the process, i.e., intestinal bacterial overgrowth which is held to trigger the cascade of events which starts from intestinal low grade inflammation to reach symptom generation. In fact, rifaximin, which is highly

Table 2 Effects of rifaximin (R) administration on symptoms in patients with diverticular disease

First author (year, ref)	Pts (n)	Treatment (type)	Duration (months)	Reduction in symptoms (%)	P
Papi (1992, 64)	217	R (400 mg daily) + glucomannan (2 g daily) vs glucomannan	12	63.9 vs 47.6	<0.001
Papi (1995, 65)	168	R (400 mg daily) + glucomannan (2 g daily) vs placebo + glucomannan	12	68.9 vs 38.5	<0.001
Latella (2003, 66)	968	R (400 mg daily) + glucomannan (4 g daily) vs glucomannan	12	56.5 vs 29.2	<0.001

effective against anaerobic bacteria^[69], is effective also in intestinal bacterial overgrowth^[70,71].

It is important, at this stage, to identify and characterize those DD patients with intestinal bacterial overgrowth and, then, to perform controlled clinical trials to evaluate the effects of antibiotic administration on symptom and complication frequency, i.e., on the natural history of this disease.

REFERENCES

- Farrell RJ, Farrell JJ, Morrin MM. Diverticular disease in the elderly. *Gastroenterol Clin North Am* 2001; **30**: 475-496
- Painter NS, Burkitt DP. Diverticular disease of the colon: a deficiency disease of Western civilization. *Br Med J* 1971; **2**: 450-454
- Sandler RS, Everhart JE, Donowitz M, Adams E, Cronin K, Goodman C, Jemmen E, Shahs A, Avdic A, Rubin R. The burden of selected digestive diseases in the United States. *Gastroenterology* 2002; **122**: 1500-1511
- Truelove SC. Movements of the large intestine. *Physiol Rev* 1966; **46**: 457-412
- Kohler L, Sauerland S, Neugebauer E. For the scientific committee of the european association for endoscopic surgery (EAES). diagnosis and treatment of diverticular disease. Results of a consensus development conference. *Surg Endosc* 1999; **13**: 430-436
- Cheskin LJ, Lamport RD. Diverticular disease. Epidemiology and pharmacological treatment. *Drugs Aging* 1995; **6**: 55-58
- Kim EH. Hiatus hernia and diverticulum of colon: their low incidence in Korea. *N Engl J Med* 1964; **271**: 764-768
- Vajrabukka T, Saksornchai K, Jimakorn P. Diverticular disease of the colon in a Far-Eastern community. *Dis Colon Rectum* 1980; **23**: 151-154
- Parks TG. Natural history of diverticular disease of the colon. *Clin Gastroenterol* 1975; **4**: 53-79
- Perry PM, Morson BC. Right-sided diverticulosis of the colon. *Br J Surg* 1971; **58**: 902-904
- Chia JG, Wilde CC, Ngoi SS, Goh PM, Ong CL. Trends of diverticular disease of the large bowel in a newly developed country. *Dis Colon Rectum* 1991; **34**: 498-501
- Lee YS. Diverticular disease of the large bowel in singapore: an autopsy study. *Dis Colon Rectum* 1986; **29**: 330-335
- Ihekwa FN. Diverticular disease of the colon in black africa. *J R Coll Surg Edin* 1992; **37**: 107-109
- Young-Fadok TM, Roberts PL, Spencer MP, Wolff BG. Colonic diverticular disease. *Curr Prob Surg* 2000; **37**: 459-464
- Larsson PA. Diverticulitis is increasing among the elderly: significant cause of morbidity and mortality. *Lakartidningen* 1997; **94**: 3837-3840
- Eide TJ, Stalsberg H. Diverticular disease of the large intestine in northern norway. *Gut* 1979; **20**: 609-615
- Kohler R. The incidence of colonic diverticulosis in Finland and Sweden. *Acta Chir Scand* 1963; **126**: 148-155
- Simpson J, Scholefield JH, Spiller RC. Pathogenesis of colonic diverticula. *Br J Surg* 2002; **89**: 546-554
- Heller SN, Hackler LR. Changes in the crude fiber content of the American diet. *Am J Clin Nutr* 1978; **31**: 1510-1514
- Gear JSS, Furdson P, Nolan DJ. Symptomless diverticular disease and intake of dietary fibre. *Lancet* 1979; **11**: 511-514
- Hodgson WJB. An interim report on the production of colonic diverticula in the rabbit. *Gut* 1972; **13**: 802-804
- Fisher N, Berry CS, Feam T, Gregory JA, Hardy J. Cereal dietary fiber consumption and diverticular disease: a lifespan study in rats. *Am J Clin Nutr* 1985; **42**: 788-804
- Brodribb AJM, Humphreys DM. Diverticular disease: Three studies. I. Relation to other disorders and fibre intake. *Br Med J* 1976; **1**: 424-430
- Aldoori WH, Giovannucci EL, Rimm EB, Wing AL, Trichopoulos, Willet WC. A prospective study of dietary fiber types and symptomatic diverticular disease in men. *Am J Clin Nutr* 1994; **60**: 757-764
- Brodribb AJM. Treatment of symptomatic diverticular disease with high-fibre diet. *Lancet* 1977; **1**: 664-666
- Painter NS, Burkitt DP. Diverticular disease of the colon a 20th century problem. *Clin Gastroenterol* 1975; **4**: 3-21
- Leahy A, Ellis RM, Quill DS, Peel ALG. High fiber diet in symptomatic diverticular disease of the colon. *Ann R Coll Surg Engl* 1985; **67**: 173-174
- Miettinen TA, Tarpila S. Fecal beta-sitosterol in patients with diverticular disease of the colon and in vegetarians. *Scand J Gastroenterol* 1978; **13**: 573-576
- Davey WW. Diet and diverticulosis. *Br Med J* 1968; **1**: 118-120
- Mendeloff AI. A critique of "fibre deficiency". *Am J Dig Dis* 1976; **21**: 109-112
- Painter NS, Truelove SC. The intraluminal pressure patterns in diverticulosis of the colon. Part I and II. *Gut* 1964; **5**: 201-213
- Painter NS, Truelove SC. The intraluminal pressure patterns in diverticulosis of the colon. Part III and IV. *Gut* 1964; **5**: 365-373
- Tarpila S, Miettinen TA, Metsaranta L. Effects of bran on serum cholesterol, fecal mass, fats, bile acids and neutral sterols and biliary lipids in patients with diverticular disease of the colon. *Gut* 1978; **19**: 137-145
- Arfwidsson S. Pathogenesis of multiple diverticula of the sigmoid colon in diverticular disease. *Acta Chir Scand* 1964; **342**: 1-68
- Slack WW. Bowel muscle in diverticular disease. *Gut* 1966; **7**: 668-670
- Whiteway J, Morson BC. Elastosis in diverticular disease of the sigmoid colon. *Gut* 1985; **26**: 258-266
- Smith AN. Colonic muscle in diverticular disease. *Clin Gastroenterol* 1986; **15**: 917-935
- Stollman NH, Raskin JB. Practice guidelines. Diagnosis and management of diverticular disease of the colon in adults. *Am J Gastroenterol* 1999; **94**: 3110-3120
- Torsoli A, Inoue M, Manousos O, Smith A, Van Steensel CJ. Diverticular disease of the colon: data relevant to management. *Gastroenterol Int* 1991; **4**: 3-20
- Wong WD, Wexner SD, Lowry A. Practice parameters for the treatment of sigmoid diverticulitis: Supporting documentation. The standards task force. The american society of colon and rectal surgeons. *Dis Colon Rectum* 2000; **43**: 290-297
- Hinchey EJ, Schaaf PH, Richards MB. Treatment of perforated diverticular disease of the colon. *Adv Surg* 1978; **12**: 85-109
- Haglund U, Hellberg R, Johnsen C, Hulten L. Complicated diverticular disease of the sigmoid colon. An analysis of short and long term outcome in 392 patients. *Ann Chir Gynaecol* 1979; **68**: 41-46
- Ambrosetti P, Robert JH, Witzig JA, Mirescu D, Mathey P, Borst F, Rohner A. Acute left colonic diverticulitis in young patients. *J Am Coll Surg* 1994; **179**: 156-160
- Farmakis N, Tudor RG, Keighley MR. The 5-year natural history of complicated diverticular disease. *Br J Surg* 1994; **81**: 733-735
- Almy TP, Howell DA. Diverticular disease of the colon. *N Engl J Med* 1980; **302**: 324-331
- Simmang CL, Shires GT. Diverticular disease of the colon. In: Feldman M, Sleisenger MH, Scharschmidt BF, Eds, Sleisenger & Fordtran's gastrointestinal and liver disease, 6th Edition, Philadelphia, WB. Saunders Company 1998: 1788-1798
- Cortesini C, Pantalone D. Usefulness of colonic motility study in identifying patients at risk for complicated diverticular disease. *Dis Colon Rectum* 1991; **34**: 339-342
- Aldoori WH, Giovannucci EL, Rimm EB. Prospective study of physical activity and the risk of symptomatic diverticular disease in men. *Gut* 1995; **36**: 276-282
- Aldoori WH, Giovannucci EL, Rimm EB. A prospective study of alcohol, smoking, caffeine, and the risk of symptomatic diverticular disease in man. *Ann Epidemiol* 1995; **5**: 221-228
- Ornstein MH, Littlewood ER, Baird IM, Fowler J, Cox AG. Are fiber supplements really necessary in diverticular disease of the colon? A controlled clinical trial. *Br Med J* 1981; **282**: 1353-1356
- Simpson J, Neal KR, Scholefield JH, Spiller RC. Relation between inflammatory and non inflammatory pain in diverticular disease. *Gut* 2000; **46** (Suppl II): A80
- Simpson J, Neal KR, Scholefield JH, Spiller RC. Symptomatology following acute diverticulitis. *Neurogastroenterol Mot* 2001; **13**: 43
- Neal KR, Hebden J, Spiller R. Prevalence of gastrointestinal symptoms six months after bacterial gastroenteritis and risk factors for development of the irritable bowel syndrome: postal survey of patients. *Br Med J* 1997; **314**: 779-782

- 54 **Isgar B**, Harman M, Kaye MD, Whorwell PJ. Symptoms of irritable bowel syndrome in ulcerative colitis in remission. *Gut* 1983; **24**: 190-192
- 55 **Barbara G**, De Giorgio R, Stanghellini V, Cremon C, Corinaldesi R. A role for inflammation in irritable bowel syndrome? *Gut* 2002; **51** (Suppl 1): i41-i44
- 56 **Collins SM**, Vallance B, Barbara G, Borgaonkar M. Putative inflammatory and immunological mechanism in functional bowel disorders. *Baillieres Best Pract Res Clin Gastroenterol* 1999; **13**: 429-436
- 57 **Ventrucci M**, Ferrieri A, Bergami R, Roda E. Evaluation of the effect of rifaximin in colon diverticular disease by means of lactulose hydrogen breath test. *Curr Med Res Opin* 1994; **13**: 202-206
- 58 **Sanovic S**, Lamb DP, Blennerhasset MG. Damage to the enteric nervous system in experimental colitis. *Am J Pathol* 1999; **155**: 1051-1057
- 59 **Watanabe T**, Kubota Y, Muto T. Substance P containing nerve fibers in rectal mucosa of ulcerative colitis. *Dis Colon Rectum* 1997; **40**: 718-725
- 60 **Di Sebastiano P**, Fink T, di Mola FF. Neuroimmune appendicitis. *Lancet* 1999; **354**: 461-466
- 61 **Brewer DB**, Thompson H, Haynes IG, Alexander-Williams J. Axonal damage in Crohn's disease is frequent but not specific. *J Pathol* 1990; **161**: 301-311
- 62 **Larson DM**, Masters SM, Spiro HM. Medical and surgical therapy in diverticular disease. A comparative study. *Gastroenterology* 1976; **71**: 734-737
- 63 **Ferzoco LB**, Raptopoulos V, Silen W. Acute diverticulitis. *N Engl J Med* 1998; **338**: 1521-1526
- 64 **Papi C**, Ciaco A, Koch M, Capurso L. And diverticular disease study group. Efficacy of rifaximin of uncomplicated diverticular disease of the colon. A pilot multicentre open trial. *Ital J Gastroenterol* 1992; **24**: 452-456
- 65 **Papi C**, Ciaco A, Koch M, Capurso L. Efficacy of rifaximin in the treatment of symptomatic diverticular disease of the colon. A multicenter double-blind placebo-controlled trial. *Aliment Pharmacol Ther* 1995; **9**: 33-39
- 66 **Latella G**, Pimpo MT, Sottili S, Zippi M, Viscido A, Chiamonte M, Frieri G. Rifaximin improves symptoms of acquired uncomplicated diverticular disease of the colon. *Int J Colorectal Dis* 2003; **18**: 55-62
- 67 **Di Stefano M**, Strocchi A, Malservisi S, Veneto G, Ferrieri A, Corazza GR. Non absorbable antibiotics for managing intestinal gas production and gas-related symptoms. *Aliment Pharmacol Ther* 2000; **14**: 1001-1008
- 68 **Pimentel M**, Chow EJ, Lin CL. Eradication of small intestinal overgrowth reduces symptoms in irritable bowel syndrome. *Am J Gastroenterol* 2000; **95**: 3505-3506
- 69 **Gillis JC**, Brogden RN. Rifaximin. *Drugs* 1995; **49**: 468-484
- 70 **Di Stefano M**, Malservisi S, Veneto G, Ferrieri A, Corazza GR. Rifaximin versus chlortetracycline in the short-term treatment of small intestine bacterial overgrowth. *Aliment Pharmacol Ther* 2000; **14**: 551-556
- 71 **Sher ME**, Agachan F, Bortul M, Noguera JJ, Weiss EG, Wexner SD. Laparoscopic surgery for diverticulitis. *Surg Endosc* 1997; **11**: 264-267

Edited by Xu XQ and Wang XL

NQO1 C609T polymorphism associated with esophageal cancer and gastric cardiac carcinoma in North China

Jian-Hui Zhang, Yan Li, Rui Wang, Helen Geddert, Wei Guo, Deng-Gui Wen, Zhi-Feng Chen, Li-Zhen Wei, Gang Kuang, Ming He, Li-Wei Zhang, Ming-Li Wu, Shi-Jie Wang

Jian-Hui Zhang, Yan Li, Rui Wang, Wei Guo, Deng-Gui Wen, Zhi-Feng Chen, Li-Zhen Wei, Gang Kuang, Ming He, Li-Wei Zhang, Ming-Li Wu, Shi-Jie Wang, Hebei Cancer Institute and the Fourth Affiliated Hospital of Hebei Medical University, Shijiazhuang 050011, Hebei Province, China

Helen Geddert, Institute of Pathology, University of Duesseldorf, Moorenstr.5 40225 Duesseldorf, Germany

Supported by the "Stiftung für Altersforschung" of Germany (grant number: 701800167) and Scientific Grant of Educational Department of Hebei Province, China (grant number: 2001150)

Correspondence to: Professor Shi-Jie Wang, The Fourth Affiliated Hospital of Hebei Medical University, Jiankanglu 12, Shijiazhuang 050011, China. wang.sj@hbmhu.edu

Telephone: +86-311-6085231 **Fax:** +86-311-6077634

Received: 2002-12-24 **Accepted:** 2003-02-11

Abstract

AIM: To investigate the association of the *NQO1* (C609T) polymorphism with susceptibility to esophageal squamous cell carcinoma (ESCC) and gastric cardiac adenocarcinoma (GCA) in North China.

METHODS: The *NQO1* C609T genotypes were determined by polymerase chain reaction-restriction fragment length polymorphism (PCR-RFLP) analysis in 317 cancer patients (193 ESCC and 124 GCA) and 165 unrelated healthy controls.

RESULTS: The *NQO1* C609T C/C, C/T and T/T genotype frequency among healthy controls was 31.5 %, 52.1 % and 16.4 % respectively. The *NQO1* T/T genotype frequency among ESCC patients (25.9 %) was significantly higher than that among healthy controls ($\chi^2=4.79$, $P=0.028$). The *NQO1* T/T genotype significantly increased the risk for developing ESCC compared with the combination of C/C and C/T genotypes, with an age, sex and smoking status adjusted odds ratio (OR) of 1.78 (1.04-2.98). This increased susceptibility was pronounced in ESCC patients with family histories of upper gastrointestinal cancers (UGIC) (adjusted OR=2.20, 95 % CI=1.18-3.98). Similarly, the susceptibility of the *NQO1* T/T genotype to GCA development was also observed among patients with family histories of UGIC, with an adjusted odds ratio of 2.55 (95 % CI=1.21-5.23), whereas no difference in *NQO1* genotype distribution was shown among patients without family histories of UGIC.

CONCLUSION: Determination of the *NQO1* C609T genotype may be used as a stratification marker to predicate the individuals at high risk for developing ESCC and GCA in North China.

Zhang JH, Li Y, Wang R, Geddert H, Guo W, Wen DG, Chen ZF, Wei LZ, Kuang G, He M, Zhang LW, Wu ML, Wang SJ. *NQO1* C609T polymorphism associated with esophageal cancer and gastric cardiac carcinoma in North China. *World J Gastroenterol* 2003; 9(7):1390-1393

<http://www.wjgnet.com/1007-9327/9/1390.asp>

INTRODUCTION

China is a country with high incidence regions of esophageal squamous cell cancer (ESCC) and gastric cardiac adenocarcinoma (GCA). Chemical carcinogenesis existed in consumed alcohol and tobacco or ingested food^[1,2], nutrition deficiency^[3], unhealthy living habits^[2] and pathogenic infections^[4-6] are in general considered as the risk factors for developing these two cancers. However, not all individuals exposed to the above exogenous risk factors will develop ESCC or GCA, indicating that the host susceptibility factors may play an important role in the cancer development. The role of a genetic background in developing these cancers was also strongly suggested by the familial clustering of upper gastrointestinal cancer (UGIC) patients in high incidence regions^[7,8].

In recent years, many polymorphic genes encoded carcinogen metabolic enzymes have been found to be associated with susceptibility to chemically induced cancers such as esophageal cancer and gastric cancer^[9-13]. NAD(P)H: quinone oxidoreductase 1 (*NQO1*) is a cytosolic enzyme which catalyzes the two-electron reduction of quinone compounds and prevents the generation of semiquinone free radicals and reactive oxygen species, thus protecting cells from oxidative damage^[14]. On the other hand, *NQO1* catalyzes the reductive activation of quinoid chemotherapeutic agents and of environmental carcinogens such as nitrosamines, heterocyclic amines and cigarette smoke condensate^[15]. The activity of the *NQO1* enzyme may be influenced by a single C to T substitution at nucleotide 609 of exon 6 of the *NQO1* cDNA that causes the Pro187Ser amino acid change^[16]. The homozygous wild-type (C/C) encodes *NQO1* protein with complete enzyme activity, whereas the protein encoded by the heterozygous phenotype (C/T) has approximately three-fold decreased activity and the homozygous mutant (T/T) phenotype has a complete lack of enzyme activity^[15-18]. The *NQO1* C609T polymorphism is correlated with the susceptibility to several chemical carcinogen induced tumors such as lung cancer^[19,20] and leukemia^[21,22]. The association of *NQO1* C609T polymorphism with the susceptibility to ESCC and GCA has not been reported so far. Therefore, the current study investigated the *NQO1* C609T genotype distribution in ESCC and GCA patients and healthy controls from North China.

MATERIALS AND METHODS

Subjects

This case-control study recruited 317 patients with histologically confirmed cancers (193 esophageal cancer and 124 gastric cardiac cancer) and 165 unrelated healthy controls. The cancer patients were hospitalized for tumor resection in the Fourth Affiliated Hospital of Hebei Medical University between 2001 and 2002. The histological pattern of the resected samples was determined by pathologists of the same hospital according to the international standard^[23]. The healthy controls were unrelated blood donors or voluntary staff of Hebei Cancer

Institute. All of the patients and controls were from Shijiazhuang city or its surrounding regions. The information about sex, age, smoking habits and family history was obtained from the cancer patients by their hospital recordings and from the healthy controls by interview directly after bleeding. The smokers were defined as ex- or current smoking 5 cigarettes per day for at least two years. The individuals with at least one first-degree relative or at least two second-degree relatives having esophageal/cardiac/gastric cancer were defined as having family histories of upper gastrointestinal cancers (UGIC). The informed consent was obtained from all the recruited subjects. The study was approved by the Ethics Committee of the Hebei Cancer Institute. The demographic data of the cancer patients and healthy controls are presented in Table 1.

DNA extraction

Five ml of venous blood from each subject was drawn in vacutainer tubes containing EDTA. The genomic DNA was extracted within one week after bleeding using proteinase K digestion followed by a salting out procedure.

NQO1 genotyping

NQO1 genotyping of healthy controls and ESCC patients was performed at the Molecular Laboratory of the Institute of Pathology, Heinrich-Heine University, Duesseldorf. The genotyping of the GCA patients was performed at the Molecular Biology Laboratory of the Hebei Cancer Institute with the same reagents and the same methods. The base change (C to T) at nucleotide 609 of NQO1 cDNA created a *Hinf*I restriction site. Therefore, the NQO1 C609T genotyping was performed by PCR and subsequent restriction fragment analysis. PCR was performed in a 25 µl volume containing 100 ng DNA template, 2.5 µl 10×PCR-buffer, 1 U Hotstar Taq-DNA-polymerase (Qiagen, Hilden, Germany), 200 µmol dNTPs and 10 pmol sense primer (5' -AAGCCAGACCAACTTCT-3') and antisense primer (5' -ATTTGAATTCGGGCGTCTGCTG-3'). Initial denaturation for 14 min at 94 °C was followed by 40 cycles at 94 °C for 1 min, at 56 °C for 1 min, and at 72 °C for 2 min. The PCR products were subsequently digested with 20 units of *Hinf*I (Boehringer, Mannheim, Germany) for 3 h at 37 °C and separated on a 2 % agarose gel (Figure 1). The NQO1 wild-type allele showed a 172-bp PCR product resistant to enzyme digestion, whereas the null allele showed a 131-bp and a 41-bp band. For quality control, each PCR reaction used distilled water instead of DNA as a negative control, and 10 % of the samples were analyzed twice.

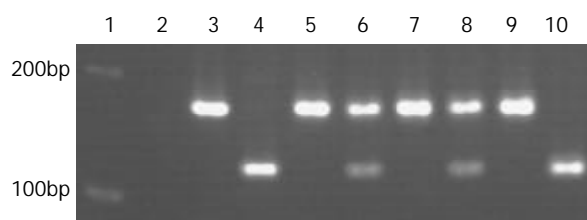


Figure 1 Genotype patterns for *NAD(P)H: quinone oxidoreductase 1 (NQO1)* C609T polymorphism analyzed by PCR-*Hinf*I digestion. Lane 1, 100bp molecular marker; lane 2, negative control; lane 3, PCR fragment containing NQO1 C609T polymorphism; lanes 4,10, homozygous null genotype (T/T); lanes 5,7,9, homozygous wild genotype (C/C); lanes 6,8, heterozygous genotype (C/T).

Statistical analysis

The comparison of NQO1 genotype distribution in the study groups was performed by means of two-sided contingency

tables using Chi-square test. Hardy-Weinberg analysis was performed to compare the observed and expected genotype frequencies using Chi-square test. A probability level of 5 % was made as statistically significant. The odds ratio (OR) and 95 % confidence interval (CI) were calculated and adjusted for age, sex and smoking status with the unconditional logistic regression model. Statistical analysis was made using SPSS software package (10.0 version).

RESULTS

As shown in Table 1, the composition of gender, age and the proportion of smokers in ESCC and GCA patients were compared with the healthy controls. Eighty-six (44.6 %) of the ESCC and 45 (36.3 %) of the GCA patients had family histories of UGIC. The proportion of age, sex and smoking status in ESCC and GCA patients with and without family histories of UGIC was also not significantly different (data not shown). None of the healthy controls had a family history of UGIC.

The NQO1 C609T genotyping was successfully performed in all study subjects. The observed NQO1 genotype frequencies were not significantly deviated from those expected from Hardy-Weinberg equilibrium in the healthy controls ($\chi^2=0.061$; $P=0.970$), ESCC patients ($\chi^2=0.166$; $P=0.920$) and GCA patients ($\chi^2=0.832$; $P=0.660$). The NQO1 C609T genotype distribution among healthy controls was 31.5 % (C/C), 52.1 % (C/T), and 16.4 % (T/T) respectively (Table 1). The genotype distribution was not correlated with gender, age and smoking status in each study group (data not shown).

Table 1 Demographic characteristics and NQO1 polymorphism among ESCC, GCA patients and controls

Groups	Control n (%)	ESCC n (%)	GCA n (%)
Sex			
Male	109(66.1)	124(64.3)	92(74.2)
Female	56(33.9)	69(35.7)	32(25.8)
Mean age \pm SD (yrs)	52 \pm 7.16	59 \pm 8.73	60 \pm 8.24
Smoking status			
Smoker	82(49.7)	104(53.9)	68(59.8)
Non-smoker	83(50.3)	89(46.1)	46(40.2)
Family history of UGIC			
Positive	0	86(44.6)	45(36.3)
Negative	165(100)	107(55.4)	79(63.7)
Genotype			
C/C	52(31.5)	51(26.4)	40(32.3)
C/T	86(52.1)	92(47.7)	55(44.3)
T/T	27(16.4)	50(25.9) ^a	29(23.4)
Allele type			
C	190(57.6)	194(50.3)	135(54.4)
T	140(42.4)	192(49.7) ^b	113(45.6)

Note. ESCC: esophageal squamous cell carcinoma; GCA: gastric cardiac adenocarcinoma; NQO1: *NAD(P)H: quinone oxidoreductase 1*; UGIC: upper gastrointestinal cancer; a. The genotype frequency was significantly higher than that in healthy controls ($\chi^2=4.79$, $P=0.028$); b. The allele frequency was marginally higher than that in healthy controls ($\chi^2=3.83$, $P=0.05$).

The overall NQO1 null-allele frequency among ESCC patients (49.7 %) was marginally higher than that among healthy controls (42.4 %) ($\chi^2=3.83$, $P=0.05$). There was no difference in allele distribution between GCA patients and healthy controls ($\chi^2=0.567$, $P=0.451$) (Table 1). The distribution of NQO1 C/C and C/T genotypes among ESCC and GCA

patients was not significantly different from that among healthy controls ($P>0.05$) (Table 1).

Interestingly, in ESCC patients, the *NQO1* T/T genotype was significantly more frequent (25.9 %) than that among healthy controls ($\chi^2=4.79$, $P=0.028$) (Table 2). The relative risk of the T/T genotype for the ESCC development was increased by about 1.8 fold compared with the combination of the C/C or C/T genotypes, with an age, sex and smoking status adjusted odds ratio of 1.78 (95 % CI=1.04-2.98). When stratified for the family history of UGIC, the *NQO1* T/T genotype was significantly more common among patients with family histories of UGIC (30.2 %) than that among healthy controls ($\chi^2=6.53$, $P=0.011$). The T/T genotype significantly increased the risk for developing ESCC among patients with family histories of UGIC, compared with the C/C and C/T genotypes (adjusted OR=2.20, 95 % CI=1.18-3.98). In contrast, the *NQO1* T/T genotype frequency was not significantly different between ESCC patients without family history of UGIC (22.4 %) and healthy controls ($\chi^2=1.49$, $P=0.223$) (Table 2).

In line with the result of ESCC, the *NQO1* T/T genotype significantly increased the risk for developing GCA compared with the C/C and C/T genotypes. However, this increased risk was only demonstrated when stratified for the family history. Thus, among GCA patients with family histories of UGIC, the T/T frequency (33.3 %) was significantly higher than that among healthy controls ($\chi^2=6.36$, $P=0.012$). In this patient group, the relative risk of the T/T genotype for developing GCA was more than two-fold higher compared with the combination of C/C and C/T genotypes (adjusted OR=2.55, 95 % CI=1.21-5.23), whereas the *NQO1* T/T genotype frequency among the overall GCA patients (23.4 %) and GCA patients without family histories of UGIC (17.7 %) remained similar to that of the healthy controls ($P>0.05$) (Table 2).

Table 2 Relative risk of the *NQO1* C609T homogenous null for ESCC and GCA development

Groups	<i>NQO1</i> genotype		aOR (95%CI) ^d
	C/C+C/T n (%)	T/T n (%)	
Healthy controls	138(83.6)	27(16.4)	
ESCC patient	143(74.1)	50(25.9) ^a	1.78 (1.04-2.98)
Family history of UGIC			
Positive	60(69.8)	26(30.2) ^b	2.20 (1.18-3.98)
Negative	83(77.6)	24(22.4)	1.46 (0.79-2.63)
GCA patient	95(76.6)	29(23.4)	1.44 (0.86-2.30)
Family history of UGIC			
Positive	30(66.7)	15(33.3) ^c	2.55 (1.21-5.23)
Negative	65(82.3)	14(17.7)	1.10 (0.80-1.34)

Note. ESCC: esophageal squamous cell carcinoma; *NQO1*:NAD(P)H: quinone oxidoreductase 1; UGIC: upper gastrointestinal cancer; a,b,c. The genotype frequency was significantly higher than that in healthy controls (a. $\chi^2=4.79$, $P=0.028$; b. $\chi^2=6.53$, $P=0.011$; c. $\chi^2=6.36$, $P=0.012$); d. The age, sex and smoking status adjusted relative risk of the *NQO1* C609T homogenous null genotype (T/T) against the combination of the heterozygote (C/T) and homozygous wild type (C/C).

To observe the different influence of the *NQO1* C609T polymorphism on the ESCC or GCA development among smokers and non-smokers, the genotype distribution was also stratified according to the smoking habits. No difference in *NQO1* genotype distribution among smoking or non-smoking ESCC and GCA patients was observed as compared with that of the healthy controls (data not shown).

DISCUSSION

Both of ESCC and GCA are characterized by a particularly poor prognosis since most of patients are diagnosed at advanced stages. Endoscopic examination is the only feasible way to detect ESCC and GCA at early and/or precancerous stages. However, the wide application of this method is limited by the high cost and painfulness of the examination. The laboratory identification of high-risk individuals, in combination with the clinical detection, will provide a promising way to detect the early tumors.

The present hospital based case control study suggests that *NQO1* C609T homozygous null genotype may increase the susceptibility to ESCC and GCA in the northern Chinese population. This result is consistent with the previous investigations, which showed that the *NQO1* homozygous null genotype increased the susceptibility to other tumor types such as lung cancer^[19], leukemia^[21,22] and cutaneous cancers^[24]. The underlying mechanism of the correlation of *NQO1* C609T polymorphism with increased risk for developing various tumors may be related to the different enzyme activities encoded by the different *NQO1* genotypes. Thus, lack of *NQO1* activity encoded by the homozygous null genotype results in a reduced detoxification of exogenous carcinogens and leads cells to be easily damaged by oxidation, and thereby increasing the susceptibility to chemically induced cancers such as ESCC and GCA. In addition, the recessive effect of the *NQO1* C609T null allele on the development of ESCC and GCA was suggested by the current study, since the heterozygous genotype frequency among tumor patients was similar to that among healthy controls. The result indicates that although the *NQO1* heterozygous genotype results in a three-fold decrease of the *NQO1* enzyme activity, it may be sufficient for protecting cells from damage by exogenous carcinogens.

In this study, the increased risk of the *NQO1* C609T homozygous null genotype for developing both of ESCC and GCA was only evident in patients with family histories of UGIC, indicating that in families aggregated with UGIC patients, a predisposition to ESCC and GCA may be inherited by lack of *NQO1* enzyme activity. A strong association of increased risk for esophageal cancer with a positive family history of UGIC in the first-degree relatives has been reported in the high incidence regions of China^[7,8]. The segregation analysis on the high-risk nuclear families suggested that the ESCC occurrence was best fit to the autosomal recessive Mendelian inheritance^[8]. However, the underlying molecular mechanisms for the familial clustering of UGIC patients have not been elucidated so far. Our results suggested, that the *NQO1* C609T polymorphic gene, together with other possible susceptible genes, might give an opportunity to challenge the genetic mechanisms of cancer development in the UGIC clustered families and provide a chance to predict high-risk individuals in the high-incidence regions. In addition, the consistent association of *NQO1* C609T polymorphism with the susceptibility to ESCC and GCA, as shown in this study, supports that there might be a common genetic background in the development of these two tumor types. However, the result should be interpreted cautiously, since the number of cases, especially in the subgroup analyses, was probably too small to draw a final conclusion.

In summary, our preliminary data suggest that the *NQO1* C609T gene polymorphism may influence the susceptibility to ESCC and CAC in a northern Chinese population. Determination of *NQO1* C609T genotype may provide a useful genetic marker in predicating high-risk individuals for the development of ESCC and CAC. It is worthwhile conducting additional population-based studies including enlarged subjects before its clinical application.

ACKNOWLEDGEMENTS

We greatly acknowledge the expert technical assistance of Mrs. C. Pawlik, Mrs. H. Huss and Mrs. B. Maruhn-Debowski. We also thank Mrs. Heyu Tong, Mr. Fanshu Meng, and Mr. Baoshan Zhao for their assistance in recruiting study subjects.

REFERENCES

- 1 **Launoy G**, Milan CH, Faivre J, Pienkowski P, Milan CI, Gignoux M. Alcohol, tobacco and oesophageal cancer: effects of the duration of consumption, mean intake and current and former consumption. *Br J Cancer* 1997; **75**: 1389-1396
- 2 **Yokokawa Y**, Ohta S, Hou J, Zhang XL, Li SS, Ping YM, Nakajima T. Ecological study on the risks of esophageal cancer in Ci-Xian, China: the importance of nutritional status and the use of well water. *Int J Cancer* 1999; **83**: 620-624
- 3 **Yang CS**. Vitamin nutrition and gastroesophageal cancer. *J Nutr* 2000; **130**(Suppl 2S): 338S-339S
- 4 **Cai L**, Yu SZ, Zhang ZF. *Helicobacter pylori* infection and risk of gastric cancer in Changle County, Fujian Province, China. *World J Gastroenterol* 2000; **6**: 374-376
- 5 **Matsha T**, Erasmus R, Kafuko AB, Mugwanya D, Stepien A, Parker MI. CANSA/MRC Oesophageal Cancer Research Group. Human papillomavirus associated with oesophageal cancer. *J Clin Pathol* 2002; **55**: 587-590
- 6 **Lavergne D**, de Villiers EM. Papillomavirus in esophageal papillomas and carcinomas. *Int J Cancer* 1999; **80**: 681-684
- 7 **Chang-Claude J**, Becher H, Blettner M, Qiu S, Yang G, Wahrendorf J. Familial aggregation of oesophageal cancer in a high incidence area in China. *Int J Epidemiol* 1997; **26**: 1159-1165
- 8 **Zhang W**, Bailey-Wilson JE, Li W, Wang X, Zhang C, Mao X, Liu Z, Zhou C, Wu M. Segregation analysis of esophageal cancer in a moderately high-incidence area of northern China. *Am J Hum Genet* 2000; **67**: 110-119
- 9 **Matsuo K**, Hamajima N, Shinoda M, Hatooka S, Inoue M, Takezaki T, Tajima K. Gene-environment interaction between an aldehyde dehydrogenase-2 (ALDH2) polymorphism and alcohol consumption for the risk of esophageal cancer. *Carcinogenesis* 2001; **22**: 913-916
- 10 **Song C**, Xing D, Tan W, Wei Q, Lin D. Methylenetetrahydrofolate reductase polymorphisms increase risk of esophageal squamous cell carcinoma in a Chinese population. *Cancer Res* 2001; **61**: 3272-3275
- 11 **Tan W**, Song N, Wang GQ, Liu Q, Tang HJ, Kadlubar FF, Lin DX. Impact of genetic polymorphisms in cytochrome P450 2E1 and glutathione S-transferases M1, T1, and P1 on susceptibility to esophageal cancer among high-risk individuals in China. *Cancer Epidemiol Biomarkers Prev* 2000; **9**: 551-556
- 12 **Cai L**, Yu SZ, Zhang ZF. Glutathione S-transferases M1, T1 genotypes and the risk of gastric cancer: a case-control study. *World J Gastroenterol* 2001; **7**: 506-509
- 13 **Cai L**, Yu SZ, Zhan ZF. Cytochrome P450 2E1 genetic polymorphism and gastric cancer in Changle, Fujian Province. *World J Gastroenterol* 2001; **7**: 792-795
- 14 **Winski SL**, Koutalos Y, Bentley DL, Ross D. Subcellular localization of NAD(P)H: quinone oxidoreductase 1 in human cancer cells. *Cancer Res* 2002; **62**: 1420-1424
- 15 **Larson RA**, Wang Y, Banerjee M, Wiemels J, Hartford C, Lebeau MM, Smith MT. Prevalence of the inactivating 609C→T polymorphism in the NAD(P)H: quinone oxidoreductase (NQO1) gene in patients with primary and therapy-related myeloid leukemia. *Blood* 1999; **94**: 803-807
- 16 **Kuehl BL**, Paterson JW, Peacock JW, Paterson MC, Rauth AM. Presence of a heterozygous substitution and its relationship to DT-diaphorase activity. *Br J Cancer* 1995; **72**: 555-561
- 17 **Moran JL**, Siegel D, Ross D. A potential mechanism underlying the increased susceptibility of individuals with a polymorphism in NAD(P)H: quinone oxidoreductase 1 (NQO1) to benzene toxicity. *Proc Natl Acad Sci USA* 1999; **96**: 8150-8155
- 18 **Smith M**. Benzene, NQO1, and genetic susceptibility to cancer. *Proc Natl Acad Sci USA* 1999; **96**: 7624-7626
- 19 **Chen H**, Lum A, Seifried A, Wilkens LR, Le Marchand L. Association of the NAD(P)H: quinone oxidoreductase 609C→T polymorphism with a decreased lung cancer risk. *Cancer Res* 1999; **59**: 3045-3048
- 20 **Xu LL**, Wain JC, Miller DP, Thurston SW, Su L, Lynch TJ, Christiani DC. The NAD(P)H: quinone oxidoreductase 1 gene polymorphism and lung cancer: differential susceptibility based on smoking behavior. *Cancer Epidemiol Biomarkers Prev* 2001; **10**: 303-309
- 21 **Wiemels JL**, Pagnamenta A, Taylor GM, Eden OB, Alexander FE, Greaves MF. A lack of a functional NAD(P)H: quinone oxidoreductase allele is selectively associated with pediatric leukemias that have MLL fusions. United Kingdom childhood cancer study investigators. *Cancer Res* 1999; **59**: 4095-4099
- 22 **Smith MT**, Wang Y, Kane E, Rollinson S, Wiemels JL, Roman E, Roddam P, Cartwright R, Morgan G. Low NAD(P)H: quinone oxidoreductase 1 activity is associated with increased risk of acute leukemia in adults. *Blood* 2001; **97**: 1422-1426
- 23 **Gabbert HE**, Shimoda T, Hainaut P, Nakamura Y, Field JK, Inoue H. Squamous cell carcinoma of the oesophagus. *Lyon IARCP Press* 2000: 11-32
- 24 **Clairmont A**, Sies H, Ramachandran S, Lear JT, Smith AG, Bowers B, Jones PW, Fryer AA, Strange RC. Association of NAD(P)H: quinone oxidoreductase (NQO1) null with numbers of basal cell carcinomas: use of a multivariate model to rank the relative importance of this polymorphism and those at other relevant loci. *Carcinogenesis* 1999; **20**: 1235-1240

Edited by Ma JY

CYP1A1, GSTs and mEH polymorphisms and susceptibility to esophageal carcinoma: Study of population from a high- incidence area in north China

Li-Dong Wang, Shu Zheng, Bin Liu, Jian-Xiang Zhou, Yan-Jie Li, Ji-Xue Li

Li-Dong Wang, Cancer Institute, Zhejiang University, Hangzhou, 310009, Zhejiang Province, China and Laboratory for Cancer Research, College of Medicine, Zhengzhou University, Zhengzhou, 450052, Henan Province, China

Shu Zheng, Cancer Institute, Zhejiang University, Hangzhou, 310009, Zhejiang Province, China

Jian-Xiang Zhou, Yan-Jie Li, Ji-Xue Li, Laboratory for Cancer Research, College of Medicine, Zhengzhou University, Zhengzhou, 450052, Henan Province, China

Bin Liu, Department of Gastroenterology, Tongren Hospital, Capital Medical University, Beijing 100013, China

Supported by National Outstanding Young Scientist Award of China 30025016 (China), State Key Project for Basic Research G1998051206 (China), Foundation of Henan Education Committee 1999125 and the U.S. NIH Grant CA65871

Correspondence to: Li-Dong Wang, M.D., Professor of Pathology and Oncology, Invited Professor of Henan Province, Director of Laboratory for Cancer Research, College of Medicine, Zhengzhou University, Zhengzhou, 450052, Henan Province, China. lidong0823@sina.com

Telephone: +86-11-371-6970165 **Fax:** +86-11-371-6970165

Received: 2003-03-12 **Accepted:** 2003-05-11

Abstract

AIM: To characterize cytochrome P4501A1 (CYP1A1), glutathione S-transferases (GSTs) and microsomal epoxide hydrolase (mEH) polymorphisms in Chinese esophageal cancer patients.

METHODS: Multiplex polymerase chain reaction (PCR) and PCR based restriction fragment length polymorphisms (PCR-RFLP) were used to detect polymorphism changes of CYP, GSTs and mEH on esophageal cancerous and precancerous lesions as well as in case control group. All the examination samples were obtained from Linzhou (formerly Linxian), Henan Province, the highest incidence area for esophageal cancer.

RESULTS: The frequency of CYP1A1 3' polymorphism in case control group (26/38, 68 %) was significantly higher than in esophageal squamous cell carcinoma group (ESCC) (29/62, 47 %) ($P < 0.05$). A significant difference in the incidence of mEH slow allele variant was observed between case control group (15/38, 39 %) and esophageal dysplasia group (22/32, 69 %) or ESCC group (39/62, 63 %) ($P < 0.05$). However, no significant difference was observed among different groups in the polymorphisms of CYP1A1 exon 7, GSTM1, GSTT1, GSTP1 and mEH fast allele.

CONCLUSION: The present results suggest that CYP1A1 3' polymorphism may be one of the promising protective factors and its wild gene type may be an indicator for higher susceptibility to esophageal cancer. mEH slow allele variant, associated with the progression of esophageal precancerous lesions, may contribute to the high susceptibility to esophageal carcinoma.

Wang LD, Zheng S, Liu B, Zhou JX, Li YJ, Li JX. CYP1A1, GSTs and mEH polymorphisms and susceptibility to esophageal carcinoma: Study of population from a high- incidence area in north China. *World J Gastroenterol* 2003; 9(7):1394-1397

<http://www.wjgnet.com/1007-9327/9/1394.asp>

INTRODUCTION

It has been revealed that carcinogenesis may be resulted from mutations or deletions in cancer-related genes. Meanwhile, a large proportion of human cancers is associated with diet, tobacco smoking and other environmental factors^[1], suggesting that a combination of endogenous and exogenous factors is responsible for human carcinogenesis. In recent years, a relatively new field of cancer research has focused on the interaction between genes and environment to understand the aetiology of cancer^[2]. Primary candidates for gene-environment interaction studies are those which encode enzymes related to the metabolism of established cancer risk factors. It has been known that most carcinogens require metabolic activation in the human body for the carcinogenic effects. There are two major enzyme systems that metabolize potential carcinogens, either synthetic or naturally occurring in the body, which have been classified as phase I and phase II. Generally, phase I enzymes can activate the carcinogen directly and produce more active metabolites. Phase II enzymes can detoxify and process the activated metabolites for final breakdown or excretion. Therefore, the genotypes with high phase I enzyme activity and low phase II enzyme level are considered to pose a high risk to cancer development^[3].

Cytochrome P450 (CYP) isoenzymes are one major kind of phase I enzymes and play an important role in the oxidation of chemical compounds, such as polycyclic aromatic hydrocarbons (PAH), often resulting in the formation of highly reactive compounds that are the ultimate carcinogens^[4]. Glutathione S-transferases (GSTs) are phase II enzymes and responsible for catalyzing the biotransformation of a variety of electrophiles, and have a central role in the detoxification of activated metabolites of procarcinogens produced by phase I reactions. GSTP1 is the main GST isoform expressed in esophageal mucosa^[5,6]. Microsomal epoxide hydrolase (mEH) plays a dual role both in detoxication and activation of procarcinogens because it is not only involved in detoxication reaction but also generates some trans-dihydrodiols that could be metabolized to highly toxic, mutagenic and carcinogenic polycyclic hydrocarbon diol epoxides^[7].

Esophageal cancer is one of the most common malignant diseases worldwide with a sharp variation in its geographic distribution^[8]. The ratio in incidence between high- and low-risk areas could be as great as 500:1. The high incidence in special areas indicates the importance of environmental factors in esophageal carcinogenesis. However, only a small part of individuals in the high-risk area for esophageal cancer develop into esophageal cancer, although all the residents in that area share very similar environment-related risk factors and lifestyle,

suggesting that host susceptibility factors, such as the polymorphisms of phase I and phase II enzymes, may play an important role in increased risk for esophageal cancer. Thus, the present study was undertaken to assess the genetic polymorphisms of CYP1A1, GSTM1, GSTT1, GSTP1 and mEH in esophageal precancerous and cancerous lesions as well as in case control group from the subjects in high-incidence area for esophageal cancer in Henan to correlate these genetic polymorphisms and susceptibility to esophageal cancer.

MATERIALS AND METHODS

Patients and controls

Sixty-two cases of esophageal squamous cell carcinoma (ESCC), including 32 males with a mean age of 55 (55±9.8) and 30 females with a mean age of 60 (66±10.5) were recruited from Yaocun Esophageal Cancer Hospital in Linzhou, who were histopathologically confirmed in 1999. All the cases were from Linzhou district and were interviewed to exclude other simultaneous malignancies. Thirty-eight subjects with matched age and sex frequencies were randomly selected as control group from the same region during the field surveys between 1998 and 1999. Thirty cases of esophageal basal cell hyperplasia (BCH), including 20 males with a mean age of 52 (52±8) and 10 females with a mean age of 54 (54±7) and thirty-two cases of esophageal dysplasia (DYS), including 18 males with a mean age of 54 (54±8) and 14 females with a mean age of 55 (55±7) were also randomly recruited from the same region during the field surveys between 1997 and 1999.

PCR analysis of CYP1A1 gene polymorphism

Genomic DNA was extracted from surgically resected ESCC specimen, BCH and DYS biopsies and buccal smear (for control group). The PCR was performed in a total volume of 25 µL with GeneAmp 9700 (Perkin-Elmer Corp., Norwalk, CT) in this study. The concentration of primers for GSTT1 was 0.3 µM, and others were 1.0 µM. The A to G transition polymorphism in exon 7 of the CYP1A1 gene was analyzed by primers 5' GAAAGGCTGGGTCCACCCTCT and 5' CCAGGAAGAAA GACCTCCCAGCGGGCCA. Briefly, 100 ng of the DNA sample was amplified in buffer (10 mM Tris-HCl, 50 mM KCl, 1.5 mM MgCl₂ pH 8.4) with 0.1 mM of each dNTP (Pharmacia, Piscataway, NJ) and 1.25 U Taq polymerase (Perkin Elmer Corp., Norwalk, CT). Pre-heated at 80 °C for 3 sec, then initial denaturation was performed at 95 °C for 10 min, followed by 35 cycles of annealing for 1 min at 55 °C, extension for 1 min at 72 °C and denaturation for 1 min at 95 °C, finally extension for 5 min at 72 °C. The PCR products were digested with NcoI (New England Biolabs, Inc., Beverly, MA) at 37 °C overnight, subjected to electrophoresis in an ethidium-bromide-stained 3 % agarose gel (Nusieve 3: 1; American Bioanalytical, Natick, MA) in TBE buffer (89 mM Tris-HCl, 0.89 mM boric acid and 2 mM EDTA, pH 8.0). PCR-RFLP analysis resulted in the following genotype classification: A predominant homozygote (Ile/Ile), a heterozygote (Ile/Val) and a rare homozygote (Val/Val).

For 3' -flank region polymorphism of CYP1A1, PCR was performed using the primers 5' CAGTCAACAGGTGTAGC and 5' GAGGCAGGTGGATCACTTGAGCTC. After preheated for 3 sec at 80 °C, initial denaturation was performed at 94 °C for 1 min, followed by 37 thermal cycles consisting of denaturation for 25 sec at 94 °C, annealing for 25 sec at 62 °C, extension for 25 sec at 72 °C and a final extension for 5 min at 72 °C. The PCR products were digested with MspI (New England Biolabs, Inc., Beverly, MA) at 37 °C overnight and subjected to electrophoresis on a 3 % agarose gel. The genotypes of CYP1A1 3' were classified as follows: Wild-type, heterozygous variant and homozygous variant.

GSTM1 and GSTT1 genotyping

GSTM1 and GSTT1 genotyping for gene deletion was carried out by a multiplex PCR using primers 5' GAACTCCCTGAAAAGCTAAAGC and 5' GTTGGGCTCAAATATACG GTGG for GSTM1, which produced a 219 bp product, primers 5' TTCCTTACTGGTCCCTCACATCTC and 5' TCACCGGATCATGGCCAGCA for GSTT1, which produced a 480 bp product. At the same time, amplification of the β -globin gene (5' ACACAACCTGTGTTTAC TAGC and 5' CTCAAAGAACCCTCTGGGTCC) was used as an internal control and produced a 299 bp product. PCR was performed in a 25 µL mixture consisting of 100 ng sample DNA, 10 mM Tris-HCl, 50 mM KCl, 1.5 mM MgCl₂ pH 8.4, 0.1 mM of each dNTP and 1.25 U Taq polymerase. After initial denaturation for 3 min at 94 °C, 35 cycles were performed at 94 °C for 1 min (denaturation), at 62 °C for 2 min (annealing) and at 72 °C for 2 min (extension), followed by a final step for 5 min at 72 °C. The amplified products were visualized by electrophoresis in ethidium-bromide-stained 3 % agarose gel in TBE buffer. For null deletions of GSTM1 and GSTT1, no amplified product could be observed.

PCR-RFLP analysis of GSTP1 gene polymorphism

The primers 5' GTATTTTGCCCAAGGTCAAG and 5' AGCCACCTGAGGGGTAAG were used to amplify exon 5 of GSTP1 gene that includes the BsmAI enzyme recognition site. The same reaction mixture as above was used, after digestion with BsmAI at 55 °C overnight, the following genotypes could be shown: Wild type (one restriction site yielded two fragments of 329 bp and 113 bp), variant with 2 restriction sites, heterozygous variant yielded 3 fragments (329, 216, 113 bp), homozygous one yielded 2 fragments (216, 113 bp).

Analysis of mEH gene polymorphism

Primers 5' GATCGATAAGTTCCGTTTCACC and 5' ATCCTTAGTCTTGAAGTGAGGAT were used to amplify mEH slow allele (113 code). Primers 5' ACATCCAC TTCATCCACGTT and 5' ATGCCTCTGAGAAGCCAT were used to amplify mEH fast allele (139 code). After two separate PCR reactions, the variant, correlated with decreased mEH activity (His 113) was identified through the presence of EcoR V restriction site, and the allele correlated with increased activity (Arg 139) was identified through the presence of RsaI site.

Statistical analysis

The χ^2 test was used to examine the differences in genotype distribution between patients and controls. The difference was considered significant in case of a two-tailed *P* value less than 0.05.

RESULTS

CYP1A1 genetic polymorphism (Table 1)

DNA samples subjected to PCR and enzymatic digestion with MspI revealed the expected fragment lengths and resulted in three genotypes of CYP1A1 3' noncoding area (Figure 1). The frequency of combined heterozygous and homozygous variant genotype detected in the groups of control, BCH, DYS and ESCC was 68 %, 63 %, 62 %, 47 %, respectively (Table 1), the difference was significant between control group and ESCC group (*P*<0.05). However, no significant difference was observed for heterozygous and homozygous variant incidence among the different groups (*P*>0.05). CYP1A1 exon 7 polymorphisms in the groups of control, BCH, DYS and ESCC were observed with an incidence of 47 %, 53 %, 50 % and 52 %, respectively, but there was no significant difference

among these groups ($P>0.05$). The corresponding heterozygous and homozygous variant frequency did not show a significant difference among these groups.

Table 1 Distribution of CYP1A1 genetic polymorphism in controls and subjects with cancer and different severity of lesions $n(\%)$

	Control ($n=38$)	BCH ($n=30$)	DYS ($n=32$)	ESCC ($n=62$)
CYP1A1 3'				
Wild type	12(32)	8(27)	9(28)	33(53)
Heterozygous	22(58)	16(53)	17(53)	25(40)
Homozygous variant	4(10)	3(10)	3(9)	4(6)
Heterozygous+	26(68)	19(63)	20(62)	29(47) ^a
Homozygous				
CYP1A1 exon 7				
Ile/Ile	20(53)	14(47)	16(50)	30(48)
Val/Ile	16(42)	14(47)	15(47)	28(45)
Val/Val	2(5)	2(7)	1(3)	4(6)
Val/Ile + Val/Val	18(47)	16(53)	16(50)	32(52)

^a $P<0.05$, vs case control group.

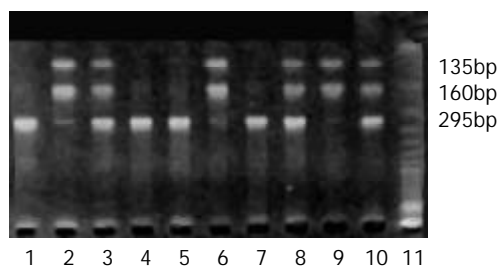


Figure 1 Examples of CYP1A1 3' polymorphism. The RFLPs of PCR-amplified fragments obtained using MspI and subjected to agarose gel electrophoresis. Wild type without MspI restriction site shows a 295 bp band (lanes 1, 4, 5, 7), variant with MspI restriction site results in two bands of 135 and 160 bp (homozygous variant, lanes 2, 6, 9) or all three bands (heterozygous variant, lanes 3, 8, 10).

GSTs genetic polymorphism (Table 2)

Table 2 shows the homozygous deletion of GSTM1 and GSTT1. A similar percentage (around 50 %) for GSTM1 and T1 homozygous deletion in the groups of control, BCH, DYS and ESCC was observed. GSTP1 polymorphism incidence in control group (37 %) was a little lower than that in other groups (about 50 %), but the difference was not significant ($P>0.05$). There was also no apparent difference for their corresponding heterozygous and homozygous variant distribution in all groups.

Table 2 Genotypes of GSTM1, GSTT1 and GSTP1 in controls and subjects with different severity of lesions and cancer $n(\%)$

	Control ($n=38$)	BCH ($n=30$)	DYS ($n=32$)	ESCC ($n=62$)
GSTM1				
+	19(50)	16(53)	18(56)	35(56)
-	19(50)	14(47)	14(44)	27(44)
GSTT1				
+	18(47)	17(57)	15(47)	28(45)
-	20(53)	13(43)	17(53)	34(55)
GSTP1				
Ile/Ile	24(63)	15(50)	15(47)	29(47)
Val/Ile	13(34)	15(50)	16(50)	30(48)
Val/Val	1(3)	0(0)	1(3)	3(5)
Val/Ile + Val/Val	14(37)	15(50)	17(53)	33(53)

mEH genetic polymorphism (Table 3)

mEH polymorphism was observed occurring frequently in exons 3 and 4, which resulted in substitution of amino acid histidine to tyrosine at residue 113 (slow allele) and arginine to histidine at residue 139 (fast allele), respectively. The variant of mEH fast allele was observed with a relatively low frequency in all groups. The homozygous and heterozygous variant for mEH was also detected with a low incidence and no significant difference was observed among different groups (Table 3, $P>0.05$). However, the different distribution of mEH slow allele variant was observed in the present study. The frequency for mEH slow allele variant (39 %) was the lowest in the control group and increased in BCH (53 %), DYS (69 %) and ECSS (63 %), the difference was significant between control group and BCH, or DYS and ESCC ($P<0.05$). Figure 2 shows slow allele polymorphism for mEH.

Another interesting result was that none of polymorphic variants of all detected genes was found to be associated with ESCC differentiation in this study.

Table 3 Slow and fast allele polymorphism of mEH in controls and subjects with different severity of lesions and cancer $n(\%)$

	Control ($n=38$)	BCH ($n=30$)	DYS ($n=32$)	ESCC ($n=62$)
mEH slow allele				
Tyr/Tyr	23(61)	14(47)	10(31)	23(37)
His/Tyr	10(26)	13(43)	15(47)	22(35)
His/His	5(13)	2(7)	7(22)	17(27)
His/Tyr+His/His	15(39)	16(53)	22(69) ^a	39(63) ^a
mEH fast allele				
His/His	32(84)	22(73)	23(72)	50(81)
Arg/His	5(13)	6(20)	7(22)	11(18)
Arg/Arg	1(3)	2(7)	2(6)	1(2)
Arg/His + Arg/Arg	6(16)	8(27)	9(28)	12(19)

^a $P<0.05$, vs case control group.

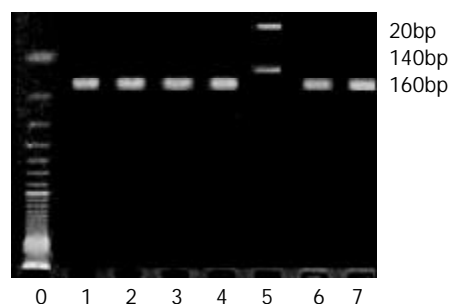


Figure 2 Example of mEH slow allele polymorphism. The RFLPs of PCR-amplified fragments obtained using EcoR V and subjected to agarose gel electrophoresis. Lane 5 is homozygote, lanes 1, 2, 3, 4, 6, 7 wild type.

DISCUSSION

In this study, a similar frequency of CYP1A1 exon 7 polymorphism was observed in the groups of control, ESCC and precancerous lesions, but the CYP1A1 3' flank polymorphic variants most frequently occurred in control group, 1.4 times that in ESCC group (68 % vs 47 %), indicating that CYP1A1 3' variants could be a protective factor for ESCC in this population. Two major relevant genetic polymorphisms have been demonstrated in the CYP1A1 gene: One is a T to C substitution in the 3' flanking region altering protein folding, whereas an Ile to Val substitution may occur in exon 7. Both substitutions were considered to result in the enhancement of

enzyme activity^[9], but polymorphism in the noncoding region of CYP1A1 was unlikely to have direct functional consequences on CYP1A1 activity^[10], even the variant of CYP1A1 exon 7 was not sure to induce an increased enzyme activity^[11]. These controversial reports suggest that the effect of CYP1A1 polymorphism on cancer development remains to be characterized.

The second interesting observation in the present study was that a high rate of GSTM1 and GSTT1 null genotype and GSTP1 polymorphic variant occurred not only in the control group but also in ESCC patients and the subjects with different precancerous lesions (BCH and DYS), suggesting that GSTs polymorphism may be responsible for the higher-risk for esophageal cancer in this population. GSTM1 and GSTT1 null genotypes have been reported to enhance the risk of developing gastric, colorectal, and lung cancers^[12,13], although other studies did not show such a genetic predisposition^[14]. Again, in normal esophageal epithelium, GSTP1 was the mean isoform for GST^[5]. An Ile to Val substitution in the GSTP1 gene has been found more often in patients with bladder and testicular cancer^[5].

The third interesting observation was that mEH sequence alteration from tyrosine to histidine at residue 113 (slow allele), but not polymorphism at residue 139, was associated with progression of esophageal lesions from normal to BCH to DYS and ESCC, and might contribute to a high susceptibility to esophageal carcinoma. mEH is involved in the metabolism of carcinogens found in cigarette smoke and cooked meat, such as PAH. Expression studies of cDNA *in vitro* indicated that mEH enzymatic activities were decreased by exon 3 polymorphism and increased by exon 4 polymorphism. Reactive and toxic epoxides are frequently generated during PAH oxidative metabolism. Epoxides can be detoxicated partly by mEH, which catalyzes their hydrolysis, thereby yielding the corresponding trans-dihydrolysis. Although hydrolysis is generally considered to represent a detoxication reaction, some trans-dihydrodiols are substrates for additional metabolic changes to highly toxic polycyclic hydrocarbon diol epoxides^[7]. It has been suggested that mEH gene His113 variant allele increases the risk of hepatocarcinoma^[15] and lung cancer^[16] but decreases the risk of ovarian cancer^[17]. Further characterization of mEH polymorphism in a larger scale population will be needed to clarify the significance of mEH in high-risk area for esophageal cancer.

Finally, it is noteworthy that the genetic variants of all detected genes in this study were not associated with ESCC differentiation, suggesting that genetic polymorphism may represent susceptibility to ESCC.

ACKNOWLEDGEMENTS

We acknowledge the help given by graduate students in Laboratory for Cancer Research, College of Medicine, Zhengzhou University (Drs. Ya-Nan Jiang, Ran Wang) in preparation of the manuscript.

REFERENCES

- Doll R**, Peto R. The causes of cancer: quantitative estimates of avoidable risks of cancer in the united states today. *J Natl Cancer Inst* 1981; **66**: 1191-1308
- Mucci LA**, Wedren S, Tamimi RM, Trichopoulos D, Adami HO. The role of gene-environment interaction in the aetiology of human cancer: examples from cancers of the large bowel, lung and breast. *J Intern Med* 2001; **249**: 477-493
- Kihara M**, Kihara M, Noda K. Risk of smoking for squamous and small cell carcinomas of the lung modulated by combinations of CYP1A1 and GSTM1 gene polymorphisms in a Japanese population. *Carcinogenesis* 1995; **16**: 2331-2336
- Guengerich FP**. Roles of cytochrome P-450 enzymes in chemical carcinogenesis and cancer chemotherapy. *Cancer Res* 1988; **48**: 2946-2954
- Peters WH**, Roelofs HM, Hectors MP, Nagengast FM, Jansen JB. Glutathione and glutathione S-transferases in Barrett's epithelium. *Br J Cancer* 1993; **67**: 1413-1417
- Nakajima T**, Wang RS, Nimura Y, Pin YM, HE M, Vinio H, Murayama N, Aoyama T, Iida F. Expresssion Of cytochrome P450s and glutathione S-transferases in human esophagus with squamous-cell carcinomas. *Carcinogenesis* 1996; **17**: 1477-1481
- Sims P**, Grover PL, Swaisland A, Pal K, Hewer A. Metabolic activation of benzo (a) pyrene proceeds by a diol-epoxide. *Nature* 1974; **252**: 326-328
- Wang LD**, Zhou Q, Feng CW, Liu B, Qi YJ, Zhang YR, Gao SS, Fan ZM, Zhou Y, Yang CS, Wei JP, Zheng S. Intervention and follow-up on human esophageal precancerous lesions in Henan, northern China, a high-incidence area for esophageal cancer. *Jpn J Cancer Chemother* 2002; **29**: 159-172
- Landi MT**, Bertazzi PA, Shields PG, Clark G, Lucier GW, GarteSJ, Cosma G, Caporaso NE. Association between CYP1A1 genotype, mRNA expression and enzymatic activity in humans. *Pharmacogenetics* 1994; **4**: 242-246
- Bailey LR**, Roodi N, Verrier CS, Yee CJ, Dupont WD, Parl FF. Breast cancer and CYP1A1, GSTM1, and GSTT1 polymorphisms: evidence of a lack of association in Caucasians and African Americans. *Cancer Res* 1998; **58**: 65-70
- Zhang ZY**, Fasco MJ, Huang L, Guengerich FP, Kaminsky LS. Characterization of purified human recombinant cytochrome P4501A1-Ile462 and -Val462: assessment of a role for the rare allele in carcinogenesis. *Cancer Res* 1996; **56**: 3926-3933
- Chenevix-Trench G**, Young J, Coggan M, Board P. Glutathione S-transferase M1 and T1 polymorphisms: susceptibility to colon cancer and age of onset. *Carcinogenesis* 1995; **16**: 1655-1657
- Deakin M**, Elder J, Hendrickse C, Peckham D, Baldwin D, Pantin C, Wild N, Leopard P, Bell DA, Jones P, Duncan H, Brannigan K, Alldersea J, Fryer AA, Strange RC. Glutathione S-transferase GSTT1 genotypes and susceptibility to cancer: studies of interactions with GSTM1 in lung, oral, gastric and colorectal cancers. *Carcinogenesis* 1996; **17**: 881-884
- Katoh T**, Nagata N, Kuroda Y, Itoh H, Kawahara A, Kuroki N, Ookuma R, Bell DA. Glutathione S-transferase M1 (GSTM1) and T1 (GSTT1) genetic polymorphism and susceptibility to gastric and colorectal adenocarcinoma. *Carcinogenesis* 1996; **17**: 1855-1859
- Mcglynn KA**, Rosvold EA, Lustbader ED, Hu Y, Clapper ML, Zhou T, Wild CP, Xia XL, Baffoe-Bonnie A, Ofori-Adjei D, Chen G, London WT, Shen F, Buetow KH. Susceptibility to hepatocellular carcinoma is associated with genetic variation in the enzymatic detoxification of aflatoxin B1. *Proc Natl Acad Sci USA* 1995; **92**: 2384-2387
- Benhamou S**, Reinikainen M, Bouchardy C, Dayer P, Hirvonen A. Association between lung cancer and microsomal epoxide hydrolase genotypes. *Cancer Res* 1998; **58**: 5291-5293
- Lancaster JM**, Brownlee HA, Bell DA, Futreal PA, Marks JR, Berchuck A, Wiseman RW, Taylor JA. Microsomal epoxide hydrolase polymorphism as a risk factor for ovarian cancer. *Mol Carcinog* 1996; **17**: 160-162

Carbonic anhydrase isozymes IX and XII in gastric tumors

Mari Leppilampi, Juha Saarnio, Tuomo J. Karttunen, Jyrki Kivelä, Silvia Pastoreková, Jaromir Pastorek, Abdul Waheed, William S. Sly, Seppo Parkkila

Mari Leppilampi, Department of Clinical Chemistry, University of Oulu, Oulu, Finland

Juha Saarnio, Department of Surgery, University of Oulu, Oulu, Finland

Tuomo J. Karttunen, Department of Pathology, University of Oulu, Oulu, Finland

Jyrki Kivelä, Department of Anatomy and Cell Biology, University of Oulu, Oulu, Finland. Institute of Dentistry, University of Helsinki, Helsinki, Finland. Research Institute of Military Medicine, Central Military Hospital, Helsinki, Finland

Silvia Pastoreková, Jaromir Pastorek, Institute of Virology, Slovak Academy of Sciences, Bratislava, Slovak Republic

Abdul Waheed, William S. Sly, Edward A. Doisy Department of Biochemistry and Molecular Biology, School of Medicine, Saint Louis University, St. Louis, Missouri, USA

Seppo Parkkila, Departments of Clinical Chemistry and Anatomy and Cell Biology, University of Oulu, Oulu, Finland. Institute of Medical Technology, University of Tampere and Tampere University Hospital, Tampere, Finland

Supported by the grants from Sigrid Juselius Foundation, from Finnish Cultural Foundation and Finnish Dental Society, from the National Institutes of Health (DK40163, GM34182, and GM53405), from Slovak Grant Agency (2/7152/20), and from Bayer Corporation
Correspondence to: Mari Leppilampi, M.Sc, Department of Clinical Chemistry, P.O.Box 5000, FIN-90014 University of Oulu, Finland. mari.leppilampi@oulu.fi

Telephone: +358-40-5164790 **Fax:** +358-8-3154494

Received: 2003-03-19 **Accepted:** 2003-04-03

Abstract

AIM: To systematically study the expression of carbonic anhydrase (CA) isozymes IX and XII in gastric tumors.

METHODS: We analyzed a representative series of specimens from non-neoplastic gastric mucosa and from various dysplastic and neoplastic gastric lesions for the expression of CA IX and XII. Immunohistochemical staining was performed using isozyme-specific antibodies and biotin-streptavidin complex method.

RESULTS: CA IX was highly expressed in the normal gastric mucosa and remained positive in many gastric tumors. In adenomas, CA IX expression significantly decreased towards the high grade dysplasia. However, the expression resumed back to the normal level in well differentiated adenocarcinomas, while it again declined in carcinomas with less differentiation. In comparison, CA XII showed no or weak immunoreaction in the normal gastric mucosa and was slightly increased in tumors.

CONCLUSION: These results demonstrate that CA IX expression is sustained in several types of gastric tumors. The variations observed in the CA IX levels support the concept that gastric adenomas and carcinomas are distinct entities and do not represent progressive steps of a single pathway.

Leppilampi M, Saarnio J, Karttunen TJ, Kivelä J, Pastoreková S, Pastorek J, Waheed A, Sly WS, Parkkila S. Carbonic anhydrase isozymes IX and XII in gastric tumors. *World J Gastroenterol* 2003; 9(7):1398-1403

<http://www.wjgnet.com/1007-9327/9/1398.asp>

INTRODUCTION

The carbonic anhydrases (CAs) catalyze the reversible hydration of carbon dioxide, $\text{CO}_2 + \text{H}_2\text{O} \rightleftharpoons \text{HCO}_3^- + \text{H}^+$, and participate in various physiological processes, including respiration, bone resorption, renal acidification, gluconeogenesis, and formation of cerebrospinal fluid and gastric acid. At present, 11 functionally active CA isozymes, differing in their tissue distribution and enzymatic activity, have been identified in mammals^[1-3].

CA IX was initially described as a tumor-associated integral plasma membrane antigen (MN)^[4]. It has been reported to contain an extracellular domain with the essential structural features and high activity of CAs^[5-7]. CA IX has been detected in the normal gastric, intestinal, and biliary mucosa^[8]. Because CA IX is more strongly expressed in the proliferating cryptal epithelium than in the upper part of the mucosa, it may play a role in the control of proliferation and differentiation of intestinal epithelial cells^[9]. Cell proliferation is abnormally increased in premalignant and malignant lesions, and therefore CA IX has been considered as a potential biomarker for tumor progression^[10]. Previous studies have shown that CA IX is expressed in a high percentage of human epithelial tumors, including carcinomas of uterine cervix, lung, kidney, biliary tract, colon, and breast^[11-20]. Most of these tumors arise from tissues with no or low CA IX expression. On the other hand, it has been proposed that CA IX is absent or reduced in most tumors originating from CA IX-positive tissues^[8].

CA XII is another transmembrane CA isozyme, whose expression has been demonstrated in normal human kidney, colon, prostate, pancreas, ovary, testis, lung, and brain^[21, 22]. By immunohistochemistry, CA XII has been detected at the basolateral plasma membrane of the superficial epithelial cells of the colon and rectum, while the small intestine has remained negative^[23]. CA XII protein has also been located in the epithelial cells of endometrium^[24], renal tubules^[25], and efferent ducts^[26]. CA XII shows a clear association with some tumors, which was first reported by Türeci *et al.*^[27]. They showed that in 10 % of patients with renal cell cancer, the CA XII transcript was expressed at much higher levels in the tumor than in the surrounding normal kidney tissue. These results have been recently confirmed by immunohistochemical staining showing CA XII expression in most cases of clear cell carcinomas and oncocytomas^[25]. In addition to renal tumors, CA XII is expressed in a number of colorectal tumors^[23] and in ductal carcinomas of the breast^[19].

CA IX and XII seem to be regulated by similar mechanisms. First, Ivanov *et al.*^[21] identified the *CA9* and *CA12* genes as von Hippel-Lindau (VHL) target genes. They observed that the wild-type VHL protein down-regulated the transcription of CA IX and XII mRNA, indicating that these isozymes may have a potential role in VHL-mediated carcinogenesis. Second, both isozymes have been induced under hypoxic conditions in tumors and cultured tumor cells^[22, 28]. Hypoxia activates transcription through hypoxia inducible factor-1 (HIF-1), which is composed of two subunits (HIF-1 α and HIF-1 β)^[29]. It is also known that VHL gene product (pVHL) interacts with HIF-1 α and is required for the destruction of HIF-1 α under normoxic conditions^[30]. Taken together, it seems plausible that

CA IX and XII are functionally connected to neoplastic processes controlled by HIF-1 and pVHL^[22]. Furthermore, high expression of CA IX and XII in tumors has suggested that they may functionally participate in the invasion process, which is facilitated by acidification of extracellular space. In favor of this hypothesis, it has been shown *in vitro* that CA inhibitors can reduce the invasion capacity and/or proliferation of cancer cells^[31-34].

The present study was designed to examine the expression of CA IX and XII in gastric tumors. Even though gastric mucosa is known to be the predominant site of CA IX expression, tumors originating from this area have not been comprehensively studied for the expression of these isozymes.

MATERIALS AND METHODS

Antibodies

The polyclonal rabbit antibodies against human CA XII have been produced earlier^[24]. The monoclonal antibody M75 against human CA IX has also been described earlier^[4]. Both antibodies have been characterized for specificity and they have shown no cross-reactivity with other CAs^[9,24].

Immunocytochemistry

The tissue samples from the non-neoplastic gastric mucosa and the corresponding benign and/or malignant neoplastic samples were obtained alongside routine histopathological specimens collected at Oulu University Hospital (Oulu, Finland). The numbers of samples in each histological category are shown in Table 1. The study was approved by the Ethics Committee of Oulu University Hospital and performed according to the guidelines of the Declaration of Helsinki.

Table 1 Number of gastric specimens analyzed for CA IX and XII expression

Diagnosis	CA IX (n)	CA XII (n)
Nonneoplastic cardia	7	5
Nonneoplastic corpus	21	15
Nonneoplastic antrum	26	17
Hyperplasia	13	3
Adenoma, slight dysplasia	11	4
Adenoma, moderate dysplasia	8	3
Adenoma, severe dysplasia	3	1
Adenocarcinoma, grade I	11	8
Adenocarcinoma, grade II	16	15
Adenocarcinoma, grade III	16	15
Diffuse carcinoma	18	15
Metastasis of gastric carcinoma	13	13
Intestinal metaplasia	33	20

The specimens were fixed in 4 % neutral-buffered formaldehyde for 24-48 h. Then they were dehydrated, embedded in paraffin in a vacuum oven at 58 °C, and 5 µm sections were placed on Superfrost microscope slides (Menzel Gläser, Braunschweig, Germany). The CA isozymes were immunostained by the biotin-streptavidin complex method, employing the following steps: (a) Pretreatment of sections with undiluted cow colostrum (Biotop Ltd, Oulu, Finland) for 30 min and rinsing in phosphate-buffered saline (PBS). (b) Incubation for 1 h with anti-CA XII serum (1:100), normal rabbit serum (1:100) or hybridoma medium with M75 antibody (1:10) in 1 % BSA-PBS. (c) Incubation for 1 h with biotinylated swine anti-rabbit IgG (Dakopatts, Glostrup, Denmark) or goat

anti-mouse IgG (Dakopatts) diluted 1:300 in 1 % BSA-PBS. (d) Incubation for 30 min with peroxidase-conjugated streptavidin (Dakopatts) diluted 1:500 in PBS and (e) incubation for 2 min in DAB solution containing 9 mg 3,3'-diaminobenzidine tetrahydrochloride (Fluka, Buchs, Switzerland) in 15 ml PBS and 5 µl 30 % H₂O₂. The sections were washed 3 times for 10 min in PBS after incubation steps b and c, and 4 times for 5 min after step d. All the incubations and washings were carried out at room temperature. After the immunostaining, the tumor sections were counterstained with hematoxylin. The stained sections were examined and photographed with Zeiss Axioplan 2 microscope (Zeiss, Göttingen, Germany).

The immunohistochemical results were semiquantitative based on the percentage of the positive cells and on the intensity of the epithelial staining evaluated in a total field of a single section. The extent of staining (EXT) was scored by four investigators (M.L., J.S., T.J.K., and S.Par.) as 1 when 1-10 % of the cells stained, 2 when 11-50 % of the cells stained, and 3 when 51-100 % of the cells stained. A negative score (0) was given to tissue sections which had no evidence of specific immunostaining. The intensity of staining (INT) was scored on a scale of 0 to 3 as follows: 0, no reaction; 1, weak reaction; 2, moderate reaction; 3, strong reaction. In the normal and hyperplastic gastric mucosa, the scores were first counted in the luminal surface, proliferative zone and glands, and relative staining indices (on the scale 0-3) were calculated separately for each histological layer using the following formula: $\sqrt{EXT \times INT}$. In the adenomas and metaplasias, the EXT and INT scores were counted separately in the deep and superficial parts of the mucosa, and the relative staining indices were calculated accordingly for both regions. Finally, the staining indices obtained in each region were used to calculate the mean values for each normal sample or lesion. The principle of these calculations is shown in Figure 1.

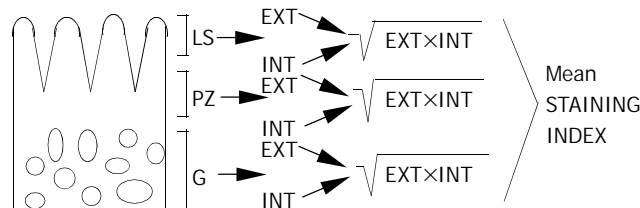


Figure 1 The principle for calculation of the relative staining index in one normal gastric sample (LS=luminal surface, PZ=proliferative zone, G=gastric glands).

Statistical analysis

Statistical analysis of the results was performed using SPSS for Windows software (SPSS Inc.). One-way analysis of variance was used to compare the staining for CA isozymes in different lesions. The pairwise comparisons between group means were performed using multiple comparison tests: Bonferroni, Tukey's honestly significant difference test, Sidak, Gabriel, Hochberg, and LSD (least significant difference).

RESULTS

Expression of CA IX

One intriguing finding of the present study was that the CA IX expression was sustained at relatively high level in many gastric tumors. Figure 2 shows some examples of CA IX immunostaining in the normal gastric mucosa (A) and different

gastric lesions (B-F). In the normal mucosa, CA IX was localized in all major cell types including parietal cells, chief cells, and mucus producing surface epithelial cells as described previously by Pastoreková *et al.*^[8]. The positive staining covered all epithelial types of the gastric mucosa including glands, proliferative zone and the superficial epithelium of the mucosa. The staining was observed to be slightly weaker in the proliferative zone (data not shown) that contrasted with previous staining results in intestine where CA IX was mainly confined to the proliferative enterocytes^[9]. Figure 2B demonstrates a typical distribution pattern of CA IX in intestinal metaplasia. It was notable that it was expressed in the crypts of metaplastic epithelium which was in line with its high expression in Lieberkühn crypts of the normal gut. Figure 3 demonstrates the mean staining indices for CA IX in the samples of normal gastric mucosa, hyperplasia, adenoma, adenocarcinoma, diffuse carcinoma, metastasis of gastric cancer, and metaplasia. The results demonstrated that the average staining reactions were quite similar in normal and hyperplastic gastric mucosa, while they became significantly weaker in dysplastic and malignant lesions. Figure 4 shows CA IX staining indices in gastric lesions grouped according to

the stages of dysplasia and grades of malignancy. This analysis surprisingly revealed that adenomas and carcinomas formed two distinct entities based on the CA IX immunostaining. In adenomas, CA IX staining indices declined from 1.3-1.4 in lesions with slight or moderate dysplasia to 0.3 in those with severe dysplasia. In grade I adenocarcinomas, the staining index remained at the same level with normal and hyperplastic mucosa, while it again declined in carcinomas with higher malignancy grades.

Expression of CA XII

Figure 5 shows examples of CA XII immunostaining in the normal gastric mucosa and different lesions. Figures 6 and 7 show the staining indices for CA XII. In the non-neoplastic gastric mucosa, CA XII showed no or weak immunoreactions. The staining indices appeared to be significantly increased in hyperplastic and adenomatous lesions as well as in grades I and II adenocarcinomas and metastases, although they did not reach the values observed with CA IX. The indices were only very slightly increased in grade III adenocarcinomas and diffuse carcinomas, but the difference was not statistically significant.

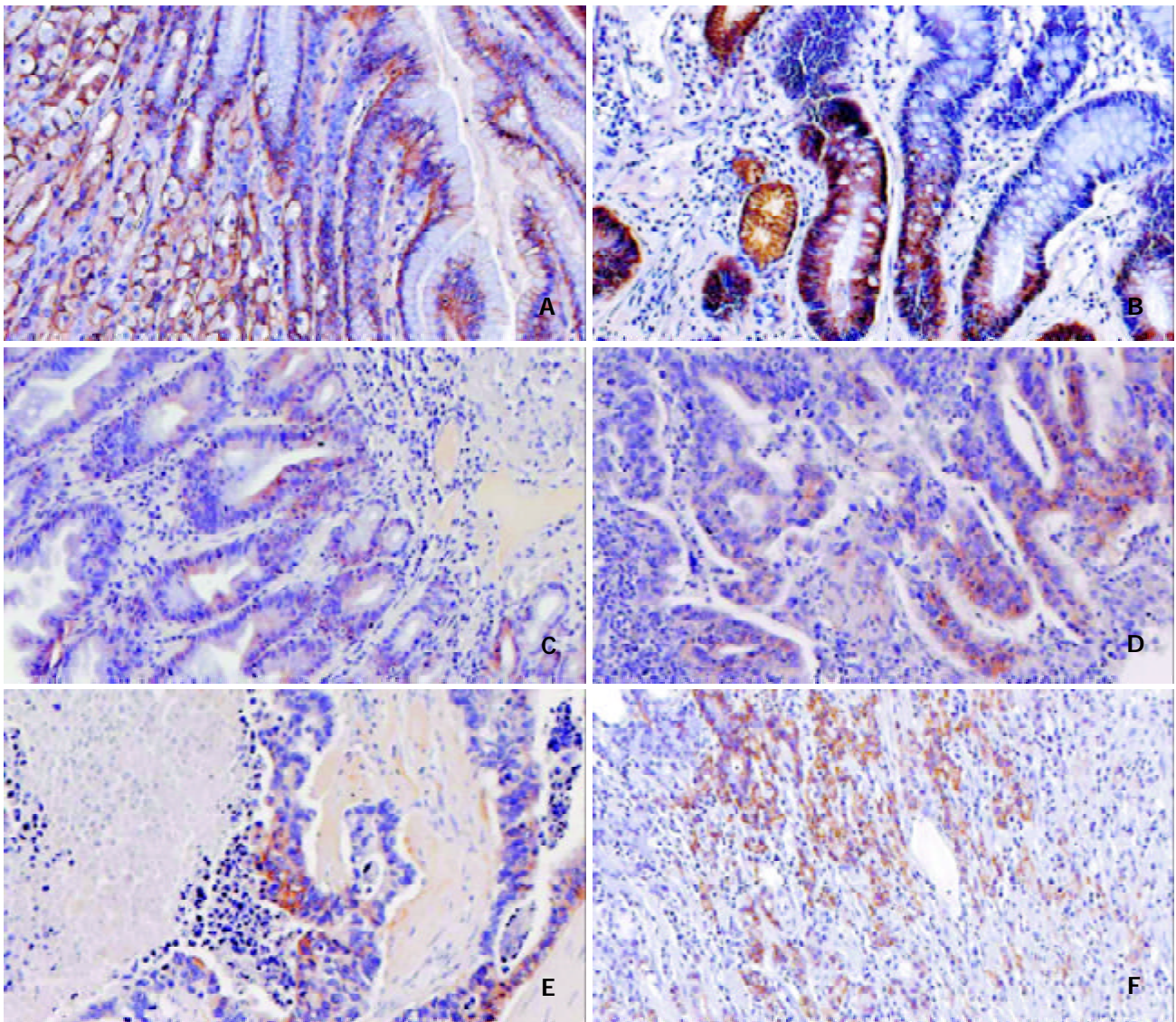


Figure 2 Immunohistochemical staining of CA IX in normal gastric mucosa (A), metaplasia (B), adenoma with moderate dysplasia (C), adenocarcinoma grade II (D), adenocarcinoma grade III (E), and diffuse carcinoma (F). In the normal mucosa, CA IX was expressed in all histological layers covering the luminal surface (LS), proliferative zone (PZ), and gastric glands (G). It was notable that CA IX was confined to deep crypts in metaplastic epithelium. The adenoma sample and all malignant lesions shown in this figure were positive for CA IX. (Original magnifications $\times 200$).

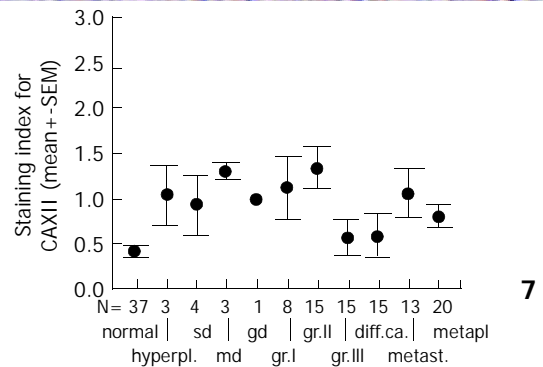
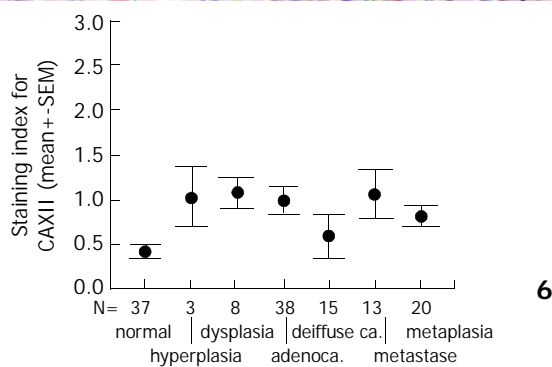
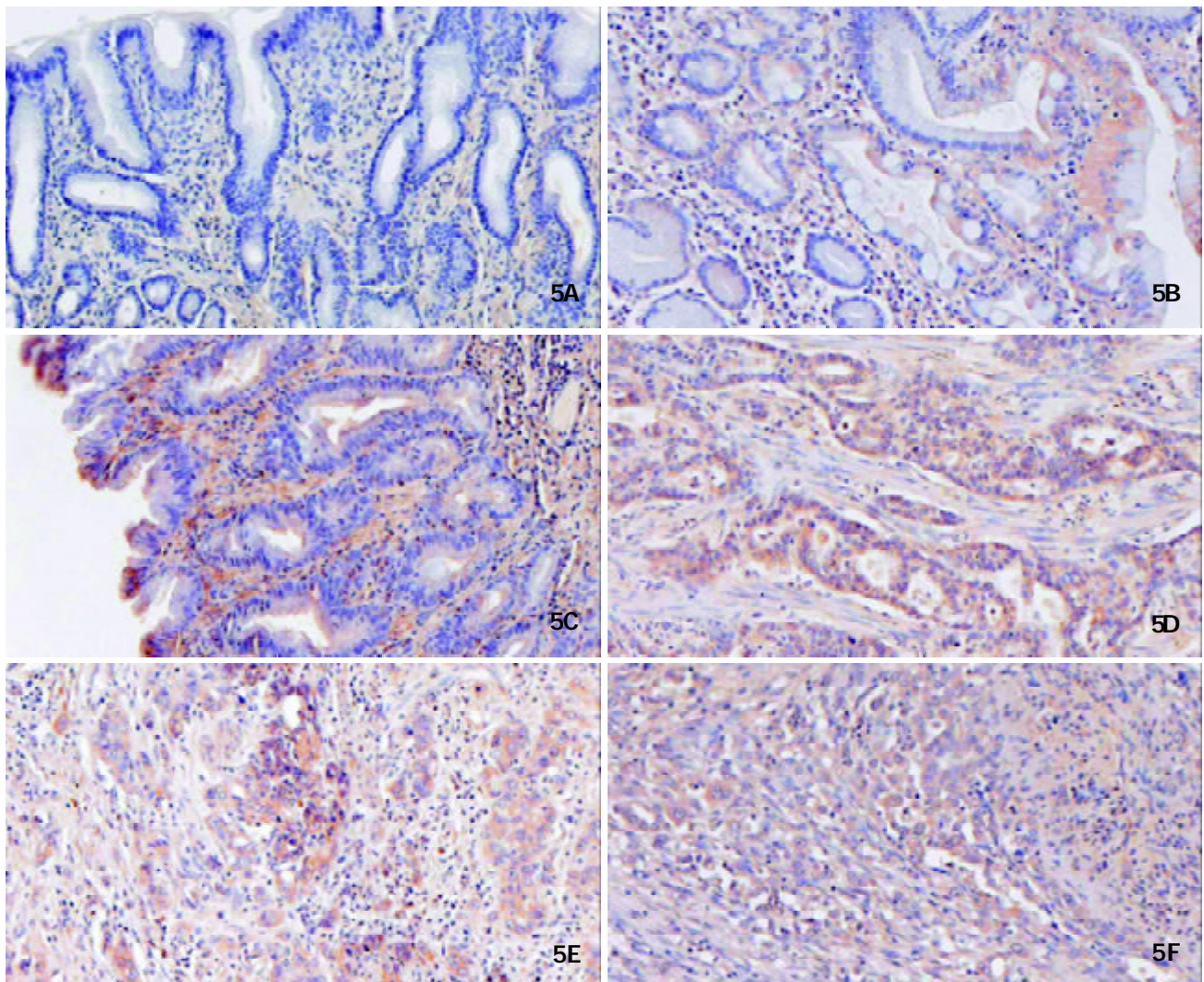
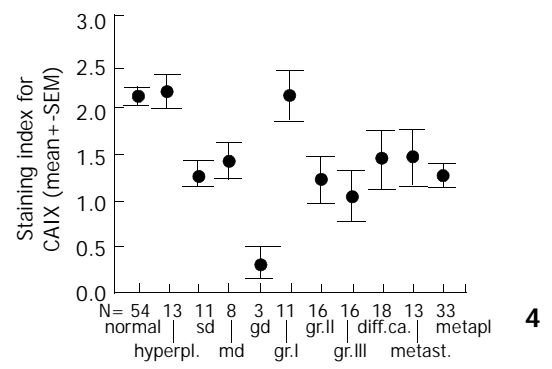
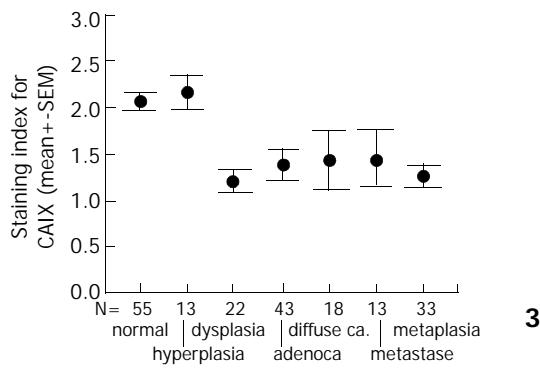


Figure 3 The mean staining indices for CA IX in the normal gastric mucosa and different gastric lesions ($P=0.002$, normal vs dysplasia, adenocarcinoma, and metaplasia).
Figure 4 The mean staining indices for CA IX in the normal gastric mucosa and lesions grouped according to the stages of dysplasia and grades of malignancy ($P<0.05$, normal vs gd, gr. II and gr. III).
Figure 5 Immunohistochemical staining of CA XII in normal gastric mucosa (A), metaplasia (B), adenoma with moderate dysplasia (C), adenocarcinoma grade II (D), adenocarcinoma grade III (E), and diffuse carcinoma (F). From these samples, CA XII was

not expressed in the normal epithelium and showed weak expression in metaplastic epithelium and diffuse carcinoma. The signal was stronger in adenoma and adenocarcinoma samples.

Figure 6 The mean staining indices for CA XII in the normal gastric mucosa and different gastric lesions ($P < 0.05$, normal vs adenocarcinoma).

Figure 7 The mean staining indices for CA XII in the normal gastric mucosa and lesions grouped according to the stages of dysplasia and grades of malignancy ($P = 0.003$, normal vs gr. II).

DISCUSSION

CA IX is present in several types of human tumors, whereas it is usually absent in the normal tissues from which these tumors originate. For example, it is expressed in neoplasias of uterine cervix and renal cell carcinomas, but not in the normal cervix or kidney^[12,13,15,35]. On the other hand, there are only a few non-cancerous tissues expressing MN/CA IX, including epithelia of stomach, intestine, and gallbladder^[8]. The present study was focused on the tumors arising from the gastric mucosa, which is normally the predominant site of CA IX expression. One interesting finding of the present study was that CA IX expression was sustained in most cases of gastric neoplasias, even though the expression indices declined compared to the normal and hyperplastic gastric mucosa.

The exact molecular mechanisms of gastric tumorigenesis are still under discussion. Some investigators have postulated that differentiated adenocarcinoma may arise from pre-existing adenoma, following a similar adenoma-carcinoma sequential axis as described for colorectal tumors^[36]. However, when gastric adenomas and adenocarcinomas were examined for loss of heterozygosity using microsatellite markers or *MUC* gene expression, the results suggested that the adenoma-carcinoma sequence was not a major pathway in gastric carcinogenesis^[37-41]. Since CA IX expression levels seemed to be very low in adenomas with severe dysplasia and normal in grade I adenocarcinoma, the present findings could support the concept that these tumor types are usually distinct entities and do not represent progressive steps from one to the other. In this respect, CA XII did not show any prominent changes in different tumor categories, although its expression was slightly increased in all pathological lesions compared to the nonneoplastic gastric mucosa.

CA IX differs from the other CA isozymes in that it has a proposed dual function as an efficient enzyme^[7] and as an adhesion molecule^[42,43]. This dual function appears to be related to the structure of CA IX molecule that consists of an extracellularly exposed N-terminal proteoglycan-like region and a CA domain. The CA domain may contribute to the regulation of acid-base homeostasis on the basolateral surfaces of the gastrointestinal epithelial cells. In tumors, CA activity has been suggested to participate in acidification of an extracellular microenvironment facilitating tumor invasion^[21]. On the other hand, the adhesion properties of CA IX may be involved in the maintenance of mucosal integrity contributing to proper intercellular contacts and communication^[42,43]. Recent studies in CA9 knockout mice have indicated that CA IX is, indeed, an important factor in gastric morphogenesis and homeostasis of the gastric epithelium possibly acting through the control of cell differentiation and proliferation^[44]. The proposed involvement of CA IX in cell differentiation agrees with our observation that high expression of CA IX was associated with a differentiated phenotype of gastric epithelial cells. However, this fact is in contrast to data from other types of tumors, e.g. breast carcinomas, where CA IX expression is increased in tumors with less differentiation, while the opposite is true for CA XII^[19].

Even though the present results indicated that CA IX and XII were not specific biomarkers for any categories of gastric tumors, and thus their clinical significance may be limited in this area, they have already revolutionized the field of the CA research in terms of the proposed functions. CA IX and XII

are not only enzymatically active isoforms, but also play several important roles in biological processes such as malignant cell invasion^[31], cell adhesion^[42,43], and cell proliferation^[9,10]. These "cancer-associated CAs" are also considered as potential targets in cancer therapy^[21,35,45] and a number of promising anticancer therapeutic agents directed to inhibition of CA activity have already been developed and await further evaluation^[32-34].

ACKNOWLEDGMENT

The technical assistance of Lissu Hukkanen is gratefully acknowledged.

REFERENCES

- 1 **Sly WS**, Hu PY. Human carbonic anhydrases and carbonic anhydrase deficiencies. *Annu Rev Biochem* 1995; **64**: 375-401
- 2 **Hewett-Emmett D**, Tashian RE. Functional diversity, conversation, and convergence in the evolution of the α -, β -, and γ -carbonic anhydrase gene families. *Mol Phylogenet Evol* 1996; **5**: 50-77
- 3 **Hewett-Emmett D**. Evolution and distribution of the carbonic anhydrase gene families. In: Chegwiddden WR, Carter ND, Edwards YH, eds. The carbonic anhydrases. New Horizons. Basel: Birkhäuser Verlag 2000: 29-76
- 4 **Pastoreková S**, Závadová Z, Kost' ál M, Babusiková O, Závada J. A novel quasi-viral agent, MaTu, is a two-component system. *Virology* 1992; **187**: 620-626
- 5 **Pastorek J**, Pastoreková S, Callebaut I, Mornon JP, Zelni k V, Opavský R, Zátövilová M, Liao S, Portetelle D, Stanbridge EJ, Závada J, Burny A, Kettman R. Cloning and characterization of MN, a human tumor-associated protein with a domain homologous to carbonic anhydrase and a putative helix-loop-helix DNA binding segment. *Oncogene* 1994; **9**: 2877-2888
- 6 **Opavský R**, Pastoreková S, Zelni k V, Gibadulinová A, Stanbridge EJ, Závada J, Kettman R, Pastorek J. MN/CA9 gene, a novel member of the carbonic anhydrase family: structure and exon to protein domain relationships. *Genomics* 1996; **33**: 480-487
- 7 **Wingo T**, Tu C, Laipis PJ, Silverman DN. The catalytic properties of human carbonic anhydrase IX. *Biochem Biophys Res Commun* 2001; **288**: 666-669
- 8 **Pastoreková S**, Parkkila S, Parkkila AK, Opavský R, Zelni k V, Saarnio J, Pastorek J. Carbonic anhydrase IX, MN/CA IX: analysis of stomach complementary DNA sequence and expression in human and rat alimentary tracts. *Gastroenterology* 1997; **112**: 398-408
- 9 **Saarnio J**, Parkkila S, Parkkila AK, Waheed A, Casey MC, Zhou ZY, Pastoreková S, Pastorek J, Karttunen T, Haukipuro K, Kairaluoma MI, Sly WS. Immunohistochemistry of carbonic anhydrase isozyme IX (MN/CA IX) in human gut reveals polarized expression in the epithelial cells with the highest proliferative capacity. *J Histochem Cytochem* 1998; **46**: 497-504
- 10 **Saarnio J**, Parkkila S, Parkkila AK, Haukipuro K, Pastoreková S, Pastorek J, Kairaluoma MI, Karttunen TJ. Immunohistochemical study of colorectal tumors for expression of a novel transmembrane carbonic anhydrase, MN/CA IX, with potential value as a marker of cell proliferation. *Am J Pathol* 1998; **153**: 279-285
- 11 **Závada J**, Závadová Z, Pastoreková S, Ciampor F, Pastorek J, Zelni k V. Expression of MaTu-MN protein in human tumor cultures and in clinical specimens. *Int J Cancer* 1993; **54**: 268-274
- 12 **Liao SY**, Brewer C, Závada J, Pastorek J, Pastoreková S, Manetta A, Bermann ML, DiSaia PJ, Stanbridge EJ. Identification of the MN antigen as a diagnostic biomarker of cervical intraepithelial squamous and glandular neoplasia and cervical carcinomas. *Am J Pathol* 1994; **145**: 598-609
- 13 **McKiernan JM**, Buttyan R, Bander NH, Stifelman MD, Katz AE,

- Chen MW, Olsson CA, Sawczuk IS. Expression of the tumor-associated gene MN: a potential biomarker for human renal cell carcinoma. *Cancer Res* 1997; **57**: 2362-2365
- 14 **Vermlyen P**, Roufosse C, Burny A, Verhest A, Bosschaerts T, Pastorekova S, Ninane V, Sculier JP. Carbonic anhydrase IX antigen differentiates between preneoplastic malignant lesions in non-small cell lung carcinoma. *Eur Respir J* 1999; **14**: 806-811
 - 15 **Liao SY**, Stanbridge EJ. Expression of the MN antigen in cervical papanicolau smears is a diagnostic biomarker of cervical dysplasia. *Cancer Epidemiol Biomarkers Prev* 1996; **5**: 549-555
 - 16 **Saarnio J**, Parkkila S, Parkkila AK, Pastorekova S, Haukipuro K, Pastorek J, Juvonen T, Karttunen TJ. Transmembrane carbonic anhydrase, MN/CA IX, is a potential biomarker for biliary tumours. *J Hepatol* 2001; **35**: 643-649
 - 17 **Giatromanolaki A**, Koukourakis MI, Sivridis E, Pastorek J, Wykoff CC, Gatter KC, Harris AL. Expression of hypoxia-inducible carbonic anhydrase-9 relates to angiogenic pathways and independently to poor outcome in non-small cell lung cancer. *Cancer Res* 2001; **61**: 7992-7998
 - 18 **Chia SK**, Wykoff CC, Watson PH, Han C, Leek RD, Pastorek J, Gatter KC, Ratcliffe P, Harris AL. Prognostic significance of a novel hypoxia-regulated marker, carbonic anhydrase IX, in invasive breast carcinoma. *J Clin Oncol* 2001; **19**: 3660-3668
 - 19 **Wykoff CC**, Beasley N, Watson PH, Campo L, Chia SK, English R, Pastorek J, Sly WS, Ratcliffe P, Harris AL. Expression of the hypoxia-inducible and tumor-associated carbonic anhydrases in ductal carcinoma *in situ* of the breast. *Am J Pathol* 2001; **158**: 1011-1019
 - 20 **Bartošová M**, Parkkila S, Pohlodek K, Karttunen TJ, Galbavý S, Mucha V, Harris AL, Pastorek J, Pastorekova S. Expression of carbonic anhydrase IX in breast is associated with malignant tissues and related to overexpression of *c-erbB2*. *J Pathol* 2002; **197**: 314-321
 - 21 **Ivanov SV**, Kuzmin I, Wei MH, Pack S, Geil L, Johnson BE, Stanbridge EJ, Lerman MI. Down regulation of transmembrane carbonic anhydrases in renal cell carcinoma cell lines by wild-type von Hippel-Lindau transgenes. *Proc Natl Acad Sci USA* 1998; **95**: 12596-12601
 - 22 **Ivanov S**, Liao SY, Ivanova A, Danilkovitch-Miagkova A, Tarasova N, Weirich G, Merrill MJ, Proescholdt MA, Oldfield EH, Lee J, Zavada J, Waheed A, Sly W, Lerman MI, Stanbridge EJ. Expression of hypoxia-inducible cell-surface transmembrane carbonic anhydrases in human cancer. *Am J Pathol* 2001; **158**: 905-919
 - 23 **Kivelä A**, Parkkila S, Saarnio J, Karttunen TJ, Kivelä J, Parkkila AK, Waheed A, Sly WS, Grubb JH, Shah G, Türeci Ö, Rajaniemi H. Expression of a novel transmembrane carbonic anhydrase isozyme XII in normal human gut and colorectal tumors. *Am J Pathol* 2000; **156**: 577-584
 - 24 **Karhumaa P**, Parkkila S, Türeci Ö, Waheed A, Grubb JH, Shah G, Parkkila AK, Kaunisto K, Tapanainen J, Sly WS, Rajaniemi H. Identification of carbonic anhydrase XII as the membrane isozyme expressed in the normal human endometrial epithelium. *Mol Hum Reprod* 2000; **6**: 68-74
 - 25 **Parkkila S**, Parkkila AK, Saarnio J, Kivelä J, Karttunen TJ, Kaunisto K, Waheed A, Sly WS, Türeci Ö, Virtanen I, Rajaniemi H. Expression of the membrane-associated carbonic anhydrase isozyme XII in the human kidney and renal tumors. *J Histochem Cytochem* 2000; **48**: 1601-1608
 - 26 **Karhumaa P**, Kaunisto K, Parkkila S, Waheed A, Pastorekova S, Pastorek J, Sly WS, Rajaniemi H. Expression of the transmembrane carbonic anhydrases, CA IX and CA XII, in the human male excurrent ducts. *Mol Hum Reprod* 2001; **7**: 611-616
 - 27 **Türeci Ö**, Sahin U, Vollmar E, Siemer S, Göttert E, Seitz G, Parkkila AK, Shah GN, Grubb JH, Pfreundschuh M, Sly WS. Human carbonic anhydrase XII, cDNA cloning, expression, and chromosomal localization of a carbonic anhydrase gene that is overexpressed in some renal cell cancers. *Proc Natl Acad Sci USA* 1998; **95**: 7608-7613
 - 28 **Wykoff CC**, Beasley N, Watson PH, Turner KJ, Pastorek J, Sibtain A, Wilson GD, Turley H, Talks K, Maxwell PH, Pugh CW, Ratcliffe PJ, Harris AL. Hypoxia inducible expression of tumor associated carbonic anhydrases. *Cancer Res* 2000; **60**: 7075-7083
 - 29 **Semenza GL**. Hypoxia, clonal selection, and the role of HIF-1 in tumor progression. *Crit Rev Biochem Mol Biol* 2000; **35**: 71-103
 - 30 **Maxwell PH**, Wiesener MS, Chang GW, Clifford SC, Vaux EC, Cockman ME, Wykoff CC, Pugh CW, Maher ER, Ratcliffe PJ. The tumour suppressor protein VHL targets hypoxia-inducible factors for oxygen-dependent proteolysis. *Nature* 1999; **399**: 271-275
 - 31 **Parkkila S**, Rajaniemi H, Parkkila AK, Kivelä J, Waheed A, Pastorekova S, Pastorek J, Sly W. Carbonic anhydrase inhibitor suppresses invasion of renal cancer cells *in vitro*. *Proc Natl Acad Sci USA* 2000; **97**: 2220-2224
 - 32 **Supuran CT**, Scozzafava A. Carbonic anhydrase inhibitors. *Curr Med Chem* 2001; **1**: 61-97
 - 33 **Supuran CT**, Briganti F, Tilli S, Chegwiddden WR, Scozzafava A. Carbonic anhydrase inhibitors: Sulfonamides as antitumor agents? *Bioorg Med Chem* 2001; **9**: 703-714
 - 34 **Supuran CT**, Scozzafava A. Applications of carbonic anhydrase inhibitors and activators in therapy. *Expert Opin Ther Patents* 2002; **12**: 217-242
 - 35 **Uemura H**, Nakagawa Y, Yoshida K, Saga S, Yoshikawa K, Hirao Y, Oosterwijk E. MN/CA IX/G250 as a potential target for immunotherapy of renal cell carcinomas. *Br J Cancer* 1999; **81**: 741-746
 - 36 **Uchino S**, Noguchi M, Ochiai A, Saito T, Kobayashi M, Hirohashi S. p53 mutation in gastric cancer: a genetic model for carcinogenesis is common to gastric and colorectal cancer. *Int J Cancer* 1993; **54**: 759-764
 - 37 **Maesawa C**, Tamura G, Suzuki Y, Ogasawara S, Sakata K, Kashiwaba M, Satodate R. The sequential accumulation of genetic alterations characteristic of the colorectal adenoma-carcinoma sequence does not occur between gastric adenoma and adenocarcinoma. *J Pathol* 1995; **176**: 249-258
 - 38 **Tamura G**, Sakata K, Maesawa C, Suzuki Y, Terashima M, Satoh K, Sekiyama S, Suzuki A, Eda Y, Satodate R. Microsatellite alterations in adenoma and differentiated adenocarcinoma of the stomach. *Cancer Res* 1995; **55**: 1933-1936
 - 39 **Tamura G**. Molecular pathogenesis of adenoma and differentiated adenocarcinoma of the stomach. *Pathol Int* 1996; **46**: 834-841
 - 40 **Semba S**, Yokozaki H, Yamamoto S, Yasui W, Tahara E. Microsatellite instability in precancerous lesions and adenocarcinomas of the stomach. *Cancer* 1996; **77**: 1620-1627
 - 41 **Tsukashita S**, Kushima R, Bamba M, Sugihara H, Hattori T. MUC gene expression and histogenesis of adenocarcinoma of the stomach. *Int J Cancer* 2001; **94**: 166-170
 - 42 **Závada J**, Závadová Z, Machon O, Kutinova L, Nemeckova S, Opavský R, Pastorek J. Transient transformation of mammalian cells by MN protein, a tumor-associated cell adhesion molecule with carbonic anhydrase activity. *Int J Oncol* 1997; **10**: 857-863
 - 43 **Závada J**, Závadová Z, Pastorek J, Biesová Z, Jezek J, Velek J. Human tumor-associated cell adhesion protein MN/CA IX: identification of M75 epitope and of the region mediating cell adhesion. *Br J Cancer* 2000; **82**: 1808-1813
 - 44 **Gut MO**, Parkkila S, Vernerová Z, Rohde E, Závada J, Höcker M, Pastorek J, Karttunen T, Gibadulinová A, Závadová Z, Knobloch KP, Wiedenmann B, Svoboda J, Horak I, Pastorekova S. Gastric hyperplasia in mice with targeted disruption of the carbonic anhydrase gene *Car9*. *Gastroenterology* 2002; **123**: 1889-1903
 - 45 **Uemura H**, Kitagawa H, Hirao Y, Okajima E, Debruyne FMJ, Oosterwijk E. Expression of tumor-associated antigen MN/G250 in urologic carcinoma: potential therapeutic target. *J Urol Suppl* 1997; **157**: 377

Spiral CT in gastric carcinoma: Comparison with barium study, fiberoptic gastroscopy and histopathology

Feng Chen, Yi-Cheng Ni, Kai-Er Zheng, Sheng-Hong Ju, Jun Sun, Xi-Long Ou, Man-Hua Xu, Hao Zhang, Guy Marchal

Feng Chen, Kai-Er Zheng, Sheng-Hong Ju, Jun Sun, Department of Radiology, Zhongda Hospital, 87 Dingjiaqiao Road, Nanjing 210009, Jiangsu Province, China

Xi-Long Ou, Man-Hua Xu, Department of Digestive Diseases, Zhongda Hospital, 87 Dingjiaqiao Road, Nanjing 210009, Jiangsu Province, China

Feng Chen, Yi-Cheng Ni, Hao Zhang, Guy Marchal, Department of Radiology, University Hospital, Herestraat 49, B-3000 Leuven, Belgium

Supported by ECR 2000-EAR-ECR Research & Education Fund Fellowship Grant

Correspondence to: Professor Yi-Cheng Ni, Department of Radiology, University Hospital, Herestraat 49, B-3000 Leuven, Belgium. yicheng.ni@med.kuleuven.ac.be

Telephone: +32-16-345940 **Fax:** +32-16-343765

Received: 2003-03-12 **Accepted:** 2003-04-11

Abstract

AIM: To evaluate spiral computed tomography (CT) including virtual gastroscopy for diagnosis of gastric carcinoma in comparison with upper gastrointestinal series (UGI), fiberoptic gastroscopy (FG) and histopathology.

METHODS: Sixty patients with histologically proven gastric carcinoma (54 advanced and 6 early) were included in this study. The results of spiral CT were compared with those of UGI and FG. Two observers blindly evaluated images of spiral CT and UGI and video recording of FG with consensus in terms of diagnostic confidence with a five-point scale. Sensitivities of lesion detection, Borrmann's classification of spiral CT, UGI and FG, as well as the accuracy of TNM staging of spiral CT were determined by comparing them to surgical and histological findings.

RESULTS: The lesion detection rate was 98 % (59/60), 95 % (57/60) and 98 % (59/60) for spiral CT, UGI and FG, respectively. There were no statistical differences in the detection sensitivity among the three techniques ($P>0.05$). For the sensitivity in Borrmann's classification, spiral CT was higher than that of UGI ($P=0.025$) and similar to that of FG ($P>0.05$). The accuracy of spiral CT in staging the gastric carcinoma was 76.7 %. Six cases of early gastric carcinoma were all detected by spiral CT as well as FG.

CONCLUSION: Spiral CT is equivalent to UGI and FG in the detection of gastric carcinoma, and superior to UGI but similar to FG in the Borrmann's classification of advanced gastric carcinoma. Spiral CT is more valuable than FG in the staging of gastric carcinoma.

Chen F, Ni YC, Zheng KE, Ju SH, Sun J, Ou XL, Xu MH, Zhang H, Marchal G. Spiral CT in gastric carcinoma: Comparison with barium study, fiberoptic gastroscopy and histopathology. *World J Gastroenterol* 2003; 9(7): 1404-1408

<http://www.wjgnet.com/1007-9327/9/1404.asp>

INTRODUCTION

Fiberoptic gastroscopy (FG) is generally regarded as a standard test for detection of gastric cancer. Upper gastrointestinal series (UGI), however, still represents a routine or survey examination for imaging gastric abnormalities although it has certain limitations in clinical use. Even though the application of conventional computed tomography (CT) in staging gastric carcinoma has been introduced, the results are unsatisfactory^[1-3]. Recently, spiral CT, including various three-dimensional (3D) reconstructions such as virtual endoscopy and axial source images (2D) has been used in imaging the alimentary tract^[2-16]. While most reports in literature laid emphasis on colon polyps^[11-12, 14-15], there have been a few studies investigating gastric carcinoma with spiral CT^[4-10]. In clinical practice, advanced gastric carcinoma is defined using Borrmann's classification, which is the pathological basis for UGI diagnosis, and the resectability of the tumor and prognosis of the patients are evaluated presurgically using TNM staging^[17], which is one of the suggested applications of spiral CT.

In this study, 2D and 3D display techniques after spiral CT scan were cross-referenced. The role of this combined spiral CT technique was compared with that of UGI and FG in the detection and Borrmann's classification of gastric carcinoma, which, to our knowledge, has not been reported in literature. The staging of gastric carcinoma with spiral CT was also correlated with histopathology.

MATERIALS AND METHODS

Patients

During a 12-month period, 60 consecutive patients (36 males, 24 females) ranging from 27 to 79 years old (mean=62 a.), who were diagnosed of gastric carcinoma with FG and subsequent biopsy were recruited. Among the 60 gastric carcinoma patients, 43 were undertaken gastrectomy or subtotal gastrectomy, 17 were undertaken surgical exploration only because of severe adhesion between tumor and surrounding tissues. This study was approved by the administrative authority of the university hospital and fully informed consent was obtained from each patient. Within one week after FG procedure, UGI was performed prior to spiral CT scanning on each patient.

Imaging acquisition

Spiral CT was performed with a Hispeed CT/i scanner (General Electric Medical Systems, Milwaukee, WI). All patients were fasted for 12 hours. Before the CT scanning, 20 mg raceanisodamine hydrochloride was intramuscularly administered and two packs (6 g) of effervescent granules were taken orally. Usually patients were immediately placed on the scanning table in an oblique supine position. A scout projection was made to confirm the stomach to be distended by gas. If insufficient distention of stomach was found, half to one pack of effervescent granules was added and a scout projection was scanned again. Then, spiral CT was performed with a 3-mm collimation and a pitch of 1.2-1.5 mm during a single breath-hold of 22-33 seconds, which produced a 3D-volume

acquisition that included the entire stomach. Tube current was 200-280 mA, voltage was 120 kVp and scan time was 1 second per rotation.

Barium double contrast technique with standard projection was used for UGI studies by an experienced radiologist. Standard FG examination was performed by an experienced gastrologist and the biopsy samples were processed as a clinical routine of pathology department.

Image reconstruction

3D-postprocessing modes including CT virtual gastroscopy (CTVG), surface shaded display (SSD) and "Raysum" Display (virtual double contrast barium study) were performed by a built-in workstation (Advantage Window 2.0, General Electric Medical Systems, Milwaukee, WI) after raw data reconstruction with 1 mm interval. For intraluminal views of the stomach, a default level of -525 (Hounsfield unit, HU) provided by the Navigator (GE Company) was chosen. SSD and "Raysum" display were obtained with a threshold of -311HU.

Image analysis

Sixty sets of hard copy of grayscale spiral CT images (including axial source images, CTVG, SSD, and "Raysum" display) and UGI radiograms from 60 patients were obtained by one radiologist and were randomly reviewed and scored with consensus by two other experienced radiologists who were blinded to clinical data, pathology, and the information of other imaging techniques. Video recording of FG examinations was reviewed and scored with consensus by two experienced gastrologists.

The diagnostic confidence, appearance, location, and size of suspected lesions on images of spiral CT, UGI and FG were

recorded. For spiral CT, the observers made the final judgments after referring to all 4 techniques including CTVG, SSD, "Raysum" and axial source images. The lesions were then classified as early and advanced gastric carcinoma according to Borrmann's classification^[2]. Based on spiral CT, TNM staging^[16] of gastric carcinoma of each case was also noted. Diagnostic confidence for detecting a lesion was rated as 1, definitely no lesion; 2, probably not a lesion; 3, possible lesion; 4, probable lesion; 5, definite lesion^[18]. Any image artifacts that degraded diagnostic confidence were also noted.

All findings of lesions with spiral CT, UGI and FG were further verified with the results of surgical exploration, dissected specimen and histology, which were used as the gold standard for detection, Borrmann's classification and spiral CT staging of gastric carcinoma.

Statistical analysis

Data entry procedures and statistical analysis were performed with a statistical software package (SAS for windows, version 6.12, SAS Institute, Cary, NC). By using only those lesions allocated with confidence rate of 3 or higher, the sensitivity of detection and classification of gastric carcinomas of each technique was assessed^[18] (Chi-square test). Significant differences were considered when the *P* value was less than or equal to 0.05.

RESULTS

The classification, size and location of the gastric cancer in this study are summarized in Table 1. A complete set of image data of a patient is exemplified in Figure 1.

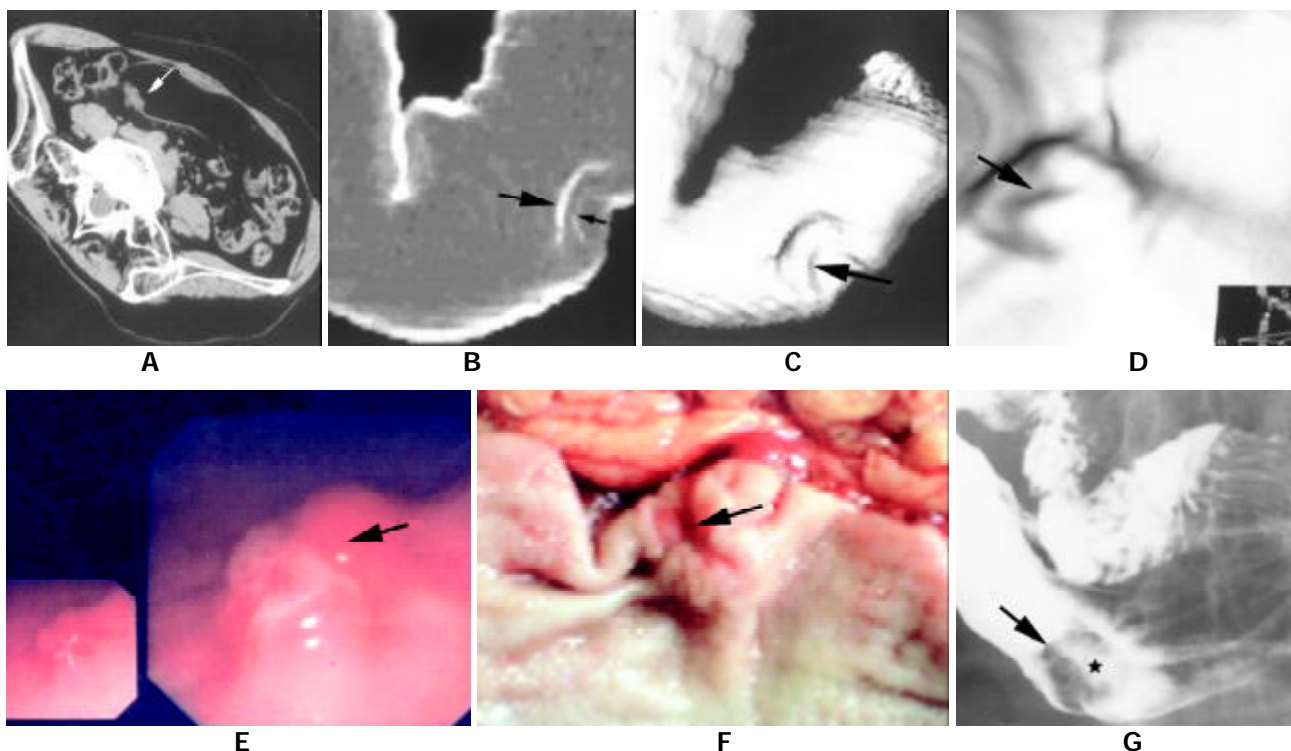


Figure 1 A complete set of image data of a patient. Spiral CT images (A-D), fiberoptic gastroscopy (E), surgical specimen (F) and corresponding barium study (G) from a patient (female, 48 a.) of Borrmann's type 2 and TNM stage 1 of advanced gastric carcinoma. (A), axial image (supine position with right side elevated) showed a focal irregular protruding (arrow) from the posterior wall of antrum. (B), "Raysum" display (virtual double contrast barium study) stressed double-margin changes at the greater curvature of antrum: tumor (large arrow) and ulcer (small arrow) margins. (C), SSD image showed depression at the antrum with a central ulcer (arrow). (D), CTVG image depicted an intraluminal irregular mass with a flat ulcer (arrow). The view angle was illustrated by the 2D image at lower right corner. (E), fiberoptic gastroscopic view showed a lobulated mass. (F), surgical specimen demonstrated a mass with a small central ulcer (arrow). (G), barium study revealed an intraluminal filling defect (arrows) with a flat ulcer (asterisk) at the greater curvature of antrum.

Table 1 Classification, size and location of gastric carcinoma (n=60)

Type 2c	Gastric cancer classification					Size of the tumor		
	Early		Advanced*			<1 cm	1-3 cm	>3 cm
	Type 3	Type 1	Type 2	Type 3	Type 4			
4 (6.7%)	2 (3.3%)	10(16.7%)	25 (41.7%)	14 (23.3%)	5 (8.3%)	6	24	30
Location of the tumor								
		Cardia area	Antrum	Great curv	Lesser curv	Antrum and body		
		29	18	5	5	3		

Notes: Numbers were patients. Curv.=curvature. *Borrmann's type of classification.

Lesion detection

In advanced gastric carcinoma, the lesion detection (with diagnostic confidence of 3 or higher) sensitivity of spiral CT was similar to that of UGI and FG ($P>0.05$). In early gastric carcinoma, it was higher than that of UGI ($P=0.031$) and similar to that of FG (Table 2). One false positive lesion (due to peristalsic wave at the lesser curvature) and one false negative lesion (with diagnostic confidence rate of 3 or lower) were noted in spiral CT. 3 and one false negative lesion was noted in UGI and FG, respectively (Table 3).

Table 2 Comparison of sensitivities on gastric carcinoma between different techniques

	Detection		Classification
	Early	Advanced	Advanced
SCT	100%	98%	77%
UGI	33%	95%	47%
FG	100%	98%	80%
Chi-Square test			
SCT vs UGI	$P=0.031$	$P>0.05$	$P=0.025$
SCT vs FG	$P>0.05$	$P>0.05$	$P>0.05$

Notes: SCT=spiral CT, UGI=upper gastrointestinal series, FG=fiberoptic gastroscopy.

Table 3 Comparison of different techniques in erroneously interpreted lesions

	n	False positive	False negative	Borrmann's classification	
				Can not be classified	Erroneously classified
SCT	60	1	1	2	12
UGI	60	0	3	9	23
FG	60	0	1	0	12

Notes: Data were the number of lesions. SCT=spiral CT, UGI=upper gastrointestinal series, FG=fiberoptic gastroscopy.

Borrmann's classification

The ability of spiral CT to correctly classify the lesions according to Borrmann's classification was statistically higher than that of UGI ($P=0.025$) and similar to that of FG ($P>0.05$) (Table 2).

For spiral CT, 12/60 lesions were erroneously classified and 2/60 could not be classified which were attributed to image artifacts of respiration movement and fluid retention in stomach. For UGI, 23/60 lesions were erroneously classified and 9/60 could not be classified. For FG, 12/60 lesions were erroneously classified (Table 3). So, a total of 47 lesions were erroneously classified from spiral CT, UGI and FG. The rates

of erroneously classified lesions in Borrmann's types 1, 2, 3, and early gastric carcinoma were 6.4 % (3/47), 61.7 % (29/47), 25.5 % (12/47), and 6.4 % (3/47), respectively. The majority of erroneously classified lesions occurred in Borrmann's type 2 (61.7 %) and type 3 (25.5 %). No erroneously classified lesion was found in Borrmann's type 4.

TNM staging of spiral CT

43 of 60 patients were included in the TNM staging. Of the 43 cases, stage I was found in 12, 6 of which were early gastric carcinoma, stage II in 7, stage III in 19 and stage IV in 5. The accuracy of spiral CT in TNM staging was 76.7 % (33/43). 5 cases of overestimation and underestimation were noted respectively in spiral CT staging (Table 4).

Table 4 Comparison of TNM staging of gastric carcinoma between spiral CT and pathology

Pathological staging	Spiral CT staging				Total
	1	2	3	4	
1	10	2	0	0	12
2	0	4	3	0	7
3	0	7	12	0	19
4	0	0	2	3	5
Total	10	13	17	3	43

DISCUSSION

The evaluation of gastric carcinoma by conventional barium studies is hampered by the following limitations: (1) the impossibility to produce endoscopic views, (2) the projective nature of the technique, (3) the quality of barium coating and the examiner's technique and skills. The disadvantage of FG examination is that it cannot evaluate the tumor involvement of gastric wall and surrounding tissues and therefore it has inability of TNM staging. Spiral CT has brought about additional possibilities for the evaluation of gastric tumors. Since the assessment of endoluminal morphology of gastric tumors is limited when only source images are used, 3D visualization techniques have been advocated^[4-10]. In a recently published paper, the SSD and virtual double contrast imaging were compared with conventional barium studies and CTVG was compared with gastroscopy in various types of gastric pathologies respectively^[6]. The present report represents a comprehensive clinical study that covers all three different 3D techniques of spiral CT (CTVG, SSD and virtual double contrast), as well as axial source images in comparison with UGI and FG focusing on the detection, classification and staging of gastric carcinoma.

We used two reconstruction algorithms for the 3D visualization of the stomach. One was SSD display, which provided outside opaque images of inner surface of the gastric

wall generated with a thresholding technique and could be interpreted similarly as in single-contrast barium study^[12]. The other was volume rendering technique including CTVG and virtual double contrast imaging as described elsewhere^[12,13]. CTVG with perspective volume rendering technique produced intraluminal view similar to those obtained from fiberoptic gastroscopy. Virtual double contrast imaging displayed somewhat translucent images similar to those of double contrast barium study.

As different 3D techniques, the advantage of SSD and virtual double contrast display was to demonstrate the overall aspect and the contour changes of the stomach, but with poor mucosal information^[6] (Figure 1 B, C), and CTVG offered the overview of the intraluminal tumors but with indiscernible surface coloration and extraluminal tumor invading (Figure 1D). Therefore, it is important to realize that information from 3D CT displays should be combined with that of source images in interpreting the gastric carcinoma clinically (Figure 1 A-D).

In our study, tumor detection sensitivities among spiral CT, UGI and FG were similar ($P>0.05$). However, the sensitivity was higher with spiral CT than that with UGI ($P=0.031$) and similar between SCG and FG ($P>0.05$) in early gastric carcinoma. Only a few studies on the detection of early gastric carcinoma with spiral CT were reported, the results so far have been controversial^[10]. The detection rate of early gastric carcinoma was 93.5 % reported by Lee^[10] with contrast enhanced SSD technique, and it was only 26 % by spiral CT according to Fukuya^[19]. Moreover, it was even lower with 3D CT than that of UGI according to Ogata^[6]. In our study, spiral CT correctly detected all 6 cases of early gastric carcinomas, the detection rate (100 %) was much higher than that of UGI (33.3 %). However, the very limited number of cases with early gastric carcinoma in this series did not allow any conclusion in this regard.

The distribution and prevalence rate of gastric tumor according to Borrmann's classification in this study was slightly different from that reported, in which the most prevalent type was Borrmann's 3 and the most common site of tumor was the posterior wall of the antrum^[8]. In our investigation, the most prevalent type was Borrmann's 2 and the most common site of tumor was the cardia and fundus. It has been reported that accurate classification of gastric tumor based on Borrmann's classification is possible with 3D CT^[7,8]. Our study indicated that Borrmann's classification with spiral CT was better than that with UGI ($P=0.025$), and similar to that of FG ($P>0.05$). In this study, the majority of misclassification occurred in Borrmann's types 2 and 3, in which UGI accounted for a highest proportion of the misclassification rate. The main reasons were most likely due to the following: (1) in the present study, cardia or fundus carcinoma was found in the highest percentage of the patients (48.3 %, 29/60), therefore Borrmann's type 2 or 3 tumors at cardia tended to be misclassified as type 1, because of the poor visualization of some small and flat ulcers within the tumor. (2) The limited capability of UGI in visualizing the ulcer and the infiltrating nature of tumors at the cardia was also a reason for the difficult differentiation between Borrmann's types 2 and 3. (3) On the contrary, Borrmann's type 2 or 3 at the antrum tended to be erroneously classified as type 4, because these tumors were poorly visualized by spiral CT^[8].

The rational work out of treatment scheme and accurate evaluation of gastric carcinoma are mainly dependent on TNM staging before surgery. Spiral CT is a practical approach in TNM staging because it can visualize the gastric wall, surrounding tissue and organs. Many studies on gastric carcinoma staging with conventional CT have been reported so far. The results in the literature were various due to the different CT scanner and materials and methods used^[20]. Using a spiral CT technique of thin slice thickness (3 mm) and plain

scanning, staging accuracy of gastric carcinoma in this study reached 76.7 %. This result was higher than that (72.0 %) obtained by conventional CT scanning with contrast enhancement^[21], and was lower than that (81 %) obtained by triphase contrast enhancement of spiral CT^[22]. Certainly, multiphase contrast enhanced spiral CT scan may further improve the staging of gastric carcinoma, the method we used, however, was simple, practical and more acceptable by the patients.

Some limitations of this study should be mentioned: (1) Since the size of more than half of the lesions in this group was large (>3 cm), the conclusions drawn from the results might not be applicable to small or flat gastric lesions. (2) Because all the CT examinations were performed in patients with known gastric carcinoma, the specificity of different imaging techniques was not investigated in our study.

In summary, the present clinical study demonstrates that spiral CT is equal to UGI and FG in the detection of gastric carcinoma. For Borrmann's classification of gastric carcinoma, spiral CT scores better than UGI and similar to FG. Spiral CT is also of value in TNM staging of gastric carcinoma. It is suggested that spiral CT is an alternative to UGI and supplement to FG in gastric carcinoma diagnosis. However, further investigations on a larger scale are necessary to confirm the role of spiral CT in the evaluation of gastric carcinoma.

REFERENCES

- 1 **Sussman SK**, Halvorsen RA Jr, Illescas FF, Cohan RH, Saeed M, Silverman PM, Thompson WM, Meyers WC. Gastric adenocarcinoma: CT versus surgical staging. *Radiology* 1988; **167**: 335-340
- 2 **Fishman EK**, Urban BA, Hruban RyH. CT of the stomach: spectrum of disease. *RadioGraphics* 1996; **16**: 1035-1054
- 3 **Balthazar EJ**, Siegel SE, Megibow AJ, Scholes J, Gordon R. CT in patients with scirrhous carcinoma of the GI tract: imaging findings and value for tumor detection and staging. *AJR* 1995; **164**: 839-845
- 4 **Lee DH**, Ko YT. Gastric lesions: evaluation with three-dimensional images using helical CT. *AJR* 1997; **169**: 787-789
- 5 **Wood BJ**, O' Malley ME, Hahn PF, Mueller PR. Virtual endoscopy of the gastrointestinal system outside the colon. *AJR* 1998; **171**: 1367-1372
- 6 **Ogata I**, Komohara Y, Yamashita Y, Mitsuzaki K, Takahashi M, Ogawa M. CT evaluation of gastric lesions with three-dimensional display and interactive virtual endoscopy: comparison with conventional barium study and endoscopy. *AJR* 1999; **172**: 1263-1270
- 7 **Lee DH**, Ko YT. Advanced gastric carcinoma: the role of three-dimensional and axial imaging by spiral CT. *Abdom Imaging* 1999; **24**: 111-116
- 8 **Lee DH**. Two-dimensional and three-dimensional imaging of gastric tumors using spiral CT. *Abdom Imaging* 2000; **25**: 1-6
- 9 **Lee DH**. Three-dimensional imaging of the stomach by spiral CT. *J Comput Assist Tomogr* 1998; **22**: 52-58
- 10 **Zheng KE**, Feng C, Ju SH, Sun J, Liu WH. CT virtual endoscopy: a preliminary clinical study in gastrointestinal tract. *World Chinese J Digestol* 1999; **7**: 629-631
- 11 **Springer P**, Stohr B, Giacomuzzi SM, Bodner G, Klingler A, Jaschke W, Zur-Nedden D. Virtual computed tomography colonoscopy: artifacts, image quality and radiation dose load in a cadaver study. *Eur Radiol* 2000; **10**: 183-187
- 12 **Rogalla P**, Bender A, Bick U, Huitema A, Terwisscha-van-Scheltinga J, Hamm B. Tissue transition projection (TTP) of the intestines. *Eur Radiol* 2000; **10**: 806-810
- 13 **Rogalla P**, Werner R, Huitema A, van-Est A, Meiri N, Hamm B. Virtual endoscopy of the small bowel: phantom study and preliminary clinical results. *Eur Radiol* 1998; **8**: 563-567
- 14 **Fletcher JG**, Luboldt W. CT colonography and MR colonography: current status, research directions and comparison. *Eur Radiol* 2000; **10**: 786-801
- 15 **Hara AK**, Johnson CD, Reed JE, Ehman RL, Ilstrup DM. Colorectal

- polyp detection with colography: two-versus three-dimensional techniques. Work in progress. *Radiology* 1996; **200**:49-54
- 16 **Wu LF**, Wang BZ, Feng JL, Cheng WR, Liu GR, Xu XH, Zheng ZC. Preoperative TN staging of esophageal cancer: Comparison of miniprobe ultrasonography, spiral CT and MRI. *World J Gastroenterol* 2003; **9**: 219-224
- 17 **Moss AA**, Schnyder P, Marks W, Margulis AR. Gastric adenocarcinoma: a comparison of the accuracy and economics of staging by computed tomography and surgery. *Gastroenterology* 1981; **80**: 45-50
- 18 **Ward J**, Chen F, Guthrie JA, Wilson D, Lodge JP, Wyatt JI, Robinson PJ. Hepatic lesion detection after superparamagnetic iron oxide enhancement: Comparison of five T2-weighted sequences at 1.0 T by using alternative-free response receiver operating characteristic analysis. *Radiology* 2000; **214**: 159-162
- 19 **Fukuya T**, Honda H, Kaneko K, Kuroiwa T, Yoshimitsu K, Irie H, Maehara Y, Masuda K. Efficacy of helical CT in T-staging of gastric cancer. *J Comput Assist Tomogr* 1997; **21**: 73-81
- 20 **Miller FH**, Kochman ML, Talamonti MS, Ghahremani GG, Gore RM. Gastric cancer: Radiologic staging. *Radiol Clin North Am* 1997; **35**: 331-349
- 21 **Minami M**, Kawauchi N, Itai Y, Niki T, Sasaki Y. Gastric tumors: radiologic-pathologic correlation and accuracy of T staging with dynamic CT. *Radiology* 1992; **185**: 173-178
- 22 **Takao M**, Fukuda T, Iwanaga S, Hayashi K, Kusano H, Okudaira S. Gastric cancer: evaluation of triphasic spiral CT and radiologic-pathologic correlation. *J Comput Assist Tomogr* 1998; **22**: 288-294

Edited by Xu XQ and Wang XL

Association of VCAM-1 overexpression with oncogenesis, tumor angiogenesis and metastasis of gastric carcinoma

Yong-Bin Ding, Guo-Yu Chen, Jian-Guo Xia, Xi-Wei Zang, Hong-Yu Yang, Li Yang

Yong-Bin Ding, Guo-Yu Chen, Jian-Guo Xia, Xi-Wei Zang, Hong-Yu Yang, Li Yang, Department of General Surgery, the First Affiliated Hospital of Nanjing Medical University, Nanjing 210029, Jiangsu Province, China

Supported by the Science Fund of Department of Science and Technology of Jiangsu Province, No.Bj 99064

Correspondence to: Yong-Bin Ding, Department of General Surgery, The First Affiliated Hospital of Nanjing Medical University, Nanjing 210029, Jiangsu Province, China. njdyb@sina.com

Telephone: +86-25-6796006

Received: 2002-12-10 **Accepted:** 2003-02-13

Abstract

AIM: To investigate the relationship between the expression of vascular cell adhesion molecule-1 (VCAM-1) and oncogenesis, tumor angiogenesis and metastasis in gastric carcinoma, and to evaluate the clinical significance of serum VCAM-1 levels in gastric cancer.

METHODS: Specimens from 41 patients with gastric cancer, 8 patients with benign gastric ulcer, and 10 healthy subjects were detected for the expression of VCAM-1 by immunohistochemistry. Microvessel density (MVD) was measured by counting the endothelial cells immunostained with the monoclonal antibody CD34 at x200 magnification. Serum VCAM-1 concentrations were measured by an enzyme linked immunosorbent assay in the 41 gastric cancer patients before surgery, and at 7 days after surgery as well as in 25 healthy controls. The association between preoperative serum VCAM-1 levels and clinicopathological features, and their changes following surgery was evaluated. In addition, serum carcinoembryonic antigen (CEA) was also examined.

RESULTS: Of the 41 gastric cancer tissues, 31 (75.6 %) were VCAM-1 positive. The VCAM-1 positive gastric cancers were more invasive and classified in the more advanced stage than the VCAM-1 negative ones. The VCAM-1 positive cancers were associated with more lymph node metastases than VCAM-1-negative ones ($P < 0.05$). The expression of VCAM-1 was detected in tissues of two of the eight patients with gastric ulcer and two of the 10 healthy controls. The expression of VCAM-1 in gastric cancer patients was significantly more frequent than that in the healthy controls and ulcer group (both $P < 0.05$). MVD in VCAM-1 expressing tissues was higher than that in VCAM-1 negative tissues ($t = 2.13, P < 0.05$). Serum VCAM-1 levels in gastric cancer patients were significantly higher than those in controls ($t = 3.4, P < 0.05$). There was a significant association between serum VCAM-1 levels and disease stage, as well as invasion depth of the tumor and the presence of distant metastases. The concentrations of serum CEA in gastric cancer were higher than normal controls. Both serum VCAM-1 and CEA levels decreased significantly after radical resection of the primary tumor ($P < 0.05$). Furthermore, the serum levels of VCAM-1 were positively correlated with the expression of VCAM-1 in the tumor tissue ($r = 0.85, P < 0.05$).

CONCLUSION: The expression of VCAM-1 is closely related to oncogenesis, tumor angiogenesis and metastasis in gastric carcinoma. Serum VCAM-1 level in gastric cancer patients is significantly increased compared with normal controls, which decreases significantly after radical resection of the primary tumor. The serum concentration of VCAM-1 may be considered as an effective marker of tumor burden of gastric cancer. Moreover, overexpression of VCAM-1 in gastric cancer tissue is likely a major source of serum VCAM-1.

Ding YB, Chen GY, Xia JG, Zang XW, Yang HY, Yang L. Association of VCAM-1 overexpression with oncogenesis, tumor angiogenesis and metastasis of gastric carcinoma. *World J Gastroenterol* 2003; 9(7):1409-1414

<http://www.wjgnet.com/1007-9327/9/1409.asp>

INTRODUCTION

Solid tumors are composed of two distinct but interdependent compartments, malignant cells themselves and the vascular and connective tissue stroma induced by malignant cells where malignant cells are dispersed. Stroma provides the vascular supply that tumors require for obtaining nutrients, gas exchange, and waste disposal. Thus, any increase in tumor mass, either primary or metastatic, must be accompanied by angiogenesis formation^[1,2]. The mechanism by which tumors induce stroma has caused considerable attention in recent years. Emphasis is increasingly placed on tumor angiogenesis. Tumor angiogenesis has been linked to tumor progression and metastasis. Many reports have suggested that cell adhesion molecules (CAM) not only play key roles in various stages of tumor angiogenesis, but also are involved in tumor progression and metastasis^[3-5].

CAMs are cell-surface glycoproteins which are critical for cell-to-cell interactions. Intercellular adhesion mediated by CAMs directly influences differentiation, and disruption of normal cell-cell contacts has been noted in neoplastic transformation and in metastasis. CAMs expressed on lymphocytes and vascular endothelial cells are thought to play an important role in lymphocyte trafficking for immune anti-infection response. There is evidence that vascular cell adhesion molecule-1 (VCAM-1) may be involved in tumor progression and metastasis^[5,6].

VCAM-1 belongs to the immunoglobulin super family group of adhesion molecules, and is one of the most important adhesion molecules which plays a crucial role in this process. VCAM-1 is an 110 KDa glycoprotein that is constitutively expressed on tissue macrophage, dendritic cells and epithelial cells, as well as on the surface of stimulated endothelial cells. Thus, VCAM-1 is a widely distributed protein. It is possible that VCAM-1 is a candidate for mediating tumor cell adhesion to vascular endothelial cells and promoting the metastatic process. Recent reports have shown that angiogenesis favors tumor growth and facilitates entry of cells into the circulation^[7,8].

It has recently been reported that the microvessel density (MVD) in a tumor correlates with tumor progression, hematogenous metastasis and recurrence of gastric carcinoma.

MVD also reflects tumor angiogenesis^[2-4,9]. In the present study, the expression of VCAM-1 and the density of microvessels were examined by immunohistochemistry in patients with gastric cancer. The association between the expression of VCAM-1 and oncogenesis, tumor angiogenesis and metastasis of gastric carcinoma was evaluated. Meanwhile we also detected the concentration of soluble forms of VCAM-1 and serum levels of carcinoembryonic antigen (CEA) in patients with gastric cancer and investigated its relation to clinical and pathological features.

MATERIALS AND METHODS

Patients

A total of 41 patients with histologically confirmed gastric cancer who had undergone curative gastrectomy at our department from March 1999 to March 2000 were included in this study. They consisted of 26 male and 15 female patients ranging in age from 35 to 74 years (mean, 58.4 years). The clinicopathologic findings were determined according to the principles set by the Japanese Society Committee on Histological Classification of Gastric Cancer. Of the 41 patients, 28 had lymph node metastasis. The patients had not received either chemotherapy or radiation therapy before operation. A tumor sample and a normal part of the stomach were obtained during surgical resection. The samples were each divided into two pieces, which were subjected to fixation in 10 % formalin for histological examination and immunohistological test. All patients had been performed distal partial gastrectomy, proximal partial gastrectomy, or total gastrectomy with regional lymph node dissection to group 1(D1), group 2(D2), group 3 (D3) with a curative intention. Gastric specimens from eight patients with gastric ulcer and 10 patients with normal gastric tissues were obtained by fiber gastroscopy.

Both the expression of VCAM-1 and the density of microvessels were examined by immunohistochemical staining. Meanwhile, blood samples from the 41 gastric cancer patients were obtained before any treatment and at 7 days after surgery. There were no infections in all these patients. Additionally, blood samples were also obtained from 25 healthy subjects as controls. The mean age of these subjects was 39.1 years (age range 20-55 years), with a ratio of male to female of 12:8.

Immunohistochemistry

Specimens were fixed in a 40 g·L⁻¹ formaldehyde solution and embedded in paraffin. Four-micrometer thick sections were cut and mounted on glass slides. Immunohistochemistry was performed using the avidin-biotin complex (ABC) method. Sections were dewaxed in xylene, dehydrated in ethanol, washed by phosphate-buffered saline solution (PBS, pH=7.4) and then heated in a microwave oven for 10 minutes to retrieve the antigens. Endogenous peroxidase activity was blocked by incubation of samples with 3 % hydrogen peroxide in methanol for 30 minutes. After being washed with PBS, 50 μl 10 % normal goat serum was added to glass slides for 10 minutes to reduce nonspecific antibody binding. Specimens were then incubated with a 1:250 dilution of anti-VCAM-1 antibody overnight at 4 °C, followed by three washes with PBS. Sections were then incubated with biotinylated goat antimouse immunoglobulin G (Nanjing Sangon Biotechnology Co.) at a dilution of 1:50 for 2 hours followed by three washes. Slides were then treated with the complex of reagent A and reagent B (ABC kit, Nanjing Sangon Biotechnology Co.) for 2 hours at a dilution of 1:50 and were washed with PBS three times. Finally, slides were incubated in PBS containing diaminobenzidine and 300 mL·L⁻¹ hydrogen peroxide for 10

minutes. Normal mouse immunoglobulin-G was substituted for primary antibody as the negative control. Immunoreactivity was graded as follows: +, more than 10 % of carcinoma cells were stained; -, no detectable expression or fewer than 10 % of carcinoma cells were stained.

Microvessel detection and counting

A detection procedure for microvessels was performed using anti-CD34 monoclonal antibody (Nanjing Sangon Biotechnology Co.). Envision-labeled polymer reagent was applied for immunoreaction. A single microvessel was defined as any brown immunostained endothelial cells, and other connective tissue elements. The stained sections were screened at ×100 magnification under a light microscope to identify the five regions of the section with the highest number of microvessels. The image was visualized on a computer display through a color video camera module and color image freezer. Microvessels were counted in this area at ×200 magnification, and the average number of microvessels in these five regions was recorded, and defined as MVD. The visualized area on the display was determined to be 0.075 mm².

Assay of soluble VCAM-1

For assay of soluble adhesion molecules venous blood samples were collected into plain tubes, allowed to clot for up to 1 hour and centrifuged at 5 000 g for 5 min. The serum was removed, aliquoted and stored at -70 °C until assayed. Concentrations of soluble VCAM-1 were measured with commercially available sandwich ELISA kits based on dual monoclonal antibodies. CEA test, a routine test in our department, was also performed.

Statistical analysis

The data were presented as $\bar{x} \pm s$. Differences in categorical variables between groups were determined by chi-square test, and differences in enumeration data between groups were determined by *t* test or by analysis of variance. Correlations between the levels of soluble adhesion molecules and the clinical and pathological variables were determined by Spearman rank correlation method.

RESULTS

Expression of VCAM-1 in gastric cancer, gastric ulcer and normal gastric tissue

VCAM-1 was positively stained in the cytoplasm or the membrane of vascular endothelial cells in brown or yellow in gastric cancer tissue. VCAM-1 was expressed not only in vascular endothelial cells, but also in the majority of gastric cancer cells. Generally, VCAM-1 expression was intense throughout the tumor, especially in keratin pearl of gastric cancer. VCAM-1 positive vessels were preferentially found in vascular-rich tumor areas. VCAM-1 expression was present in 31 (75.6 %) out of 41 gastric cancer tissues and in 5 (12.2 %) adjacent normal gastric tissue. The rate of expression of VCAM-1 in gastric cancer tissue was significantly higher than that in adjacent normal gastric tissue ($\chi^2=52.1$, $P<0.05$).

VCAM-1 expression was present in 25 % (2/8) of gastric ulcer tissue, and in 20 % (2/10) of healthy subjects ($\chi^2=0.1$, $P>0.05$). However, The rate of VCAM-1 expression in gastric cancer was remarkably higher than that in gastric ulcer and healthy subjects (both $P<0.05$).

CD34 was positively stained mainly in the cytoplasm of vascular endothelial cells as brown or yellow granules. MVD ranged from 21.5 to 71.2, with a mean value of 30.2 in gastric cancer tissues, and ranged from 2 to 14, with a mean value of

11.5 in normal gastric tissues. MVD in tumor tissue was significantly higher than that in normal tissues ($t=3.1$, $P<0.05$).

Association of the expressions of VCAM-1 and MVD with pathological features of gastric carcinoma

As shown in Table 1, VCAM-1 expression was present in 26 (92.9 %) of the 28 gastric cancer patients with lymph node metastasis, but in only 5 (34.5 %) of the 13 gastric cancer patients without lymph node metastasis. The rate of VCAM-1 in patients with lymph node metastasis was significantly higher than that in patients without lymph node metastasis ($\chi^2=11.4$, $P<0.05$). Meanwhile VCAM-1 expression in the gastric cancer patients was also associated with clinicopathological stage and depth of infiltration (both $P<0.05$).

Furthermore, microvessel count in patients with gastric cancer was related to clinicopathological stage, depth of infiltration and lymph node metastasis (all $P<0.05$). The rate of expression of VCAM-1 and MVD in gastric carcinoma tissue had no significant differences among the size, location, age and gender (data not shown).

Table 1 Association of expressions of VCAM-1 and MVD with pathological features of gastric carcinoma

Pathological characteristics	<i>n</i>	Positive VCAM-1(%)	MVD($x\pm s$)
Size of tumor			
<3 cm	10	6	37.1 \pm 12.1
3 cm	31	25	39.5 \pm 12.7
Location			
Lower third	10	7	39.4 \pm 7.3
Middle third	20	17	36.2 \pm 11.3
Upper third	11	7	41.4 \pm 13.3
Depth of invasion			
Mucosa and submucosa	11	5	28.4 \pm 8.1
Muscle and subserosa	12	9	36.9 \pm 10.7
Serosa	18	17 ^a	49.6 \pm 15.1 ^b
Clinicopathologic stage			
I	7	3	29.3 \pm 3.54
II	12	7	33.9 \pm 9.3
III	16	15	46.3 \pm 10.3
IV	6	6 ^c	55.4 \pm 8.1 ^d
Lymph node metastasis			
Present	28	26	45 \pm 9.8
Absent	13	5 ^e	28.5 \pm 5.5 ^f

MVD and expression of VCAM-1 had no significant difference in the size, location. The rate of positive VCAM-1 expression and MVD were positively correlated with depth of invasion (^a $P<0.05$, ^b $P<0.05$ respectively). There was a significant difference between the rate of positive VCAM-1 expression, MVD and clinic pathological stage (^c $P<0.05$, ^d $P<0.05$). The rate of positive VCAM-1 expression and MVD were significantly higher than that in those without lymph node metastasis (^e $P<0.05$, ^f $P<0.05$ respectively).

Correlation between expression of VCAM-1 and MVD

MVD was 46.5 \pm 11.3 in VCAM-1 positive tissue in gastric cancer, while it was 31.2 \pm 8.4 in negative VCAM-1 tissue. MVD in VCAM-1-positive tumors was significantly higher than that in VCAM-1-negative tumors ($t=2.13$, $P<0.05$).

Association of soluble VCAM-1 with gastric cancer

In gastric cancer patients, soluble VCAM-1 was significantly elevated in comparison with that in healthy subjects (878 \pm 46 μ g/lm vs 297 \pm 35 μ g/ml, $P<0.05$, Table 2). The difference in serum concentration of soluble VCAM-1 was also significant

between patients with stage I-II and those with stage III-IV gastric cancer, indicating that soluble VCAM-1 concentration correlated well with the staging of gastric cancer. No significant difference was found between ulcer group and controls ($P>0.05$). Concentrations of serum CEA in gastric cancer patients were higher than those in control group and ulcer group (both $P<0.05$). But no significant difference was found between stage I-II and stage III-IV gastric cancer.

Table 2 Soluble levels of VCAM-1, CEA in gastric cancer patients, ulcer patients and control group

	<i>n</i>	Soluble VCAM-1(μ g/ml) ($x\pm s$)	CEA
Gastric cancer	41	878 \pm 46 ^a	4.7 \pm 0.43
I-II	17	764 \pm 24 ^b	4.1 \pm 0.23
III-IV	24	1006 \pm 78 ^c	4.9 \pm 0.31
Ulcer	8	301 \pm 21	4.5 \pm 0.41
Control	25	297 \pm 35	2.3 \pm 0.28

^a $P<0.05$, ^b $P<0.05$, ^c $P<0.05$, (vs control group).

The concentration of soluble VCAM-1 was higher in the patients with lymph node metastasis than that in those without lymph node metastasis ($P<0.05$). Positive correlation was found between concentration of soluble VCAM-1 and depth of invasion of gastric cancer. In contrast, no significant association was found between concentration of soluble VCAM-1 and location, size, age and gender (data not shown).

Levels of postoperative soluble VCAM-1 in gastric cancer patients were reduced significantly compared to preoperative levels (578 \pm 39 μ g/lm vs 878 \pm 46 μ g/ml, $P<0.05$, Table 3). It was noteworthy that concentration of soluble VCAM-1 was positively correlated with expression of VCAM-1 in the tumor tissue ($r=0.85$, $P<0.05$). The level of serum CEA was also decreased significantly after radical resection of the primary tumor ($P<0.05$).

Table 3 Concentrations of soluble VCAM-1 and CEA at preoperative and postoperative stages

	$x\pm s$ (ng/L)	<i>P</i>
sVCAM-1		
preoperative	878 \pm 46	
postoperative	578 \pm 39	0.0001
CEA		
preoperative	10.3 \pm 18.4	
postoperative	6.3 \pm 11.5	0.0031

Serum VCAM-1 and CEA levels decreased significantly after radical resection of the primary tumor ($P<0.05$).

DISCUSSION

Gastric carcinoma, as one of the most common human malignant tumors, ranks worldwide the first leading cause of gastrointestinal cancer-related mortality. In China, it now ranks the second among all malignant tumors. Recent important advance in oncology is the finding that tumor angiogenesis plays an important role in tumor genesis, growth and metastasis, and an increasing number of studies have proven that vascular targeting therapy is very effective^[9-11]. Many factors are involved in tumor angiogenesis, one of the most important factors is VCAM-1, which is capable of promoting and maintaining the establishment of tumor vascular system^[12]. Thus it can directly stimulate tumor growth and metastasis. Generation of new blood vessels, or angiogenesis, plays a key role in the growth

of malignant disease and has drawn great interest in developing agents that inhibit angiogenesis. Angiogenesis is characterized by invasion, migration, and proliferation of endothelial cells, processes that depend on cell interactions with extracellular matrix components^[12-14]. Our current study has shown VCAM-1 is a key player by providing a vasculature-specific target for antiangiogenic treatment strategies.

Expression of VCAM-1 may facilitate oncogenesis

Recent advances in molecular biology and genetic technology studies on adhesion molecules have demonstrated that cell-cell and cell-extracellular matrix interactions play an important role in cancer metastasis. In addition to activation of oncogenes and inactivation of tumor suppressor genes, alteration of adhesion molecules seems to be critical for the development of gastric cancer^[15]. Tumour development is a multi-step process during which genetic and epigenetic events determine the transition from a normal to a malignant cellular state. In the past decade, extensive effort has been made not only to define the molecular mechanisms underlying progression to malignancy but also to predict the development of the disease and to identify possible molecular targets for therapy. Common to most tumours, several regulatory circuits are altered during multistage tumour progression of gastric cancer, which includes control of proliferation, balance between cell survival and programmed cell death (apoptosis), communication with neighbouring cells and extracellular matrix, induction of tumour neovascularization (angiogenesis) and tumour cell migration, invasion and metastatic dissemination. Deregulation of each of these processes represents a rate-limiting step for tumour development and, hence, has to be achieved by tumour cells in a highly selective manner during tumour progression. In this complex process, more attention has been placed on adhesion molecules, because adhesion molecules are necessary to mediate cell-matrix and cell-cell interactions, metabolism, and differentiation. Moreover, adhesive interactions between tumor cell surface receptors and endothelial cell adhesion molecules are thought to contribute to tumor cell arrest and extravasation during hematogenous metastasis^[14-17]. Changes in expression and function of adhesion molecules are important characteristics in the development of gastrointestinal malignancies and might be used in future as prognostic factors or as new targets in diagnosis and therapy. VCAM-1, one of the adhesion molecules involved in malignant tumor, is found to be expressed mainly in activated endothelial cells, and dendritic cells.

Maurer *et al.* confirmed that VCAM-1 protein was over-expressed in colorectal cancers at the mRNA level by Northern blotting. In comparison to normal controls, the expression of VCAM-1 mRNA was increased by 3.4 fold in colorectal cancers. Our study found that the expression of VCAM-1 in gastric tumor tissue was higher than that in adjacent-cancer tissue, and the ratio of positive VCAM-1 in gastric cancer tissue was higher than that in gastric ulcer and normal mucosa, suggesting that VCAM-1 may play a key role in the growth of gastric cancer.

However, we noted that VCAM-1 expression was positive in one healthy subject, and in two patients with gastric ulcer, indicating that there are other factors involved in the expression of VCAM-1. Some studies believed that *Helicobacter pylori* infection of gastric mucosa was one of the causes responsible for VCAM-1 expression^[18,19].

VCAM-1 expression stimulates tumor angiogenesis

Angiogenesis is of key importance in the process of tumour progression in a number of tumour types. Angiogenesis is a biological process by which new capillaries are formed from

pre-existing vessels. It occurs in physiological conditions such as embryo development, and cyclically in wound repair of female genital system, and during pathological conditions, such as arthritis, diabetic retinopathy and tumors. In the both physiological conditions, angiogenesis is mediated accurately by feedback system. However, in solid tumor growth, a specifically critical turning point is the transition from the vascular to the vascular phase. Having developed an intrinsic vascular network, the neoplastic mass is able to grow indefinitely (unlike other forms of cell growth, tumor angiogenesis is not limited in time) both *in situ* and at distant sites (metastasis). Thus, tumor angiogenesis cannot be controlled by feedback. Angiogenesis is capable of providing continuous nutrients, gas exchange, and waste disposal for tumors growth. Any increase in tumor mass, either primary or metastatic, must be accompanied by vascular formation. Therefore, tumor angiogenesis is a very complex process. At present, an increasing number of studies have shown that abnormal adhesion molecules contribute to tumor angiogenesis by stimulating neoplastic cells to produce growth factors specific for endothelial cells and able to stimulate growth of the host's blood vessels^[6,8,13,15]. Recent studies have demonstrated that VCAM-1 may contribute to tumor angiogenesis. MVD, a reliable index of tumor angiogenesis, has been confirmed to be linked to tumor progression, hematogenous metastasis, and tumor recurrence.

Our study indicated that MVD of gastric cancer tissues with VCAM-1 expression was significantly higher than that in tissues negative for VCAM-1, suggesting that VCAM-1 expression may be one of the factors mediating the activation of angiogenesis. Several reports have observed that gastric cancer cells are capable of activating vessel endothelial cells, which leads to expression of VCAM-1, and thus the induction of tumour neovascularization. Maeds *et al.* proposed that VCAM-1 binding to its ligand VLA4 not only results in activation of vessel endothelial cells, but also leads to shedding of tumor cells and invasion of adjacent tissue^[20,21]. Byrne *et al.* suggested that VCAM-1 was expressed on endothelial cells as a result of stimulation by vascular endothelial growth factor (VEGF). In general, these findings suggest that VCAM-1 may be used for sustained angiogenesis and tissue invasion and metastasis via autocrine/paracrine manners^[7].

However, in some tumors, high MVD VCAM-1 expression was not detected, which suggests that other factors such as extracellular matrix, and metabolic and mechanical factors also contribute to tumor angiogenesis. Hence anti-angiogenesis therapy should utilize multiangiogenesis tactics^[23,24].

MVD may be different according to the observer, and cut-off values are also different. In addition, it has been reported that different MVD could be obtained with different antibodies used in different studies. Therefore, MVD that was observed in this study may be different from those previously reported.

VCAM-1 favors lymph node metastasis of gastric cancer

It is generally accepted that the presence or absence of regional lymph node involvement is one of the important factors influencing survival in respectable gastric cancer. Lymph node metastasis occurs even in some patients with early gastric cancer. Recently, studies have confirmed that prognosis of gastric cancer patients with lymph node metastasis is very poor. Gastric cancer patients with lymph node metastasis have been commonly reported to have poorly differentiated adenocarcinoma, and deeper invasion, in comparison with gastric cancer patients without lymph node metastasis. In our present study, we observed that VCAM-1 expression in 26 of 28 cases with lymph node metastasis, whereas in only 5 of 13 gastric cancer patients without lymph node metastasis. There

was a significant difference between the two groups ($P < 0.05$), indicating that expression of VCAM-1 may be associated with lymph node metastasis of gastric cancer. VCAM-1 is predominantly expressed on gastric carcinoma cells, giving these tumor cells the ability to perform lymph-node metastasis. Meanwhile, expression of VCAM-1 significantly alters malignant transformation^[11,20,21].

Tumor metastasis involves the release of cells from primary tumor due to a firmly formed cluster of tumor cells probably by detaching from the tumor nests with unstable adhesiveness, followed by their migration in extracellular matrix, adhesion to vessel walls, arrest in microcirculation of distant organs, and subsequent extravasation. Extravasation of metastatic tumor cells from bloodstream of the tissue space in a secondary organ is related specific binding to determinants on endothelial cell surface. Each step requires cell adhesive interactions involving specific adhesion molecules and receptors. Several families of adhesion molecules have now been identified, some of which are promising candidates for a role in neoplasia. So tumor metastasis is a very complex process, Colette *et al.* thought that VCAM-1 overexpression stimulated tumour neovascularization, and angiogenesis was necessary for tumor growth and metastasis, VCAM-1 expression was linked to lymph node metastasis^[2,3,21-24].

We observed that VCAM-1 expression was present in 5 of the 13 cases without lymph node metastasis, which may be related to lymph node micrometastasis. It has been demonstrated that micrometastases consisting of one to a few cells in lymph nodes resected during gastrectomy are difficult to identify using conventional hematoxylin and eosin (H&E) stains^[25,26].

Concentration of soluble VCAM-1 may be one of the important markers for gastric carcinoma

Our study demonstrated that serum concentration of VCAM-1 was elevated in patients with gastric cancer before treatment in comparison with the healthy group; hence, the concentration of soluble VCAM-1 may be of significance in diagnosis of gastric carcinoma. In addition, a positive correlation was observed between levels of soluble VCAM-1 and tumor stage, and invasion depth. More important was that the concentration of soluble VCAM-1 in patients with lymph node metastasis was significantly higher than that in patients without lymph node metastasis. These findings suggest that the levels of soluble VCAM-1 are linked to tumor growth and metastasis. Our results are consistent with the findings by Velikova *et al.*, who also reported elevated serum levels of VCAM-1 in gastric cancer, and proposed that patients with elevated serum VCAM-1 have a poorer survival rate. Measurement of circulating VCAM-1 may bring additional prognostic information for patients with gastric cancer in relation to different stages and tumor pathology, and it should be included in future large multivariate analyses of prognostic factors should be performed whenever possible^[27,28]. Animal experiments have confirmed that soluble VCAM-1 promotes angiogenesis in rat cornea, which is supported by our findings^[29,30].

Additionally, It was first observed that postoperative concentrations of soluble VCAM-1 decreased significantly in patients with gastric cancer in comparison with preoperative concentrations ($P < 0.05$). This finding suggests that measurement of circulating VCAM-1 may play a critical role in prognosis of gastric cancer patient. It is likely that tumor burden in patients with gastric cancer is decreased after operation, so the concentration of soluble VCAM-1 is reduced. If the levels of soluble VCAM-1 increase again after operation, we should pay great attention to tumor recurrence. Therefore, soluble VCAM-1 may be considered as a marker for tumor

burden. Some investigators have reported a positive correlation between serum concentration of VCAM-1 and age of patients, but no such a correlation was found in healthy subjects. Our study did not confirm this although we noted that the median age in healthy group was lower than that of gastric cancer patients. Therefore, the effect of age on serum levels of VCAM-1 can not be excluded, and future studies should take it into account^[31].

In our department, CEA is one of the routine tests in gastric cancer. It is well accepted that CEA is one of the most important marks of gastrointestinal carcinoma, and preoperative positivity for CEA is an independent risk factor for hematogenous recurrence of gastric carcinoma. Our finding on CEA is consistent with those previously reported^[32,33].

Expression of VCAM-1 in tumor tissue is one of the sources of soluble VCAM-1 in gastric cancer

The source of soluble VCAM-1 is not yet known. VCAM-1 is known to be expressed predominantly on activated endothelial cells, dendritic cells and renal proximal tubule cells. We found that strong VCAM-1 expression occurred in gastric cancer cells and endothelial cells in tumor tissues, especially in vessel abundant regions. Some studies have reported that VCAM-1 has been found in malignant epithelial tissue, including metastasis gastric cancer cells, melanoma cell lines and hepatocellular cells. In our study, a strong correlation was found between expression of VCAM-1 in gastric cancer tissue and serum concentration of soluble VCAM-1 ($r = 0.85$, $P < 0.05$). Increased expression of VCAM-1 in gastric cancer cells and their shedding into circulation may be the factor accounting for the significantly elevated serum levels of VCAM-1. Other studies have reported that soluble VCAM-1 may be related to the white cell count. To eliminate this possibility, blood tests were performed, and gastric cancer patients with normal blood tests were included. We observed that expression of VCAM-1 in gastric carcinoma tissue was positively correlated with concentration of soluble VCAM-1, indicating that expression of VCAM-1 in gastric cancer tissue is a major source of soluble VCAM-1. VCAM-1 is expressed on endothelial cells as a result of vascular endothelial growth factor (VEGF) stimulation^[4,6,19-21,34,35].

In conclusion, VCAM-1 may be involved in the progression of human gastric carcinoma, particularly via lymphangiogenesis. VCAM-1 expression at invading edge of gastric carcinoma may be a sensitive marker for metastasis to lymph nodes. Differentially expressed vascular molecules may influence the functional characteristics of extravasating leukocytes and represent new targets in anti-gastric cancer therapy. In general, an increasing number of studies on a variety of malignant diseases have suggested that VCAM-1 may play a role in the process of adhesion of tumor cells to endothelial cells and neovascularization. Expression of VCAM-1 is associated with oncogenesis, tumor angiogenesis and metastasis in gastric carcinoma. MVD in gastric carcinoma tissue is closely associated with lymph node metastasis, clinical stage and depth of invasion. Expression of VCAM-1 is closely related to MVD in gastric cancer, and thus VCAM-1 can act as an important index reflecting the biological behaviors of gastric carcinoma. VCAM-1 may be used as a metastasis marker and/or a target for antiangiogenic therapy. VCAM-1 has been shown to be a key player by providing a vasculature-specific target for antiangiogenic treatment strategies. Concentration of soluble VCAM-1 correlates well with tumor growth and metastasis. Expression of VCAM-1 in gastric cancer tissue is positively correlated with concentration of soluble VCAM-1. Elevated soluble VCAM-1 is decreased significantly in gastric cancer patients after operation, and thus soluble VCAM-1 may be one of the markers for gastric carcinoma tumor burden, and

serum VCAM-1 may be considered as an effective diagnostic and prognostic factor.

REFERENCES

- Ghossein RA**, Bhattacharya S, Rosai J. Molecular detection of micrometastases and circulating tumor cells in solid tumors. *Clin Cancer Res* 1999; **5**: 1950-60
- Liu DH**, Zhang XY, Fan DM, Huang YX, Zhang JS, Huang WQ, Zhang YQ, Huang QS, Ma WY, Chai YB, Jin M. Expression of vascular endothelial growth factor and its role in oncogenesis of human gastric carcinoma. *World J Gastroenterol* 2001; **7**: 500-505
- Saito H**, Tsujitani S, Kondo A, Ikeguchi M, Maeta M, Kaibara N. Expression of vascular endothelial growth factor correlates with hematogenous recurrence in gastric carcinoma. *Surgery* 1999; **125**: 195-201
- Ren J**, Dong L, Xu CB, Pan BR. The role of KDR in the interactions between human gastric carcinoma cell and vascular endothelial cell. *World J Gastroenterol* 2002; **8**: 596-601
- Alexiou D**, Karayiannakis AJ, Syrigos KN, Zbar A, Kremmyda A, Bramis I, Tsigris C. Serum levels of E-selectin, ICAM-1 and VCAM-1 in colorectal cancer patients: correlations with clinicopathological features, patient survival and tumour surgery. *Eur J Cancer* 2001; **37**: 2392-2397
- Maurer CA**, Friess H, Kretschmann B, Wildi S, Muller C, Graber H, Schilling M, Buchler MW. Over-expression of ICAM-1, VCAM-1 and ELAM-1 might influence tumor progression in colorectal cancer. *Int J Cancer* 1998; **79**: 76-81
- Byrne GJ**, Bundred NJ. Surrogate markers of tumoral angiogenesis. *Int J Biol Markers* 2000; **15**: 334-339
- Li DY**, Sorensen LK, Brooke BS, Urness LD, Davis EC, Taylor DG, Boak BB, Wendel DP. Defective angiogenesis in mice lacking endoglin. *Science* 1999; **284**: 1534-1537
- Kakeji Y**, Koga T, Sumiyoshi Y, Shibahara K, Oda S, Maehara Y, Sugimachi K. Clinical significance of vascular endothelial growth factor expression in gastric cancer. *J Exp Clin Cancer Res* 2002; **21**: 125-129
- Tao HQ**, Lin YZ, Wang RN. Significance of vascular endothelial growth factor messenger RNA expression in gastric cancer. *World J Gastroenterol* 1998; **4**: 10-13
- Takahashi N**, Haba A, Matsuno F, Seon BK. Antiangiogenic therapy of established tumors in human skin/severe combined immunodeficiency mouse chimeras by anti-endoglin (CD105) monoclonal antibodies, and synergy between anti-endoglin antibody and cyclophosphamide. *Cancer Res* 2001; **61**: 7846-7854
- Muller AM**, Weichert A, Muller KM. E-cadherin, E-selectin and vascular cell adhesion molecule: immunohistochemical markers for differentiation between mesothelioma and metastatic pulmonary adenocarcinoma? *Virchows Arch* 2002; **441**: 41-46
- Brandvold KA**, Neiman P, Ruddell A. Angiogenesis is an early event in the generation of myc-induced lymphomas. *Oncogene* 2000; **19**: 2780-2785
- Langley RR**, Carlisle R, Ma L, Specian RD, Gerriten ME, Granger DN. Endothelial expression of vascular cell adhesion molecule-1 correlates with metastatic pattern in spontaneous melanoma. *Microcirculation* 2001; **8**: 335-345
- Maehara Y**, Kabashima A, Koga T, Tokunaga E, Takeuchi H, Kakeji Y, Sugimachi K. Vascular invasion and potential for tumor angiogenesis and metastasis in gastric carcinoma. *Surgery* 2000; **128**: 408-416
- Park HJ**, Lee YW, Hennig B, Toborek M. Linoleic acid-induced VCAM-1 expression in human microvascular endothelial cells is mediated by the NF-kappa B-dependent pathway. *Nutr Cancer* 2001; **41**: 126-134
- Seon BK**, Takahashi N, Haba A, Matsuno F, Haruta Y, She XW, Harada N, Tsai H. Angiogenesis and metastasis marker of human tumors. *Rinsho Byori* 2001; **49**: 1005-1013
- Ohnita K**, Isomoto H, Mizuta Y, Maeda T, Haraguchi M, Miyazaki M, Murase K, Murata I, Tomonaga M, Kohno S. *Helicobacter pylori* infection in patients with gastric involvement by adult T-cell leukemia/lymphoma. *Cancer* 2002; **94**: 1507-1516
- Mori N**, Wada A, Hirayama T, Parks TP, Stratowa C, Yamamoto N. Activation of intercellular adhesion molecule 1 expression by *Helicobacter pylori* is regulated by NF-kappaB in gastric epithelial cancer cells. *Infect Immun* 2000; **68**: 1806-1814
- Kwon S**, Kim GS. Prognostic significance of lymph node metastasis in advanced carcinoma of the stomach. *Br J Surg* 1996; **83**: 1600-1603
- Gulubova MV**. Expression of cell adhesion molecules, their ligands and tumour necrosis factor alpha in the liver of patients with metastatic gastrointestinal carcinomas. *Histochem J* 2002; **34**: 67-77
- Charpin C**, Garcia S, Andrac L, Horschowski N, Choux R, Lavaut MN. VCAM (IGSF) adhesion molecule expression in breast carcinoma detected by automated and quantitative immunocytochemical assays. *Hum Pathol* 1998; **29**: 896-903
- Hemmerlein B**, Scherbening J, Kugler A, Radzun HJ. Expression of VCAM-1, ICAM-1, E- and P-selectin and tumour-associated macrophages in renal cell carcinoma. *Histopathology* 2000; **37**: 78-83
- Lode HN**, Moehler T, Xiang R, Jonczyk A, Gillies SD, Cheresch DA, Reisfeld RA. Synergy between an antiangiogenic integrin alpha antagonist and an antibody-cytokine fusion protein eradicates spontaneous tumor metastases. *Proc Natl Acad Sci USA* 1999; **96**: 1591-1596
- Vlems FA**, Diepstra JH, Cornelissen IM, Ruers TJ, Ligtenberg MJ, Punt CJ, van Krieken JH, Wobbes T, van Muijen GN. Limitations of cytokeratin 20 RT-PCR to detect disseminated tumour cells in blood and bone marrow of patients with colorectal cancer: expression in controls and downregulation in tumour tissue. *Mol Pathol* 2002; **55**: 156-163
- Lee E**, Chae Y, Kim I, Choi J, Yeom B, Leong AS. Prognostic relevance of immunohistochemically detected lymph node micrometastasis in patients with gastric carcinoma. *Cancer* 2002; **94**: 2867-2873
- Alexiou D**, Karayiannakis AJ, Syrigos KN, Zbar A, Sekara E, Michail P, Rosenberg T, Diamantis T. Clinical significance of serum levels of E-selectin, intercellular adhesion molecule-1, and vascular cell adhesion molecule-1 in gastric cancer patients. *Am J Gastroenterol* 2003; **98**: 478-485
- Karayiannakis AJ**, Syrigos KN, Polychronidis A, Zbar A, Kouraklis G, Simopoulos C, Karatzas G. Circulating VEGF levels in the serum of gastric cancer patients: correlation with pathological variables, patient survival, and tumor surgery. *Ann Surg* 2002; **236**: 37-42
- Velikova G**, Banks RE, Gearing A, Hemingway I, Forbes MA, Preston SR, Hall NR, Jones M, Wyatt J, Miller K, Ward U, Al-Maskatti J, Singh SM, Finan PJ, Ambrose NS, Primrose JN, Selby PJ. Serum concentrations of soluble adhesion molecules in patients with colorectal cancer. *Br J Cancer* 1998; **77**: 1857-1863
- Yoo NC**, Chung HC, Chung HC, Park JO, Rha SY, Kim JH, Roh JK, Min JS, Kim BS, Noh SH. Synchronous elevation of soluble intercellular adhesion molecule-1 (ICAM-1) and vascular cell adhesion molecule-1 (VCAM-1) correlates with gastric cancer progression. *Yonsei Med J* 1998; **39**: 27-36
- Locker GJ**, Stoiser B, Losert H, Wenzel C, Ohler L, Kabrna E, Geissler K. Decrease of circulating hematopoietic progenitor cells During interleukin-2 treatment is associated with an increase of vascular cell adhesion molecule-1, a critical molecule for progenitor cell adhesion. *Leuk Lymphoma* 2000; **39**: 355-364
- Marrelli D**, Pinto E, De Stefano A, Farnetani M, Garosi L, Roviello F. Clinical utility of CEA, CA 19-9, and CA 72-4 in the follow-up of patients with resectable gastric cancer. *Am J Surg* 2001; **181**: 16-19
- Kinugasa T**, Kuroki M, Takeo H, Matsuo Y, Ohshima K, Yamashita Y, Shirakusa T, Matsuoka Y. Expression of four CEA family antigens (CEA, NCA, BGP and CGM2) in normal and cancerous gastric epithelial cells: up-regulation of BGP and CGM2 in carcinomas. *Int J Cancer* 1998; **76**: 148-153
- Kaptur S**, Riedel F, Erhardt T, Hormann K. Serum concentrations of soluble adhesion molecules sICAM-1 and sVCAM-1 in patients with malignant ENT tumors. *HNO* 2001; **49**: 910-913
- Ikeda M**, Furukawa H, Imamura H, Shimizu J, Ishida H, Masutani S, Tatsuta M, Kawasaki T, Satomi T. Surgery for gastric cancer increases plasma levels of vascular endothelial growth factor and von Willebrand factor. *Gastric Cancer* 2002; **5**: 137-141

Expression of Fas ligand and Caspase-3 contributes to formation of immune escape in gastric cancer

Hua-Chuan Zheng, Jin-Min Sun, Zheng-Li Wei, Xue-Fei Yang, Yin-Chang Zhang, Yan Xin

Hua-Chuan Zheng, Jin-Min Sun, Xue-Fei Yang, Yin-Chang Zhang, Yan Xin, The Fourth Lab. Cancer Institute, the First Affiliated Hospital of China Medical University, Shenyang 110001, Liaoning Province, China

Zheng-Li Wei, Department of Oncology, Affiliated Hospital of China Medical University, Shenyang 110001, Liaoning Province, China

Correspondence to: Dr. Hua-Chuan Zheng, the Fourth Lab. Cancer Institute, The First Affiliated Hospital of China Medical University, Shenyang 110001, Liaoning Province, China. zheng_huachuan@hotmail.com

Telephone: +86-24-23256666 Ext. 6351 **Fax:** +86-24-23253443

Received: 2002-12-22 **Accepted:** 2003-01-18

Abstract

AIM: To study the role of Fas ligand (FasL) and Caspase-3 expression in carcinogenesis and progression of gastric cancer and molecular mechanisms of relevant immune escape.

METHODS: FasL and Caspase-3 expression was studied in adjacent epithelial cells, cancer cells and lymphocytes of primary foci, and cancer cells of metastatic foci from 113 cases of gastric cancer by streptavidin-biotin-peroxidase (S-P) immunohistochemistry. Expression of both proteins in cancer cells of primary foci was compared with clinicopathological features of gastric cancer. The relationship between FasL expression in cancer cells and Caspase-3 expression in cancer cells or infiltrating lymphocytes of primary foci was investigated.

RESULTS: Cancer cells of primary foci expressed FasL in 53.98 % (61/113) of gastric cancers, more than their adjacent epithelial cells (34.51 %, 39/113) ($P=0.003$, $\chi^2=8.681$), while the expression of Caspase-3 in cancer cells of primary foci was detected in 32.74 % (37/113) of gastric cancers, less than in the adjacent epithelial cells (50.44 %, 57/113) ($P=0.007$, $\chi^2=7.286$). Infiltrating lymphocytes of the primary foci showed positive immunoreactivity to Caspase-3 in 70.80 % (80/113) of gastric cancers, more than their corresponding adjacent epithelial cells ($P=0.001$, $\chi^2=10.635$) or cancer cells of primary foci ($P=0.000$, $\chi^2=32.767$). FasL was less expressed in cancer cells of metastases (51.16 %, 22/43) than in those of the corresponding primary foci (81.58 %, 31/38) ($P=0.003$, $\chi^2=9.907$). Conversely, Caspase-3 was more expressed in cancer cells of metastases (58.14 %, 25/43) than in those of the corresponding primary foci (34.21 %, 13/38) ($P=0.031$, $\chi^2=4.638$). FasL expression was significantly correlated with tumor size ($P=0.035$, $rs=0.276$), invasive depth ($P=0.039$, $rs=0.195$), metastasis ($P=0.039$, $rs=0.195$), differentiation ($P=0.015$, $rs=0.228$) and Lauren's classification ($P=0.038$, $rs=0.196$), but not with age or gender of patients, growth pattern or TNM staging of gastric cancer ($P>0.05$). In contrast, Caspase-3 expression showed no correlation with any clinicopathological parameters described above in cancer cells of the primary foci ($P>0.05$). Interestingly, FasL expression in primary gastric cancer cells paralleled to Caspase-3 expression in infiltrating lymphocytes

of the primary foci ($P=0.016$, $\chi^2=5.825$).

CONCLUSION: Up-regulated expression of FasL and down-regulated expression of Caspase-3 in cancer cells of primary foci play an important role in gastric carcinogenesis. As an effective marker to reveal the biological behaviors, FasL is implicated in differentiation, growth, invasion and metastasis of gastric cancer by inducing apoptosis of infiltrating lymphocytes. Chemical substances derived from the primary foci and metastatic microenvironment can inhibit the growth of metastatic cells by enhancing Caspase-3 expression and diminishing FasL expression.

Zheng HC, Sun JM, Wei ZL, Yang XF, Zhang YC, Xin Y. Expression of Fas ligand and Caspase-3 contributes to formation of immune escape in gastric cancer. *World J Gastroenterol* 2003; 9(7): 1415-1420

<http://www.wjgnet.com/1007-9327/9/1415.asp>

INTRODUCTION

Gastric cancer is one of the commonest malignancies in China, and even in the world^[1-7]. Although early diagnosis and treatment have somewhat improved the patients' outcome, gastric cancer still remains the major killer among Chinese^[8,9]. The stepwise transitions during gastric carcinogenesis and progression show that growth-limited gastric epithelial cells become immortalized and in turn exhibit malignant phenotypes^[10,11]. It is obvious that the intrinsic regulatory systems for normal cell survival and death are perturbed in these sequential changes of gastric carcinogenesis and progression, so a further understanding of aberrant apoptosis of gastric epithelial cells and cancer cell will be of great significance in the prevention, diagnosis and treatment of gastric cancer.

Fas ligand (FasL) is a family member of tumor necrosis factor (TNF) and nerve growth factor (NGF), which maps to human chromosome 1^[12]. When membrane FasL (mFasL) crosslinks with membrane Fas (mFas), cellular apoptosis is induced. However, soluble Fas is released into tumor microenvironment to neutralize FasL on tumor infiltrating lymphocytes and consequently blocks their apoptotic induction, leading to tumor immune escape^[13]. Some matrix metalloproteinases can hydrolyze the mFasL into impotent soluble FasL, which can resist apoptosis-induced effect by lymphocytes^[14]. In Fas/FasL pathway, association of Fas with FasL can activate the Fas-associated death domain (FADD) and make mitochondrion release cytochrome C^[15], which eventually initiates the key Caspase-3 in catalyzing the specific cleavage of many important cellular proteins during apoptosis^[16,17].

Caspase-3/ CPP32 is a member of the interleukin-1 β -converting enzyme (ICE) family, which specifically cleaves substrates at the C-terminal of aspartic acid residues. Caspase-3 includes two types of CPP32 α and CPP32 β with cysteine protease activity, and shows a high homology to the pro-apoptotic ced-3 of *C. elegans*^[18,19]. Several members of the Caspase family have been implicated in apoptosis, among

which Caspase-3 is thought to act as a central mediator of programmed cell death (PCD) in mammalian cells^[20]. Caspase-3 is synthesized as an inactive 32 kd proenzyme and processed during apoptosis into its active form that is composed of two subunits, p17-20 and p10-12. Activated Caspase-3 is responsible for the cleavage of poly (ADP-ribose) polymerase (PARP), actin and sterol regulatory element binding protein (SREBP), which relate to apoptosis^[19,21-23]. Inhibition of the CPP32-induced proteolytic breakdown of PARP has been demonstrated to result in the attenuation of apoptosis^[15].

Previous study suggested that high expression of Fas and FasL was involved in gastroduodenal carcinogenesis^[24]. In the current study, we aimed to evaluate the expression of FasL and Caspase-3 in adjacent epithelial cells, cancer cells and lymphocytes of the primary foci, and cancer cells of the metastatic foci of gastric cancer and to find out if there is any relationship between their expressions in cancer cells of the primary foci and clinicopathological features of gastric cancer, as well as between FasL expression in cancer cells of the primary foci and Caspase-3 expression in cancer cells or its infiltrating lymphocytes of the primary foci in order to clarify the role of FasL and Caspase-3 expression in carcinogenesis and progression of gastric cancer and the molecular mechanism of relevant immune escape.

MATERIALS AND METHODS

Subjects

Surgical specimens of 113 gastric cancers were studied from the Second Affiliated Hospital of China Medical University from Sep. 1997 to Feb. 2001. None of the patients underwent radiotherapy or chemotherapy before operation. Adjacent mucosa and primary tumors of all the cases, as well as 43 metastases from 38 cases were fixed in 4 % formaldehyde solution, embedded in paraffin and cut into 4 μ m sections.

Evaluation of clinicopathological features

Hematoxylin-and-eosin-stained sections were examined by two pathologists to confirm the histological diagnosis and other microscopic characteristics. These cancers were histologically classified into differentiated and undifferentiated cancers. Their growth pattern was classified into mass, nest, or diffuse types, as reported previously^[6]. Penetration of gastric wall, lymph node and distal metastases were routinely described in each patient. Tumor staging was assessed according to TNM classification system.

Immunohistochemistry

The representative and consecutive sections from each adjacent mucosa, primary and secondary tumor were immunostained with streptavidin-peroxidase technique (S-P kit, Zhongshan Biotech.). Anti-FasL antibody (Boster Biotech.) and anti-Caspase-3 antibody (DAKO Biotech.) were diluted in phosphate-buffered saline (PBS, 0.01 mol/L, pH7.4) at the

dilution ratio of 1:50 and 1:100 respectively. All procedures were implemented according to the product illustration. For negative controls, sections were processed as the above but with PBS instead of the primary antibodies.

Evaluation of FasL and Caspase-3 staining

The immunoreactivity to FasL or Caspase-3 was localized in the cytoplasm. From 5 randomly selected representative fields of each section, one hundred cells were counted by two independent observers, who did not know the clinicopathological features of these gastric cancers. According to proportion of positive cells, the degree of staining achieved with their antibodies was graded as follows: negative (-), ≤ 5 %; weakly positive (+), 5-25 %; moderately positive (++), 25-50 %; and strongly positive (+++), ≥ 50 %.

Statistical analysis

Statistical evaluation was performed using *chi*-square to differentiate the rates of different groups and using Spearman's test to analyze ranking correlation. $P < 0.05$ was considered statistically significant. SPSS 10.0 software for Windows was employed to analyze all data.

RESULTS

FasL and Caspase-3 expression in adjacent epithelial cells, cancer cells and lymphocytes of the primary foci, and cancer cells of the metastatic foci of gastric cancer

Cancer cells of the primary foci expressed FasL in 53.98 % (61/113) of gastric cancers, more than the adjacent epithelial cells (34.51 %, 39/113) ($P=0.003$, $\chi^2=8.681$), while Caspase-3 in cancer cells of primary foci was expressed in 32.74 % (37/113) of gastric cancers, less than in the adjacent epithelial cells (50.44 %, 57/113) ($P=0.007$, $\chi^2=7.286$). Infiltrating lymphocytes in the primary foci showed strong immunoreactivity to Caspase-3 in 70.80 % (80/113) of gastric cancers, more than that in the corresponding adjacent epithelium ($P=0.001$, $\chi^2=10.635$) or cancer cells of the primary foci ($P=0.000$, $\chi^2=32.767$). FasL was less expressed in cancer cells of metastases (51.16 %, 22/43) than in those of the corresponding primary foci (81.58 %, 31/38) ($P=0.003$, $\chi^2=9.907$). Conversely, Caspase-3 was more positively expressed in cancer cells of metastases (58.14 %, 25/43) than in those of the corresponding primary foci (34.21 %, 13/38) ($P=0.031$, $\chi^2=4.638$) (Table 1, Figures 1-4).

Relationship between FasL and Caspase-3 expression in cancer cells of the primary foci and the clinicopathological features of gastric cancer

FasL expression was significantly correlated with tumor size ($P=0.035$, $r_s=0.276$), invasive depth ($P=0.039$, $r_s=0.195$), metastasis ($P=0.039$, $r_s=0.195$), histological classification ($P=0.015$, $r_s=0.228$) and Lauren's classification ($P=0.038$,

Table 1 Expression of FasL and Caspase-3 in adjacent epithelial cells, cancer cells of primary and metastatic foci of gastric cancer

	n	FasL expression			Caspase-3 expression		
		-	+~+++	PR(%)	-	+~+++	PR(%)
Adjacent epithelial cells	113	74	39	34.51	56	57	50.44
Cancer cells of primary foci	113	52	61	53.98 ^a	76	37	32.74 ^b
Cancer cells of metastatic foci	43	21	22	51.16 ^c	18	25	58.14 ^d

^a $P=0.003$ ($\chi^2=8.681$, Pearson's $R=0.176$), vs adjacent epithelial cells; ^b $P=0.007$ ($\chi^2=7.286$, Pearson's $R=0.180$), vs adjacent epithelial cells; ^c $P=0.003$ ($\chi^2=9.907$, Pearson's $R=0.245$), vs cancer cells of the corresponding primary foci; ^d $P=0.031$ ($\chi^2=4.638$, Pearson's $R=0.239$), vs cancer cells of the corresponding primary foci; PR, positive rate.

$r_s=0.196$) of gastric cancer in cancer cells of the primary foci, whereas not with growth pattern or TNM staging of gastric cancer, gender or age of patients ($P>0.05$). Comparatively, Caspase-3 expression showed no significant correlation with tumor size, invasive depth, metastasis, histological classification, TNM staging, age and gender of patients in cancer cells of the primary foci ($P>0.05$) (Table 2).

Relationship between FasL and Caspase-3 expression in gastric cancer

Interestingly, our results showed FasL expression in cancer cells of the primary foci was positively associated with Caspase-3 expression in their infiltrating lymphocytes ($P=0.016$, $\chi^2=5.825$), not with Caspase-3 expression in cancer cells of the primary foci ($P>0.05$) (Table 3).

Table 2 Relationship between the expression of FasL, Caspase-3 in cancer cells of primary foci and clinicopathological features of gastric cancer

Clinicopathological features	n	FasL expression					Caspase-3 expression						
		-	+	++	+++	PR(%)	P value	-	+	++	+++	PR(%)	P value
Age							0.318						0.414
<50 years	33	13	7	6	7	60.61		21	3	3	6	36.36	
≥50 years	80	39	17	14	10	51.25		55	13	4	8	31.25	
Gender							0.548						0.514
Male	83	37	16	16	14	55.42		57	12	5	9	31.32	
Female	30	15	5	7	3	50.00		19	4	2	5	36.37	
Tumor size							0.035						0.802
<4 cm	47	27	8	7	5	42.55		33	3	5	6	29.79	
≥4 cm	66	25	13	16	12	62.12		43	13	2	8	34.84	
Invasive depth							0.039						0.987
Above submucosa	26	16	4	4	2	38.46		18	3	3	2	30.76	
Muscularis propria	34	16	6	8	4	52.94		22	6	0	6	32.35	
Below subserosa	53	20	11	11	11	62.26		36	7	4	6	33.96	
Metastasis							0.039						0.913
-	75	40	12	15	8	46.67		51	9	3	12	32.00	
+	38	12	9	8	9	68.42		25	7	4	2	34.21	
TNM staging							0.312						0.506
O	18	10	3	3	2	44.44		12	3	1	2	33.33	
I	28	13	4	8	3	53.57		18	3	2	5	35.71	
II	40	19	8	8	5	52.50		26	7	2	5	35.00	
III	17	7	2	2	6	58.82		13	1	1	2	23.53	
IV	10	3	4	2	1	70.00		7	2	1	0	30.00	
Growth pattern							0.338						0.735
Mass	23	8	5	10	0	65.22		17	3	1	2	26.09	
Nest	30	12	4	5	9	60.00		18	5	1	6	40.00	
Diffuse	34	18	7	3	6	47.06		23	5	2	4	32.35	
Lauren's classification							0.038						0.333
Intestinal type	36	12	7	13	4	66.67		27	3	1	5	25.00	
Diffuse type	57	32	10	8	7	43.86		36	9	5	7	36.84	
Mixed type	20	8	4	2	6	60.00		13	4	1	2	35.00	
Histological classification							0.015						0.754
Differentiated	53	19	9	14	11	64.15		37	6	2	8	30.18	
Undifferentiated	60	33	12	9	6	45.00		39	10	5	6	35.00	

PR, positive rate.

Table 3 Relationship between FasL and Caspase-3 expression in gastric cancer

FasL expression In CC of PF	n	Caspase-3 expression in CC of PF			Caspase-3 expression in ILC of PF		
		-	+~++++	PR(%)	-	+~++++	PR(%)
-	52	39	13	26.92	21	31	65.38
+~++++	61	37	24	37.70	12	49	75.41 ^a
Total	113	76	37	32.74	33	80	70.80

^a $P=0.016$ ($\chi^2=5.825$, Pearson' $R=0.227$), vs FasL-negative cases; CC, cancer cells; PF, primary foci; ILC, infiltrating lymphocytes; PR, positive rate.

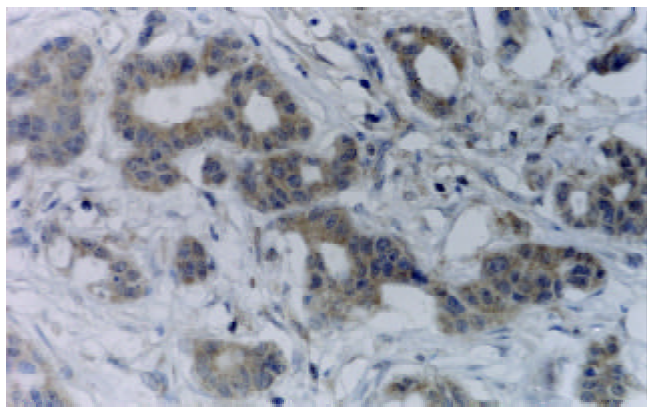


Figure 1 FasL was strongly expressed in moderately differentiated adenocarcinoma of stomach (+++). S-P \times 400.

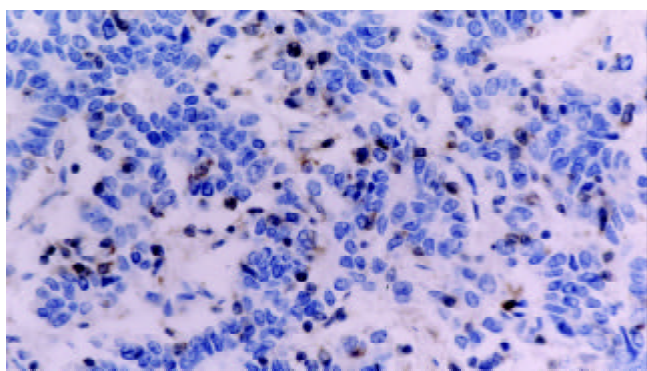


Figure 2 Caspase-3 was negatively expressed in poorly differentiated adenocarcinoma of stomach (-), while strongly positive in tumor infiltrating lymphocytes (+++). S-P \times 400.

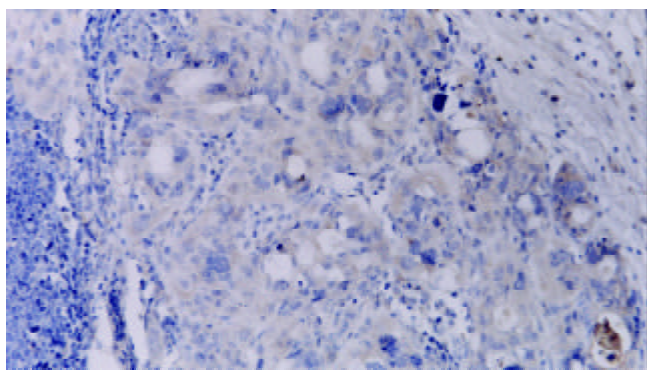


Figure 3 FasL was strongly expressed in gastric cancer cells of lymph node metastasis (+++). S-P \times 400.

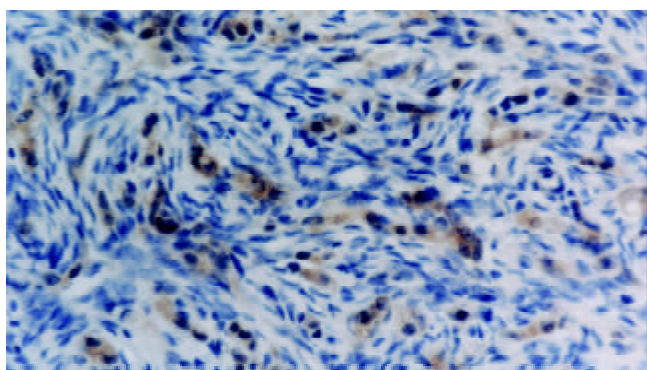


Figure 4 Caspase-3 was strongly expressed in gastric cancer cells of ovary metastasis (+++). S-P \times 400.

DISCUSSION

As a transmembrane type II protein, FasL initiates PCD through activating FADD when coupled with mFas, so FasL greatly contributes to apoptotic induction in most cells^[25]. During the course, Caspase-3 will be activated by a series of cascade reactions, and eventually DNase (CAD, CPAN, or DEF40) is activated, which belongs to the Mg²⁺-dependent endonuclease and acts as a killer in apoptosis. Some previous studies demonstrated that esophageal and colon cancers highly expressed FasL at the levels of mRNA and protein. Furthermore, increased FasL can bind to mFas in infiltrating lymphocytes, which is eliminated by inducing their apoptosis^[26,27]. Therefore, cancer cells can form an immune escape.

In this study, we found that FasL and Caspase-3 were expressed in 34.51 % (39/113) and 50.44 % (57/113) of adjacent epithelial of gastric cancer respectively, most of which exhibited inflammation, regeneration, or intestinal metaplasia. Li *et al.*^[24] detected FasL expression in normal gastric mucosa and atrophic gastritis. It was previously documented that most cells from human organs showed positive immunoreactivity to Caspase-3, including cryptal cells of gastric pit. These data indicate that FasL and Caspase-3 play an important role in regulating the balance of cellular proliferation and apoptosis in gastric mucosa by inducing apoptosis.

Moreover, FasL is more frequently expressed in cancer cells of primary foci than in their adjacent epithelial cells ($P < 0.05$). Belluco *et al.*^[28] found that FasL was overexpressed in adenoma-adenocarcinoma of colorectum and FasL expression paralleled to malignant degrees. These results suggest that up-regulated expression of FasL contributes to gastric carcinogenesis. On the other hand, Caspase-3 expression was less frequently detected in cancer cells of the primary foci, than in the adjacent epithelial cells ($P < 0.05$), as described previously^[29]. Hoshi *et al.*^[30] also found the positive rate of Caspase-3 expression was lower in gastric cancers than in their adjacent mucosa and gastric adenoma, and was correlated negatively with proliferative index of Ki-67, as well as positively with apoptotic index labeled by TUNEL. These studies reveal that down-regulated expression of Caspase-3 is implicated in gastric carcinogenesis.

Additionally, our results also indicated that Caspase-3 expression in infiltrating lymphocytes was found in 70.80 % of gastric cancers, significantly more than in cancer cells and adjacent epithelial cells of their primary foci ($P < 0.05$). So most of primary gastric cancers showed strong expression of Caspase-3 in infiltrating lymphocytes, whereas weak or no expression of Caspase-3 in primary cancer cells. Interestingly, we found that FasL expression in primary cancer cells was closely correlated with Caspase-3 expression in infiltrating lymphocytes of the primary cancer ($P < 0.05$). Although FasL-positive gastric cancer expressed more Caspase-3 than FasL-negative one, the positive rates of Caspase-3 expression in FasL-positive and FasL-negative carcinomas were of no significant difference ($P > 0.05$). The more FasL was expressed in cancer cells, the more Caspase-3 was expressed in lymphocytes in the primary foci. Some investigators found that FasL-positive cancer showed increased apoptosis in its infiltrating lymphocytes and decreased apoptosis in cancer cells^[31]. Our study showed that more expression of Caspase-3 in infiltrating lymphocytes of gastric cancer demonstrated its critical contribution to Fas-mediated immune escape. However, FasL-positive gastric cancer also showed high expression of Caspase-3, suggesting there were other mechanisms that played an important role in Fas-Caspase apoptotic pathway of gastric cancer cells.

In our study, FasL expression in cancer cells of primary foci was not correlated with gender or age of patients with gastric cancer ($P > 0.05$), suggesting that FasL expression in

the primary cancer cells genetically did not depend on the gender or age of patients, and they therefore had no effect on relationship between FasL expression and patho-biological behaviors of gastric cancer. Our results showed that FasL expression in cancer cells of primary foci was closely associated with tumor size, invasive depth, metastasis, histological differentiation and Lauren's classification ($P < 0.05$), but not with growth pattern or TNM staging of gastric cancer ($P > 0.05$). Tsutsumi *et al*^[32] found serum content of soluble FasL (sFasL) was correlated with invasive depth, lymph node and distal metastasis. These indicate that FasL is implicated in progression of gastric cancer by forming immune counterattack. Although FasL expression in primary cancer cells was not significantly associated with growth pattern of gastric cancer, higher expression of FasL in mass-type than in nest-type or diffuse-type gastric cancer revealed that increased FasL expression in cancer cells responded to elevated infiltrating lymphocytes in gastric cancer with mass growth. Notably, FasL was expressed more in intestinal-type gastric cancers than in diffuse-type ones ($P < 0.05$), indicating that both types of gastric cancer have different histogenetic pathways. Furthermore, this study showed no relationship between down-regulated expression of Caspase-3 and clinicopathological features of gastric cancer described above ($P > 0.05$), suggesting that Caspase-3 expression is genetically independent of gender or age and is not implicated in progression.

FasL was significantly expressed in cancer cells of the primary foci than in corresponding metastatic foci ($P < 0.05$), while Caspase-3 was less expressed in cancer cells of primary foci than in corresponding metastatic foci of gastric cancer ($P < 0.05$), demonstrating that decreased ability of metastatic cancer cells to induce apoptosis of lymphocytes and increased apoptosis in metastatic cancer cells, might be influenced by tumor microenvironment. It was documented that metastases grew rapidly after the primary foci of tumor were removed, and a kind of substance from the primary foci could inhibit growth of metastases^[33]. If so, another reason for this phenomenon might be that primary foci regulate the expression of Caspase-3 and FasL of metastatic cancer cells so as to suppress their ability to proliferate.

In conclusion, up-regulation of FasL expression and down-regulation of Caspase-3 expression in cancer cells of primary carcinoma are involved in gastric carcinogenesis. As an effective marker to reveal the patho-biological behaviors, FasL contributes to differentiation, growth, invasion and metastasis of gastric cancer by inducing apoptosis of infiltrating lymphocytes. Chemical substances from primary foci and metastatic microenvironment can induce apoptosis of metastatic cancer cells or weaken ability of metastatic cancer cells to counterattack adjacent lymphocytes by decreasing FasL expression and increasing Caspase-3 expression of metastatic cancer cells, eventually resulting in the inhibition of their growth.

ACKNOWLEDGEMENT

We thank Mrs Zhao Yuhong and Mrs Huang Yaming for their contribution to the preparation of this manuscript.

REFERENCES

- Zhou YN**, Xu CP, Han B, Li M, Qiao L, Fang DC, Yang JM. Expression of E-cadherin and beta-catenin in gastric carcinoma and its correlation with the clinicopathological features and patient survival. *World J Gastroenterol* 2002; **8**: 987-993
- Fang DC**, Luo YH, Yang SM, Li XA, Ling XL, Fang L. Mutation analysis of APC gene in gastric cancer with microsatellite instability. *World J Gastroenterol* 2002; **8**: 787-791
- Song ZJ**, Gong P, Wu YE. Relationship between the expression of iNOS, VEGF, tumor angiogenesis and gastric cancer. *World J Gastroenterol* 2002; **8**: 591-595
- Yao XX**, Yin L, Sun ZC. The expression of hTERT mRNA and cellular immunity in gastric cancer and precancerosis. *World J Gastroenterol* 2002; **8**: 586-590
- Niu WX**, Qin XY, Liu H, Wang CP. Clinicopathological analysis of patients with gastric cancer in 1200 cases. *World J Gastroenterol* 2001; **7**: 281-284
- Xin Y**, Li XL, Wang YP, Zhang SM, Zheng HC, Wu DY, Zhang YC. Relationship between phenotypes of cell-function differentiation and pathobiological behavior of gastric carcinomas. *World J Gastroenterol* 2001; **7**: 53-59
- Jiang BJ**, Sun RX, Lin H, Gao YF. Study on the risk factors of lymphatic metastasis and the indications of less invasive operations in early gastric cancer. *World J Gastroenterol* 2000; **6**: 553-556
- Jemal A**, Thomas A, Murray T, Thun M. R. Cancer statistics, 2002. *CA Cancer J Clin* 2002; **52**: 23-47
- Theuer CP**. Asian gastric cancer patients at a southern California comprehensive cancer center are diagnosed with less advanced disease and have superior stage-stratified survival. *Am Surg* 2000; **66**: 821-826
- Schmidt PH**, Lee JR, Joshi V, Playford RJ, Poulsom R, Wright NA, Goldenring JR. Identification of a metaplastic cell lineage associated with human gastric adenocarcinoma. *Lab Invest* 1999; **79**: 639-646
- Bajtai A**, Hidvegi J. The role of gastric mucosal dysplasia in the development of gastric carcinoma. *Pathol Oncol Res* 1998; **4**: 297-300
- Sakata K**, Sakata A, Kong L, Dang H, Talal N. Role of Fas/FasL interaction in physiology and pathology: the good and the bad. *Clin Immunol Immunopathol* 1998; **87**: 1-7
- O'Connell J**, Bennett MW, O' Sullivan GC, Roche D, Kelly J, Collins JK, Shanahan F. Fas ligand expression in primary colon adenocarcinomas: evidence that the Fas counterattack is a prevalent mechanism of immune evasion in human colon cancer. *J Pathol* 1998; **186**: 240-246
- Mitsiades N**, Yu WH, Poulaki V, Tsokos M, Stamenkovic I. Matrix metalloproteinase-7-mediated cleavage of Fas ligand protects tumor cells from chemotherapeutic drug cytotoxicity. *Cancer Res* 2001; **61**: 577-581
- Wilson MR**. Apoptosis: unmasking the executioner. *Cell Death Differ* 1998; **5**: 646-652
- Slee EA**, Adrain C, Martin SJ. Serial killers: ordering caspase activation events in apoptosis. *Cell Death Differ* 1999; **6**: 1067-1074
- Porter AG**, Janicke RU. Emerging roles of caspase-3 in apoptosis. *Cell Death Differ* 1999; **6**: 99-104
- Shaham S**, Reddien PW, Davies B, Horvitz HR. Mutational analysis of the *Caenorhabditis elegans* cell-death gene *ced-3*. *Genetics* 1999; **153**: 1655-1671
- Tian R**, Zhang GY, Yan CH, Dai YR. Involvement of poly (ADP-ribose) polymerase and activation of caspase-3-like protease in heat shock-induced apoptosis in tobacco suspension cells. *FEBS Lett* 2000; **474**: 11-15
- Kutsyi MP**, Kuznetsova EA, Gaziev AI. Involvement of proteases in apoptosis. *Biochemistry (Mosc)* 1999; **64**: 115-126
- Truong-Tran AQ**, Carter J, Ruffin RE, Zalewski PD. The role of zinc in caspase activation and apoptotic cell death. *Biometals* 2001; **14**: 315-330
- Fujii Y**, Matura T, Kai M, Matsui H, Kawasaki H, Yamada K. Mitochondrial cytochrome c release and caspase-3-like protease activation during indomethacin-induced apoptosis in rat gastric mucosal cells. *Proc Soc Exp Biol Med* 2000; **224**: 102-108
- Umeda T**, Kouchi Z, Kawahara H, Tomioka S, Sasagawa N, Maeda T, Sorimachi H, Ishiura S, Suzuki K. Limited proteolysis of filamin is catalyzed by caspase-3 in U937 and Jurkat cells. *J Biochem (Tokyo)* 2001; **130**: 535-542
- Li H**, Liu N, Guo L, Li JW, Liu JR. Frequent expression of soluble Fas and Fas ligand in Chinese stomach cancer and its preneoplastic lesions. *Int J Mol Med* 2000; **5**: 473-476
- Chang HY**, Yang X. Proteases for cell suicide: functions and regulation of caspases. *Microbiol Mol Biol Rev* 2000; **64**: 821-846
- O'Connell J**, Bennett MW, Nally K, Houston A, O' Sullivan GC, Shanahan F. Altered mechanisms of apoptosis in colon cancer: Fas resistance and counterattack in the tumor-immune conflict. *Ann N Y Acad Sci* 2000; **910**: 178-192

- 27 **Izban KF**, Wrone-Smith T, Hsi ED, Schnitzer B, Quevedo ME, Alkan S. Characterization of the interleukin-1beta-converting enzyme/ced-3-family protease, caspase-3/ CPP32, in Hodgkin's disease: lack of caspase-3 expression in nodular lymphocyte predominance Hodgkin's disease. *Am J Pathol* 1999; **154**: 1439-1447
- 28 **Belluco C**, Esposito G, Bertorelle R, Alaggio R, Giacomelli L, Bianchi LC, Nitti D, Lise M. Fas ligand is up-regulated during the colorectal adenoma-carcinoma sequence. *Eur J Surg Oncol* 2002; **28**: 120-125
- 29 **Bennett MW**, O'Connell J, Houston A, Kelly J, O'Sullivan GC, Collins JK, Shanahan F. Fas ligand upregulation is an early event in colonic carcinogenesis. *J Clin Pathol* 2001; **54**: 598-604
- 30 **Hoshi T**, Sasano H, Kato K, Yabuki N, Ohara S, Konno R, Asaki S, Toyota T, Tateno H, Nagura H. Immunohistochemistry of Caspase3/ CPP32 in human stomach and its correlation with cell proliferation and apoptosis. *Anticancer Res* 1998; **18**: 4347-4353
- 31 **Bennett MW**, O'Connell J, O'Sullivan GC, Brady C, Roche D, Collins JK, Shanahan F. The Fas counterattack *in vivo*: apoptotic depletion of tumor-infiltrating lymphocytes associated with Fas ligand expression by human esophageal carcinoma. *J Immunol* 1998; **160**: 5669-5675
- 32 **Tsutsumi S**, Kuwano H, Shimura T, Morinaga N, Mochiki E, Asao T. Circulating soluble Fas ligand in patients with gastric carcinoma. *Cancer* 2000; **89**: 2560-2564
- 33 **Torosian MH**, Bartlett DL. Inhibition of tumor metastasis by a circulating suppressor factor. *J Surg Res* 1993; **55**: 74-79

Edited by Zhang JZ

Prognostic significance of expression of cyclooxygenase-2 and vascular endothelial growth factor in human gastric carcinoma

Hai Shi, Jian-Ming Xu, Nai-Zhong Hu, Hui-Jun Xie

Hai Shi, Jian-Ming Xu, Nai-Zhong Hu, Hui-Jun Xie, Department of Gastroenterology, the First Affiliated Hospital, Anhui Medical University, Hefei 23022, Anhui Province, China

Correspondence to: Dr. Hai Shi, Department of Gastroenterology, the First Affiliated Hospital, Anhui Medical University, Hefei 23022, Anhui Province, China. shmdah@hotmail.com

Telephone: +86-551-2922039

Received: 2002-12-28 **Accepted:** 2003-02-18

Abstract

AIM: To investigate the role of cyclooxygenase-2(COX-2) and vascular endothelial growth factor (VEGF) in the development of gastric carcinoma and correlation between expression of COX-2 and VEGF and clinicopathologic features in tissues from patients with gastric carcinoma.

METHODS: 281 patients with gastric carcinoma who underwent surgical resection between 1990 and 1999 at the First Affiliated Hospital, Anhui Medical University, PRC, were followed up. Expression of COX-2 and VEGF was investigated retrospectively in 232 gastric carcinoma tissues and 60 noncancerous specimens by using immunohistochemistry.

RESULTS: The 5-year survival rates of early gastric carcinoma (EGC) and advanced gastric carcinoma (AGC) were 93.4 % and 59.0 %, respectively. Survival time was highly correlated with lymph node metastasis, vascular invasion, depth of invasion and treatment with chemotherapy. Compared with paired noncancerous tissues, expression of COX-2 and VEGF and microvessel density (MVD) value in carcinoma tissue were significantly higher. The MVD value was much higher in COX-2-positive group and VEGF-positive group than that in COX-2-negative group and VEGF-negative group. Expression of COX-2 and VEGF, as well as MVD value were highly correlated with lymph node metastasis and vascular invasion. The 5-year survival rate of patients with expression of COX-2 or VEGF was significantly lower than that of patients without COX-2 or VEGF expression. Multivariate analysis revealed that VEGF overexpression, lymph node metastasis, COX-2 overexpression, depth of invasion and vascular invasion were all independent prognostic factors of gastric carcinoma.

CONCLUSION: Overexpression of COX-2 and VEGF in patients with gastric carcinoma can enhance the possibility of invasion and metastasis, implicating a poor prognosis. They may serve as the fairly good prognostic factors to indicate biologic behaviors of gastric carcinoma.

Shi H, Xu JM, Hu NZ, Xie HJ. Prognostic significance of expression of cyclooxygenase-2 and vascular endothelial growth factor in human gastric carcinoma. *World J Gastroenterol* 2003; 9(7):1421-1426

<http://www.wjgnet.com/1007-9327/9/1421.asp>

INTRODUCTION

Gastric carcinoma is one of the most common malignancies

worldwide. Carcinogenesis and progression of carcinoma are believed to be from multi-stage processes involving the activation of oncogenes and/or the loss of suppressor genes. Epidemiologic studies have shown that nonsteroidal anti-inflammatory drugs (NSAIDs) can reduce the incidence rate and mortality of digestive tract carcinomas, including esophageal, gastric, colon, and rectal lesions^[1,2]. The prostaglandin synthetic enzyme cyclooxygenase (COX) is a target for NSAIDs therapy, and a key enzyme in the conversion of arachidonic acid to prostaglandins. Recent studies have confirmed the presence of two forms of COX, constitutively produced COX-1 and inducible COX-2^[3]. COX-1 is a constitutively expressed gene in many tissues, and levels of this protein do not fluctuate in response to stimuli^[4]. COX-2 is induced by pathologic stimuli, such as inflammation, various growth factors, and cytokines produced by tumor cells^[5]. Human gastric mucosa, however, normally expresses barely detectable levels of COX-2 protein^[6]. To date, whether COX-2 is involved in the growth of gastric carcinoma remains to be clarified, although COX-2 overexpression has recently been reported in human gastric adenocarcinoma^[7].

Recently, many studies have reported on the relation between the malignant potential of neoplasms and tumor angiogenesis^[8-10]. Vascular endothelial growth factor (VEGF) is one of these angiogenic factors, and is known to play a crucial role in the formation of neovasculature^[11]. VEGF expression is correlated significantly with tumor vascularity and a marker for tumor angiogenesis^[12,13]. In the current study, we examined COX-2 and VEGF expression in primary gastric carcinoma tissues at various stages to investigate the relations between COX-2 and VEGF expression and clinicopathologic features of these tumors. We also investigated the prognostic value of these two biologic factors in gastric carcinoma and compared them with the conventional clinicopathologic factors.

MATERIALS AND METHODS

Clinical materials

Totally 281 patients with gastric carcinoma who received gastrectomy without preoperative chemotherapy between 1990 and 1999 at our university hospital were followed up. Among the 281 patients, there were 110 patients with early gastric carcinoma (EGC) in which carcinoma invasion was confined to the mucosa or submucosa and 171 patients with advanced gastric carcinoma (AGC) that invaded beyond the submucosal layer (but not to serosa in our study) according to the criteria of the Japanese Research Society for Gastric Cancer^[14]. The patients were comprised of 198 men and 83 women with an average age of 55.6 years (range, 22 to 80 years). Of these 281 patients, 66 had lymph node metastasis and 39 had vascular invasion. Patients who died of other disease were excluded from the study. 60 paired control samples (including 30 cases of chronic atrophic gastritis (CAG) and 30 cases of gastric epithelial dysplasia) were obtained from the antrum.

Immunohistochemical techniques

In brief, archival paraffin-embedded tissue specimens and controls were sectioned at a thickness of 4 μ m, deparaffinized,

and rehydrated. The slides were incubated with 3 % hydrogen peroxide in methanol for 10 minutes to block endogenous peroxidase activity, and then washed in phosphate-buffered saline (PBS) and incubated in 10 % normal rabbit serum for 5 minutes to reduce nonspecific antibody binding. Rabbit polyclonal antibody specific for human COX-2 (H-62; Santa Cruz Biotechnology, Inc. Santa Cruz, CA) was applied as the primary antibody at a dilution of 1:100. Mouse monoclonal antibody against VEGF (A-20, Santa Cruz Biotechnology, Inc. Santa Cruz, CA) or Factor VIII related antigen (PC-10, Maxim Biotech, Inc.) was also applied as the primary antibody. These slides were incubated with primary antibody for 60 minutes at room temperature, followed by 3 washes with PBS. Sections then were incubated with biotinylated IgG for 20 minutes followed by 3 washes. Slides then were treated with streptavidin-peroxidase reagent for 20 minutes and washed with PBS 3 times. Finally, slides were incubated in PBS containing diaminobenzidine and 1 % hydrogen peroxide for 5-10 minutes, counterstained with Mayer hematoxylin, and mounted. PBS was substituted for primary antibody as the negative control.

Staining analysis

COX-2 staining The expression of COX-2 was semiquantified. The degree of immunostaining for COX-2 was considered positive when unequivocal staining of the cytoplasm was observed in tumor cells^[7].

VEGF staining Immunoreactivity was graded as follows^[12]: Positive, unequivocal staining of the membrane or the cytoplasm was seen in more than 5 % of carcinoma cells, negative, no detectable expression or less than 5 % of tumor cells were stained.

Microvessel staining and counting Intratumoral microvessels were highlighted by immunostaining with anti-Factor VIII related antigen monoclonal antibody. Any single brownly-stained cell or cluster of endothelial cells that was clearly separated from adjacent microvessels, tumor cells, and other connective tissue elements were considered a vessel^[12]. Branching structures were counted as a single vessel unless there was a discontinuity in the structure. The stained sections were screened at $\times 100$ magnification under a light microscope to identify the 5 regions of the section with the highest vascular density. Vessels were counted in the 5 regions at $\times 200$ magnification, and the average numbers of microvessels were recorded^[12]. Two observers did the counting, and the mean value was used for the analysis.

Statistical analysis

Data were analyzed using the chi-square test for categorical variables and Student's *t* test for continuous variables. Five-year survival was compared using the Kaplan-Meier method and analyzed by the log rank test. Factors affecting survival were analyzed by Cox proportional hazards model using the SPSS statistic package Version 10.0. Differences with *P* values < 0.05 were considered statistically significant.

RESULTS

The detection rates of EGC between 1990 and 1999 fluctuated between 1.1 % and 6.6 %. The average detection rate was 4.3 % (110/2533). In patients with EGC, cardia gastric tumors more frequently occurred than corpus and antrum gastric carcinoma in 60-69 age group (50.0 % vs 28.9 %, 21.3 %, $P < 0.05$).

Five-year survival rate

The follow-up rates of EGC and AGC were 88.2 % (97/110) and 84.8 % (145/171), respectively. The overall disease-specific 5-year survival rates for patients with EGC and AGC

were 93.4 % and 59.0 %, respectively. The 5-year survival rates for patients with EGC with different tumor location were as follows: cardia, 90.9 %; corpus, 91.3 %; and antrum, 96.3 %. The 5-year survival rate for patients with EGC with different depth of invasion was 96.7 % for mucosa invasion and 90.3 % for submucosa invasion. The 5-year survival rates for patients with AGC with different tumor location were as follows: cardia, 45.0 %; corpus, 69.6 %; and antrum, 60.0 %.

Correlation between postoperative survival time and clinicopathologic factors

Table 1 shows the clinicopathologic data of 106 patients who survived for ≥ 5 years and 47 patients who died within 5 years. There were no differences with respect to gender, age, location of the tumor, or histology between patients with long and short survival time. But survival time was highly correlated with depth of invasion, lymph node metastasis, vascular invasion, and treatment with chemotherapy ($P < 0.05-0.01$).

Table 1 Correlation between clinicopathologic factors and survival time

Variables	Alive more than 5 years <i>n</i> =106	Died within 5 years <i>n</i> =47	<i>P</i> value
Gender			
Male	76(71.7)	33(70.2)	NS
Female	30(28.3)	14(29.8)	
Age(years)			
<60	28(26.4)	18(38.3)	NS
≥ 60	78(73.6)	29(61.7)	
Location of tumor			
Cardia	19(17.9)	11(23.4)	NS
Corpus	37(34.9)	17(31.9)	
Antrum	50(47.2)	21(44.7)	
Depth of invasion			
Mucosa or submucosa	57(53.8)	6(12.8)	< 0.01
Muscularis propria	49(46.2)	41(87.2)	
Histology			
Differentiated	41(38.7)	19(40.4)	NS
Undifferentiated	65(61.3)	28(59.6)	
Lymph node metastasis			
Present	21(19.8)	38(80.9)	< 0.01
Absent	85(80.2)	9(19.1)	
Vascular invasion			
Present	9(8.5)	26(55.3)	< 0.01
Absent	97(91.5)	21(44.7)	
Chemotherapy			
Yes	69(65.1)	20(42.6)	< 0.05
No	37(34.9)	27(57.4)	

Note: NS, not significant.

Immunohistochemical analysis

Correlation between expression of COX-2 and clinicopathologic factors Immunoreactivity for COX-2 protein was present in the cytoplasm of tumor cells, smooth muscle cells, and surrounding glands, but not in the surrounding stroma (Figure 1). Positive immunostaining for COX-2 was also seen in some CAG (23.3 %) and mucosal atypical hyperplasia (60.0 %) specimens (Figure 2). However, it was observed more frequently in tumor cells (Table 2), which showed that the expression of COX-2 was significantly higher in mucosal atypical hyperplasia than that in CAG ($P < 0.01$).

Compared with paired noncancerous specimens, COX-2 levels in carcinoma tissue were significantly higher ($P<0.05-0.01$). There was no significant association between COX-2 expression and gender, age, location of the tumor, or depth of invasion. However, significant difference was noted with respect to histologic type, lymph node metastasis, and vascular invasion. The COX-2-positive rate was significantly higher in patients with lymph node metastasis or vascular invasion than that in those without such metastasis or invasion ($P<0.05-0.01$). Similar results were obtained in relationship between the histologic type and the COX-2-positive rate ($P<0.01$, Table 2).

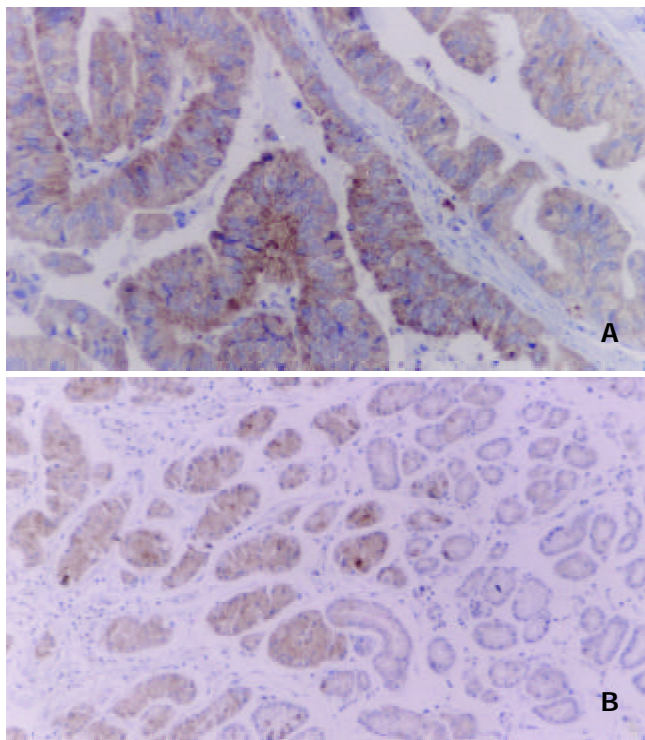


Figure 1 Immunohistochemical staining of COX-2 protein in gastric carcinoma. Immunoreactivity for COX-2 protein was present in the cytoplasm of tumor cells, smooth muscle cells (A, $\times 200$), and surrounding glands (B, $\times 100$).

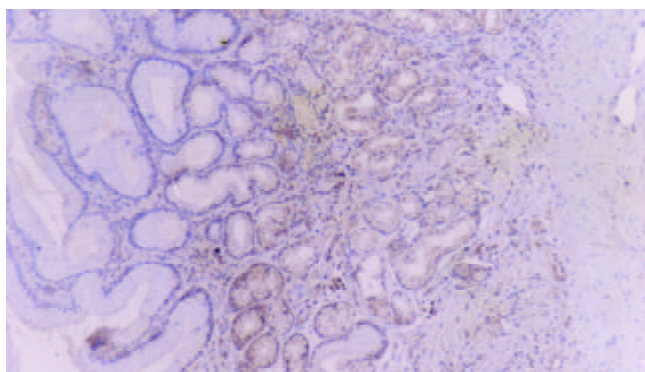


Figure 2 Positive immunostaining for COX-2 was observed in some CAG specimens ($\times 100$).

Correlations between expression of VEGF, microvessel counting and clinicopathologic factors VEGF was mainly localized in the cytoplasm or on the membrane of carcinoma cells (Figure 3). Tumor cells that were strongly immunopositive for VEGF were observed more often in the invasive front than that in the center of the tumors. Weakly positive VEGF staining was seen in some endothelial cells and noncancerous specimens. VEGF expression was detected in 122 (52.6 %)

tumors and significantly higher ($P<0.01$) than that in noncancerous specimens (13.3 %). Correlations between VEGF expression, MVD and different clinicopathologic variables are shown in Table 3. VEGF-positive rate and MVD value were significantly correlated with depth of invasion, lymph node metastasis, and invasion of blood vessels ($P<0.01$). There was no significant association among VEGF expression, MVD value and histologic type. The microvessel count in COX-2-positive or VEGF-positive tumors (28.76 ± 8.58 and 26.23 ± 8.47 , respectively) was significantly higher than that in COX-2-negative or VEGF-negative tumors (19.27 ± 8.36 and 18.91 ± 8.12 , respectively), $P<0.01$.

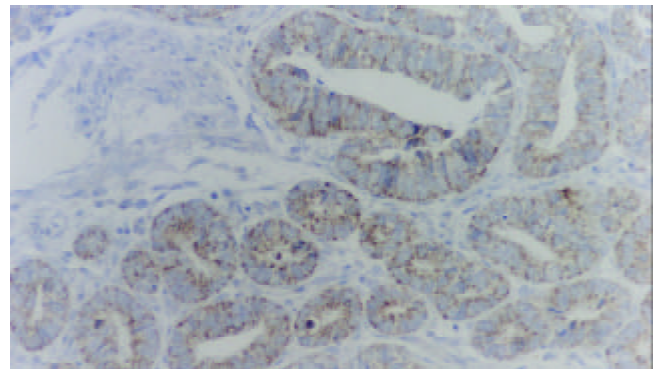


Figure 3 Immunohistochemical staining for VEGF in gastric carcinoma. VEGF was mainly localized on the membrane of the carcinoma cells or in the cytoplasm ($\times 200$).

Table 2 Correlation between COX-2 expression and clinicopathologic factors

Variables	n	COX-2 n(%)		P value
		Positive	Negative	
Gender				
Male	168	30(17.9)	138(82.1)	NS
Female	64	12(18.7)	52(81.3)	
Age(years)				
<60	145	25(17.2)	120(82.8)	NS
≥ 60	87	17(19.5)	70(80.5)	
Location of tumor				
Cardia	61	7(11.5)	54(88.5)	NS
Corpus	77	19(24.7)	58(75.3)	
Antrum	94	16(17.1)	78(82.9)	
Histology				
Differentiated	129	7(5.4)	122(94.6)	<0.01
Undifferentiated	103	35(33.9)	68(66.1)	
Lymph node metastasis				
Present	64	2(3.1)	62(96.9)	<0.01
Absent	168	40(23.8)	128(76.2)	
Vascular invasion				
Present	39	2(5.1)	37(94.9)	<0.05
Absent	193	40(20.7)	153(79.3)	
Depth of invasion				
Mucosa or submucosa	94	19(20.2)	75(79.8)	NS
Muscularis propria	138	23(16.7)	115(83.3)	
Noncancerous tissue				
CAG	30	23(76.7)	7(23.3)	<0.01
Atypical hyperplasia	30	12(40.0)	18(60.0)	

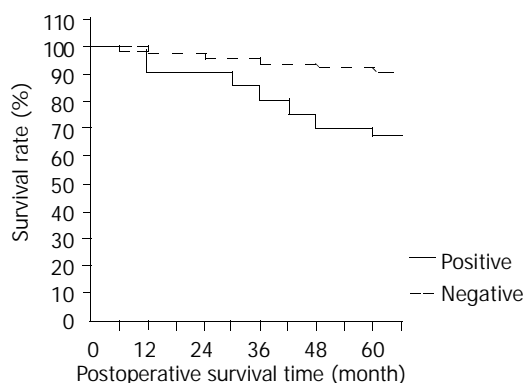
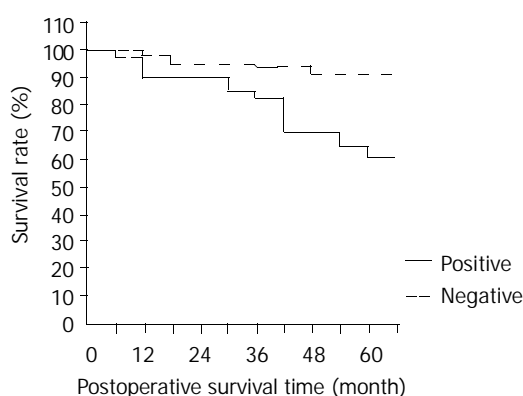
Notes: NS, not significant; CAG, chronic atrophic gastritis.

Table 3 Correlation between VEGF, MVD and clinicopathologic factors

Variables	n	VEGF n (%)		MVD	
		Positive	P value	$\bar{x}\pm s$	P value
Gender					
Male	168	88(52.4)	NS	22.11±9.14	NS
Female	64	34(53.1)		24.21±8.85	
Tumor size (cm)					
<5 cm	163	87(53.4)	NS	23.17±9.53	NS
≥5 cm	69	35(50.7)		23.69±8.26	
Depth of invasion					
Mucosa or submucosa	94	26(27.7)	<0.01	18.08±8.32	<0.01
Muscularis propria	138	96(69.6)		26.41±8.44	
Histology					
Differentiated	129	70(54.3)	NS	23.48±9.01	NS
Undifferentiated	103	52(50.5)		23.25±9.06	
Lymph node metastasis					
Present	64	47(73.4)	<0.01	28.52±4.39	<0.01
Absent	168	75(44.6)		19.73±8.47	
Vascular invasion					
Present	39	29(74.4)	<0.01	28.94±5.03	<0.01
Absent	193	93(48.2)		21.67±9.12	
Noncancerous tissue					
CAG	30	3(10.0)	NS	10.43±4.22	NS
Atypical hyperplasia	30	5(16.7)		11.56±6.17	

Notes: NS, not significant; CAG, chronic atrophic gastritis

Correlations between postoperative survival time and expression of COX-2 and VEGF COX-2 or VEGF positive rate was significantly higher in patients who died within 5 years (93.6 % and 78.7 %, respectively) than that in those survived ≥5 years (69.8 % and 49.1 %, respectively, $P<0.01$). Expression of COX-2 or VEGF was highly correlated with postoperative survival time. The 5-year survival rate was 67.9 % in patients with COX-2-positive tumors and 91.4 % in patients with COX-2-negative tumors. Accordingly, the prognosis for patients with a COX-2-negative tumor was significantly better than that for patients with a COX-2-positive tumor (Figure 4, $P<0.01$). The survival curves subdivided according to VEGF expression are shown in Figure 5. The 5-year survival rate was 61.2 % in patients with VEGF-positive tumors, which was significantly lower than the rate in those patients with VEGF-negative tumors (91.5 %, $P<0.01$).

**Figure 4** Kaplan-Meier survival curves of patients with gastric carcinoma with regard to COX-2 expression (positive and negative), $\chi^2=7.56$, $P<0.01$.**Figure 5** Kaplan-Meier survival curves of patients with gastric carcinoma with regard to VEGF expression (positive and negative), $\chi^2=16.51$, $P<0.01$.

Multivariate analysis

The effects of variables presumably associated with prognosis were studied by multivariate analysis using the Cox model. As a result, the depth of wall invasion, lymph node metastasis, vascular invasion, COX-2 expression, and VEGF expression emerged as independent prognostic factors (Table 4). Among these parameters, VEGF expression was the most important factor for predicting overall survival, followed by lymph node metastasis and COX-2 expression.

Table 4 Risk factors affecting survival determined by multivariate analysis using the Cox proportional hazards model

Variables	Regression coefficient	Standard error	Odds ratio (95% confidence interval)	P value
Histology (differentiated/undifferentiated)	0.564	0.337	1.758 (1.583-2.147)	NS
Depth of invasion (EGC/muscularis propria)	0.524	0.248	1.688 (1.638-1.714)	<0.05
Lymph node metastasis (present/absent)	0.796	0.1934	2.220 (1.518-3.239)	<0.01
Vascular invasion (present/absent)	0.413	0.213	2.003 (1.499-2.460)	<0.01
COX-2 expression (positive/negative)	0.776	0.194	2.173 (1.486-3.178)	<0.01
VEGF expression (positive/negative)	1.071	0.254	2.917 (1.774-4.796)	<0.01

Note: NS, not significant.

DISCUSSION

Recently, detection of gastric cancer at an early stage has been widely used in diagnostic procedures such radiography and endoscopy with targeted biopsy. In Japan, more than 50 % patients with gastric carcinoma were EGC^[15]. However, in U.S., the proportion of EGC was approximately 20 %^[16]. In the current study, our detection rate of EGC (4.3 %) was lower than that in above reports. This indicates the need to upgrade diagnostic efforts in the future. The incidence of adenocarcinoma of the gastric cardia has increased gradually in the West^[17]. In our study, carcinoma of the gastric cardia accounted for 16.4 % of EGC and 30.4 % of AGC. The absolute number and the rates of cardia carcinoma have been increasing significantly and this increase may be derived from advances in endoscopic techniques and equipment. Our data also showed that carcinoma of the gastric cardia more frequently occurred in 60-69 age group than distal gastric cancer. Thus, we should pay attention to those patients who are older than 60 years in

the diagnosis of early carcinoma of the gastric cardia during an endoscopic examination.

The prognosis for EGC is universally excellent. Almost all Western and Japanese authors reported 5-year survival rates were over 90 % for EGC if relative survival or deaths from gastric carcinoma alone were considered. The results of the current study indicate that prognosis of patients with AGC was poorer than that with EGC and that prognosis of patients with submucosa invasion was poorer than that with mucosa invasion. The survival of patients with tumors in the upper third of the stomach was significantly worse compared with that of patients with tumors in the middle third and lower third of the stomach^[16,18]. Our study disclosed that the 5-year survival rate of patients with tumors in the upper third of the stomach was lower than that of patients with tumors in the middle third and lower third of the stomach, especially in patients with AGC. However, there were no statistically significant differences among them (data not shown).

The depth of wall invasion, lymph node metastasis, and vascular invasion were reported to be the most important prognostic parameters in gastric carcinoma^[19]. The current study demonstrated that long or short survival time was highly correlated not only with depth of invasion, lymph node metastasis, and vascular invasion, but also with adjuvant chemotherapy. The results were in agreement with other reports.

However, preoperative diagnosis of the extent of wall invasion or the presence of lymph node metastasis and vascular invasion is difficult in some cases. Therefore, not only conventional clinicopathologic factors but also biologic factors should be examined for the prediction of clinical outcome. Recently, some studies^[20,21] found an increase in COX-2 protein levels in gastric carcinoma beyond the levels in paired normal gastric mucosa samples. The present study demonstrated that expression of COX-2 was significantly higher in mucosal atypical hyperplasia than that in CAG and that its expression was significantly higher in carcinoma tissue compared with noncancerous specimens. These indicate that COX-2 is involved in the growth of gastric carcinoma and that COX-2 promotes malignant transformation in human gastric carcinoma.

Recent studies have found that overexpression of COX-2 protein is associated significantly with lymph node metastasis^[22,23] and depth of invasion^[24,25] and that there is no correlation between the histologic types of gastric carcinoma and the expression of COX-2 protein^[24,26]. We found that COX-2 expression was associated with lymph node metastasis, vascular invasion, and the degree of tumor cell differentiation and did not connect to depth of invasion. The results suggest that COX-2 might enhance the metastatic potential as well as tumorigenicity and might be mainly involved in the progression of well-differentiated gastric carcinoma. The different conclusions of our study and above reports might have two explanations. First, differences in the methods employed (COX-2 mRNA level or protein immunoreactivity) and subjects may well influence the results of these studies. Second, there may have been discrepancies in the histologic type distribution among different areas.

Solid tumors need angiogenesis for growth and metastasis. Tumor angiogenesis may be regulated by angiogenic factors that are secreted by tumor cells, and VEGF is thought to be such a factor^[27,28]. VEGF is a selective mitogen for endothelial cells and may directly stimulate the growth of new blood vessels^[27]. Numerous studies have demonstrated that the expression of VEGF is a significant predictor of an increased risk of metastatic disease and overall survival by stimulating angiogenesis in gastric carcinoma^[9,28] and other carcinomas^[29]. In this study, we found that VEGF expression and microvessel count were significantly associated with lymph node metastasis, depth of invasion, and vascular invasion. The

finding that the microvessel count in VEGF-positive or COX-2-positive tumors was significantly higher than that in VEGF-negative or COX-2-negative tumors suggests that COX-2 as well as VEGF may facilitate tumor progression by promoting tumor angiogenesis^[9,30].

With regard to prognosis, many studies have shown that expression of VEGF is an independent prognostic indicator^[12,31]. However, there have been few studies on the association of COX-2 expression and the postoperative survival rate of patients with gastric carcinoma^[32]. The current study demonstrated that the 5-year survival rate in patients with COX-2-positive or VEGF-positive tumors was significantly lower than that in patients with COX-2-negative or VEGF-negative tumors. The results suggest that the presence of COX-2 or VEGF expression, as well as conventional clinicopathologic factors, are prognostic indicators in patients with gastric carcinoma. Multivariate analysis revealed five independent prognostic factors. Combination analysis of these pathologic and biologic features of gastric carcinoma will give aid to the improvement of the prognosis of some patients. If these assessments of COX-2 and VEGF expression are confirmed in long term follow-up of a larger group of patients, COX-2 and VEGF staining using endoscopically biopsied specimens prior to surgery could be used for the prediction of clinical outcome and in the preoperative selection of treatment for patients with gastric carcinoma. Accordingly, the inhibition of COX-2 activity may have an important therapeutic benefit in the control of gastric carcinoma^[33].

ACKNOWLEDGMENTS

We thank Drs. Li-Xing Zhu, Ji-Fong Wu, Hong-Fu Zhang and Xi-Yu Gong for their excellent technical support.

REFERENCES

- 1 **Thun MJ**, Namboodiri MM, Calle EE, Flanders WD, Health CW Jr. Aspirin use and risk of fatal cancer. *Cancer Res* 1993; **53**: 1322-1327
- 2 **Boolbol SK**, Dannenberg AJ, Cadburn A, Martucci C, Guo XJ, Ramovetti JT, Abreu-Goris M, Newmark HL, Lipkin ML, Decosse JJ, Bertagnolli MM. Cyclooxygenase-2 overexpression and tumor formation are blocked by sulindac in a murine model of familial adenomatous polyposis. *Cancer Res* 1996; **56**: 2556-2560
- 3 **Smith WL**, Garavito RM, DeWitt DL. Prostaglandin endoperoxide H synthases (cyclooxygenase) -1 and -2. *J Biol Chem* 1996; **271**: 33157-33160
- 4 **Vane J**. Towards a better aspirin. *Nature* 1994; **367**: 215-216
- 5 **Eberhart CE**, Dubois RN. Eicosanoids and the gastrointestinal tract. *Gastroenterology* 1995; **109**: 285-301
- 6 **Mizuno H**, Sakamoto C, Matsuda K, Wada K, Uchida T, Noguchi H, Akamatsu T, Kasuga M. Induction of cyclooxygenase-2 in gastric mucosal lesions and its inhibition by the specific antagonist delays healing in mice. *Gastroenterology* 1997; **112**: 387-397
- 7 **Ristimaki A**, Honkanen N, Jankala H, Sipponen P, Harkonen M. Expression of cyclooxygenase-2 in human gastric carcinoma. *Cancer Res* 1997; **57**: 1276-1280
- 8 **Weidner N**, Folkman J, Pozza F, Bevilacqua P, Allred EN, Moore DH, Meli S, Gasparini G. Tumor angiogenesis: a new significant and independent prognostic indicator in early-stage breast carcinoma. *J Natl Cancer Inst* 1992; **84**: 1875-1887
- 9 **Song ZJ**, Gong P, Wu YE. Relationship between the expression of iNOS, VEGF, tumor angiogenesis and gastric cancer. *World J Gastroenterol* 2002; **8**: 591-595
- 10 **Dvorak HF**, Brown LF, Detmar M, Dvorak AM. Vascular permeability factor/vascular endothelial growth factor, microvascular hyperpermeability, and angiogenesis. *Am J Pathol* 1995; **146**: 1029-1039
- 11 **Folkman J**. What is the evidence that tumors are angiogenesis dependent? *J Natl Cancer Inst* 1990; **82**: 4-6

- 12 **Maeda K**, Chung YS, Ogawa Y, Takatsuka S, Kang SM, Ogawa M, Sawada T, Sowa M. Prognostic value of vascular endothelial growth factor expression in gastric carcinoma. *Cancer* 1996; **77**:858-863
- 13 **Tao HQ**, Lin YZ, Wang RN. Significance of vascular endothelial growth factor messenger RNA expression in gastric cancer. *World J Gastroenterol* 1998; **4**: 10-13
- 14 **Japanese Research Society for Gastric Cancer**. Japanese classification of gastric carcinoma. First English edition. Tokyo: Kanehara & Co., Ltd., 1993
- 15 **Maehara Y**, Kakeji Y, Oda S, Takahashi I, Akazawa K, Sugimachi K. Time trends of surgical treatment and the prognosis for Japanese patients with gastric cancer. *Br J Cancer* 2000; **83**: 986-991
- 16 **Noguchi Y**, Yoshikawa T, Tsuburaya A, Motohashi H, Karpeh MS, Brennan MF. Is gastric carcinoma different between Japan and the United States? *Cancer* 2000; **89**: 2237-2246
- 17 **Ekstrom AM**, Signorello LB, Hansson LE, Bergstrom R, Lindgren A, Nyren O. Evaluating gastric cancer misclassification: a potential explanation for the rise in cardia cancer incidence. *J Natl Cancer Inst* 1999; **91**: 786-790
- 18 **Okabayashi T**, Gotoda T, Kondo H, Inui T, Ono H, Saito D, Yoshida S, Sasako M, Shimoda T. Early carcinoma of the gastric cardia in Japan: Is it different from that in the West? *Cancer* 2000; **89**: 2555-2559
- 19 **Adachi Y**, Yasuda K, Inomata M, Sato K, Shiraishi N, Kitano S. Pathology and prognosis of gastric carcinoma: well versus poorly differentiated type. *Cancer* 2000; **89**: 1418-1424
- 20 **Uefuji K**, Ichikura T, Mochizuki H, Shinomiya N. Expression of cyclooxygenase 2 protein in gastric adenocarcinoma. *J Surg Oncol* 1998; **69**: 168-172
- 21 **Guo XL**, Wang LE, Du SY, Fan CL, Li L, Wang P, Yuan Y. Association of cyclooxygenase-2 expression with HP-cagA infection in gastric cancer. *World J Gastroenterol* 2003; **9**: 246-249
- 22 **Murata H**, Kawano S, Tsuji S, Tsujii M, Sawaoka H, Kimura Y, Shiozaki H, Hori M. Cyclooxygenase, 2 overexpression enhances lymphatic invasion and metastasis in human gastric carcinoma. *Am J Gastroenterol* 1999; **94**: 451-455
- 23 **Xue YW**, Zhang QF, Zhu ZB, Wang Q, Fu SB. Expression of cyclooxygenase-2 and clinicopathologic features in human gastric adenocarcinoma. *World J Gastroenterol* 2003; **9**: 250-253
- 24 **Ohno R**, Yoshinaga K, Fujita T, Hasegawa K, Iseki H, Tasunozaki H, Ichikawa W, Nihei Z, Sugihara K. Depth of invasion parallels increased cyclooxygenase-2 levels in patients with gastric carcinoma. *Cancer* 2001; **91**: 1876-1881
- 25 **Gao HJ**, Yu LZ, Sun L, Miao K, Bai JF, Zhang XY, Lu XZ, Zhao ZQ. Expression of cyclooxygenase-2 oncogene proteins in gastric cancer and paracancerous tissues. *Shijie Huaren Xiaohua Zazhi* 2000; **8**: 578-579
- 26 **Yamamoto H**, Itoh F, Fukushima H, Hinoda Y, Imai K. Overexpression of cyclooxygenase-2 protein is less frequent in gastric cancers with microsatellite instability. *Int J Cancer* 1999; **84**: 400-403
- 27 **Leung DW**, Cachianes G, Kuang WJ, Goedel DV, Ferrara N. Vascular endothelial growth factor is a secreted angiogenic mitogen. *Science* 1989; **246**: 1306-1309
- 28 **Liu DH**, Zhang XY, Fan DM, Huang YX, Zhang JS, Huang WQ, Zhang YQ, Huang QS, Ma WY, Chai YB, Jin M. Expression of vascular endothelial growth factor and its role in oncogenesis of human gastric carcinoma. *World J Gastroenterol* 2001; **7**: 500-505
- 29 **Fontanini G**, Vignati S, Boldrini L, Chine S, Silvestri V, Lucchi M, Mussi A, Angeletti CA, Bevilacqua G. Vascular endothelial growth factor is associated with neovascularization and influences progression of non-small cell lung carcinoma. *Clin Cancer Res* 1997; **3**: 861-865
- 30 **Fosslien E**. Molecular pathology of cyclooxygenase-2 in cancer-induced angiogenesis. *Ann Clin Lab Sci* 2001; **31**: 325-348
- 31 **Maeda K**, Kang SM, Onoda N, Ogawa M, Kato Y, Sawada T, Chung KH. Vascular endothelial growth factor expression in preoperative biopsy specimens correlate with disease recurrence in patients with early gastric carcinoma. *Cancer* 1999; **86**: 566-571
- 32 **Chen CN**, Sung CT, Lin MT, Lee PH, Chang KJ. Clinicopathologic association of cyclooxygenase 1 and cyclooxygenase 2 expression in gastric adenocarcinoma. *Ann Surg* 2001; **233**: 183-188
- 33 **Fosslien E**. Biochemistry of cyclooxygenase (COX)-2 inhibitors and molecular pathology of COX-2 in neoplasia. *Crit Rev Clin Lab Sci* 2000; **37**: 431-502

Edited by Xu XQ

Preventive effect of hydrotalcite on gastric mucosal injury in rats induced by taurocholate

Bao-Ping Yu, Jun Sun, Mu-Qi Li, He-Sheng Luo, Jie-Ping Yu

Bao-Ping Yu, Jun Sun, Mu-Qi Li, He-Sheng Luo, Jie-Ping Yu,
Department of Gastroenterology, Renmin Hospital of Wuhan University, Wuhan 430060, Hubei Province, China

Correspondence to: Professor Bao-Ping Yu, Department of Gastroenterology, Renmin Hospital of Wuhan University, Wuhan 430060, Hubei Province, China. yubaoping62@yahoo.com.cn

Telephone: +86-27-88041911-2135

Received: 2002-05-13 **Accepted:** 2002-06-12

Abstract

AIM: To study the preventive effect of hydrotalcite on gastric mucosal injury in rat induced by taurocholate, and to investigate the relationship between the protective mechanism of hydrotalcite and the expression of trefoil factor family 2 (TFF2) mRNA and c-fos protein.

METHODS: Forty five male Wistar rats were randomly divided into hydrotalcite group, ranitidine group and control group. Gastric mucosal injury was induced by introgastric acidified taurocholate. OD value of TFF2 mRNA expression in gastric mucous cells was determined by hybridization and computer image analysis system. OD value of c-fos protein expression in gastric mucous cells was measured by immunohistochemistry and computer image analysis system.

RESULTS: The gross mucosal injury index in hydrotalcite group was significantly lower than that in ranitidine group and control group (8.60 ± 2.20 vs 16.32 ± 4.27 , 29.53 ± 5.39 ; $P < 0.05$, $P < 0.01$). The expression level of TFF2 mRNA in hydrotalcite group was markedly higher than that in ranitidine group and control group (0.56 ± 0.09 vs 0.30 ± 0.05 , 0.28 ± 0.03 , $P < 0.05$). The OD value of c-fos protein in hydrotalcite group was higher than that in ranitidine group and control group (0.52 ± 0.07 vs 0.31 ± 0.04 , 0.32 ± 0.05 , $P < 0.05$).

CONCLUSION: Hydrotalcite can protect gastric mucosal injury in rats induced by taurocholate, which may be related to the increased expression of TFF2 and c-fos protein.

Yu BP, Sun J, Li MQ, Luo HS, Yu JP. Preventive effect of hydrotalcite on gastric mucosal injury in rats induced by taurocholate. *World J Gastroenterol* 2003; 9(7): 1427-1430 <http://www.wjgnet.com/1007-9327/9/1427.asp>

INTRODUCTION

Hydrotalcite is one kind of protective agents for gastric mucosal^[1,2], it neutralizes the gastric acid^[29], stimulates the synthesis of prostaglandin and the release of epidermal growth factor^[3] from gastric mucosa^[4]. Because hydrotalcite binds to cholic acid in the stomach^[5,6], it is effective on bile reflux gastritis. Trefoil factor family 2 (TFF2)^[7-9] is one of the members in the trefoil peptide factor family^[10-13] mainly produced by mucus-secreting cells in the gastrointestinal tract^[1,14,15]. It

involves restitution of epithelial lining after epithelial cell injury^[16,17], mucosal defense^[18,19] and healing of ulcer^[20-23]. c-fos gene^[24,25] is one of the earlier expressed genes after gastric mucosa injury. c-fos protein relates to mucosal repair after mucosal injury^[26]. In the present study, we aimed to study the preventive effect of hydrotalcite on gastric mucosal injury in rat induced by taurocholate and the relationship between the protective mechanism of hydrotalcite and the expression of TFF2 mRNA and c-fos protein.

MATERIALS AND METHODS

Methods

Animals model Forty-five adult male Wistar rats weighing 200-250 g were divided into three groups randomly: hydrotalcite group, ranitidine group and control group, 15 rats in each group. The animals were housed at the Experimental Animal Center of Wuhan University. Taurocholate was dissolved in normal saline and HCl was added to a final concentration of 0.2 mol/L with pH value of 1.4^[27]. The rats in hydrotalcite group were given 100 mg/kg hydrotalcite. The rats in control group were given 1.5 ml normal saline at the same time. The rats in ranitidine group were given 30 mg/kg ranitidine twice 12 hrs the day before. After one hour of hydrotalcite administration, gastric mucosal damage in three groups was induced by introgastric administration of 1.5 ml taurocholate^[1] at 15 mmol/L. Two hours later, the animals were killed by cervical dislocation. The abdomen was opened, and the stomach was removed and incised along the greater curvature. The mucosal surface was gently washed with normal saline. Gastric lesions were scored by a previously described scoring system^[28] as follows: one point, point erosion; two point, <1 mm of erosion; three point, 1-2 mm of erosion; four point, 3-4 mm of erosion; five point, >4 mm of erosion. The mucosa injury index was calculated on the totally accumulated points. After scored, the mucosa was obtained and prepared for histological examination and other tests.

TFF2 mRNA *in situ* hybridization Gastric mucosa tissue immersion-fixed in neutral buffered formaldehyde was dehydrated, oriented in cross section and embedded in wax. Four micrometer sections were cut, dewaxed, and rehydrated to PBS. Sections were permeabilized with proteinase K, postfixed in 4 % paraformaldehyde in PBS, and acetylated with acetic anhydride in 0.1 mol/L triethanolamine. The tissues were then dehydrated for hybridization. Hybridization was performed according to the instructions of text kit (Sigma Co). Oligo-nucleotide probe sequence was 5' - GTAGTGACAAATCTTCCACAGA. The optic density (OD) value of the hybridization signals was assessed by image analysis system.

Immunohistochemistry of c-fos protein Sections of gastric mucosa tissues were incubated with monoclonal antibody against human c-fos protein for four hours at 37 °C. Immunostaining of c-fos protein was revealed using a commercially available peroxidase-based method (SP vectastain, Zhongshan Co.) according to the instructions of the manufacturer. The optic density of immunosignals was determined by image analysis system.

RESULTS

Gross inspection showed that there were obvious hyperemia, edema, sheet or strip of necrosis and spot hemorrhage in the gastric mucosa of control groups. There were milder lesions after hydrotalcite pretreatment, and microscopic examination confirmed marked protection against taurocholate-induced gastric injury. The degree of lesion in ranitidine group fell in-between the two groups. The gastric mucosa injury index was 8.60 ± 2.20 , 16.32 ± 4.27 , 29.53 ± 5.39 in hydrotalcite, ranitidine and control groups, respectively. The gastric mucosa index in hydrotalcite group was significantly lower than that in ranitidine group ($P < 0.05$) and control group ($P < 0.01$).

In all three groups TFF2 mRNA was expressed in the atrium of stomach as revealed by *in situ* hybridization. TFF2 mRNA was mainly confined in gastric epithelial cells and gastric gland mucous neck cells, especially in the margin of the injury region (Figure 1-2).

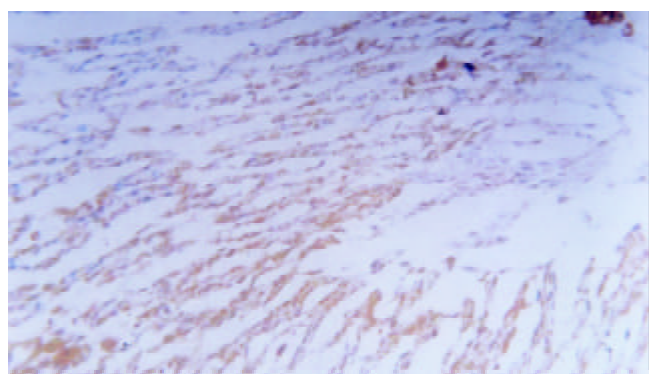


Figure 1 TFF2 mRNA in situ hybridization in hydrotalcite group Positive cells were stained brown-yellow $\times 200$.

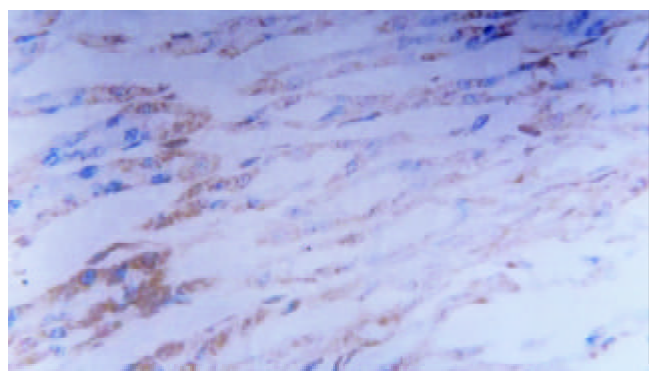


Figure 2 TFF2 mRNA in situ hybridization in hydrotalcite group Positive cells were stained brown-yellow $\times 400$.

Immunocytochemistry showed that c-fos protein localized in nuclei of positively stained cells, which were mainly gastric gland mucous neck cells (Figure 3-4). The OD values of TFF2 mRNA and c-fos protein in the three groups are shown in Table 1.

Table 1 OD values of TFF2 mRNA staining and c-fos protein staining

Group	Animal number	TFF2 mRNA	c-fos protein
Hydrotalcite	15	0.56 ± 0.09^a	0.52 ± 0.07^a
Ranitidine	15	0.30 ± 0.05^b	0.31 ± 0.04^b
Control	15	0.28 ± 0.03	0.32 ± 0.05

^a $P < 0.05$ vs control, ^b $P > 0.05$ vs control.

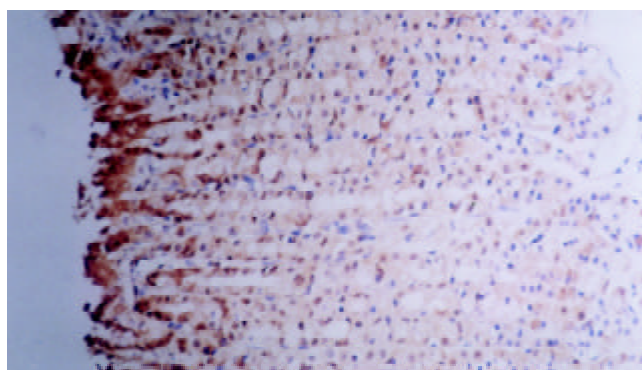


Figure 3 c-fos protein Immunostaining in hydrotalcite group Nuclei of positive cells were stained brown-yellow $\times 200$.

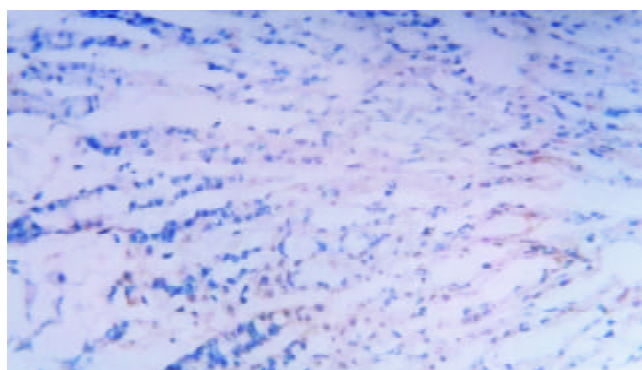


Figure 4 c-fos protein Immunostaining in ranitidine group Nuclei of positive cells were stained buff $\times 200$.

DISCUSSION

Hydrotalcite is a complex comprised of aluminum hydroxide, magnesium hydroxide, carbonate and H_2O , which neutralizes gastric acid^[29], binds pepsin^[30,31] and cholic acid^[5,31], etc. Our study showed that hydrotalcite could markedly protect gastric mucosa against taurocholate-induced lesions. The mucosal injury index in hydrotalcite group was significantly lower than that in ranitidine and control groups. Cholic acid has been thought to elicit gastric injury by degrading the difference of potential in gastric mucosa, increasing inversed diffusion of acid, and stimulating mast cell to release histamine. Recent researches indicated that transforming growth factor was related to the recovery of gastric mucosal injury induced by taurocholate^[27,32,33]. Hydrotalcite has been shown to enhance the synthesis and release of prostaglandin and to increase the amount of epidermal growth factor in mucosal blood^[4].

The mechanism of the protective and healing effect of TFF2 on gastric mucosa is still not fully elucidated. *In vitro* studies, TFF2 was shown to stimulate cell migration^[34]. Recently hTFF was shown to decrease proton permeation through interacting with mucus in both *in vivo* and *in vitro* studies^[35]. Orally-administrated TFF2 was found to bind to the mucus layer of the stomach^[36,37], which accelerates the healing of gastric ulcer in the rat^[38-41]. In this study, we have shown that hydrotalcite reduces gastric injury induced by taurocholate in rats, and it also increases expression of TFF2 mRNA in margin of the injury region, suggesting that the protective effect of hydrotalcite on gastric mucosa is related to the increase of TFF2 expression. The reason why hydrotalcite increases expression of TFF2 is not yet fully understood. Previous studies indicate that TFF expression and secretion are regulated by neuropeptides and acetylcholine^[42], and hydrotalcite increases the amount of epidermal growth factor in gastric mucosa^[4]. It is presumed

that hydrotalcite regulates TFF2 mRNA expression through the increase of epidermal growth factor.

C-fos gene is one of the immediate early genes which are involved in the control of cell proliferation in a variety of cell types^[43-46]. Change of c-fos mRNA expression is found as early as two hours in the healing of gastric mucosal stress ulcer^[26,47]. In this study, the expression of c-fos protein was found two hours later in gastric mucosal damage induced by taurocholate. The amount of c-fos protein in hydrotalcite was higher than that in ranitidine and control groups, suggesting that c-fos protein participates in the mechanism of the protective effect of hydrotalcite in gastric mucosa. It has been shown that EGF^[48,49] stimulates the proliferation^[50] of cells derived from gastric fundus and induces the expression of c-fos and c-myc, and hydrotalcite increases the amount of epidermal growth factor in gastric mucosa. It may be presumed that hydrotalcite increases c-fos protein through the increase of the amount of epidermal growth factor in gastric mucosa.

REFERENCES

- Rankin BJ**, Zhu H, Webb M, Roberts NB. The development and in-vitro evaluation of novel mixed metal hydroxy-carbonate compounds as phosphate binders. *J Pharm Pharmacol* 2001; **53**: 361-369
- Holtermuller KH**, Liszky M, Bernard I, Haese W. [Therapy of stomach ulcer-a comparison between the low dosage antacid hydrotalcite and ranitidine-results of a randomized multicenter double-blind study. Talcivent Study Group]. *Z Gastroenterol* 1992; **30**: 717-721
- Lambrecht N**, Trautmann M, Korolkiewicz R, Liszky M, Peskar BM. Role of eicosanoids, nitric oxide, and afferent neurons in antacid induced protection in the rat stomach. *Gut* 1993; **34**: 329-337
- Schmassmann A**, Tarnawski A, Gerber HA, Flogerzi B, Sanner M, Varga L, Halter F. Antacid provides better restoration of glandular structures within the gastric ulcer scar than omeprazole. *Gut* 1994; **35**: 896-904
- Tarnawski AS**, Tomikawa M, Ohta M, Sarfeh IJ. Antacid talcid activates in gastric mucosa genes encoding for EGF and its receptor. The molecular basis for its ulcer healing action. *J Physiol Paris* 2000; **94**: 93-98
- Dreyer M**, Marwinski D, Wolf N, Dammann HG. [Acidity profile in humans after multiple oral administration of hydrotalcite]. *Arzneimittel Forschung* 1991; **41**: 738-741
- Vatier J**, Ramdani A, Vitre MT, Mignon M. Antacid activity of calcium carbonate and hydrotalcite tablets. Comparison between in vitro evaluation using the "artificial stomach-duodenum" model and in vivo pH-metry in healthy volunteers. *Arzneimittel Forschung* 1994; **44**: 514-518
- Simoneau G**. Absence of rebound effect with calcium carbonate. *Eur J Drug Metab Pharmacokinet* 1996; **21**: 351-357
- Watters KJ**, Murphy GM, Tomkin GH, Ashford JJ. An evaluation of the bile acid binding and antacid properties of hydrotalcite in hiatus hernia and peptic ulceration. *Curr Med Res Opin* 1979; **6**: 85-87
- Mendelsohn D**, Mendelsohn L. Hydrogen ion, pepsin and bile acid binding properties of hydrotalcite. *S Afr Med J* 1975; **49**: 1011-1014
- Poulsom R**. Trefoil peptides. *Baillieres Clin Gastroenterol* 1996; **10**: 113-134
- Podolsky DK**. Mechanisms of regulatory peptide action in the gastrointestinal tract: trefoil peptides. *J Gastroenterol* 2000; **35** (Suppl 12): 69-74
- Taupin D**, Wu DC, Jeon WK, Devaney K, Wang TC, Podolsky DK. The trefoil gene family are coordinately expressed immediate-early genes: EGF receptor- and MAP kinase-dependent interregulation. *J Clin Invest* 1999; **103**: R31-R38
- Dignass A**, Lynch-Devaney K, Kindon H, Thim L, Podolsky DK. Trefoil peptides promote epithelial migration through a transforming growth factor beta-independent pathway. *J Clin Invest* 1994; **94**: 376-383
- Al-azzeah ED**, Fegert P, Blin N, Gott P. Transcription factor GATA-6 activates expression of gastroprotective trefoil genes TFF1 and TFF2. *Biochim Biophys Acta* 2000; **1490**: 324-332
- Sommer P**, Blin N, Gott P. Tracing the evolutionary origin of the TFF-domain, an ancient motif at mucous surfaces. *Gene* 1999; **236**: 133-136
- McKenzie C**, Thim L, Parsons ME. Topical and intravenous administration of trefoil factors protect the gastric mucosa from ethanol-induced injury in the rat. *Aliment Pharmacol Ther* 2000; **14**: 1033-1040
- Farrell JJ**, Taupin D, Koh TJ, Chen D, Zhao CM, Podolsky DK, Wang TC. TFF2/SP-deficient mice show decreased gastric proliferation, increased acid secretion, and increased susceptibility to NSAID injury. *J Clin Invest* 2002; **109**: 193-204
- Tran CP**, Cook GA, Yeomans ND, Thim L, Giraud AS. Trefoil peptide TFF2 (spasmolytic polypeptide) potently accelerates healing and reduces inflammation in a rat model of colitis. *Gut* 1999; **44**: 636-642
- Taupin D**, Pedersen J, Familiari M, Cook G, Yeomans N, Giraud AS. Augmented intestinal trefoil factor (TFF3) and loss of pS2 (TFF1) expression precedes metaplastic differentiation of gastric epithelium. *Lab Invest* 2001; **81**: 397-408
- Kawanaka H**, Tomikawa M, Baatar D, Jones MK, Pai R, Szabo IL, Sugimachi K, Sarfeh IJ, Tarnawski AS. Despite activation of EGF-receptor-ERK signaling pathway, epithelial proliferation is impaired in portal hypertensive gastric mucosa: relevance of MKP-1, c-fos, c-myc, and cyclin D1 expression. *Life Sci* 2001; **69**: 3019-3033
- Fu X**, Gu X, Sun T. [mRNA and protein expression of three growth-related factors and their possible signal transduction pathways in wound healing] *Zhonghua Waike Zazhi* 2001; **39**: 714-717
- Schuligoj R**, Herzeg G, Wachter C, Jovic M, Holzer P. Differential expression of c-fos messenger RNA in the rat spinal cord after mucosal and serosal irritation of the stomach. *Neuroscience* 1996; **72**: 535-544
- Polk WH Jr**, Dempsey PJ, Russell WE, Brown PI, Beauchamp RD, Barnard JA, Coffey RJ Jr. Increased production of transforming growth factor alpha following acute gastric injury. *Gastroenterology* 1992; **102**: 1467-1474
- Lanza FL**, Royer GL Jr, Nelson RS. Endoscopic evaluation of the effects of aspirin, buffered aspirin, and enteric-coated aspirin on gastric and duodenal mucosa. *N Engl J Med* 1980; **303**: 136-138
- Vatier J**, Vitre MT, Lionnet F, Poitevin C, Mignon M. Assessment of antacid characteristics of drugs containing a combination of aluminium and magnesium salts using the "artificial stomach" model. *Arzneimittel Forschung* 1990; **40**: 42-48
- Kokot ZJ**. Effect of pepsin on the kinetics of HCl neutralization by dihydroxyaluminum sodium carbonate, hydrotalcite and dihydroxyaluminum aminoacetate. *Acta Pol Pharm* 1991; **48**: 27-31
- Murphy MS**. Growth factors and the gastrointestinal tract. *Nutrition* 1998; **14**: 771-774
- Jones MK**, Tomikawa M, Mohajer B, Tarnawski AS. Gastrointestinal mucosal regeneration: role of growth factors. *Front Biosci* 1999; **4**: D303-D309
- Hahn KB**, Lee KM, Kim YB, Hong WS, Lee WH, Han SU, Kim MW, Ahn BO, Oh TY, Lee MH, Green J, Kim SJ. Conditional loss of TGF-beta signalling leads to increased susceptibility to gastrointestinal carcinogenesis in mice. *Aliment Pharmacol Ther* 2002; **16**(Suppl 2): 115-127
- Fukuda M**, Ikuta K, Yanagihara K, Tajima M, Kuratsune H, Kurata T, Sairenji T. Effect of transforming growth factor-beta1 on the cell growth and Epstein-Barr virus reactivation in EBV-infected epithelial cell lines. *Virology* 2001; **288**: 109-118
- Kanai M**, Konda Y, Nakajima T, Izumi Y, Takeuchi T, Chiba T. TGF-alpha inhibits apoptosis of murine gastric pit cells through an NF-kappaB-dependent pathway. *Gastroenterology* 2001; **121**: 56-67
- Ebert MP**, Yu J, Miehlke S, Fei G, Lendeckel U, Ridwelski K, Stolte M, Bayerdorffer E, Malfertheiner P. Expression of transforming growth factor beta-1 in gastric cancer and in the gastric mucosa of first-degree relatives of patients with gastric cancer. *Br J Cancer* 2000; **82**: 1795-1800
- Kang B**, Alderman BM, Nicoll AJ, Cook GA, Giraud AS. Effect of omeprazole-induced achlorhydria on trefoil peptide expression in the rat stomach. *J Gastroenterol Hepatol* 2001; **16**: 1222-1227

- 35 **Dignass A**, Lynch-Devaney K, Kindon H, Thim L, Podolsky DK. Trefoil peptides promote epithelial migration through a transforming growth factor beta-independent pathway. *J Clin Invest* 1994; **94**: 376-383
- 36 **Playford RJ**, Marchbank T, Chinery R, Evison R, Pignatelli M, Boulton RA, Thim L, Hanby AM. Human spasmodic polypeptide is a cytoprotective agent that stimulates cell migration. *Gastroenterology* 1995; **108**: 108-116
- 37 **Kato K**, Chen MC, Nguyen M, Lehmann FS, Podolsky DK, Soll AH. Effects of growth factors and trefoil peptides on migration and replication in primary oxyntic cultures. *Am J Physiol* 1999; **276**: G1105-G1116
- 38 **Goke MN**, Cook JR, Kunert KS, Fini ME, Gipson IK, Podolsky DK. Trefoil peptides promote restitution of wounded corneal epithelial cells. *Exp Cell Res* 2001; **264**: 337-344
- 39 **Langer G**, Walter S, Behrens-Baumann W, Hoffmann W. [TFF peptides. New mucus-associated secretory products of the conjunctiva]. *Ophthalmologie* 2001; **98**: 976-979
- 40 **Wright NA**. Aspects of the biology of regeneration and repair in the human gastrointestinal tract. *Philos Trans R Soc Lond B Biol Sci* 1998; **353**: 925-933
- 41 **Poulsen SS**, Thulesen J, Christensen L, Nexø E, Thim L. Metabolism of oral trefoil factor 2 (TFF2) and the effect of oral and parenteral TFF2 on gastric and duodenal ulcer healing in the rat. *Gut* 1999; **45**: 516-522
- 42 **Ogata H**, Podolsky DK. Trefoil peptide expression and secretion is regulated by neuropeptides and acetylcholine. *Am J Physiol* 1997; **273**: G348-354
- 43 **Chen L**, Tong A, Yu D. [Effects of fluoride on the expression of c-fos and c-jun genes and cell proliferation of rat osteoblasts] *Zhonghua Yufang Yixue Zazhi* 2000; **34**: 327-329
- 44 **Di Toro R**, Campana G, Murari G, Spampinato S. Effects of specific bile acids on c-fos messenger RNA levels in human colon carcinoma Caco-2 cells. *Eur J Pharm Sci* 2000; **11**: 291-298
- 45 **Osaki M**, Tsukazaki T, Yonekura A, Miyazaki Y, Iwasaki K, Shindo H, Yamashita S. Regulation of c-fos gene induction and mitogenic effect of transforming growth factor-beta1 in rat articular chondrocyte. *Endocr J* 1999; **46**: 253-261
- 46 **Li G**, Wu D, Xiao B, Li J. Effect of lead on the expression of immediate early genes in different regions of rat brain. *Weisheng Yanjiu* 1999; **28**: 65-69
- 47 **Fu X**, Jiang L, Sun T. The significance and characteristics of the gene expressions of c-fos and c-jun in hypertrophic scar and chronic ulcer tissues] *Zhonghua Shaoshang Zazhi* 2000; **16**: 300-302
- 48 **Tarnawski AS**, Pai R, Wang H, Tomikawa M. Translocation of MAP (Erk-1 and -2) kinases to cell nuclei and activation of c-fos gene during healing of experimental gastric ulcers. *J Physiol Pharmacol* 1998; **49**: 479-488
- 49 **Yanaka A**, Suzuki H, Shibahara T, Matsui H, Nakahara A, Tanaka N. EGF promotes gastric mucosal restitution by activating Na (+)/H(+) exchange of epithelial cells. *Am J Physiol Gastrointest Liver Physiol* 2002; **282**: G866-G876
- 50 **Wong BC**, Wang WP, So WH, Shin VY, Wong WM, Fung FM, Liu ES, Hiu WM, Lam SK, Cho CH. Epidermal growth factor and its receptor in chronic active gastritis and gastroduodenal ulcer before and after *Helicobacter pylori* eradication. *Aliment Pharmacol Ther* 2001; **15**: 1459-1465
- 51 **Hsieh JS**, Wang JY, Huang TJ. The role of epidermal growth factor in gastric epithelial proliferation in portal hypertensive rats exposed to stress. *Hepatogastroenterology* 1999; **46**: 2807-2811
- 52 **Miyazaki Y**, Hiraoka S, Tsutsui S, Kitamura S, Shinomura Y, Matsuzawa Y. Epidermal growth factor receptor mediates stress-induced expression of its ligands in rat gastric epithelial cells. *Gastroenterology* 2001; **120**: 108-116

Edited by Bo XN

Expression of NGF family and their receptors in gastric carcinoma: A cDNA microarray study

Jian-Jun Du, Ke-Feng Dou, Shu-You Peng, Bing-Zhi Qian, Hua-Sheng Xiao, Feng Liu, Wei-Zhong Wang, Wen-Xian Guan, Zhi-Qing Gao, Ying-Bin Liu, Ze-Guang Han

Jian-Jun Du, Ke-Feng Dou, Wei-Zhong Wang, Wen-Xian Guan, Zhi-Qing Gao, Department of General Surgery, Xijing Hospital, The Fourth Military Medical University, Xi'an 710032, Shanxi Province, China

Shu-You Peng, Ying-Bin Liu, Department of General Surgery, the Second Affiliated Hospital, Medical College, Zhejiang University, Hangzhou 310009, Zhejiang Province, China

Bing-Zhi Qian, Hua-Sheng Xiao, Feng Liu, Ze-Guang Han, China Human Genome Center at Shanghai, Shanghai 201203, China

Correspondence to: Dr. Ze-Guang Han, China Human Genome Center at Shanghai, 351 Guo Shou Jing Road, Zhangjiang High-Tech Park, Shanghai 201203, China. hanzg@chgc.sh.cn

Telephone: +86-29-3375256

Received: 2003-02-26 **Accepted:** 2003-03-28

Abstract

AIM: To investigate the expression of NGF family and their receptors in gastric carcinoma and normal gastric mucosa, and to elucidate their effects on gastric carcinoma.

METHODS: RNA of gastric cancer tissues and normal gastric tissues was respectively isolated and mRNA was purified. Probes of both mRNA reverse transcription product cDNAs labeled with α -³²P dATP were respectively hybridized with Atlas Array membrane where NGF and their family genes were spotted on. Hybridized signal images were scanned on phosphor screen with ImageQuant 5.1 software after hybridization. Normalized values on spots were analyzed with ArrayVersion 5.0 software. Differential expression of NGF family and their receptors mRNA was confirmed between hybridized Atlas Array membranes of gastric cancer tissues and normal gastric mucosa, then their effects on gastric carcinoma were investigated.

RESULTS: Hybridization signal images on Atlas Array membrane appeared in a lower level of nonspecific hybridization. Both of NGF family and their receptors Trk family mRNA were expressed in gastric cancer and normal gastric mucosa. But adversely up-regulated expression in other tissues and organs. NGF, BDGF, NT-3, NT-4/5, NT-6 and TrkA, B and C were down-regulated simultaneously in gastric carcinoma in comparison with normal gastric mucosa. Degrees of down-regulation in NGF family were greater than those in their receptors Trk family. Down-regulation of NT-3 and BDGF was the most significant, and TrkC down-regulation level was the lowest in receptors Trk family.

CONCLUSION: Down-regulated expression of NGF family and their receptors Trk family mRNA in gastric cancer is confirmed. NGF family and their receptors Trk family probably play a unique role in gastric cancer cell apoptosis by a novel Ras or Raf signal transduction pathway. Their synchronous effects are closely associated with occurrence and development of gastric carcinoma induced by reduction of signal transduction of programmed cell death.

Du JJ, Dou KF, Peng SY, Qian BZ, Xiao HS, Liu F, Wang WZ, Guan WX, Gao ZQ, Liu YB, Han ZG. Expression of NGF family and their receptors in gastric carcinoma: A cDNA microarray study. *World J Gastroenterol* 2003; 9(7): 1431-1434
<http://www.wjgnet.com/1007-9327/9/1431.asp>

INTRODUCTION

Recently, NGF family and their receptors family have been found in other non-neural tissues of the body, and more and more attentions are being paid to their effects on these tissues, especially on tumor tissues. Gene expression of NGF and Trk families in gastric tissue and gastric carcinoma has been seldom documented. Simultaneous detection of NGF family and their receptors family expression has become possible since cDNA microarray was developed^[1]. As abnormal expression of many genes is involved in gastric carcinogenesis^[2-11], it contributes to a better understanding of their roles in the occurrence and development of gastric cancer and helps reveal mRNA expression of the family genes in gastric tissue and gastric carcinoma.

MATERIALS AND METHODS

RNA extraction and mRNA purification

RNA of gastric cancer tissues and normal gastric mucosa was respectively isolated with Trizol (Gibco) in five cases of gastric cancer from Xijing Hospital, Fourth Military Medical University. To ensure good total RNA quality 28S/18S ≥ 1.5 , samples were immediately placed into liquid nitrogen after being removed intraoperatively, and trituration of the samples was performed in liquid nitrogen. Then, mRNA was purified in Oligotex mRNA Kit (Qiagen). An equal mRNA mixture of gastric cancer tissues and normal gastric mucosa from five patients respectively constituted gastric cancer group and normal gastric mucosa group. At last, reverse transcription product (the first stranded cDNAs) of mRNA mixture was electrophoresed to evaluate its size and quality.

Probe labeling

One μ g of mRNA mixture of gastric cancer tissue and normal gastric mucosa from five patients was respectively transcribed into cDNAs as a probe labeled with 3.5 μ l α -³²P dATP (>2 , 500 kCi·mol⁻¹, 10 Ci·L⁻¹, Dupont) and 1 μ l CDS primer 1 (Clontech) in a mixture containing 1 μ l MMLV, 1 μ l 10 \times dNTP Mix (for dATP label), 0.5 μ l DTT (100 mM), and 2 μ l 5 \times reaction buffer in a final volume of 10 μ l was incubated for 0.25 h at 50 °C using an unregulated heat block (Eppendorf). Labeled reaction was stopped by adding 1 μ l 10 \times Termination Mix. To purify the labeled cDNA from unincorporated ³²P-labeled nucleotides and small (<0.1 kb) cDNA fragments, the above probe synthetic reactions were diluted to 200 μ l total volume with Buffer NT2 included in Atlas cDNA Expression Arrays (Clontech), then transferred to a NucleoSpin Extraction Spin Column. 400 μ l Buffer NT3 was added into the column after centrifugation at 14 000 rpm for 1 min and the flowthrough

was discarded. The procedure was repeated twice. To elute the labeled probe, 100NE was added into the column, centrifuged at 14 000 rpm for 1 min. The flowthrough was obtained as the labeled probe.

Prehybridization and hybridization

Prehybridization of Atlas Array membrane was carried out in 0.5 mg heat-denatured sheared salmon DNA, and 5 ml prewarmed ExpressHyb solution (Clontech) in a hybridization bottle was incubated for 0.5 h at 68 °C. Then, heat-denatured cDNA probes were added into the above prehybridization bottle together with 5 µl heat-denatured C₀t-1 DNA. The hybridization reactions were performed at 68 °C overnight. The next day, the Atlas Array membrane was washed three times in prewarmed wash solution 1 (2×SSC, 1 % SDS) with continuous agitation at 68 °C for 0.5 h, and in prewarmed wash solution 2 (0.1×SSC, 0.5 % SDS) at 68 °C for 0.5 h. The damp Atlas Array membrane was wrapped in a plastic wrap after the last washing in 2×SSC at room temperature for 5 min.

Exposure of hybridization signals to phosphorimager and result analyses

Atlas Array hybridization membrane was exposed to phosphor screen at room temperature overnight. The hybridization signals were analyzed with ArrayVersion 5.0 software (MD) after the phosphor screen was scanned with ImageQuant 5.1 software (MD). Quantitative data of each hybridization signals were obtained.

RESULTS

Identification of mRNA quality

Good total RNA quality was confirmed by 28S/18S \geq 1.5. Size range of reverse transcription product cDNAs represented a smear from 0.2-4kb both in gastric cancer and normal gastric mucosa (Figure 1).

Image of scan on hybridization signals of phosphor screen

Hybridization signal images on Atlas Array membrane appeared in lower levels of nonspecific hybridization (Figure 2).

Expression of NGF family and their receptors Trk family mRNA

To quantify hybridization signals, signal intensity was detected after hybridized signal normalization of two hybridization Atlas Array membranes between gastric cancer and the normal mucosa. Signal intensity of NGF family and their receptors Trk family on Atlas Array membranes represented their mRNA expression level. NGF, BDGF, NT-3, NT-4/5, NT-6 and TrkA, B and C were down-regulated in gastric carcinoma in comparison with normal gastric mucosa. Degrees of down-regulation in NGF family were greater than those in their receptors Trk family. Down-regulation of NT-3 and BDGF was the most significant, and TrkC down-regulation level was the lowest in receptors Trk family (Table 1).

Table 1 Signal intensity of NGF family and their receptors Trk family

Dot	Gene	CAVOL	NORnVOL	NORnVOL/CAVOL
D07n	NT-3,BDGF	0.031	0.311	10.128
D11n	NGF	0.045	0.272	6.036
D08n	NT-4/5, NT-6	0.06	0.352	5.822
D02i	TrkC	0.029	0.119	4.172
D03k	Trk	0.038	0.157	4.093
D14h	TrkA	0.043	0.141	3.252
D01i	TrkB	0.026	0.051	1.926

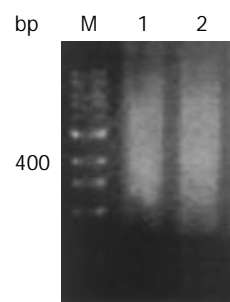


Figure 1 Size range of mRNA on 2 % agarose gel electrophoresis. Normal gastric mucosa mRNA (lane 1) and gastric carcinoma mRNA (lane 2). 100 bp size marker (lane M).

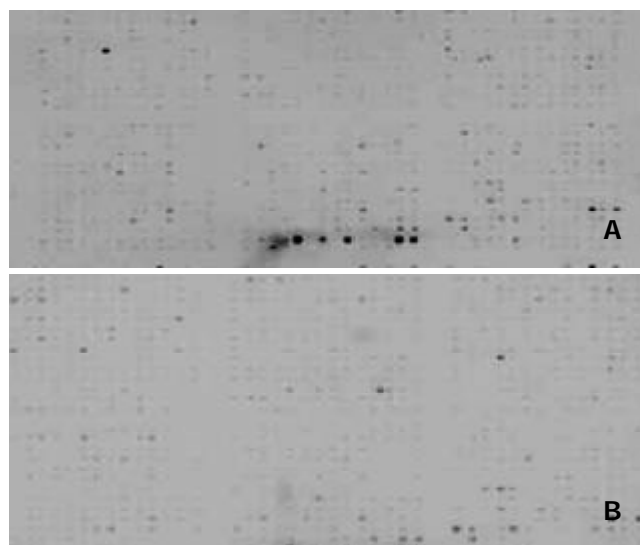


Figure 2 Hybridization signals of reverse transcription products cDNAs hybridized with Atlas Array membrane. A: hybridization signals of reverse transcription products cDNAs of normal gastric mucosa mRNA hybridized with Atlas Array membrane. B: hybridization signals of reverse transcription products cDNAs of gastric cancer mRNA hybridized with Atlas Array membrane.

DISCUSSION

Gene microarray has been rapidly and extensively used in detecting expression of genes, DNA sequence, novel genes and gene mutants, DNA polymorphism, and in screening drugs, diagnosing diseases and mapping gene library since Schena reported it in 1995^[12-28]. Profiling of differentially expressed genes in human gastric carcinoma by cDNA expression array was also reported^[29]. The study detected expression of NGF family and their receptors Trk family mRNA by using cDNA microarray. The Atlas Array membranes were provided by Clontech. A set of housekeeping genes was included on the Atlas Array membranes to normalize mRNA expression levels. Our good total RNA and mRNA quality, as well as successful synthesis and labeling of a cDNA probe with highly specific activity ensured the best possible results. ExpressHybTM hybridization solution was used in our hybridization experiments, a low-viscosity hybridization solution that significantly enhances the sensitivity of detection and reduces background.

NGF is composed of three subunit proteins (α , β and γ) among which β subunit represents an active form. NGF produced by targets of sympathetic neuron, sensory central neuron exerts an important effect on growth, development, differentiation of these neurons. Brain-derived nerve growth factor (BDNF), NT-3, NT-4/5 and NT-6 are members of the

NGF family, and NGF has 50 % of homology with BDNF. Difference between members of the family comes from the distribution of tissues, the early and/or later expression, and different receptors. NGF family receptors are subdivided into three types: Trk A, TrkB and TrkC. The structure of the three receptors consists of cellular external region, transcellular membrane region and cellular internal region. The receptors all are tyrosine kinase, and there is 66-68 % of homology between them. NGF binds TrkA, and BDNF, NT-3, NT-4/5 and NT-6 bind TrkB, in which binding of NT-3 is weaker and mainly with TrkC. As the functions of NGF family, TrkA, TrkB and TrkC can regulate growth, development and differentiation of corresponding neurons while receiving signals of NGF, BDNF, NT-3, NT-4/5 and NT-6. NT-3 and its receptor TrkC play a role in early growth, development and differentiation of neural systems.

Recently NGF family and their receptors family were found in other non-neural tissues of the body, and more and more attentions are being paid to their effects. It was reported that dermal pigment cells expressed NGF and Trk^[30], hepatic cells expressed BDNF, NT-3, NT-4/5 as well as TrkA, which were related to liver pathophysiology. Hepatic stellate cells expressed BDNF, NT-3, NT-4/5, TrkB and TrkC that were involved in liver remodeling^[31]. NT-3, NT-4/5, TrkB and TrkC expressed by microphages played a role in tissue inflammatory reaction and repair^[32]. Cardiac myocytes expressed TrkC and NT-3, and early growth and development of the heart were retarded when blockage of TrkC was used^[33]. Schneider *et al*^[34] demonstrated TrkA and TrkC expression in pancreatic ducts and pancreatic islets, TrkB in apha-cells of islets, NGF in pancreatic ducts and pancreatic acinar cells, NT-3 and NT-4 respectively in capillary endothelia and ductule cells. Additionally, TrkB and TrkC were found in endocrine cells of gut epithelium and neural tissues in fish^[35,36], and TrkA, TrkB and TrkC were all expressed in testis of rats. A current study also indicated NGF family and their receptors played an essential role in the development of tubulogenesis in embryonic kidney, spermatogenesis, hair follicle, heart and vascular differentiation and maintenance of blood and immune cells^[37].

Similarly, more attentions are being paid to their effects on tumors. Antagonists of NGF family and their receptors are being applied to kill tumor cells experimentally. It was noted that NGF family and their receptors were not expressed in some normal tissues, but expressed in their corresponding tumors. For example, up-regulated expression of Trk was present in tumors originating from thyroid and ovary while absent in the normal tissues. When chromosomal translocation occurred, a fusion protein of Trk-T1 composed of carboxyl terminal tyrosine kinase domain of NTRK1 and amino terminal portion of TPR (translocated promoter region) was formed. Trk-T1 was oncogenic *in vivo* and contributed to the papillary neoplastic transformation of the thyroid^[38]. These results suggest that NGF family and their receptors are involved in tumorigenicity. A recent study showed that pancreatic carcinoma cells could express NGF, TrkA and TrkC^[34]. It is interesting that Trk was highly expressed in esophageal carcinoma, thyroid carcinoma and prostate carcinoma, and adversely Trk expression revealed significantly lower in gastric carcinoma and colon carcinoma^[39,40]. Difference between NGF and Trk expression in various tumors suggests that NGF family and their receptors may play a different role or have directly reverse effects on various carcinoma originating from different tissues. Some studies verified the assumption that occurrence of apoptosis could be inhibited and/or enhanced while cascade effect was brought out by intracellular signal transduction pathway blocking or inducing programmed cell death^[41,42]. Its signal transduction pathways include Ras, the Cdc42/Rac/RhoG protein family, MAPK, PI3K and PLC-gamma.

Adversely, other novel Ras and/or Raf pathways participate in signal transduction paths mediating programmed cell death. For example, prostate growth depends on autocrine NGF interaction with Trk expressed by itself, otherwise, apoptosis occurred in medulloblastoma when NGF was bound to Trk^[43]. Therefore, inhibition or enhancement of apoptosis induced by Trk depended on cellular types and development periods of cells^[44].

The study showed that expression of NGF family and their receptors were simultaneously down-regulated in gastric cancer tissues. NT-3 and BDGF down-regulation was the lowest in NGF family, Trk C down-regulation was the lowest in Trk family. The evidences support that NGF family and their receptors Trk family may play a unique apoptotic role in gastric cancer by a new Ras or Raf signal transduction pathway. These further substantiate that NGF family and Trk family have synchronous effects on the occurrence and development of gastric carcinoma induced by reduction in signal transduction of programmed cell death brought out by simultaneously down-regulated expression of NGF family and Trk family. It remains unclear that which cells in gastric mucosa secrete NGF family, and whether NGF plays a role in the occurrence and development of gastric carcinoma in autocrine or paracrine way.

REFERENCES

- 1 **Schena M**, Shalon D, Davis RM, Brown PO. Quantitative monitoring of gene expression patterns with a complementary DNA microarray. *Science* 1995; **270**: 467-470
- 2 **Liu HF**, Liu WW, Fang DC, Men RP. Expression and significance of proapoptotic gene Bax in gastric carcinoma. *World J Gastroenterol* 1999; **5**: 15-17
- 3 **To KF**, Leung WK, Lee TL, Yu J, Tong JH, Chan MW, Ng EK, Chung SC, Sung JJ. Promoter hypermethylation of tumor-related genes in gastric intestinal metaplasia of patients with and without gastric cancer. *Int J Cancer* 2002; **102**: 623-628
- 4 **Gao HJ**, Yu LZ, Bai JF, Peng YS, Sun G, Zhao HL, Miu K, Lü XZ, Zhang XY, Zhao ZQ. Multiple genetic alterations and behavior of cellular biology in gastric cancer and other gastric mucosal lesions: *H. pylori* infection, histological types and staging. *World J Gastroenterol* 2000; **6**: 848-854
- 5 **Liu DH**, Zhang XY, Fan DM, Huang YX, Zhang JS, Huang WQ, Zhang YQ, Huang QS, Ma WY, Chai YB, Jin M. Expression of vascular endothelial growth factor and its role in oncogenesis of human gastric carcinoma. *World J Gastroenterol* 2001; **7**: 500-505
- 6 **He XS**, Su Q, Chen ZC, He XT, Long ZF, Ling H, Zhang LR. Expression, deletion and mutation of p16 gene in human gastric cancer. *World J Gastroenterol* 2001; **7**: 515-521
- 7 **Kaneda A**, Kaminishi M, Yanagihara K, Sugimura T, Ushijima T. Identification of silencing of nine genes in human gastric cancers. *Cancer Res* 2002; **62**: 6645-6650
- 8 **Ficorella C**, Cannita K, Ricevuto E, Toniato E, Fusco C, Sinopoli NT, De Galitiis F, Di Rocco ZC, Porzio G, Frati L, Gulino A, Martinotti S, Marchetti P. P16 hypermethylation contributes to the characterization of gene inactivation profiles in primary gastric cancer. *Oncol Rep* 2003; **10**: 169-173
- 9 **Li HL**, Chen DD, Li XH, Zhang HW, Lu YQ, Ye CL, Ren XD. Changes of NF- κ B, p53, Bcl-2 and caspase in apoptosis induced by JTE-522 in human gastric adenocarcinoma cell line AGS cells: role of reactive oxygen species. *World J Gastroenterol* 2002; **8**: 431-435
- 10 **Xia L**, Yuan YZ, Xu CD, Zhang YP, Qiao MM, Xu JX. Effects of epidermal growth factor on the growth of human gastric cancer cell and the implanted tumor of nude mice. *World J Gastroenterol* 2002; **8**: 455-458
- 11 **Fang DC**, Luo YH, Yang SM, Li XA, Ling XL, Fang L. Mutation analysis of APC gene in gastric cancer with microsatellite instability. *World J Gastroenterol* 2002; **8**: 787-791
- 12 **Eisen MB**, Brown PO. DNA arrays for analysis of gene expression. *Methods Enzymol* 1999; **303**: 179-205
- 13 **Brown PO**, Botstein D. Exploring the new world of the genome with DNA microarrays. *Nat Genet* 1999; **21**(Suppl): 33-37

- 14 **Hannon MF**, Rao S. Transcription: of chips and ChIPs. *Science* 2002; **296**: 666-669
- 15 **Duggan DJ**, Bittner M, Chen Y, Meltzer P, Trent JM. Expression profiling using cDNA microarrays. *Nat Genet* 1999; **21** (Suppl): 10-14
- 16 **Iyer VR**, Eisen MB, Ross DT, Schuler G, Moore T, Lee JC, Trent JM, Staudt LM, Hudson J Jr, Boguski MS, Lashkari D, Shalon D, Botstein D, Brown PO. The transcriptional program in the response of human fibroblasts to serum. *Science* 1999; **283**: 83-87
- 17 **Favis R**, Barany F. Mutation detection in K-ras, BRCA1, BRCA2, and p53 using PCR/LDR and a universal DNA microarray. *Ann N Y Acad Sci* 2000; **906**: 39-43
- 18 **Wang K**, Gan L, Jeffery E, Gayle M, Gown AM, Skelly M, Nelson PS, Ng WV, Schummer M, Hood L, Mulligan J. Monitoring gene expression profile changes in ovarian carcinomas using cDNA microarray. *Gene* 1999; **229**: 101-108
- 19 **Xu S**, Mou H, Lu G, Zhu C, Yang Z, Gao Y, Lou H, Liu X, Cheng Y, Yang W. Gene expression profile differences in high and low metastatic human ovarian cancer cell lines by gene chip. *Chin Med J (Engl)* 2002; **115**: 36-41
- 20 **Wellmann A**, Thieblemont C, Pittaluga S, Sakai A, Jaffe ES, Siebert P, Raffeld M. Detection of differentially expressed genes in lymphomas using cDNA arrays: identification of clusterin as a new diagnostic marker for anaplastic large-cell lymphomas. *Blood* 2000; **96**: 398-404
- 21 **Golub TR**, Slonim DK, Tamayo P, Huard C, Gaasenbeek M, Mesirov JP, Coller H, Loh ML, Downing JR, Caligiuri MA, Bloomfield CD, Lander ES. Molecular classification of cancer: Class discovery and class prediction by gene expression monitoring. *Science* 1999; **286**: 531-537
- 22 **Alizadeh AA**, Eisen MB, Davis RE, Ma C, Lossos IS, Rosenwald A, Boldrick JC, Sabet H, Tran T, Yu X, Powell JL, Yang L, Marti GE, Moore T, Hudson J Jr, Lu L, Lewis DB, Tibshirani R, Sherlock G, Chan WC, Greiner TC, Weisenburger DD, Armitage JO, Warnke R, Staudt LM. Distinct type of diffuse large B-cell lymphoma identified by gene expression profiling. *Nature* 2000; **403**: 503-511
- 23 **Assersohn L**, Gangi L, Zhao Y, Dowsett M, Simon R, Powles TJ, Liu ET. The feasibility of using fine needle aspiration from primary breast cancers for cDNA microarray analyses. *Clin Cancer Res* 2002; **8**: 794-801
- 24 **Hippo Y**, Yashiro M, Ishii M, Taniguchi H, Tsutsumi S, Hirakawa K, Kodama T, Aburatani H. Differential gene expression profiles of scirrhous gastric cancer cells with high metastatic potential to peritoneum or lymph nodes. *Cancer Res* 2001; **61**: 889-895
- 25 **Tiwari G**, Sakaue H, Pollack JR, Roth RA. Gene expression profiling in prostate cancer cells with akt activation reveals fra-1 as an akt-inducible gene. *Mol Cancer Res* 2003; **1**: 475-484
- 26 **Mycko MP**, Papoian R, Boschert U, Raine CS, Selmaj KW. cDNA microarray analysis in multiple sclerosis lesions: detection of genes associated with disease activity. *Brain* 2003; **126**: 1048-1057
- 27 **Man K**, Lo CM, Lee TK, Li XL, Ng IO, Fan ST. Intra-graft gene expression profiles by cDNA microarray in small-for-size liver grafts. *Liver Transpl* 2003; **9**: 425-432
- 28 **Kawaguchi K**, Kaneko S, Honda M, Kawai HF, Shiota Y, Kobayashi K. Detection of hepatitis B virus DNA in sera from patients with chronic hepatitis B virus infection by DNA microarray method. *J Clin Microbiol* 2003; **41**: 1701-1704
- 29 **Liu LX**, Liu ZH, Jiang HC, Qu X, Zhang WH, Wu LF, Zhu AL, Wang XQ, Wu M. Profiling of differentially expressed genes in human gastric carcinoma by cDNA expression array. *World J Gastroenterol* 2002; **8**: 580-585
- 30 **Innominato PF**, Libbrecht L, van den Oord JJ. Expression of neurotrophins and their receptors in pigment cell lesions of the skin. *J Pathol* 2001; **194**: 95-100
- 31 **Cassiman D**, Deneff C, Desmet VJ, Roskams T. Human and rat hepatic stellate cells express neurotrophins and neurotrophin receptors. *Hepatology* 2001; **33**: 148-158
- 32 **Barouch R**, Appel E, Kazimirsky G, Brodie C. Macrophages express neurotrophins and neurotrophin receptors. Regulation of nitric oxide production by NT-3. *J Neuroimmunol* 2001; **112**: 72-77
- 33 **Lin MI**, Das I, Schwartz GM, Tsoulfas P, Mikawa T, Hempstead BL. Trk C receptor signaling regulates cardiac myocyte proliferation during early heart development *in vivo*. *Dev Biol* 2000; **226**: 180-191
- 34 **Schneider MB**, Standop J, Ulrich A, Wittel U, Friess H, Andren-Sandberg A, Pour PM. Expression of nerve growth factors in pancreatic neural tissue and pancreatic cancer. *J Histochem Cytochem* 2001; **49**: 1205-1210
- 35 **Radaelli G**, Domeneghini C, Arrighi S, Castaldo L, Lucini C, Mascarello F. Neurotransmitters, neuromodulators, and neurotrophin receptors in the gut of pantex, a hybrid sparid fish (*Pagrus major* x *Dentex dentex*). Localizations in the enteric nervous and endocrine systems. *Histol Histopathol* 2001; **16**: 845-853
- 36 **De Girolamo P**, Lucini C, Vega JA, Andreozzi G, Coppola L, Castaldo L. Co-localization of Trk neurotrophin receptors and regulatory peptides in the endocrine cells of the teleostean stomach. *Anat Rec* 1999; **256**: 219-226
- 37 **Sariola H**. The neurotrophic factors in non-neuronal tissues. *Cell Mol Life Sci* 2001; **58**: 1061-1066
- 38 **Russell JP**, Powell DJ, Cunnane M, Greco A, Portella G, Santoro M, Fusco A, Rothstein JL. The TRK-T1 fusion protein induces neoplastic transformation of thyroid epithelium. *Oncogene* 2000; **19**: 5729-5735
- 39 **Koizumi H**, Morita M, Mikami S, Shibayama E, Uchikoshi T. Immunohistochemical analysis of TrkA neurotrophin receptor expression in human non-neuronal carcinomas. *Pathol Int* 1998; **48**: 93-101
- 40 **Weeraratna AT**, Arnold JT, George DJ, DeMarzo A, Isaacs JT. Rational basis for Trk inhibition therapy for prostate cancer. *Prostate* 2000; **45**: 140-148
- 41 **Patapoutian A**, Reichardt LF. Trk receptors: mediators of neurotrophin action. *Curr Opin Neurobiol* 2001; **11**: 272-280
- 42 **Chou TT**, Trojanowski JQ, Lee VM. A novel apoptotic pathway induced by nerve growth factor-mediated TrkA activation in medulloblastoma. *J Biol Chem* 2000; **275**: 565-570
- 43 **Muragaki Y**, Chou TT, Kaplan DR, Trojanowski JQ, Lee VM. Nerve growth factor induces apoptosis in human medulloblastoma cell lines that express TrkA receptors. *J Neurosci* 1997; **17**: 530-542
- 44 **Nakagawara A**. Trk receptor tyrosine kinases: a bridge between cancer and neural development. *Cancer Lett* 2001; **169**: 107-114

Edited by Zhang JZ and Wang XL

Expression of survivin in human gastric carcinoma and gastric carcinoma model of rats

Xiao-Dong Zhu, Geng-Jin Lin, Li-Ping Qian, Zhong-Qing Chen

Xiao-Dong Zhu, Geng-Jin Lin, Li-Ping Qian, Department of Gastroenterology, Huashan Hospital, Fudan University, Shanghai, 200040, China

Zhong-Qing Chen, Department of Pathology, Huashan Hospital, Fudan University, Shanghai, 200040, China

Correspondence to: Dr. Geng-Jin Lin, Department of Gastroenterology, Huashan Hospital, Fudan University, NO.12 wulumuqi Road, Shanghai, 200040, China. xddr@netease.com

Telephone: +86-021-62489999

Received: 2003-01-04 **Accepted:** 2003-02-18

Abstract

AIM: To study the expression of survivin, an inhibitor of apoptosis protein, in human gastric carcinomas and gastric carcinoma models of rats.

METHODS: With the method of immunohistochemical staining, we studied the expression of survivin in 20 cases of chronic gastritis and 56 cases of gastric carcinomas. We used N-methyl-N'-nitro-N-nitrosoguanidine (MNNG) and high dose sodium-chloride diet to induce rat gastric carcinomas. Survivin expression was studied in glandular stomachs of normal rats, adenocarcinomas and tissues adjacent to the tumor, as well as in rats during the induction period.

RESULTS: Survivin was expressed in 27 of 56 (48.2 %) cases of human gastric carcinoma tissues and 1 of 20 (5 %) cases of chronic gastritis. It was found that the expression of survivin had no relation with the elements of age, tumor depth, tumor size, and disease stage, but was significantly related to histological type. The positive rate of survivin expression in cases of intestinal type was significantly higher than that in cases of diffuse type ($P < 0.05$). In animal experiments, survivin expression in glandular stomachs of normal rats, of rats in middle induction period, in adenocarcinomas and tissues adjacent to tumor were 0, 40.0 %, 78.3 % and 38.9 %, respectively. Compared with the survivin expression in normal rats, the differences were significant.

CONCLUSION: These data imply that survivin plays an important role in the onset of gastric carcinoma and that high survivin expression is an early event of gastric carcinoma.

Zhu XD, Lin GJ, Qian LP, Chen ZQ. Expression of survivin in human gastric carcinoma and gastric carcinoma model of rats. *World J Gastroenterol* 2003; 9(7): 1435-1438
<http://www.wjgnet.com/1007-9327/9/1435.asp>

INTRODUCTION

Survivin, a member of the inhibitors of apoptosis protein (IAP) family, is a mitotic spindle-associated protein involved in linking mitotic spindle function to the activation of apoptosis

in mammalian cells. The structure of full-length human survivin determined by X-ray crystallography is 2.7 \AA . The structure forms a very unusual bow tie-shaped dimer. The unusual shape and dimensions of survivin suggest that it serves as an adaptor through its alpha-helical extensions^[1]. Just like other IAP members, survivin can suppress apoptosis through combination with Caspase3, Caspase7 by baculoviral IAP repeat (BIR)^[2,3]. The common pathway of apoptosis is the activation of Caspase3, Caspase7 or Caspase 6, hence high expression of survivin may protect cells from many apoptosis signals and help cells survive^[4,5]. Now, substantial data have shown that inhibition of apoptosis plays a great role in carcinogenesis^[6-10], so survivin may be an important factor in the development of cancer. It has reported that survivin is undetectable in terminally differentiated adult tissues and becomes prominently expressed in transformed cell lines and in most common human cancers of lung, colon, pancreas, prostate and breast^[2]. Some data indicate that high expression of survivin is correlated with poor prognosis and chemotherapy resistance^[11-13]. In this study, we investigated the expression of survivin in human gastric carcinoma and its relationship with clinicopathological factors, as well as the expression of survivin in gastric carcinoma models of rats.

MATERIALS AND METHODS

Patients and samples

A total of fifty-six cases of gastric carcinoma were involved in this study including 46 males and 10 females. The age range was 26-79 years, mean age was 59.8 years. The patients with gastric carcinoma, having undergone potentially curative tumor resection at Huashan Hospital from 2000 to 2001, had received neither chemotherapy nor radiation therapy before surgery. The histological types of tumors were classified according to Lauren as intestinal type and diffuse type, and the disease stage was defined in accordance with the tumor-node-metastasis (TNM) classification^[14]. There were 32 cases of intestinal type and 24 cases of diffuse type. Materials were composed of 19 cases of stage I, 8 cases of stage II, and 29 cases of stage III. The tissues containing principal tumor were selected and fixed with formalin, embedded in paraffin routinely. Serial sections of $4 \mu\text{m}$ were prepared for immunohistochemical examination and histopathological study. The expression of survivin was investigated in these 56 gastric carcinoma patients and 20 cases of chronic gastritis by immunohistochemical examination.

Animal experiment

Forty-six male 6-week-old Wistar rats were divided into 2 groups. Thirty rats in group A were fed with a diet supplemented with 8 % NaCl for 20 weeks and simultaneously given N-methyl-N'-nitro-N-nitrosoguanidine (MNNG) in drinking water at a concentration of 100 $\mu\text{g/ml}$ for the first 17 weeks. From week 18, these rats were given normal water. From week 21, these rats were fed with normal diet for 15 weeks. The other sixteen rats in group B were fed with normal diet for 35 weeks and served as the control. At week 20, 10 rats in group A were killed and all the rest animals were killed

at the end of week 35. The whole stomach and a part of duodenum were sampled and cut open along the greater curvature. The number of tumors with their locations and sizes were recorded in details. All the specimens were histopathologically investigated and the expression of survivin was examined with immunohistochemical analysis as they were done in human specimens.

Immunohistochemical staining for survivin and assessment of its expression

Anti-survivin polyclonal antibody was purchased from Santa Cruz Company. Immunohistochemical analysis was carried out with the standard streptavidin-biotin-peroxidase (SP) complex technique using the Ultra sensitive™ S-P kit (Maixin-Bio Company). One case of stage III gastric carcinoma intensively and reproducibly stained for survivin expression in more than 50 % of tumor cells served as positive control. Negative control slides were stained without primary antibody. To assess the expression of survivin in various samples examined, a 4-grade-method was established according to the mean percentage of positive tumor cells and their intensity. Moderately stained slides with a mean percentage of positive tumor cells no less than 30 % were scored as positive (+). Moderately or intensively stained slides with a mean percentage of positive tumor cells more than 70 % were scored as intensely positive (+++). Slightly or moderately stained slides with a mean percentage of positive tumor cells between 30 % and 70 % were scored as moderately positive (++) . Slightly or moderately stained slides with a mean percentage of positive tumor cells less than 30 % were scored as negative (-).

Statistical analysis

Software Stata (version 6.0, STATA Corp, College Station) was applied to compare the rates.

RESULTS

Correlation between expression of survivin and clinicopathological factors in human gastric carcinomas

Positive staining for survivin was located in cytoplasm of tumor cells (Figure 1). A clinicopathological analysis of survivin-positive cases is shown in Table 1. The expression of survivin was positive in 27 of 56 (48.2 %) cases of gastric carcinoma tissues and 1 of 20 (5 %) cases of chronic gastritis. Expression of survivin had no relation with age, tumor depth, tumor size, and disease stage ($P>0.05$), but it was significantly related to histological type. The positive rate of survivin expression in cases of intestinal type was significantly higher than that in cases of diffuse type ($P<0.05$).

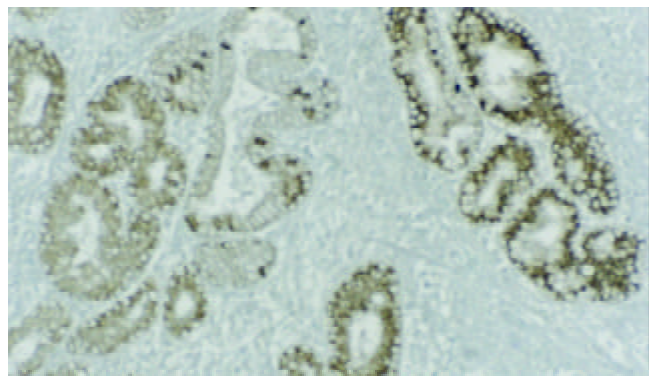


Figure 1 Immunohistochemical staining for the expression of survivin in human gastric carcinoma. Positive staining for survivin was located in cytoplasm ($\times 50$).

Table 1 Correlation between expression of survivin and clinicopathological factors in human gastric carcinomas

Variables	Cases	Survivin expression n (%)	P
Chronic gastritis	20	1(5%)	<0.001
Gastric carcinoma	56	27(48.2%)	
Age			
<55	18	11(61.1%)	0.184
>55	38	16(42.1%)	
Invasion size			
<12.3 cm ²	31	16(51.6%)	0.571
>12.3 cm ²	25	11(44.0%)	
Invasion depth			
Muscular layer unaffected	14	5(35.7%)	0.280
Muscular layer affected	42	22(52.4%)	
Lymph node metastasis			
Regional lymph Node unaffected	20	9(45.0%)	0.720
Regional lymph Node affected	36	18(50%)	
Histological type (Lauren) intestinal	32	20(62.5%)	0.013
Diffuse	24	7(29.2%)	
Disease stage(TMN)			
I	19	8(42.1%)	0.873
II	8	4(50.0%)	
III	29	15(51.7%)	

Notes: The disease stage of each tumor was defined in accordance with the tumor-node-metastasis (TNM) classification, the histological type was classified according to Lauren, and other pathological variables were defined in accordance with the Gastric Carcinoma^[14].

The expression of survivin in gastric carcinoma models of rats

By the end of week 35, neoplastic foci were found in antral mucosa in 18 rats of group A which were histologically determined to be adenocarcinomas. Of these 18 rats, the total number of adenocarcinomas was 23, and 22 were very well differentiated, which could be classified as intestinal type according to Lauren classification. Just like human gastric carcinoma, positive staining for survivin was located in cytoplasm of tumor cells (Figure 2). No survivin expression was detected in antral mucosa of normal rats (group B). As shown in Table 2, in antral mucosa of those rats at week 20, survivin expression was positive in 4 of 10 rats. In adenocarcinomas and tissues adjacent to the tumor, the ratio was 78.3 % and 38.9 %, respectively. Compared to normal tissue, the difference was significant (Table 2).

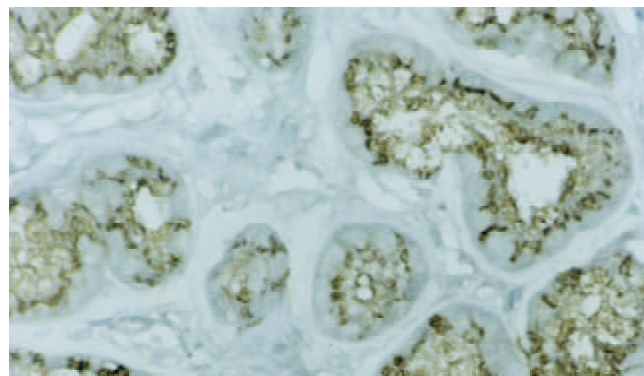


Figure 2 Immunohistochemical staining for the expression of survivin in gastric carcinoma of rat model. Positive staining for survivin was also located in cytoplasm. ($\times 100$).

Table 2 Survivin expression in experimental gastric carcinoma

	Cases	Survivin expression	Positive rate(%)
Control (group B)	16	0	0
Group A			
Antral mucosa of rats at week 20	10	4	40% ^a
Adenocarcinomas	23	18	78.3% ^b
Tissues adjacent to tumor	18	7	38.9% ^c

Ten rats of group A were killed at week 20, and the antral mucosa were examined. At week 35, all rats in both group A and B were killed and investigated. Tissues adjacent to tumor were defined as the tissues 5 mm away from the edge of tumor.

^a $P < 0.05$ vs control group, ^b $P < 0.001$ vs control group, ^c $P < 0.01$ vs control group.

DISCUSSION

Survivin is expressed in a series of human cancers, and it has been widely accepted that survivin is highly related to the onset and development of cancer. In this study, we adopted human gastric carcinoma specimens and experimental gastric carcinoma models to discuss the effect of survivin on gastric cancer.

Survivin was expressed in 27 of 56 (48.2 %) cases of human gastric carcinoma tissues and only 1 of 20 (5 %) cases of chronic gastritis. In experimental gastric carcinoma, the positive rate rose to 78.3 %. These data suggest that high expression of survivin is a common phenomenon in gastric cancer and inhibition of apoptosis resulted from survivin expression may play an important role in carcinogenesis.

Our data on human gastric carcinoma proved that the expression of survivin in intestinal type cases is significantly higher than that in diffuse type cases and the expression of survivin is correlated with intestinal histological type. This result is consistent with Lu^[15]. The Lauren histological classification has a specific epidemiological significance because the epidemiological study has determined that intestinal type cases are dominant in high risk areas while diffuse type cases are dominant in low risk areas. Substantial data suggest that intestinal type cases are highly related to circumstances and diffuse type cases are related to heredity. At present, Correa's theory of an atrophy-metaplasia-dysplasia-carcinoma sequence in the development of intestinal type gastric carcinoma has been widely accepted^[16-22]. The fact that the expression of survivin in intestinal type was higher than that in diffuse type suggests that survivin plays a more important role in the former and indicate that survivin may be an important factor contributing to the conversion from atrophy to carcinoma. Our animal experiment provided further evidences.

In our animal experiment, 95.7 % of the induced gastric carcinomas were intestinal type, and we did find atrophy and dysplasia lesions during the induction period. These data suggest that our rat model could simulate the development of human gastric carcinoma (intestinal type). We dynamically investigated the expression of survivin during the induction period and found 4 cases were positive in 10 rats at week 20, and 78.3% was positive in gastric carcinoma. These data indicate a rising trend of survivin expression during the development of gastric cancer, and suggest an important role of survivin expression in tumor formation.

Some scholars concluded that survivin could only be found in tumor^[15], but others thought it could be found in precancerous lesions^[23,24]. Our results supported the latter. In our experiment, the expression of survivin was positive in some gastritis patients, and in some rats during the induction period, as well as in some tissues adjacent to tumor. Hence, we may conclude

that survivin is not only expressed in cancer tissues but also in damaged tissues. The expression of survivin occurs before the formation of adenocarcinomas, and is an early event in carcinoma development.

Recently, some studies have partly explained why survivin was highly expressed in cancer. According to the study of Hoffman *et al*^[25], the anti-apoptotic gene, survivin, is a p53-repressed gene. Chromatin immunoprecipitations indicate that wild type p53 binds survivin promoter *in vivo*, which results in transcriptional repression. Mirza *et al*^[26] study implicated that wild-type p53 suppresses survivin expression at both mRNA and protein levels. It is widely accepted that mutated p53 loses its function as a tumor inhibitor and this may contribute to the loss of inhibition to survivin. Due to the high incidence of p53 mutation in gastric cancer, we put forward the hypothesis that long term effect of carcinogen should lead to p53 or other important gene damage, which results in survivin expression and apoptosis inhibition. Abnormal apoptosis leads to carcinogenesis.

According to our clinical data, age and prognostic factors such as different tumor size, tumor depth, lymph node metastasis or disease stage have no significant correlation with survivin expression, which indicates that survivin has little impact on tumor biological behavior.

Survivin plays an important role in gastric carcinoma and is a key molecule of cell cycle, mitosis and apoptosis^[27]. Moreover, inhibition of survivin function will result in cell apoptosis^[28-30]. The antisense oligonucleotide targeting survivin expression sensitizes lung cancer cells to chemotherapy^[30]. All these data suggest that survivin may be an attractive target for gastric cancer therapy.

REFERENCES

- 1 **Chantalat L**, Skoufias DA, Kleman JP, Jung B, Dideberg O, Margolis RL. Crystal structure of human survivin reveals a bow tie-shaped dimer with two unusual alpha-helical extensions. *Mol Cell* 2000; **6**: 183-189
- 2 **Ambrosini G**, Adida C, Altieri DC. A novel anti-apoptosis gene, survivin, expressed in cancer and lymphoma. *Nat Med* 1997; **3**: 917-921
- 3 **Johnson AL**, Langer JS, Bridgham JT. Survivin as a cell cycle-related and antiapoptotic protein in granulosa cells. *Endocrinology* 2002; **143**: 3405-3413
- 4 **Tamm I**, Wang Y, Sausville E, Scudiero DA, Vigna N, Oltersdorf T, Reed JC. IAP-family protein survivin inhibits caspase activity and apoptosis induced by Fas (CD95), Bax, caspases, and anti-cancer drugs. *Cancer Res* 1998; **58**: 5315-5320
- 5 **Conway EM**, Pollefeyt S, Steiner-Mosonyi M, Luo W, Devriese A, Lupu F, Bono F, Leducq N, Dol F, Schaeffer P, Collen D, Herbert JM. Deficiency of survivin in transgenic mice exacerbates Fas-induced apoptosis via mitochondrial pathways. *Gastroenterology* 2002; **123**: 619-631
- 6 **Xu AG**, Li SG, Liu JH, Gan AH. Function of apoptosis and expression of the proteins Bcl-2, p53 and C-myc in the development of gastric cancer. *World J Gastroenterol* 2001; **7**: 403-406
- 7 **Wu MY**, Liang YR, Wu XY, Zhuang CX. Relationship between Egr-1 gene expression and apoptosis in esophageal carcinoma and precancerous lesions. *World J Gastroenterol* 2002; **8**: 971-975
- 8 **Shan CM**, Li J. Study of apoptosis in human liver cancers. *World J Gastroenterol* 2002; **8**: 247-252
- 9 **Zhang Z**, Yuan Y, Gao H, Dong M, Wang L, Gong YH. Apoptosis, proliferation and p53 gene expression of *H. pylori* associated gastric epithelial lesions. *World J Gastroenterol* 2001; **7**: 779-782
- 10 **Xu HY**, Yang YL, Guan XL, Song G, Jiang AM, Shi LJ. Expression of regulating apoptosis gene and apoptosis index in primary liver cancer. *World J Gastroenterol* 2000; **6**: 721-724
- 11 **Ikeguchi M**, Kaibara N. Survivin messenger RNA expression is a good prognostic biomarker for oesophageal carcinoma. *Br J Cancer* 2002; **87**: 883-887
- 12 **Chakravarti A**, Noll E, Black PM, Finkelstein DF, Finkelstein DM,

- Dyson NJ, Loeffler JS. Quantitatively determined survivin expression levels are of prognostic value in human gliomas. *J Clin Oncol* 2002; **20**: 1063-1068
- 13 **Zaffaroni N**, Pennati M, Colella G, Perego P, Supino R, Gatti L, Pilotti S, Zunino F, Daidone MG. Expression of the anti-apoptotic gene survivin correlates with taxol resistance in human ovarian cancer. *Cell Mol Life Sci* 2002; **59**: 1406-1412
- 14 **Chen B**, Wang SB. The clinical manifestation and disease stage of gastric cancer In: Zhang WF, Zhang YC, Chen JQ, eds. Gastric cancer. 2nd ed. Shanghai: Shanghai Science and Technology Publishing Company 2001: 249-255
- 15 **Lu CD**, Altieri DC, Tanigawa N. Expression of a novel antiapoptosis gene, survivin, correlated with tumor cell apoptosis and p53 accumulation in gastric carcinomas. *Cancer Res* 1998; **58**:1808-1812
- 16 **Su Q**, Luo ZY, Teng H, Yun WD, Li YQ, He XE. Effect of garlic and garlic-green tea mixture on serum lipids in MNNG-induced experimental gastric carcinoma and precancerous lesion. *World J Gastroenterol* 1998; **4**: 29
- 17 **Cui RT**, Cai G, Yin ZB, Cheng Y, Yang QH, Tian T. Transretinoic acid inhibits rats gastric epithelial dysplasia induced by N-methyl-N-nitro-N-nitrosoguanidine: influences on cell apoptosis and expression of its regulatory genes. *World J Gastroenterol* 2001; **7**:394-398
- 18 **Zhou HP**, Wang X, Zhang NZ. Early apoptosis in intestinal and diffuse gastric carcinomas. *World J Gastroenterol* 2000; **6**: 898-901
- 19 **Goldstein NS**, Lewin KJ. Gastric epithelial dysplasia and adenoma: historical review and histological criteria for grading. *Hum Pathol* 1997; **28**: 127-133
- 20 **Walker MM**. Is intestinal metaplasia of the stomach reversible? *Gut* 2003; **52**: 1-4
- 21 **Ming SC**. Cellular and molecular pathology of gastric carcinoma and precursor lesions: A critical review. *Gastric Cancer* 1998; **1**:31-50
- 22 **Lauwers GY**, Riddell RH. Gastric epithelial dysplasia. *Gut* 1999; **45**: 784-790
- 23 **Grossman D**, McNiff JM, Li F, Altieri DC. Expression of the apoptosis inhibitor, survivin, in nonmelanoma skin cancer and gene targeting in a keratinocyte cell line. *Lab Invest* 1999; **79**: 1121-1126
- 24 **Kawasaki H**, Toyoda M, Shinohara H, Okuda J, Watanabe I, Yamamoto T, Tanaka K, Tenjo T, Tanigawa N. Expression of survivin correlates with apoptosis, proliferation, and angiogenesis during human colorectal tumorigenesis. *Cancer* 2001; **91**: 2026-2032
- 25 **Hoffman WH**, Biade S, Zilfou JT, Chen J, Murphy M. Transcriptional repression of the anti-apoptotic survivin gene by wild type p53. *J Biol Chem* 2002; **277**: 3247-3257
- 26 **Mirza A**, McGuirk M, Hockenberry TN, Wu Q, Ashar H, Black S, Wen SF, Wang L, Kirschmeier P, Bishop WR, Nielsen LL, Pickett CB, Liu S. Human survivin is negatively regulated by wild-type p53 and participates in p53-dependent apoptotic pathway. *Oncogene* 2002; **21**: 2613-2622
- 27 **Li F**, Ambrosini G, Chu EY, Plescia J, Tognin S, Marchisio PC, Altieri DC. Control of apoptosis and mitotic spindle checkpoint by survivin. *Nature* 1998; **396**: 580-584
- 28 **Xia C**, Xu Z, Yuan X, Uematsu K, You L, Li K, Li L, McCormick F, Jablons DM. Induction of apoptosis in mesothelioma cells by antisurvivin oligonucleotides. *Mol Cancer Ther* 2002; **1**: 687-694
- 29 **Grossman D**, Kim PJ, Schechner JS, Altieri DC. Inhibition of melanoma tumor growth in vivo by survivin targeting. *Proc Natl Acad Sci U S A* 2001; **98**: 635-640
- 30 **Olie RA**, Simoes-Wust AP, Baumann B, Leech SH, Fabbro D, Stahel RA, Zangemeister-Wittke U. A novel antisense oligonucleotide targeting survivin expression induces apoptosis and sensitizes lung cancer cells to chemotherapy. *Cancer Res* 2000; **60**: 2805-2809

Edited by Xu XQ and Wang XL

cDNA suppression subtraction library for screening down-regulated genes in gastric carcinoma

Jian-Jun Du, Ke-Feng Dou, Shu-You Peng, Hua-Sheng Xiao, Wei-Zhong Wang, Wen-Xian Guan, Zhong-Hua Wang, Zhi-Qing Gao, Ying-Bin Liu

Jian-Jun Du, Ke-Feng Dou, Wei-Zhong Wang, Wen-Xian Guan, Zhong-Hua Wang, Zhi-Qing Gao, Department of General Surgery, Xijing Hospital, The Fourth Military Medical University, Xian 710032, Shaanxi Province, China

Hua-Sheng Xiao, Department of Neurobiology, The Fourth Military Medical University, Xi an 710032, Shaanxi Province, China

Shu-You Peng, Ying-Bin Liu, Department of General Surgery, the Second Affiliated Hospital, Medical College, Zhejiang University, Hangzhou 310009, Zhejiang Province, China

Correspondence to: Dr. Ke-Feng Dou, Department of General Surgery, Xijing Hospital, The Fourth Military Medical University, Xian 710032, Shaanxi Province, China. zhongmrh@yahoo.com

Telephone: +86-029-3375256

Received: 2003-01-04 **Accepted:** 2003-02-16

Abstract

AIM: To establish cDNA suppression subtraction library with a high subtraction efficiency by counterpart normal gastric mucosa mixture mRNA subtracting gastric cancer cells mixture mRNA for screening down-regulated genes in gastric carcinoma.

METHODS: RNA of gastric cancer tissues and counterpart normal gastric mucosa were respectively isolated in five patients with gastric cancer, and their mRNA was purified. cDNA suppression subtraction library was established by counterpart normal gastric mucosa mixture mRNA (tester) subtracting gastric cancer tissues mixture mRNA (driver) of five patients with gastric carcinoma. The library plasmids were transformed into competent bacteria DH5a after ligation of the library cDNA fragments with T vectors. Library plasmids were extracted after picking colonies and shaking bacteria overnight. Its subtraction efficiency was confirmed by PCR and reverse hybridization of a nylon filter onto which the colonies of bacteria were transferred with probes of reverse transcription products cDNA of gastric cancer tissues mRNA and counterpart normal gastric mucosa mRNA labeled with α -³²P dCTP.

RESULTS: mRNA purified from total RNA of gastric cancer tissues and counterpart normal gastric mucosa in five patients with gastric carcinoma revealed a good quality. cDNA suppression subtraction library constructed for screening down-regulated genes in gastric carcinoma represented a high subtraction efficiency. 86 % of differential expression in down-regulated genes between counterpart normal gastric mucosa and gastric carcinoma was confirmed.

CONCLUSION: cDNA suppression subtraction library with a high subtraction efficiency for screening down-regulated genes in gastric carcinoma is successfully established.

Du JJ, Dou KF, Peng SY, Xiao HS, Wang WZ, Guan WX, Wang ZH, Gao ZQ, Liu YB. cDNA suppression subtraction library for screening down-regulated genes in gastric carcinoma. *World J Gastroenterol* 2003; 9(7): 1439-1443

<http://www.wjgnet.com/1007-9327/9/1439.asp>

INTRODUCTION

High incidence of 50-80 % LOH (loss of hybridization) in gastric carcinoma cells reveals obvious chromosome fragments loss^[1,2], e.g 8p, 18q12.2, 21q22, 1p35-pter of regions of LOH were currently found^[2-8]. These suggest the novel tumor suppressor genes in the regions of LOH are involved in gastric tumorigenicity^[9]. But these novel tumor suppressor gene candidates have not been cloned. To reach the targets, we screened down-regulated genes in a suppression subtraction cDNA library established by counterpart normal gastric mucous membrane mixture mRNA (tester) subtracting gastric cancer cells mixture mRNA (driver) of five patients with gastric cancer based on the suppression subtractive hybridization (SSH) technique^[10]. These down-regulated genes obtained from the library probably are tumor suppressor gene candidates. Up to now, down-regulated genes in gastric cancer cloned from gastric tissues have been seldom documented except CA11, LDOC1^[11-13].

MATERIALS AND METHODS

RNA extraction and mRNA purification

RNA of gastric cancer tissues and counterpart normal gastric mucosa was respectively isolated with Trizol (Gibco) in five patients with gastric cancer from Xijing Hospital, Fourth Military Medical University. To ensure good total RNA quality 28S/18S ≥ 1.5 , samples were immediately placed into liquid nitrogen after being removed intraoperatively, and trituration of the samples must be performed in liquid nitrogen. Then, mRNA was purified in Oligotex mRNA Kit (Qiagen). An equal mRNA mixture of gastric cancer tissues and counterpart normal gastric mucosa in five patients with gastric cancer contributed to driver group (gastric cancer tissues) and tester group (counterpart normal gastric mucosa) respectively. At last, reverse transcription products (the first stranded cDNAs) of mRNA mixture were electrophoresed to evaluate their size range and quality.

Suppression subtraction library construction

First-strand was synthesized with 1 μ l cDNA synthesis primer (10 μ mol \cdot L⁻¹, Clontech) in a mixture containing 2 μ g mRNA mixture, 20U AMV, 2 μ l 5 \times first-strand buffer in a final volume of 10 μ l at 42 $^{\circ}$ C for 1.5 h. Then, second-strand synthesis was carried out in 10 μ l first strand react volume, 4.0 μ l 20 \times second-strand enzyme cocktail, 48.4 μ l of sterile H₂O, 1.6 μ l dNTP Mix (10 mM \cdot L⁻¹), 16.0 μ l 5 \times second-strand buffer solution for 2 h at 16 $^{\circ}$ C. Polymeric reaction was performed at 16 $^{\circ}$ C for 0.5 h after 2 μ l (6 units) of T4 DNA polymerase was added into the above reaction volume. The second-strand synthesis was terminated by adding 4 μ l of 20 \times EDTA/Glycogen Mix (Clontech). After phenol:chloroform: isoamyl alcohol (25:24:1) and chloroform: isoamyl alcohol (24:1) extraction twice respectively, and 4 M NH₄OAc and 95 % ethanol precipitation of the second stranded cDNAs, the pellet was dissolved in 50 μ l of sterile H₂O when precipitate was washed in 80 % ethanol and residual ethanol was evaporated after the supernatant was removed.

The second double-stranded cDNA was digested with 15U *RsaI* in a final volume of 50 μ l at 37 $^{\circ}$ C for 1.5 h. Enzyme digestion was terminated by adding 2.5 μ l 20 \times EDTA/Glycogen Mix. After extraction and precipitation of digested second-strand cDNAs, the pellet was dissolved in 5.5 μ l of sterile H₂O when precipitate was washed in 80 % ethanol and residual ethanol was evaporated after the supernatant was removed.

One μ l of digested first-strand cDNAs of normal gastric mucosa was diluted with 5 μ l of sterile H₂O. Each 2 μ l of the cDNA was acted as tester1-1 and tester1-2 that were respectively mixed with adaptor1 and adaptor 2, and 1 μ l T4 DNA ligase (400 kU \cdot L⁻¹) in a final volume of 10 μ l, while mixture of 2 μ l of each tester1-1 and tester1-2 was taken as control (Tester C). Ligation to adaptors completed at 16 $^{\circ}$ C overnight.

Then, 1.5 μ l of tester1-1 with adaptor 1 and tester1-2 with adaptor 2 was respectively hybridized with 1.5 μ l digested first-stranded driver cDNA of gastric cancer in 1.0 μ l 4 \times hybridization buffer solution at 68 $^{\circ}$ C for 10 h. Tester1-2 hybridization sample was drawn into the pipette tip. Afterwards, 1 μ l denatured mixture from 1 μ l digested second-stranded driver cDNA, 2 μ l H₂O, 1 μ l 4 \times hybridization buffer solution at 98 $^{\circ}$ C was drawn into the pipette tip with a slight air space below the droplet of the above tester1-2 hybridization sample. Sequentially, the entire mixture of pipette tip was transferred to a tube containing the above tester1-1 hybridization sample overnight at 68 $^{\circ}$ C. After second hybridization, 200 μ l dilution buffer was added into the tube. One μ l of tester C was diluted with 1 000 μ l of sterile H₂O. 1 μ l of diluted tester C and the secondary hybridization sample were amplified with PCR primer 1 and 50 \times advantage cDNA polymerase mix in a final volume of 25 μ l respectively after adaptors were extended at 75 $^{\circ}$ C. 3 μ l of primary PCR product was diluted with 27 μ l of sterile H₂O. 1 μ l of diluted primary PCR products was again amplified with nested PCR primer 1, 2R and 50 \times advantage cDNA polymerase mix in a final volume of 25 μ l for 12 cycles.

Analyses of adaptor ligation efficiency and subtraction efficiency by PCR

One 1 μ l of tester1-1 and tester1-2 with adaptors was diluted with 200 μ l of sterile H₂O respectively. 1 μ l of diluted tester1-1 and tester1-2 was repeatedly amplified respectively using G3PDH 3' primer, PCR primer 1 as well as G3PDH 3' primer, G3PDH 5' primer after adaptors were extended at 75 $^{\circ}$ C. 1 μ l of subtraction cDNA and secondary PCR product of tester C was diluted with 9 μ l of sterile H₂O. 1 μ l of diluted subtraction cDNA and secondary PCR product of tester C was respectively amplified with G3PDH 3' primer, G3PDH 5' primer. 5 μ l of PCR products collected at 18, 23, 28, and 33 cycles was electrophoresed on 2 % agarose gel respectively.

Identification of suppression subtraction library

Six μ l of secondary PCR product of subtraction cDNA was ligated to T vectors in a mixture containing 2 μ l T vectors, 1 μ l T4DNA ligase in a final volume of 10 μ l at 16 $^{\circ}$ C for 36 h. Then, 5 μ l of ligated product was transformed into 100 μ l of competent DH5a (stratgene) for electroporation. Competent DH5a transformed by ligated product was grown on LB medium plates. White colonies were placed into LB medium and shaken overnight at 37 $^{\circ}$ C. In a large scale, fragments inserted into library plasmids were identified by PCR amplification with SP6 and T7 primers after library plasmids were extracted. Each colony of plasmids with inserted fragments was inoculated twice on a LB medium plate (100 colonies per plate, and one pair of positive and negative controls per plate) and grown until colony diameter reached to 3 mm.

At time, colonies were transferred onto a nylon filter (NEN), then the nylon filter was cross-linked by using an UV stratalinker (CL-1000, Upland). Each 200 ng mRNA of the normal mucosa and gastric carcinoma was reverse transcribed with 1 μ g Oligo (dT)₁₅ and super transcriptase II as a probe labeled with α -³²PdCTP, hybridized respectively with filters. The filters were exposed to phosphore screen and analyzed.

RESULTS

Identification of mRNA quality

Good total RNA quality was confirmed by 28S/18S \geq 1.5. Size range of reverse transcription product cDNAs was represented in a smear from 0.2-4kb both in gastric cancer and normal mucosa (Figure 1).

RsaI enzyme digestion

Size range of double-strand cDNA without digestion showed a normal size as expected. By comparison, *RsaI* enzyme digested double-strand cDNA on electrophoresis represented a smear from 0.2-2kb caused by complete digestion (Figure 2).

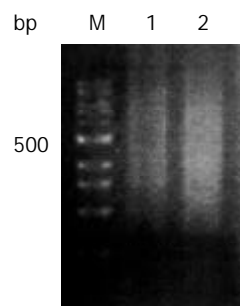


Figure 1 Size range of mRNA on 2 % agarose gel electrophoresis. Normal gastric mucosa mRNA (lane1) and gastric carcinoma mRNA (lane 2). 100 bp size marker (lane M).

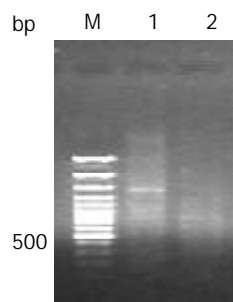


Figure 2 Digested and undigested double strands cDNA products. Undigested double strands cDNA products (lane 1) and *RsaI* digested double strands cDNA products (lane 2). 100bp size marker (lane M).

Detection of adaptor ligation efficiency and analyses of PCR products

A 0.75 kb band of tester1-1 and tester1-2 PCR product accorded with the theoretic size as expected when they were amplified with G3PDH3' primer and PCR1 primer respectively. The 0.75 kb band intensity of tester1-1 and tester1-2 PCR product also was as same as the band of tester1-1 and tester1-2 PCR product amplified with G3PDH3' and G3PDH5' primers (Figure 3). Secondary PCR product of subtraction sample exhibited a smear from 0.2-2 kb with some distinct bands that were greatly different from that appeared in unsubtraction samples (Figure 4).

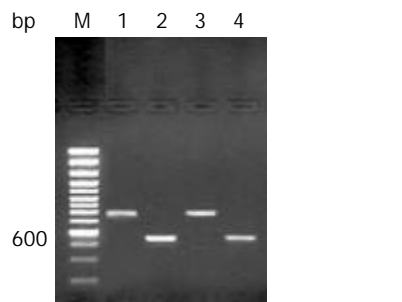


Figure 3 Detection of adaptors ligation efficiency. Tester1-1 was amplified with G3PDH3' primer, PCR primer1 (lane 1) and tester1-1 with G3PDH3', 5' primers (lane 2). Tester1-2 was amplified with G3PDH3' primer, PCR primer1 (lane 3) and tester1-2 with G3PDH3', 5' primers (lane 4). 100 bp size marker (lane M).

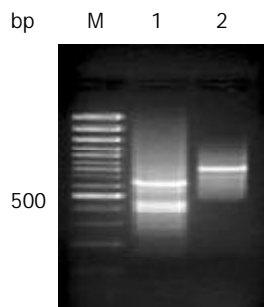


Figure 4 Analyses of PCR products. Secondary PCR products of subtraction samples (lane 1) and unsubtraction samples (lane 2). 100 bp size marker (lane M).

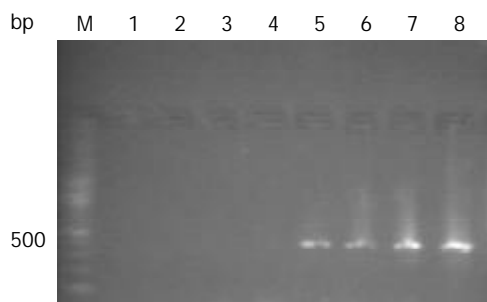


Figure 5 Identification of subtraction efficiency by PCR. G3PDH PCR products of subtracted samples at 18, 23, 28 and 33 cycles (lanes 1, 2, 3 and 4) respectively and G3PDH PCR products of unsubtracted samples respectively at 18, 23, 28 and 33 cycles (lanes 5, 6, 7 and 8). 100 bp size marker (lane M).

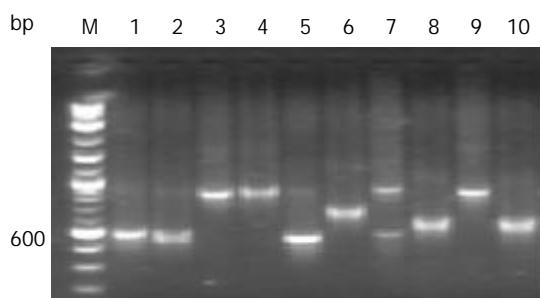


Figure 6 Identification of inserted fragments in plasmids of library by PCR. Inserted fragments in plasmids of library (lanes 1-10). 100 bp size marker (lane M).

Analyses of subtraction efficiency by PCR

G3PDH persistently was expressed at 18, 23, 28 and 33 cycles

of PCR and the bands exhibited greater and greater intensity with increasing cycle numbers in unsubtraction control group, but not expressed in subtraction group (Figure 5).

Identification of inserted fragments in plasmids of library by PCR and positive clone by reverse hybridization

PCR products of library plasmids amplified with SP6 and T7 primers on a larger scale showed that each plasmid included one inserted fragment ranging from 300-700 bp (Figure 6). 86 % of down-regulated genes between normal gastric mucosa and gastric carcinoma were confirmed by hybridization of a transferred filter with probes of reverse transcription product cDNAs.

DISCUSSION

Many genes involves in gastric tumorigenicity and tumor metastasis^[14-24]. Occurrence and development of gastric carcinoma are closely associated with loss or lower expression of suppressor genes^[25,26]. It contributes to a better understanding of the molecular mechanism of gastric tumorigenicity, and the expression profiles of down-regulated genes in gastric carcinoma, as well as cloning of novel genes, especially human stomach-specific gene. The novel genes usually express in lower abundance, and play an important role in cell differentiation and development. We have successfully established the cDNA suppression subtraction library to screen down-regulated genes in gastric carcinoma.

It is an important step to guarantee mRNA quality in constructing cDNA suppression subtraction library with a high subtraction efficiency because it is directly related to subtraction efficiency. Good mRNA quality depends on total RNA quality except for mRNA purification. To ensure good total RNA quality of 28S/18S ≥ 1.5 , samples must be immediately placed into liquid nitrogen after removed intraoperatively, and trituration of samples must be performed also in liquid nitrogen. At last, reverse transcription products (the first stranded cDNAs) of mRNA were electrophoresed to evaluate its size and quality. The mRNA size range should accord with its theoretic value.

Each step for establishing cDNA suppression subtraction library was verified by corresponding methods provided by Clontech to ensure subtraction efficiency. Many reports have shown that the suppression subtractive technique has successfully constructed a lots of cDNA suppression subtraction library with high efficiency, and cloned many novel genes^[27-45]. Our experiments were carried out strictly according to the rule. Identifications of experimental results step by step revealed complete enzyme cutting, and enzyme digested size of double-strand cDNA accorded with theoretic size range, enough ligation of the digested fragments of double-strand cDNA and adaptors. It demonstrated that, in cDNA suppression subtraction library with high subtractive efficiency, G3PDH was persistently expressed at 18, 23, 28 and 33 cycles of PCR and the bands exhibited greater and greater intensity with increasing cycles in unsubtraction control group, but not expressed in subtraction group.

After establishment of the cDNA suppression subtraction library with a high efficiency, maximum cloning of novel down-regulated genes in gastric cancer depends on highly efficient plasmid transformation method and competent bacteria cells. Lower abundance of gene fragments will be likely cloned if commercially available high concentration competent cells are used ($1 \times 10^{12} \cdot L^{-1}$) for transformation with a high transformation rate ($1-2 \times 10^8 / \mu g$ PUC19). Use of electroporation method can greatly enhance library plasmids transformation rate by obtaining $10^8 / \mu g$ PUC19. Additionally, it especially fits transformation of the small fragments produced in cDNA suppression subtraction library.

Several identified methods for cDNA suppression subtraction library were described below. The expression pattern of individual clones could be confirmed by Northern blot analysis. 10-20 clones were randomly picked from the subtracted library as probes on Northern blots. If less than two clones were confirmed as differentially expressed genes, the differential screening procedure should be performed to eliminate false positives. Dot or Southern blot analysis was performed. Secondary PCR products of the unsubtracted tester cDNA, the unsubtracted driver cDNA, and the subtracted cDNA were electrophoresed on a 1.5 % agarose gel, transferred onto nylon filters and hybridized respectively with differential expressing genes as probes labeled with α -³²PdCTP. But more background bands of unpredicted sizes often appeared. Nylon filters onto which the library colonies of bacteria were transferred and hybridized with reverse transcript product cDNA of gastric cancer tissues mRNA and normal gastric mucosa mRNA were used as probes labeled with α -³²PdCTP respectively. This method has been extensively used. The disadvantage is that only a high abundance of mRNA can be detected. Another approach can bypass the problem of losing a low-abundance of sequences. By this method, the subtracted library was hybridized with forward- and reversely-subtracted cDNA probes. To make reversely-subtracted probes, subtractive hybridization was performed with the original tester cDNA as a driver and the driver cDNA as a tester. Plasmids colonies that are truly differentially expressed will hybridize only with the forward-subtracted probe. Plasmids colonies that hybridize with the reversely-subtracted probe may be considered as the background. This approach requires one additional step: before it can be used as probes, the forward- and reversely-subtracted probes must undergo restriction enzyme digestion to remove the adaptor sequences. Despite their small size, these adaptors can cause a very high background when the subtracted probes are hybridized to the subtracted cDNA library.

REFERENCES

- Park WS**, Oh RR, Park JY, Yoo NJ, Lee SH, Shin MS, Kim SY, Kim YS, Lee JH, Kim HS, An WG, Lee JY. Mapping of a new target region of allelic loss at 21q22 in primary gastric cancers. *Cancer Lett* 2000; **159**: 15-21
- Kim HS**, Woo DK, Bae SI, Kim YI, Kim WH. Allelotype of the adenoma-carcinoma sequence of the stomach. *Cancer Detect Prev* 2001; **25**: 237-244
- Baffa R**, Santoro R, Bullrich F, Mandes B, Ishii H, Croce CM. Definition and refinement of chromosome 8p regions of loss of heterozygosity in gastric cancer. *Clin Cancer Res* 2000; **6**: 1372-1377
- Igarashi J**, Nimura Y, Fujimori M, Mihara M, Adachi W, Kageyama H, Nakagawara A. Allelic loss of the region of chromosome 1p35-pter is associated with progression of human gastric carcinoma. *Jpn J Cancer Res* 2000; **91**: 797-801
- Wang Q**, Chen H, Bai J, Wang B, Wang K, Gao H, Wang Z, Wang S, Zhang Q, Fu S. Analysis of loss of heterozygosity on 19p in primary gastric cancer. *Zhonghua Yixue Yichuanxue Zazhi* 2001; **18**: 459-461
- Sud R**, Wells D, Talbot IC, Delhanty JD. Genetic alterations in gastric cancers from British patients. *Cancer Genet Cytogenet* 2001; **126**: 111-119
- Chung YJ**, Choi JR, Park SW, Kim KM, Rhyu MG. Evidence for two modes of allelic loss: Multifocal analysis on both early and advanced gastric carcinomas. *Virchows Arch* 2001; **438**: 31-38
- Han HS**, Kim HS, Woo DK, Kim WH, Kim YI. Loss of heterozygosity in gastric neuroendocrine tumor. *Anticancer Res* 2000; **20**: 2849-2854
- Nishioka N**, Yashiro M, Inoue T, Matsuoka T, Ohira M, Chung KH. A candidate tumor suppressor locus for scirrhous gastric cancer at chromosome 18q 12.2. *Int J Oncol* 2001; **18**: 317-322
- Diatchenko L**, Lau YF, Campbell AP, Chenchik A, Moqadam F, Huang B, Lukyanov S, Lukyanov K, Gurskaya N, Sverdlov ED, Siebert PD. Suppression subtractive hybridization: A method for generating differentially regulated or tissue-specific cDNA probes and libraries. *Proc Natl Acad Sci USA* 1996; **93**: 6025-6030
- Yoshikawa Y**, Mukai H, Hino F, Asada K, Kato I. Isolation of two novel genes, down-regulated in gastric cancer. *Jpn J Cancer Res* 2000; **91**: 459-463
- Nagasaki K**, Manabe T, Hanzawa H, Maass N, Tsukada T, Yamaguchi K. Identification of a novel gene, LDOC1, down-regulated in cancer cell lines. *Cancer Lett* 1999; **140**: 227-234
- Jung MH**, Kim SC, Jeon GA, Kim SH, Kim Y, Choi KS, Park SI, Joe MK, Kimm K. Identification of differentially expressed genes in normal and tumor human gastric tissue. *Genomics* 2000; **69**: 281-286
- Wang B**, Shi LC, Zhang WB, Xiao CM, Wu JF, Dong YM. Expression and significance of P16 gene in gastric cancer and its pre-cancerous lesions. *Shijie Huaren Xiaohua Zazhi* 2001; **9**: 39-42
- Wang RQ**, Fang DC, Liu WW. MUC2 gene expression in gastric cancer and preneoplastic lesion tissues. *Shijie Huaren Xiaohua Zazhi* 2000; **8**: 285-288
- Machado JC**, Oliveira C, Carvalho R, Soares P, Berx G, Caldas C, Seruca R, Carneiro F, Sobrinho-Simoes M. E-cadherin gene (CDH1) promoter methylation as the second hit in sporadic diffuse gastric carcinoma. *Oncogene* 2001; **20**: 1525-1528
- Liu HF**, Liu WW, Fang DC, Yang SM, Wang RQ. Bax gene expression and its relationship with apoptosis in human gastric carcinoma and precancerous lesions. *Shijie Huaren Xiaohua Zazhi* 2000; **8**: 665-668
- He XS**, Su Q, Chen ZC, He XT, Long ZF, Ling H, Zhang LR. Expression, deletion [was deletion] and mutation of p16 gene in human gastric cancer. *World J Gastroenterol* 2001; **7**: 515-521
- Liu DH**, Zhang XY, Fan DM, Huang YX, Zhang JS, Huang WQ, Zhang YQ, Huang QS, Ma WY, Chai YB, Jin M. Expression of vascular endothelial growth factor and its role in oncogenesis of human gastric carcinoma. *World J Gastroenterol* 2001; **7**: 500-505
- Gu HP**, Ni CR, Zhan RZ. Relationship between CD15 mRNA and its protein expression and gastric carcinoma invasion. *Shijie Huaren Xiaohua Zazhi* 2000; **8**: 851-854
- Endo K**, Maejara U, Baba H, Tokunaga E, Koga T, Ikeda Y, Toh Y, Kohnoe S, Okamura T, Nakajima M, Sugimachi K. Heparanase gene expression and metastatic potential in human gastric cancer. *Anticancer Res* 2001; **21**: 3365-3369
- Nesi G**, Palli D, Pernice LM, Saieva C, Paglierani M, Kroning KC, Catarzi S, Rubio CA, Amorosi A. Expression of nm23 gene in gastric cancer is associated with a poor 5-year survival. *Anticancer Res* 2001; **21**: 3643-3549
- Murahashi K**, Yashiro M, Takenaka C, Matsuoka T, Ohira M, Chung KH. Establishment of a new scirrhous gastric cancer cell line with loss of heterozygosity at E-cadherin locus. *Int J Oncol* 2001; **19**: 1029-1033
- Wang CD**, Chen YL, Wu T, Liu YR. Association between lower expression of somatostatin receptor II gene and lymphoid metastasis in patients with gastric cancer. *Shijie Huaren Xiaohua Zazhi* 1999; **7**: 864-866
- Yamamoto M**, Tsukamoto T, Sakai H, Shirai N, Ohgaki H, Furihata C, Donehower LA, Yoshida K, Tatematsu M. p53 knock-out mice (-/-) are more susceptible than (+/-) or (+/+) mice to N-methyl-N-nitrosourea stomach carcinogenesis. *Carcinogenesis* 2000; **21**: 1891-1897
- Xu X**, Brodie SG, Yang X, Im YH, Parks WT, Chen L, Zhou YX, Weinstein M, Kim SJ, Deng CX. Haploid loss of the tumor suppressor Smad4/Dpc4 initiates gastric polyposis and cancer in mice. *Oncogene* 2000; **19**: 1868-1874
- Osheroov N**, Mathew J, Romans A, May GS. Identification of conidial transcripts in *Aspergillus nidulans* using suppression subtractive hybridization. *Fungal Genet Biol* 2002; **37**: 197-204
- Petersen S**, Petersen I. Expression profiling of lung cancer based on suppression subtraction hybridization (SSH). *Methods Mol Med* 2003; **75**: 189-207
- Liu ZW**, Zhao MJ, Li ZP. Identification of Up-regulated genes in rat regenerating liver tissue by suppression subtractive hybridization. *Shenwu Huaxue Yu Shengwu Wuli Xuebao (Shanghai)* 2001; **33**: 191-197
- Ji W**, Wright MB, Cai L, Flament A, Lindpaintner K. Efficacy of SSH PCR in isolating differentially expressed genes. *BMC Genomics* 2002; **3**: 12-14

- 31 **Shridhar V**, Sen A, Chien J, Staub J, Avula R, Kovats S, Lee J, Lillie J, Smith DI. Identification of underexpressed genes in early- and late-stage primary ovarian tumors by suppression subtraction hybridization. *Cancer Res* 2002; **62**: 262-270
- 32 **Tanaka F**, Hori N, Sato K. Identification of differentially expressed genes in rat hepatoma cell lines using subtraction and microarray. *J Biochem (Tokyo)* 2002; **131**: 39-44
- 33 **Lin S**, Chugh S, Pan X, Wallner EI, Wada J, Kanwar YS. Identification of up-regulated Ras-like GTPase, Rap1b, by suppression subtractive hybridization. *Kidney Int* 2001; **60**: 2129-2141
- 34 **Majda BT**, Meloni BP, Rixon N, Knuckey NW. Suppression subtraction hybridization and northern analysis reveal upregulation of heat shock, trkB, and sodium calcium exchanger genes following global cerebral ischemia in the rat. *Brain Res Mol Brain Res* 2001; **93**: 173-179
- 35 **Shi J**, Cai W, Chen X, Ying K, Zhang K, Xie Y. Identification of dopamine responsive mRNAs in glial cells by suppression subtractive hybridization. *Brain Res* 2001; **910**: 29-37
- 36 **Wang X**, Feuerstein GZ. Suppression subtractive hybridisation: Application in the discovery of novel pharmacological targets. *Pharmacogenomics* 2000; **1**: 101-108
- 37 **Dey R**, Son HH, Cho MI. Isolation and partial sequencing of potentially odontoblast-specific/enriched rat cDNA clones obtained by suppression subtractive hybridization. *Arch Oral Biol* 2001; **46**: 249-260
- 38 **Ye Z**, Connor JR. Identification of iron responsive genes by screening cDNA libraries from suppression subtractive hybridization with antisense probes from three iron conditions. *Nucleic Acids Res* 2000; **28**: 1802-1807
- 39 **Kim JY**, Chung YS, Paek KH, Park YI, Kim JK, Yu SN, Oh BJ, Shin JS. Isolation and characterization of a cDNA encoding the cysteine proteinase inhibitor, induced upon flower maturation in carnation using suppression subtractive hybridization. *Mol Cells* 1999; **9**: 392-397
- 40 **Diatchenko L**, Lukyanov S, Lau YF, Siebert PD. Suppression subtractive hybridization: A versatile method for identifying differentially expressed genes. *Methods Enzymol* 1999; **303**: 349-380
- 41 **Fang J**, Shi GP, Vaghy PL. Identification of the increased expression of monocyte chemoattractant protein-1, cathepsin S, UPIX-1, and other genes in dystrophin-deficient mouse muscles by suppression subtractive hybridization. *J Cell Biochem* 2000; **79**: 164-172
- 42 **Zhang L**, Cilley RE, Chinoy MR. Suppression subtractive hybridization to identify gene expressions in variant and classic small cell lung cancer cell lines. *J Surg Res* 2000; **93**: 108-119
- 43 **Chim SS**, Cheung SS, Tsui SK. Differential gene expression of rat neonatal heart analyzed by suppression subtractive hybridization and expressed sequence tag sequencing. *J Cell Biochem* 2000; **80**: 24-36
- 44 **Porkka KP**, Visakorpi T. Detection of differentially expressed genes in prostate cancer by combining suppression subtractive hybridization and cDNA library array. *J Pathol* 2001; **193**: 73-79
- 45 **Villalva C**, Trempat P, Zenou RC, Delsol G, Brousset P. Gene expression profiling by suppression subtractive hybridization (SSH): A example for its application to the study of lymphomas. *Bull Cancer* 2001; **88**: 315-319

Edited by Zhang JZ

Observation of DNA damage of human hepatoma cells irradiated by heavy ions using comet assay

Li-Mei Qiu, Wen-Jian Li, Xin-Yue Pang, Qing-Xiang Gao, Yan Feng, Li-Bin Zhou, Gao-Hua Zhang

Li-Mei Qiu, Wen-Jian Li, Yan Feng, Li-Bin Zhou, Gao-Hua Zhang, Institute of Modern Physics, the Chinese Academy of Sciences, Lanzhou 730000, Gansu Province, China
Xin-Yue Pang, Qing-Xiang Gao, School of Life Science, Lanzhou University, Lanzhou 730000, Gansu Province, China
Supported by President Special Foundation of Chinese Academy of Sciences, grant No. TB990601

Correspondence to: Li-Mei Qiu, Institute of Modern Physics, the Chinese Academy of Sciences, Lanzhou 730000, Gansu Province, China. qiuqiu69@sina.com

Telephone: +86-931-4969338 **Fax:** +86-931-4969201

Received: 2002-10-22 **Accepted:** 2002-11-28

Abstract

AIM: Now many countries have developed cancer therapy with heavy ions, especially in GSI (Gesellschaft für Schwerionenforschung mbH, Darmstadt, Germany), remarkable results have obtained, but due to the complexity of particle track structure, the basic theory still needs further researching. In this paper, the genotoxic effects of heavy ions irradiation on SMMC-7721 cells were measured using the single cell gel electrophoresis (comet assay). The information about the DNA damage made by other radiations such as X-ray, γ -ray, UV and fast neutron irradiation is very plentiful, while little work have been done on the heavy ions so far. Hereby we tried to detect the reaction of liver cancer cells to heavy ion using comet assay, meanwhile to establish a database for clinic therapy of cancer with the heavy ions.

METHODS: The human hepatoma cells were chosen as the test cell line irradiated by 80Mev/u $^{20}\text{Ne}^{10+}$ on HIRFL (China), the radiation-doses were 0, 0.5, 1, 2, 4 and 8 Gy, and then comet assay was used immediately to detect the DNA damages, 100-150 cells per dose-sample (30-50 cells were randomly observed at constant depth of the gel). The tail length and the quantity of the cells with the tail were put down. EXCEL was used for statistical analysis.

RESULTS: We obtained clear images by comet assay and found that SMMC-7721 cells were all damaged apparently from the dose 0.5Gy to 8Gy (*t*-test: $P < 0.001$, vs control). The tail length and tail moment increased as the doses increased, and the number of cells with tails increased with increasing doses. When doses were higher than 2Gy, nearly 100 % cells were damaged. Furthermore, both tail length and tail moment, showed linear equation.

CONCLUSION: From the clear comet assay images, our experiment proves comet assay can be used to measure DNA damages by heavy ions. Meanwhile DNA damages have a positive correlation with the dose changes of heavy ions and SMMC-7721 cells have a great radiosensitivity to $^{20}\text{Ne}^{10+}$. Different reactions to the change of doses indicate that comet assay is a useful tool to detect DNA damage induced by heavy ions.

Qiu LM, Li WJ, Pang XY, Gao QX, Feng Y, Zhou LB, Zhang GH. Observation of DNA damage of human hepatoma cells irradiated

by heavy ions using comet assay. *World J Gastroenterol* 2003; 9(7): 1450-1454

<http://www.wjgnet.com/1007-9327/9/1450.asp>

INTRODUCTION

During the past few decades, radiation research has developed into specialized sub-disciplines, from basic physics and chemistry to tumor biology and experimental radiation therapy^[1]. Although the radiobiological effects are extensively investigated for X-ray and γ -ray, little work has been directed towards heavy ion beams. With the exploration of the outer space, the research of high linear energy transfer (LET) has attracted more and more attention. Since heavy ions were first applied in the mid-1970s to cure cancer at Bevalac of Lawrence Berkeley Laboratory (LBL), United States, promising results have been reported when compared with the conventional radiotherapy for soft tissue sarcoma, bone sarcoma and prostate cancer^[2]. Now scientists in many countries (GSI in Germany, HIMAC in Japan^[25,26], HIRFL in China) have designed accelerators to deliver beams of ions for the treatment and started basic researches of cancer therapy with heavy ions such as carbon, neon, oxygen and argon.

The aim of our present study was to investigate DNA damages induced by heavy ions by comet assay. The theoretical value was then compared to responses to external X-ray or γ -ray and other irradiations, so that we could establish the data base for clinical therapy.

Comet assay, the alkaline version in particular, has become a very popular method for the analysis of DNA damage caused by various chemical and physical agents because of its simplicity and rapidity^[4-10]. DNA damages consisted of DNA strand breakage, alkali-labile sites and incomplete excision repair sites^[11]. Although the direct DNA-breaking capacity can be estimated by alkaline elution, nick translation and alkaline single cell gel electrophoresis (SCGE), SCGE has been shown to be more sensitive than the former two. It had been proved that the sensitivity of SCGE is significantly higher than that of cytokinesis-blocked micronucleus (CBMN) test^[12]. The most important point is that comet assay is an electrophoretic technique, which allows measurements of DNA damages as well as DNA repair rates on an individual cell. Therefore its contribution to DNA damages by irradiating cells with heavy ions at once or after a while can be reflected as initial damages or residual DNA damages, if time is allowed for enzymatic repairs of initial DNA strand break. In our lab, we focused on the radiobiological effects of heavy ions on tumor cells. Previous experiments were mainly on cell survival measurements and could not explain the underlying radiosensitization mechanism at molecular level^[2]. To verify the radiobiological effects of heavy ions on cellular DNA, SCGE also called comet assay was used to directly measure DNA damages in cells.

MATERIALS AND METHODS

Cells and cell culture

Human hepatoma cells SMMC-7721, purchased from Second Military Medical University in Shanghai, were cultivated in

RMIP-1640 medium (Gibco product) supplemented with 15 % calf serum in a standard incubator at 37 °C. One passage of cells every 2-3 days and change of the medium everyday were performed, to ensure the cells growth in good conditions. Two days before the irradiation, the cells were shifted to Φ 35 mm petri-dishes, each had 2 ml cell suspension, and the density of the cells was 5×10^4 cells/ml. Each dose had 5 petri-dishes. Before irradiation, cells in each petri-dish were examined under the inverted light microscope to select materials good in growth and even in density, and medium 1640 in petri-dishes was removed, only Dulbecc' s phosphate -buffered saline medium (PBS) was left to keep the moisture of the cells when irradiated.

Selection of ion beams

Irradiation was performed using $^{20}\text{Ne}^{10+}$ with energy of 80 Mev/u and intensity of 0.00136nA (2.1×10^6 p/s). The cells were irradiated at the doses of 0, 0.5, 1, 2, 4, 8Gy. The doses of cells were measured by an air ionization chamber.

Preparation of single cell suspension and comet assay

As soon as irradiation ended, the cells were washed and collected, the final concentration of cells was adjusted to $(5-10) \times 10^6$ by adding Dulbecc' s phosphate -buffered saline medium (PBS) to the single cell suspension.

The alkaline version of comet assay was carried out based on the work of Ostling and Johansson with some minor modifications as followings: On the day of electrophoresis, an aliquot of 10 μ l freshly prepared suspension of cells was mixed with 30 μ l 0.5 % low- melting-agarose in Dulbecc' s PBS (pH 7.4). The mixture was layered on top of an ordinary microscope slide precoated with 0.5 % normal-melting -agorose, which was allowed to dry at room temperature protected from dust and other particles. After low-melting-agarose was solidified in a refrigerator for 10 minutes, the coverslip was carefully removed and the slide was gently immersed in a freshly prepared lysing solution (2.5MNaCl, 10mM Tris, 1 % sodium lauryl sarcosinate, 100mM Na₂EDTA, with 1 % Triton-100 and 10 % DMSO added just before use). From this moment until the end of neutralization, all steps needed to avoid the sunlight.

After lysis for 1-1.5 h, the microscopy slides were transferred to electrophoresis session, 18 microscopy slides from 6 samples (3 slides/each sample) were randomly placed in a electrophoretic unit.

After 20-30 minutes of DNA unwinding in electrophoresis buffer (1 mM EDTA-Na₂, 300 mM NaOH, pH>13), single cell gel electrophoresis was performed in the same buffer (20 min, 20 V, 300 nA). After electrophoresis the slides were neutralized with 0.4 M Tris buffer (pH7.5).

Evaluation of DNA damage

The microscopy slides were stained with ethidium bromide in water (40 μ g/ml, 50 μ l/slide). After application of a coverslip was removed, each slide was examined at 10 \times 20 magnification in a fluorescence microscope (excitation filter: 400nm, barrier filter: 590nm). 100-150 cells per dose-sample (30-50 cell were randomly observed at constant depth of the gel, avoiding the edges of the gel on each of three replicate slides). The tail length and the quantity of the cells with the tail were put down, at the same time, photos were taken with 135# black and white film (ISO 400). Then analysis was done using EXCEL.

RESULTS AND DISCUSSION

Formation of comet assay images-DNA loops and alkaline unwinding

The comet assay is attractive for many reasons. Apart from

being a quick, simple, sensitive, reliable and fairly inexpensive way of measuring, it also produces appealing images.

There are two explanations about what the comet tails consist of. One is that it is a fragment DNA, the other is that the length of such a fragment is about 1 μ m, but the length of the tail of a comet is a few percentages of it^[13-16], as to our experiment the longest mean length of tail was no more than 200 μ m. Nuclear DNA is not a tangle of string, even after treatment with detergents and a strong salt solution, as in the SCGE procedure, the nuclear (or nucleoid) had a structure, the DNA was organized as loops, which retained the super coils that were contained in the nucleosome. Cook *et al*^[17] deduced the presence of supercoiled loops and then they observed that, when DNA was broken by irradiation, supercoiling was relaxed and loops spilled out into a 'halo' around the nucleoid. By analogy, it is assumed that the Comet tail is made up of relaxed loops, and that the number of loops in the tail indicates the number of DNA breaks.

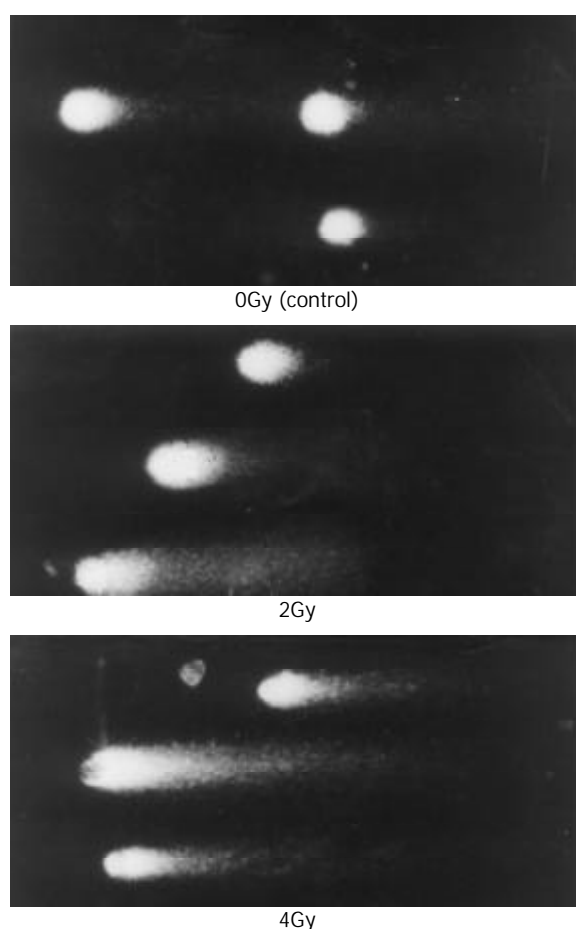


Figure 1 Comet assay image at different doses.

The alkaline comet assay can detect DNA breaks including single and double DNA strand breaks, and AP sites, which are alkali-labile and probably converted to breaks while DNA is in the electrophoretic solution at high pH^[14-16]. The present comet assay is generally practiced including incubation of DNA at high pH before and during electrophoresis, different from the original work of Ostling and Johansson who employed near-neutral pH. Collins AR^[13] proved that both the neutral and alkaline methods could detect low levels of DNA damage, however, the breaks by higher levels of damage were more clearly resolved from the head under alkaline conditions^[18]. Thus in our experiment, the alkaline version was used.

Furthermore, breaks will be transiently present when cells repair lesions via base excision or nucleotide excision so that

a high level of breaks in the Comet assay may indicate either severe damage or efficient repair^[13]. In fact, much useful information can be obtained by exploiting cellular repair to produce DNA breaks and thus to reveal or amplify the effect of radiation that otherwise may not show positive effects by the comet assay. This will be discussed in our later work on the repair effects of heavy ions.

DNA damage caused by heavy ions

The SCGE test or comet assay is a straightforward visual method for the detection of DNA damage of cells in interphase. This technique is especially sensitive in detecting DNA single-strand breaks, alkali-labile damage and excision repair sites in individual cells^[13-16]. The Comet assay has been widely applied in the following fields: radiation biology^[5-6,9-12,19], excisable DNA damage, DNA cross-links^[20], oxidative damage^[21,22], genetic toxicology and apoptosis^[23,24].

Ionizing radiation is a ubiquitous environmental agent. Its physiochemical interaction with cellular DNA produces a variety of primary lesions, such as single-strand breaks (SSB), double-strand breaks (DSB), DNA-DNA and DNA-protein crosslinks, and damage to purine and pyrimidine bases. And using ionizing radiation may avoid complications of drug metabolism, intracellular distribution, membrane permeability and drug efflux. Although the technique of SCGE is very sensitive to ionizing radiation, information about DNA damage made by other radiations such as X-ray^[10,12], γ -ray^[8,9], UV^[9] and fast neutron^[19] irradiation is very plentiful, little work has been done on heavy ions so far.

Microdosimetric considerations suggest that, in a given type of radiation, the yield DNA damage must be proportional to dose, so that besides the influence of changing repair efficiency, the magnitude of the dose might not be expected to be critical in comparison of the results. Heavy ion is a kind of high LET (Linear Energy Transfer) irradiation, as emphasized long ago by Lea, high-LET radiation could, through the increased frequency of DSB in close proximity, cause interactive damages and misrepair^[27-28]. We anticipated that heavy ions probably had strong effects on the cellular DNA, but we wonder if it can make the linear equation after irradiation by heavy ions.

In our experiment, the data for DNA damages induced by heavy ions at the doses of 0-8Gy are presented in Table 1. The dose-response curves for tail length and tail moment (the fraction of DNA in the tail multiplied by tail length) are shown in Figure 2. We could see tail length and tail moment showed linear equation. It proved that SMMC-7721 cells have high radiosensitivity to heavy ions and comet assay is very useful to detect DNA damages induced by heavy ions.

Figure 3 shows the change of tail DNA as the dose increased. It was found that almost 100 % cells were damaged when the dose reached at 2Gy. But the details were unknown about how badly DNA was damaged when the dose was higher than 2Gy. To completely evaluate DNA damages by different doses, comets of every dose-sample were sorted visually into classes 0-4, representing increasing amount of damage. Figure 4, result shows that with increase of the dose, slighter damage of DNA tail (class 0-2) converted to more severe change of DNA (DNA migrated from the head to form longer and longer tail).

We should pay more attention to the dose of 2Gy, which is the conventional choice of γ -ray radiotherapy. At the dose of 2 Gy, 100 % cells were damaged, with different grade of DNA damage (classes 1-4). Among them nearly 25 % cells were badly damaged. It is known that a central phenomenon in radiobiology is the efficiency of densely ionizing radiation for cellular effects. As in our experiment, chromosomal aberrations or cell killing occurred on these badly damaged cells^[27-30, 33-35]. Additionally, we noticed that nearly 80 % cells

were most severely damaged (class 4) at the dose of 8Gy. It showed that 8Gy might be or near the highest dose that the cells could withstand.

Table 1 Values of damages detected by Comet assay after 80Mev/u ²⁰Ne¹⁰⁺ irradiation

Dose Gy	Tail length mean \pm S.E. μ m	Tail DNA mean \pm S.E. %	Tail moment mean \pm S.E.	t-test P
0	29.44 \pm 1.46	38.50 \pm 3.50	11.53 \pm 1.45	
0.5	54.18 \pm 11.74	59.21 \pm 9.21	33.02 \pm 11.80	2.06227E-07
1	90.16 \pm 6.66	85.54 \pm 2.21	76.96 \pm 3.44	8.7291E-21
2	115.09 \pm 3.26	100.00 \pm 0.00	115.09 \pm 3.25	6.97944E-31
4	134.17 \pm 8.18	98.86 \pm 1.07	134.17 \pm 8.10	4.48617E-68
8	194.08 \pm 15.58	100.00 \pm 0.00	194.08 \pm 15.58	6.4087E-104

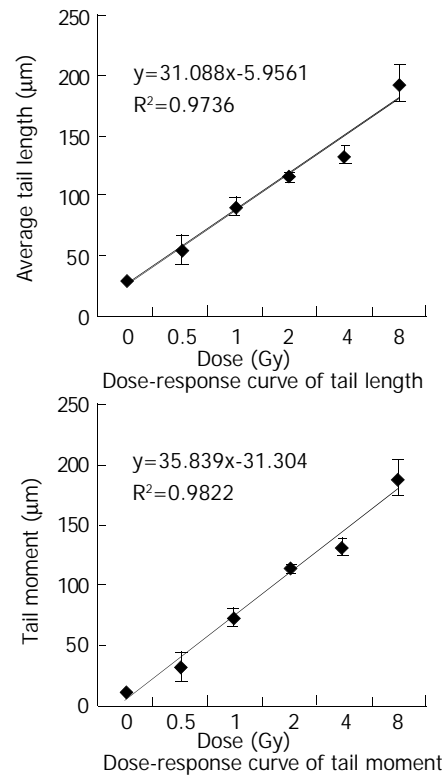


Figure 2 Curve of tail length and tail moment.

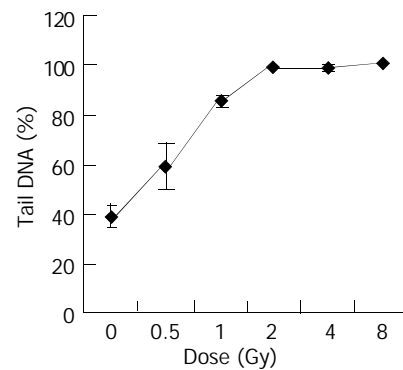


Figure 3 Dose-response curve of tail DNA.

One thing to be mentioned here is that the relative biological effectiveness (RBE) tends to increase with linear energy transfer (LET). For very heavy ions with LET in excess of about 100-200 keV/ μ m, a more complex dependence on particle track structure emerges^[31,32]. Therefore, the study on particle track structure is very important for further research.

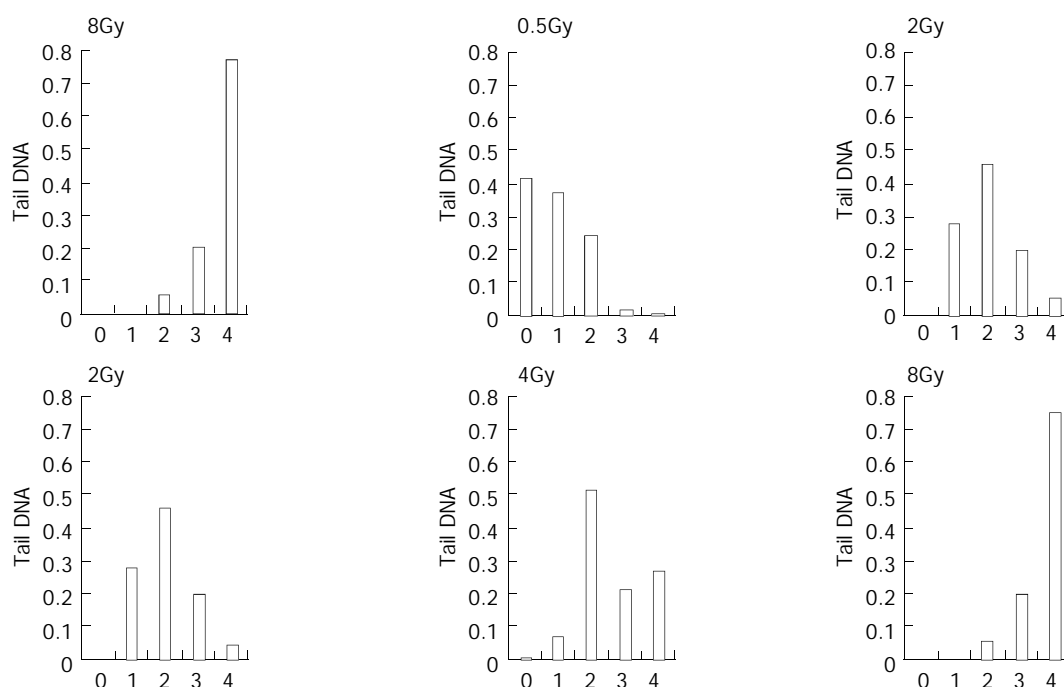


Figure 4 Comet class at the dose of 0-8Gy of heavy ions irradiation.

REFERENCES

- Dorr W**, Dorschel B, Sprinz H. Report on the third annual meeting of the Society for Biological Radiation Research, GBS '99. *Radiat Environ Biophys* 2000; **39**: 147-152
- Li WJ**, Gao QX, Zhou GM, Wei ZQ. Micronuclei and cell survival in human liver cancer cells irradiated by 25MeV/u $^{40}\text{Ar}^{14+}$. *World J Gastroenterol* 1999; **5**: 365-368
- Zhou GM**, Chen WQ, Gao QX, Li WJ, Li Q, Wei ZQ. Biological effects of hepatoma cells irradiated by 25MeV/u $^{40}\text{Ar}^{14+}$. *World J Gastroenterol* 1998; **4**: 271-272
- Wojewodzka M**, Kruszewski M, Iwanenko T, Collins AR, Szumiel I. Application of the comet assay for monitoring DNA damage in workers exposed to chronic low-dose irradiation. I. Strand breakage. *Mutat Res* 1998; **416**: 21-35
- Kruszewski M**, Wojewodzka M, Iwanenko T, Collins AR, Szumiel I. Application of the comet assay for monitoring DNA damage in workers exposed to chronic low-dose irradiation. II. Base damage. *Mutat Res* 1998; **416**: 37-57
- Muller WU**, Bauch T, Stuben G, Sack H, Streffer C. Radiation sensitivity of lymphocytes from healthy individuals and cancer patients as measured by the comet assay. *Radiat Environ Biophys* 2001; **40**: 83-89
- Wojewodzka M**, Kruszewski M, Iwanenko T, Collins AR, Szumiel I. Lack of adverse effect of smoking habit on DNA strand breakage and base damage, as revealed by the alkaline comet assay. *Mutat Res* 1999; **440**: 19-25
- Mayer C**, Popanda O, Zelezny O, von Brevern MC, Bach A, Bartsch H, Schmezer P. DNA repair capacity after gamma-irradiation and expression profiles of DNA repair genes in resting and proliferating human peripheral blood lymphocytes. *DNA Repair (Amst)* 2002; **1**: 237-250
- Mohankumar MN**, Paul SF, Venkatachalam P, Jeevanram RK. Influence of in vitro low-level gamma-radiation on the UV-induced DNA repair capacity of human lymphocytes-analysed by unscheduled DNA synthesis (UDS) and comet assay. *Radiat Environ Biophys* 1998; **37**: 267-275
- Koppen G**, Angelis KJ. Repair of X-ray induced DNA damage measured by the comet assay in roots of *Vicia faba*. *Environ Mol Mutagen* 1998; **32**: 281-285
- Cebulska-Wasilewska A**, Nowak D, Niedzwied ZW, Anderson D. Correlations between DNA and cytogenetic damage induced after chemical treatment and radiation. *Mut Res* 1998; **421**: 83-91
- He JL**, Chen WL, Jin LF, Jin HY. Comparative evaluation of the *in vitro* micronucleus test and the comet assay for the detection of genotoxic effects of X-ray radiation. *Mut Res* 2000; **469**: 223-231
- Collins AR**, Dobson VL, Dusinska M, Kennedy G, Stetina R. The comet assay: what can it really tell us? *Mutat Res* 1997; **375**: 183-193
- McNamee JP**, McLean JR, Ferrarotto CL, Bellier PV. Comet assay: rapid processing of multiple samples. *Mutat Res* 2000; **466**: 63-69
- Godard T**, Gauduchon P, Debout C. A first step in visual identification of different cell populations by a modified alkaline comet assay. *Mutat Res* 2002; **520**: 207-211
- Mariano Ruiz de Almodovar J**, Guirado D, Isabel Nunez M, Lopez E, Guerrero R, Teresa Valenzuela M, Villalobos M, del Moral R. Individualization of radiotherapy in breast cancer patients: possible usefulness of a DNA damage assay to measure normal cell radiosensitivity. *Radiation Oncol* 2002; **62**: 327-333
- Cook PR**, Brazell IA, Jost E. Characterization of nuclear structures containing superhelical DNA. *J Cell Sci* 1976; **22**: 303-324
- Hartmann A**, Agurell E, Beevers C, Brendler-Schwaab S, Burlinson B, Clay P, Collins A, Smith A, Speit G, Thybaud V, Tice RR. Recommendations for conducting the *in vivo* alkaline Comet assay. *Mutagenesis* 2003; **18**: 45-51
- Gajendiran N**, Tanaka K, Kamada N. Comet assay to sense neutron 'fingerprint'. *Mutat Res* 2000; **452**: 179-187
- Merk O**, Reiser K, Speit G. Analysis of chromate-induced DNA-protein crosslinks with the comet assay. *Mutat Res* 2000; **471**: 71-80
- Guertens G**, De Boeck G, Highley M, van Oosterom AT, de Bruijn EA. Oxidative DNA damage: biological significance and methods of analysis. *Crit Rev Clin Lab Sci* 2002; **39**: 331-457
- Godard T**, Deslandes E, Sichel F, Poul JM, Gauduchon P. Detection of topoisomerase inhibitor-induced DNA strand breaks and apoptosis by the alkaline comet assay. *Mutat Res* 2002; **520**: 47-56
- Heng Z**, Li R, Zhang Z. Distinguishing apoptotic cells from DNA strand-broken cells by comet assay. *Weisheng Yanjiu* 2001; **30**: 149-151
- Roser S**, Pool-Zobel BL, Rechkemmer G. Contribution of apoptosis to responses in the comet assay. *Mutat Res* 2001; **497**: 169-175
- Ando K**. High LET radiobiology at NIRS-current status and future plan. *Phys Med* 2001; **17**(Suppl): 292-295
- Imamura M**, Murata T, Akagi K, Tanaka Y, Imamura M, Inoue K, Mizuma N, Kobayashi Y, Watanabe H, Hachiya M, Akashi M, Furusawa Y, Yamanaka H, Takahashi S, Nakano T, Nagaoka S, Ohnishi T, Obiya Y, Harada K. Relationship between LET and

- RBE values for *Escherichia coli* determined using carbon ion beams from the TIARA cyclotron and HIMAC synchrotron. *J Gen Appl Microbiol* 1997; **43**: 175-177
- 27 **Sutherland BM**, Bennett PV, Schenk H, Sidorkina O, Laval J, Trunk J, Monteleone D, Sutherland J. Clustered DNA damages induced by high and low LET radiation, including heavy ions. *Phys Med* 2001; **17**(Suppl): 202-204
- 28 **Goodwin EH**, Blakely EA. Heavy ion-induced chromosomal damage and repair. *Adv Space Res* 1992; **12**: 81-89
- 29 **Blakely EA**. New measurements for hadrontherapy and space radiation: biology. *Phys Med* 2001; **17**(Suppl): 50-58
- 30 **Suzuki M**, Kase Y, Yamaguchi H, Kanai T, Ando K. Relative biological effectiveness for cell-killing effect on various human cell lines irradiated with heavy-ion medical accelerator in Chiba (HIMAC) carbon-ion beams. *Int Radiat Oncol Biol Phys* 2000; **48**: 241-250
- 31 **Katz R**, Cucinotta FA. Tracks to therapy. *Radiat Meas* 1999; **31**: 379-388
- 32 **Kraxenberger F**, Weber KJ, Friedl AA, Eckardt-Schupp F, Flentje M, Quicken P, Kellerer AM. DNA double-strand breaks in mammalian cells exposed to gamma rays and very heavy ions. Fragment-size distributions determined by pulsed-field gel electrophoresis. *Radiat Environ Biophys* 1998; **37**: 107-115
- 33 **Edwards AA**. RBE of radiations in space and the implications for space travel. *Phys Med* 2001; **17**(Suppl): 147-152
- 34 **Rydberg B**, Loblrich M, Cooper PK. Repair of clustered DNA damage caused by high LET radiation in human fibroblasts. *Phys Med* 1998; **14**(Suppl): 24-28
- 35 **Belli M**. An overview of recent charged-particle radiation biology in Italy. *Phys Med* 2001; **17**(Suppl): 278-282

Edited by Zhao P, Zhu LH and Wang XL

Preparation and characterization of polyclonal antibodies against ARL-1 protein

Jun-Fei Jin, Liu-Di Yuan, Li Liu, Zhu-Jiang Zhao, Wei Xie

Jun-Fei Jin, Liu-Di Yuan, Li Liu, Zhu-Jiang Zhao, Wei Xie, Genetics Research Center, Medical School, Southeast University, Nanjing 210009, Jiangsu Province, China

Supported by Health Department Grant of Jiang Su Province (H9925) and National Award for Excellent Research and Teaching from the Ministry of Education (2001/182)

Correspondence to: Dr. Wei Xie, Genetics Research Center, Medical School, Southeast University, Nanjing 210009, Jiangsu Province, China. wei.xie@seu.edu.cn

Telephone: +86-25-3220761 **Fax:** +86-25-3220761

Received: 2002-11-19 **Accepted:** 2002-12-18

Abstract

AIM: To prepare and characterize polyclonal antibodies against aldose reductase-like (ARL-1) protein.

METHODS: ARL-1 gene was inserted into the *E. coli* expression vector pGEX-4T-1(His)₆C and vector pQE-30. Recombinant ARL-1 proteins named ARL-(His)₆ and ARL-GST were expressed. They were purified by affinity chromatography. Sera from domestic rabbits immunized with ARL-(His)₆ were purified by CNBr-activated sepharose 4B coupled ARL-GST. Polyclonal antibodies were detected by Western blotting.

RESULTS: Recombinant proteins of ARL-(His)₆ with molecular weight of 35.7 KD and ARL-GST with molecular weight of 60.8 KD were highly expressed. The expression levels of ARL-GST and ARL-(His)₆ were 15.1 % and 27.7 % among total bacteria proteins, respectively. They were soluble, predominantly in supernatant. After purification by non-denatured way, SDS-PAGE showed one band. In the course of polyclonal antibodies purification, only one elution peak could be seen. Western blotting showed positive signals in the two purified proteins and the bacteria transformed with pGEX-4T-1(His)₆C-ARL and pQE-30-ARL individually.

CONCLUSION: Polyclonal antibodies are purified and highly specific against ARL-1 protein. ARL-GST and ARL-(His)₆ are highly expressed and purified.

Jin JF, Yuan LD, Liu L, Zhao ZJ, Xie W. Preparation and characterization of polyclonal antibodies against ARL-1 protein. *World J Gastroenterol* 2003; 9(7): 1455-1459
<http://www.wjgnet.com/1007-9327/9/1455.asp>

INTRODUCTION

Aldose reductase (AR) is a NADPH-dependent enzyme that is involved in diabetic complications^[1-17]. Some reports showed that AR was induced in rat hepatoma, suggesting that it may be essential for detoxifying harmful metabolites produced by fast growing cancer cells^[18-27]. Partial sequence determination of a protein induced in rat hepatoma called Spot 17 showed that it was highly homologous to the rat AR^[28,29]. Cao *et al.*^[22] found about 29 % of liver cancers over-expressed AR. Moreover, they identified a novel human protein that was

highly homologous to AR, then submitted it to GenBankTM (HARL U37100). This protein, known as ARL-1, consists of 316 amino acids, the same size as AR, and its amino acid sequence is 71 % identical to that of AR. About 54 % of hepatocellular carcinoma (HCC) over-express ARL-1 gene. These suggest ARL-1 might be related to liver cancers.

ARL-1 is a novel gene, its function and exact relationship with liver cancers are unclear. In order to clarify the role of ARL-1 in HCC, two recombinant proteins of ARL-(His)₆ and ARL-GST were expressed, and highly specific polyclonal antibodies against ARL-1 protein were prepared.

MATERIALS AND METHODS

Restrictive endonuclease and T4 DNA polymerase enzymes were purchased from TaKaRa Biotech Corp. Glutathione sepharose 4B, CNBr-activated sepharose 4B and pGEX-4T-1(His)₆C were obtained from Pharmacia Biotech. Rainbow markers and mid-range protein molecular weight markers were obtained from Amersham Pharmacia Biotech and Promega, respectively. PVDF membrane was from Schleicher & Schüll. T4 DNA ligase and GeneRulerTM 100 bp DNA ladder plus were products of MBI Fermentas. TALON^R metal affinity resin was obtained from Clontech. Freund's adjuvant incomplete and Freund's adjuvant complete were purchased from Sigma. *E. coli* strains were from Stratagene. Horseradish peroxidase (HRP)-conjugated anti-rabbit secondary antibody was from New England Biolabs Inc.

The following primers used in this study were made by HaoJia Corp: cg gaa ttc atg gcc acg ttt gtg gag c, cg ctc gag tca ata ttc tgc atc gaa ggg according to GenBankTM (accession number HARLU37100).

RT-PCR to subclone cDNA of ARL-1

According to the reference^[22], cDNA of ARL-1 was obtained by RT-PCR (data not shown).

Expression of ARL-1 in *E. coli*

ARL-1 polymerase chain reaction-amplified products were inserted into the *E. coli* expression vector pGEX-4T-1(His)₆C, and their proteins would be translated in-frame from the vector's start codon. The plasmid DNA was then transformed into bacteria host BL21. Induction of expression of ARL-1 inserts and purification of the recombinant proteins named ARL-GST were done according to the manufacturer's manual. Briefly, bacteria growing to $A_{600}=0.4$ were induced by 0.05 mM isopropyl-1-thio- β -D-galactopyranoside at 30 °C overnight. Cells were harvested and lysed by sonication. After centrifugation to remove debris, the supernatant was mixed with a 50 % slurry of glutathione sepharose 4B, which bound to the glutathione S-transferase (GST) at the amino terminus of the recombinant protein. The slurry was then loaded onto a column and eluted with 5 bed volumes of elution buffer (10 mM reduced glutathione in 50 mM Tris-HCL, pH 8.0). Fractions of 500 μ L were collected, and samples from the column were analyzed in 15 % SDS-polyacrylamide gel electrophoresis. Fractions containing the recombinant protein ARL-GST were stored at -20 °C.

We subcloned ARL-1 gene into another *E. coli* expression vector pQE-30 (Qiagen), expressed another recombinant protein named ARL-(His)₆. According to the user manual, ARL-(His)₆ was purified with TALON[®] metal affinity resin whose cobaltions bound to the 6-histidine residues at the amino terminus of the recombinant protein. Briefly, TALON[®] metal affinity resin was saturated with a bacterial polyhistidine-tagged GFPuv lysate in extraction buffer (pH 8.0). The resin was then washed twice with 5 mL of wash buffer (pH 7.0). At last, bound protein was eluted by washing three times with 1 mL elution buffer (pH 7.0), a sample of each eluate was analyzed by electrophoresis on a 15 % SDS-polyacrylamide gel to verify the purity of elution protein. The purified ARL-(His)₆ was stored at -20 °C.

Preparation of polyclonal antibodies against ARL-1 protein

Domestic rabbits were injected with 0.4 mg recombinant protein ARL-(His)₆ with Freund's complete adjuvant. Three weeks later, they were injected with 0.16 mg ARL-(His)₆ with Freund's incomplete adjuvant, which was repeated four times at 2-week intervals. After a little serum was collected from rabbit ear and proved positive by double agar diffusion test, rabbit sera were taken by carotid intubation and stored in 0.1 % sodium azide at -20 °C.

According to the manufacturer's manual, polyclonal antibodies against ARL-1 protein were purified with CNBr-activated sepharose 4B. Firstly, rabbit sera were filtered through a 0.22 μm filter and diluted one to four times with phosphate-buffered saline (PBS, pH 7.4). Secondly, the gel was prepared with 1mM HCL. The purified recombinant protein ARL-GST was then coupled with the prepared gel in coupling buffer (0.1M NaHCO₃, pH 8.3, containing 0.5M NaCl). Finally, the prepared rabbit sera were mixed with the sepharose coupled ARL-GST in a stopped vessel. The mixture was rotated end-over-end overnight at 4 °C and subsequently stood at room temperature for hours. The gel was washed with 1×PBS (pH 7.4), 2M NaCl in 1×PBS (pH 7.4) and 1×PBS (pH 4.5) till the OD₂₈₀ of washed solution was zero, respectively. At last, it was eluted with 0.1M glycine (pH 2.8). The polyclonal antibodies were collected in 0.05 mM Tris-base (pH 9.5) and stored in 0.1 % sodium azide at -20 °C.

Western blotting

All plasmids including pGEX-4T-1(His)₆C-ARL, pGEX, pQE-30-ARL and pET-CTF that encoded protein ARL-GST, GST, ARL-(His)₆ and CTF-(His)₆, were transformed to BL21, respectively. After bacteria grew to A₆₀₀=0.4, they were induced by 0.05 mM isopropyl-1-thio-β-D-galactopyranoside at 37 °C for 3 h. A 1/4 volume of SDS sample buffer containing Tris-HCl 0.33 mol·L⁻¹, 10 % SDS (w/v), 40 % glycerol (v/v), and 0.4 % bromophenol blue was added to cell lysates above and purified ARL-(His)₆ and ARL-GST. After being boiled for 5-10 min, 10 μg protein was electrophoresed on 15 % SDS-polyacrylamide gel. The protein was transferred to PVDF membrane, which was then blocked for 1 h at room temperature with 5 % BSA in TBST (100 mmol/L Tris-HCl and 0.9 % NaCl containing 0.05 % Tween-20). The blots were incubated with the primary polyclonal antibodies against ARL-1 protein (1:2 000 in TBST) and subsequently with HRP-labeled second antibody (1:5 000 in TBST) at room temperature for 1 h, respectively. At last, immunoreactive signals were visualized by DAB in 0.03% H₂O₂.

RESULTS

Construction of pGEX-4T-1(His)₆C-ARL and pQE-30-ARL

The recombinant plasmids were identified by restrictive

endonuclease and/or polymerase chain reaction. All products of pGEX-4T-1(His)₆C-ARL amplified by polymerase chain reaction and digested by *EcoRI* only or *EcoRI* and *XhoI* in combination, underwent 1.5 % agarose electrophoresis. The expected 950 bp could be seen, which was ARL-1 gene (Figure 1). In the same way, pQE-30-ARL was identified by restrictive endonuclease. All fragments were expected including 4.5kb fragment of pQE-30-ARL which was digested by *HindIII* alone, 0.7kb and 3.8kb fragments of pQE-30-ARL digested by *BamHI* only, and 3.4kb, 0.7kb and 0.3kb fragments of pQE-30-ARL digested by *BamHI* and *HindIII* in combination (Figure 2).

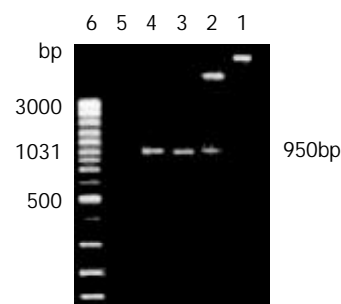


Figure 1 Recombinant plasmid pGEX-4T-1(His)₆C-ARL was identified by restrictive endonuclease and polymerase chain reaction (1.5 % agarose electrophoresis). Lane 1: The recombinant plasmid pGEX-4T-1(His)₆C-ARL digested by *EcoRI* only, about 5.9 kb fragment could be seen; Lane 2: The recombinant plasmid pGEX-4T-1(His)₆C-ARL digested by *EcoRI* and *XhoI*, two fragments of 5.0 kb and 950 bp could be seen; Lane 3: pGEX-4T-1(His)₆C-ARL being template, 950 bp was amplified by polymerase chain reaction; Lane 4: positive control of PCR; Lane 5: negative control of PCR; Lane 6: GeneRuler[™] 100 bp DNA ladder plus.

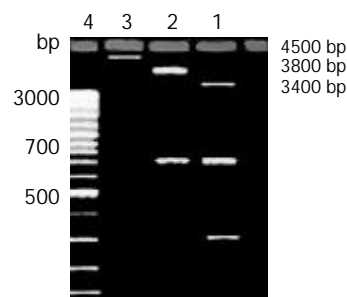


Figure 2 Recombinant plasmid pQE-30-ARL was identified by restrictive endonuclease (1.5 % agarose electrophoresis). Lane 1: 3.4 kb and 0.7 kb and 0.3 kb fragments of pQE-30-ARL digested by *BamHI* and *HindIII* together; Lane 2: 0.7 kb and 3.8 kb fragments of pQE-30-ARL digested by *BamHI* only; Lane 3: 4.5 kb fragment of pQE-30-ARL digested by *HindIII* alone; Lane 4: GeneRuler[™] 100 bp DNA ladder plus.

Expression of recombinant proteins ARL-GST and ARL-(His)₆

The transformed pGEX-4T-1(His)₆C-ARL BL21 induced by 0.05 mM isopropyl-1-thio-β-D-galactopyranoside could express the protein with molecular weight of 60.8 KD, which was recombinant protein ARL-GST. Its expression level was 15.1 % of total bacteria proteins. Under the same conditions, the transformed pQE-30-ARL BL21 expressed recombinant protein ARL-(His)₆ with molecular weight of 35.7 KD. Among total bacteria proteins, ARL-(His)₆ expression level was 27.7 %. Two recombinant proteins were purified by non-denatured method because they were soluble, predominantly in supernatant. After purification, only one band could be seen,

indicating that ARL-GST and ARL-(His)₆ were highly purified (Figures 3 and 4).

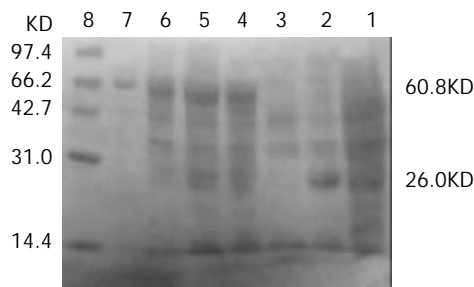


Figure 3 The transformed pGEX-4T-1(His)₆C-ARL BL21 induced by 0.05 mM isopropyl-1-thio-β-D-galactopyranoside. Lane 1: BL21 transformed with pGEX-4T-1(His)₆C, no IPTG induced; Lane 2: BL21 transformed with pGEX-4T-1(His)₆C, IPTG induced, GST (26KD) was expressed; Lane 3: BL21 transformed with pGEX-4T-1(His)₆C-ARL, no IPTG induced; Lane 4: BL21 transformed with pGEX-4T-1(His)₆C-ARL, IPTG induced, recombinant protein ARL-GST (about 60.8 KD) was expressed; Lane 5: supernatant; Lane 6: pellet; Lane 7: purified ARL-GST; Lane 8: mid-range protein molecular weight markers.

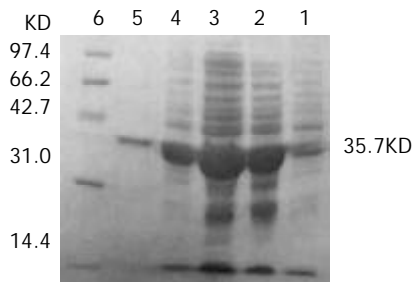


Figure 4 The transformed pQE-30-ARL BL21 induced by 0.05 mM isopropyl-1-thio-β-D-galactopyranoside. Lane 1: BL21 transformed with pQE-30-ARL, no IPTG induced; Lane 2: BL21 transformed with pQE-30-ARL, IPTG induced, ARL-(His)₆ (35.7KD) could express; Lane 3: supernatant; Lane 4: pellet; Lane 5: purified ARL-(His)₆; Lane 6: mid-range protein molecular weight markers.

Preparation of polyclonal antibodies against ARL-1 protein

Purification of polyclonal antibodies against ARL-1 protein: The rabbit sera immunized with ARL-(His)₆ were purified by CNBr-activated sepharose 4B coupled ARL-GST. After mixed with sera, washed with solution as described above, the gel was eluted with 0.1 M glycine (pH 2.8), only one elution peak could be seen in the elution curve (Figure 5), suggesting that polyclonal antibodies against ARL-1 protein were highly purified.

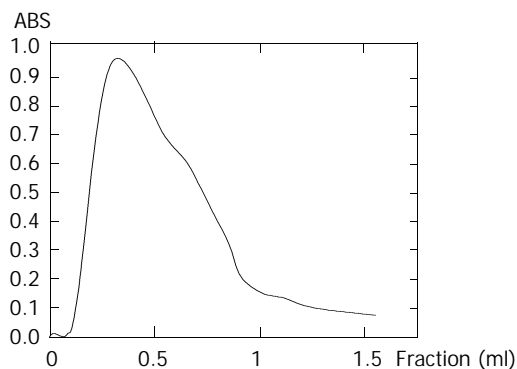


Figure 5 The gel eluted with 0.1 M glycine (pH 2.8).

Specification of polyclonal antibodies against ARL-1 protein: Proteins of all bacteria described were tested by Western blotting using polyclonal antibodies against ARL-1. Figure 6 displays that positive signals could be seen in the two purified proteins and the bacteria transformed with pGEX-4T-1(His)₆C-ARL and pQE-30-ARL individually.

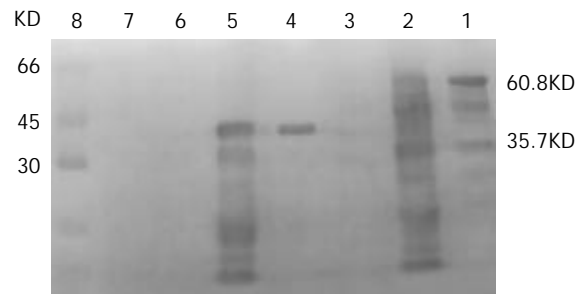


Figure 6 Proteins of all bacteria described were tested by Western blotting using polyclonal antibodies against ARL-1. Lane 1: purified ARL-GST; Lane 2: BL21 transformed with pGEX-4T-1(His)₆C-ARL; Lane 3: BL21 transformed with pGEX-4T-1(His)₆C; Lane 4: purified ARL-(His)₆; Lane 5: BL21 transformed with pQE-30-ARL; Lane 6: BL21 transformed with pET-CTF; Lane 7: BL21; Lane 8: Rainbow markers.

DISCUSSION

The cDNA of ARL-1 gene was cloned and identified by Cao *et al.* The amino acid sequence of this protein called ARL-1 was 71 % identical to that of AR. It is more homologous to a group of AR-like proteins. Its amino acid sequence was 80 %, 82 %, 83 %, and 94 % identical to that of the mouse vas deferens protein (MVDP), the mouse fibroblast growth factor-regulated protein (FR-1), the Chinese hamster ovary (CHO) reductase, and Spot 17 in rat hepatoma, respectively^[22].

ARL-1 is a new member of AKR1B group of aldoketo reductases including AR, MVDP, FR-1, CHO reductase, Spot 17, etc. The gene expression spectrum is not the same. MVDP gene was primarily expressed in the vas deferens and the adrenal gland^[30-37]. AR, was different. In adults, AR message was most abundant in the prostate, testis, skeletal muscle, and the heart. Substantial amounts were found in the ovary, small intestines, colon, thymus, spleen, kidney, and the placenta. Lower levels were found in the brain, lung, leukocytes, and the pancreas. Of the four fetal tissues tested, AR mRNA was most abundant in the kidneys, a substantial amount was found in the brain, and a low level in the lung and liver^[38,39]. FR-1 was expressed quite strongly in the small intestines, and it was expressed in testis, ovary, brain, heart, liver, kidney, and muscle, but FR-1 expression has not been screened in urinary bladder and jejunum^[40-44]. CHO reductase mRNA was quite abundant in the urinary bladder and the jejunum, this gene was also expressed in the testis and the ovary. However, CHO reductase mRNA was not detectable in brain, heart, liver, kidney, and muscle^[45-47]. ARL-1 was not expressed in many tissues. Its message was most abundant in the small intestines and colon, and a low level of its mRNA was found in the liver, thymus, prostate, testis, and skeletal muscle. No ARL-1 mRNA was detected in the four fetal tissues tested including the kidney, brain, lung and liver. Moreover, ARL-1 mRNA was not present in human vas deferens. Although many functions of all these AR-like genes are not known, different expression spectrums indicate that their physiological functions are quite different^[22].

Not only 71 % of ARL-1 amino acid sequence was identical to that of AR, but also all of the key amino acids being responsible for AR's enzymatic activities were conserved in

this protein. They included Ser¹⁵⁹, Asn¹⁶⁰, Gln¹⁸³, and Lys²⁶² for cofactor NADPH binding, Tyr⁴⁸ and His¹¹⁰ as potential hydrogen donors, and active site residues Lys⁷⁷, Tyr²⁰⁹, and Cys²⁹⁸. The enzymatic activity of ARL-1 was similar to that of the well-characterized human AR. In terms of pH optimum, salt requirement, and kinetics in reducing some substrates, these two proteins were different. For example, the activity of ARL-1 was not affected by 0.3 M sulfate ion, which was the optimum concentration for stimulating AR activity^[22]. In the present project, two recombinant ARL-1 proteins were expressed and highly purified, polyclonal antibodies against ARL-1 were prepared and characterized. Polyclonal antibodies prepared by us were only against ARL-1 protein, the yeast and fly tissues were detected by Western blotting using our antibodies, no signals were visualized (data not shown), suggesting that these polyclonal antibodies were highly specific. Other characters of ARL-1 protein should be studied, as well as the relation between ARL-1 and human diseases.

AR is thought to be involved in diabetic complications such as cataract, retinopathy, neuropathy, and nephropathy. It is not clear if ARL-1 also contributes to these diabetic complications. So two recombinant ARL-1 proteins and polyclonal antibodies against ARL-1 prepared in our research would help determine the relationship between ARL-1 and diabetes. AR and an AR-like protein called Spot 17 were induced in rat hepatomas, suggesting that these proteins may be needed to detoxify methylglyoxal or other metabolites generated by fast growing cancer cells. About 29 % of individual human HCCs over-expressed AR and 54 % of them over-expressed ARL-1. The deduced protein sequence of ARL-1 was 94 % identical to that of Spot 17, indicating that it is most likely the human homologue of that protein^[22]. In our studies, ARL-1 protein was detected in 94.4 % (17/18) liver cancer tissues, but only in 82.4 % (14/17) surrounding nontumorous tissues. Moreover, in all normal liver tissues (5 cases), ARL-1 protein was negative, ARL-1 expression in all detected liver cancer tissues was up-regulated (data not shown). All these studies suggest that ARL-1 is closely related to liver cancers.

In conclusion, two recombinant ARL-1 proteins and polyclonal antibodies against ARL-1 protein were prepared. As a basic research, these would help us identify the function of ARL-1, the exact relationship between ARL-1 and liver cancers. The life expectancy of HCC patients is hard to predict because of the high possibility of postoperative recurrence. Many factors, such as patients' general conditions, macroscopic tumor morphology, as well as tumor histopathological features, have been proven of prognostic significance^[48-58]. With the progress in ARL-1 studies, the early diagnosis rate and the therapy level of liver cancers might be elevated, which will improve the prognosis of patients with liver cancer in the future.

REFERENCES

- Fanelli A**, Hadjadj S, Gallois Y, Fumeron F, Betoule D, Grandchamp B, Marre M. Polymorphism of aldose reductase gene and susceptibility to retinopathy and nephropathy in Caucasians with type 1 diabetes. *Arch Mal Coeur Vaiss* 2002; **95**: 701-708
- Cisarik-Fredenburg P**. Discoveries in research on diabetic keratopathy. *Optometry* 2001; **72**: 691-704
- Chandra D**, Jackson EB, Ramana KV, Kelley R, Srivastava SK, Bhatnagar A. Nitric oxide prevents aldose reductase activation and sorbitol accumulation during diabetes. *Diabetes* 2002; **51**: 3095-3101
- Naya Y**, Soh J, Ochiai A, Mizutani Y, Kawauchi A, Fujito A, Ushijima S, Ono T, Iwamoto N, Aoki T, Imada N, Nakamura N, Yabe-Nishimura C, Miki T. Erythrocyte aldose reductase correlates with erectile dysfunction in diabetic patients. *Int J Impot Res* 2002; **14**: 213-216
- Jung SH**, Lee YS, Lee S, Lim SS, Kim YS, Shin KH. Isoflavonoids from the rhizomes of *Belamcanda chinensis* and their effects on aldose reductase and sorbitol accumulation in streptozotocin induced diabetic rat tissues. *Arch Pharm Res* 2002; **25**: 306-312
- Kryvko Iula**, Kozyts' kyi ZIa, Serhiienko OO, Kuchmerovs' ka TM, Velykyi MM. Diabetic neuropathies. Metabolism of sorbitol in sciatic nerve tissue in streptozotocin diabetes. *Ukr Biokhim Zh* 2001; **73**: 69-74
- Chang KC**, Paek KS, Kim HJ, Lee YS, Yabe-Nishimura C, Seo HG. Substrate-induced up-regulation of aldose reductase by methylglyoxal, a reactive oxoaldehyde elevated in diabetes. *Mol Pharmacol* 2002; **61**: 1184-1191
- Aukunuru JV**, Sunkara G, Ayalasomayajula SP, DeRuijter J, Clark RC, Kompella UB. A biodegradable injectable implant sustains systemic and ocular delivery of an aldose reductase inhibitor and ameliorates biochemical changes in a galactose-fed rat model for diabetic complications. *Pharm Res* 2002; **19**: 278-285
- Park HK**, Ahn CW, Lee GT, Kim SJ, Song YD, Lim SK, Kim KR, Huh KB, Lee HC. (AC)(n) polymorphism of aldose reductase gene and diabetic microvascular complications in type 2 diabetes mellitus. *Diabetes Res Clin Pract* 2002; **55**: 151-157
- Kaul CL**, Ramarao P. The role of aldose reductase inhibitors in diabetic complications: recent trends. *Methods Find Exp Clin Pharmacol* 2001; **23**: 465-475
- Colciago A**, Negri-Cesi P, Celotti F. Pathogenesis of diabetic neuropathy-do hyperglycemia and aldose reductase inhibitors affect neuroactive steroid formation in the rat sciatic nerves? *Exp Clin Endocrinol Diabetes* 2002; **110**: 22-26
- Hansen SH**. The role of taurine in diabetes and the development of diabetic complications. *Diabetes Metab Res Rev* 2001; **17**: 330-346
- Raptis AE**, Viberti G. Pathogenesis of diabetic nephropathy. *Exp Clin Endocrinol Diabetes* 2001; **109**(Suppl): 424-437
- Hotta N**, Toyota T, Matsuoka K, Shigetani Y, Kikkawa R, Kaneko T, Takahashi A, Sugimura K, Koike Y, Ishii J, Sakamoto N. Clinical efficacy of fidarestat, a novel aldose reductase inhibitor, for diabetic peripheral neuropathy: a 52-week multicenter placebo-controlled double-blind parallel group study. *Diabetes Care* 2001; **24**: 1776-1782
- Rippin JD**, Patel A, Bain SC. Genetics of diabetic nephropathy. *Best Pract Res Clin Endocrinol Metab* 2001; **15**: 345-358
- Kubo E**, Maekawa K, Tanimoto T, Fujisawa S, Akagi Y. Biochemical and morphological changes during development of sugar cataract in otsuka long-evans tokushima fatty (OLETF) rat. *Exp Eye Res* 2001; **73**: 375-381
- Wallner EI**, Wada J, Tramonti G, Lin S, Srivastava SK, Kanwar YS. Relevance of aldo-keto reductase family members to the pathobiology of diabetic nephropathy and renal development. *Ren Fail* 2001; **23**: 311-320
- Zeindl-Eberhart E**, Klugbauer S, Dimitrijevic N, Jungblut PR, Lamer S, Rabes HM. Proteome analysis of rat hepatomas: carcinogen-dependent tumor-associated protein variants. *Electrophoresis* 2001; **22**: 3009-3018
- Lee KW**, Ko BC, Jiang Z, Cao D, Chung SS. Overexpression of aldose reductase in liver cancers may contribute to drug resistance. *Anticancer Drugs* 2001; **12**: 129-132
- Kelly VP**, Ireland LS, Ellis EM, Hayes JD. Purification from rat liver of a novel constitutively expressed member of the aldo-keto reductase 7 family that is widely distributed in extrahepatic tissues. *Biochem J* 2000; **348**: 389-400
- Muzio G**, Salvo RA, Taniguchi N, Maggiora M, Canuto RA. 4-Hydroxynonenal metabolism by aldo/keto reductase in hepatoma cells. *Adv Exp Med Biol* 1999; **463**: 445-452
- Cao D**, Fan ST, Chung SS. Identification and characterization of a novel human aldose reductase-like gene. *J Biol Chem* 1998; **273**: 11429-11435
- Scuric Z**, Stain SC, Anderson WF, Hwang JJ. New member of aldose reductase family proteins overexpressed in human hepatocellular carcinoma. *Hepatology* 1998; **27**: 943-950
- Zeindl-Eberhart E**, Jungblut PR, Otto A, Kerler R, Rabes HM. Further characterization of a rat hepatoma-derived aldose-reductase-like protein-organ distribution and modulation *in vitro*. *Eur J Biochem* 1997; **247**: 792-800
- Takahashi M**, Hoshi A, Fujii J, Miyoshi E, Kasahara T, Suzuki K,

- Aozasa K, Taniguchi N. Induction of aldose reductase gene expression in LEC rats during the development of the hereditary hepatitis and hepatoma. *Jpn J Cancer Res* 1996; **87**: 337-341
- 26 **Takahashi M**, Fujii J, Miyoshi E, Hoshi A, Taniguchi N. Elevation of aldose reductase gene expression in rat primary hepatoma and hepatoma cell lines: implication in detoxification of cytotoxic aldehydes. *Int J Cancer* 1995; **62**: 749-754
- 27 **Canuto RA**, Ferro M, Muzio G, Bassi AM, Leonarduzzi G, Maggiora M, Adamo D, Poli G, Lindahl R. Role of aldehyde metabolizing enzymes in mediating effects of aldehyde products of lipid peroxidation in liver cells. *Carcinogenesis* 1994; **15**: 1359-1364
- 28 **Zeindl-Eberhart E**, Jungblut PR, Otto A, Rabes HM. Identification of tumor-associated protein variants during rat hepatocarcinogenesis. Aldose reductase. *J Biol Chem* 1994; **269**: 14589-14594
- 29 **Zeindl-Eberhart E**, Jungblut P, Rabes HM. Expression of tumor-associated protein variants in chemically induced rat hepatomas and transformed rat liver cell lines determined by two-dimensional electrophoresis. *Electrophoresis* 1994; **15**: 372-381
- 30 **Martinez A**, Aigueperse C, Val P, Dussault M, Tournaire C, Berger M, Veyssiere G, Jean C, Lefrancois Martinez A. Physiological functions and hormonal regulation of mouse vas deferens protein (AKR1B7) in steroidogenic tissues. *Chem Biol Interact* 2001; **130-132**: 903-917
- 31 **Ho HT**, Jenkins NA, Copeland NG, Gilbert DJ, Winkles JA, Louie HW, Lee FK, Chung SS, Chung SK. Comparisons of genomic structures and chromosomal locations of the mouse aldose reductase and aldose reductase-like genes. *Eur J Biochem* 1999; **259**: 726-730
- 32 **Fabre S**, Darne C, Veyssiere G, Jean C. Protein kinase C pathway potentiates androgen-mediated gene expression of the mouse vas deferens specific aldose reductase-like protein (MVDP). *Mol Cell Endocrinol* 1996; **124**: 79-86
- 33 **Lau ET**, Cao D, Lin C, Chung SK, Chung SS. Tissue-specific expression of two aldose reductase-like genes in mice: abundant expression of mouse vas deferens protein and fibroblast growth factor-regulated protein in the adrenal gland. *Biochem J* 1995; **312**: 609-615
- 34 **Gui T**, Tanimoto T, Kokai Y, Nishimura C. Presence of a closely related subgroup in the aldo-ketoreductase family of the mouse. *Eur J Biochem* 1995; **227**: 448-453
- 35 **Fabre S**, Manin M, Pailhoux E, Veyssiere G, Jean C. Identification of a functional androgen response element in the promoter of the gene for the androgen-regulated aldose reductase-like protein specific to the mouse vas deferens. *J Biol Chem* 1994; **269**: 5857-5864
- 36 **Pailhoux E**, Martinez A, Veyssiere G, Tournaire C, Berger M, Jean C. Characterization of cDNA and of the gene corresponding to androgen-dependent protein of the vas deferens in mice. *Ann Endocrinol (Paris)* 1991; **52**: 437-440
- 37 **Pailhoux EA**, Martinez A, Veyssiere GM, Jean CG. Androgen-dependent protein from mouse vas deferens. cDNA cloning and protein homology with the aldo-keto reductase superfamily. *J Biol Chem* 1990; **265**: 19932-19936
- 38 **Moczulski DK**, Scott L, Antonellis A, Rogus JJ, Rich SS, Warram JH, Krolewski AS. Aldose reductase gene polymorphisms and susceptibility to diabetic nephropathy in Type 1 diabetes mellitus. *Diabet Med* 2000; **17**: 111-118
- 39 **Bain SC**, Chowdhury TA. Genetics of diabetic nephropathy and microalbuminuria. *J R Soc Med* 2000; **93**: 62-66
- 40 **Glickman M**, Malek RL, Kwitek-Black AE, Jacob HJ, Lee NH. Molecular cloning, tissue-specific expression, and chromosomal localization of a novel nerve growth factor-regulated G-protein-coupled receptor, nrg-1. *Mol Cell Neurosci* 1999; **14**: 141-152
- 41 **Winkles JA**. Serum- and polypeptide growth factor-inducible gene expression in mouse fibroblasts. *Prog Nucleic Acid Res Mol Biol* 1998; **58**: 41-78
- 42 **Frank S**, Werner S. The human homologue of the yeast CHL1 gene is a novel keratinocyte growth factor-regulated gene. *J Biol Chem* 1996; **271**: 24337-24340
- 43 **De Boer WI**, Schuller AG, Vermey M, van der Kwast TH. Expression of growth factors and receptors during specific phases in regenerating urothelium after acute injury *in vivo*. *Am J Pathol* 1994; **145**: 1199-1207
- 44 **Quelle DE**, Ashmun RA, Shurtleff SA, Kato JY, Bar-Sagi D, Roussel MF, Sherr CJ. Overexpression of mouse D-type cyclins accelerates G1 phase in rodent fibroblasts. *Genes Dev* 1993; **7**: 1559-1571
- 45 **Kaneko M**, Carper D, Nishimura C, Millen J, Bock M, Hohman TC. Induction of aldose reductase expression in rat kidney mesangial cells and Chinese hamster ovary cells under hypertonic conditions. *Exp Cell Res* 1990; **188**: 135-140
- 46 **Li H**, Nobukuni Y, Gui T, Yabe-Nishimura C. Characterization of genomic regions directing the cell-specific expression of the mouse aldose reductase gene. *Biochem Biophys Res Commun* 1999; **255**: 759-764
- 47 **Ye Q**, Hyndman D, Li X, Flynn TG, Jia Z. Crystal structure of CHO reductase, a member of the aldo-keto reductase superfamily. *Proteins* 2000; **38**: 41-48
- 48 **Qin LX**, Tang ZY. The prognostic significance of clinical and pathological features in hepatocellular carcinoma. *World J Gastroenterol* 2002; **8**: 193-199
- 49 **Tang ZY**. Hepatocellular carcinoma-Cause, treatment and metastasis. *World J Gastroenterol* 2001; **7**: 445-454
- 50 **Wu MC**, Shen F. Progress in research of liver surgery in China. *World J Gastroenterol* 2000; **6**: 773-776
- 51 **Rabe C**, Pilz T, Klostermann C, Berna M, Schild HH, Sauerbruch T, Caselmann WH. Clinical characteristics and outcome of a cohort of 101 patients with hepatocellular carcinoma. *World J Gastroenterol* 2001; **7**: 208-215
- 52 **Yip D**, Findlay M, Boyer M, Tattersall MH. Hepatocellular carcinoma in central Sydney: a 10 year review of patients seen in a medical oncology department. *World J Gastroenterol* 1999; **5**: 483-487
- 53 **Sithinamsuwan P**, Piratvisuth T, Tanomkiat W, Apakupakul N, Tongyoo S. Review of 336 patients with hepatocellular carcinoma at Songklanagarind Hospital. *World J Gastroenterol* 2000; **6**: 339-343
- 54 **Niu Q**, Tang ZY, Ma ZC, Qin LX, Zhang LH. Serum vascular endothelial growth factor is a potential biomarker of metastatic recurrence after curative resection of hepatocellular carcinoma. *World J Gastroenterol* 2000; **6**: 565-568
- 55 **Jiang YF**, Yang ZH, Hu JQ. Recurrence or metastasis of HCC: predictors, early detection and experimental antiangiogenic therapy. *World J Gastroenterol* 2000; **6**: 61-65
- 56 **He P**, Tang ZY, Ye SL, Liu BB. Relationship between expression of α -fetoprotein messenger RNA and some clinical parameters of human hepatocellular carcinoma. *World J Gastroenterol* 1999; **5**: 111-115
- 57 **Parks RW**, Garden OJ. Liver resection for cancer. *World J Gastroenterol* 2001; **7**: 766-771
- 58 **Wu ZQ**, Fan J, Qiu SJ, Zhou J, Tang ZY. The value of postoperative hepatic regional chemotherapy in prevention of recurrence after radical resection of primary liver cancer. *World J Gastroenterol* 2000; **6**: 131-133

Characteristics and application of established luciferase hepatoma cell line that responds to dioxin-like chemicals

Zhi-Ren Zhang, Shun-Qing Xu, Xi Sun, Yong-Jun Xu, Xiao-Kun Cai, Zhi-Wei Liu, Xiang-Lin Tan, Yi-Kai Zhou, Jun-Yue Zhang, Hong Yan

Zhi-Ren Zhang, Shun-Qing Xu, Xi Sun, Yong-Jun Xu, Xiao-Kun Cai, Zhi-Wei Liu, Xiang-Lin Tan, Yi-Kai Zhou, Jun-Yue Zhang, Hong Yan, Institute of Environmental Medicine, Tongji Medical College, Huazhong University of Science and Technology, Wuhan, 430030, Hubei Province, China

Supported by the National Natural Science Foundation of China, No. 29877020 and 20107002

Correspondence to: Dr. Shun-Qing Xu, Institute of Environmental Medicine, Tongji Medical College, Huazhong University of Science and Technology, Wuhan, 430030, Hubei Province, China. shunqing@public.wh.hb.cn

Telephone: +86-27-83693417 **Fax:** +86-27-83657705

Received: 2002-01-28 **Accepted:** 2002-05-11

Abstract

AIM: To establish a luciferase reporter cell line that responds to dioxin-like chemicals (DLCs) and on this basis to evaluate its characteristics and application in the determination of DLCs.

METHODS: A recombinant luciferase reporter plasmid was constructed by inserting dioxin-responsive element (DREs) and MMTV promoter segments into the pGL₃-promoter plasmid immediately upstream of the luciferase gene, which was structurally demonstrated by fragment mapping analysis in gel electrophoresis and transfected into the human hepatoma cell line HepG₂, both transiently and stably, to identify the inducible expression of luciferase by 2, 3, 7, 8-tetrachlorodibenzo-*p*-dioxin (TCDD). The time course, responsive period, sensitivity, structure-inducibility and dose-effect relationships of inducible luciferase expression to DLCs was dynamically observed in HepG₂ cells stably transfected by the recombinant vector (HepG₂-Luc) and compared with that assayed by ethoxyresorufin-*O*-deethylase (EROD) in non-transfected HepG₂ cells (HepG₂-wt).

RESULTS: The inducible luciferase expression of HepG₂-Luc cells was noted in a time-, dose-, and AhR-dependent manner, which peaked at 4 h and then decreased to a stable level at 14 h after TCDD treatment. The responsiveness of HepG₂-Luc cells to TCDD induction was decreased with culture time and became undetectable at 10th month of HepG₂-Luc cell formation. The fact that luciferase activity induced by 3, 3', 4, 4'-PCB in HepG₂-Luc cells was much less than that induced by TCDD suggests a structure-inducibility relationship existing among DLCs. Within the concentrations from 3.5×10⁻¹² to 5×10⁻⁹ mol/L, significant correlations between TCDD doses and EROD activities were observed in both HepG₂-luc and HepG₂-wt cells. The correlation between TCDD doses from 1.1×10⁻¹³ to 1×10⁻⁸ mol/L and luciferase activities was also found to be significant in HepG₂-luc cells ($r=0.997$, $P<0.001$), but not in their HepG₂-wt counterparts. For the comparison of the enzyme responsiveness between cell lines to TCDD, the luciferase sensitivity and reproducibility in HepG₂-luc cells were both better than that of EROD in HepG₂-wt cells, the former was at 1.1×10⁻¹³

mol/L and 3.5×10⁻¹² mol/L, and the coefficients of variation (CV) of the latter was 15-30 % and 22-38 %, respectively.

CONCLUSION: The luciferase expression of HepG₂-luc cells established in the present study could sensitively respond to the DLCs stimulation and might be a prospective tool for the determination of DLCs.

Zhang ZR, Xu SQ, Sun X, Xu YJ, Cai XK, Liu ZW, Tan XL, Zhuo YK, Zhang JY, Yan H. Characteristics and application of established luciferase hepatoma cell line that responds to dioxin-like chemicals. *World J Gastroenterol* 2003; 9(7): 1460-1464 <http://www.wjgnet.com/1007-9327/9/1460.asp>

INTRODUCTION

It has been well known in recent years that dioxin-like chemicals (DLCs) such as 2,3,7,8-tetrachlorodibenzo-*p*-dioxin (TCDD) can produce a wide variety of species- and tissue-specific toxic and biological effects, such as epidermal lesion, wasting syndrome, birth defect, hepatotoxicity, lethality, alteration in endocrine homeostasis, tumor promotion, myelotoxicity, immunotoxicity and induction of numerous enzymes (e.g. cytochrome P4501A1)^[1-4]. Many of these responses are mediated by the cytosolic aryl hydrocarbon receptor (AhR) and modulated by the interaction of DLCs: AhR complex with its DNA recognition sequence [the dioxin-responsive element (DRE)]^[5-9]. Generally, the combination of DLCs with cytoplasmic AhR is the initial step of DLCs-triggered cell signaling pathway. After that, two molecules of hsp90 dissociate from DLCs: AhR complex, and the latter enters the nucleus to form a new complex with AhR nuclear translocator protein (ARNT), which further binds to the DRE, leading to the transcriptional activation of adjacent genes and toxic effects^[10,11]. Therefore, AhR and its related signal pathway have been usually taken as the useful targets to be investigated for the determination of DLCs in different situations. Till now, the DLCs-responsive receptor assays have been established in mammalian cell lines^[12] and in mice^[13].

However, not all of these assays have been considered to be satisfactory yet. For example, the ethoxyresorufin-*O*-deethylase (EROD) induced as a common and rapid response to DLCs under DREs control has been widely used to evaluate the relatively toxicological potency of a complex mixture containing DLCs^[14-16] except that higher concentrations appear when the enzyme activity is inhibited. Some detecting methods are time-consuming, expensive and inadequate to be used for screening and diagnosing dioxin and dioxin-like compounds in large numbers of samples^[17-19]. Even if the chemical-activated luciferase expression (CALUX) bioassay method based on the pGL₂ vector^[20] is to a certain extent lack of sensitivity and needs to be improved.

We therefore conducted the present study in an attempt to establish a more effective luciferase reporter cell line that responds to the alteration of DLCs concentrations and to evaluate its characteristics and applications in measurement of DLCs.

MATERIALS AND METHODS

Materials

Plasmids pHAV and pMcat were generously provided by Dr. James P. Whitlock Jr., Stanford University. Restriction endonuclease and other reagents used for molecular cloning were from Huamei Ltd. (China, Shanghai) or Promega Corporation. 2,3,7,8-TCDD and 3',4,4'- polychlorinated biphenyl (PCB) were purchased from Accustanfards Inc. (New Haven, CT). Dimethylsulphoxide (DMSO) was from BIB Corporation. Luciferase assay reagents came from Promega Corporation.

Construction of inducible luciferase expression vector

Plasmid pHAV containing DREs was cleaved with *HindIII*. Following purification by agarose gel electrophoresis, the smaller *HindIII* fragment was further digested by *BamHI* and *EcoRV* to produce a 630-bp segment containing DREs, which was then ligated with *BglIII* linkers and cleaved with *BglIII* to create cohesive ends. To get the MMTV promoter, plasmid pMcat was cleaved with *HindIII* and the smaller *HindIII* fragment was then cleaved with *BglIII* to produce cohesive 5' *BglIII* and 3' *HindIII* termini. The two segments containing DREs and MMTV promoter were connected with T₄ DNA ligase to form a 1 020 bp fragment with cohesive 5' *BglIII* and 3' *HindIII* termini, which was further subcloned into the *BglIII*-*HindIII* site immediately upstream of the luciferase gene in the pGL₃-promoter plasmid (Promega). As such, the luciferase's expression was under the control of DREs. The recombinant vector was identified structurally with restriction endonuclease analysis.

Inducible expression of recombinant vector

HepG₂ cells were seeded in a 60 mm culture dish at a density of 3×10⁵ cells in 5 ml of RPMI1640 supplemented with 10 % heat-inactivated fetal calf serum at 37 °C with saturated humidity and a 5 % (v/v) CO₂ atmosphere^[21]. After cultured for 24 h, the cells were transiently or stably transfected by 15 µg of recombinant vector with calcium phosphate mediated method^[22]. For transient transfection, the cells were allowed to grow for 48 h, followed by adding 0.5 % DMSO or 0.1-1 nmol/L TCDD dissolved in DMSO. After cultivated for another 24 h^[22], cells were harvested to determine luciferase expression.

For the establishment of stable transfection, HepG₂ cells were cotransfected with the selective plasmid PTK-Hyg and the recombinant vector simultaneously. Following 24 h of cultivation in nonselective medium, the transfected cells were transferred into a selective medium containing hygromycin and cultured for 4 weeks when TCDD-induced luciferase expression was conducted. The clone with the largest ratio of inducible to constitutive expression of luciferase was selected for further study^[23]. To identify the time course of inducible luciferase expression, the stably transfected cells (HepG₂-Luc) were cultured with exposure to 0.5 % DMSO or 1 nmol/L TCDD and the induced luciferase activities were determined at every 2 h up to 28 h post-exposure. For determination of the responsive period of luciferase induction, the HepG₂-Luc cells were treated with the same kinds of inducers for 24 h and their luciferase activity was assayed, which was performed at every month up to 12 months. The structure-inducibility and dose-effect relationships of different inducers that might represent their ability to bind AhR were also analyzed in HepG₂-Luc cells with the indicated concentrations of 3, 3', 4, 4'-PCB, another member of DLCs, and TCDD.

Luciferase assay was performed by the routine procedures. Briefly, after removal of the culture medium, the incubated cells were washed twice with phosphate buffered saline (PBS) and lysed using luciferase lysis reagent for 15 min at room

temperature. Following centrifugation, 20 µl of supernatant was added into 100 µl luciferase assay reagent, the resulting bioluminescence was quantified immediately with Lumate LB 9570 luminometer over 3 s. The concentration of the sample protein was determined with Bio-Rad method^[24]. The luciferase activity was finally expressed as relative light unit (RLU) per microgram protein^[21, 25].

Comparative study with EROD determination

EROD activity was employed as a variable to evaluate the effectiveness of HepG₂-luc cells in response to TCDD and to compare with luciferase. HepG₂ (HepG₂-wt) and HepG₂-luc cells were seeded in 6-well dishes at a density of 2×10⁵ cells in 3 ml of medium and cultivated for 24 h, then they were exposed to the indicated concentrations of TCDD in DMSO and further incubated for 72 h. Following removal of the culture medium, the cells were washed twice with PBS and stored at -80 °C. EROD activity was assayed using fluorescent method. The concentrations of sample protein were determined with Bio-Rad method^[24]. EROD activity was finally expressed as pmol resorufin production per microgram protein per minute^[26, 27].

Statistical analysis

Data values in the present study were presented as the mean for each independent determination of four replicates. The detection limit was expressed as the average value plus three times of standard deviations (SD). Coefficients of variation (CV) were calculated by SD/mean ×100 %. Correlation coefficients (*r*) were obtained using least-squares linear regression analysis.

RESULTS

Identification of inducible expression of recombinant vector

Structurally, segment analysis by restriction endonuclease digestion confirmed that the inserted fragment sequences containing DREs and MMTV promoter in the constructed plasmids were completely consistent with that of the theoretical calculations as shown in Figure 1.

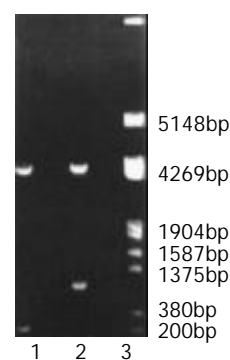


Figure 1 Fragment mapping analysis of recombinant plasmid digested with *BglIII* and *HindIII* in gel electrophoresis. Lane 1: pGL₃ plasmid was cleaved into two fragments, which showed about 5 000 bp and 200 bp respectively. Lane 2: Recombinant plasmid was cut into a fragment of about 5 000 bp and the one of about 1 000 bp. Lane 3: DNA marker.

Inducible expression of luciferase by the recombinant plasmid was identified in transiently transfected HepG₂ cells, which produced a significantly higher induction of luciferase activity (80-fold, data not shown) compared with that of their non-transfected counterparts when exposed to TCDD. Dynamically, TCDD-induced luciferase activity in HepG₂-Luc cells peaked at 4 h and then decreased to a stable level at about

14 h after TCDD treatment (Figure 2). Responsiveness of HepG₂-Luc cells to the TCDD induction was decreased with culture time and became undetectable at 10th month of HepG₂-Luc cell formation (Figure 3), which indicates that the recombinant plasmid could not integrate stably with HepG₂ chromosome. The structure-inducibility relationship of different DLCs inducers was demonstrated by the fact that the luciferase activity induced by 3, 3', 4, 4' -PCB was much less than that induced by TCDD and a dose-dependent increase of luciferase activity was evoked by both of the DLCs inducers as shown in Figure 4.

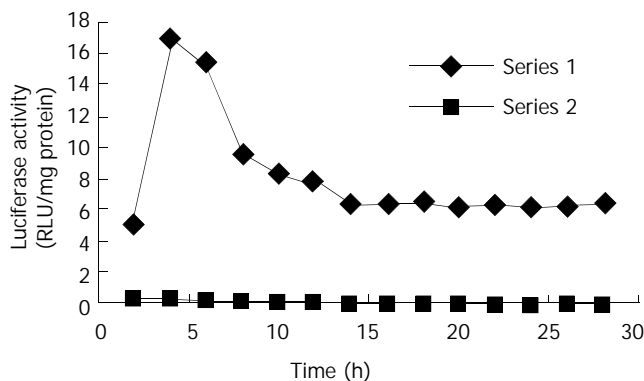


Figure 2 The time course of luciferase activities induced by TCDD and DMSO in stably transfected cells. The TCDD-induced luciferase activity in HepG₂-Luc cells peaked at about 4 h, and then decreased to a stable level at about 14 h after TCDD treatment.

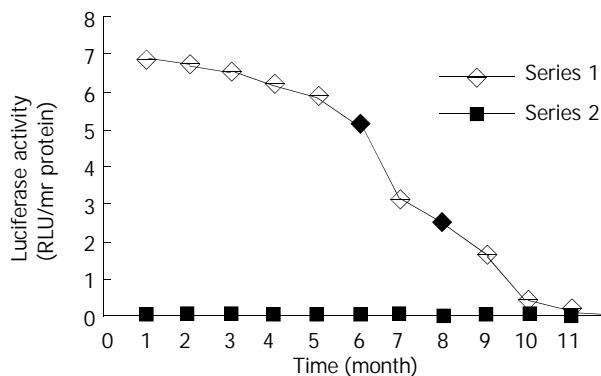


Figure 3 Responsive period of HepG₂-Luc cells to TCDD induction. The responsiveness of HepG₂-Luc cells to TCDD induction was decreased with culture time and became undetectable at about 10th month.

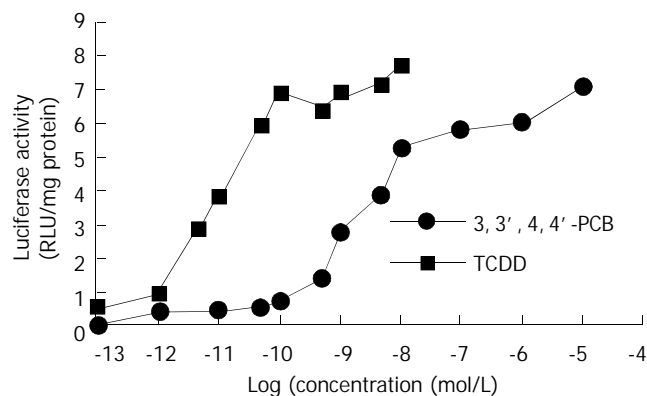


Figure 4 Comparison of luciferase activity induced by TCDD and 3, 3', 4, 4' -PCB in HepG₂-Luc cells. The luciferase activity induced by indicated concentrations of 3, 3', 4, 4' -PCB was much less than that induced by TCDD.

Comparative study

Within concentrations from 3.5×10^{-12} to 5×10^{-9} mol/L, significant correlations between TCDD doses and EROD activities were observed in both HepG₂-luc and HepG₂-wt cells. The correlation between TCDD doses from 1.1×10^{-13} to 1×10^{-8} mol/L and luciferase activities was also found to be significant in HepG₂-luc cells ($r=0.997$, $P<0.001$), but not in their HepG₂-wt counterparts. For comparison of the enzyme responsiveness between cell lines to TCDD, the luciferase sensitivity and reproducibility in HepG₂-luc cells were better than those of EROD in HepG₂-wt cells, which were 1.1×10^{-13} mol/L and 3.5×10^{-12} mol/L, whose CV was 15-30 % and 22-38 % (data not shown), respectively.

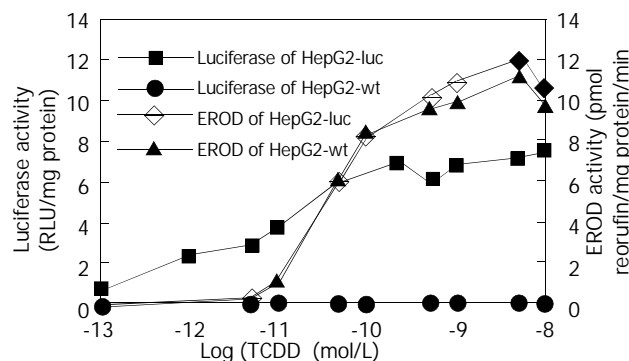


Figure 5 Comparison of EROD and luciferase responsiveness to the induction of TCDD in both HepG₂-luc and HepG₂-wt cells.

DISCUSSION

Few environmental compounds have generated much interest within the scientific community and in the lay public as polychlorinated dibenzo-p-dioxins (PCDDs) and polychlorinated dibenzofurans (PCDFs). Their ubiquitous presence in the environment and the risk of accidental exposure have raised concern over a possible threat of PCDDs or PCDFs to human health. The most extensively studied potent isomer is TCDD or dioxin, which is known to induce a wide range of toxic and biochemical responses in laboratory animals and humans^[8, 11]. Therefore, monitoring the levels of DLCs in environmental pollutants is important for assessing and maintaining the safety of food and the health of environment. Exploring new biotectors such as bioassays, biomarkers, enzyme immunoassays (EIAs), or other bioanalytical tools has been a continuously growing area in recent years^[15]; in which, however, establishing luciferase reporter cell lines for bioassays has been considered as the rapid, sensitive and inexpensive methods for the screening and diagnosis of dioxin and dioxin-like compounds^[20, 28].

In the present study, we constructed a recombinant expression plasmid that contained the luciferase gene under TCDD-inducible control of several DREs and responded to DLCs with the induction of firefly luciferase, which has been identified by both transient and stable transfection of this vector into HepG₂ cells. Our results indicate that this established HepG₂-luc cell bioassay reporter system can respond sensitively to DLCs with the induction of luciferase in a time-, dose-, and AhR-dependent manner and harbors lots of better features. Firstly, it bears higher level of sensitivity and can detect TCDD within the linear range from 1.1×10^{-13} to 1×10^{-8} mol/L, which is 10-fold more sensitive than that of previously similar studies and 30-fold more sensitive than the EROD assay. This is partially because the vector plasmid employed in the study is pGL₃, whose expression efficiency of luciferase is 10-100 times more than that of pGL₂. In addition, no post-transcriptional procedures are needed to regulate the expression of prokaryotic

luciferase, thus its linear relationship is better than that of endogenous gene. Secondly, its pronounced accuracy has been demonstrated by the significant correlation between inducible luciferase activities and TCDD doses ($r=0.997$, $P<0.001$), and by the satisfactory reproducibility of TCDD determination with HepG₂-luc cells (CV=15-30 %). Finally, the simplicity and facility of HepG₂-luc cells in analytical methodology make it possible to perform a rapid screening and semi-quantitation of DLCs^[29,30] and to deal with lots of samples in a short period of time.

Besides the detection of DLCs described above, HepG₂-luc cells can also be applied to many other DLCs-related research fields. Since ARNT is required to exert biological effects by some TCDD and related ligands, interactions between AhR and hypoxia signaling pathways can be studied by using luciferase transfected cell line^[31]. In accordance with the fact that the toxic factor of 3,3',4,4'-PCB equivalent to TCDD is 0.01^[32], our results showed that the ability of 3,3',4,4'-PCB to induce luciferase expression was much less than that of TCDD, suggesting that the structure-inducibility relationship existing in some DLCs could be reflected by HepG₂-luc cells, and the latter can be used alone or with chromatographer to evaluate the relative toxicity of DLCs^[19,33,34]. In addition, this kind of recombinant cell lines can also be used for the detection and relative quantitation of AhR agonists/antagonists in complex mixtures of environmental and biological samples, for identification and characterization of novel AhR agonists, and for examination of species differences in DLCs responsiveness^[12].

One limitation of the present study is the relatively short duration of responsiveness to DLCs by established HepG₂-luc cells, although it is in accordance with that reported by most of the other studies. Up to the present, many established luciferase reporter cell lines such as MLE/BV, H4IIE, GPC16 and HGL1.1c3 responding to DLCs maintain their stable TCDD responsiveness for 6-12 months, except for Hepa1 which maintains its sensitivity for over 3 years^[27]. Therefore, our further study has been designed aiming at improving and maintaining the sensitivity of HepG₂-luc cells to DLCs for a longer time.

ACKNOWLEDGEMENTS

We thank Dr. James P. Whitlock Jr. (Stanford University) for his kind gift of plasmids pHAV and pMcat.

REFERENCES

- Couture LA**, Abbott BD, Birnbaum LS. A critical review of the developmental toxicity and teratogenicity of 2,3,7,8-tetrachlorodibenzo-p-dioxin: advances toward understanding the mechanism. *Teratology* 1990; **42**: 619-627
- Martinez JM**, Afshari CA, Bushel PR, Masuda A, Takahashi T, Walker NJ. Differential toxicogenomic responses to 2, 3, 7, 8-tetrachlorodibenzo-p-dioxin in malignant and nonmalignant human airway epithelial cells. *Toxicol Sci* 2002; **69**: 409-423
- Dong W**, Teraoka H, Yamazaki K, Tsukiyama S, Imani S, Imagawa T, Stegeman JJ, Peterson RE, Hiraga T. 2, 3, 7, 8-tetrachlorodibenzo-p-dioxin toxicity in the zebrafish embryo: local circulation failure in the dorsal midbrain is associated with increased apoptosis. *Toxicol Sci* 2002; **69**: 191-201
- Kerkvliet NI**. Recent advances in understanding the mechanisms of TCDD immunotoxicity. *Int Immunopharmacol* 2002; **2**: 277-291
- Lindstrom G**, Hooper K, Petreas M, Stephens R, Gilman A. Workshop on perinatal exposure to dioxin-like compounds. I. Summary. *Environ Health Perspect* 1995; **103**(Suppl): S135-S142
- Legare ME**, Hanneman WH, Barhoumi R, Burghardt RC, Tiffany-Castiglioni E. 2, 3, 7, 8-Tetrachlorodibenzo-p-dioxin alters hippocampal astroglia-neuronal gap junctional communication. *Neurotoxicology* 2000; **21**: 1109-1116
- Hankinson O**. The aryl hydrocarbon receptor complex. *Annu Rev Pharmacol Toxicol* 1995; **35**: 307-340
- Wilson CL**, Safe S. Mechanisms of ligand-induced aryl hydrocarbon receptor-mediated biochemical and toxic responses. *Toxicol Pathol* 1998; **26**: 657-671
- Unkila M**, Pohjanvirta R, Tuomisto J. Biochemical effects of 2, 3, 7, 8-tetrachlorodibenzo-p-dioxin (TCDD) and related compounds on the central nervous system. *Int J Biochem Cell Biol* 1995; **27**: 443-455
- Dragan YP**, Schrenk D. Animal studies addressing the carcinogenicity of TCDD (or related compounds) with an emphasis on tumor promotion. *Food Addit Contam* 2000; **17**: 289-302
- Vanden Heuvel JP**, Lucier G. Environmental toxicology of polychlorinated dibenzo-p-dioxins and polychlorinated dibenzofurans. *Environmental Health Perspectives* 1993; **100**: 189-200
- Garrison PM**, Tullis K, Aarts JM, Brouwer A, Giesy JP, Denison MS. Species-specific recombinant cell lines as bioassay systems for the detection of 2, 3, 7, 8-tetrachlorodibenzo-p-dioxin-like chemicals. *Fundamental and Applied Toxicology* 1996; **30**: 194-203
- Willey JJ**, Stripp BR, Baggs RB, Gasiewicz TA. Aryl hydrocarbon receptor activation in genital tubercle, palate and other embryonic tissues in 2, 3, 7, 8-tetrachlorodibenzo-p-dioxin-responsive lacZ mice. *Toxicol Appl Pharmacol* 1998; **151**: 33-44
- Whyte JJ**, Jung RE, Schmitt CJ, Tillitt DE. Ethoxyresorufin-O-deethylase (EROD) activity in fish as a biomarker of chemical exposure. *Crit Rev Toxicol* 2000; **30**: 347-570
- Behnisch PA**, Hosoe K, Sakai S. Bioanalytical screening methods for dioxins and dioxin-like compounds: a review of bioassay/biomarker technology. *Environ Int* 2001; **27**: 413-439
- Whitlock JP**. Induction of cytochrome P4501A1. *Annu Rev Pharmacol Toxicol* 1999; **39**: 103-125
- Diehl-Jones WL**, Bols NC. Use of response biomarkers in milk for assessing exposure to environmental contaminants: the case for dioxin-like compounds. *J Toxicol Environ Health B Crit Rev* 2000; **3**: 79-107
- Schwirzer SM**, Hofmaier AM, Ketrup A, Nerdinger PE, Schramm KW, Thoma H, Wegenke M, Wiebel FJ. Establishment of a simple cleanup procedure and bioassay for determining 2,3,7,8-tetrachlorodibenzo-p-dioxin toxicity equivalents of environmental samples. *Ecotoxicol Environ Saf* 1998; **41**: 77-82
- Behnisch PA**, Hosoe K, Brouwer A, Sakai S. Screening of dioxin-like toxicity equivalents for various matrices with wildtype and recombinant rat hepatoma H4IIE cells. *Toxicol Sci* 2002; **69**: 125-130
- Sanderson JT**, Aarts JM, Brouwer A, Froese KL, Denison MS, Giesy JP. Comparison of Ah receptor-mediated luciferase and ethoxyresorufin-O-deethylase induction in H4IIE cells: implications for their use as bioanalytical tools for the detection of polyhalogenated aromatic hydrocarbons. *Toxicol Appl Pharmacol* 1996; **137**: 316-325
- Chen CA**, Okayama H. Calcium phosphate-mediated gene transfer: a highly efficient transfection system for stably transforming cells with plasmid DNA. *Bio Techniques* 1988; **6**: 632-639
- Zhang ZR**, Xu SQ, Zhou YK, Ren S, Lu B. Construction of luciferase reporter plasmid which is under the control of dioxin-responsive enhancers. *Shengwu Gongcheng Xuebao* 2001; **17**: 170-174
- Chen C**, Okayama H. High-efficiency transformation of mammalian cells by plasmid DNA. *Mol Cell Biol* 1987; **7**: 2745-2752
- Bradford MM**. A rapid and sensitive method for the quantitation of microgram quantities of protein utilizing the principle of protein-dye binding. *Anal Biochem* 1976; **72**: 248-254
- Murk AJ**, Legler J, Denison MS, Giesy JP, Van De Guchte C, Brouwer A. Chemical-activated luciferase gene expression (CALUX): a novel in vitro bioassay for Ah receptor active compounds in sediments and pore water. *Fundam Appl Toxicol* 1996; **33**: 149-160
- Li W**, Wu WZ, Xu Y, Li L, Schramm KW, Ketrup A. Measuring TCDD equivalents in environmental samples with the micro-EROD assay: comparison with HRGC/HRMS data. *Bull Environ Contam Toxicol* 2002; **68**: 111-117
- Postlind H**, Vu TP, Tukey RH, Quattrochi LC. Response of hu-

- man CYP1-luciferase plasmids to 2, 3, 7, 8-tetrachlorodibenzo-p-dioxin and polycyclic aromatic hydrocarbons. *Toxicol Appl Pharmacol* 1993; **118**: 255-262
- 28 **Hahn ME**. Biomarkers and bioassays for detecting dioxin-like compounds in the marine environment. *Sci Total Environ* 2002; **289**: 49-69
- 29 **Allen SW**, Mueller L, Williams SN, Quattrochi LC, Raucy J. The use of a high-volume screening procedure to assess the effects of dietary flavonoids on human cyp1a1 expression. *Drug Metab Dispos* 2001; **29**: 1074-1079
- 30 **Khim JS**, Lee KT, Villeneuve DL, Kannan K, Giesy JP, Koh CH. In vitro bioassay determination of dioxin-like and estrogenic activity in sediment and water from Ulsan Bay and its vicinity, Korea. *Arch Environ Contam Toxicol* 2001; **40**: 151-160
- 31 **Nie M**, Blankenship AL, Giesy JP. Interactions between aryl hydrocarbon receptor (AhR) and hypoxia signaling pathways. *Environ Toxicol Pharmacol* 2001; **10**: 17-27
- 32 **Safe SH**. Polychlorinated biphenyls (PCBs): environmental impact, biochemical and toxic responses, and implications for risk assessment. *Crit Rev Toxicol* 1994; **24**: 87-149
- 33 **Machala M**, Vondracek J, Blaha L, Ciganek M, Neca JV. Aryl hydrocarbon receptor-mediated activity of mutagenic polycyclic aromatic hydrocarbons determined using in vitro reporter gene assay. *Mutat Res* 2001; **497**: 49-62
- 34 **Hamers T**, van Schaardenburg, Felzel EC, Murk AJ, Koeman JH. The application of reporter gene assays for the determination of the toxic potency of diffuse air pollution. *Sci Total Environ* 2000; **262**: 159-174

Edited by Zhu L

Construction and expression of recombinant human AFP eukaryotic expression vector

Li-Wang Zhang, Jun Ren, Liang Zhang, Hong-Mei Zhang, Bin Jin, Bo-Rong Pan, Xiao-Ming Si, Yan-Jun Zhang, Zhong-Hua Wang, Yang-Lin Pan, Stephen M Festein

Li-Wang Zhang, Jun Ren, Liang Zhang, Hong-Mei Zhang, Bin Jin, Bo-Rong Pan, Xiao-Ming Si, Yan-Jun Zhang, Department of Oncology, Xijing Hospital, Fourth Military Medical University, Xi' an 710032, Shaanxi Province, China

Zhong-Hua Wang, Department of Hepatobiliary Surgery, Xijing Hospital, Fourth Military Medical University, Xi' an 710032, Shaanxi Province, China

Yang-Lin Pan, Department of Gastroenterology, Xijing Hospital, Fourth Military Medical University, Xi' an 710032, Shaanxi Province, China

Stephen M Festein, Department of Biology, Hamilton College, 198 College Hill Road Clinton, New York 13323, USA

Supported by Teaching and Research Award Program for Outstanding Young Teacher in Higher Education Institutes, No. TRAPOYT99-016, and the Fund for Distinguished Young Scholars of Chinese PLA, No.01J016

Correspondence to: Dr. Jun Ren, Department of Oncology, Xijing Hospital, Fourth Military Medical University, Xi' an 710032, Shaanxi Province, China. renjun@fmmu.edu.cn

Telephone: +86-29-3375407

Received: 2003-01-11 **Accepted:** 2003-03-05

Abstract

AIM: To construct a recombinant human AFP eukaryotic expression vector for the purpose of gene therapy and target therapy of hepatocellular carcinoma (HCC).

METHODS: The full length AFP-cDNA of prokaryotic vector was digested, and subcloned to the multi-clony sites of the eukaryotic vector. The constructed vector was confirmed by enzymes digestion and electrophoresis, and the product expressed was detected by electrochemiluminescence and immunofluorescence methods.

RESULTS: The full length AFP-cDNA successfully cloned to the eukaryotic vector through electrophoresis, 0.9723 IU/ml AFP antigen was detected in the supernatant of AFP-CHO by electrochemiluminescence method. Compared with the control groups, the differences were significant ($P < 0.05$). AFP antigen molecule was observed in the plasma of AFP-CHO by immunofluorescence staining.

CONCLUSION: The recombinant human AFP eukaryotic expression vector can express in CHO cell line. It provides experimental data for gene therapy and target therapy of hepatocellular carcinoma.

Zhang LW, Ren J, Zhang L, Zhang HM, Jin B, Pan BR, Si XM, Zhang YJ, Wang ZH, Pan YL, Festein SM. Construction and expression of recombinant human AFP eukaryotic expression vector. *World J Gastroenterol* 2003; 9(7): 1465-1468

<http://www.wjgnet.com/1007-9327/9/1465.asp>

INTRODUCTION

Hepatocellular carcinoma (HCC) is a very common

malignancy in China^[1-5], and it has a very poor prognosis^[6-9]. Only a minority of patients are eligible for surgical therapies due to advanced tumors or extrahepatic diseases at primary diagnosis^[10,11]. Therefore, it is urgent to find a novel strategy to prevent the proliferation of malignant cells. It is a hot spot at present to study prophylactic vaccination targeting the tumor-associated antigen (TAA) or tumor-specific antigen (TSA). This approach has been successful in mouse models, such as the tyrosinase-related protein (TRP)-2 in murine melanoma^[12,13]. A colon cancer specific DNA vaccination directed against the carcinoembryonic antigen (CEA) is in phase I clinical trial^[14].

The oncofetal alpha-fetoprotein (AFP) may be a possible target for an HCC-specific vaccination. It is a 70-ku to 80-ku secretory protein that is heterogeneously glycosylated. AFP is usually expressed at high concentrations in fetal liver, gastrointestinal tract, and the yolk sack. It is transcriptionally down-regulated after birth, and frequently re-expressed in HCC and therefore, used as a diagnostic marker for this tumor^[15-21]. Serum AFP is useful not only for diagnosis, but also a prognostic indicator for HCC patients^[22,23]. AFP mRNA has been proposed as a predictive marker of HCC cells disseminated into the circulation and for metastatic recurrence^[24-27]. Some experiments *in vitro* have also demonstrated that AFP promotes cell proliferation of hepatoma cell lines^[28,29].

AFP may be used as a target molecule for immunotherapy or prophylaxis against HCC. For this purpose, we constructed the recombinant human AFP eukaryotic expression vector, and hope that it will provide experimental data for the treatment of HCC.

MATERIALS AND METHODS

Cell line and culture condition

CHO cell line was provided by the Department of Biochemistry, Fourth Military Medical University. Cells were maintained in RPMI 1640 medium, supplemented with 10 mL/L FCS, 1 mmol/L glutamine, and 100 kU/L penicillin.

Plasmids

The prokaryotic expression vector pRESTA-AFP containing human full-length AFP-cDNA was presented by Dr. Stephen M Festein, Hamilton College, USA. The eukaryotic vector pCEFL was provided by Dr. Pan YL, Fourth Military Medical University.

Amplification of pRESTA-AFP

Transformation of competent bacterial DH5- α was carried out with pRESTA-AFP. The transformed cell DH5- α was transferred onto LB medium which was anti-aminobenzyl penicillin, cultured overnight in an incubator at 37 °C. Four-five clones were selected and maintained in LB medium, and shaken overnight at 37 °C.

Evaluation of pRESTA-AFP

Five mL bacterial medium was picked up, and the plasmid

DNA was extracted following the procedures of EZNA plasmid miniprep kit (Omega). The extracted DNA was digested by *Bam*H I and *Eco*R I (TaKaRa). The digested products were evaluated with 10 g/L agarose gel electrophoresis.

Construction of recombinant human AFP eukaryotic expression vector

The human full-length AFP-cDNA was retrieved following the procedures of UNIQ-10 centrifugation column type gel retrieve kit (Sangon, Shanghai) and ligated to the multi-clony sites of pCEFL that was digested by *Bam*H I and *Eco*R I at a ratio of 10:1 with T4 DNA ligase (TaKaRa). Amplification, extraction, digestion and evaluation were performed according to the above-mentioned methods. It demonstrated that the full-length AFP-cDNA was inserted into pCEFL successfully, and named pCEFL-AFP.

Transfections of CHO cells

CHO cells were transiently transfected with pCEFL-AFP by liposome, Lipofectamine™ 2000 (Gibco). All the procedures were performed according to the guidance of the reagent. CHO cells were also transfected with pCEFL as control group, CHO cells not being transfected also served as control.

Detection of AFP expression by electrochemiluminescence

The supernatants of the cells from the three groups were collected, and detected by electrochemiluminescence method with Elecsys 1010 (Roche) and AFP electrochemiluminescence detection kit (Roche).

Detection of AFP expression by immunofluorescence

The transfected cells were stabilized with 10 g/L formaldehydum polymerisatum for 30 minutes at 4 °C, and blocked with 100 g/L bovine serum albumin (BSA) for 1 hour at room temperature, then coated with rabbit anti-human AFP antibody (Dako) for 45 minutes at 37 °C, followed by goat anti-rabbit IgG-FITC (Boster, Wuhan) for 30 minutes at 37 °C. The antibody-coated cells were observed under fluorescence microscope (Optiphot XIF, Nikon, Japan) within 24 hours.

Statistical analysis

Student's *t* test was used to compare the difference of AFP molecule in the supernatants between control groups and transfected pCEFL-AFP group. *P* value less than 0.05 was considered statistically significant.

RESULTS

Evaluation of pRESTA-AFP

pRESTA-AFP was digested by *Bam*H I and *Eco*R I and evaluated with electrophoresis. Figure 1 shows that pRESTA-AFP contained the full-length human AFP-cDNA.

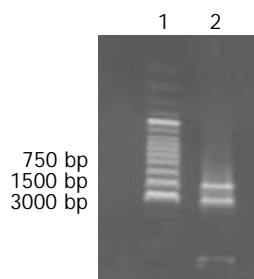


Figure 1 Electrophoresis of pRESTA-AFP. 1. Marker, 2. Full length AFP-cDNA in the upper, pRESTA in the lower.

Evaluation of pCEFL-AFP

To demonstrate that the full-length human AFP-cDNA was inserted into the multi-clony sites of pCEFL correctly, pCEFL-AFP was digested by *Bam*H I and *Eco*R I and evaluated with electrophoresis. Figure 2 shows that AFP-cDNA was inserted into pCEFL successfully.

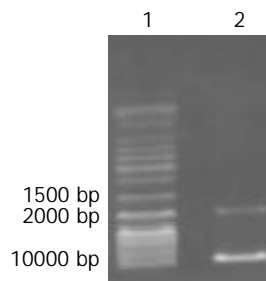


Figure 2 Electrophoresis of pCEFL-AFP. 1. Marker, 2. Full length AFP-cDNA in the upper, pCEFL in the lower.

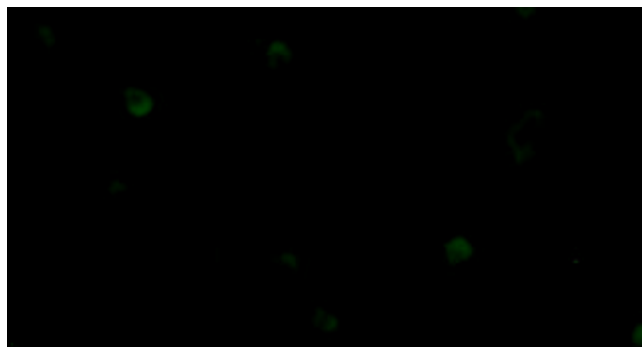


Figure 3 CHO transfected with pCEFL-AFP. The fluorescence staining in the cytoplasm was positive. $\times 400$.

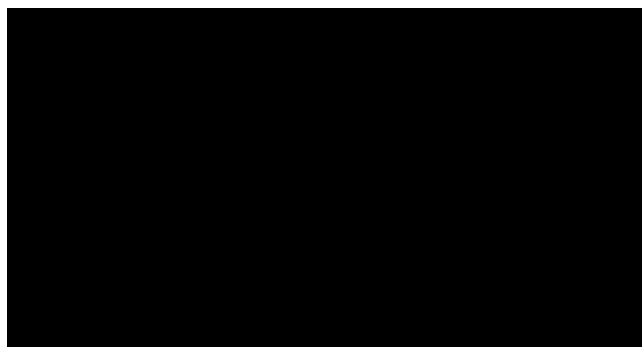


Figure 4 CHO transfected with pCEFL. The fluorescence staining in the cytoplasm was negative. $\times 400$.



Figure 5 Non-transfected CHO. The fluorescence staining in the cytoplasm was negative. $\times 400$.

AFP molecule expression in the supernatant

CHO cells were transfected with pCEFL-AFP. To demonstrate that the transfection was successful, the supernatant of CHO cells was detected by electrochemiluminescence method. The results showed that AFP molecule expression in the supernatant of CHO cells transfected with pCEFL-AFP was higher (972.3 ± 69.9 IU/L) than that transfected with pCEFL (556.3 ± 60.2 IU/L, $P < 0.05$) and also higher than that not being transfected (582.3 ± 58.0 IU/L, $P < 0.05$). The differences were significant.

Immunofluorescence staining of transfected cells

The transfected cells were coated with AFP antibody and fluorescent antibody. Under fluorescence microscope, it could be observed that the fluorescence staining was positive in the cytoplasm of CHO cells transfected with pCEFL-AFP and negative in the controls (Figures 3-5).

DISCUSSION

In China, the incidence of HCC is very high, and surgical operation, chemotherapy, and interventional therapy are the common therapies. But only a few patients of earlier stage without extrahepatic malignancy are indicated for operation, and for the advanced cases, chemotherapy and interventional therapy usually cannot achieve a satisfactory effect. AFP is a TAA of HCC, which may be used as a target for treatment.

Vollmer *et al.*^[30] firstly showed a prophylactic effect of an AFP-specific DNA vaccination on the growth of AFP-positive tumor cells in C57BL/6 mice. In their experiments, only 7.4 % of mice were fully protected from tumor growth. In the remaining animals, a prolonged time until tumors reached diameters of 10 mm was observed. Wang *et al.*^[31] found that antisense S-ODNs targeting AFP gene treatment led to reduced AFP gene expression. Specific antisense S-ODNs, but not control S-ODNs, inhibited the growth of hepatoma cells *in vitro*. *In vitro*, only antisense S-ODNs exhibited obvious antitumor activities. Guo *et al.*^[32] found that the dendritic cells (DCs) based vaccine with HLA-A2 restricted peptide epitope derived from hAFP have marked cytotoxicity against AFP positive primary HCC. In their experiments, after stimulated by DCs loaded with CTL epitope based peptide derived from hAFP, lymphocytes showed good characteristics and the culture medium of activated lymphocytes contained a high level of Th1 type cytokines of IL-12 and TNF. Activated lymphocytes not only specifically lysed HLA-A2 (+) HepG2 line but also had the cytotoxicity against T2 target cells loaded with peptide of hAFP. Hanke *et al.*^[33] demonstrated that DNA vaccination with AFP-encoding plasmid DNA could prevent the growth of subcutaneous AFP-expressing tumors and not interfere with liver regeneration in mice. Grimm *et al.*^[34] achieved similar outcomes.

Since immunotherapy or gene therapy targeting TAA or TSA is a direction of tumor therapy, AFP as a TAA of HCC, has shown its profound effect on HCC treatment in animal models. In our experiment, we constructed the recombinant human AFP eukaryotic expression vector successfully. This, we believe, provides experimental data for gene therapy and immunotherapy of HCC. It may be used as a treatment target of human HCC.

REFERENCES

- 1 **Wu W**, Lin XB, Qian JM, Ji ZL, Jiang Z. Ultrasonic aspiration hepatectomy. For 136 patients with hepatocellular carcinoma. *World J Gastroenterol* 2002; **8**: 763-765
- 2 **Jiang HC**, Liu LX, Piao DX, Xu J, Zheng M, Zhu AL, Qi SY, Zhang WH, Wu LF. Clinical short-term results of radiofrequency ablation in liver cancers. *World J Gastroenterol* 2002; **8**: 624-630
- 3 **Zhang G**, Long M, Wu ZZ, Yu WQ. Mechanical properties of hepatocellular carcinoma cells. *World J Gastroenterol* 2002; **8**: 243-246
- 4 **Tang ZY**. Hepatocellular carcinoma-cause, treatment and metastasis. *World J Gastroenterol* 2001; **7**: 445-454
- 5 **Rabe C**, Pilz T, Klostermann C, Berna M, Schild HH, Sauerbruch T, Caselmann WH. Clinical characteristics and outcome of a cohort of 101 patients with hepatocellular carcinoma. *World J Gastroenterol* 2001; **7**: 208-215
- 6 **Jiang YF**, Yang ZH, Hu JQ. Recurrence or metastasis of HCC: predictors, early detection and experimental antiangiogenic therapy. *World J Gastroenterol* 2000; **6**: 61-65
- 7 **Zhao WH**, Ma ZM, Zhou XR, Feng YZ, Fang BS. Prediction of recurrence and prognosis in patients with hepatocellular carcinoma after resection by use of CLIP score. *World J Gastroenterol* 2002; **8**: 237-242
- 8 **Qin LX**, Tang ZY. The prognostic molecular markers in hepatocellular carcinoma. *World J Gastroenterol* 2002; **8**: 385-392
- 9 **Zeng WJ**, Liu GY, Xu J, Zhou XD, Zhang YE, Zhang N. Pathological characteristics, PCNA labeling index and DNA index in prognostic evaluation of patients with moderately differentiated hepatocellular carcinoma. *World J Gastroenterol* 2002; **8**: 1040-1044
- 10 **Durr R**, Caselmann WH. Carcinogenesis of primary liver malignancies. *Langenbecks Arch Surg* 2000; **385**: 154-161
- 11 **Caselmann WH**, Blum HE, Fleig WE, Huppert PE, Ramadori G, Schirmacher P, Sauerbruch T. Guidances of the german society of digestive and metabolic diseases for diagnosis and therapy of hepatocellular carcinoma. German society of digestive and metabolic diseases. *Z Gastroenterol* 1999; **37**: 353-365
- 12 **Bronte V**, Apolloni E, Ronca R, Zamboni P, Overwijk WW, Surman DR, Restifo NP, Zanovello P. Genetic vaccination with "self" tyrosinase-related protein 2 causes melanoma eradication but not vitiligo. *Cancer Res* 2000; **60**: 253-258
- 13 **Tuting V**, Gambotto A, DeLeo A, Lotze MT, Robbins PD, Storkus WJ. Induction of tumor antigen-specific immunity using plasmid DNA immunization in mice. *Cancer Gene Ther* 1999; **6**: 73-80
- 14 **Conry RM**, LoBuglio AF, Loechel F, Moore SE, Sumerel LA, Barlow DL, Pike J, Curiel DT. A carcinoembryonic antigen polynucleotide vaccine for human clinical use. *Cancer Gene Ther* 1995; **2**: 33-38
- 15 **Shen LJ**, Zhang ZJ, Ou YM, Zhang HX, Huang R, He Y, Wang MJ, Xu GS. Computed morphometric analysis and expression of alpha-fetoprotein in hepatocellular carcinoma and its related lesion. *World J Gastroenterol* 2000; **6**: 415-416
- 16 **Sithinamsuwan P**, Piratvisuth T, Tanomkiat W, Apakupakul N, Tongyoo S. Review of 336 patients with hepatocellular carcinoma at Songklanagarind Hospital. *World J Gastroenterol* 2000; **6**: 339-343
- 17 **Wawrzynowicz-Syczewska M**, Leonciuk A, Jurczyk K, Karpinska E, Boron-Kaczmarek A. Increased incidence of hepatocellular carcinoma. *Pol Merkuriusz Lek* 2002; **13**: 100-102
- 18 **Chou SF**, Hsu WL, Hwang JM, Chen CY. Production of monoclonal and polyclonal antibodies against human alpha-fetoprotein, a hepatocellular tumor marker. *Hybrid Hybridomics* 2002; **21**: 301-305
- 19 **Chu PG**, Ishizawa S, Wu E, Weiss LM. Hepatocyte antigen as a marker of hepatocellular carcinoma: an immunohistochemical comparison to carcinoembryonic antigen, CD10, and alpha-fetoprotein. *Am J Surg Pathol* 2002; **26**: 978-988
- 20 **Nguyen MH**, Garcia RT, Simpson PW, Wright TL, Keeffe EB. Racial differences in effectiveness of alpha-fetoprotein for diagnosis of hepatocellular carcinoma in hepatitis C virus cirrhosis. *Hepatology* 2002; **36**: 410-417
- 21 **Ma J**, Gong Q, Lin M. Combined five tumor markers in detecting primary hepatic carcinoma. *Zhonghua Waikao Zazhi* 2000; **38**: 14-16
- 22 **Qin LX**, Tang ZY. The prognostic significance of clinical and pathological features in hepatocellular carcinoma. *World J Gastroenterol* 2002; **8**: 193-199
- 23 **Song BC**, Suh DJ, Yang SH, Lee HC, Chung YH, Sung KB, Lee YS. Lens culinaris agglutinin-reactive alpha-fetoprotein as a prognostic marker in patients with hepatocellular carcinoma undergoing transcatheter arterial chemoembolization. *J Clin Gastroenterol* 2002; **35**: 398-402

- 24 **Witzigmann H**, Geissler F, Benedix F, Thiery J, Uhlmann D, Tannapfel A, Wittekind C, Hauss J. Prospective evaluation of circulating hepatocytes by alpha-fetoprotein messenger RNA in patients with hepatocellular carcinoma. *Surgery* 2002; **131**: 34-43
- 25 **Ijichi M**, Takayama T, Matsumura M, Shiratori Y, Omata M, Makuuchi M. Alpha-Fetoprotein mRNA in the circulation as a predictor of postsurgical recurrence of hepatocellular carcinoma: a prospective study. *Hepatology* 2002; **35**: 853-860
- 26 **Wu X**, Lin Z, Fan J, Lu J, Wang L, Tang Z. Quantitation of alpha-fetoprotein messenger RNA in peripheral blood of nude mice and its relationship with tumor recurrence and metastasis after curative resection of hepatocellular carcinoma. *Zhonghua Ganzangbing Zazhi* 2002; **10**: 189-191
- 27 **He P**, Tang ZY, Ye SL, Liu BB. Relationship between expression of alpha-fetoprotein messenger RNA and some clinical parameters of human hepatocellular carcinoma. *World J Gastroenterol* 1999; **5**: 111-115
- 28 **Li MS**, Li PF, He SP, Du GG, Li G. The promoting molecular mechanism of alpha-fetoprotein on the growth of human hepatoma Bel7402 cell line. *World J Gastroenterol* 2002; **8**: 469-475
- 29 **Li MS**, Li PF, Li G, Du GG. Enhancement of Proliferation of HeLa Cells by the alpha-Fetoprotein. *Shengwuhuaxue Yu Shengwuwuli Xuebao* 2002; **34**: 769-774
- 30 **Vollmer CM Jr**, Eliber FC, Butterfield LH, Ribas A, Dissette VB, Koh A, Montejo LD, Lee MC, Andrews KJ, McBride WH, Glaspy JA, Economou JS. Alpha-fetoprotein-specific genetic immunotherapy for hepatocellular carcinoma. *Cancer Res* 1999; **59**: 3064-3069
- 31 **Wang XW**, Yuan JH, Zhang RG, Guo LX, Xie Y, Xie H. Antihepatoma effect of alpha-fetoprotein antisense phosphorothioate oligodeoxyribonucleotides *in vitro* and in mice. *World J Gastroenterol* 2001; **7**: 345-351
- 32 **Guo J**, Cai M, Wei D, Qin L, Huang J, Wang X. Immune responses of dendritic cells after loaded with cytotoxicity T lymphocyte epitope based peptide of human alpha-fetoprotein (hAFP). *Zhonghua Ganzangbing Zazhi* 2002; **10**: 178-180
- 33 **Hanke P**, Serwe M, Dombrowski F, Sauerbruch T, Caselmann WH. DNA vaccination with AFP-encoding plasmid DNA prevents growth of subcutaneous AFP-expressing tumors and does not interfere with liver regeneration in mice. *Cancer Gene Ther* 2002; **9**: 346-355
- 34 **Grimm CF**, Ortmann D, Mohr L, Michalak S, Krohne TU, Meckel S, Eisele S, Encke J, Blum HE, Geissler M. Mouse alpha-fetoprotein-specific DNA-based immunotherapy of hepatocellular carcinoma leads to tumor regression in mice. *Gastroenterology* 2000; **119**: 1104-1112

Edited by Ma JY

Mast cells and human hepatocellular carcinoma

Fabio Grizzi, Barbara Franceschini, Maurizio Chiriva-Internati, Young Liu, Paul L. Hermonat, Nicola Dioguardi

Fabio Grizzi, Barbara Franceschini, Nicola Dioguardi, Scientific Direction, Istituto Clinico Humanitas, Rozzano, Milan, Italy. Fondazione "M. Rodriguez", Istituto Scientifico per le Misure Quantitative in Medicina, Milan, Italy

Maurizio Chiriva-Internati, Health Sciences Center, Texas Tech University, Amarillo, Texas, USA

Young Liu, Paul L. Hermonat, Department of Obstetrics and Gynecology, Division of Gynecologic Oncology, University of Arkansas, Little Rock, Arkansas, USA

Supported by the grants from the Foundation "Michele Rodriguez". Istituto Scientifico per le Misure Quantitative in Medicina, Milan, Italy

Correspondence to: Fabio Grizzi, Ph.D., Scientific Direction, Istituto Clinico Humanitas, Via Manzoni, 56 20089 Rozzano, Milano, Italy. fabio.grizzi@humanitas.it

Telephone: +390282244548 **Fax:** +390282244590

Received: 2002-11-30 **Accepted:** 2002-12-22

Abstract

AIM: To investigate the density of mast cells (MCs) in human hepatocellular carcinoma (HCC), and to determine whether the MCs density has any correlations with histopathological grading, staging or some baseline patient characteristics.

METHODS: Tissue sections of 22 primary HCCs were histochemically stained with toluidine blue, in order to be able to quantify the MCs in and around the neoplasm using a computer-assisted image analysis system. HCC was staged and graded by two independent pathologists. To identify the sinusoidal capillarisation of each specimen 3 µm thick sections were histochemically stained with sirius red, and semi-quantitatively evaluated by two independent observers. The data were statistically analysed using Spearman's correlation and Student's *t*-test when appropriate.

RESULTS: MCs density did not correlate with the age or sex of the patients, the serum alanine aminotransferase (ALT) or aspartate aminotransferase (AST) levels, or the stage or grade of the HCC. No significant differences were found between the MCs density of the patients with and without hepatitis C virus infection, but they were significantly higher in the specimens showing marked sinusoidal capillarisation.

CONCLUSION: The lack of any significant correlation between MCs density and the stage or grade of the neoplastic lesions suggests that there is no causal relationship between MCs recruitment and HCC. However, as capillarisation proceeds concurrently with arterial blood supply during hepatocarcinogenesis, MCs may be considered of primary importance in the transition from sinusoidal to capillary-type endothelial cells and the HCC growth.

Grizzi F, Franceschini B, Chiriva-Internati M, Liu Y, Hermonat PL, Dioguardi N. Mast cells and human hepatocellular carcinoma. *World J Gastroenterol* 2003; 9(7): 1469-1473
<http://www.wjgnet.com/1007-9327/9/1469.asp>

INTRODUCTION

Mast cells (MCs) have fascinated the biomedical sciences ever since they were first recognised by Paul Ehrlich in the late 1800s^[1]. MCs originate from haematopoietic stem cells in bone marrow^[2, 3]. MCs circulate in the blood only as progenitors, and it is not until they enter the tissues that they undergo their terminal differentiation into mature cells. MCs provide granule and membrane mediators as well as different cytokines during the course of many human and experimental diseases^[4-8]. It has recently been shown that MCs play an important role in antigen presentation to T cells, and that there is a direct interaction between them and the B cells signalling immunoglobulin E (IgE) production. Although a number of studies have shown that MCs play different roles in human tumours^[9-26], the exact nature of the relationship between them and HCC has still to be established. The aim of the present study was to investigate MCs density in HCC and compare it with stage and grade of the neoplasia, and some clinical and histopathological characteristics of the patients.

MATERIALS AND METHODS

Patient profiles and surgical specimens

The study was conducted in accordance with the guidelines of the Ethics Committee of the hospital treating the patients (Istituto Clinico Humanitas, Rozzano, Milan, Italy), all of whom were informed of the possible discomforts and risks of surgical treatment.

The study involved 22 primary HCC patients (15 men and 7 women, mean age: 68.22 years, range 48-80 years) who were surgically treated between 1997 and 2001 (Table 1). Tumours were independently graded and staged by two experienced histopathologists. The study was performed on surgical specimens fixed in formalin and embedded in paraffin.

Histochemical detection of MCs and capillarisation

Sections of 3 µm were cut, mounted on glass slides, de-waxed in xylene and re-hydrated using graded alcohol/water baths. They were then rinsed in distilled water for 5 minutes and incubated for 30 minutes at room temperature with a freshly made staining aqueous solution consisting of 0.1 % toluidine blue (Sigma Chem. Co., MO, USA) and 0.005 % acetic acid. The number of MCs detectable on the whole surface of the available liver sections at a magnification of 200× was quantified using a computer-assisted image analysis system consisting of an Axiophot light microscope (Zeiss, Germany), a 3-CCD camera (JVC KY-F55BE, Italy), a Pentium 600 computer (Hewlett-Packard, Italy) with an incorporated frame-grabber board (Imascan, USA), and Image-Pro Plus image analysis software (Imaginie Computer, Rho, Italy). The digitized image, which was composed of a variable number of fields tiled together to form a unique final image, represent all of the histological materials available for examination (>30 mm² for each slide). The Image Pro-Plus software automatically selected stained MCs as single objects on the basis of similarities in the color of adjacent pixels, the image intensity was the same throughout the study. MCs density (d) was automatically calculated using the formula: d=(number of

MCs)/(sample surface), where the sample surface was expressed in μm^2 .

In order to evaluate the hepatic sinusoid capillarisation of each specimen, a $3\ \mu\text{m}$ section was stained with Direct-red 80 (Sigma Chem. Co., MO, USA; 0.1 % in saturated picric acid). The sections were subsequently washed in running tap water for 30 minutes to remove excess staining, counter-stained in Mayer's hemallum solution, dehydrated, and mounted in Eukitt (Bio-Optica, Milan, Italy). Sinusoid capillarisation was independently scored as strong (+++), moderate (++), weak (+) or absent (0) by two experienced histopathologists.

Statistical analysis

Linear regression analysis was used to assess the statistical correlation between MCs density and the other histopathological and clinical data. The relationships were determined using Spearman's correlation and Student's *t*-test when appropriate. Statistical analysis was performed using Statistica software (StatSoft Inc., Tulsa, OK, USA). $P < 0.05$ was considered statistically significant.

RESULTS

Table 1 shows the baseline characteristics of the 22 patients involved in the study. MCs were strongly identified in 18 cases (82 %). They were found in and around the neoplastic tissue. MCs density did not correlate with the patients' age ($r = 0.1698$). It correlated non-significantly with disease stage (Figure 1A) and disease grade (Figure 1B), nor with serum alanine aminotransferase (ALT, $r = 0.20765$) or aspartate aminotransferase (AST, $r = -0.0439$) (Figure 2). There was no significant difference in the density of MCs between the patients with and without chronic hepatitis C virus disease (Figure 3), but a semi-quantitative evaluation showed that MCs density did correlate significantly with the capillarisation process (Table 2). MCs were found abundantly in tissues showing a higher capillarisation phenomenon (Figure 4).

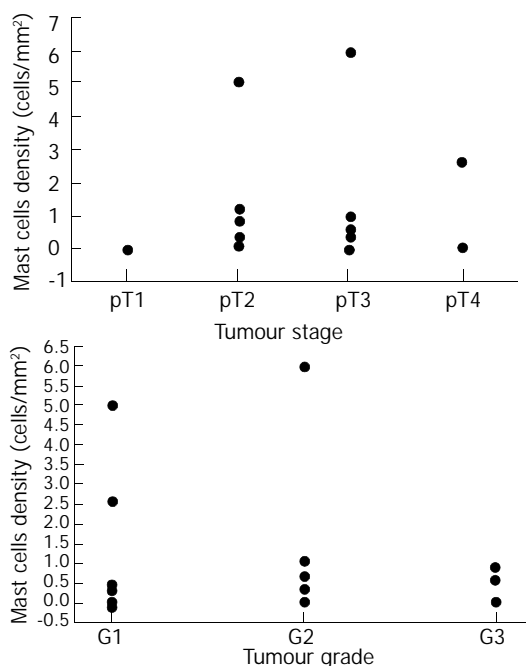


Figure 1 Relationship between MCs density and tumour stage (A) and tumour grade (B).

Table 2 Semi-quantitative evaluation of sinusoidal capillarisation related to MCs density (cells/mm²)

MC density	Presence of capillarisation			
	Absent	Weak	Moderate	Strong
0-0.01	3	2	0	0
0.01-0.1	3	0	0	0
0.1-1	1	5	1	0
>1	0	0	2	3 ^a

^a $P < 0.005$ vs the other categories.

Table 1 Baseline characteristics of the patients involved in the study

<i>n</i>	Age	Sex	ALT(UI/l)	AST	Histology	Stage	Grade	Angioinvasivity	HCV-Ab	MCs density(cells/mm ²)
1	73	m	98	37	TR	G1	pT2	absent	-	0
2	70	m	61	37	PS	G2	pT2	peritumoural	-	0
3	76	f	97	94	TR	G2	pT3	peritumoural	+	0
4	59	m	169	48	TR	G3	pT4	peritumoural	+	0
5	72	f	40	29	TR	G1	pT3	peritumoural	nd	0.0053
6	51	f	20	32	TR	G3	pT3	peritumoural	-	0.0061
7	70	f	62	66	C	G1	pT1	absent	+	0.0062
8	67	m	108	82	TR	G3	pT3	peritumoural	+	0.0483
9	71	m	48	64	PS	G1	pT2	peritumoural	-	0.0625
10	78	m	75	116	TR	G3	pT2	absent	+	0.0726
11	71	m	199	110	C	G1	pT4	peritumoural	+	0.253
12	74	m	40	25	TR	G1	pT2	absent	nd	0.3846
13	76	f	75	94	TR	G2	pT3	intratumoural	+	0.446
14	77	m	286	95	TR	G3	pT3	absent	+	0.55
15	63	m	97	78	TR	G2	pT3	peritumoural	+	0.625
16	69	m	55	74	C	G3	pT3	absent	+	0.894
17	80	f	58	64	TR	G3	pT3	peritumoural	+	0.9422
18	51	m	103	153	C	G2	pT2	absent	+	1.1
19	68	f	79	113	TR	G1	pT2	absent	+	1.15
20	48	f	149	76	TR	G1	pT2	absent	-	2.58
21	73	m	116	45	TR	G1	pT3	absent	-	5.041
22	64	m	131	70	C	G2	pT3	absent	+	6.006

TR=trabecular, PS=pseudoglandular, C= combined.

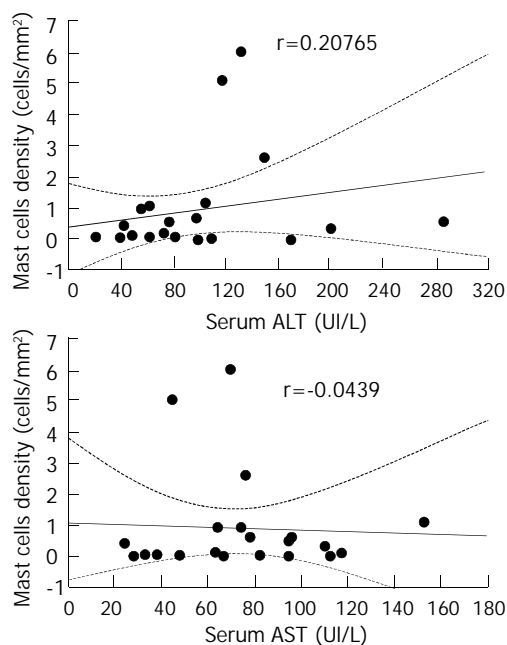


Figure 2 Correlation between MCs densities and serum ALT (A) and AST (B).

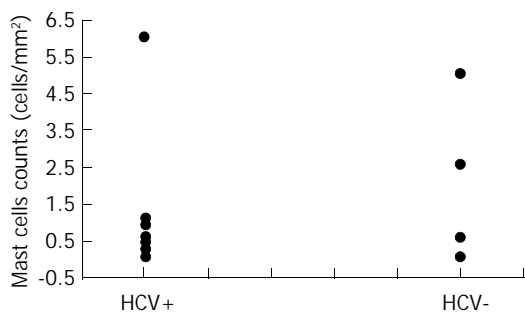


Figure 3 MCs densities in patients with and without hepatitis C virus (HCV) infection.

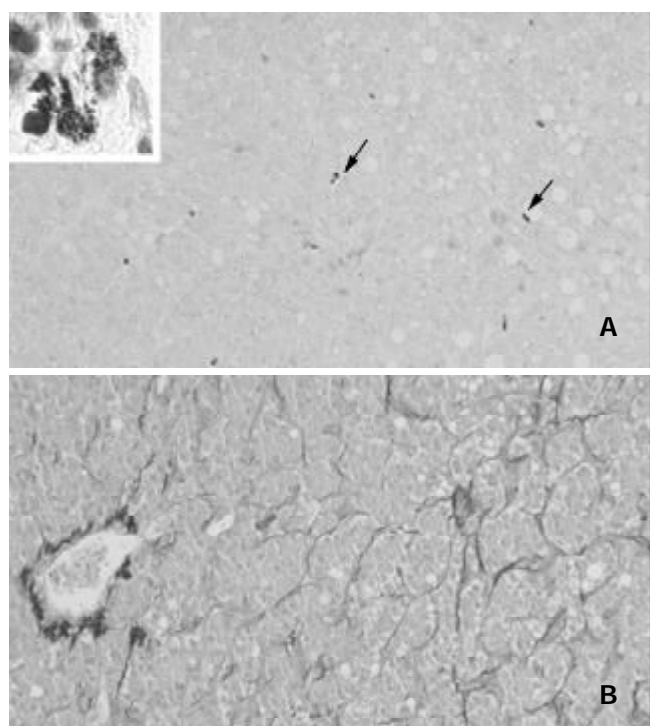


Figure 4 MCs were found abundantly in tissues showing a

higher capillarisation phenomenon. (a) High densities of stained MCs (arrows) in human HCC tissues (toluidine blue, objective magnification 5x; insert, objective magnification, 100x). (b) Sinusoidal capillarisation in HCC tissue (sirius red, objective magnification 20x).

DISCUSSION

MCs are a group of long-living cells of bone marrow origin that are commonly found in the skin and the gastrointestinal and respiratory systems. These cells produce, store and release a high number of bioactive mediators, such as TNF- α , IL-1, IL-4, IL-5, IL-6, IL-8, IL-13, NGF, β -FGF and TGF- β , histamine, and the serine proteases, trypsin and chymase^[3, 4, 27].

MCs are known to be present in normal and pathological livers. In normal human livers, there are a few resident MCs located near the portal tracts which are more densely distributed around the biliary tree. Large amounts of MCs have been detected in the fibrotic septa and portal regions in cirrhotic human livers. A number of studies have indicated that MCs are associated with hepatic fibrosis as they promote fibroblast growth, collagen synthesis and may inhibit extracellular matrix degradation by means of inhibitors of metalloproteases (TIMPs)^[6, 27-32]. MCs density is a valid index of acute liver inflammation^[7, 8].

MCs were recognized in various human tumours^[8, 26]. The accumulation of MCs around the neoplasia is a well-known phenomenon in basal cell carcinoma, melanoma, lung, prostate and breast cancer.

Although the functions of intra-tumour MCs are yet unclear (some MCs have been evidenced in close apposition to tumour cells, suggesting the existence of direct cell-to-cell interactions), two main hypotheses have been proposed: The first is that MCs may accelerate tumour growth, invasion and neovascularity. Contrarily, the second is that MCs have cytotoxic activity for some tumours (especially those sensitive to TNF- α), as a result of cytotoxic products or the enhancement of the cytotoxic activation of mainly peri-tumoural eosinophils and macrophages^[33-36].

Experimental studies have shown that an increase in MCs density is stimulated by IL-3 and IL-4, thus suggesting that their defensive role against tumour growth may be particularly associated with T cells^[37-39]. IL-4 is essential for the triggering of Th2 lymphocytes that they themselves produce to initiate inflammatory cell accumulation and B lymphocyte immunoglobulin class switching to IgE^[40].

However, the well documented relationship between MCs and angiogenesis makes the first hypothesis more persuasive^[23, 27]. Secreting MCs are able to induce and enhance angiogenesis via multiple in part interacting pathways^[27]. The supporting evidence includes: (a) The fact that tumour cells produce agents promoting MC chemotaxis. Moreover, most of the tumour-infiltrating MCs exhibit anaphylactic or piecemeal degranulation, indicating that the MCs are activated *in situ*. (b) MCs degranulation facilitates the endothelial cell invasion in connective tissue. (c) MC heparin stimulates the endothelial cell motility essential for the angiogenic process. (d) The *metachromasia* that is determined by the presence of highly sulphated proteoglycans in the secretory granules of MCs, is commonly found at the tumour periphery, suggesting the release of vasoactive substances around the tumour. (e) Histamine, VEGF, and certain lipid-derived mediators that induce microvascular hyperpermeability having pro-angiogenic effects.

In the present paper, we showed that HCC contained a higher density of toluidine blue stained MCs, thus suggesting that the recruitment of MCs increases during the development of HCC. However, the results obtained from 22 HCC patients

did not indicate any significant correlation between MCs density and disease stage. We hypothesize that the lower density observed in the most severe stage may be due to the massive degranulation of a large number of MCs.

Moreover, the obtained results allow the following conclusions to be drawn: (a) MCs density did not significantly correlate with disease grade, but there was a trend towards a decrease in MCs number as the grade increased. (b) There was no correlation between MCs density and some baseline characteristics of the patients, such as the sex or age of the patients, since the tumour evolves more slowly in older patients, we expected to find a higher density in younger cases. This hypothesis was partially substantiated by an albeit statistically non-significant negative correlation between MCs density and age. This behaviour was in line with theoretical models showing that a large number of biological events were age-dependent^[7]. (c) MCs density did not correlate with serum ALT or AST levels. HCV, cirrhosis and HCC were associated with persistent or fluctuating elevations in ALT levels, but did not distinguish among these conditions. (d) There was no significant difference in the density of MCs between patients with and without HCV disease. As it is known that there is a close relationship between HCC and hepatitis C virus infection, it is not surprising that we had more HCV-positive than HCV-negative cases. Nevertheless, MCs density was similar in both groups, suggesting that HCV infection did not increase MC recruitment. (e) The close proximity of MCs and surrounding tumour cells suggested the existence of roles of MCs in the development of HCC, including tumour growth as well as host immunity and stromal reaction. (f) The density of MCs was higher in the specimens showing a greater capillarisation of sinusoidal endothelial cells.

A number of studies have indicated that the sinusoidal endothelial cells tend to show phenotypic changes in the early stage of hepatocarcinogenesis. In HCC, endothelial fenestrae are diminished and basement membrane become thick: due to the fact that as the arterial blood supply for HCC increases, the sinusoidal endothelial cells may form basement membranes, mainly consisting of type IV collagen and laminin, and take on the morphological appearance of capillaries^[41-44].

Capillarisation of sinusoids has also constant features such as the appearance of new junctions between endothelial cells, deposition of fibrillary material in Disse's spaces, and flattening of hepatocyte microvilli. Capillarisation of the sinusoid may also cause a disturbance in exchanges of many bioactive substances between the sinusoidal blood and liver cells across the Disse space. Capillarisation, resulting in impairment of microcirculation, subsequently, affecting the exchange of the oxygen and substance of the liver cell seriously, thus brings about or aggravates the damage of liver cell^[45]. Capillarisation may contribute to the HCC metastatic process. The angiogenesis of liver metastases may progress stepwise as the metastases enlarge, and capillarisation of sinusoidal endothelium around the liver metastases may occur. A number of papers have suggested that (a) tumour vessels in metastatic liver cancers consist of endothelium, collagenic basement membrane and pericytes, (b) the sinusoids adjacent to tumours undergo capillarisation, and (c) VEGF, a well-demonstrated mediator secreted by MCs may contribute to angiogenesis in metastatic HCC.

It is well documented that heparin, combined to a range of heparin-binding factors such as b-FGF or TGF- β , or other potent factors, such as IL-8 and VEGF, are able to promote neovascularity, and that MC proteases cause loss of the extracellular matrix integrity^[27].

All these comments suggest that MCs accumulation at the tumour site may lead to increased rates of tumour vascularity and, consequently, increased rates of tumour growth and

metastasis.

In conclusion, since capillarisation proceeds concurrently with arterial blood supply during hepatocarcinogenesis, MCs may be considered as a key element in the process of transition from sinusoidal endothelial cells into capillary-type endothelial cells and concurrently in the development of collagen's basement membrane. MCs mediated capillarisation may thus be of pathogenic significance in tumor growth.

ACKNOWLEDGMENTS

The authors are grateful to prof. Massimo Roncalli and Dr Piergiuseppe Colombo for supplying the HCC specimens, and for their grading and staging classification. They would also like to thank Giorgia Ceva-Grimaidi for her precious technical support.

REFERENCES

- 1 **Ehrlich P.** Beitrage zur kenntniss der quilinfarbunger und ihrer verivendung in der mickroskopischen technik. *Alch Mikros Anat* 1877; **13**: 263-267
- 2 **Welle M.** Development, significance, and heterogeneity of mast cells with particular regard to the mast cell-specific proteases, chymase and tryptase. *J Leukoc Biol* 1997; **61**: 233-245
- 3 **Fodiger M,** Fritsch G, Winkler K, Emminger W, Mitterbauer G, Gadner H, Valent P, Mannhalter C. Origin of human mast cells: development from transplanted hematopoietic stem cells after allogenic bone marrow transplantation. *Blood* 1994; **84**: 2954-2959
- 4 **Galli SJ.** Mast cells and basophils. *Curr Opinion Haematol* 2000; **7**: 32-39
- 5 **Metcalfe DD,** Baram D, Mekori YA. Mast cells. *Physiol Rev* 1997; **77**: 1033-1079
- 6 **Farrell DJ,** Hines JE, Walls AF, Kelly PJ, Bennett MK, Burt AD. Intrahepatic mast cells in chronic liver diseases. *Hepatology* 1995; **22**: 1175-1181
- 7 **Grizzi F,** Franceschini B, Gagliano N, Barbieri B, Arosio B, Annoni G, Chiriva-Internati M, Dioguardi N. Mast cell density: a quantitative index of liver acute inflammation. *Anal Quant Cytol Histol* 2002; **24**: 63-69
- 8 **Grizzi F,** Franceschini B, Gagliano N, Moscheni C, Annoni G, Vergani C, Hermonat PL, Chiriva-Internati M, Dioguardi N. Mast cell density, hepatic stellate cell activation and TGF- β_1 transcript in aging Sprague-Dowely rat during the early acute liver injury. *Toxicol Pathol* 2003; **31**: 173-178
- 9 **Sari A,** Serri TA, Candir O, Ozturk A, Kosar A. Mast cell variations in tumour tissue and with histopathological grading in specimens of prostatic adenocarcinoma. *BJU International* 1999; **84**: 851-853
- 10 **Imada A,** Shijubo N, Kojima H, Abe S. Mast cells correlate with angiogenesis and poor outcome in stage lung adenocarcinoma. *Eur Respir J* 2000; **15**: 1087-1093
- 11 **Tomita M,** Matsuzaki Y, Onitsuka T. Effect of mast cells on tumor angiogenesis in lung cancer. *Ann Thorac Surg* 2000; **69**: 1686-1690
- 12 **Simak R,** Capodiec P, Cohen DW, Fair WR, Scher H, Melamed J, Drobnjak M, Heston WD, Stix U, Steiner G, Cordon-Cardo C. Expression of c-kit and kit-ligand in benign and malignant prostatic tissues. *Histol Histopathol* 2000; **15**: 365-374
- 13 **Toth-Jakatics R,** Jimi S, Takebayashi S, Kawamoto N. Cutaneous malignant melanoma: correlation between neovascularization and peritumor accumulation of mast cells overexpressing vascular endothelial growth factor. *Hum Pathol* 2000; **31**: 955-960
- 14 **Terada T,** Matsunaga Y. Increased mast cells in hepatocellular carcinoma and intrahepatic cholangiocarcinoma. *J Hepatol* 2000; **33**: 961-966
- 15 **Demitsu T,** Inoue T, Kakurai M, Kiyosawa T, Yoneda K, Manabe M. Activation of mast cells within a tumor of angiosarcoma: ultrastructural study of five cases. *J Dermatol* 2002; **29**: 280-289
- 16 **Yano H,** Kinuta M, Tateishi H, Nakano Y, Matsui S, Monden T, Okamura J, Sakai M, Okamoto S. Mast cell infiltration around gastric cancer cells correlates with tumor angiogenesis and metastasis. *Gastric Cancer* 1999; **2**: 26-32

- 17 **Cabanillas-Saez A**, Schalper JA, Nicovani SM, Rudolph MI. Characterization of mast cells according to their content of tryptase and chymase in normal and neoplastic human uterine cervix. *Int J Gynecol Cancer* 2002; **12**: 92-98
- 18 **Yavuz E**, Gulluoglu MG, Akbas N, Tuzlali S, Ilhan R, Iplikci A, Akhan SE. The values of intratumoral mast cell count and Ki-67 immunoreactivity index in differential diagnosis of uterine smooth muscle neoplasms. *Pathol Int* 2001; **51**: 938-941
- 19 **Elpek GO**, Gelen T, Aksoy NH, Erdogan A, Dertsiz L, Demircan A, Keles N. The prognostic relevance of angiogenesis and mast cells in squamous cell carcinoma of the oesophagus. *J Clin Pathol* 2001; **54**: 940-944
- 20 **Fukushima N**, Satoh T, Sano M, Tokunaga O. Angiogenesis and mast cells in non-Hodgkin's lymphoma: a strong correlation in angioimmunoblastic T-cell lymphoma. *Leuk Lymphoma* 2001; **42**: 709-720
- 21 **Tomita M**, Matsuzaki Y, Edagawa M, Shimizu T, Hara M, Sekiya R, Onitsuka T. Association of mast cells with tumor angiogenesis in esophageal squamous cell carcinoma. *Dis Esophagus* 2001; **14**: 135-138
- 22 **Erkilic S**, Erbagci Z. The significance of mast cells associated with basal cell carcinoma. *J Dermatol* 2001; **28**: 312-315
- 23 **Ribatti D**, Vacca A, Nico B, Crivellato E, Roncali L, Dammacco F. The role of mast cells in tumour angiogenesis. *Br J Haematol* 2001; **115**: 514-521
- 24 **Nielsen HJ**, Hansen U, Christensen II, Reimert CM, Brunner N, Moesgaard F. Independent prognostic value of eosinophil and mast cell infiltration in colorectal cancer tissue. *J Pathol* 1999; **189**: 487-495
- 25 **Reynolds JL**, Akhter JA, Magarey CJ, Schwartz P, Adams WJ, Morris DL. Histamine in human breast cancer. *Br J Surg* 1998; **85**: 538-541
- 26 **Kankkunen JP**, Harvima IT, Naukkarinen A. Quantitative analysis of tryptase and chymase containing mast cells in benign and malignant breast lesions. *Int J Cancer* 1997; **72**: 385-388
- 27 **Norby K**. Mast cells and angiogenesis. *APMIS* 2002; **110**: 355-371
- 28 **Cairns JA**, Walls AF. Mast cell tryptase stimulates the synthesis of type 1 collagen in human lung fibroblast. *J Clin Invest* 1997; **99**: 1313-1321
- 29 **Inoue Y**, King TE Jr, Barker E, Daniloff E, Newman LS. Basic fibroblast growth factor and its receptors in idiopathic pulmonary fibrosis and lymphangiomyomatosis. *Am J Respir Crit Care Med* 2002; **166**: 765-773
- 30 **Armbrust T**, Batusic D, Burkhardt R, Ramadori G. Mast cells distribution in human liver disease and experimental rat liver fibrosis. Indications for mast cell participation in development of liver fibrosis. *J Hepatol* 1997; **26**: 1042-1054
- 31 **Yamashiro M**, Kouda W, Kono N, Tsuneyama K, Matsui O, Nakanuma Y. Distribution of intrahepatic mast cells in various hepatobiliary disorders. An immunohistochemical study. *Virchows Arch* 1998; **433**: 471-479
- 32 **Neubauer K**, Saile B, Ramadori G. Liver fibrosis and altered matrix synthesis. *Can J Gastroenterol* 2001; **15**: 187-193
- 33 **Tani K**, Ogushi F, Shimizu T, Sone S. Protease-induced leukocyte chemotaxis and activation: roles in host defense and inflammation. *J Med Invest* 2001; **48**: 133-141
- 34 **Coussens LM**, Werb Z. Inflammatory cells and cancer: think different. *J Exp Med* 2001; **193**: F23-F26
- 35 **Montemurro P**, Nishioka H, Dundon WG, de Bernard M, Del Giudice G, Rappuoli R, Montecucco C. The neutrophil-activating protein (HP-NAP) of *Helicobacter pylori* is a potent stimulant of mast cells. *Eur J Immunol* 2002; **32**: 671-676
- 36 **Dimitriadou V**, Koutsilieris M. Mast cell-tumor cell interactions: for or against tumour growth and metastasis? *Anticancer Res* 1997; **17**: 1541-1549
- 37 **Bradding P**, Feather IH, Wilson S, Bardin PG, Heusser CH, Holgate ST, Howarth PH. Immunolocalization of cytokines in the nasal mucosa of normal and perennial rhinitic subjects. The mast cell as a source of IL-4, IL-5, and IL-6 in human allergic mucosal inflammation. *J Immunol* 1993; **151**: 3853-3865
- 38 **Bradding P**, Roberts JA, Britten KM, Montefort S, Djukanovic R, Mueller R, Heusser CH, Howarth PH, Holgate ST. Interleukin-4, -5, and -6 and tumor necrosis factor-alpha in normal and asthmatic airways: evidence for the human mast cell as a source of these cytokines. *Am J Respir Cell Mol Biol* 1994; **10**: 471-480
- 39 **Okayama Y**, Petit-Frere C, Kassel O, Semper A, Quint D, Tunon-de-Lara MJ, Bradding P, Holgate ST, Church MK. IgE-dependent expression of mRNA for IL-4 and IL-5 in human lung mast cells. *J Immunol* 1995; **155**: 1796-1808
- 40 **Wilson SJ**, Shute JK, Holgate ST, Howarth PH, Bradding P. Localization of interleukin (IL) -4 but not IL-5 to human mast cell secretory granules by immunoelectron microscopy. *Clin Exp Allergy* 2000; **30**: 493-500
- 41 **Kin M**, Torimura T, Ueno T, Inuzuka S, Tanikawa K. Sinusoidal capillarization in small hepatocellular carcinoma. *Pathol Int* 1994; **44**: 771-778
- 42 **Yamamoto T**, Kaneda K, Hirohashi K, Kinoshita H, Sakurai M. Sinusoidal capillarization and arterial blood supply continuously proceed with the advance of the stages of hepatocarcinogenesis in the rat. *Jpn J Cancer Res* 1996; **87**: 442-450
- 43 **Zimmermann A**, Zhao D, Reichen J. Myofibroblast in the cirrhotic rat liver reflects hepatic remodelling and correlates with fibrosis and sinusoidal capillarization. *J Hepatol* 1999; **30**: 646-652
- 44 **Park YN**, Yang CP, Fernandez GJ, Cubukcu O, Thung SN, Theise ND. Neoangiogenesis and sinusoidal "capillarization" in dysplastic nodules of the liver. *Am J Surg Pathol* 1998; **22**: 656-662
- 45 **Huang GW**, Yang LY. Metallothionein expression in hepatocellular carcinoma. *World J Gastroenterol* 2002; **8**: 650-653

Antitumor and immunomodulatory activity of resveratrol on experimentally implanted tumor of H22 in Balb/c mice

Hong-Shan Liu, Cheng-En Pan, Wei Yang, Xue-Min Liu

Hong-Shan Liu, Cheng-En Pan, Wei Yang, Xue-Min Liu, Department of Hepatobiliary Surgery, First Affiliated Hospital, Xi'an Jiaotong University, Xi'an 710061, Shaanxi Province, China
Correspondence to: Dr. Hong-Shan Liu, Department of Hepatobiliary Surgery, First Affiliated Hospital, Xi'an Jiaotong University, Xi'an 710061, Shaanxi Province, China. doctorliuqi@yahoo.com.cn
Telephone: +86-29-5324009 **Fax:** +86-29-5324009
Received: 2002-10-17 **Accepted:** 2002-12-07

Abstract

AIM: To study the antitumor and immunomodulatory activity of resveratrol on experimentally implanted tumor of H22 in Balb/c mice

METHODS: The cytotoxicity of peritoneal macrophages (M ϕ) against H22 cells was measured by the radioactivity of [³H]TdR assay, mice with H22 tumor were injected with different concentrations of resveratrol, and the inhibitory rates were calculated and IgG contents were determined by single immunodiffusion method. the plaque forming cell (PFC) was measured by improved Cunningham method, the levels of serum tumor necrosis factor- α (TNF- α) were measured by cytotoxic assay against L929 cells.

RESULTS: Resveratrol 2.5 mg·L⁻¹, 5.0 mg·L⁻¹, 10.0 mg·L⁻¹, 20.0 mg·L⁻¹ (E:T=10:1, 20:1) promoted the cytotoxicity of M ϕ against H22 cells. Resveratrol ip 500 mg·kg⁻¹, 1 000 mg·kg⁻¹ and 1 500 mg·kg⁻¹ could curb the growth of the implanted tumor of H22 in mice. The inhibitory rates were 31.5 %, 45.6 % and 48.7 %, respectively ($P < 0.05$), which could raise the level of serum IgG and PFC response to sheep red blood cell. Resveratrol 1 000 mg·kg⁻¹ and 1 500 mg·kg⁻¹ and BCG 200 mg·kg⁻¹ ip could increase the production of serum TNF- α in mice H22 tumor. However, the effect of resveratrol was insignificant ($P > 0.05$).

CONCLUSION: Resveratrol could inhibit the growth of H22 tumor in Balb/c mice. The antitumor effect of resveratrol might be related to directly inhibiting the growth of H22 cells and indirectly inhibiting its potential effect on nonspecific host immunomodulatory activity.

Liu HS, Pan CE, Yang W, Liu XM. Antitumor and immunomodulatory activity of resveratrol on experimentally implanted tumor of H22 in Balb/c mice. *World J Gastroenterol* 2003; 9(7): 1474-1476
<http://www.wjgnet.com/1007-9327/9/1474.asp>

INTRODUCTION

Recently, considerable attention has been focused on identifying naturally occurring chemopreventive substances capable of inhibiting, retarding, or reversing the multi-stage carcinogenesis. Resveratrol (3,5,4'-trihydroxy-trans-stilbene), a phytoalexin found in grapes and other dietary and medicinal plants, has been shown to have anti-inflammatory, antioxidant

and antitumor activities^[1-7]. Many of these beneficial effects of resveratrol require participation of the cells of the immune system. However, the effect of resveratrol on the development of immunological responses remains unknown.

In the present study, the antitumor activity and immunomodulatory actions of resveratrol, including M ϕ against H22 cells, serum IgG and the plaque forming cells and tumor necrosis factor (TNF- α) content in Balb/C mice with experimentally implanted tumor of H22 were investigated.

MATERIALS AND METHODS

Materials

Resveratrol, MTT, IPS and dimethylsulfoxide (DMSO) were purchased from SGMA Co. Mouse hepatocellular carcinoma cells H22, L929 and sheep red blood cell (SRBC) were kindly supplied by Cheng Wei (Center of Molecular Biology, First Affiliated Hospital, Xi'an Jiaotong University). Cells were subcultured in RPMI 1640 (Gibco) which was supplemented with 10 % fetal bovine serum, penicillin (100 IU·ml⁻¹) and streptomycin (100 mg·l⁻¹). Stock solution of resveratrol was made in dimethylsulfoxide (DMSO) at a concentration of 10 g·L⁻¹. Working dilutions were directly made in the tissue culture medium. [³H]TdR was purchased from Shanghai Nuclear Research Institute. IL test kit and LPS were purchased from Gibco Co. Balb/C mice, 2.5 month old, weighing 20±2 g, were purchased from the Animal Center, Xi'an Jiaotong University.

Methods

Effect of resveratrol on cytotoxicity of peritoneal macrophages (M ϕ) against H22 cells M ϕ was collected from the peritoneal cavity of Balb/c mice 3 days after ip 10 % sheep red blood cells (SRBC, 1 ml/mouse). The cells were washed twice and resuspended in RPMI 1640 culture medium. H22 cells were cultured for 12 h, and 100 μ l M ϕ suspension and different concentrations of resveratrol were added to each well of 96-well plates at a ratio of effectors: target (E:T) cell 10:1 or 25:1. After cultured for 24 h, each well was added with [³H]TdR (9.3 kBq/well), and then was incubated for another 6 h. Cells were placed onto the glass fiber filter and [³H]TdR incorporation was determined by liquid scintillation. The cytotoxicity was calculated with the following formula: the cytotoxicity of M ϕ = (control-treatment)/control × 100 % (dpm).
Anti-tumor activity of resveratrol and its effect on serum antibody IgG, plaque forming cells (PFC) in Balb/C mice with implanted tumor of H22 Mouse ascites (including 2 × 10⁵ cells) were injected into the right axilla of 40 Balb/c mice. On the second day, 40 Balb/c mice were divided into 4 groups randomly, and then were injected with resveratrol at a dose of 500 mg·kg⁻¹, 1000 mg·kg⁻¹, 1 500 mg·kg⁻¹ and normal saline for 10 d. Mice were sensitized to ip SRBC (3 × 10⁷ cells). After 4 d, the mice were bled to obtain serum for IgG investigation. At the same time, spleens were excised for PFC counting. IgG contents were determined by single immunodiffusion method. PFC was measured by modified Cunningham method.
Effect of resveratrol on serum tumor necrosis factor alpha

(TNF- α) production induced by LPS in Balb/c mice Ascites cells of 2×10^5 were injected into the Balb/c mice. Resveratrol at a dose a $500 \text{ mg} \cdot \text{kg}^{-1}$, $1\,000 \text{ mg} \cdot \text{kg}^{-1}$ and $1\,500 \text{ mg} \cdot \text{kg}^{-1}$ was injected for 10 d, and BCG of $200 \text{ mg} \cdot \text{kg}^{-1}$ as a positive control agent was injected ip on d 1. On d 11, 90 minutes after ip LPS of $0.1 \text{ mg} \cdot \text{kg}^{-1}$, the mice were exsanguinated. Blood was centrifuged ($400 \times g$, 10 min). The levels of serum TNF- α were measured by cytotoxic assay against L929 cells as described previously. The TNF- α activity was calculated with the following formula: cytotoxicity = $(A_{\text{control}} - A_{\text{test}}) / A_{\text{control}} \times 100 \%$.

RESULTS

Effect of resveratrol on cytotoxicity of peritoneal macrophages (M ϕ) against H22 cells

Resveratrol at $2.5 \text{ mg} \cdot \text{l}^{-1}$ could decrease the cytotoxicity of M ϕ against H22 cells ($P > 0.05$). Resveratrol at $12.5 \text{ mg} \cdot \text{l}^{-1}$, $5.0 \text{ mg} \cdot \text{l}^{-1}$, $10.0 \text{ mg} \cdot \text{l}^{-1}$ could enhance insignificantly the cytotoxicity of M ϕ against H22 cells ($P > 0.05$) concentration-dependently. However, resveratrol at $20.0 \text{ mg} \cdot \text{l}^{-1}$ could raise significantly the cytotoxicity of M ϕ against H22 cells ($P < 0.05$) (Table 1).

Table 1 Effect of resveratrol on cytotoxicity of peritoneal macrophages (M ϕ) against H22 cells *in vitro* ($n=3$)

Resveratrol (mg \cdot l $^{-1}$)	Cytotoxicity of M ϕ : H22 (10:1)	ϕ (%) M ϕ : H22 (25:1)
Control	12.6 \pm 7.9	15.6 \pm 6.0
1.25	10.9 \pm 2.9 ^a	10.6 \pm 5.4 ^a
2.50	12.5 \pm 3.2 ^a	16.4 \pm 1.8 ^a
5.0	13.4 \pm 2.8 ^a	27.6 \pm 2.6 ^a
10.0	14.6 \pm 3.7 ^a	18.3 \pm 4.2 ^a
20.0	16.7 \pm 4.7 ^b	20.2 \pm 3.1 ^b

^a $P > 0.05$, ^b $P < 0.05$ vs control.

Anti-tumor activity of resveratrol and its effect on serum antibody IgG, plaque forming cells (PFC) in Balb/c mice with implanted tumor of H22

Resveratrol ip at a dose $500 \text{ mg} \cdot \text{kg}^{-1}$, $1\,000 \text{ mg} \cdot \text{kg}^{-1}$ and $1\,500 \text{ mg} \cdot \text{kg}^{-1}$ could significantly curb the growth of implanted tumor of H22 in mice. The inhibitory rates were 31.5 %, 45.6 % and 48.7 %, respectively ($P < 0.05$, Table 2).

Table 2 Inhibitory rates of resveratrol on H22 in mice *in vivo*

Group	Dose mg \cdot kg $^{-1}$	Route	Mice begin/end	Tumor weight ($\bar{x} \pm s$) (g)	Inhibitory rate (%)	P value
Control		ip	10/9 ^b	1.81 \pm 0.62		
Resveratrol 1	500	ip	10/8 ^b	1.24 \pm 0.40	31.5	<0.05 ^a
Resveratrol 2	1000	ip	10/9 ^b	0.99 \pm 0.35	45.6	<0.05 ^a
Resveratrol 3	1500	ip	10/10	0.93 \pm 0.25	48.7	<0.05 ^a

^a $P < 0.05$ vs control; ^bkilled by other mice.

The result also showed that the immunity of mice with tumor could be more significantly inhibited than that of normal mice, and resveratrol ip could raise the level of serum LgG and number of PFC in Balb/c mice with implanted tumor of H22 *in vivo*. Resveratrol, however, could insignificantly increase the immunity of mice with tumor ($P > 0.05$, Table 3).

Effect of resveratrol on serum tumor necrosis factor alpha (TNF- α) production induced by LPS in Balb/c mice

The ability of TNF- α production of mice with H22 tumor was significantly stronger than that of normal mice.

Furthermore, the group of control and BCG at $200 \text{ mg} \cdot \text{kg}^{-1}$ ip had an increase in the at production of serum TNF- α in mice with H22 tumor ($P < 0.05$), but resveratrol at a dose of $500 \text{ mg} \cdot \text{kg}^{-1}$, $1\,000 \text{ mg} \cdot \text{kg}^{-1}$ and $1\,500 \text{ mg} \cdot \text{kg}^{-1}$ had less effect on mice with H22 tumor ($P > 0.05$, Table 4).

Table 3 Effects of resveratrol on serum antibody IgG, plaque forming cells (PFC) in Balb/c mice with implanted tumor of H22 *in vivo*

Group	Dose mg \cdot kg $^{-1}$	Route	IgG/g \cdot L $^{-1}$	PFC/10 ⁶ cells
Normal mice	NS	ip	27 \pm 8	441 \pm 32
Control	NS	ip	19 \pm 6 ^a	297 \pm 57 ^a
Resveratrol 1	500	ip	20 \pm 8 ^a	305 \pm 53 ^a
Resveratrol 2	1000	ip	23 \pm 6 ^a	328 \pm 49 ^a
Resveratrol 3	1500	ip	24 \pm 5 ^a	348 \pm 46 ^a

^a $P > 0.05$ vs normal mice or control.

Table 4 Effect of resveratrol on TNF- α production induced by LPS in Balb/c mice

Group	Dose (mg \cdot kg $^{-1}$)	Route	TNF- α activity specific lysis
Normal mice	NS	ip	7.1 \pm 3.2
Control	NS	ip	16.3 \pm 2.3 ^a
Resveratrol 1	500	ip	15.8 \pm 2.0 ^{ab}
Resveratrol 2	1000	ip	17.7 \pm 2.9 ^{ab}
Resveratrol 3	1500	ip	19.5 \pm 3.1 ^{ab}
Control+BCG	200	ip	29.8 \pm 3.7 ^{ab}

^a $P < 0.05$ vs normal mice; ^b $P > 0.05$ vs control.

DISCUSSION

Resveratrol is a phytopolyphenol isolated from the seeds and skin of grapes. Recent studies have indicated that resveratrol can block the process of multistage carcinogenesis, namely, tumor initiation, promotion and progression. Resveratrol can also reduce the risk of cardiovascular diseases in man. These activities have been identified by some authors^[8-13]. Roberto *et al*^[14] have shown that PBMC exposure to resveratrol produced a biphasic effect on the anti-CD3/anti-CD28-induced development of both IFN- γ -IL-2 and IL4-producing CD8⁺ and CD4⁺T cells, with stimulation at low resveratrol concentrations and suppression at high concentrations. Similarly, the compound was found to induce a significant enhancement at low concentrations and suppression at high concentrations of both CTL and NK cell cytotoxic activity. Gao *et al*^[15] found that mitogen-, IL-2- or alloantigen-induced proliferation of splenic lymphocytes, induction of cytotoxic T lymphocytes (CTLs) and lymphokine activated killer (LAK) cells, and production of the cytokine interferon (IFN)- γ , interleukin (IL)-2, tumor necrosis factor (TNF)- α were significantly suppressed at 25-50 μM resveratrol, but in some cases mitogen/IL-2-induced production and CTL generation were enhanced following pretreatment of cells with resveratrol. The effects of resveratrol on immune function of mice *in vivo* have not been reported yet.

Our results indicate that resveratrol of $2.5 \text{ mg} \cdot \text{l}^{-1}$ could decrease the cytotoxicity of M ϕ against H22 cells ($P > 0.05$). Resveratrol of $2.5 \text{ mg} \cdot \text{l}^{-1}$, $5.0 \text{ mg} \cdot \text{l}^{-1}$ and $10.0 \text{ mg} \cdot \text{l}^{-1}$ could insignificantly enhance the cytotoxicity of M ϕ against H22 cells concentration-dependently ($P > 0.05$). However, resveratrol of $20.0 \text{ mg} \cdot \text{l}^{-1}$ could raise significantly the cytotoxicity of M ϕ against H22 cells ($P < 0.05$). So, resveratrol could alone affect the [³H]TDR uptake by H22 cells *in vitro*,

suggesting that the antitumor action of resveratrol had a direct cytotoxic effect. This result is coincident with the previous studies^[16-18]. Resveratrol ip could insignificantly increase the host nonspecific immunological defense of mice with H22 tumor, by raising the level of serum IgG and TNF- α and the number of PFC ($P>0.05$). *In vivo* resveratrol could also augment the cytotoxicity of peritoneal macrophages against H22 cells, and there was an insignificant difference compared with the control group ($P>0.05$). Therefore, resveratrol could inhibit the growth of H22 cells *in vivo*, but it could not significantly enhance the host immune defense against tumor. Based on the results of the present study, it can be suggested that the antitumor activity of resveratrol might be due to direct cytotoxic/antiproliferative activity against tumor cells, but not to the augmentation of immune response against tumors. It has demonstrated that resveratrol inhibits cell proliferation, cell-mediated cytotoxicity, and cytokine production, at least in part through the inhibition of NF-kappa B activation. But the molecular mechanism by which resveratrol imparts cancer chemopreventive effects has not been clearly defined and further studies are needed.

REFERENCES

- Kris-Etherton PM**, Hecker KD, Bonanome A, Coval SM, Binkoski AE, Hilpert KF, Griel AE, Etherton TD. Bioactive compounds in foods: their role in the prevention of cardiovascular disease and cancer. *Am J Med* 2002; **30**: 71S-88S
- Park EJ**, Pezzuto JM. Botanicals in cancer chemoprevention. *Cancer Metastasis Rev* 2002; **21**: 231-255
- Olas B**, Wachowicz B, Saluk-Juszczak J, Zielinski T. Effect of resveratrol, a natural polyphenolic compound, on platelet activation induced by endotoxin or thrombin. *Thromb Res* 2002; **107**: 141-145
- Martinez J**, Moreno JJ. Effect of resveratrol, a natural polyphenolic compound, on reactive oxygen species and prostaglandin production. *Biochem Pharmacol* 2000; **59**: 865-870
- Latruffe N**, Delmas D, Jannin B, Malki MC, Passilly-Degrace P, Berlot JP. Molecular analysis on the chemopreventive properties of resveratrol, a plant polyphenol microcomponent. *Int J Mol Med* 2002; **10**: 755-760
- Ding XZ**, Adrian TE. Resveratrol inhibits proliferation and induces apoptosis in human pancreatic cancer cells. *Pancreas* 2002; **25**: 71-76
- Cal C**, Garban H, Jazirehi A, Yeh C, Mizutani Y, Bonavida B. Resveratrol and Cancer: Chemoprevention, Apoptosis, and Chemo-immunosensitizing Activities. *Curr Med Chem Anti-Canc Agents* 2003; **3**: 77-93
- Asensi M**, Medina I, Ortega A, Carretero J, Bano MC, Obrador E, Estrela JM. Inhibition of cancer growth by resveratrol is related to its low bioavailability. *Free Radic Biol Med* 2002; **33**: 387-398
- De-Ledinghen V**, Monvoisin A, Neaud V, Krisa S, Payrastre B, Bedin C, Desmouliere A, Bioulac-Sage P, Rosenbaum J. Trans-resveratrol, a grapevine-derived polyphenol, blocks hepatocyte growth factor-induced invasion of hepatocellular carcinoma cells. *Int J Oncol* 2001; **19**: 83-88
- Tian XM**, Zhang ZX. The anticancer activity of resveratrol on implanted tumor of HepG2 in nude mice. *Shijie Huaren Xiaohua Zazhi* 2001; **9**: 161-164
- Liu HS**, Pan CE, Qi Y, Liu QG, Liu XM. Effect of resveratrol with 5-FU on growth of implanted H22 tumor in mice. *Shijie Huaren Xiaohua Zazhi* 2002; **10**: 32-35
- Sun ZJ**, Pan CE, Liu HS, Wang GJ. Anti-hepatoma activity of resveratrol *in vitro*. *World Gastroenterol* 2002; **8**: 79-81
- Zhou HB**, Yan Y, Sun YN, Zhu JR. Resveratrol induces apoptosis in human esophageal carcinoma cells. *World J Gastroenterol* 2003; **9**: 408-411
- Falchetti R**, Fuggetta MP, Lanzilli G, Tricarico M, Ravagnan G. Effects of resveratrol on human immune cell function. Effect of resveratrol on human immune cell function. *Life Sciences* 2001; **70**: 81-96
- Gao X**, Xu YX, Janakiraman N, Chapman RA, Gautam SC. Immunomodulatory activity of resveratrol: suppression of lymphocyte proliferation, development of cell-mediated cytotoxicity, and cytokine production. *Biochemical Pharmacol* 2001; **62**: 1299-1308
- Delmas D**, Jannin B, Malki MC, Latruffe N. Inhibitory effect of resveratrol on the proliferation of human and rat hepatic derived cell lines. *Oncol Rep* 2000; **7**: 847-352
- Brakenhielm E**, Cao R, Cao Y. Suppression of angiogenesis, tumor growth, and wound healing by resveratrol, a natural compound in red wine and grapes. *FASEB J* 2001; **15**: 1798-1800
- Dong Z**. Molecular mechanism of the chemopreventive effect of resveratrol. *Mutat Res* 2003; **523-524**: 145-150

Edited by Ma JY

Laparoscopic total mesorectal excision of low rectal cancer with preservation of anal sphincter: A report of 82 cases

Zong-Guang Zhou, Zhao Wang, Yong-Yang Yu, Ye Shu, Zhong Cheng, Li Li, Wen-Zhang Lei, Tian-Cai Wang

Zong-Guang Zhou, Zhao Wang, Yong-Yang Yu, Ye Shu, Zhong Cheng, Li Li, Wen-Zhang Lei, Tian-Cai Wang, Department of General Surgery and Institute of Digestive Surgery, West China Hospital, Sichuan University, Chengdu 610041, Sichuan Province, China

Supported by the Key Project of National Outstanding Youth Foundation of China, No. 39925032

Correspondence to: Zong-Guang Zhou, Department of General Surgery and Institute of Digestive Surgery, West China Hospital, Sichuan University, Chengdu 610041, Sichuan Province, China. zhou767@21cn.com

Telephone: +86-28-85422484

Received: 2002-06-14 **Accepted:** 2002-07-19

Abstract

AIM: To assess the feasibility and efficacy of laparoscopic total mesorectal excision (LTME) of low rectal cancer with preservation of anal sphincter.

METHODS: From June 2001 to June 2003, 82 patients with low rectal cancer underwent laparoscopic total mesorectal excision with preservation of anal sphincter. The lowest edge of tumors was below peritoneal reflection and 1.5-7 cm from the dentate line (1.5-5 cm in 48 cases, 5-7 cm in 34 cases).

RESULTS: LTME with anal sphincter preservation was performed on 82 randomized patients with low rectal cancer, and 100 % sphincter preservation rate was achieved. There were 30 patients with laparoscopic low anterior resection (LLAR) at the level of the anastomosis below peritoneal reflection and 2 cm above from the dentate line; 27 patients with laparoscopic ultralow anterior resection (LULAR) at the level of anastomoses 2 cm below from the dentate line; and 25 patients with laparoscopic coloanal anastomoses (LCAA) at the level of the anastomoses at or below the dentate line. No defunctioning ileostomy was created in any case. The mean operating time was 120 minutes (ranged from 110-220 min), and the mean operative blood loss was 20 mL (ranged from 5-120 mL). Bowel function was restored and diet was resumed on day 1 or 2 after operation. The mean hospital stay was 8 days (ranged from 5-14). Postoperative analgesics were used in 45 patients. After surgery, 2 patients had urinary retention, one had anastomotic leakage, and another 2 patients had local recurrence one year later. No intraoperative complication was observed.

CONCLUSION: LTME with preservation of anal sphincter is a feasible, safe and minimally invasive technique with less postoperative pain and rapid recovery, and importantly, it has preserved the function of the sphincter.

Zhou ZG, Wang Z, Yu YY, Shu Y, Cheng Z, Li L, Lei WZ, Wang TC. Laparoscopic total mesorectal excision of low rectal cancer with preservation of anal sphincter: A report of 82 cases. *World J Gastroenterol* 2003; 9(7): 1477-1481

<http://www.wjgnet.com/1007-9327/9/1477.asp>

INTRODUCTION

The optimal operation for rectal cancer still remains controversial. Surgical management of rectal cancer has undergone a significant change during the past two decades, a new concept of total mesorectal excision (TME) was introduced^[1], and its feasibility and efficacy had been confirmed by a series of clinical trials^[2-5]. Compared with conventional procedure, TME markedly improved both oncological and functional outcomes of rectal cancer^[6-9], therefore, this procedure has been used as a golden standard for rectal cancer.

Laparoscopic approach has been employed in colorectal surgery for ten years, and its feasibility has been shown in a variety of colorectal operations^[10-14]. However, for inadequate operative vision and limitation of the narrow pelvis, total laparoscopic TME with construction of colo-anal anastomosis for low rectal cancer has been regarded as being difficult and time-consuming, and mainly used for upper rectal cancer for a long time^[15,16]. Few cases about laparoscopic TME with anal sphincter preservation (SP) for low rectal cancer were reported^[17]. The current study was performed to assess the feasibility and efficacy of laparoscopic total mesorectal excision (LTME) for low rectal cancer with preservation of anal sphincter.

MATERIALS AND METHODS

Patients

Between June 2001 and June 2003, randomized 82 patients with low rectal cancer underwent laparoscopic total mesorectal excision with anal sphincter preservation at Department of General Surgery of West China Hospital. The lowest edges of tumors were below peritoneal reflection and 1.5-7 cm from the dentate line (1.5-5 cm in 46 cases, and 5-7 cm in 36 cases). Patients with previous abdominal surgery, obese body, and other surgical benign diseases were not excluded from the laparoscopic procedure. Clinical and demographic data including age, sex, tumor diameter, distances of tumor from the dentate line, concomitant diseases are shown in Table 1.

Table 1 Clinical and demographic data

Parameters	Data
Age, mean (years)	26-85, 44
Sex (No. of patients)	
Male	46
Female	36
Tumor diameter, mean (cm)	1.5-13, 5.6
Distance of the tumor from the dentate line (cm)	1.5-7
1.5-5 cm from lowest edge of tumors to the dentate line (No. of patients)	48
5-7 cm from lowest edge of tumors to the dentate line (No. of patients)	34
Concomitant diseases (No. of patients)	
Chronic cholecystitis, cholecystolithiasis, torsion of ovarian cyst and diabetes	2
Chronic cholecystitis and cholecystolithiasis	6
Previous lower abdominal operation	7

Preoperative examinations including flexible endoscopes, biopsy, ultrasonography, CT scan, radiography of the chest were performed routinely. All patients underwent preoperative bowel preparation (1L 10 % mannite electrolyte solution). Prophylactic antibiotics (ciprofloxacin and metronidazole) were given three days before operation routinely. A urinary catheter and a nasogastric tube were used.

Operative techniques

Under general anesthesia, 82 patients were operated in lithotomic position with 15° head-down tilt by the same surgeon (ZZ ZHOU) with two assistants (YY. YU and Y. SHU). Pneumoperitoneum was introduced through subumbilical incision to maintain pressure at 12-14 mmHg (1 mmHg=0.133 Kpa). A camera port was created in subumbilical zone with trocar, then an operative port in the right midclavicular line at the level of umbilicus, and an other two operative ports in the left and right McBurney point were created.

Laparoscope was inserted at 25° or 30° into abdominal cavity via the camera port. Routine intra-abdominal exploration was performed. All sharp dissections and divisions on peritoneum, fascia, and connective tissue in retroperitoneal space were performed with a harmonic scalpel. Left lateral peritoneal was divided first, and then sigmoid and descending colon were mobilized completely to ensure the subsequent colo-anal anastomosis free of tension. Then the bowel and its mesentery by a cotton tape at the level 8-10 cm above the upper margin of the tumor were tied, lymph nodes around inferior mesenteric vessels were dissected, and inferior mesenteric vessels were ligated at the high level.

With the operation proceeding of total mesorectal excision, division was moved downward into the pelvis along the anatomic space between visceral and parietal endopelvic fascia. Lateral ligaments of the rectum containing the middle rectal artery or its branches (Figure 1) were gradually divided with the harmonic scalpel from the inner limit of the inferior hypogastric nerve fibers (Figure 2). The pelvic splanchnic nerves were preserved intact as far as possible. Anteriorly, Denonvilliers' fascia was dissected and the seminal vesicles and prostate or the posterior wall of the vagina were exposed (Figure 3). At posterior, the rectosacral ligament, anococcygeal ligament, and pubococcygeus muscle were divided, and S₂, S₃, and S₄ sacral splanchnic nerves were identified and protected carefully. The mesorectum, especially the distal mesorectum (DMR), was excised completely till levator ani. Thus, longitudinal muscle layer of the distal precutting rectum and levator ani could be clearly visualized under laparoscopic view, so-called 'denudation' and 'muscularization'. For low bulky tumor, the 'denudation' should be performed under intra-anal finger-guidance to avoid inadvertent damage of adjacent structures. The rectal cross clamping was performed 1.5-3.5 cm below the tumor with endo-cutter (Figure 4).

To extract the bowel loop of the tumor, the port incision was extended at the left McBurney's point to about 3.5 cm long, and isolated the tumor routinely by inserting in a sheath-shaped plastic bag through the incision. The tumor and the proximal colon was extracted through the bag, and then transected the bowel at the level of 10-15 cm above upper margin of the tumor. After inserting the anvil of 29 or 30 mm-sized circular stapler into the end of proximal bowel and securing with 2/0 prolene purse-string suture, the proximal bowel was internalized and the extended incision was closed. Pneumoperitoneum was induced again. Laparoscopic colo-anal or colo-rectal anastomosis was done with CDH 29 circular stapler. After the circular stapler was inserted into the anus, its puncturing cone was pricked through the midpoint of the distal

occluding line of the rectum (Figure 5), and fitted into the anvil of the stapler in the pelvic cavity. The stapler was then closed slowly with extreme cautions to avoid inadvertent stapling of adjacent important structures. In this way, the low/ultralow/colo-anal anastomoses were accomplished smoothly. A 10 mm-sized latex tube was routinely put into pelvic cavity through the port at the right McBurney point. No defunctioning ileostomy was created in any case. Distal clearance measurements were taken in an unfixed and unpinned status of surgical specimen in the operating room. The specimen was routinely checked if the visceral endopelvic fascia was dissected completely, and then sent for pathologic examination (Figure 6).

Laparoscopic cholecystectomy and ovariectomy could be performed simultaneously for patients with cholecystolithiasis, chronic cholecystitis, ovarian cyst, and torsion of the ovary.

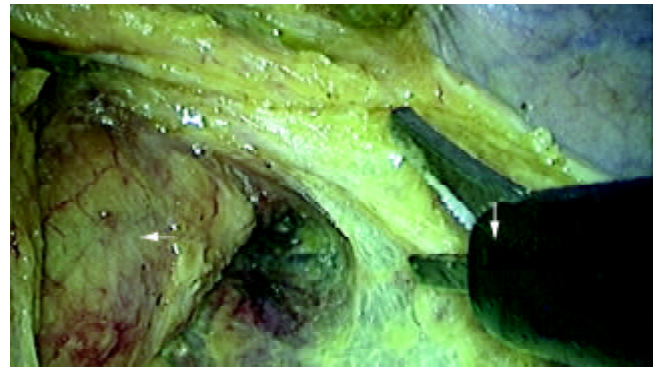


Figure 1 The "lateral ligaments" (→) of rectum containing middle rectal artery or its branches, and mesorectum (←) were dissected completely with a harmonic scalpel (↓).

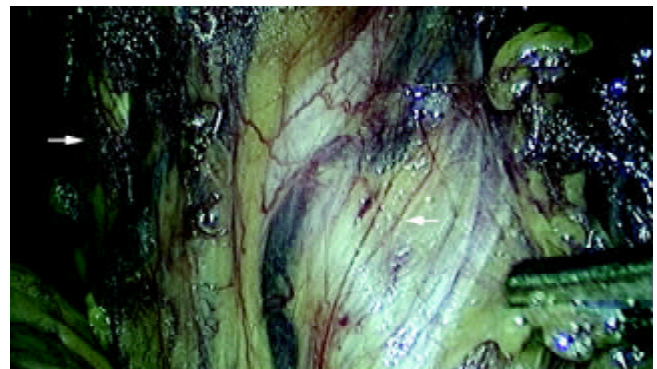


Figure 2 The left pelvic splanchnic nerves were preserved intact as far as possible. Inset shows the inferior hypogastric nerve fibers (←) and the ureter (→).

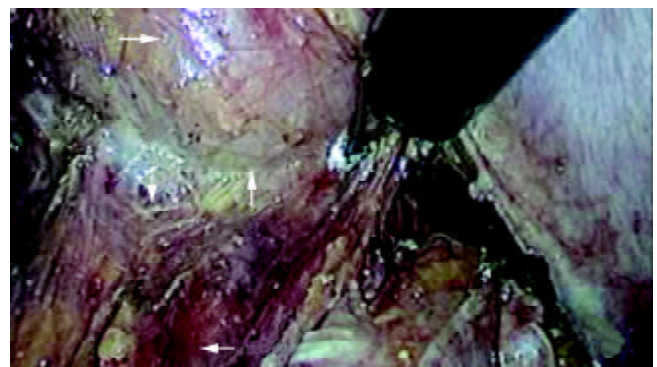


Figure 3 Denonvilliers' fascia (↓) was dissected along the space (↑) between the posterior wall of vagina (→) and the rectum (←).

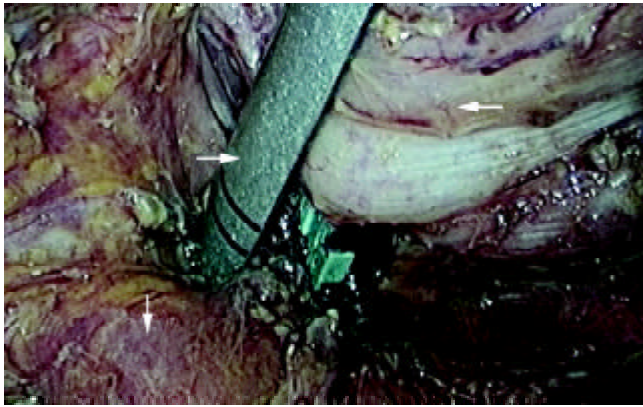


Figure 4 The cross clamping of the rectum (←) was performed 1.5~3.5cm below the tumor with endo-cutter (→). Pelvic floor 'muscularization' was shown (↓).

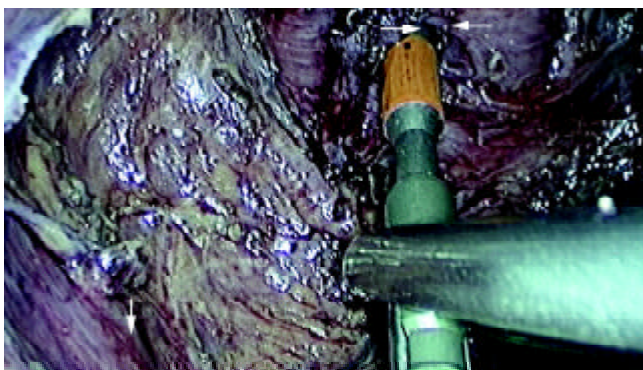


Figure 5 The puncturing cone (→) of the circular stapler pricked through the midpoint of occluding line of the distal rectum(←). Levator ani muscles were exposed (↓).

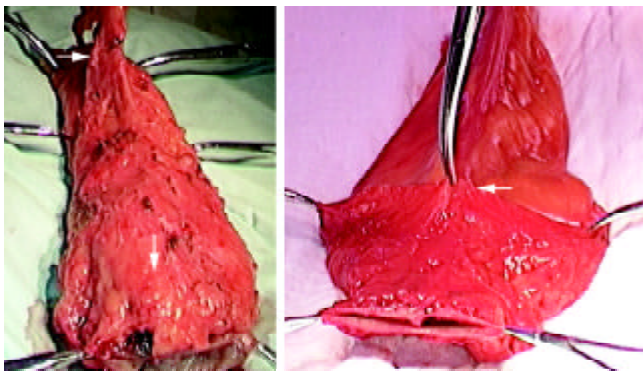


Figure 6 The dorsal mesorectum (→) and distal mesorectum (↓) of the rectal specimen were shown (6a). The anterior side of the specimen and distal margin (←) were shown (6b).

RESULTS

TME with anal sphincter preservation was accomplished with laparoscope in 82 randomized patients with low rectal cancer, and 100 % sphincter preservation rate was achieved. There were 30 patients by laparoscopic low anterior resection (LLAR) at the level of the anastomosis below peritoneal reflection and 2 cm above the dentate line; 27 patients by laparoscopic ultralow anterior resection (LULAR) at the level of the anastomosis 2 cm below the dentate line; and 25 patients by laparoscopic coloanal anastomoses (LCAA) at the level of the anastomosis at/below the dentate line (Figure 7). No defunctioning ileostomy was created in any case. The mean operating time was 120 minutes (ranged from 110-220 min),

and the mean operative blood loss was 20 mL (ranged from 5-120 mL). Both bowel function recovery and diet resumption occurred within 1-2 days after surgery, and the mean hospital stay were 8 days (ranged from 5-14). Postoperative analgesics were used in 45 patients. One patient was converted to open surgery due to dysfunction of coagulation. After operation, 2 patients had urinary retention, one had anastomotic leakage, 2 patients had local recurrence one year later, and no intraoperative complication was observed. Clinical and surgical details in this study including tumor and anastomotic levels from anal verge, stage of disease, duration of surgery, length of specimen removed, duration of parenteral analgesia, time to passage of flatus, time to resumption of liquids and solids, and length of post-operative stay are shown in Tables 2,3 and 4.

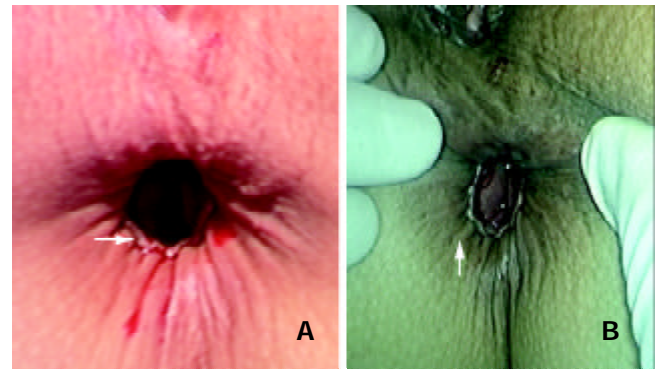


Figure 7 The anastomotic ring (→) could be shown easily in the patient receiving colo-anal anastomosis (a). Satisfactory contractive function of the saved anus (↑) was achieved in the patients receiving laparoscopic TME with anal sphincter preservation at the first day after operation (b).

Table 2 Clinical parameters for patients with LTME and SP

Parameters	Data
Dukes stage (No. of patients)	
A	5
B	10
C1	33
C2	30
D	4
Pathologic types (No. of patients)	
High differentiated adenocarcinoma	24
Moderately differentiated adenocarcinoma	37
Low differentiated adenocarcinoma	21
Multiple primary carcinomas on the bowel wall	3
Distance of the tumor from the section edge (cm)	1.5-4
Cancer cell found in the cut margins (No. of patients)	1
Colo-rectal/anal anastomotic height (cm) (No. of patients)	
LLAR, below peritoneal reflection and 2 cm above the dentate line	30
LULAR, 2 cm below the dentate line	27
LCAA, at/below the dentate line	25

Table 3 Early results for laparoscopic TME and SP

Parameters	Data
Operation time (min)	120(110-220)
Operative bleeding (ml)	20(5-120)
Time for bowel function recovery (d)	1-2
Time to resume normal diet (d)	1-2
Post-operative analgesic requirement (No. Of patients)	45
Total hospital stay (d)	8 (5-14)
Sphincter preservation rate (%)	100 %
Mortality (%)	0

Table 4 Complications of laparoscopic TME and SP

Complications	No. of patients
Total number of patients	82
Perforation of rectum	0
Urethra damage	0
Intra-abdominal bleeding	0
Pelvic abscess	0
Urinary retention	2
Anastomotic Leakage	1
Local recurrence	2

The patients were mobilized two days after operation. Oral intake was gradually increased with the recovery of intestinal function. Most of the patients with low anastomosis as well as about 1/2 of the patients with ultralow or colo-anal anastomosis experienced a quick recovery in anal sphincter's function and controlling of defecation, while 50 % of patients with ultralow anastomosis or colo-anal anastomosis suffered from urgent defecation about 5-10 times per day, and their defecation was controlled gradually by proper medication and functional exercise of anal sphincter and levator ani around half a year.

There were no portal site recurrence and mortality observed during follow-up, which ranged from 1 to 24 months.

DISCUSSION

Study on the management of rectal cancer has progressed greatly in both clinical practice^[18-23] and basic research^[24-27] in recent years. Multiple clinical studies have demonstrated the correlation of high pelvic recurrence with the degree of mesorectal excision^[28]. Residual mesorectum, especially inadequate excision of distal mesorectum (DMR), contributed to poor oncologic outcomes. Regarding DMR, histopathological evidence revealed a high metastasis rate in this region, and it was also found that patients with metastasis in this region would experience a poor prognosis. This is why the principle of TME should be followed in the treatment of rectal cancer^[29-31]. Since clinical application of TME, the local recurrence rate of the cancer has decreased dramatically to 5-7.1 %^[7,32,33], while that of conventional operative procedure remains 18.5 %.

Up to now, there are only a few reports on laparoscopic procedure for low rectal cancer in the literatures, which was mainly due to inadequate surgical vision and limitation of the narrow pelvis. The area 5-8 cm from anal verge and below peritoneal reflection has ever been considered as a blind zone and that within 5 cm from anal verge as a forbidden zone. The current study revealed that the so-called blind and forbidden zones could be broken through, and minimally invasive TME with anal sphincter preservation could be performed safely for patients with rectal cancer based on our success of the large number of open TME and low/ultralow/colo-anal anastomosis and proficient laparoscopic skill. This study is concerned with our experience in colorectal surgery and deals with special laparoscopic colorectal techniques including LLAR, LULAR and LCAA.

Based on our clinical experiences, laparoscopic TME and SP have the following advantages: (1) it helps surgeons identify accurately the interspace of loose connective tissue between visceral and parietal pelvic fascia, and select operative access by amplifying inner image on the monitors. (2) 25° or 30° laparoscope, the third eye of the surgeon, can reach the narrow lesser pelvis and magnify the local vision; (3) it is more definite to identify and protect the pelvic autonomic nerve fiber and plexus due to its magnifying function. (4) hemostatic benefit was owed to minimally invasive sharp dissection with minimal blood loss under laparoscopic view.

However, the laparoscopic technique has its disadvantages,

such as long operative time, short of direct hand feeling, technical constraints of the narrow pelvis, difficulty in assessing adequate surgical margins and in ultralow rectal cross clamping, and a long learning course for surgeons.

Good experience with laparoscopic surgery leads to shorter operating time and encouraging results. A bulky tumor or a thickening mesentery usually occupies the most space of narrow pelvic cavity and often influence the operation. To avoid this impact, the camera operator should try his best to adjust laparoscope constantly by 25-30°, which keeps the operator at a correct position. Crack sight and smog are other troublesome problems. Crack sight often occurs after the operation moving into lesser pelvis and it can be solved by adjusting the angle of laparoscope properly. Smog results from the operation of using the harmonic scalpel or cautery, which often distracts operator's vision, even breaks the operative process. The camera operator should withdraw the laparoscope and disperse the smog in time when smog is too heavy or obscures the lens of laparoscope. Therefore, the role of the camera operator is so important that his skill can directly influence the operative processes and results.

The anastomosis is a critical step for the success of this minimally invasive technique with anal sphincter preservation^[28]. Double stapling technique (DST) is the remarkable progress in the anastomosis for the operation of low rectal cancer in recent years. Research showed that local recurrence rate was much lower in patients treated with DST than those treated with conventional anastomosis^[34]. Low/ultralow/colo-anal anastomoses in all cases of laparoscopic procedure were achieved with DST at this hospital. Based on our experience, there are two special points regarding the anastomosis with DST: (1) denudation of the distal rectal tube, and (2) selection of the pricking point on the occluding line. By denuding the pre-cutting part of the rectal tube, the fat and lymphatic tissue within the mesorectum of distal rectum could be thoroughly excised, the denuded rectal longitudinal muscle could be visualized, and the distal rectum could easily be divided and occluded with endo-stapler. The pricking point of the cone on the stapler should locate at midpoint of the occluding line, because too much displacement of the pricking point may result in ischemia and leakage of the anastomosis, or stapling of adjacent important structures. These two steps can effectively prevent rectal wall from damage and dehiscence of the anastomosis, reduce the use of endo-staplers, and decrease local recurrence.

Special training on TME technique is necessary for surgeons to have enough experience of TME and SP^[35]. Proficient skills of laparoscopic operation in pelvis and plentiful experience of open TME are important factors for the success of LTME and SP.

REFERENCES

- 1 **Heald RJ**, Husband EM, Ryall RDH. The mesorectum in rectal cancer surgery - the clue to pelvic recurrence? *Br J Surg* 1982; **69**: 613-616
- 2 **Goldberg S**, Klas JV. Total mesorectal excision in the treatment of rectal cancer: a view from the USA. *Semin Surg Oncol* 1998; **15**: 87-90
- 3 **MacFarlane JK**, Ryall RD, Heald RJ. Mesorectal excision for rectal cancer. *Lancet* 1993; **341**: 457-460
- 4 **Ceelen W**, Pattyn P. Total mesorectal excision in the treatment of rectal cancer: a review. *Acta Chir Belg* 2000; **100**: 94-99
- 5 **Kapiteijn E**, van De Velde CJ. European trials with total mesorectal excision. *Semin Surg Oncol* 2000; **19**: 350-357
- 6 **Lazuskas T**, Lelcuk S, Michowitz M, Rabau M. Anterior resection with colo-anal anastomosis for low rectal cancer. *Harefuah* 1994; **126**: 505-506
- 7 **Killingback M**, Barron P, Dent OF. Local recurrence after curative resection of cancer of the rectum without total mesorectal excision. *Dis Colon Rectum* 2001; **44**: 473-483

- 8 **Bolognese A**, Cardi M, Muttillio IA, Barbarosos A, Bocchetti T, Valabrega S. Total mesorectal excision for surgical treatment of rectal cancer. *J Surg Oncol* 2000; **74**: 21-23
- 9 **Kapiteijn E**, Putter H, van de Velde CJ. Impact of the introduction and training of total mesorectal excision on recurrence and survival in rectal cancer in The Netherlands. *Br J Surg* 2002; **89**: 1142-1149
- 10 **Monson JR**, Darzi A, Carey PD, Guillou PJ. Prospective evaluation of laparoscopic-assisted colectomy in an unselected group of patients. *Lancet* 1992; **340**: 831-833
- 11 **Huscher C**, Silecchia G, Croce E, Farello GA, Lezoche E, Morino M, Azzola M, Feliciotti F, Rosato P, Tarantini M, Basso N. Laparoscopic colorectal resection. A multicenter Italian study. *Surg Endosc* 1996; **10**: 875-879
- 12 **Kwok SP**, Lau WY, Carey PD, Kelly SB, Leung KL, Li AK. Prospective evaluation of laparoscopic-assisted large bowel excision for cancer. *Ann Surg* 1996; **223**: 170-176
- 13 **Barlehner E**, Decker T, Anders S, Heukrodt B. Laparoscopic surgery of rectal carcinoma. Radical oncology and late results. *Zentralbl Chir* 2001; **126**: 302-306
- 14 **Watanabe M**, Teramoto T, Hasegawa H, Kitajima M. Laparoscopic ultralow anterior resection combined with per anum intersphincteric rectal dissection for lower rectal cancer. *Dis Colon Rectum* 2000; **43**(Suppl): S94-S97
- 15 **Hartley JE**, Mehigan BJ, Qureshi AE, Duthie GS, Lee PW, Monson JR. Total mesorectal excision: assessment of the laparoscopic approach. *Dis Colon Rectum* 2001; **44**: 315-321
- 16 **Weiser MR**, Milsom JW. Laparoscopic total mesorectal excision with autonomic nerve preservation. *Semin Surg Oncol* 2000; **19**: 396-403
- 17 **Chung CC**, Ha JP, Tsang WW, Li MK. Laparoscopic-assisted total mesorectal excision and colonic J pouch reconstruction in the treatment of rectal cancer. *Surg Endosc* 2001; **15**: 1098-1101
- 18 **Cao GW**, Qi ZT, Pan X, Zhang XQ, Miao XH, Feng Y, Lu XH, Kuriyama S, Du P. Gene therapy for human colorectal carcinoma using human CEA promoter controlled bacterial ADP-ribosylating toxin genes human CEA: PEA & DTA gene transfer. *World J Gastroenterol* 1998; **4**: 388-391
- 19 **Mao AW**, Gao ZD, Xu JY, Yang RJ, Xiao XS, Jiang TH, Jiang WJ. Treatment of malignant digestive tract obstruction by combined intraluminal stent installation and intraarterial drug infusion. *World J Gastroenterol* 2001; **7**: 587-592
- 20 **Makin GB**, Breen DJ, Monson JR. The impact of new technology on surgery for colorectal cancer. *World J Gastroenterol* 2001; **7**: 612-621
- 21 **Deng YC**, Zhen YS, Zheng S, Xue YC. Activity of boanmycin against colorectal cancer. *World J Gastroenterol* 2001; **7**: 93-97
- 22 **Wang SH**, Zheng YQ. A clinicopathologic analysis of 354 cases of large intestinal cancer in western. *Hunan Xin Xiaohuabingxue Zazhi* 1996; **4**: 325-326
- 23 **Kapiteijn E**, Marijnen CA, Nagtegaal ID, Putter H, Steup WH, Wiggers T, Rutten HJ, Pahlman L, Glimelius B, van Krieken JH, Leer JW, van de Velde CJ. Preoperative radiotherapy combined with total mesorectal excision for resectable rectal cancer. *N Engl J Med* 2001; **345**: 638-646
- 24 **Yuan HY**, Li Y, Yang GL, Bei DJ, Wang K. Study on the causes of local recurrence of rectal cancer after curative resection: analysis of 213 cases. *World J Gastroenterol* 1998; **4**: 527-529
- 25 **Qing SH**, Jiang HY, Qi DL, Zhou ZD, Huang XC, Zhang FM, Sheng QG. Relationship between related factors with lymph node metastasis of colorectal cancer. *Shijie Huaren Xiaohua Zazhi* 2000; **8**: 654-657
- 26 **Gao ZS**, Yin CH, Song DY, Liu FZ, Gu YZ, Liu YP. Clinical significance of pedicled greater omentum transplantation in radical resection of rectal cancer. *Huaren Xiaohua Zazhi* 1998; **6**: 875-876
- 27 **Yang JH**, Rao BQ, Wang Y, Tu XH, Zhang LY, Chen SH, Ou Yang XN, Dai XH. Clinical significance of detecting the circulating cancer cells in peripheral blood from colorectal cancer. *Shijie Huaren Xiaohua Zazhi* 2000; **8**: 187-189
- 28 **Wexner SD**, Rotholtz NA. Surgeon influenced variables in resectional rectal cancer surgery. *Dis Colon Rectum* 2000; **43**: 1606-1627
- 29 **Choi JS**, Kim SJ, Kim YI, Min JS. Nodal metastasis in the distal mesorectum: need for total mesorectal excision of rectal cancer. *Yonsei Med J* 1996; **37**: 243-250
- 30 **Tocchi A**, Mazzoni G, Lepre L, Liotta G, Costa G, Agostini N, Miccini M, Scucchi L, Frati G, Tagliacozzo S. Total mesorectal excision and low rectal anastomosis for the treatment of rectal cancer and prevention of pelvic recurrences. *Arch Surg* 2001; **136**: 216-220
- 31 **Scott N**, Jackson P, al-Jaberi T, Dixon MF, Quirke P, Finan PJ. Total mesorectal excision and local recurrence: a study of tumour spread in the mesorectum distal to rectal cancer. *Br J Surg* 1995; **82**: 1031-1033
- 32 **Heald RJ**. Total mesorectal excision (TME). *Acta Chir Iugosl* 2000; **47**(4 Suppl 1): 17-18
- 33 **McCall JL**, Cox MR, Wattchow DA. Analysis of local recurrence rates after surgery alone for rectal cancer. *Int J Colorectal Dis* 1995; **10**: 126-132
- 34 **Law WL**, Chu KW. Impact of total mesorectal excision on the results of surgery of distal rectal cancer. *Br J Surg* 2001; **88**: 1607-1612
- 35 **Heald RJ**. Total mesorectal excision is optimal surgery for rectal cancer: a Scandinavian consensus. *Br J Surg* 1995; **82**: 1297-1299

Expression of proliferating cell nuclear antigen and CD44 variant exon 6 in primary tumors and corresponding lymph node metastases of colorectal carcinoma with Dukes' stage C or D

Ji-Cheng Zhang, Zuo-Ren Wang, Yan-Juan Cheng, Ding-Zhong Yang, Jing-Sen Shi, Ai-Lin Liang, Ning-Na Liu, Xiao-Min Wang

Ji-Cheng Zhang, Zuo-Ren Wang, Ding-Zhong Yang, Jing-Sen Shi, Department of Hepatobiliary Surgery, First Hospital of Xi'an Jiaotong University, Xi'an 710061, Shannxi Province, China

Yan-Juan Cheng, Department of Medical Education, Shannxi Provincial Cancer Hospital, Xi'an 710061, Shannxi Province, China

Ai-Lin Liang, Ning-Na Liu, Xiao-Min Wang, Department of Pathology, Shannxi Provincial Cancer Hospital, Xi'an 710061, Shannxi Province, China

Correspondence to: Professor Zuo-Ren Wang, Department of Hepatobiliary Surgery, First Hospital of Xi'an Jiaotong University, Xi'an 710061, Shannxi Province, China. zjc1986@hotmail.com

Telephone: +86-29-5324009

Received: 2002-10-09 **Accepted:** 2002-11-12

Abstract

AIM: To study changes in characteristics of colorectal carcinoma during the metastatic process and to investigate the correlation between cell proliferation activity and metastatic ability of patients with Dukes' stage C or D.

METHODS: Formalin fixed and paraffin embedded materials of primary tumors and corresponding lymph node metastases resected from 56 patients with Dukes' stage C or D of colorectal carcinoma were stained immunohistochemically with proliferating cell nuclear antigen (PCNA) and CD44 variant exon 6 (CD44v6).

RESULTS: Thirty-one of 56 patients (55.4 %) expressed PCNA in the primary sites and 36 of 56 patients (64.3 %) expressed PCNA in the metastatic lymph nodes. A significant relation in PCNA expression was observed between the primary site and the metastatic lymph node ($0.010 < P < 0.025$). Forty-one of 56 patients (73.2 %) expressed CD44v6 in the primary site and 39 of 56 patients (69.6 %) expressed CD44v6 in the metastatic lymph node. There was also a significant relationship of CD44v6 between the primary site and the metastatic lymph node ($0.005 < P < 0.010$). No difference was observed between expression of CD44v6 and PCNA in the primary site ($0.250 < P < 0.500$).

CONCLUSION: This study partially demonstrates that tumor cells in metastatic lymph node of colorectal carcinoma still possess cell proliferation activity and metastatic ability of tumor cells in primary site. There may be no association between cell proliferation activity and metastatic ability in colorectal carcinoma.

Zhang JC, Wang ZR, Cheng YJ, Yang DZ, Shi JS, Liang AL, Liu NN, Wang XM. Expression of proliferating cell nuclear antigen and CD44 variant exon 6 in primary tumors and corresponding lymph node metastases of colorectal carcinoma with Dukes' stage C or D. *World J Gastroenterol* 2003; 9(7): 1482-1486
<http://www.wjgnet.com/1007-9327/9/1482.asp>

INTRODUCTION

Colorectal carcinoma appears to be increasing in Chinese populations and is characterised by an aggressive course and frequent metastases resulting in death. To reduce morbidity and mortality, identification of those patients with a high propensity to develop distant metastases is of great importance, since they might benefit from adjuvant chemotherapy and/or radiotherapy^[1,2]. Although Dukes' classification is still considered as the most accurate predictor of prognosis after resection, even within a group of tumors of a specified stage, tumor behaviour and prognosis of the disease is not uniform^[3-5]. For this reason, additional markers that predict tumor metastatic behaviour are needed^[6-9]. At present, PCNA has been described as a significant factor in the prognosis of colorectal carcinoma in several studies^[10-12]. On the other hand, many studies demonstrated that expression of CD44v6 correlated with poor survival and was an independent prognosticator in patients who underwent radical surgery^[13-17]. However, to our knowledge questions concerning metastases, characteristic changes that occur during the metastatic process, and the correlation between tumor characteristics have to be clarified in detail^[18-20]. To our knowledge, there has been neither any study regarding patients with Dukes' stage C or D analyzing both primary sites and corresponding metastatic lymph nodes genetically or immunohistologically nor a study assessing their relationship.

We examined the expression of these two factors in both primary sites and metastatic lymph nodes to elucidate the characteristic changes of the tumor during metastases and to evaluate the correlation between cell proliferation activity and metastatic ability of the tumor in patients with Dukes' stage C or D of colorectal carcinoma.

MATERIALS AND METHODS

Materials

175 consecutive patients with colorectal carcinoma admitted to our department underwent resection between 1989 and 1996. The total rate of lymph node metastasis was 33.7 %, 77.2 %, of which lymph node metastasis next to the colorectum was, 17.9 % and 4.9 % mesentery and mesenteric artery ligation point respectively. Of these 175 patients, 62 (35.8 %) were diagnosed with Dukes' stage C or D. Among these 62 patients, 56 whose primary site and metastatic node tissues were immunohistochemically evaluable were enrolled in the study. They were comprised of 30 males and 26 females with a mean age of 51.3 ± 14.2 years. Forty nine patients with Dukes' stage C underwent a complete tumor resection with lymph node dissection and 7 patients with Dukes' stage D underwent a palliative tumor resection with lymph node dissection in the Department of Gastroenterology, Shannxi Provincial Cancer Hospital in Xi'an, China. The patients had not been treated before. Their respective clinical data were collected through the review of their medical records. Histologic typing revealed 12 papillary adenocarcinomas, 27 tubular adenocarcinomas, 10 mucinous adenocarcinomas, 5 signet-ring cell carcinomas

and 2 undifferentiated carcinomas. Of these patients, there were 49 patients with Dukes' stage C, whose average number of metastatic lymph nodes was 5.3 ± 2.1 and 7 patients with Dukes' stage D, whose average number of metastatic sites including lymph node, liver, greater omentum and peritoneum was 8.7 ± 2.6 . The paraffin-embedded blocks and histological slides were taken from the Department of Pathology, Shaanxi Provincial Cancer Hospital (Table 1).

Table 1 Characteristics of patients with Dukes' stage C or D colorectal carcinoma

Gender	Male	30
	Female	26
Age(yrs) (mean \pm SD)	51.3 \pm 14.2	
Histology	Papillary adenocarcinoma	12
	Tubular adenocarcinoma	27
	Mucinous adenocarcinoma	10
	Signet-ring cell carcinoma	5
	Undifferentiated carcinoma	2
Dukes' classification	Stage C	49
	Stage D	7

Methods

Formalin fixed, paraffin embedded sections of samples were stained immunohistochemically with labeled streptavidin-biotin (LSAB) using a LSAB Kit (Doctor Biotechnology Company, Wuhan, Hubei Province, China). The samples were thinly sectioned (4 μ m thick). After deparaffinization, the sections were hydrolyzed with ethanol and endogenous peroxidase activity was inhibited with 0.3 % hydrogen peroxide-containing methanol at room temperature for 15 minutes. For antigen retrieval, the sections were mounted in 300 mL 0.01 M sodium citrate buffer (pH 6.0) in a container and microwaved for 15 minutes at maximum power in a Sharp microwave oven (850 W). Nonspecific binding sites were blocked with 10 % nonimmune goat serum. For PCNA, PC10 (Zymed Laboratories, California) whose optimal dilution was 1:150 was used for the first antibody and allowed to react at 4 $^{\circ}$ C for 12 hours. For CD44v6, CD44 variant exon 6 (VFF-18; Bender Co.) whose optimal dilution was 1:100 was used for the first antibody and allowed to react at 4 $^{\circ}$ C for 12 hours. After the second antibody was made to react, peroxidase-labeled streptavidin was finally allowed to react as an enzyme reagent. Diaminobenzidine was used for coloring. Sections of human tonsils and submucosal lymphoid follicles were used as positive control for PCNA. Positive control of CD44v6 was normal human stratified squamous epithelium which could be strongly stained by anti-CD44v6 antibodies^[15]. Sections stained by omitting the primary antibody were used as their negative controls. At least 5 visual fields of the immunohistochemically stained sample were observed at random at $\times 100$ or $\times 400$ magnification. More than 1000 tumor cells were counted by two investigators who were blinded to the clinical outcome. The number of positive cells was counted and expressed as percentage. For PCNA, when the percentage of positive cells was ≤ 50 %, the specimen was diagnosed as negative, and when >50 %, the specimen was diagnosed as positive. We also determined the percentage of cells positively stained for CD44v6, as well as the intensity of this staining. Negative, ≤ 10 % of cells were positively stained, and positive, >10 % cells were positively stained^[21]. The data were analyzed using χ^2 test and a *P* value <0.05 was considered significant.

RESULTS

Immunohistochemical staining with PCNA showed a selective nuclear pattern (Figures 1,2). Thirty-one of 56 patients (55.4 %) expressed PCNA in the primary site and 36 of 56 patients (64.3 %)

expressed PCNA in the metastatic lymph node. Among these 56 patients, twenty-four expressed PCNA in both the primary site and metastatic lymph node, seven patients expressed PCNA in the primary site but did not express it in the metastatic lymph node, whereas twelve patients did not express PCNA in the primary site but expressed it in the metastatic lymph node, thirteen patients expressed PCNA in neither the primary site nor metastatic lymph node (Table 2). For expression of PCNA in these 56 patients, a significant relation was observed between the primary site and the metastatic lymph node ($0.010 < P < 0.025$).

Table 2 Expression of PCNA in colorectal carcinoma at primary sites and metastatic lymph nodes

Metastatic lymph nodes	Primary sites	
	-	+
-	13	7
+	12	24

Note: $\chi^2=5.21$, $0.010 < P < 0.025$.

Intensely positive staining with CD44v6 mainly occurred on the cell membrane surface of tumor cells (Figure 3). Forty-one of 56 patients (73.2 %) expressed CD44v6 in the primary site and 39 of 56 patients (69.6 %) expressed CD44v6 in the metastatic lymph node (Figure 4). Among these 56 patients, thirty-three expressed CD44v6 in both the primary site and metastatic lymph node, eight expressed CD44v6 in the primary site but did not express it in the metastatic lymph node, whereas six did not express CD44v6 in the primary site but expressed it in the metastatic lymph node, nine expressed CD44v6 in neither primary site nor metastatic lymph node (Table 3). For expression of CD44v6 in these 56 patients, there was also a significant relationship between the primary site and the metastatic lymph node ($0.005 < P < 0.010$).

Table 3 Expression of CD44v6 in colorectal carcinoma at primary sites and metastatic lymph nodes

Metastatic lymph nodes	Primary sites	
	-	+
-	9	8
+	6	33

Note: $\chi^2=6.71$, $0.005 < P < 0.010$.

Table 4 Expression of PCNA and CD44v6 in colorectal carcinoma at primary sites

PCNA	CD44v6	
	-	+
-	5	20
+	10	21

Note: $\chi^2=1.06$, $0.250 < P < 0.500$

To evaluate the correlation between cell proliferation activity and metastatic ability, we studied expression of PCNA and CD44v6 in the primary site. Among these 56 patients, twenty-one expressed both PCNA and CD44v6 and 5 expressed neither PCNA nor CD44v6 in the primary site, twenty expressed CD44v6 but did not express PCNA, whereas ten did not express CD44v6 but expressed PCNA in the primary site (Table 4).

No difference was observed between expression of CD44v6 and PCNA in the primary site ($0.250 < P < 0.500$).

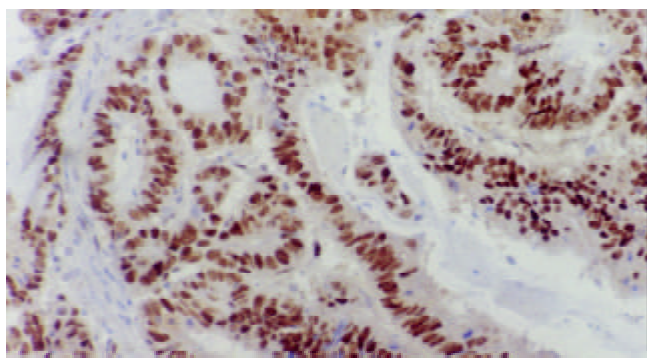


Figure 1 Positive expression of PCNA in primary colorectal carcinoma tissue (LSAB×100).

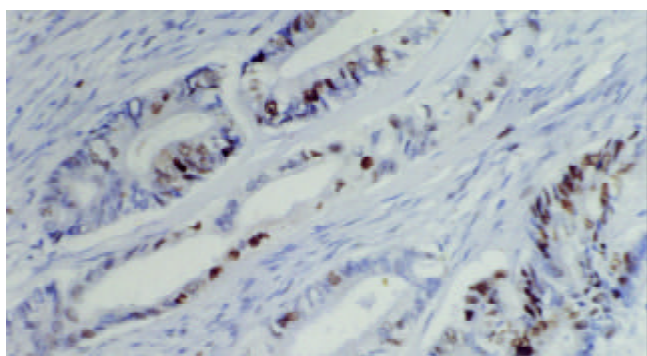


Figure 2 Negative expression of PCNA in primary site (LSAB×100).

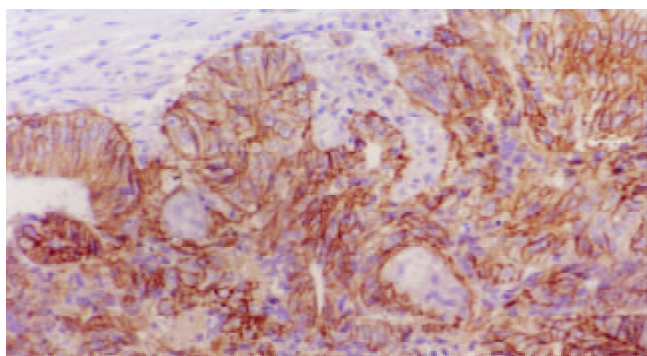


Figure 3 CD44v6 was observed on the cell membrane of tumor cells (LSAB×100).

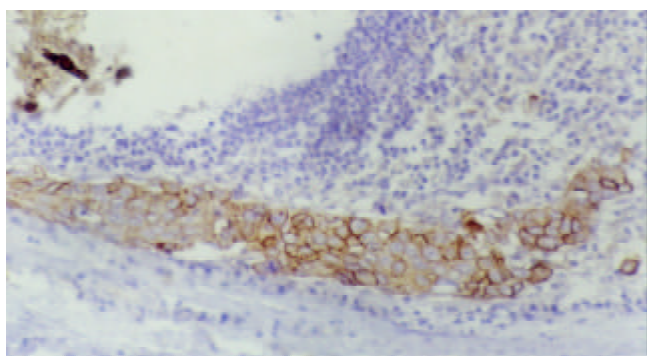


Figure 4 Expression of CD44v6 in corresponding metastatic lymph node, showing that tumor cells were invading lymph node from periphery. (LSAB×100).

Cell morphology

Immunohistochemical staining with PCNA showed a selective nuclear pattern (Figures 1,2). Intensely positive staining with CD44v6 mainly occurred on the cell membrane surface of tumor cells (Figure 3). Expression of CD44v6 in corresponding metastatic lymph node showed that tumor cells were invading lymph node from periphery (Figure 4).

DISCUSSION

One of the first steps in multistage colonic carcinogenesis is increased cell proliferation. PCNA, which is a nonhistone nuclear protein of 36 kilodaltons, also is known as cyclin and an auxiliary factor in DNA polymerase, plays a very important role in DNA replication^[22]. Because of this direct relation with cell proliferation, PCNA is considered to be an important factor in prognosis. In fact, it has been described as a significant factor in the prognosis of colorectal carcinoma in several studies^[10-12]. CD44, a glycoprotein of the membrane penetration type, functions as an extracellular matrix glycan receptor and a hyaluronate receptor^[23]. As a consequence of studies in rats showed that CD44v6 could confer metastatic potential to rat pancreatic carcinoma cell lines^[24], studies addressing the prognostic and biological significance of CD44 variant expression in human cancer have largely been focused on CD44v6. Overexpression of CD44v6 has been demonstrated in colorectal neoplasia by immunohistochemistry, RT-PCR and *in situ* hybridization. Their expression was found to correlate with tumor stage^[13-17]. As for prognosis, it was shown that expression of CD44v6 correlate with poor survival rate and was an independent prognosticator in patients who underwent radical surgery. Hence, it identifies individuals with a high propensity to develop metastases. These patients might benefit from adjuvant therapy^[16].

Despite intensive research in recent years, very little is known about the characteristic changes of malignant colorectal tumor cells during the process of metastases. We examined expression of these two factors in both primary site and metastatic lymph node. Among these 56 patients, twenty-four expressed PCNA in both the primary site and metastatic lymph node and thirteen expressed PCNA in neither the primary site nor metastatic lymph node. The concordance rate of PCNA expression in the primary site and in the metastatic lymph node was 66.1 % ($0.010 < P < 0.025$). That is to say, compared with primary site, PCNA expression in metastatic lymph node had no significant change. This suggests that cell proliferation activity revealed by PCNA still exists in the tumor cells of metastatic lymph nodes. Similarly, the concordance rate of CD44v6 expression in the primary site and in the metastatic lymph node was 75.0 % ($0.005 < P < 0.010$). This also means that metastatic ability revealed by CD44v6 still exists in the tumor cells of metastatic lymph nodes.

Although cell proliferation and metastasis are a very complicated problem involving many molecular mechanisms and biologic factors, our study partially showed that tumor cells in metastatic lymph node of colorectal carcinoma still possessed cell proliferation activity and metastatic ability of tumor cells in primary site. However, Kimball *et al*^[25] isolated a cellular subpopulation from a human colonic carcinoma cell line and Brattain *et al*^[26] reported that malignant cells from a human colonic carcinoma possessed heterogeneity. A question rises: do tumor cells of colorectal carcinoma not possess heterogeneity between the primary site and the metastatic lymph node? It is well known that cancer cell population, either as a solid tumor mass *in vivo* or as a continuous cell line *in vitro*, is an ever-changing entity due to their genetic instability and selective environmental pressure. A tumor mass consists of different cell clones, a phenomenon known as tumor

heterogeneity^[27,28]. Based on this phenomenon, tumor cell clones with different biological properties have been isolated from a number of human and animal tumor cell lines. The differences included a variety of biological characteristics such as tumor cell morphology, karyotypes, *in vitro* and *in vivo* growth patterns^[29,30], DNA ploidy^[31], tumorigenicity, metastatic patterns and metastatic potentials^[32]. Cancer metastasis is the ultimate display of complex interactions between the malignant cells and the host defense mechanism. The process of metastasis consists of selection and sequential steps that include angiogenesis, detachment, motility, invasion of the extracellular matrix, intravasation, circulation, adhesion, extravasation into the organ parenchyma and growth^[28]. The ability of cancer cells to form metastasis depends on a set of unique biological properties that enable the malignant cells to complete all those steps of metastatic cascade. But this basically biological theory is not in contradiction with our present study, because our results are a clinicopathologic outcome depending upon experiment.

Our study showed that there was no significant association between expression of CD44v6 and PCNA in the primary site ($0.250 < P < 0.500$). This result partially indicated that there existed no absolute association between cell proliferation activity and metastatic ability in colorectal carcinoma. At present, whether tumor cell growth rate is directly related to metastasis is not clear yet. Yasoshima *et al.*^[33] using metastatic gastric cancer cell line, and Samiei *et al.*^[34] using metastatic mammary clones found that metastasis was independent of tumor cell growth, while other works^[35-37] showed a close association between tumor cell growth rate and metastasis. Further study of the correlation between cell proliferation activity and metastatic ability in colorectal carcinoma is therefore needed.

In conclusion, we have partially demonstrated in the present study that tumor cells in metastatic lymph node of colorectal carcinoma still possess cell proliferation activity and metastatic ability in primary site. There may be no association between cell proliferation activity and metastatic ability in colorectal carcinoma.

REFERENCES

- 1 **Mayer RJ**, O'Connell MJ, Tepper JE, Wolmark N. Status of adjuvant therapy for colorectal cancer. *J Natl Cancer Inst* 1989; **81**: 1359-1364
- 2 **Moertel CG**. Chemotherapy for colorectal cancer. *N Engl J Med* 1994; **330**: 1136-1142
- 3 **Steele G Jr**. Advances in the treatment of early- to late-stage colorectal cancer: 20 years of progress. *Ann Surg Oncol* 1995; **2**: 77-88
- 4 **Greene FL**, Stewart AK, Norton HJ. A new TNM staging strategy for node-positive (stage III) colon cancer: an analysis of 50, 042 patients. *Ann Surg* 2002; **236**: 416-421
- 5 **Fisher ER**, Sass R, Palekar A, Fisher B, Wolmark N. Dukes' classification revisited. Findings from the National Surgical Adjuvant Breast and Bowel Projects (Protocol R-01). *Cancer* 1989; **64**: 2354-2360
- 6 **Douglass HO Jr**, Moertel CG, Mayer RJ, Thomas PR, Lindblad AS, Mittleman A, Stablein DM, Bruckner HW. Survival after postoperative combination treatment of rectal cancer. *N Engl J Med* 1986; **315**: 1294-1295
- 7 **Laurie JA**, Moertel CG, Fleming TR, Wieand HS, Leigh JE, Rubin J, McCormack GW, Gerstner JB, Krook JE, Mailliard J. Surgical adjuvant therapy of large-bowel carcinoma: an evaluation of levamisole and the combination of levamisole and fluorouracil. The North Central Cancer Treatment Group and the Mayo Clinic. *J Clin Oncol* 1989; **7**: 1447-1456
- 8 **Krook JE**, Moertel CG, Gunderson LL, Wieand HS, Collins RT, Beart RW, Kubista TP, Poon MA, Meyers WC, Mailliard JA. Effective surgical adjuvant therapy for high-risk rectal carcinoma. *N Engl J Med* 1991; **324**: 709-715
- 9 **Harris GJ**, Church JM, Senagore AJ, Lavery IC, Hull TL, Strong SA, Fazio VW. Factors affecting local recurrence of colonic adenocarcinoma. *Dis Colon Rectum* 2002; **45**: 1029-1034
- 10 **Kanazawa Y**, Onda M, Tanaka N, Seya T. Proliferating cell nuclear antigen and p53 protein expression in submucosal invasive colorectal carcinoma. *J Nippon Med Sch* 2000; **67**: 242-249
- 11 **Onodera H**, Maetani S, Kawamoto K, Kan S, Kondo S, Imamura M. Pathologic significance of tumor progression in locally recurrent rectal cancer: different nature from primary cancer. *Dis Colon Rectum* 2000; **43**: 775-781
- 12 **Seong J**, Chung EJ, Kim H, Kim GE, Kim NK, Sohn SK, Min JS, Suh CO. Assessment of biomarkers in paired primary and recurrent colorectal adenocarcinomas. *Int J Radiat Oncol Biol Phys* 1999; **45**: 1167-1173
- 13 **Wielenga VJ**, Heider KH, Offerhaus GJ, Adolf GR, van den Berg FM, Ponta H, Herrlich P, Pals ST. Expression of CD44 variant proteins in human colorectal cancer is related to tumor progression. *Cancer Res* 1993; **53**: 4754-4756
- 14 **Finn L**, Dougherty G, Finley G, Meisler A, Becich M, Cooper DL. Alternative splicing of CD44 pre-mRNA in human colorectal tumors. *Biochem Biophys Res Commun* 1994; **200**: 1015-1022
- 15 **Fox SB**, Fawcett J, Jackson DG, Collins I, Gatter KC, Harris AL, Gearing A, Simmons DL. Normal human tissues, in addition to some tumors, express multiple different CD44 isoforms. *Cancer Res* 1994; **54**: 4539-4546
- 16 **Mulder JW**, Kruyt PM, Sewnath M, Oosting J, Seldenrijk CA, Weidema WF, Offerhaus GJ, Pals ST. Colorectal cancer prognosis and expression of exon-v6-containing CD44 proteins. *Lancet* 1994; **344**: 1470-1472
- 17 **Gotley DC**, Fawcett J, Walsh MD, Reeder JA, Simmons DL, Antalis TM. Alternatively spliced variants of the cell adhesion molecule CD44 and tumour progression in colorectal cancer. *Br J Cancer* 1996; **74**: 342-351
- 18 **Fukuse T**, Hirata T, Tanaka F, Yanagihara K, Hitomi S, Wada H. Prognosis of ipsilateral intrapulmonary metastases in resected nonsmall cell lung cancer. *Eur J Cardiothorac Surg* 1997; **12**: 218-223
- 19 **Ichinose Y**, Hara N, Ohta M. Synchronous lung cancers defined by deoxyribonucleic acid flow cytometry. *J Thorac Cardiovasc Surg* 1991; **102**: 418-424
- 20 **Martini N**, Melamed MR. Multiple primary lung cancers. *J Thorac Cardiovasc Surg* 1975; **70**: 606-612
- 21 **Nanashima A**, Yamaguchi H, Sawai T, Yasutake T, Tsuji T, Jibiki M, Yamaguchi E, Nakagoe T, Ayabe H. Expression of adhesion molecules in hepatic metastases of colorectal carcinoma: relationship to primary tumours and prognosis after hepatic resection. *J Gastroenterol Hepatol* 1999; **14**: 1004-1009
- 22 **Bravo R**, Frank R, Blundell PA, Macdonald-Bravo H. Cyclin/PCNA is the auxiliary protein of DNA polymerase-delta. *Nature* 1987; **326**: 515-517
- 23 **Aruffo A**, Stamenkovic I, Melnick M, Underhill CB, Seed B. CD44 is the principal cell surface receptor for hyaluronate. *Cell* 1990; **61**: 1303-1313
- 24 **Gunther U**, Hofmann M, Rudy W, Reber S, Zoller M, Haussmann I, Matzku S, Wenzel A, Ponta H, Herrlich P. A new variant of glycoprotein CD44 confers metastatic potential to rat carcinoma cells. *Cell* 1991; **65**: 13-24
- 25 **Kimball PM**, Brattain MG. Isolation of a cellular subpopulation from a human colonic carcinoma cell line. *Cancer Res* 1980; **40**: 1574-1579
- 26 **Brattain MG**, Fine WD, Khaled FM, Thompson J, Brattain DE. Heterogeneity of malignant cells from a human colonic carcinoma. *Cancer Res* 1981; **41**: 1751-1756
- 27 **Fidler IJ**. Tumor heterogeneity and the biology of cancer invasion and metastasis. *Cancer Res* 1978; **38**: 2651-2660
- 28 **Fidler IJ**. Critical factors in the biology of human cancer metastasis: twenty-eighth G.H.A. Clowes memorial award lecture. *Cancer Res* 1990; **50**: 6130-6138
- 29 **Dexter DL**, Spremulli EN, Fligiel Z, Barbosa JA, Vogel R, VanVoorhees A, Calabresi P. Heterogeneity of cancer cells from a single human colon carcinoma. *Am J Med* 1981; **71**: 949-956
- 30 **Dexter DL**, Kowalski HM, Blazar BA, Fligiel Z, Vogel R, Heppner GH. Heterogeneity of tumor cells from a single mouse mammary

- tumor. *Cancer Res* 1978; **38**: 3174-3181
- 31 **Bonsing BA**, Corver WE, Fleuren GJ, Cleton-Jansen AM, Devilee P, Cornelisse CJ. Allelotype analysis of flow-sorted breast cancer cells demonstrates genetically related diploid and aneuploid subpopulations in primary tumors and lymph node metastases. *Genes Chromosomes Cancer* 2000; **28**: 173-183
- 32 **Solimene AC**, Carneiro CR, Melati I, Lopes JD. Functional differences between two morphologically distinct cell subpopulations within a human colorectal carcinoma cell line. *Braz J Med Biol Res* 2001; **34**: 653-661
- 33 **Yasoshima T**, Denno R, Kawaguchi S, Sato N, Okada Y, Ura H, Kikuchi K, Hirata K. Establishment and characterization of human gastric carcinoma lines with high metastatic potential in the liver: changes in integrin expression associated with the ability to metastasize in the liver of nude mice. *Jpn J Cancer Res* 1996; **87**: 153-160
- 34 **Samiei M**, Waghorne CG. Clonal selection within metastatic SP1 mouse mammary tumors is independent of metastatic potential. *Int J Cancer* 1991; **47**: 771-775
- 35 **Li Y**, Tang ZY, Ye SL, Liu YK, Chen J, Xue Q, Chen J, Gao DM, Bao WH. Establishment of cell clones with different metastatic potential from the metastatic hepatocellular carcinoma cell line MHCC97. *World J Gastroenterol* 2001; **7**: 630-636
- 36 **Price JE**, Bell C, Frost P. The use of a genotypic marker to demonstrate clonal dominance during the growth and metastasis of a human breast carcinoma in nude mice. *Int J Cancer* 1990; **45**: 968-971
- 37 **Suzuki N**, Frapart M, Grdina DJ, Meistrich ML, Withers HR. Cell cycle dependency of metastatic lung colony formation. *Cancer Res* 1977; **37**: 3690-3693

Edited by Zhao M and Wang XL

Gastric autoimmune disorders in patients with chronic hepatitis C before, during and after interferon-alpha therapy

Carlo Fabbri, M. Francesca Jaboli, Silvia Giovanelli, Francesco Azzaroli, Alessandro Pezzoli, Esterita Accogli, Stefania Liva, Giovanni Nigro, Anna Miracolo, Davide Festi, Antonio Colecchia, Marco Montagnani, Enrico Roda, Giuseppe Mazzella

Carlo Fabbri, M. Francesca Jaboli, Silvia Giovanelli, Francesco Azzaroli, Alessandro Pezzoli, Esterita Accogli, Stefania Liva, Giovanni Nigro, Anna Miracolo, Antonio Colecchia, Marco Montagnani, Enrico Roda, Giuseppe Mazzella, Department of Internal Medicine and Gastroenterology, University of Bologna, Bologna, Italy

Davide Festi, Department of Medicine and Aging, University "G D' Annunzio" Chieti, Italy

Correspondence to: Professor Giuseppe Mazzella, Department of Internal Medicine and Gastroenterology, University of Bologna, Ospedale S. Orsola- Malpighi, via Massarenti 9, I-40138 Bologna, Italy. mazzella@med.unibo.it

Telephone: +39-51-6363276 **Fax:** +39-51-343398

Received: 2003-02-25 **Accepted:** 2003-03-16

Abstract

AIM: To explore the prevalence of autoimmune gastritis in chronic hepatitis C virus (HCV) patients and the influence of α -interferon (IFN) treatment on autoimmune gastritis.

METHODS: We performed a prospective study on 189 patients with positive anti-HCV and viral RNA enrolled in a 12-month IFN protocol. We evaluated: a) the baseline prevalence of autoimmune gastritis, b) the impact of IFN treatment on development of biochemical signs of autoimmune gastritis (at 3, 6 and 12 months), c) the evolution after IFN withdrawal (12 months) in terms of anti-gastric-parietal-cell antibodies (APCA), gastrin, anti-thyroid, and anti-non-organ-specific antibodies.

RESULTS: APCA positivity and 3-fold gastrin levels were detected in 3 (1.6 %) and 9 (5 %) patients, respectively, at baseline, in 25 (13 %) and 31 (16 %) patients at the end of treatment (both $P < 0.001$, vs baseline), and in 7 (4 %) and 14 (7 %) patients 12 months after withdrawal ($P = 0.002$ and $P = 0.01$ respectively, vs baseline; $P =$ not significant vs end of treatment). The development of autoimmune gastritis was strictly associated with the presence of autoimmune thyroiditis ($P = 0.0001$), no relationship was found with other markers of autoimmunity.

CONCLUSION: In HCV patients, IFN frequently precipitates latent autoimmune gastritis, particularly in females. Following our 12-month protocol, the phenomenon generally regressed. Since APCA positivity and high gastrin levels are associated with the presence of antithyroid antibodies, development of autoimmune thyroiditis during IFN treatment may provide a surrogate preliminary indicator of possible autoimmune gastritis to limit the need for invasive examinations.

Fabbri C, Jaboli MF, Giovanelli S, Azzaroli F, Pezzoli A, Accogli E, Liva S, Nigro G, Miracolo A, Festi D, Colecchia A, Montagnani M, Roda E, Mazzella G. Gastric autoimmune disorders in patients with chronic hepatitis C before, during and after interferon-alpha therapy. *World J Gastroenterol* 2003; 9(7): 1487-1490 <http://www.wjgnet.com/1007-9327/9/1487.asp>

INTRODUCTION

Chronic hepatitis C virus (HCV) infection can lead to the development of chronic liver disease, cirrhosis and hepatocellular carcinoma (HCC)^[1]. Chronic HCV patients frequently have a broad spectrum of autoantibodies and/or concurrent autoimmune disease^[2-4], apparently not closely associated with the HCV genotype^[5] or to the severity of liver disease^[6]. Several studies have indicated that immunological abnormalities are sometimes unmasked by interferon- α (IFN) therapy^[7-12]. Although autoimmune thyroiditis is one of the most common immunological side effects of IFN treatment, with very close monitoring, its presence is not an absolute contraindication for the therapy. A close association has been reported between autoimmune thyroiditis and autoimmune (i. e. type A) gastritis^[13]. Autoimmune gastritis involves the fundus and the body of the stomach while sparing the antrum. It is associated with pernicious anemia, autoantibodies to gastric parietal cells, achlorhydria, low serum pepsinogen I with normal serum pepsinogen II concentrations^[14] and high serum gastrin concentration, the latter is resulted from hyperplasia of gastrin-producing cells. It is thought that *Helicobacter pylori* (*H. pylori*) could be implicated in the development of autoimmune gastritis^[15,16], since it induces antigenic mimicry^[17] and antibodies against *H. pylori* can cross-react with both antral mucosal and gastrin-producing cells.

The frequencies of thyroiditis manifestations during IFN treatment of chronic hepatitis C infection are well documented^[7,9,10]. However, the impact of IFN therapy on the development of autoimmune and other types of gastric disease is unknown. To address this issue, we designed a prospective study on 189 chronic HCV patients treated with IFN. In particular, we investigated: a) the baseline prevalence of autoimmune gastritis, b) the impact of IFN on the development of biochemical signs of autoimmune gastritis, c) the outcome of twelve months after withdrawal of IFN. We also examined the presence of antithyroid, antigastric parietal-cell and anti-non-organ-specific (anti-NOS) antibodies. Finally, we investigated whether the presence of *H. pylori* affected the development of autoimmune gastritis.

MATERIALS AND METHODS

Patients and study design

We prospectively studied a group of 189 consecutive IFN-treated chronic hepatitis C patients (95 males, 94 females, mean age 58 ± 18 years) who entered an IFN therapeutic program at our institution from September 1996 to July 1998 (Table 1). Criteria for the diagnosis of chronic HCV infection were: 1) presence of anti-HCV antibodies and polymerase chain reaction (PCR) positivity for HCV-RNA, 2) histological confirmation of chronic hepatitis C, 3) exclusion of other causes of chronic liver diseases (alcoholism, Wilson's disease, drugs, hemochromatosis, $\alpha 1$ antitrypsin deficiency, autoimmune hepatitis, PBC). Criteria for inclusion in the IFN treatment program were the generally recognized ones (transaminase levels over two times the upper limit, age between 18 and 70

years, absence of pregnancy and psychiatric history or other chronic severely invalidating conditions). None of the patients had received immunosuppressive or immunostimulatory therapy before entry into the study. All the patients were negative for human immunodeficiency virus (HIV) antibodies and hepatitis B surface antigen (HBsAg). Disease activity and stage were evaluated according to Scheuer's histological score. None of the patients were receiving proton pump inhibitors or anti-H₂ antagonist drugs. Informed consent was obtained from each patient and approval for the study protocol was granted by the Ethical Committee of our institution.

Table 1 Baseline characteristics of patients

Patients (n)	189	
Age (year) ± SD	58±18	
Sex (M/F)	95/94	
ALT (U/L) ± SE	142±8	
AST (U/L) ± SE	103±7	
Genotype 1-4 vs others	115 vs 74	61 vs 39%
Anti- <i>Hp</i> positive antibody	60	31.8%
Gastrin (pg/ml)(median±SE)	52.0±10.4	
TSH (UI/ml)	2.2±0.15	
ANA positive (n)	34	18%
AMA positive (n)	-	
ASMA positive (n)	57	30%
LKM positive (n)	1	0.5%
APCA positive (n)	3	1.6%
ATM positive (n)	15	7.8%
Liver histology (n)		
CAH without cirrhosis (n)	138	73%
CAH with cirrhosis (n)	51	27%

All the patients received 6 MU of recombinant IFN daily for the first month, followed by 6 MU each alternate day for 5 months and then 3 MU each alternate day for a further 6 months. In the event of side-effects, the dosage was decreased. If side effects were severe or sustained, IFN treatment was suspended.

Serum samples were analyzed in all the patients for presence of gastric parietal cell autoantibodies and gastrin at the following time points: baseline, after 3 and 6 months of treatment, the end of IFN treatment (i.e. at 12 months, or at the time of suspension, if earlier), 12 months after suspension of IFN. Multiple endoscopic gastric biopsies were always performed when positive anti-gastric parietal cell autoantibodies and/or serum levels of gastrin were found to be over 3 times the normal upper limit, presence of gastrinoma was excluded by the secretin stimulation test. In all patients, *Helicobacter pylori* status was serologically tested before the start of treatment. Criteria for diagnosis of autoimmune gastritis were according to Sidney classification system^[18,19].

Biochemical and virological assays

Serum samples were analyzed for routine biochemical liver function tests with a multichannel autoanalyzer. HBsAg and anti-HBs and anti-hepatitis B core (HBc) antibodies were tested using a commercial solid-phase radioimmunoassay (Abbott Laboratories, North Chicago, IL). HIV determination was done according to a standard enzyme-linked immunosorbent assay (ELISA) procedure (HIV ELISA, Abbott Laboratories, North Chicago, IL). Anti-HCV antibodies were tested using a second-generation ELISA procedure (ELISA-2, Ortho Diagnostic Test Systems, Raritan, NJ). HCV RNA was detected by nested PCR analysis using primers from the highly conserved 5' non-coding

region of the HCV genome (Shindo *et al*, 1991). HCV genotype was determined by InnoLipa.

Immunoserological evaluation

Anti-nuclear, anti-mitochondrial, smooth-muscle and liver-kidney microsome-1 auto-antibodies (ANA, AMA, SMA and LKM-1) were determined using indirect immunofluorescence assays on unfixed cryostat frozen sections of mouse liver, kidney and stomach. Sera were screened for anti-parietal cell autoantibodies (APCA) by immunofluorescence reactivity with paraffin-embedded sections of mouse stomach and for H⁺/K⁺-ATPase autoantibodies by ELISA. A positive result required a titer of at least 1/40. Basal serum gastrin and thyroid serum hormone (TSH) concentration were measured by radioimmunological assay (RIA), which detects sulfated and non-sulfated human heptadecapeptide (hG-17), as well as human big gastrin (hG-34). Gastrin results were expressed as pg/ml. Thyroid microsomal and thyroglobulin autoantibodies (TMA and TGA) were analyzed using hemagglutination tests (Ames, Elkhart, IN, USA). The cut-off points for both TMA and TGA were 1:100.

H. pylori investigation

Serum immunoglobulin G (IgG) response to *H. pylori* purified antigens was measured by ELISA, the cut-off value used was an optical density ratio >1.0. The presence or absence of *H. pylori* was also defined by histological examination of multiple gastric biopsy specimens from the antrum, fundus, or cardia in all the patients with positive APCA and/or elevated levels of gastrin. All biopsy specimens were fixed in Hollande's fixative and stained with H&E and Giemsa.

Statistical analysis

Intent-to-treat analysis was adopted. To analyze associations among groups the Fisher's exact test and the χ^2 test with Yates' correction were used. A two-tailed *P* value less than 0.05 was considered significant.

RESULTS

Treatment outcome

The entire 12-month treatment schedule was completed by 168/189 (89%) of patients. In 21 patients, the IFN dose was reduced due to the severity of side effects (severe thrombocytopenia and/or severe leukopenia with neutrophil count <800/mm³, continuous fever unresponsive to paracetamol, or severe myalgia). At least three months of treatment were completed by all but two of the patients (one suspended due to severe depression and suicidal tendency, the other due to side effects coupled with lack of motivation). None of the patients who discontinued therapy was positive for APCA.

Abdominal symptoms

In 164/189 (87%) patients, no abdominal symptoms were reported. The most frequently reported symptoms were epigastric pain and/or abdominal discomfort. Presence of abdominal symptoms was not affected by positivity/negativity for *H. pylori*.

APCA and hypergastrinemia outcome (Tables 2, 3)

At the start of treatment, APCA positivity was detected in 3 (1.6%) patients, and hypergastrinemia (i.e. serum gastrin levels over three times the normal upper limit) was found in a further 9 (5%). At the end of treatment, these incidences rose to 25 (13%) and 31 (16%) patients, respectively (both *P*<0.001 vs baseline values). Thus, 22 patients developed both APCA and hypergastrinemia, mostly by the third month of therapy. Twelve

months after suspension of IFN, APCA and hypergastrinemia were still present in 7 (4 %) and 14 (7 %) patients, respectively ($P=0.002$ and $P=0.01$, respectively, *vs* end of IFN treatment; both P =not significant *vs* baseline). During IFN treatment, females were more prone to have increased APCA ($P=0.017$) or increased serum gastrin levels ($P=0.011$) than males.

Serum gastrin levels (defined as median \pm Standard Error) increased during administration of IFN (from 52 ± 10.4 pg/ml to 57 ± 17.2 pg/ml, $P=0.001$). Twelve months after withdrawal of therapy, serum gastrin levels (56 ± 12.6 pg/ml) were still higher than those at baseline ($P=0.001$), although they were significantly lower than those at the end of treatment ($P=0.001$). Serum TSH levels increased during administration of IFN (from 2.6 ± 0.13 MCU/ml to 3.2 ± 0.17 MCU/ml, $P=0.02$), and subsequently remained higher than the baseline values at 12 months from withdrawal of therapy (3.2 ± 0.3 MCU/ml, $P=0.02$ *vs* baseline, P =not significant *vs* withdrawal). As can be seen from Tables 2 and 3, the behavior of the antithyroid autoantibodies TPO was very similar to that of APCA. By contrast, IFN did not affect the non-organ-specific antibodies ANA, SMA and AMA.

Table 2 Variations of APCA positivity and hypergastrinemia in IFN treated patients

	Before IFN <i>n</i> (%)	IFN withdrawal <i>n</i> (%)	12 months after withdrawal <i>n</i> (%)
APCA positivity	3 (1.6%)	25 (13%) ^a	7 (4%) ^{b,d}
Hypergastrinemia	9 (5%)	31 (16%) ^a	14 (7%) ^{c,d}

^a $P<0.001$ *vs* before IFN; ^b $P<0.002$ *vs* IFN withdrawal; ^c $P<0.01$ *vs* IFN withdrawal; ^d P =not significant *vs* before IFN.

Table 3 Organ-specific and non-organ-specific autoantibodies

	Before IFN + (%)	IFN withdrawal + (%)	12 months after withdrawal+ (%)
Organ-specific antibodies			
TPO	14 (8.0%)	39 (20.6%) ^a	23 (12.2%)
Non-organ-specific antibodies			
ANA	34 (18.0%)	45 (24.0%)	41 (22.0%)
SMA	56 (30.0%)	62 (33.0%)	60 (31.0%)
AMA	-	1 (0.5%)	1 (0.5%)
LMK 1	1 (0.5%)	3 (1.6%)	2 (1.1%)

^a $P<0.001$ *vs* before IFN; $P=0.036$ *vs* 12 months after IFN withdrawal.

H. pylori status

At baseline, 61/189 (32.3 %) patients had a positive serum IgG response to *H. pylori* whole-cell antigen. These included 3 of the 9 (33.3 %) patients with autoimmune gastritis and 12 of the 31 (38.7 %) who developed biochemical signs of autoimmune gastritis during treatment.

Histology

Multiple endoscopic gastric biopsies were performed when positive APCA and/or serum levels of gastrin were found to be over 3 times the normal upper limit. At biopsy, all the patients with either baseline APCA positivity ($n=3$) or hypergastrinemia ($n=9$) showed a histological picture consistent with autoimmune gastritis. Among the 22 patients who developed both APCA positivity and hypergastrinemia during IFN therapy, the histology of the fundus was consistent with autoimmune gastric atrophy in 13 (59 %). Four other patients who were persistently consistent with presence of gastric atrophy maintained histological lesions at 12 months from IFN withdrawal.

Outcome of HCV infection

At baseline, 115/189 (61.0 %) patients were found to be infected with HCV genotype 1 or 4, while the remaining 74 (39.0 %) were infected with more IFN-responsive strains. Overall, 37/189 (19.5 %) patients showed a long-term virological response to IFN (at 12 months from withdrawal). In particular, long-term response was observed in 8/109 (7.3 %) patients with genotype 1, 21/39 (53 %) with genotype 2, 7/14 (50 %) with genotype 3, and 1/6 (16 %) with genotype 4, respectively. No difference in responsive rate was observed among the patients who developed hypothyroidism and/or hypergastrinemia and those who did not. No relationships were observed between HCV genotype and the development of autoimmune gastritis.

DISCUSSION

The prevalence of autoimmune gastritis in chronic HCV patients is currently unknown. Autoimmune gastritis can be associated with thyroid autoimmune abnormalities. The hypothesis that IFN therapy encourages the development of autoimmune gastritis in these patients has never been tested.

In this prospective study, we investigated the occurrence of autoimmune gastritis in 189 chronic HCV patients treated with IFN. The baseline prevalence of biochemical signs and histological features of autoimmune gastritis was similar to that found in the general population. However, the number of patients who displayed biochemical and/or histological signs of autoimmune gastritis significantly increased during IFN treatment. By 12 months after interruption of IFN, the number of patients showing these signs had partially regressed, although it still remained higher than the baseline value. Seven more patients continued to have elevated APCA and gastrinemia, all with histological evidence of autoimmune gastritis. These findings are in line with the hypothesis that IFN can unmask patients with latent autoimmune gastritis and sometimes may even induce permanent alterations consistent with autoimmune gastritis. Our findings also support the concept that these abnormalities are more frequent in females.

Patients with autoimmune gastritis have a 3-fold increased risk of gastric carcinoma and a 13-fold higher risk of gastric carcinoid tumours^[20]. However, it is not known whether hypergastrinemia or mucosal damage plays a dominant etiologic role^[21]. Evidence exists that endogenous hypergastrinemia is associated with stimulation of rectal^[21] and liver cell proliferation^[22,23], as also occurs in conditions that are known to raise the risk of colon cancer and HCC. HCV patients are at increased risk of developing HCC anyway^[1] but IFN treatment seems to prevent or delay its onset^[24]. Hence, the implications of the occurrence of hypergastrinemia followed by autoimmune gastritis during IFN treatment of HCV infection require careful consideration.

Although 13/22 of our patients developed histological signs of autoimmune gastritis during the 12-month period of therapy, in the majority of cases, these signs regressed in the following year. Persistent histological and biochemical hallmarks of autoimmune gastritis were only eventually found in 4 % (7 of 189) of our patients. The relatively short duration of immunostimulation by IFN may explain why the autoimmune gastritis regressed in most cases. Therefore, our findings may only be applicable to the effects of short-term treatment.

The presence of antithyroid antibodies does not absolutely contraindicate the use of IFN^[25], even though it has to be remembered that IFN leads to permanent thyroid alterations in more than one-fifth patients^[26,27]. Likewise, although the presence of autoimmune gastritis does not contraindicate IFN treatment, it has to be considered that some patients may develop permanent gastric alterations.

In the present study, we also investigated the possibility that *H. pylori* infection might play a pathogenetic role in the onset of autoimmune gastritis in IFN-treated chronic HCV patients^[15,16]. Our data provided no support for this hypothesis. Indeed, in our series of patients, there was no observable difference in the frequencies of autoimmune gastritis between chronic HCV patients with and without *H. pylori* infection, either before, during or after IFN treatment.

Furthermore, we were unable to find any association between the presence of non-organ specific antibodies and that of antithyroid antibodies or APCA. This finding is of clinical interest because positivity for antithyroid antibodies or APCA reveals autoimmune thyroid or gastric disease, whereas the presence of anti-NOS antibodies may only refer to an autoimmune epiphenomenon. This underlines the importance of testing antithyroid antibodies and APCA as well as the anti-NOS ones.

In conclusion, IFN treatment for chronic hepatitis C does appear to be associated with frequent occurrence of autoimmune gastritis, particularly in female patients. In the majority of cases, autoimmune gastritis in the wake of our protocol appeared to be a transient phenomenon. However, this may depend on the limited (12 month) duration of treatment, and this point requires further investigation, especially in regard to the effects of long-term treatment. Autoimmune gastritis is an asymptomatic disease, but in the long run increases the risk for developing a variety of tumors especially in the stomach. Our experience underlines the importance of measuring APCA and/or gastrin levels in chronic HCV patients treated with IFN, and especially those who develop thyroid dysfunction. Development of autoimmune thyroiditis during IFN treatment might provide a surrogate indicator of possible autoimmune gastritis, limiting the need for invasive gastric procedures.

ACKNOWLEDGMENT

We thank Robin MT Cooke's help for working up the manuscript.

REFERENCES

- Fattovich G**, Giustina G, Degos F, Tremolada F, Diodati G, Almasio P, Nevens F, Solinas A, Mura D, Brouwer JT, Thomas H, Njapoum C, Casarin C, Bonetti P, Fuschi P, Basho J, Tocco A, Bhalla A, Galassini R, Noventa F, Schalm SW, Realdi G. Morbidity and mortality in compensated cirrhosis type C: a retrospective follow-up study of 284 patients. *Gastroenterology* 1997; **112**: 463-472
- Meyer zum Buschenfelde KH**, Loshse AW, Gerken G, Treichel U, Lohr HF, Mohr H, Grosse A, Dienes HP. The role of autoimmunity in hepatitis C infection. *J Hepatol* 1995; **22**(Suppl 1): 93-96
- Hadziyannis SJ**. Non hepatic manifestations and combined diseases in HCV infection. *Dig Dis Sci* 1996; **41**: 63S-74S
- Eddleston AL**. Hepatitis C infection and autoimmunity. *J Hepatol* 1996; **24**(Suppl 2): 55-60
- Pawlotsky JM**, Roudot-Thoraval F, Simmonds P, Mellor J, Ben Yahia MB, Andre C, Voisin MC, Intrator L, Zafrani ES, Duval J, Dhumeaux D. Extrahepatic immunologic manifestations in chronic hepatitis C and Hepatitis C serotypes. *Ann Int Med* 1995; **122**: 169-173
- Czaja AJ**, Carpenter HA, Santrach PJ, Moore SB. DR human leukocyte antigens and disease severity in chronic hepatitis C. *J Hepatol* 1996; **24**: 666-673
- Nagayama Y**, Ohta K, Tsuruta M, Takeshita A, Kimura H, Hamasaki K, Ashizawa K, Nakata K, Yokoyama N, Nagataki S. Exacerbation of thyroid autoimmunity by interferon alpha treatment in patients with chronic viral hepatitis: our studies and review of the literature. *Endocr J* 1994; **41**: 565-572
- Chakrabarti D**, Hultgren B, Steward TA. IFN-alpha induces autoimmune T cells through the induction of intracellular adhesion molecule-1 and B7.2. *J Immunol* 1996; **157**: 522-528
- Marcellin P**, Pouteau M, Messian O, Bok B, Erlinger S, Benhamou. Hepatitis C virus, interferon alpha, and dysthyroidism. *Gastroenterol Clin Biol* 1993; **17**: 887-891
- Lisker-Melman M**, Di Bisceglie AM, Usala SJ, Weintraub B, Murray LM, Hoofnagle JH. Development of thyroid disease during therapy of chronic viral hepatitis with interferon alfa. *Gastroenterology* 1992; **102**: 2155-2160
- Ronblom LE**, Alm GV, Oberg KE. Autoimmunity after alpha-interferon therapy for malignant carcinoid tumors. *Ann Int Med* 1991; **115**: 178-183
- Mazzella G**, Salzetta A, Casanova S, Morelli MC, Villanova N, Miniero R, Sottili S, Novelli V, Cipolla A, Festi D, Roda E. Treatment of chronic sporadic-type non-A, non-B hepatitis with lymphoblastoid interferon: gamma GT levels predictive for response. *Dig Dis Sci* 1994; **39**: 866-870
- Centanni M**, Marignani M, Gargano L, Corleto VD, Casini A, Delle Fave G, Andreoli M, Annibale B. Atrophic body gastritis in patients with autoimmune thyroid disease: an underdiagnosed association. *Arch Intern Med* 1999; **159**: 1726-1730
- Samloff IM**, Varis K, Ihama K, Siurala M, Rotter JI. Relationships among serum pepsinogen I, serum pepsinogen II, and gastric mucosal histology. A study in relatives of patients with pernicious anemia. *Gastroenterology* 1982; **83**: 204-209
- Faller G**, Steininger H, Kranzlein J, Maul H, Kerkau T, Hensen J, Hahn EG, Kirchner T. Antigastric autoantibodies in *Helicobacter pylori* infection: implications of histological and clinical parameters of gastritis. *Gut* 1997; **41**: 619-623
- Negrini R**, Savio A, Appelmelk BJ. Autoantibodies to gastric mucosa in *Helicobacter pylori* infection. *Helicobacter* 1997; **2**: S13-S16
- Ierardi E**, Francavilla R, Balzano T, Negrini R, Francavilla A. Autoantibodies reacting with gastric antigens in *Helicobacter pylori* associated body gastritis of dyspeptic children. *Ital J Gastroenterol Hepatol* 1998; **30**: 478-480
- Price AB**. The Sidney system: histological division. *J Gastroenterol Hepatol* 1991; **6**: 209-222
- Dixon MF**, Genta RM, Yardley JH, Correa P. The participants in the international workshop on the histopathology of gastritis, houston 1994. *Am J Surg Pathol* 1996; **20**: 1161-1181
- Toh BH**, van Driel IR, Gleeson PA. Pernicious anemia. *New Engl J Med* 1997; **337**: 1441-1448
- Penston J**, Wormsley KG. Achlorhydria: hypergastrinemia: carcinoids-a flawed hypothesis? *Gut* 1987; **28**: 488
- Renga M**, Brandi G, Paganelli GM, Calabrese C, Papa S, Tosti A, Tomassetti P, Miglioli M, Biasco G. Rectal cell proliferation and colon cancer risk in patients with hypergastrinemia. *Gut* 1997; **41**: 330-332
- Rasmussen TN**, Jorgensen PE, Almdal T, Poulsen SS, Olsen PS. Effect of gastrin on liver regeneration after partial hepatectomy in rats. *Gut* 1990; **31**: 92-95
- Caplin M**, Khan K, Savage K, Rode J, Varro A, Michaeli D, Grimes S, Brett B, Pounder R, Dhillon A. Expression and processing of gastrin in hepatocellular carcinoma, fibrolamellar carcinoma and cholangiocarcinoma. *J Hepatol* 1999; **30**: 519-526
- Mazzella G**, Accogli E, Sottili S, Festi D, Orsini M, Salzetta A, Novelli V, Cipolla A, Fabbri C, Pezzoli A, Roda E. Alpha interferon treatment may prevent hepatocellular carcinoma in HCV-related liver cirrhosis. *J Hepatol* 1996; **24**: 141-147
- Saracco G**, Touscoz A, Durazzo M, Rosina F, Donegani E, Chiandussi L, Gallo V, Petrino R, De Micheli AG, Solinas A. Autoantibodies and response to α -interferon in patients with chronic viral hepatitis. *J Hepatol* 1990; **11**: 339-343
- Ganne-Carrie N**, Medini A, Coderc E, Seror O, Christidis C, Grimbert S, Trinchet JC, Beaugrand M. Latent autoimmune thyroiditis in untreated patients with HCV chronic hepatitis: a case-control study. *J Autoimmun* 2000; **14**: 189-193

Long-term alpha interferon and lamivudine combination therapy in non-responder patients with anti-HBe-positive chronic hepatitis B: Results of an open, controlled trial

M. Francesca Jaboli, Carlo Fabbri, Stefania Liva, Francesco Azzaroli, Giovanni Nigro, Silvia Giovanelli, Francesco Ferrara, Anna Miracolo, Sabrina Marchetto, Marco Montagnani, Antonio Colecchia, Davide Festi, Letizia Bacchi Reggiani, Enrico Roda, Giuseppe Mazzella

M. Francesca Jaboli, Stefania Liva, Francesco Azzaroli, Giovanni Nigro, Silvia Giovanelli, Francesco Ferrara, Anna Miracolo, Sabrina Marchetto, Marco Montagnani, Antonio Colecchia, Enrico Roda, Mazzella Giuseppe, Department of Internal Medicine and Gastroenterology, University of Bologna, Italy

Carlo Fabbri, Department of Gastroenterology and Gastrointestinal Endoscopy, Bellaria Hospital, Bologna, Italy

Davide Festi, Department of Medicine and Aging, University of Chieti, Italy

Letizia Bacchi Reggiani, Department of Cardiology, University of Bologna, Italy

Correspondence to: Professor Giuseppe Mazzella, Department of Internal Medicine and Gastroenterology, University of Bologna, Ospedale S. Orsola- Malpighi, via Massarenti 9, 40138 Bologna, Italy. mazzella@med.unibo.it

Telephone: +39-51-6363276 **Fax:** +39-51-300700

Received: 2003-02-25 **Accepted:** 2003-03-16

Jaboli MF, Fabbri C, Liva S, Azzaroli F, Nigro G, Giovanelli S, Ferrara F, Miracolo A, Marchetto S, Montagnani M, Colecchia A, Festi D, Reggiani LB, Roda E, Mazzella G. Long-term alpha interferon and lamivudine combination therapy in non-responder patients with anti-HBe-positive chronic hepatitis B: Results of an open, controlled trial. *World J Gastroenterol* 2003; 9(7): 1491-1495 <http://www.wjgnet.com/1007-9327/9/1491.asp>

INTRODUCTION

Chronic hepatitis B virus (HBV) infection remains a major worldwide public health problem. Over 300 million people are affected by the disease^[1], which is associated with high mortality and morbidity due to the associated risk of cirrhosis and hepatocellular carcinoma^[2]. In addition, HBV infection is becoming an increasingly relevant problem for transplanted and immunodeficient patients, who are prone to develop more severe, accelerated liver disease^[3].

Until recently, interferon- α (IFN) was the only drug approved throughout the world for chronic HBV infection^[4,5]. Unfortunately, relapse with return of viremia and hepatitis occurs in up to 50 % of cases^[6]. The hepatitis B s antigen (HBsAg) may become negative in months to years after the end of treatment, suggesting total viral clearance^[7]. IFN is less effective in the presence of HBeAg negativity^[8], or in patients who have already developed cirrhosis or have had recurrence of HBV after a hepatic allograft.

Lamivudine (3TC) is the first potentially non-cytotoxic^[9,10] oral nucleoside analogue approved for the treatment of chronic hepatitis B. It suppresses viral DNA replication by means of chain termination, and competitively inhibits viral polymerase, but does not act on supercoiled DNA. For these reasons, lamivudine rapidly reduces serum HBV DNA, enhances transaminase normalization, and improves the histological picture^[11-13]. But only 16 % achieve full HBeAg seroconversion, and after suspension of therapy serum HBV DNA levels and transaminases generally return to pretreatment values^[14]. Furthermore, after clearance of HBV DNA, mutations in the sequence of the YMDD locus of the HBV RNA-dependent DNA polymerase appear in 15 % of cases after one year of therapy, leading to recurrence of viremia^[15]. Onset of resistance generally occurs after six months to several years of lamivudine therapy^[16].

Combination therapy with IFN and lamivudine is being investigated in order to take advantage of the drugs' different mechanisms of action^[17-21]. However, the results of short-term treatment studies have been not altogether encouraging^[18]. The aim of the present study was to investigate whether long-term combination therapy was safe and well tolerated, and whether it could provide additional therapeutic benefits with respect to either of the single drug regimens. In particular, we set out to evaluate efficacy in terms of primary and sustained viremia and transaminase responses. We also assessed histological response, incidence of YMDD-variant HBV, and safety.

Abstract

AIM: To investigate the safety and efficacy of long-term combination therapy with alpha interferon and lamivudine in non-responsive patients with anti-HBe-positive chronic hepatitis B.

METHODS: 34 patients received combination treatment (1 month lamivudine, 12 month lamivudine+interferon, 6 month lamivudine), 24 received lamivudine (12 months), 24 received interferon (12 months). Interferon was administered at 6 MU tiw and lamivudine at 100 mg orally once daily. Patients were followed up for 6 months after treatment.

RESULTS: At the end of treatment, HBV DNA negativity rates were 88 % with lamivudine+interferon, 99 % with lamivudine and 55 % with interferon, ($P=0.004$, combination therapy vs. interferon, and $P=0.001$ lamivudine vs. interferon), and serum transaminase normalization rates were 84 %, 91 % and 53 % ($P=0.01$ combination therapy vs. interferon, and $P=0.012$ lamivudine vs. interferon). Six months later, HBV DNA negativity rates were 44 % with lamivudine+interferon, 33 % with lamivudine and 25 % with interferon, and serum transaminase normalization rates were 61 %, 42 % and 45 %, respectively, without statistical significance. No YMDD variants were observed with lamivudine+interferon (vs. 12 % with lamivudine). The combination therapy appeared to be safe.

CONCLUSION: Although viral clearance and transaminase normalization are slower with long-term lamivudine+interferon than that with lamivudine alone, the combination regimen seems to provide more lasting benefits and to protect against the appearance of YMDD variants. Studies with other regimens regarding sequence and duration are needed.

MATERIALS AND METHODS

Patients

This open trial concerned 82 adult Italian patients with chronic anti-HBe positive hepatitis B (68 males, 14 females) enrolled between February 1997 and February 1999 who had either not responded to or had relapsed after previous interferon treatment. The experimental protocol was carried out in accordance with the Helsinki Declaration, and was approved by the Ethics Review Committee, and all patients gave written informed consent to participate in a trial involving long-term treatment either with interferon plus lamivudine or with lamivudine or interferon alone.

Inclusion criteria for the study were: age between 18 and 70 years, detectable hepatitis B surface antigen (HBsAg) in serum at the time of screening and for at least six months before the start of the study, serum HBV DNA levels of at least 5 pg/ml at screening, raised alanine transaminase values within three months before the start of therapy. Exclusion criteria were: presence of co-infection with hepatitis C and D virus or HIV, signs of hepatic decompensation or hepatocellular carcinoma, other possible causes of chronic liver damage (i.e. alcohol abuse, hemochromatosis, Wilson's disease, α 1-antitrypsin deficiency, autoimmune diseases, drug-induced hepatotoxicity and congestive heart failure), assumption of immunosuppressive or antiviral therapy within six months before the study. Needle biopsy performed in all cases within 2 years of the study, showed that 33 patients had a Scheuer score for fibrosis >3 .

The patients were divided into three groups: group A ($n=34$) for combination treatment, group B ($n=24$) for treatment with lamivudine alone, group C ($n=24$) for treatment with interferon alone.

Treatment protocols and study design

Patients in group A received 100 mg/day of lamivudine (Glaxo-Wellcome Inc, Research Triangle Park, NC, USA) orally for one month, followed by lamivudine (100 mg/day) in association with six million units three times per week of natural interferon (Wellferon, Glaxo-Wellcome Inc, Research Triangle Park, NC, USA) for twelve months, and then lamivudine (100 mg/day) alone for six months. Patients in group B received lamivudine (100 mg/day) orally for twelve months. Patients in group C received six million units three times per week of natural interferon for twelve months. Interferon was administered subcutaneously by the patients after adequate training. Patients were followed up after the end treatment for twenty-four weeks. All patients had a liver biopsy within 2 years of entering the study, and were requested to have another at the end of treatment. Hepatitis flare up was defined as an increase in serum ALT during therapy and classified as mild, moderate or severe (>1.5 , 5, 10 times respectively) according to the preceding ALT value.

The main end point of the study was to evaluate the end-of-treatment and sustained response, defined as HBV DNA loss and serum ALT normalization at the end of therapy and follow-up, respectively. Secondary variables included histological response, incidence of YMDD-variant HBV, and safety.

Laboratory methods

Blood samples were obtained immediately before therapy, after 15 days, and then every month during treatment and follow-up. Routine biochemical tests and blood cell counts were performed. HBsAg, HBeAg, and anti-HBs and anti-HBe antibodies were determined by enzyme immunoassay. Serum HBV DNA was measured quantitatively by a solution-hybridization assay (Abbott, Chicago, USA) with a lower limit of 3.0 pg/ml of serum.

Presence of the YMDD variant was evaluated by a restriction

fragment length polymorphism assay in all ends of treatment samples and in cases where initial loss of HBV DNA was followed by a return to positivity, regardless of transaminase values. The biopsy specimens were scored according to the Scheuer histological activity index^[22].

Statistical analysis

Baseline characteristics of the patients were presented as mean values \pm standard error (SE). Statistical evaluations were conducted according to the intention-to-treat procedure. The Chi-square test or the Fisher's exact test was used to compare differences in proportion between treatment groups. Continuous data were analyzed using Kruskal-Wallis test and Mann-Whitney test. A two-tailed P value of less than 0.05 was considered to be statistically significant.

RESULTS

Study population

All treatment arms were well matched with regard to baseline characteristics (Table 1). Of the 82 patients, 79 completed the treatment schedule, while the remaining 3 dropped out of the study: one group A patient withdrew, one group B patient and one group C patient experienced depression.

Table 1 Baseline characteristics of patients

Characteristics	Lamivudine+ interferon ($n=34$)	Lamivudine alone ($n=24$)	Interferon alone ($n=24$)
Age (year)	44.0 \pm 2.0	48.7 \pm 2.4	44.4 \pm 2.5
Sex (m/f)	30/4	18/6	20/4
ALT (U/l)	151 \pm 21	160 \pm 39	130 \pm 17
AST (U/l)	81 \pm 10	111 \pm 37	66 \pm 10
GT (U/l)	48 \pm 3	57 \pm 6	47 \pm 3
Albumin (gr/dl)	3.94 \pm 0.04	3.97 \pm 0.04	4.01 \pm 0.03
HBV DNA (pg/ml)	60 \pm 25	85 \pm 43	73 \pm 36
Histology:			
Cirrhosis	13 (38%)	10 (42%)	10 (42%)
Severe activity	10 (29%)	7 (29%)	9 (37%)

P value was not significant for all comparisons.

Virological response (Figure 1)

End-of-treatment response HBV DNA negativity was observed at the end of treatment in 30 (88 %) patients who received combination therapy (i.e. group A), 23 (99 %) who had lamivudine alone (i.e. group B), and 13 (55 %) who had interferon alone (i.e. group C). HBV DNA negativity was achieved in week 12, 4 and 32, respectively, in the three groups. Two differences in primary response among the three groups were highly significant [combination vs. interferon: OR 6.34 (95 % CI: 1.7-23 %), $P=0.004$; lamivudine vs. interferon: OR 19.46 (95 % CI: 3.3-113 %), $P=0.001$].

Sustained response A total of 15 (44 %) patients in group A, 8 (33 %) in group B and 6 (25 %) in group C were HBV DNA negative at the end of the follow-up. None of the differences in sustained virological response among the three groups reached statistical significance.

Biochemical response (Figure 2)

End-of-treatment response Serum transaminases became normal at the end of treatment in 29 (84 %) patients in group A, 21 (91 %) in group B and 13 (53 %) in group C [combination vs. interferon: OR 4.9 (95 % CI: 1.4-17 %), $P=0.01$; lamivudine vs. interferon: OR 5.92 (95 % CI: 1.28-25.3 %), $P=0.012$]. Normalization was achieved in week 20, 8 and 38, respectively,

in the three groups. A mild flare-up without bilirubin alteration was observed only in 8 group A patients. In all cases, serum transaminase normalization was preceded by a rise of HBV DNA at 2-8 months of therapy. The flare-up was always followed 1-2 months later by serum HBV DNA negativization and transaminase normalization. None of these patients had a YMDD variant.

Sustained response Sustained serum transaminase normalization was observed in 21 (61 %) patients in group A, 10 (42 %) in group B and 11 (45 %) in group C. None of the differences in sustained transaminase response among the three groups had statistical significance. Only 4 of the 8 patients who experienced a flare-up during combined therapy maintained their primary response.

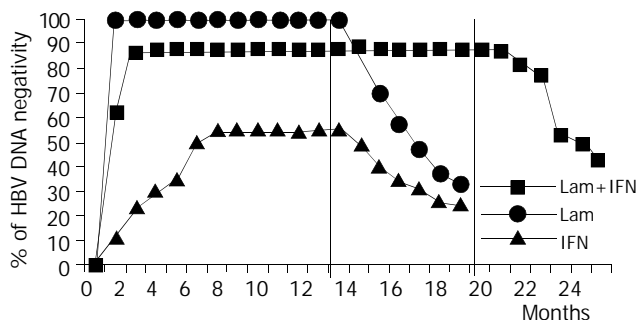


Figure 1 Virological response. Percentages of patients with HBV DNA negativity related either to the treatment or to the follow-up times. The vertical lines were drawn at the end of each treatment (19 months for interferon and lamivudine in combination, and 12 months for lamivudine and interferon monotherapy).

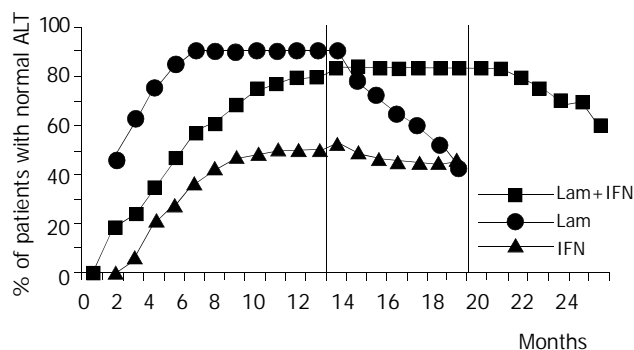


Figure 2 Biochemical response. Percentages of patients with normal ALT levels related either to the treatment or to the follow-up times. The vertical lines were drawn at the end of each treatment (19 months for interferon and lamivudine in combination, and 12 months for lamivudine and interferon monotherapy).

Secondary criteria of efficacy

Histological findings Paired pre- and post-treatment liver biopsies were available for 22 (65 %), 15 (62 %) and 14 (58 %) patients in groups A, B and C, respectively. None of the post-treatment biopsies showed a worsening or unchanged histological picture. Significant improvements in necro-inflammatory activity in parenchyma ($P < 0.01$) and portal space ($P < 0.01$) were observed in each group. Significant improvements in fibrosis were found in groups A and B ($P < 0.05$), but not in group C.

Incidence of YMDD variant HBV YMDD variants of HBV were not detected in any of the patients who received combination or IFN therapy. 3 of the 24 (12 %) patients treated with lamivudine alone had a YMDD variant after 6-9 months of therapy. In particular, two had a YVDD variant and the other

had a YIDD variant. They continued lamivudine therapy and were monitored weekly. After a progressive rise of serum HBV DNA, two of the patients showed 5 times of elevation of transaminases (with respect to the upper limit) and another showed 1.5 times of elevation. However, after the emergence of the variant, the HBV DNA and transaminase levels always remained lower than the baseline.

Safety

The whole treatment program was completed by 33 (98 %), 23 (96 %) and 23 (94 %) patients in groups A, B and C, respectively. No patient received reduced dosage but we directly stopped treatment. The side effects of the combination regimen were generally similar to those of interferon treatment. In addition, among the 34 patients in group A, symptomatic and reversible rises in serum levels of amylase, lipase and creatinine phosphokinase were recorded in 9 (28 %), 2 (5 %) and 1 (3 %) cases, respectively. Worsening of pre-existing hypertriglyceridemia was recorded in 2 (7 %) cases. By comparison, among the 24 patients in group B, lamivudine therapy was associated with an asymptomatic and reversible rise in amylase, lipase or creatinine phosphokinase in 6 (25 %), 1 (4 %) and 1 (4 %), respectively. No case of hepatocellular carcinoma, liver decompensation or death was recorded, and no patient requested orthotopic liver transplantation (Table 2).

Table 2 Adverse events documented during treatment

Adverse events	Lamivudine+interferon (n=34), n (%)	Lamivudine alone (n=24), n (%)	Interferon alone (n=24), n (%)
Influenza-like symptoms	24 (70%)	none	19 (79%)
Hair loss	8 (23%)	none	9 (38%)
Weight loss	5 (16%)	none	4 (15%)
Depression	none	1 (4%)	1 (6%)
Low white-cell count	19 (56%)	none	14 (59%)
Low platelet count	14 (42%)	none	10 (44%)
Amylase rise	9 (28%)	6 (25%)	none
Lipase rise	2 (5%)	1 (4%)	none
CPK rise	1 (3%)	1 (4%)	none
Hypertriglyceridemia	2 (7%)	none	none

DISCUSSION

The development of effective treatment strategies for patients with HBV remains a major clinical challenge. We investigated the possible benefits of a long-term interferon/lamivudine combination treatment regimen in a cohort of patients who had already received unsuccessful treatment with interferon alone. The effects of this long-term combination regimen were compared with single-agent treatment with either interferon or lamivudine in three similar groups of patients. In regard to virological response, we found that at the end of therapy, HBV DNA had become undetectable in 88 % of the patients receiving combination treatment, as compared with 99 % and 55 % of those who had single-line therapy with lamivudine or interferon, respectively. These differences in end-of-treatment response were statistically significant in comparison of the combination therapy and lamivudine monotherapy with interferon monotherapy. The analysis of sustained response showed that 44 % patients in the combination therapy group maintained DNA clearance as compared with only 33 % in the lamivudine group and 25 % in the interferon group. Although these differences did not have statistical significance, there was a trend in favor of the combination regimen. Similarly, although the end-of-treatment transaminase normalization rate was significantly higher in the combination

treatment (84 %) group and in the lamivudine group of patients (91 %) than that in interferon (53 %) group, the sustained response showed a non-significant trend in favor of the combination regimen (61 % in the combination group vs. 42 % and 45 % with lamivudine or interferon alone, respectively).

As has been reported for short-term treatment^[23], during our long-term combination therapy regimen there was a progressive viral decline, whereas with single-line lamivudine therapy the HBV DNA levels leveled off. Our data are in keeping with the concept that lamivudine therapy is more rapid and effective on virological and biochemical response than interferon alone or even in combination with lamivudine. However, after discontinuation of therapy, virological and biochemical relapses were considerably more common with lamivudine alone than those with the combination regimen (even though this difference did not actually reach statistical significance). Moreover, there was a trend suggesting that combination therapy delays relapse. The non-significant status of these trends could be due to the relatively small cohort sizes.

Among the two monotherapy options, interferon appeared less effective than lamivudine. In our study, interferon provided less end-of-treatment responses than lamivudine, and no advantages in terms of sustained response. The relatively poor capacity of interferon monotherapy to promote viral clearance may be explained by an inability to induce an efficient immune response.

After about 5 months of combination therapy, we observed a mild flare-up in 8 patients following a rise in serum HBV DNA. The flare-up was always followed, after a further one to two months of therapy by a return to serum HBV DNA negativity and normalization of transaminases. They may have been caused by enhanced immune responses prompted by increased mutant viral replication other than YMDD, which however were unable to permanently eradicate the virus.

As regards the secondary criteria of response, all the patients who underwent a post-treatment biopsy derived histological benefit in terms of necro-inflammatory activity in parenchyma and in portal space, regardless of their serological response. However, in keeping with other reports^[24], interferon monotherapy provided no improvement in fibrosis.

YMDD HBV variants were not detected in any of the patients who received combination therapy or interferon alone. After 6-9 months of lamivudine monotherapy, 3 (12 %) patients had YMDD, a rate similar to that reported in Asian patients. Interferon therapy seemed to exert a protective effect against the emergence of variants, probably because it lowers viral replication and enhances immunological response. In any case, in the three affected patients, the serum HBV DNA levels did not return completely to pretreatment levels. Thus, the mutant strains of HBV DNA that break through during prolonged therapy with lamivudine may not be as replicative-efficient or as pathogenic as wild-type strains. As in other reports^[25], we found that 3 to 4 months after lamivudine treatment was stopped, there was disappearance of this HBV mutant and re-emergence of the wild type virus. Honkoop *et al.*^[26] observed acute exacerbation of chronic HBV infection after withdrawal of lamivudine therapy and concluded that the relationship between the development of "lamivudine-withdrawal hepatitis" and the lamivudine-resistant mutant virus was currently unclear, since both the emergence of a lamivudine resistant viral mutant and the resurgence of wild-type virus after withdrawal of therapy were able to induce severe hepatitis exacerbations. Studies of rechallenge with lamivudine have yet to be reported, and the significance of YMDD variant is being evaluated in the ongoing follow-up clinical trials.

As regards safety, the combination therapy was well tolerated and no serious side effects were observed. The side

effects observed during the course of the long-term combination regimen were those that were commonly associated with the two drugs. As expected, in the two monotherapy groups, the incidence of drug-related adverse events was much lower with lamivudine than that with interferon.

In conclusion, these results suggest that for patients who have already been unsuccessfully treated with interferon, long-term combination therapy may have some advantages over single-line treatment with lamivudine or interferon^[27]. Other studies with other regimens regarding dose, sequence and duration of interferon and lamivudine are needed. Finally, correct staging of patients according to the particular phases in the natural history of chronic hepatitis B appears to be important to personalise patients' management. It is possible that combinations of two^[28,29] or more nucleoside analogs may reduce the development of viral resistance, increase overall response rates, decrease adverse events. In general, multi-drug therapies^[30] that take advantage of different modes of action concurrently may provide a more appropriate approach for particular subgroups of patients.

ACKNOWLEDGMENT

We are grateful to Robin MT Cooke for editing.

REFERENCES

- 1 **Maynard JE.** Hepatitis B: global importance and need for control. *Vaccine* 1990; **8**: (Suppl): S18-S20
- 2 **De Jongh FE,** Jansen HL, de Man RA, Hop WC, Schalm SW, van Blankenstein M. Survival and prognostic indicators of hepatitis B surface antigen-positive cirrhosis of the liver. *Gastroenterology* 1992; **103**: 1630-1635
- 3 **Davies SE,** Portmann BC, O'Grady JG, Aldis PM, Chaggar K, Alexander GJ, Williams R. Hepatic histological findings after transplantation for chronic hepatitis B virus infection, including a unique pattern of fibrosing cholestatic hepatitis. *Hepatology* 1991; **13**: 150-157
- 4 **Dusheiko GM.** Treatment and prevention of chronic viral hepatitis. *Pharmacol Ther* 1995; **65**: 47-73
- 5 **Korenman J,** Baker B, Waggoner J, Everhart JE, Di Bisceglie AM, Hoofnagle JH. Long term remission of chronic hepatitis B after interferon therapy. *Ann Intern Med* 1991; **114**: 629-634
- 6 **Hoofnagle JH,** Lau D. Chronic viral hepatitis-benefits of current therapies. *N Eng J Med* 1996; **334**: 1470-1471
- 7 **Mazzella G,** Saracco G, Festi D, Rosina F, Marchetto S, Jaboli F, Sostegni R, Pezzoli A, Azzaroli F, Cancellieri C, Montagnani M, Roda E, Rizzetto M. Long term results with interferon therapy in chronic type B hepatitis: a prospective randomized trial. *Am J Gastroenterol* 1999; **94**: 2246-2250
- 8 **Hadziyannis SJ.** Hepatitis B e antigen negative chronic hepatitis B: from clinical recognition to pathogenesis and treatment. *Viral Hepatitis Rev* 1995; **1**: 7-15
- 9 **Cui L,** Yoon S, Schinazi RF, Sommadossi JP. Cellular and molecular events leading to mitochondrial toxicity of 1-(2-deoxy-2-fluoro-1-beta-D-arabinofuranosyl)-5-iodouracil in human liver cells. *J Clin Invest* 1995; **95**: 555-563
- 10 **Nicoll A,** Locarini S. Review: present and future directions in the treatment of chronic hepatitis B infection. *J Gastroenterol Hepatol* 1997; **12**: 843-854
- 11 **Dienstag JL,** Perrillo RP, Schiff ER, Bartholomew M, Vicary C, Rubin M. A preliminary trial of lamivudine for chronic hepatitis B infection. *N Eng J Med* 1995; **333**: 1657-1661
- 12 **Lai CL,** Chien RN, Leung NWY, eta Chang TT, Guan R, Tai DI, Ng KY, Wu PC, Dent JC, Barber J, Stephenson SL, Gray DF. A one year trial of lamivudine for chronic hepatitis B. *N Eng J Med* 1998; **339**: 61-68
- 13 **Kweon YO,** Goodman ZD, Dienstag JL. Lamivudine decreases fibrogenesis in chronic hepatitis B: an immunohistochemical study of paired liver biopsies. *Hepatology* 2000; **32**: 870P
- 14 **Honkoop P,** de Man RA, Heitjink RA, Schalm SW. Hepatitis B reactivation after lamivudine. *Lancet* 1995; **346**: 1156-1157

- 15 **Dienstag JL**, Schiff ER, Mitchell M, Casey DE Jr, Gitlin N, Lissos T, Gelb LD, Condeay L, Crowther L, Rubin M, Brown N. Extended lamivudine re-treatment for chronic hepatitis B: maintenance of viral suppression after discontinuation of therapy. *Hepatology* 1999; **30**: 1082-1087
- 16 **Hoofnagle J**. Therapy of viral hepatitis. *Digestion* 1998; **59**: 563-578
- 17 **Schiff E**, Karayalcin S, Grimm I, Grimm IS, Perrillo RP, Husa P, de Man RA, Goodman Z, Condeay LD, Crowther LM, Woessner MA, McPhillips PJ, Brown NA. Lamivudine and 24 weeks of lamivudine/interferon combination therapy for hepatitis B e antigen-positive chronic hepatitis B in interferon nonresponders. *J Hepatol* 2003; **38**: 818-826
- 18 **Mutimer D**, Naoumov N, Honkoop P, Marinos G, Ahmed M, de Man R, McPhillips P, Johnson M, Williams R, Elias E, Schalm S. Combination alpha-interferon and lamivudine therapy for alpha-interferon-resistant chronic hepatitis B infection: results of a pilot study. *J Hepatol* 1998; **28**: 923-929
- 19 **Heathcote J**, Schalm SW, Cianciara J, G Farrell, V Feinmann, M Shermann, AP Dhillon, AE Moorat and DF Gray. Lamivudine and Intron A combination treatment in patients with chronic hepatitis B infection. *EASL* April, 1998, Lisbon
- 20 **Schalm SW**, Heathcote J, Cianciara J, Farrell G, Sherman M, Willems B, Dhillon A, Moorat A, Barber J, Gray DF. Lamivudine and alpha interferon combination treatment of patients with chronic hepatitis B infection: a randomised trial. *Gut* 2000; **46**: 562-568
- 21 **Farrell G**. Hepatitis B e antigen seroconversion: effects of lamivudine alone or in combination with interferon alpha. *J Med Virol* 2000; **61**: 374-379
- 22 **Scheuer P**. Classification of chronic viral hepatitis: a need for reassessment. *J Hepatology* 1991; **13**: 372-374
- 23 **van Nunen AB**, Hansen BE, Mutimer DJ. Viral kinetics during 16 weeks of interferon and lamivudine monotherapy versus interferon-lamivudine combination therapy in chronic hepatitis B patients. *Hepatology* 2000; **32**: 878
- 24 **Brook MG**, Petrovic L, McDonald JA, Scheuer PJ, Thomas HC. Histological improvement after anti-viral treatment for chronic hepatitis B virus infection. *J Hepatol* 1989; **8**: 218-225
- 25 **Chayama K**, Suzuki Y, Kobayashi M, Kobayashi M, Tsubota A, Hashimoto M, Miyano Y, Koike H, Kobayashi M, Koida I, Arase Y, Saitoh S, Murashima N, Ikeda K, Kumada H. Emergence and takeover of YMDD motif mutant hepatitis B virus during long-term lamivudine therapy and re-takeover by wild type after cessation of therapy. *Hepatology* 1998; **27**: 1711-1716
- 26 **Honkoop P**, de Man RA, Niesters HGM, Zondervan PE, Schalm SW. Acute exacerbation of chronic hepatitis B virus infection after withdrawal of lamivudine therapy. *Hepatology* 2000; **32**: 635-639
- 27 **Janssen HLA**, Schalm SW, Berk L, de Man RA, Heijntink RA. Repeated courses of alpha-interferon for treatment of chronic hepatitis B. *J Hepatol* 1993; **17**(Suppl 3): S47-51
- 28 **Perrillo R**, Schiff E, Yoshida E, Statler A, Hirsch K, Wright T, Gutfreund K, Lamy P, Murray A. Adefovir dipivoxil for the treatment of lamivudine-resistant hepatitis B mutants. *Hepatology* 2000; **32**: 129-134
- 29 **Lau GK**, Tsiang M, Hou J, Yuen S, Carman WF, Zhang L, Gibbs CS, Lam S. Combination therapy with lamivudine and famciclovir for chronic hepatitis B-infected Chinese patients: a viral dynamics study. *Hepatology* 2000; **32**: 394-399
- 30 **Marques AR**, Lau DT, McKenzie R, Straus SE, Hoofnagle JH. Combination therapy with famciclovir and alpha-interferon for the treatment of chronic hepatitis B. *The J Infect Dis* 1998; **178**: 1483-1487

Edited by Xu XQ

Acute hepatitis C in a chronically HIV-infected patient: Evolution of different viral genomic regions

Diego Flichman, Veronica Kott, Silvia Sookoian, Rodolfo Campos

Diego Flichman, Veronica Kott, Rodolfo Campos, Catedra de Virologia, Facultad de Farmacia y Bioquímica, Universidad de Buenos Aires, Argentina

Silvia Sookoian, Unidad de Hígado, Hospital "Dr. Cosme Argerich", Argentina

Supported by the grants from the Universidad de Buenos Aires (SECyT-UBA, TB14), Consejo Nacional de Investigaciones Científicas y Técnicas (CONICET, PIP723), Agencia Nacional de Promoción Científica y Tecnológica (ANPCyT, PICT 01610) and Ministerio de Salud Pública de la Nación (Beca Carrillo-Oñativia)

Correspondence to: Dr. Rodolfo Campos, Facultad de Farmacia y Bioquímica, Junin 956, 4th floor, (1113), Capital Federal, Argentina. rcampos@ffyb.uba.ar

Telephone: +5411-49648264 **Fax:** +5411-45083645

Received: 2003-02-26 **Accepted:** 2003-03-16

Abstract

AIM: To analyze the molecular evolution of different viral genomic regions of HCV in an acute HCV infected patient chronically infected with HIV through a 42-month follow-up.

METHODS: Serum samples of a chronically HIV infected patient that seroconverted to anti HCV antibodies were sequenced, from the event of superinfection through a period of 17 months and in a late sample (42nd month). Hypervariable genomic regions of HIV (V3 loop of the gp120) and HCV (HVR-1 on the E2 glycoprotein gene) were studied. In order to analyze genomic regions involved in different biological functions and with the cellular immune response, HCV core and NS5A were also chosen to be sequenced. Amplification of the different regions was done by RT-PCR and directly sequenced. Confirmation of sequences was done on reamplified material. Nucleotide sequences of the different time points were aligned with CLUSTAL W 1.5, and the corresponding amino acid ones were deduced.

RESULTS: Hypervariable genomic regions of both viruses (HVR1 and gp120 V3 loop) presented several nonsynonymous changes but, while in the gp120 V3 loop mutations were detected in the sample obtained right after HCV superinfection and maintained throughout, they occurred following a sequential and cumulative pattern in the HVR1. In the NS5A region of HCV, two amino acid changes were detected during the follow-up period, whereas the core region presented several amino acid replacements, once the HCV chronic infection had been established.

CONCLUSION: During the HIV-HCV superinfection, each genomic region analyzed shows a different evolutionary pattern. Most of the nucleotide substitutions observed are non-synonymous and clustered in previously described epitopes, thus suggesting an immune-driven evolutionary process.

Flichman D, Kott V, Sookoian S, Campos R. Acute hepatitis C in a chronically HIV-infected patient: Evolution of different viral genomic regions. *World J Gastroenterol* 2003; 9(7): 1496-1500 <http://www.wjgnet.com/1007-9327/9/1496.asp>

INTRODUCTION

It has been proven that patients with HIV infection are frequently coinfecting with other viruses, including that of HCV. Both HIV and HCV share the same route of transmission, and thus, coinfection with these two viruses is rather common among intravenous drug users or transfused patients^[1,2]. HCV infection is considered as an HIV opportunistic disease^[3].

The clinical impact of HIV-HCV coinfection has been widely studied^[4]. However, the viral molecular interaction during the establishment of HCV superinfection is not yet well understood as the acute phase is frequently a subclinical event.

HCV, an RNA virus, shows a marked variability but nucleotide substitutions are unevenly distributed along the entire genome^[5]. HCV diversity is the greatest in the envelope proteins E1 and E2, especially in a 27 amino-acid segment at the N-terminus of E2 designated hypervariable region 1 (HVR1). The variation of this region is thought to be related to the maintenance of persistent infection by emerging escape variants^[6] and it is considered as the main target for humoral immunity as well as an immunologic decoy^[7].

A similar degree of heterogeneity is found within the gp120 V3 loop region of HIV, an RNA virus that also causes persistent infections in the host. This region has been found to elicit neutralizing antibodies as well as cytotoxic and Th-cell responses, properties that are also ascribed to the HVR1^[8].

NS5A is an HCV nonstructural protein that is associated with several functions such as being an *in vitro* transcriptional repressor^[9] and tightly associated via the "interferon sensitivity determining region" (ISDR), with the subversion of the IFN activity. ISDR inhibits the cellular double-stranded RNA-activated protein kinase R^[10], an effector of the IFN antiviral activity. There is also evidence that the C-terminal domain of NS5A including the ISDR contains transcriptional activity^[11], suggesting that NS5A might function as a viral transactivator. The core gene is located in the 5' end of the HCV genome and its primary function is to form the viral nucleocapsid. The core protein has many effects on host-cell signalling pathways that includes the host-cell gene expression^[12], apoptosis by interaction with the cytoplasmic tail of the lymphotoxin receptor and with TNF receptor^[13,14], transforming activity^[15], modulation of lipid metabolism^[16,17]. Several studies have shown that the region contains multiple and highly immunogenic humoral^[18,19] and cellular^[19,20] epitopes.

In a previous report we described the *in vivo* down regulation of HIV replication in an HIV-infected patient after HCV superinfection^[21]. Herein we presented a further study of this patient through the analysis of hypervariable regions of both viruses, and the less variable core and NS5A regions of HCV.

MATERIALS AND METHODS

Patient

A 16 year-old HIV patient was referred to the Liver Unit because of an acute hepatitis-like illness with the manifestations of jaundice, nausea, abdominal pain, fever, diarrhea, itching and elevated ALT and AST levels. She was in the 30th week of gestation and her prenatal course had been uneventful until this episode. Diagnosis of acute hepatitis C was established by

seroconversion of HCV antibodies by an EIA test (HCV EIA 2.0; Ortho Diagnostics) and confirmed with a strip immunoblot assay (RIBA HCV 2.0; Chiron Corporation). HIV and HCV were thought to be acquired by intravenous drug use. Serum HCV and HIV RNAs were detected by RT-PCR using primers for the 5NC and the gag regions, respectively^[21] (Table 1).

Thereafter, the patient was followed up for 42 months and serum samples were taken monthly during the first 17 months of the analyzed period and in the 42nd month as a late specimen. Serum samples before HCV superinfection were also available. Liver function tests (AST, ALT, γ -glutamyl-transferase, alkaline phosphatase, albumin, gamma globulin, bilirubin and prothrombin time) were routinely performed using automatic standard procedures.

A liver biopsy was obtained at the 15th month of follow-up showing a histological picture of chronic hepatitis (Knodell score 5) without fibrosis.

No antiviral therapy was implemented during the study period because of the patient's refusal. This study followed the ethical standards of the World Medical Association Helsinki Declaration adopted in 1964 and amended in 1996 and was approved by the local Ethics Committee. At all times, written consents were obtained from the woman.

Methods

RNA extraction RNA was recovered from 150 μ l aliquots as described by Chomczynski and Sacchi^[22] using components from a commercially available RNA extraction kit (Trizol® Life Technologies) and resuspended in 20 μ l dH₂O.

cDNA synthesis and PCRs RNA was used as templates in randomly primed reverse transcription reactions to produce cDNA in the following conditions: 50 mM TrisHCl (pH 8.3), 25 mM KCl, 3 mM MgCl₂, 0.1 mM DTT, 1.0 mM dNTPs, 18

U RNasin ribonuclease inhibitor (Promega) and 100 U Moloney murine leukemia virus RT (Life Technologies). The reactions were performed for 90 min at 37 °C. After heat inactivation at 95 °C for 5 min and chilling on ice, the cDNA was amplified.

Different genomic viral regions -gp120 V3 loop region of HIV and the HVR1, core and NS5A regions of HCV- were amplified and directly sequenced. The PCR reaction (50 μ l) contained 20 mM TrisHCl, 50 mM KCl, 50 pmol of each primer and 1.25 U *Taq* DNA polymerase (Promega). Nested PCR was performed with 2 μ l PCR product as a template, using internal primers under the same conditions as the first round. The first and second round primers and cycling parameters for each region are shown in Table 1 and were made according to Kwok and Higuchi's recommendations^[23].

Nucleotide sequencing Each DNA was purified and directly sequenced with a Thermo Sequenase radiolabeled-terminator-cycle sequencing kit (U.S. Biochemical Corporation) using the same cycling parameters of the second PCR round. Confirmatory sequencing was performed on reamplified DNA.

RESULTS

The genomic regions of HCV: HVR1, core and NS5A and the gp120 V3 loop of HIV were sequenced during a 42 month follow-up of a chronically HIV patient acutely infected with HCV. Phylogenetic analysis of core and NS5A grouped the HCV sequences into genotype 1a (data not shown).

After alignment and comparison of genomic sequences obtained before and after HCV superinfection, the nucleotide sequence of HIV gp120 V3 loop showed three nonsynonymous mutations (I309L, T317A and E320D) that appeared in the sample obtained 2 months after HCV superinfection and

Table 1 Oligonucleotide primers used to amplify various HIV and HCV regions

Viral region	Nucleotide position	Primer sequence (5' → 3')	PCR cycling parameters
HIV			
gag			5 min at 94 °C, 40 cycles of 30 s at 94 °C, 30 s at 55 °C and 45 s at 72 °C and a final extension of 7 min at 72 °C
OS	4653 - 4675	CCCTACAATCCCCAAAGTCAAGG	
OA	4956 - 4976	TACTGCCCTTCACCTTTCCA	
V3 loop			
OS	6957 - 6976	GTACAATGTACACATGGAAT	
OA	7357 - 7376	GTAGAAAAATTCCCCTCCAC	Idem HIV-gag PCR
IS	7010 - 7029	TGGCAGTCTAGCAGAAGAAG	
IA	7319 - 7339	ACAATTTCTGGGTCCCCTCCT	
HCV			
5UT			
OS	44 - 69	CCTGTGAGGAACTACTGTCTTCACGC	Idem HIV-gag PCR
OA	321 - 341	GGTGCACGGTCTACGAGACCT	
HVR1			
OS	1273 - 1296	GCCATATAACGGGTCACCGCATGG	
OA	1681 - 1704	TCTCAGGACAGCCTGAAGMGTGA	Idem HIV-gag PCR
IS	1296 - 1379	GCATGGGATATGATGATGAAGTGG	
IA	1623 - 1646	GGTGTGAGGCTATCATTGCARTT	
core			
OS	272 - 291	CGAAAGGCCTTGTGGTACTG	5 min at 94 °C, 30 cycles of 1 min at 94 °C, 1 min at 50 °C and 2 min at 72 °C and a final extension of 10 min at 72 °C
OA	1020 - 1037	CTCGGRACGCAAGGGAC	
IS	281 - 302	TTGTGGTACTGCCTGATAGGGT	
IA	956 - 976	ATACTCGAGTTAGGGCAATCA	
NS5A			
OS	6716 - 6739	TAGATGGGGTGCCTGCAYAGGTT	
OA	7310 - 7332	GCTTCTCCGRGGCGGAGGCACWG	Idem HCV core PCR
IS	6734 - 6753	TAGGTTTGCCTCCCTGMA	
IA	7287 - 7306	GGGGACYKTGGAGGTGGAAG	

Notes: OS: outer sense primer; OA: outer antisense; IS: inner sense; IA: inner antisense. Nucleotide positions were according to HIVHXB2 (K03455) for the HIV region and to HCV-1 (M62321) for HCV regions. Degenerate bases were indicated with standard codes of the International Union of Pure and Applied Chemistry.

maintained thereafter for the rest of the period (Figure 1).

As far as HCV sequences were concerned, in the HVR1 three nonsynonymous mutations were observed (F399L, G393S and A397S) in the acute phase of the infection, conversely, the mutation dynamics followed a sequential and cumulative pattern, occurring at the 6th, 8th and 12th follow-up months. Each mutation was associated with an ALT flare-up (Figure 1). In the last sample, 42 months after HCV superinfection, two more amino acid changes were selected (G398A and L399F).

Different patterns of substitutions were observed in the HCV core and NS5A regions. In the core, three nonsynonymous substitutions (Q63P, H69R and R74G) appeared at the 17th month of the follow-up (Figure 2), once chronic hepatitis was fully established. Late on the follow-up, four mutations were selected: P63Q, A68V, G74R and G152A. The amino acids that were resulted from the modifications in positions 63 and 74 were the same as that which was present in the earliest samples.

In the portion of NS5A sequenced (nt 6632-7077), one amino acid substitution was observed in the acute phase (E2227Q) and remained thereafter, and another one was selected at the end of the follow-up (V2251I).

The sequences were submitted to GenBank and assigned accession numbers: AF361170 through AF361176 and AF359345 through AF359354.

DISCUSSION

In this study, we analyzed the evolution of different viral genomic regions during HCV superinfection of a chronically HIV infected patient.

Most of the nucleotide substitutions fixed during the HCV superinfection process were nonsynonymous and located at described epitopes, suggesting a positive immune selection mechanism driving their molecular evolution.

We found that hypervariable regions of both HCV and HIV had several amino acid modifications during the acute phase of superinfection. However, these changes occurred simultaneously on the gp120 V3 loop whereas they were sequentially selected and showed a cumulative pattern in the HVR1.

The selection of an HIV viral population with three amino acid modifications in the V3 loop region right after HCV superinfection maybe resulted from the overgrowth of markedly different but minor HIV quasispecies from the initial sample.

In contrast, the HVR1 evolved showed a cumulative pattern of mutations during the 17 month period. Each time of sequential incorporation of a nonsynonymous mutation was associated with an ALT flare up and resulted from the selection process, also exerted by the evolving host immune response^[24].

It has been proposed that the evolution of hypervariable regions may be caused by the successive accumulation of point substitutions as we have seen in the HVR1-HCV or, alternatively from the selection of a pre-existing minor subpopulations, which was different from the previous one, as observed in V3 loop of HIV^[25].

Once the chronic infection was established, two extra amino acid mutations were observed in the HVR1, the first one was at position 398 (G→A), and the second one was at position 399 (L→F). F or L occupied the last position alternatively in most of the HVR sequences published elsewhere^[26] and may be considered as a return to a previous state of the quasispecies equilibrium.

The timing of the substitutions observed in the core region, which were late (after 17 months and 42 months of infection), implied its involvement in the infection once persistence had been established. Non-synonymous changes clustered in HCV

epitopes that stimulated the humoral and cellular response and were previously described^[18, 20, 27], suggesting an active participation of these epitopes in the persistence of HCV infection. Moreover, the sample at the end of the follow-up showed two modifications (aa 63 and 74 of the core protein) that recovered the early amino acid sequences. As far as the HVR sequences concerned, this effect that might be due to the return to a quasispecies equilibrium state favored the outgrowth of the fittest quasispecies for that particular host conditions, as a consequence from the interplaying of virus populations in every situation.

Two substitutions were selected in the NS5A region. One of them occurred at the early phase of the infection whereas the second appeared at the end of the follow-up. The first mutation selected (E2227Q) was located in the ISDR, described as related to the IFN resistance of some HCV genotypes by means of its interactions with the cellular PKR and in a cellular epitope, as previously described^[19].

In conclusion, during the HCV superinfection process, each genomic region analyzed presents a different pattern of evolution, and is probably related to their functions in the viral life cycle. The localization of mutations at described epitopes suggests the participation of the host immune system drives the balance of the viral subpopulations towards escape and better fitness ones. In order to study this hypothesis, a quasispecies analysis is worth to be done to address the changes showed during the coinfection by means of the population equilibriums.

REFERENCES

- 1 **Waldrep TW**, Summers KK, Chiliade PA. Coinfection with HIV and HCV: more questions than answers? *Pharmacotherapy* 2000; **20**: 1499-1507
- 2 **Laskus T**, Radkowski M, Piasek A, Nowicki M, Horban A, Cianciara J, Rakela J. Hepatitis C virus in lymphoid cells of patients coinfecting with human immunodeficiency virus type 1: evidence of active replication in monocytes/macrophages and lymphocytes. *J Infect Dis* 2000; **181**: 442-448
- 3 **Centers for Disease Control and Prevention**. 1999 USPHS/IDSA guidelines for the prevention of opportunistic infections in persons infected with human immunodeficiency virus: disease-specific recommendations. USPHS/IDSA Prevention of Opportunistic Infections Working Group: U.S. Public Health Services/ Infectious Diseases Society of America. *Morbidity and Mortality Weekly Report* 1999; **48**: 1-82
- 4 **Rockstroh JK**, Woitas RP, Spengler U. Human immunodeficiency virus and hepatitis C virus coinfection. *Europ J Med Res* 1998; **3**: 269-277
- 5 **Rispeter K**, Lu M, Behrens SE, Fumiko C, Yoshida T, Roggendorf M. Hepatitis C virus variability: sequence analysis of an isolate after 10 years of chronic infection. *Virus Genes* 2000; **21**: 179-188
- 6 **Smith DB**. Evolution of the hypervariable region of hepatitis C virus. *J Viral Hepatitis* 1999; **6**(Suppl 1): 41-46
- 7 **Ray SC**, Wang YM, Laeyendecker O, Ticehurst JR, Villano SA, Thomas DL. Acute hepatitis C virus structural gene sequences as predictors of persistent viremia: hypervariable region 1 as a decoy. *J Virol* 1999; **73**: 2938-2946
- 8 **Hwang SS**, Boyle TJ, Lysterly HK, Cullen BR. Identification of the envelope V3 loop as the primary determinant of cell tropism in HIV-1. *Science* 1991; **253**: 71-74
- 9 **Ghosh AK**, Steele R, Meyer K, Ray R, Ray RB. Hepatitis C virus NS5A protein modulates cell cycle regulatory genes and promotes cell growth. *J General Virol* 1999; **80**: 1179-1183
- 10 **Gale MJ Jr**, Korh MJ, Tang NM, Tan SL, Hopkins DA, Dever TE, Polyak SJ, Gretch DR, Katze MG. Evidence that hepatitis C virus resistance to interferon is mediated through repression of the PKR protein kinase by the nonstructural 5A protein. *Virology* 1997; **230**: 217-227
- 11 **Kato N**, Lan KH, Ono-Nita SK, Shiratori Y, Omata M. Hepatitis C virus nonstructural region 5A protein is a potent transcriptional activator. *J Virol* 1997; **71**: 8856-8859

- 12 **McLauchlan J.** Properties of the hepatitis C virus core protein: a structural protein that modulates cellular processes. *J Viral Hepat* 2000; **7**: 2-14
- 13 **Matsumoto M,** Hsieh TY, Zhu N, VanArsdale T, Hwang SB, Jeng KS, Gorbalyena AE, Lo SY, Ou JH, Ware CF, Lai MM. Hepatitis C virus core protein interacts with the cytoplasmic tail of lymphotoxin-beta receptor. *J Virol* 1997; **71**: 1301-1309
- 14 **Zhu N,** Khoshnan A, Schneider R, Matsumoto M, Dennert G, Ware C, Lai MM. Hepatitis C virus core protein binds to the cytoplasmic domain of tumor necrosis factor (TNF) receptor 1 and enhances TNF-induced apoptosis. *J Virol* 1998; **72**: 3691-3697
- 15 **Jin DY,** Wang HL, Zhou Y, Chun AC, Kibler KV, Hou YD, Kung H, Jeang KT. Hepatitis C virus core protein-induced loss of LZIP function correlates with cellular transformation. *EMBO J* 2000; **19**: 729-740
- 16 **Barba G,** Harper F, Harada T, Kohara M, Goulinet S, Matsuura Y, Eder G, Schaff Z, Chapman MJ, Miyamura T, Brechot C. Hepatitis C virus core protein shows a cytoplasmic localization and associates to cellular lipid storage droplets. *Proceed Natl Acad Sci USA* 1997; **94**: 1200-1205
- 17 **Sabile A,** Perlemuter G, Bono F, Kohara K, Demaugre F, Kohara M, Matsuura Y, Miyamura T, Brechot C, Barba G. Hepatitis C virus core protein binds to apolipoprotein AII and its secretion is modulated by fibrates. *Hepatology* 1999; **30**: 1064-1076
- 18 **Akatsuka T,** Donets M, Scaglione L, Ching WM, Shih JW, Di Bisceglie AM, Feinstone SM. B-cell epitopes on the hepatitis C virus nucleocapsid protein determined by human monospecific antibodies. *Hepatology* 1993; **18**: 503-510
- 19 **Ward S,** Lauer G, Isba R, Walker B, Klenerman P. Cellular immune responses against hepatitis C virus: the evidence base 2002. *Clin Experimental Immunol* 2002; **128**: 195-203
- 20 **Koziel MJ,** Dudley D, Afdhal N, Choo QL, Houghton M, Ralston R, Walker BD. Hepatitis C virus (HCV)-specific cytotoxic T lymphocytes recognize epitopes in the core and envelope proteins of HCV. *J Virol* 1993; **67**: 7522-7532
- 21 **Flichman D,** Cello J, Castano G, Campos R, Sookoian S. *In vivo* down regulation of HIV replication after hepatitis C superinfection. *Medicina* 1999; **59**: 364-366
- 22 **Chomczynski P,** Sacchi N. Single-step method of RNA isolation by acid guanidinium thiocyanate-phenol-chloroform extraction. *Analytical Biochemistry* 1987; **162**: 156-159
- 23 **Kwok S,** Higuchi R. Avoiding false positives with PCR. *Nature* 1989; **339**: 237-238
- 24 **Hjalmarsson S,** Blomberg J, Grillner L, Pipkorn R, Allander T. Sequence evolution and cross-reactive antibody responses to hypervariable region 1 in acute hepatitis C virus infection. *J Med Virol* 2001; **64**: 117-124
- 25 **Lu L,** Nakano T, Orito E, Mizokami M, Robertson BH. Evaluation of accumulation of hepatitis C virus mutations in a chronically infected chimpanzee: comparison of the core, E1, HVR1, and NS5b regions. *J Virol* 2001; **75**: 3004-3009
- 26 **Penin F,** Combet C, Germanidis G, Frainais PO, Deleage G, Pawlotsky JM. Conservation of the conformation and positive charges of hepatitis C virus E2 envelope glycoprotein hypervariable region 1 points to a role in cell attachment. *J Virol* 2001; **75**: 5703-5710
- 27 **Beld M,** Penning M, van Putten M, Lukashov V, van den Hoek A, McMorrow M, Goudsmit J. Quantitative antibody responses to structural (Core) and nonstructural (NS3, NS4, and NS5) hepatitis C virus proteins among seroconverting injecting drug users: impact of epitope variation and relationship to detection of HCV RNA in blood. *Hepatology* 1999; **29**: 1288-1298

Edited by Xu XQ and Wang XL

Interruption of HBV intrauterine transmission: A clinical study

Xiao-Mao Li, Yue-Bo Yang, Hong-Ying Hou, Zhong-Jie Shi, Hui-Min Shen, Ben-Qi Teng, Ai-Min Li, Min-Feng Shi, Ling Zou

Xiao-Mao Li, Yue-Bo Yang, Hong-Ying Hou, Zhong-Jie Shi, Hui-Min Shen, Ben-Qi Teng, Ai-Min Li, Ling Zou, Department of Obstetrics and Gynecology, The Third Affiliated Hospital, Sun Yat-Sen University, Guangzhou 510630, Guangdong Province, China
Min-Feng Shi, Maternity Hospital, School of Medicine, Zhejiang University, Hangzhou 310006, Zhejiang Province, China

Supported by the Science and Research Foundations of Sun Yat-Sen University and Guangzhou Science Committee, No.1999-J-005-01

Correspondence to: Xiao-Mao Li, Department of Obstetrics and Gynecology, The Third Affiliated Hospital, Sun Yat-Sen University, Guangzhou 510630, Guangdong Province, China. tigerli777@163.com

Telephone: +86-20-85515609 **Fax:** +86-20-87565575

Received: 2003-03-13 **Accepted:** 2003-04-11

Abstract

AIM: To investigate the effect of hepatitis B virus (HBV) specific immunoglobulin (HBIG) and lamivudine on HBV intrauterine transmission in HBsAg positive pregnant women.

METHODS: Each subject in the HBIG group (56 cases) was given 200 IU HBIG intramuscularly (im.) every 4 weeks from 28-week (wk) of gestation, while each subject in the lamivudine group (43 cases) received 100 mg lamivudine orally (po.) every day from 28-wk of gestation until the 30th day after labor. Subjects in the control group (52 cases) received no specific treatment. Blood specimens were tested for HBsAg, HBeAg, and HBV-DNA in all maternities at 28-wk of gestation, before delivery, and in their newborns 24 hours before the administration of immune prophylaxis.

RESULTS: Reductions of HBV DNA in both treatments were significant ($P < 0.05$). The rate of neonatal intrauterine HBV infection was significantly lower in HBIG group (16.1 %) and lamivudine group (16.3 %) compared with control group (32.7 %) ($P < 0.05$), but there was no significant difference between HBIG group and lamivudine group ($P > 0.05$). No side effects were found in all the pregnant women or their newborns.

CONCLUSION: The risk of HBV intrauterine infection can be effectively reduced by administration of HBIG or Lamivudine in the 3rd trimester of HBsAg positive pregnant women.

Li XM, Yang YB, Hou HY, Shi ZJ, Shen HM, Teng BQ, Li AM, Shi MF, Zou L. Interruption of HBV intrauterine transmission: A clinical study. *World J Gastroenterol* 2003; 9(7): 1501-1503
<http://www.wjgnet.com/1007-9327/9/1501.asp>

INTRODUCTION

It is of vital importance to interrupt the transmission of viral hepatitis B from mother to fetus in control of its prevalence^[1-3], including HBV intrauterine infection^[4-7]. This study investigated the effect of administration of HBIG (im.) and lamivudine (po.) on the interruption of HBV intrauterine infection from the 3rd trimester of gestation.

MATERIALS AND METHODS

Subjects

One hundred and fifty one pairs of women and their newborns who followed the antepartum care were selected and admitted for labor in our hospital from January of 1999 to December of 2001. These pregnant women were HBsAg positive, with normal liver and kidney function. Serial tests were negative for HAV, HCV, HDV and HEV in these women and no other severe complications were found and no other drugs, including the ones that were studied, anti-virus, cytotoxic, steroid hormones, or immune regulating drugs were administered. The patients were randomly allocated into 3 groups. There were 56 patients in the HBIG group (22 were both HBsAg and HBeAg positive) and 43 in the lamivudine group (33 were both HBsAg and HBeAg positive). There were 52 patients in the control group (17 were both HBsAg and HBeAg positive). No significant differences were found in age, race, time of gestation and parturition, gestational age, way of delivery, and incidence of threatened abortion, threatened labor or pregnancy-induced hypertension syndrome (PIH). The 151 pregnant women delivered 151 newborns.

Methods

Patients in the HBIG group were administered HBIG 200IU intramuscularly (im.) from 28-wk of gestation, once every 4 weeks till labor. Patients in the lamivudine group were administered 100 mg (po.) lamivudine orally daily till the 30th day after labor. Patients in the control group were given no specific treatment. Blood specimens were tested for HBsAg, HBeAg, and HBV-DNA in all the subjects at 28-wk and before delivery, and their newborns (blood from the femoral vein) 24 hours before administration of immune prophylaxis.

HBsAg and HBeAg were assessed by ELISA, the assay kits were produced by Zhongshan Biological and Engineering Co. Ltd. HBV-DNA was assessed by fluorogenic quantitative polymerase chain reaction (FQ-PCR), and the assay kits were produced by Da'an Gene Diagnosis Center, Sun Yat-Sen University.

Before the administration of positive and/or active prophylaxis at 24 hours after delivery, intrauterine HBV infection would be considered if HBsAg and/or HBeAg were tested positive in neonatal peripheral blood.

Statistics

The *t*-test and χ^2 test were used to analyze our data using Excel software. Statistical significance was set at $P < 0.05$. HBV DNA values were expressed as $\bar{x} \pm s$, and neonatal intrauterine HBV infection rates were expressed as percentage of total cases in each group.

RESULTS

Changes of HBsAg, HBeAg and HBV DNA

HBsAg turned negative in 1 case of the HBIG group, but HBeAg turned negative in no case. HBsAg and HBeAg turned negative in 1 case of the lamivudine group. No cases turned negative of HBsAg or HBeAg in the control group.

Before administration of agents, there was no significant difference in the values of HBV DNA among 3 groups

($P>0.05$). But there was significant difference between the values of HBV DNA in HBIG group and lamivudine group after administration of either reagent respectively (both values reduced, $P<0.05$). The reduction of value before and after administration of the reagents was significantly different between the administered groups and control group ($P<0.05$). (Table 1).

Table 1 Comparison of HBV DNA values before and after administration of the reagents

Group	<i>n</i>	Log10 HBV DNA before administration of drugs (copies/ml)	Log10 HBV DNA before labor (copies/ml)	Minus value of log10 HBV DNA before and after administration of agents (copies/ml)
HBIG	56	7.38±1.17 ^a	5.28±2.77 ^{bd}	2.09±2.28 ^b
Lamivudine	43	7.49±0.54 ^a	5.33±1.34 ^{bd}	2.16±1.27 ^b
Conrol	52	7.05±1.29 ^a	6.23±3.66 ^c	0.82±2.73 ^c

^a $P>0.05$ vs other groups; ^b $P>0.05$ between HBIG group and lamivudine group; ^c $P<0.05$ vs HBIG group or lamivudine group; ^d $P<0.05$ (before vs after administration).

Incidence of HBV intrauterine infection

Three newborns were HBsAg positive, and 7 cases were HBeAg positive, one of them was doubly positive for HBsAg and HBeAg in HBIG group. Corresponding cases in lamivudine group and control group were 1, 7, and 1, or 8, 11, and 2 respectively. The infection rates of HBIG, lamivudine, and control groups were 16.1 %, 16.3 %, and 32.7 %, respectively. There were significant differences between the incidence of HBV intrauterine infection in either reagent administrated group and control group ($P<0.05$), while there was no significant difference between HBIG group and lamivudine group ($P>0.05$). (Table 2).

Table 2 Incidence of neonatal intrauterine infection in 3 groups

Group	<i>n</i>	HBsAg(+) <i>n</i>	HBeAg(+) <i>n</i>	Intrauterine infection	
				<i>n</i>	%
HBIG	56	3	7	9	16.1 ^a
Lamivudine	43	1	7	7	16.3 ^a
Control	52	8	11	17	32.7 ^b

^a $P>0.05$ between HBIG group and lamivudine group; ^b $P<0.05$ vs HBIG group or lamivudine group.

Safety

There were no incidences of fever, rigor, rash, or other complaints and dysfunction of the liver and kidney in subjects throughout administration and follow-ups. There were no significant differences in gestational age, severity of postpartum hemorrhage, rate of cesarean section, neonatal weight, neonatal height, circumference of neonatal head and Apgar score ($P>0.05$).

DISCUSSION

There are several thoughts about the mechanisms of HBV intrauterine transmission, including placental infection^[8], placental exudation and transudation^[9-11], peripheral blood monocyte (PBMC)^[12] infection, fraternal transmission, etc. Infection through placenta is the most active pathway in maternity-fetus transmission. It is suggested that infection mainly occurs in the 3rd trimester. This might be resulted from the fact that the layer of trophoblastic cells becomes thinner and turns into chorion-vessel membrane, which makes it easier for HBV to pass the placental barrier^[13]. The organs of fetus during this period have already developed, therefore, it is safe

for the administration of reagents. So we chose this period to begin the interruption of infection. Lamivudine (po.) or HBIG (im.) was administered from 28-wk of gestation.

Barrier-destroying factors, such as threatened abortion, threatened premature labor and TORCH (toxoplasmosis, others, rubella, cytomegalovirus, herpes) infection, were the highly risk factors for HBV intrauterine infection^[14]. It is generally considered that intrauterine infection might be the general effect of maternity and virus. In this study, there were no significant differences among the 3 groups in the highly risk factors (threatened abortion, threatened premature labor) or age, time of gestation and delivery, pregnant complication, medical or surgical complication, gestational age at labor or way of delivery.

It has been clinically accepted to administer joint immune reagents (HBIG together with HBV vaccine) to neonates with high risks, but the immune failure rate is still about 10-20 %^[15,16], the main reason is intrauterine infection. So, it is important to study the mechanism of HBV intrauterine infection, and we further investigated the intrauterine prevention and interruption of HBV infection.

HBIG is a highly effective immune globulin^[17], which is purified from highly effective plasma or serum taken from healthy individuals after the use of HBV vaccine. HBs antibody can bind HBsAg, activate the complimentary system at the same time and strengthen humoral immune, clear HBV, and reduce the number of virus in the maternal blood. It can prevent and decrease the incidence of normal cell infection and might reduce HBV copy in the body. Placenta has the function of transmitting antibody in the form of IgG to the fetus. It is suggested that after maternal administration of HBIG (im.), HBsAb can be transmitted to fetus, which makes it possible for the fetus to obtain the protection of intrauterine passive immunization and to prevent intrauterine infection^[18]. The results of this study suggest that regular administration of HBIG (im.) to HBV positive pregnant women might reduce the amount of HBV DNA in blood, and neonatal intrauterine infection rate also reduced significantly when compared with control group. DNA polymerase of HBV has many functions in the process of virus replication. After infection of liver cells by HBV, the incomplete double strand DNA integrates into a complete one, enters the nuclei, forming super helix covalent closed circular DNA (cccDNA). cccDNA is extremely stable, and is the resource of viral DNA and directs the formation of viral protein. The whole mRNA replicated from cccDNA model can form a single strand minus-DNA by reverse-transcription of the HBV DNA polymerase. This DNA can form incomplete double strand DNA through DNA polymerase. The latter can also integrate with antigen proteins in the endoplast, forming new, contagious mature viral particles and be released into blood, or migrate into the nuclei to supply cccDNA there. The multiple functions of HBV polymerase enable it to become one of the most prosperous anti-virus targets.

Lamivudine is a potent anti-virus nucleotide analogue to HBV and HIV. Through competitive inhibition of HBV DNA polymerase and formation of new HBV DNA strand, it can terminate the synthesis of new strand^[19,20]. After several days of the administration of lamivudine, the level of HBV DNA drops dramatically, and throughout the treatment, HBV DNA will be suppressed continuously. It can reduce the necrosis and inflammation of the liver and bring ALT level to normal without significant side effects or malformation-causing effects^[21-31]. We found the amount of HBV DNA in blood and the rate of neonatal intrauterine infection after administration of lamivudine in the 3rd trimester were significantly lower than that in control group. This suggests that administration of lamivudine of HBV positive pregnant women in the 3rd trimester can effectively decrease the rate of intrauterine HBV infection.

As a passive antibody, the main effect of HBIG is to neutralize HBV in the body, prevent and decrease infection of normal cells^[32]; while lamivudine is a potent anti-virus agent, which can suppress the replication of HBV actively, decrease HBV level during pregnancy. Our data showed that the neonatal infection rates, after these two reagents were used in the 3rd trimester to interrupt intrauterine HBV infection, were 16.1 % and 16.3 %, respectively, with no significant difference between these 2 groups ($P>0.05$). But compared with control group, the infection rates of both groups were significantly lower. These data indicate that both of them are safe and effective in the interruption of intrauterine HBV infection.

We found in our previous studies that HBV DNA level in maternal serum was an important factor for intrauterine infection^[1]. Especially when HBV DNA is $\geq 10^8$ copies/ml, it has significant correlation with neonatal HBV infection^[33]. Administration of HBIG in combination with lamivudine in these patients might decrease the neonatal HBV infection rate more effectively. Further studies are required to improve our understanding about this problem.

REFERENCES

- 1 **Li XM**, Liu SL, Li X, Huang HJ, Lu JX, Gao ZL. The level of HBV DNA in peripheral, umbilical, and milk of maternal and its correlation. *Zhongshan Yike Daxue Xuebao* 2000; **21**: 233-235
- 2 **Merle P**, Trepo C, Zoulim F. Current management strategies for hepatitis B in the elderly. *Drugs Aging* 2001; **18**: 725-735
- 3 **Hamdani-Belghiti S**, Bouazzaou NL. Mother-child transmission of hepatitis B virus. State of the problem and prevention. *Arch Pediatr* 2000; **7**: 879-882
- 4 **Zhang SL**, Han XB, Yue YF. Relationship between HBV viremia level of pregnant women and intrauterine infection: nested PCR for detection of HBV DNA. *World J Gastroenterol* 1998; **4**: 61-63
- 5 **Shiraki K**. Perinatal transmission of hepatitis B virus and its prevention. *J Gastroenterol Hepatol* 2000; **15** (Suppl): E11-15
- 6 **Michielsen PP**, Van Damme P. Viral hepatitis and pregnancy. *Acta Gastroenterol Belg* 1999; **62**: 21-29
- 7 **Tang JR**, Hsu HY, Lin HH, Ni YH, Chang MH. Hepatitis B surface antigenemia at birth: a long-term follow-up study. *J Pediatr* 1998; **133**: 374-377
- 8 **Xu DZ**, Yan YP, Zou S, Choi BC, Wang S, Liu P, Bai G, Wang X, Shi M, Wang X. Role of placental tissues in the intrauterine transmission of hepatitis B virus. *Am J Obstet Gynecol* 2001; **185**: 981-987
- 9 **Kroes AC**, Quint WG, Heijntink RA. Significance of isolated hepatitis B core antibodies detected by enzyme immunoassay in a high risk population. *J Med Virol* 1991; **35**: 96-100
- 10 **Suga M**, Shibata K, Kodama T, Arima K, Yamada S, Yachi A. A case of HBs antigen negative fulminant hepatitis with IgM antibody to hepatitis B core antigen persisting more than seven years. *Gastroenterol Jpn* 1991; **26**: 661-665
- 11 **Wang JS**, Zhu QR. Infection of the fetus with hepatitis B e antigen via the placenta. *Lancet* 2000; **355**: 989
- 12 **Leung NW**, Tam JS, Lau GT, Leung TW, Lau WY, Li AK. Hepatitis B virus DNA in peripheral blood leukocytes. A comparison between hepatal cellulo carcinoma and other hepatitis B virus-related chronic liver diseases. *Cancer* 1994; **73**: 1143-1148
- 13 **Yan YP**, Xu DZ, Wang WL, Liu B, Liu ZH, Men K, Zhang JX, Xu JQ. The relation between HBV placenta infection and intrauterine transmission. *Zhonghua Fuchanke Zazhi* 1999; **34**: 392-395
- 14 **Del Canho R**, Grosheide PM, Schalm SW, de Vries RR, Heijntink RA. Failure of neonatal hepatitis B vaccination: the role of HBV-DNA levels in hepatitis B carrier mothers and HLA antigens in neonates. *J Hepatol* 1994; **20**: 483-486
- 15 **Zhu Q**, Lu Q, Gu X, Xu H, Duan S. A preliminary study on interruption of HBV transmission in uterus. *Chin Med J (Engl)* 1997; **110**: 145-147
- 16 **Xu DZ**, Yan YP, Choi BC, Xu JQ, Men K, Zhang JX, Liu ZH, Wang FS. Risk factors and mechanism of transplacental transmission of hepatitis B virus: A case-control study. *J Med Virol* 2002; **67**: 20-26
- 17 **Ghendon Y**. Perinatal transmission of hepatitis B virus in high-incidence countries. *J Virol Methods* 1987; **17**: 69-79
- 18 **Yue YF**, Yang XJ, Zhang SL, Han XB. Clinical research of the effect of intramuscular administration of HBIG on HbsAg positive pregnant women to prevent vertical transmission. *Zhongguo Shiyong Fuke Yu Chanke Zazhi* 1999; **15**: 547-548
- 19 **Yao GB**, Wang SB, Cui ZY, Yao JL, Zeng MD. A multi-center random double-blind case-control study of the treatment of chronic hepatitis B by Lamivudine. *Zhongguo Xinyao Yu Linchuang Zazhi* 1999; **18**: 131-135
- 20 **Johnson MA**, Moore KH, Yuen GJ, Bye A, Pakes GE. Clinical pharmacokinetics of lamivudine. *Clin Pharmacokinet* 1999; **36**: 41-66
- 21 **Rizzetto M**. Efficacy of lamivudine in HBeAg-negative chronic hepatitis B. *J Med Virol* 2002; **66**: 435-451
- 22 **Ricceri L**, Venerosi A, Valanzano A, Sorace A, Alleva E. Prenatal AZT or 3TC and mouse development of locomotor activity and hot-plate responding upon administration of the GABA(A) receptor agonist muscimol. *Psychopharmacology (Berl)* 2001; **153**: 434-442
- 23 **Calamandrei G**, Venerosi A, Branchi I, Valanzano A, Alleva E. Prenatal exposure to anti-HIV drugs. long-term neurobehavioral effects of lamivudine (3TC) in CD-1 mice. *Neurotoxicol Teratol* 2000; **22**: 369-379
- 24 **Culnane M**, Fowler M, Lee SS, McSherry G, Brady M, O'Donnell K, Mofenson L, Gortmaker SL, Shapiro DE, Scott G, Jimenez E, Moore EC, Diaz C, Flynn PM, Cunningham B, Oleske J. Lack of long-term effects of in utero exposure to zidovudine among uninfected children born to HIV-infected women. *JAMA* 1999; **281**: 151-157
- 25 **Conner EM**, Sperling RS, Gelber R, Kiselev P, Scott G, O'Sullivan MJ, VanDyke R, Bey M, Shearer W, Jacobson RL. Reduction of maternal-infant transmission of human immunodeficiency virus type-1 with zidovudine. *N Engl J Med* 1994; **331**: 1173-1180
- 26 **Vuthipongse R**, Bhadrakom C, Roongpisuthipong P. Administration of Zidovudine during late pregnancy and delivery to prevent perinatal HIV transmission-Thailand 1996-1998. *MMWR* 1998; **47**: 151-154 // *JAMA* 1998; **279**: 1061-1062
- 27 **Moodley J**, Moodley D, Pillay K, Coovadia H, Saba J, van Leeuwen R, Goodwin C, Harrigan PR, Moore KH, Stone C, Plumb R, Johnson MA. Pharmacokinetics and antiretroviral activity of lamivudine alone or when coadministered with zidovudine in human immunodeficiency virus type 1-infected pregnant women and their offspring. *J Infect Dis* 1998; **178**: 1327-1333
- 28 **van Leeuwen R**, Lange JM, Nijhuis M, Schuurman R, Reiss P, Danner SA, Boucher CA. Results of long-term follow-up of HIV-infected patients treated with lamivudine monotherapy, followed by a combination of lamivudine and zidovudine. *Antivir Ther* 1997; **2**: 79-90
- 29 **Dienstag JL**, Perillo RP, Schiff ER, Bartholomew M, Vicary C, Rubin M. A preliminary trial of lamivudine for chronic hepatitis B infection. *N Engl J Med* 1995; **333**: 1657-1661
- 30 **Liaw YF**. Current therapeutic trends in therapy for chronic viral hepatitis. *J Gastroenterol Hepatol* 1997; **12**: S346-353
- 31 **Lai CL**, Ching CK, Tung AK, Li E, Young J, Hill A, Wong BC, Dent J, Wu PC. Lamivudine is effective in suppressing hepatitis B virus DNA in Chinese hepatitis B surface antigen carriers: a placebo-control trial. *Hepatology* 1997; **25**: 241-244
- 32 **Yue Y**, Yang X, Zhang S. Prevention of intrauterine infection by hepatitis B virus with hepatitis B immunoglobulin: efficacy and mechanism. *Chin Med J (Engl)* 1999; **112**: 37-39
- 33 **Ngui SL**, Andrews NJ, Underhill GS, Heptonstall J, Teo CG. Failed postnatal immunoprophylaxis for hepatitis B: characteristics of maternal hepatitis B virus as risk factors. *Clinical Infectious Diseases* 1998; **27**: 100-106

Inhibition of HBV targeted ribonuclease enhanced by introduction of linker

Wei-Dong Gong, Jun Liu, Jin Ding, Ya Zhao, Ying-Hui Li, Cai-Fang Xue

Wei-Dong Gong, Jun Liu, Jin Ding, Ya Zhao, Ying-Hui Li, Cai-Fang Xue, Department of Pathogenic Organisms, Fourth Military Medical University, Xi'an 710033, Shaanxi Province, China

Supported by National Natural Scientific Foundation of China, No. 30100157 and Innovation Project of FMMU, No. CX99005

Correspondence to: Professor Cai-Fang Xue or Dr. Jun Liu, Department of Pathogenic Organisms, Fourth Military Medical University, Xi'an 710033, Shaanxi Province, China. etiology@fmmu.edu.cn

Received: 2003-03-05 **Accepted:** 2003-04-01

Abstract

AIM: To construct human eosinophil-derived neurotoxin (hEDN) and HBV core protein (HBVc) eukaryotic fusion expression vector with a linker (Gly₄Ser)₃ between them to optimize the molecule folding, which will be used to inhibit HBV replication *in vitro*.

METHODS: Previously constructed pcDNA3.1(-)/TR was used as a template. Linker sequence was synthesized and annealed to form dslinker, and cloned into pcDNA3.1(-)/TR to produce plasmid pcDNA3.1(-)/Hbc-linker. Then the hEDN fragment was PCR amplified and inserted into pcDNA3.1(-)/Hbc-linker to form pcDNA3.1(-)/TNL in which the effector molecule and the target molecule were separated by a linker sequence. pcDNA3.1(-)/TNL expression was identified by indirect immunofluorescence staining. Radioimmunoassay was used to analyse anti-HBV activity of pcDNA3.1(-)/TNL. Meanwhile, metabolism of cells was evaluated by MTT colorimetry.

RESULTS: hEDN and HBVc eukaryotic fusion expression vector with a linker (Gly₄Ser)₃ between them was successfully constructed. pcDNA3.1(-)/TNL was expressed in HepG2.2.15 cells efficiently. A significant decrease of HBsAg concentration from pcDNA3.1(-)/TNL transfectant was observed compared to pcDNA3.1(-)/TR ($P=0.036$, $P<0.05$). MTT assay suggested that there were no significant differences between groups ($P=0.08$, $P>0.05$).

CONCLUSION: Linker introduction enhances the inhibitory effect of HBV targeted ribonuclease significantly.

Gong WD, Liu J, Ding J, Zhao Y, Li YH, Xue CF. Inhibition of HBV targeted ribonuclease enhanced by introduction of linker. *World J Gastroenterol* 2003; 9(7): 1504-1507
<http://www.wjgnet.com/1007-9327/9/1504.asp>

INTRODUCTION

Hepatitis B virus (HBV) remains a major public health problem worldwide^[1-6] and causes transient and chronic infection of liver^[7-9]. Transient infection may produce serious illness, and chronic infection may also have serious consequences: nearly 25% of chronic HBV infected patients terminate in untreatable liver cancer of 350 million chronic HBV infected patients. The available treatments are of limited efficacy, such as interferon-

α (INF- α)^[10-12], nucleoside analogues^[13-15] and gene therapy strategy^[16,17]. Alternative approaches to inhibit HBV replication are urged. Capsid-targeted viral inactivation (CTVI, also called virion-targeted viral inactivation) was established by Natsoulis and Boeke in 1991, in which a viral capsid protein or other virion associated protein as a carrier guides a degradative enzyme into virus particles specifically to inhibit virus replication or kill it^[18]. CTVI has been thoroughly investigated in experimental treatment for retrovirus, such as Moloney murine leukemia virus (MMLV) and HIV, showing a promising prospect as an antiviral treatment^[19,20]. Previously we fused HBV core protein (HBVc) to human eosinophil-derived neurotoxin (hEDN), and after transfection of the fusion protein encoding plasmid into HepG2.2.15 cells HBV replication was inhibited, due to the fact that HBV pregenome RNA (pgRNA) was degraded by the effector molecule, hEDN, *via* the guiding of the target molecule, HBVc^[21,22]. Here we reported the further enhancement of the degradative effect by introduction of a linker sequence (Gly₄Ser)₃ to separate the effector molecule and the target one.

MATERIALS AND METHODS

Reagents and equipments

pcDNA3.1(-)/TR was constructed in our laboratory^[21]. HepG2.2.15 cells were kindly provided by Dr. Hao (Tangdu Hospital, Fourth Military Medical University). Restriction enzymes, alkaline phosphatase, *TaKaRa Ex Taq*TM, DNA marker-DL2000 and T₄ DNA ligase (*TaKaRa* Biotechnology Co., Ltd., Dalian), Plasmid Miniprep Kit, Agarose Gel Extraction kit (Watson Biotechnology, Shanghai), LipofectinMine2000 (GIBCO), mouse anti-HA and rabbit anti-mouse IgG labeled with FITC (Sino-American Biotechnology Company), Radioimmunoassay Kit (Beijing Bei Mian Dongya Biotech Institute), GeneAmp PCR System 9600 (Perkin Elmer).

Linker and primers

All the oligomers were synthesized by Sangon (Shanghai).
LinkerF 5' -gcg cgg atc cgg tgg cgg tgg ctc ggg cgg tgg tgg gtc ggg tgg cgg cgg atc tga tga gct cgc gc- 3' (*Bam*HI, *Sac*I)
LinkerR 5' -gcg cga gctc aga tcc gcc gcc acc cga ccc acc gcc cga gcc acc gcc acc gga tcc gcg c- 3' (*Sac*I, *Bam*HI)
P1: 5' -gcg gga tcc acc atg aaa cct cca cag tt- 3' (*Bam*HI)
P2: 5' -gcg agatct gat gat tct atc cag gtg aa- 3' (*Bgl*II)

Cell culture

HepG2.2.15 cells integrated full-length HBV genome were cultured in DMEM medium containing 150 mL/L fetal bovine serum at 37 °C, in 50 mL/L CO₂. G418 was added to screen cells at the final concentration of 100 g/L. The media were freshed once every two days and the cells were passaged every six days.

Introduction of linker

To prepare double stranded linker, linkerF and linkerR were annealed by heating at 100 °C for 5 min and then slowly cooling to room temperature, and dissolved at a concentration of 0.1 g/L.

Dslinker bearing *Bam*HI and *Sac*I restriction sites was digested and cloned into pcDNA3.1(-)/TR digested by the same restrictions, to produce plasmid pcDNA3.1(-)/Hbc-linker.

hEDN fragment acquired from pcDNA3.1(-)/TR was PCR amplified by using primers and taking pcDNA3.1(-)/TR as a template. The PCR products digested by *Bam*HI/*Bgl*II were inserted into pcDNA3.1(-)/Hbc-linker which was restricted by *Bam*HI and dephosphorated, and the direction of hEDN was identified by enzyme restriction. The constructed plasmid was called pcDNA3.1(-)/TNL in which the effector molecule and the target molecule were separated by a linker sequence. The linker sequence and the PCR products were confirmed by sequencing by gencore (Shanghai).

Transfection and indirect immunofluorescence

Transfections were performed as described by the provider of LipofectinMine2000 and the transfecting condition had already been optimized by our laboratory^[21]. The cell density of 4×10^8 /L was added by 500 μ L/well in 24-well plate in which the cover glasses were put in advance. Transfecting work was performed when cells were adhered, usually after 24 hours^[18]. The experiment was divided into 3 groups: test group in which pcDNA3.1(-)/TNL was used, and two control groups in which blank vector pcDNA3.1(-) was used in the second group and the third was taken for mock transfection. Tri-wells were contained in each group. 48 hours post-transfection cells were quickly washed with 1mL sterile PBS (pH8.0) for 5 minutes, fixed in 1 g/L TritonX-100 diluted with 20 g/L paraformaldehyde and put on ice for 30 minutes. The fixed cells were washed three times with cold PBS, incubated with mouse anti-HA (1:100) for 15 minutes at 4 °C, and then washed three times in cold PBS, followed by incubation in rabbit anti-mouse IgG labeled with FITC (1:100) for 10 minutes at 4 °C. After rinsed with PBS for 1 hour, the slides were mounted with cover ships by using 500 g/L glycerol/PBS. The results were observed by fluoroscopy and pictures were taken.

Analysis of anti-HBV activity for pcDNA3.1(-)/TNL

24 hours before transfection, HepG2.2.15 cells were plated into a 96 well-plate with of 4×10^4 cells per well. Transfections were performed as described above. To determine HBsAg concentration, transfection experiment was divided into 7 groups, they were pcDNA3.1(-)/TNL, pcDNA3.1(-)/TR, pcDNA3.1(-)/hEDN_{mut}-HBVc, pcDNA3.1(-)/HBVc, pcDNA3.1(-)/hEDN, pcDNA3.1(-) and mock transfection, named as A to G respectively. Each transfection was performed in triplicate. After 48 hours of transfection the cell suspension was taken and HBsAg concentration was determined by RIA kit (completed by Nuclear Medicine Department of Xijing Hospital). Meanwhile the transfected cells were used to analyze the metabolic activity in order to analyze the effect of expressing protein on host cells. The data obtained were analyzed by SPSS software.

MTT assay

Metabolism of cells was evaluated by MTT colorimetry. 48 hours following transfections, 20 μ L of MTT solution (5 g/L) was added into each well and incubated at 37 °C for another 4 h. 150 μ L DMSO was added and surged for 10 min to dissolve the crystal completely. Absorbance values were identified at 490 nm wavelength by ELISA reader.

RESULTS

Linker introduction

To separate Hbc and hEDN, a linker was introduced. Both the linker sequence cloned into plasmid pcDNA3.1(-)/Hbc-linker

and hEDN fragment from PCR products, were subsequently inserted into pcDNA3.1(-)/TNL, and confirmed by sequencing. plasmid pcDNA3.1(-)/TNL was identified by restrictions of *Bam*HI/*Sac*I and *Sac*I/*Hind*III, the results suggested the construction was successful (Figure 1).

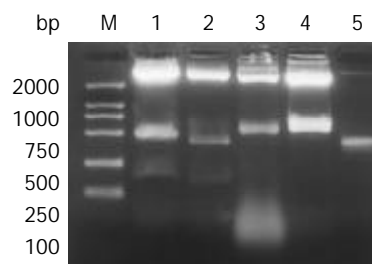


Figure 1 Identifications of plasmids in construction of pcDNA3.1(-)/TNL. 1: pcDNA3.1(-)/TNL digested by *Sac*I/*Hind*III; 2: pcDNA3.1(-)/TR by *Bam*HI/*Sac*I; 3: pcDNA3.1(-)/TR by *Sac*I/*Hind*III; 4: pcDNA3.1(-)/TNL by *Bam*HI/*Sac*I; 5: PCR products of hEDN.

Indirect immunofluorescence

To observe the expression of linker-separated fusion protein of pcDNA3.1(-)/TNL, indirect immunofluorescence was performed after 48 h of transfection (Figure 2).

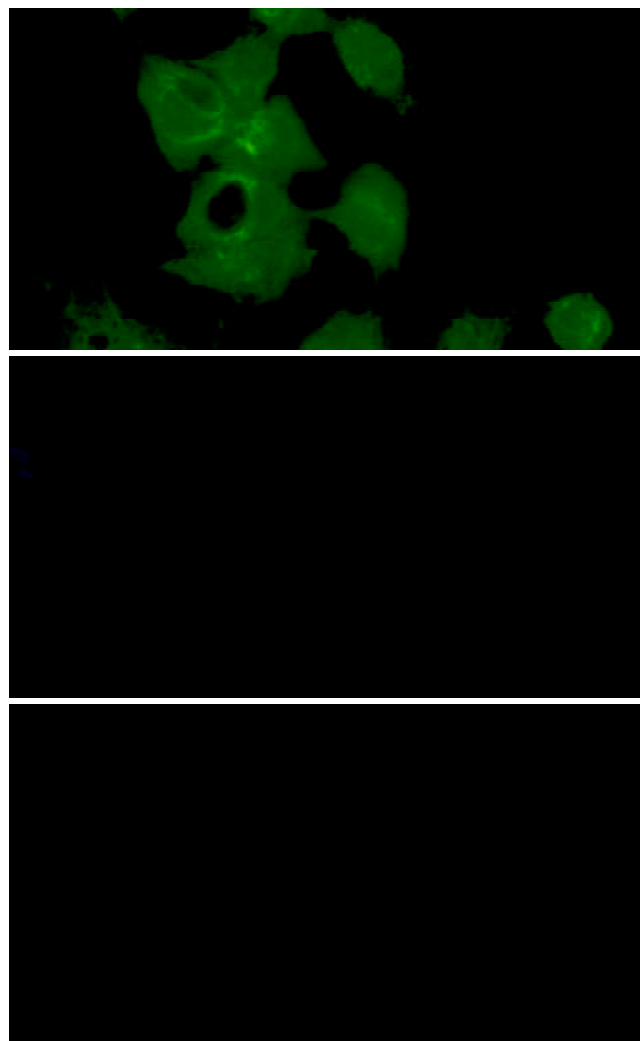


Figure 2 Detection of fusion protein by indirect immunofluorescence. 1: Green fluorescence in cells transfected by pcDNA3.1(-)/TNL; 2, 3: No fluorescence was observed in pcDNA3.1(-) transfectant and mock transfection.

Linker effect

To analyze the digestion effect of hEDN separated by a linker with HBVc. HBsAg concentration was determined by RIA after transfection. The significant decrease of HBsAg concentration in pcDNA3.1(-)/TNL transfectant, compared to pcDNA3.1(-)/TR ($P=0.036$, $P<0.05$, Figure 3), suggested that linker introduction enhanced hEDN digestion effect, which may be due to optimization of the folding of both hEDN and HBVc molecules. Also there were significant differences between groups A, B and groups C, D, E, F, G ($P=0.0054$, $P<0.01$), and no significant difference was found between groups C, D, E, F and group G ($P=0.085$, $P>0.05$).

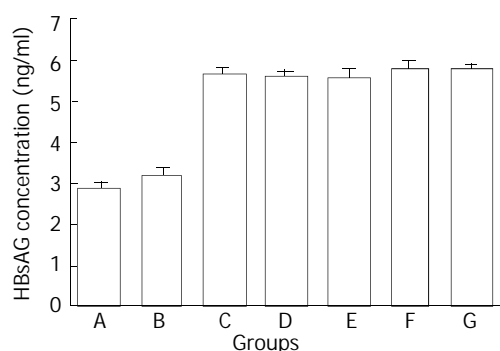


Figure 3 Comparison of HBsAg concentration in transfection groups.

Cell toxicity effect

48 hours post-transfection cell growth was observed and cell toxic effect of linker-separated fusion protein on host hepatocytes was detected by MTT assay. The A_{490} value of HepG2.2.15 cells transfected with pcDNA3.1(-)/TNL, pcDNA3.1(-)/TR, pcDNA3.1(-)/hEDN_{mut}-HBVc, pcDNA3.1(-)/HBVc, pcDNA3.1(-)/hEDN, pcDNA3.1(-) and mock transfection was 0.62 ± 0.16 , 0.69 ± 0.10 , 0.70 ± 0.05 , 0.64 ± 0.04 , 0.75 ± 0.08 , 0.78 ± 0.04 , 0.54 ± 0.16 , respectively ($\bar{x}\pm s$, $n=3$). The results suggested that there were no significant differences between groups ($P=0.08$, $P>0.05$).

DISCUSSION

HBV infection is an important health problem worldwide. Interferons and nucleosides analogues are effective drugs for chronic HBV infection, but only 20-30% of treated patients maintain a long-lasting response to anti-viral drugs^[23]. The expense of prolonged treatment makes these therapies poorly suitable for people in developing countries, where the prevalence of chronic HBV infection is often high. Therefore, new therapy strategy for HBV infection is urgent.

A new strategy called CTVI was established to guide effector molecule to target molecule and inhibit virus replication^[18]. Previously we fused HBVc to hEDN, and after transfection of the fusion protein encoding plasmid into HepG2.2.15 cells, HBV replication was inhibited due to the fact that HBV pregenome RNA (pgRNA) was degraded by the effector molecule, hEDN, by guiding the target molecule, HBVc^[21,22]. To further enhance the degradative effect of targeted ribonuclease, the classic linker (Gly₄Ser)₃ was introduced to separate the effector molecule and the target one. In our investigation, HBsAg concentration decreased significantly in pcDNA3.1(-)/TNL transfectant compared to pcDNA3.1(-)/TR transfectant due to linker introduction which may augment the digestion effect of hEDN significantly ($P=0.036$, $P<0.05$) via optimizing the protein folding.

Linker introduction, one of the gene fusion techniques, has become an increasingly useful tool in a variety of biomedical

researches^[24]. Many naturally occurring enzymes are composed of two or more distinct modules that are joined into a single macromole by stretches of amino acids referred to as linkers^[25]. In structural biology, construction of recombinant fusion proteins has been used as a means to increase the expression of soluble proteins and to facilitate protein purification^[26-28]. In recent years, a wide range of applications of gene fusion techniques has been reported in the fields of biotechnology. These applications include selection and production of antibodies and proteins with specialized functions, such as proteins that target specific genes^[29-31]. Recent studies have provided examples of linkers that are important in establishing the structural and functional assembly of multi-domain proteins^[32]. These interdomain linkers are relatively long and probably flexible in order to allow the two modules to perform independent functions. Recombinant production of chimeric enzymes requires stable linkers to join fusion partners without interfering with their function. The use of long linkers may result in low yield of active fusion protein since unprotected and flexible regions are often susceptible to proteolytic cleavage during recombinant protein production. A shorter linker might overcome problems associated with protease degradation. On the other hand, there is a risk that a shorter linker brings the modules too close to each other, resulting in a loss of function^[25]. In many studies functional single-chain antibodies (scFvs) were engineered by linking immunoglobulin heavy and light chain variable domains (V_H and V_L) via (Gly₄Ser)₃, which satisfies the needs above. Further enhancement of hEDN digestion and inhibitory effect may be completed by further linker design and screening, and the work involved in this field is in progress in our lab.

REFERENCES

- 1 **Fleming J**. Current treatments for hepatitis. *J Infus Nurs* 2002; **25**: 379-382
- 2 **elSaadany S**, Tepper M, Mao Y, Semenciw R, Giulivi A. An epidemiologic study of hepatocellular carcinoma in Canada. *Can J Public Health* 2002; **93**: 443-446
- 3 **Hassan MM**, Hwang LY, Hatten CJ, Swaim M, Li D, Abbruzzese JL, Beasley P, Patt YZ. Risk factors for hepatocellular carcinoma: synergism of alcohol with viral hepatitis and diabetes mellitus. *Hepatology* 2002; **36**: 1206-1213
- 4 **Torbenson M**, Thomas DL. Occult hepatitis B. *Lancet Infect Dis* 2002; **2**: 479-486
- 5 **Lok AS**. Hepatitis B infection: Pathogenesis and management. *J Hepatol* 2000; **32**(Suppl 1): 89-97
- 6 **Mazumdar TN**. Management of chronic hepatitis B infection: an update. *J Indian Med Assoc* 2001; **99**: 306-308, 310
- 7 **Chen N**, Zhu C, Hu D, Zeng F. The clinical significance of negative serological markers of hepatitis B infection in hepatitis B virus carriers with chronic hepatic disease. *Zhonghua Neike Zazhi* 2002; **41**: 653-655
- 8 **Hino O**, Kajino K, Umeda T, Arakawa Y. Understanding the hypercarcinogenic state in chronic hepatitis: a clue to the prevention of human hepatocellular carcinoma. *J Gastroenterol* 2002; **37**: 883-887
- 9 **Esteban R**. Management of chronic hepatitis B: an overview. *Semin Liver Dis* 2002; **22**(Suppl 1): 1-6
- 10 **Wai CT**, Chu CJ, Hussain M, Lok AS. HBV genotype B is associated with better response to interferon therapy in HBeAg(+) chronic hepatitis than genotype C. *Hepatology* 2002; **36**: 1425-1430
- 11 **Manns MP**. Current state of interferon therapy in the treatment of chronic hepatitis B. *Semin Liver Dis* 2002; **22**(Suppl 1): 7-14
- 12 **Shindo M**, Hamada K, Koya S, Sokawa Y, Okuno T. The clinical significance of core promoter and precore mutations during the natural course and interferon therapy in patients with chronic hepatitis B. *Am J Gastroenterol* 1999; **94**: 2237-2245
- 13 **Liaw YF**. Therapy of chronic hepatitis B: current challenges and opportunities. *J Viral Hepat* 2002; **9**: 393-399
- 14 **Wolters LM**, Hansen BE, Niesters HG, de Man RA. Viral dynamics in chronic hepatitis B patients treated with lamivudine,

- lamivudine-famciclovir or lamivudine-ganciclovir. *Eur J Gastroenterol Hepatol* 2002; **14**: 1007-1011
- 15 **Santantonio T**, Mazzola M, Iacovazzi T, Miglietta A, Guastadisegni A, Pastore G. Long-term follow-up of patients with anti-HBe/HBV DNA-positive chronic hepatitis B treated for 12 months with lamivudine. *J Hepatol* 2000; **32**: 300-306
- 16 **Song YH**, Lin JS, Liu NZ, Kong XJ, Xie N, Wang NX, Jin YX, Liang KH. Anti-HBV hairpin ribozyme-mediated cleavage of target RNA *in vitro*. *World J Gastroenterol* 2002; **8**: 91-94
- 17 **Chiou HC**, Lucas MA, Coffin CC, Banaszczyk MG, Ill CR, Lollo CP. Gene therapy strategies for the treatment of chronic viral hepatitis. *Expert Opin Biol Ther* 2001; **1**: 629-639
- 18 **Natsoulis G**, Boeke JD. New antiviral strategy using capsid-nuclease fusion proteins. *Nature* 1991; **352**: 632-635
- 19 **VanBrocklin M**, Federspiel MJ. Capsid-targeted viral inactivation can eliminate the production of infectious murine leukemia virus *in vitro*. *Virology* 2000; **267**: 111-123
- 20 **Wu X**, Liu H, Xiao H, Kim J, Seshiah P, Natsoulis G, Boeke JD, Hahn BH, Kappes JC. Targeting foreign proteins to human immunodeficiency virus particles via fusion with Vpr and Vpx. *J Virol* 1995; **69**: 3389-3398
- 21 **Li YH**, Liu J, Xue CF. Construction of HBV targeted ribonuclease and its expression in 2.2.15 cell line. *Xibao yu Fenzi Mianyixue Zazhi* 2002; **18**: 217
- 22 **Ding J**, Liu J, Xue CF, Li YH, Gong WD. Construction and expression of prokaryotic expression vector for pTAT-HBV targeted ribonuclease. fusion protein. *Xibao yu Fenzi Mianyixue Zazhi* 2003; **19**: 49-51
- 23 **Raj V**. Treatment of hepatitis B. *Clin Cornerstone* 2001; **3**: 24-36
- 24 **Arai R**, Ueda H, Kitayama A, Kamiya N, Nagamune T. Design of linkers which effectively separate domains of a bifunctional fusion protein. *Protein Eng* 2001; **14**: 529-532
- 25 **Gustavsson M**, Lehtio J, Denman S, Teeri TT, Hult K, Martinelle M. Stable linker peptides for a cellulose-binding domain-lipase fusion protein expressed in *Pichia pastoris*. *Protein Eng* 2001; **14**: 711-715
- 26 **Stein A**, Dalal Y, Fleury TJ. Circle ligation of *in vitro* assembled chromatin indicates a highly flexible structure. *Nucleic Acids Res* 2002; **30**: 5103-5109
- 27 **Kiczak L**, Kasztura M, Koscielska-Kasprzak K, Dadlez M, Otlewski J. Selection of potent chymotrypsin and elastase inhibitors from M13 phage library of basic pancreatic trypsin inhibitor (BPTI). *Biochim Biophys Acta* 2001; **1550**: 153-163
- 28 **Reiter Y**, Schuck P, Boyd LF, Plaksin D. An antibody single-domain phage display library of a native heavy chain variable region: isolation of functional single-domain VH molecules with a unique interface. *J Mol Biol* 1999; **290**: 685-698
- 29 **Rojas G**, Almagro JC, Acevedo B, Gavilondo JV. Phage antibody fragments library combining a single human light chain variable region with immune mouse heavy chain variable regions. *J Biotechnol* 2002; **94**: 287-298
- 30 **Klug A**. Zinc finger peptides for the regulation of gene expression. *J Mol Biol* 1999; **293**: 215-218
- 31 **Tang L**, Li J, Katz DS, Feng JA. Determining the DNA bending angle induced by non-specific high mobility group-1 (HMG-1) proteins: a novel method. *Biochemistry* 2000; **39**: 3052-3060
- 32 **Gokhale RS**, Khosla C. Role of linkers in communication between protein modules. *Curr Opin Chem Biol* 2000; **4**: 22-27

Edited by Ren SY and Wang XL

Detection of anti-HAV antibody with dot immunogold filtration assay

Zhong-Jun Shao, De-Zhong Xu, Yong-Ping Yan, Jing-Hua Li, Jing-Xia Zhang, Zhi-Ying Zhang, Bo-Rong Pan

Zhong-Jun Shao, De-Zhong Xu, Yong-Ping Yan, Jing-Hua Li, Jing-Xia Zhang, Zhi-Ying Zhang, Department of Epidemiology, Fourth Military Medical University, Xi'an 710032, Shaanxi Province, China

Jing-Hua Li, Department of Traditional Chinese Medicine, Xijing Hospital, Fourth Military Medical University, Xi'an 710032, Shaanxi Province, China

Bo-Rong Pan, Oncology Center, Xijing Hospital, Fourth Military Medical University, Xi'an 710032, Shaanxi Province, China

Supported by National Natural Science Foundation of China, No 30230320

Correspondence to: De-Zhong Xu, Department of Epidemiology, Fourth Military Medical University, 169 Changle West Road, Xi'an 710032, China. xudezh@fmmu.edu.cn

Telephone: +86-29-3374871 **Fax:** +86-29-3374868

Received: 2003-03-04 **Accepted:** 2003-04-03

Abstract

AIM: To establish a rapid, sensitive and specific immunogold assay for detection of hepatitis A virus infection.

METHODS: Rabbit monoclonal antibodies to anti-human IgM and IgG (Dako) were dotted on a nitrocellulose membrane (NCM) respectively to capture the human sera IgM and IgG. Then the captured antibodies would conjugate to HAV antigen, which was revealed by mouse anti-HAV IgG conjugated to gold particles. Final results were assessed by blind method.

RESULTS: Sera from 96 patients with acute hepatitis were used for our study. Compared with well-recognized standard (Abbott Laboratory, USA), the sensitivity and specificity of IgM-DIGFA (self-made) were 91.3 % (42/46) and 96.0 % (48/50), and those of IgM-ELISA (Kehua, Shanghai) were 97.8 % (45/46) and 100.0 % (50/50). The identical results were produced from the study with reagents at different conditions, and the study was repeated in 15 negative sera and 10 positive sera. The serum anti-HAV IgG was tested with DIGFA at the same time. In comparison with ELISA, the sensitivity and specificity of DIGFA for IgG anti-HAV were 87.2 % (41/47) and 91.8 % (45/49), respectively.

CONCLUSION: This assay can detect anti-HAV IgM and IgG simultaneously, and be done within 3 minutes. The simplicity, rapidity and specificity of the assay were useful for screening and epidemiological study.

Shao ZJ, Xu DZ, Yan YP, Li JH, Zhang JX, Zhang ZY, Pan BR. Detection of anti-HAV antibody with dot immunogold filtration assay. *World J Gastroenterol* 2003; 9(7): 1508-1511
<http://www.wjgnet.com/1007-9327/9/1508.asp>

INTRODUCTION

Hepatitis A is a self-limiting disease and often a subclinical disorder^[1,2]. Since symptomatic hepatitis A infection can be clinically undistinguished from hepatitis B, C or E, serological

testing is an important tool in its diagnosis^[3-6]. Diagnosis of HAV infection depends mainly on the detection of specific antibody^[3,4]. Although enzyme linked immunosorbent assay (ELISA) and RT-PCR are currently used for the detection of HAV infection and meet most of the clinical requirements^[7-11], the two methods provide little information on prevention of diseases^[12-15]. Dot immunogold filtration assay for the detection of anti-HAV IgM was established^[16,17]. In our study a dot immunogold filtration assay was established to detect both anti-HAV IgM and IgG simultaneously.

MATERIALS AND METHODS

Sera

Blood samples were continuously collected from acute hepatitis inpatients in Xi'an Infectious Disease Hospital from March to October 2000 with permission of both the hospital and patients. Five milliliters of blood were drawn from each patient and the specimen was centrifuged at 3 000 r/min for 15 minutes to separate the serum. Ninety-six sera specimens were collected by the end of study. Anti-HAV IgM was detected as positive in 46, anti-HBc IgM in 31, anti-hepatitis C in 15, transmission-transmitted virus (TTV) in 3 by RT-PCR^[18]. No hepatitis virus markers were found in 6 specimens, and positive anti-HAV and HBV were detected simultaneously in 2 sera.

Preparation of probe

Colloidal gold was produced by citromalic acid trisodium recovery method. The colloidal gold solution was scanned between 400 nm and 700 nm by using a spectrophotometer. The batch with λ_{max} between 519 and 520 was used subsequently for conjugating with mouse anti-HAV IgG (CAPM). The pH was adjusted to 8.0 with 0.2 mol/L K_2CO_3 . Then mouse anti-HAV IgG (1 μ g per milliliter) was added into the colloidal gold solution and mixed for 30 minutes, then stored at 4 °C overnight. The pellet was collected by centrifugation at 15 000 r/min for 60 minutes, and the absorbance (A) was regulated by 0.02 mol/L PBS to the value of 1.5.

ELISA test for anti-HAV IgM and IgG

ELISA test was performed strictly according to instructions of the kit (anti-IgM kit from Kehua Biotech Co. and anti-IgG kit from Huaguang Biotech Co). Diluted sera (1:1 000) were incubated at 37 °C for one hour in a reactive well, and after washed, HAV Ag and anti-HAV peroxidase conjugates were added and incubated at 37 °C for 10 minutes, and followed by washing. Then the substrate was added, and the reaction was stopped by diluted sulfuric acid 10 minutes later. The absorbance was measured at 540 nm. An absorbance of 2.1 times the negative control value was considered as positive. The detecting procedures for HAV IgG were the same as for IgM except for serum dilution (1:50).

AXSYM HAVAB-M (Abbott Laboratory) was based on microparticle enzyme immunoassay technology^[19-21]. Samples and all AXSYM HAVAb-M reagents required for one test were pipetted with the sampling probe into wells in reactive vessel in the sampling center. The reaction vessel was immediately

transferred into the processing center. Further pipetting was done in the processing center by the processing probe. All steps were completed automatically and the diagnostic results were reported immediately.

DIGFA

There were 4 components in the kit: solid phase reaction board (SPRD, self-made), HAV Ag, color-developing reagents and lotion. Anti-human IgM and IgG antibodies (Dako, USA) were blotted onto small round nitrocellulose membranes (Hyclone, USA) separately, air-dried at room temperature, and then incubated in 20 g/L bovine serum albumin (BSA) overnight, and finally washed and air dried. These nitrocellulose membranes prepared were fitted in SPRD with coated side facing exteriorly. Then SPRD was filled with water-absorbed stuff. One drop of lotion (PBS-T, pH8.0 containing 05 g/L Tween20 and 20 g/L BSA) was added to prepare SPRD. 100 μ L of serum with dilution of 1:100 was added to each reaction well, and then washed with one drop of lotion. Then one drop of HAV Ag was added, and then was washed. Finally two drops of anti-HAV IgG colloidal gold conjugates were added, and then washed with one drop of lotion. A reddish dot with sharp margin was considered as positive.

Statistical analysis

The following definitions and formulae were used in this study. A true positive (a) sample was both reactive by DIGFA/ELISA and ABBOTT. A true negative (d) sample was nonreactive by both DIGFA/ELISA and ABBOTT. A false positive (b) sample was reactive by DIGFA/ELISA but negative by ABBOTT and a false negative (c) sample was negative by DIGFA/ELISA but positive by ABBOTT. The sensitivity of DIGFA was defined as the probability that a sample containing anti-HAV antibodies would be positive in DIGFA/ELISA. The specificity of DIGFA/ELISA was defined as the probability that a sample without anti-HAV antibodies would be negative in DIGFA/ELISA. Chi-square test was used.

RESULTS

Preparation of probe

Transmission electron microscopic studies revealed that the average diameter of the gold particle was 15 nm (15 \pm 0.7 nm). The maximum absorbing wavelength was 519 nm, indicating that the colloid gold met the experimental requirements. After purification of labeling anti-HAV IgG to gold particle, one drop of probe was added to SPRD coated by goat anti-mouse IgG and a pink dot appeared 30 seconds later, indicating effectiveness of the probe.



Figure 1 Detection of 24 sera from acute hepatitis inpatients by DIGFA. Red dot: positive; Left: anti-human IgG; Right: anti-human IgM.

Comparison of three diagnostic methods (Tables 1, 2 and 3)

Abbott kit has been widely recognized in the world, but its usage was limited in China due to the relatively high cost. The comparative analysis of 96 serum specimens showed that the sensitivity and specificity of IgM-ELISA were higher than those of IgM-DIGFA (Table 1). Statistical analysis (two tailed binomial probability test) showed no significant differences in sensitivity and specificity (Figure 1). Cross-reaction was found in DIGFA for anti-HAV IgM in a serum specimen, which was diagnosed as anti-HBV positive by ELISA.

Table 1 Comparison of DIGFA, ELISA and AXSYM HAVAb-M

	IgM	HAVAB-M (Abbott laboratory)		Total
		+	-	
DIGFA	+	42	2	44
	-	4	48	52
ELISA	+	45	0	45
	-	1	50	51

Sensitivity of IgM-DIGFA was 91.3 % (42/46) and specificity was 96.0 % (48/50). Sensitivity of IgM-ELISA was 97.8 % (45/46) and specificity was 100.0 % (50/50). There were no significant differences in sensitivity ($P=0.36$) and specificity ($P=0.49$).

Anti-HAV IgG and IgM were detected in all sera. ELISA kit was purchased from Huaguang Biotech Co, Xi'an, China. Forty-one of 96 sera specimens were detected as positive with both methods and 86 were diagnosed coincidentally. The sensitivity and specificity were 87.2 % (41/47) and 91.8 % (45/49), respectively (Table 2).

Table 2 Comparison of IgG-DIGFA with IgG-ELISA

IgG-DIGFA	IgG-ELISA		Total
	+	-	
+	41	4	45
-	6	45	51
Total	47	49	96

In this study, twenty-three sera specimens were detected as positive for IgG, and 30 as negative for both IgM and IgG, which indicated that some individuals in general population were possibly susceptible to HAV infection (Table 3).

Table 3 Analysis of anti-HAV IgG and IgM by DIGFA method

Anti-HAV IgG	Anti-HAV IgM		Total
	+	-	
+	23	22	45
-	21	30	51
Total	44	52	96

Repeatability and stability

All reagents could be stored effectively at 4 $^{\circ}$ C for 3 months, at room temperature for 15 days and at 48 $^{\circ}$ C for 2 days. Fifteen negative and ten positive sera samples were selected randomly and detected with reliable results.

DISCUSSION

Detection of antibody against hepatitis A virus

DIGFA is a new technique of solid phase labeled immunoassay,

in which NCM is used as a support and colloidal gold as the label, and the principle of filtration is adapted for the rapid reaction of antigen and antibody^[22,23]. The use of visible gold-conjugated monoclonal antibody instead of enzyme in ELISA makes the test simple^[24]. The sensitivity of DIGFA is lower than that of ELISA. This method can detect two kinds of anti-HAV antibodies simultaneously that are similar to protein biochip, but the cost is much lower than that of biochip^[25]. It is very suitable for screening and vaccination program^[26-29]. IgM antibody persists for 3 to 6 months afterwards, and is seldom found after vaccination. Patients with asymptomatic hepatitis A may have detectable anti-HAV IgM for a shorter period than patients with symptomatic diseases^[30]. Although anti-HAV IgG may be present at early stage of infection, it is always accompanied by anti-HAV IgM at the onset of illness. Anti-HAV IgG alone indicates a past infection and persists for decades after acute HAV infection, reflecting recovery and resistance to reinfection^[31,32]. However, detection of anti-HAV IgG is often ignored due to its limited clinical value, but it can show whether a person is susceptible to HAV and offer a good instruction to health workers. Twenty-two sera were detected as negative for both anti-HAV IgM and IgG, which indicated that these people need to be vaccinated.

Comparison with ELISA

The sensitivity and specificity of IgM-DIGFA for HAV in these sera were lower than those of IgM-ELISA. However, there was no significant difference in specificity of both assays. IgM-DIGFA can be used as an eligible assay to screen HAV infection for its rapidity and specificity. It takes a few minutes to complete the whole process by DIGFA, and the detection of 30 sera specimens can be done within 30 minutes. Shortened reaction time gives a proper explanation to the lower sensitivity of IgM-DIGFA. A cost-analysis of DIGFA and ELISA was done, and found that pure reagents cost of DIGFA was 0.75 Yuan (RMB) and that of anti-HAV IgM ELISA was 1.20 Yuan (RMB). It was not as expensive as expected and two kinds of antibodies were detected at one time^[33]. All the reagents leaked through NCM and took a full reaction with antibodies attached to NCM. This was due to the effect of immunoenhancement^[34]. It is easy to tell the results without the help of extra apparatus. Therefore, it can be widely used in an epidemiological survey.

REFERENCES

- 1 **De Paula VS**, Saback FL, Gaspar AM, Niel C. Mixed infection of a child care provider with hepatitis A virus isolates from subgenotypes IA and IB revealed by heteroduplex mobility assay. *J Virol Methods* 2003; **107**: 223-228
- 2 **Sedyaningsih-Mamahit ER**, Larasati RP, Laras K, Sidemen A, Sukri N, Sabaruddin N, Didi S, Saragih JM, Myint KS, Endy TP, Sulaiman A, Campbell JR, Corwin AL. First documented outbreak of hepatitis E virus transmission in Java Indonesia. *Trans R Soc Trop Med Hyg* 2002; **96**: 398-404
- 3 **Yayli G**, Kilic S, Ormeci AR. Hepatitis agents with enteric transmission an epidemiological analysis. *Infection* 2002; **30**: 334-337
- 4 **Koff RS**. Prevention of Viral Hepatitis. *Curr Treat Options Gastroenterol* 2002; **5**: 451-463
- 5 **Han LH**, Sun WS, Ma CH, Zhang LN, Liu SX, Zhang Q, Gao LF, Chen YH. Detection of soluble TRAIL in HBV infected patients and its clinical implications. *World J Gastroenterol* 2002; **8**: 1077-1080
- 6 **Jiang YG**, Wang YM, Li QF. Expression and significance of HLA-DR antigen and heat shock protein 70 in chronic hepatitis B. *Shijie Huaren Xiaohua Zazhi* 2001; **9**: 907-910
- 7 **Jean J**, Blais B, Darveau A, Fliss I. Simultaneous detection and identification of hepatitis A virus and rotavirus by multiplex nucleic acid sequence-based amplification (NASBA) and microtiter plate hybridization system. *J Virol Methods* 2002; **105**: 123-132
- 8 **Li JW**, Wang XW, Yuan CQ, Zheng JL, Jin M, Song N, Shi XQ, Chao FH. Detection of enteroviruses and hepatitis A virus in water by consensus primer multiplex RT-PCR. *World J Gastroenterol* 2002; **8**: 699-702
- 9 **Vernozy-Rozand C**, Feng P, Montet MP, Ray-Gueniot S, Villard L, Bavai C, Meyrand A, Mazuy C, Atrache V. Detection of *Escherichia coli* O157:H7 in heifers' faecal samples using an automated immunoenrichment system. *Lett Appl Microbiol* 2000; **30**: 217-222
- 10 **Rood JC**, Lovejoy JC, Tulley RT. Comparison of a radioimmunoassay with a microparticle enzyme immunoassay of insulin for use with the minimal model method of determining whole-body insulin sensitivity. *Diabetes Technol Ther* 1999; **1**: 463-468
- 11 **Koraka P**, Zeller H, Niedrig M, Osterhaus AD, Groen J. Reactivity of serum samples from patients with a flavivirus infection measured by immunofluorescence assay and ELISA. *Microbes Infect* 2002; **4**: 1209-1215
- 12 **Nikolova M**, Liubomirova M, Iliev A, Krasteva R, Andreev E, Radenkova J, Minkova V, Djerassi R, Kiperova B, Vlahov ID. Clinical significance of antinuclear antibodies, anti-neutrophil cytoplasmic antibodies and anticardiolipin antibodies in heroin abusers. *Isr Med Assoc J* 2002; **4**: 908-910
- 13 **Nikolaeva LI**, Blokhina NP, Tsurikova NN, Voronkova NV, Miminoshvili MI, Braginsky DM, Yastrebova ON, Boynitskaya OB, Isaeva OV, Michailov MI, Archakov AI. Virus-specific antibody titres in different phases of hepatitis C virus infection. *J Viral Hepat* 2002; **9**: 429-437
- 14 **Zhao YL**, Meng ZD, Xu ZY, Guo JJ, Chai SA, Duo CG, Wang XY, Yao JF, Liu HB, Qi SX, Zhu HB. H2 strain attenuated live hepatitis A vaccines: Protective efficacy in a hepatitis A outbreak. *World J Gastroenterol* 2000; **6**: 829-832
- 15 **Santos DC**, Souto FJ, Santos DR, Vitral CL, Gaspar AM. Seroepidemiological markers of enterically transmitted viral hepatitis A and E in individuals living in a community located in the North Area of Rio de Janeiro, RJ. *Brazil Mem Inst Oswaldo Cruz* 2002; **97**: 637-640
- 16 **Han FC**, Hou Y, Yan XJ, Xiao LY, Guo YH. Dot immunogold filtration assay for rapid detection of anti-HAV IgM in Chinese. *World J Gastroenterol* 2000; **6**: 400-401
- 17 **Wu W**, Xu DZ, Yan YP, Zhang JX, Liu Y, Li RL. Evaluation of dot immunogold filtration assay for anti-HAV IgM antibody. *World J Gastroenterol* 1999; **5**: 132-134
- 18 **Hu ZJ**, Lang ZW, Zhou YS, Yan HP, Huang DZ, Chen WR, Luo ZX. Clinicopathological study on TTV infection in hepatitis of unknown etiology. *World J Gastroenterol* 2002; **8**: 288-293
- 19 **el Saadany S**, Gully P, Giulivi A. Hepatitis A, B, and C in Canada. Results from the national sentinel health unit surveillance system, 1993-1995. *Can J Public Health* 2002; **93**: 435-438
- 20 **Keevil BG**, McCann SJ, Cooper DP, Morris MR. Evaluation of a rapid micro-scale assay for tacrolimus by liquid chromatography-tandem mass spectrometry. *Ann Clin Biochem* 2002; **39**: 487-492
- 21 **Dietemann J**, Berthoux P, Gay-Montchamp JP, Batie M, Berthoux F. Comparison of ELISA method versus MEIA method for daily practice in the therapeutic monitoring of tacrolimus. *Nephrol Dial Transplant* 2001; **16**: 2246-2249
- 22 **Hirota WK**, Duncan MB, Hirota WK, Tsuchida A. The utility of prescreening for hepatitis A in military recruits prior to vaccination. *Mil Med* 2002; **167**: 907-910
- 23 **Yang SS**, Wu CH, Chen TH, Huang YY, Huang CS. TT viral infection through blood transfusion: retrospective investigation on patients in a prospective study of post-transfusion hepatitis. *World J Gastroenterol* 2000; **6**: 70-73
- 24 **Lu J**, Xu WX, Zhan YQ, Cui XL, Cai WM, He FC, Yang XM. Identification and characterization of a novel isoform of hepatopietin. *World J Gastroenterol* 2002; **8**: 353-356
- 25 **Moreno-Bondi MC**, Alarie JP, Vo-Dinh T. Multi-analyte analysis system using an antibody-based biochip. *Anal Bioanal Chem* 2003; **375**: 120-124
- 26 **Acharya SK**, Batra Y, Saraya A, Hazari S, Dixit R, Kaur K, Bhatkal B, Ojha B, Panda SK. Vaccination for hepatitis A virus is not re-

- quired for patients with chronic liver disease in India. *Natl Med J India* 2002; **15**: 267-268
- 27 **Wang KX**, Li CP, Wang J, Tian Y. Cyclospore cayetanensis in Anhui, China. *World J Gastroenterol* 2002; **8**: 1144-1148
- 28 **Ohno H**, Ujiie N, Takeuchi C, Sato A, Hayashi A, Ishiko H, Nishizawa T, Okamoto H. Vertical transmission of hepatitis viruses collaborative study group. TT virus infection during childhood. *Transfusion* 2002; **42**: 892-898
- 29 **Fleming J**. Current treatments for hepatitis. *J Infus Nur* 2002; **25**: 379-382
- 30 **Jarvis B**, Figgitt DP. Combined Two-Dose Hepatitis A and B Vaccine (AmBrix trade mark). *Drugs* 2003; **63**: 207-213
- 31 **Hu NZ**, Hu YZ, Shi HJ, Liu GD, Qu S. Mutational characteristics in consecutive passage of rapidly replicating variants of hepatitis A virus strain H2 during cell culture adaptation. *World J Gastroenterol* 2002; **8**: 872-878
- 32 **Edoute Y**, Malberger E, Tibon-Fishe O, Assy N. Non-imaging-guided fine-needle aspiration of liver lesions: a retrospective study of 279 patients. *World J Gastroenterol* 1999; **5**: 98-102
- 33 **Shyu RH**, Shyu HF, Liu HW, Tang SS. Colloidal gold-based immunochromatographic assay for detection of ricin. *Toxicon* 2002; **40**: 255-258
- 34 **Vernozzy-Rozand C**, Ray-Gueniot S, Ragot C, Bavai C, Mazuy C, Montet MP, Bouvet J, Richard Y. Prevalence of Escherichia coli O157:H7 in industrial minced beef. *Lett Appl Microbiol* 2002; **35**: 7-11

Edited by Ren SY and Wang XL

Generation of cytotoxic T cell against HBcAg using retrovirally transduced dendritic cells

Chuan-Lin Ding, Kun Yao, Tian-Tai Zhang, Feng Zhou, Lin Xu, Jiang-Ying Xu

Chuan-Lin Ding, Kun Yao, Feng Zhou, Department of Microbiology and Immunology, Nanjing Medical University, Nanjing 210029, Jiangsu Province, China

Tian-Tai Zhang, Department of Medicine, Affiliated Hospital of Lanzhou Medical College, Lanzhou 730000, Gansu Province, China
Lin Xu, Jiang-Ying Xu, Gene Center of Nanjing Military Medical College, Nanjing 210099, Jiangsu Province, China

Supported by a grant from Key Lab Programs of Jiangsu Province, No. k2030

Correspondence to: Professor Kun Yao, Department of Microbiology and Immunology, Nanjing Medical University, Nanjing 210029, Jiangsu Province, China. yaokun@njmu.edu.cn

Telephone: +86-25-6662901 **Fax:** +86-25-6508960

Received: 2003-01-14 **Accepted:** 2003-03-05

Abstract

AIM: Cytotoxic T lymphocytes (CTLs) play an important role in resolving HBV infection. In the present study, we attempted to evaluate the efficiency of bone marrow-derived dendritic cells (DCs) transduced with recombinant retroviral vector bearing hepatitis B virus (HBV) core gene and the capability of generating CTLs against HBcAg by genetically modified DCs *in vivo*.

METHODS: A retroviral vector containing HBV core gene was constructed. Replicating DC progenitor of C57BL/6 mice was transduced by retroviral vector and continually cultured in the presence of recombinant mouse granulocyte-macrophage colony-stimulating factor (rmGM-CSF) and interleukin-4 (IL-4) for 6 days. LPS was added and cultured for additional two days. The efficiency of gene transfer was determined by PCR, Western blot and FACS. Transduced DCs immunized C57BL/6 mice subcutaneously 2 times at an one-week interval. Intracellular IFN- γ and IL-4 of immunized mice lymphocytes were analyzed. Generation of CTLs in lymphocytes stimulated with mitomycin C-treated EL4-C cell which stably expresses HBcAg was determined by LDH release assays.

RESULTS: Recombinant retroviral expression vector (pLCSN) was positively detected by PCR as well as enzyme digestion with *EcoRI* and *BamHI*. Retroviruses were generated by pLCSN transfection packing cell and the virus titer was 3×10^5 CFU/ml. Indirect immunofluorescence and FACS showed that HBV core gene was expressed in murine fibroblasts. Transduced bone marrow cells had capability of differentiating into DCs *in vitro* in the presence of rmGM-CSF and rmIL-4. The result of PCR showed that HBV core gene was integrated into the genome of transduced DCs. Western blot analysis showed that HBV core gene was expressed in DCs. The transduction rate was 28 % determined by FACS. Retroviral transduction had no influence on DCs expressions of CD80 and MHC class II. HBcAg specific CTLs and Th1 type immune responses could be generated in the mice by using transduced DCs as antigen presenting cells (APCs).

CONCLUSION: Retroviral transduction of myeloid DCs

progenitors expresses efficiently HBcAg, and genetically modified DCs evoke a higher CTLs response than HBcAg *in vivo*.

Ding CL, Yao K, Zhang TT, Zhou F, Xu L, Xu JY. Generation of cytotoxic T cell against HBcAg using retrovirally transduced dendritic cells. *World J Gastroenterol* 2003; 9(7): 1512-1515
<http://www.wjgnet.com/1007-9327/9/1512.asp>

INTRODUCTION

Individuals with chronic hepatitis B virus (HBV) infection have a high risk of developing liver cirrhosis and primary hepatocellular carcinoma. Current treatments for chronic HBV infection are poorly efficacious^[1-3].

Cytotoxic T lymphocytes (CTLs) are thought to contribute to HBV clearance by killing infected hepatocytes and secreting antiviral cytokines. Acutely infected patients characteristically produce a vigorous, polyclonal, and multispecific CTLs response that is usually sufficient to clear the infection, while persistently infected patients produce a weak or undetectable HBV-specific CTLs response. The cumulated data suggest that CTLs activity may play an important role in resolving HBV infection^[4-13]. Based on these observations, therapeutic enhancement of T cell responsiveness to HBV has the potential to terminate chronic HBV infection.

Dendritic cells (DCs) are highly specialized antigen presenting cells (APCs) that possess unique immunostimulatory properties and function as the principal activators of naïve T cells^[14,15]. DCs are distributed throughout the body and can be expanded with granulocyte-macrophage CSF (GM-CSF) and IL-4. When DCs are pulsed with antigen protein or peptide, they can induce specific antibody and CTLs responses both *in vitro* and *in vivo*. Since activated DCs express a high level of costimulatory molecules and secrete inflammatory cytokines, they have the potential to activate anergic T cells.

In the present study, we attempted to induce CTLs response using retrovirally transduced DCs. The results demonstrated that administration of retrovirally transduced DCs could evoke HBcAg-specific CTLs responses in mice.

MATERIALS AND METHODS

Generating expression vector

The full-length HBV core gene was generated by PCR amplification from pADR (kindly provided by Prof. Zheng-Hong Yuan) which contains complement nucleotide sequence of HBV subtype adr with a pair of primers (5' - TGTGAATTC TGGCTTTGGGCATGGACATTG - 3', corresponding to the nucleotide sequence 1891-1912 of HBV genome with an additional *EcoRI* restriction site, and 5' - GCTGGATCCAGTTTCCCACCTTATGAGTCCA - 3', corresponding to the nucleotide sequence 2462-2483 of HBV genome with an additional *BamHI* restriction site). After digestion with *EcoRI* and *BamHI*, PCR products were inserted downstream of LTR of retroviral vector pLXSN (Clontech, USA) to obtain a recombinant retroviral expression vector pLCSN.

Virus production

To produce retroviral virus, packing cell (PT67, Clontech, USA) was cultured in a 24 well culture plate with D-MEM containing 10 % heat-inactivated FBS and transfected with 1 µg of retroviral vector plCSN by lipofectAMINE2000 (GIBCO, USA). Colonies were isolated by neomycin selectin (G418, Amresco, USA) and expanded. Supernatants of cloned packing cells were harvested, filtered (0.45 µm pore size), and tested for the presence of virus. Viral titration was performed on NIH3T3 according to the instructions of the manufacturer yielding a titer of 3×10^5 infectious particles/ml.

DC culture, transduction and immunization

Bone marrow cells were collected from femurs of C57BL/6 mouse and depleted of red cells with ammonium chloride. After extensively washed with RPMI1640, cells (5×10^5 cells/ml) in RPMI1640 supplemented with 10 % FBS, 500 U/ml rmGM-CSF and 250 U/ml rmIL-4 were plated in a 24 well culture plate, incubated at 37 °C in 5 % CO₂-atmosphere. After 24-h incubation, the cells were transduced with retroviral supernatants and polybrene (Sigma, USA) at a final concentration of 8 µg/ml. The cells were incubated at 37 °C, in 5 % CO₂ atmosphere for 2-3 h. The supernatant was replaced with RPMI1640 supplemented with 10 % FBS, 500 U/ml rmGM-CSF and 250 U/ml rmIL-4 overnight. The transduction procedure was repeated 3 times. After 6 days, LPS (1 µg/ml) was added and mature DC was obtained after additional culture for 2 days. The cells were washed three times, and 5×10^5 DCs suspended in 0.5 ml of PBS were injected subcutaneously. The immunization was repeated after 7 days.

Polymerase chain reaction

DNA from retrovirally transduced and untransduced DCs was isolated according to the manufacturer's protocol (Boehringer, Germany). DNA was isolated from the G418 resistant PT67 cell line as positive control. Primers used for amplification of HBcAg were mentioned above. PCR was performed for 1 min at 94 °C, for 1 min at 54 °C, and for 1 min at 72 °C for 30 cycles, followed by a final extension time of 6 min at 72 °C. The PCR product was resolved on a 1.5 % agarose gel.

Western blot analysis of HBcAg

Cell lysates were made from retrovirally transduced and untransduced DCs. Protein samples were separated by SDS-PAGE and transferred to nitrocellulose. HBcAg protein was identified using the anti-HBc positive serum as primary Ab and goat anti-human IgG peroxidase-conjugate (1:500, volume ratio) as secondary Ab. The blots were developed using substrate solution containing DAB and H₂O₂.

Intracellular cytokine analysis

Spleen lymphocytes were stimulated with Con A at 20 µg/ml, and 1 µl GolgiPlug™ was added for every 1 ml of cell culture to inhibit cytokine secretion. Lymphocytes were incubated for 6 hours, then harvested and washed with staining buffer. Cells were thoroughly resuspended and 100 µl of cytofix/cytoperm solution was added into each well for 20 min at 4 °C. Cells were washed and stained with FITC-labeled anti-mouse IFN-γ and PE-labeled anti-mouse IL-4, incubated at 4 °C for 30 min in the dark, then washed twice and analyzed with a flow cytometer.

CTL_s assay

The tumor cell line EL4 (H-2^b) was transduced with recombinant retrovirus and then selected in the presence of 400 µg/ml G418. The G418-resistant clones (EL4-C) were screened for HBcAg expression by PCR and indirect

immunofluorescence. Spleen cells obtained from individual mice were stimulated with EL4-C treated by 25 µg/ml mitomycin C at effector:stimulator ratio of 20. The specific CTLs were expanded by adding 50 IU/ml of IL-2 for 7 days. The CTLs activity in the cultures was measured in triplicate in a standard four-hour LDH release assay using EL4-C cells as target cells according to the manufacturer's instructions (Roche, Switzerland).

RESULTS

Generation of retroviral expression vector and retrovirus

The HBV core gene fragment generated by PCR amplification and digested with *EcoRI* and *BamHI* was successfully cloned into downstream of LTR of pLXSN to obtain recombinant retroviral expression vector pLCSN (Figure 1). Recombinant retroviral vector was positively detected by PCR as well as enzyme digestion with *EcoRI* and *BamHI*. To produce retroviral virus, packing cells were transfected with retroviral expression vector pLCSN. Colonies were isolated by neomycin selectin and expanded. Supernatants of G418 resistant cells were harvested. The virus titer was 3×10^5 infectious particles/ml. It was found that retroviruses could infect a number of eukaryotic cells, such as NIH3T3, EL4, and SP2/0 (data not shown).

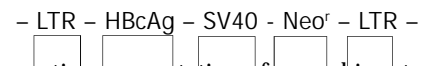


Figure 1 Schematic representation of recombinant retroviral vector pLCSN.

Retroviral transduction of bone marrow cells and differentiation into DCs

To assess the expression of HBcAg in DCs, we transduced bone marrow cells from C57BL/6 mice in packing cell supernatants. The transduced cells were then cultured in the presence of rmGM-CSF, rmIL-4 and LPS for the purpose of differentiation into mature DCs. After cultured for 8 days, the majority of cells displayed distinct DC morphology with many fine dendrites. Retroviral transduction had no influence on DCs expressions of CD80 and class II molecule of MHC (72.94 % versus 73.43 %, 86.54 % versus 91.75 %, respectively). T-cell stimulatory activity of DCs in MLR was expressed as stimulation index (SI) value, at a T cell:DC ratio of 80:1, 40:1, 20:1 and 10:1. The SI values were 3.16, 7.26, 23.99, 31.70, respectively. The HBV core gene in transduced DCs was demonstrated by PCR (Figure 2). Approximately 28 % of the bone marrow derived cells could express HBcAg determined by flow cytometric analysis. Finally, Western blot analysis demonstrated that HBcAg was expressed in transduced DCs (Figure 3).

Induction of CTLs responses *in vivo*

Next we evaluated the capability of retrovirally transduced DCs to induce CTLs responses *in vivo*. C56BL/6 mice were immunized subcutaneously with 5×10^5 DCs transduced with HBcAg. The immunization was repeated after one week. 7 days after the last immunization, the mice were sacrificed and splenocytes were collected. Splenocytes were restimulated *in vitro* for 7 days in the presence of mitomycin C-treated EL4-C cell and IL-2, and then cocultivated with different target cells at varied E:T ratios to measure target cell lysis with LDH release cytotoxic assay. As shown in Figure 4, splenocytes from mice immunized with transduced DCs demonstrated significantly higher cytotoxicity than those from controlled mice. To determine the type of Th responses, we measured the lymphocyte which could secrete IFN-γ or IL-4 with intracellular cytokine analysis. After immunization of retrovirally transduced DCs in mice, lymphocyte producing IFN-γ was significantly higher than that from mice injected

only with untransduced DCs (1.15 % versus 0.28 %). At the same time, lymphocyte producing IL-4 in both mice with injections of transduced and untransduced DCs was similar (0.74 % versus 0.47 %).

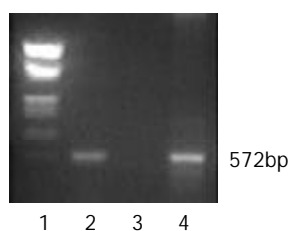


Figure 2 PCR analysis of HBV core gene in retrovirally transduced DCs. 1. Marker; 2. Transduced DCs; 3. Untransduced DCs; 4. G418 resistant PT67 cell.

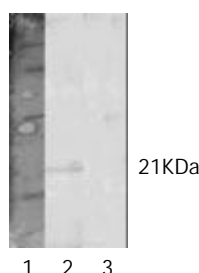


Figure 3 Western blot analysis of HBcAg expression in retrovirally transduced DCs. 1. Marker; 2. Transduced DCs; 3. Untransduced DCs.

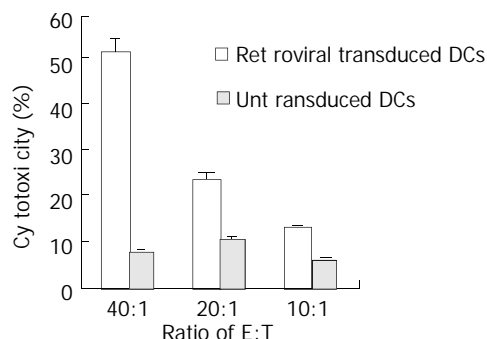


Figure 4 Induction of CTLs against HBcAg responses *in vivo*.

DISCUSSION

Chronic HBV infection has a significant association with liver cirrhosis and hepatocellular carcinoma. Studies on immunological mechanisms have demonstrated that CTLs play a critical role in the control and termination of HBV infection. CTLs are thought to contribute to HBV clearance by killing infected hepatocytes and secreting antiviral cytokines. Acutely infected patients characteristically produce a vigorous, polyclonal, and multispecific CTLs response that is usually sufficient to clear the infection, while persistently infected patients produce weak or undetectable HBV-specific CTLs responses^[4-13]. Based on these observations, therapeutic enhancement of T cell responsiveness to HBV has the potential to terminate chronic HBV infection.

A number of experimental reports showed that CTLs responses could be induced. Vaccination with HBsAg-anti-HBs immune complex could affect HBeAg seroconversion and clearance of serum HBV DNA in patients^[16]. Sallberg *et al*^[17] observed a marked decrease of HBV DNA level and seroconversion of HBeAg to anti-HBe in sera of experimental

chimpanzees after immunization of HBV core gene using retrovirus. Plasmid DNA immunization has been shown to induce specific antibody and CTLs responses in normal mice and rhesus monkeys^[18-20]. ISCOMS-based hepatitis B polypeptide vaccine could also induce a higher CTLs response *in vivo*^[21].

DCs play a central role in humoral and cellular immunity because they can take up and process antigen in peripheral tissues and present the antigen to T cells in secondary lymphoid tissues, such as lymph nodes. The mature DCs screen for passing antigen-specific naïve T cell, and induce primary T cell-mediated immune response. Mature DCs are thought to be functionally competent and have been used in clinical studies to induce antigen-specific T cells^[14,15,22,23]. In this study, we used DCs as an attractive approach for immunotherapy of chronic HBV infection. In developing strategies to optimize the use of DCs in immunotherapy, viral transduction of DCs with antigen genes may offer more advantages over peptide-pulsed DCs. The efficacy of peptide-pulsed DCs might be limited *in vivo*, because peptides pulsed onto DCs stay bound to MHC molecules only transiently. Additionally, use of peptide-pulsed DCs is dependent on the knowledge of the HLA haplotype of patients. Transduction of DCs by viral vectors can produce a high level of antigen expression, and endogenous protein synthesis may allow presentation of antigens by class I molecules of MHC, resulting in induction of CD8⁺ CTLs responses. Several viruses have the potential for use in immunotherapy, such as vaccinia virus, adenovirus, and retrovirus^[24]. Retroviral transduction of DCs may allow constitutive expression of protein leading to prolonged antigen presentation *in vivo*, and presentation of multiple or unidentified antigen epitopes in the context of class I and II molecules of MHC. But as nonreplicating, mature DCs are poor candidates for retroviral gene modification. However, dividing bone marrow progenitor cells can be efficiently transduced with retroviral vectors^[25-29]. In this study, rapidly dividing bone marrow progenitor cells were used as targets for retroviral transduction and cultured in the presence of GM-CSF and IL-4 plus LPS. Our results showed that retrovirally transduced progenitor cells could differentiate into mature DCs *in vitro*, transduced or untransduced dendritic cells expressed comparable levels of CD80 and class II of MHC, the transduction efficiency was about 28%. Retrovirally transduced DCs could be used to induce strong CTLs responses in C57BL/6 mice *in vivo*.

Previous studies showed that Th1 type response was beneficial for the clearance of chronically infected viruses^[30,31]. The profiles of cytokine production were indicators of helper T cell responses. IFN- γ and IL-4 were observed in the present experiment as Th1 and Th2 type cytokines, respectively. After immunization of retroviral transduced DCs, lymphocyte producing IFN- γ was significantly higher than that from mice injected only with untransduced DCs, indicating Th1 type immune responses occurred in mice immunized with retroviral transduced DCs.

These results together with other studies support the ongoing efforts to develop genetically modified DCs for immunotherapy of chronic HBV infection. Further study is underway to determine whether this genetically modified DCs can break the immune tolerance in the HBV transgenic mouse model.

REFERENCES

- Gow PJ, Mutimer D. Treatment of chronic hepatitis. *BMJ* 2001; **323**: 1164-1167
- Malik AH, Lee WM. Chronic hepatitis B virus infection: treatment strategies for the next millennium. *Ann Intern Med* 2000; **132**: 723-731

- 3 **Locamini SA**, Bartholomeusz A, Delaney WE. Evolving therapies for the treatment of chronic hepatitis B virus infection. *Expert Opin Investig Drugs* 2002; **11**: 169-187
- 4 **Sette AD**, Oseroff C, Sidney J, Alexander J, Chesnut RW, Kakimi K, Guidotti LG, Chisari FV. Overcoming T cell tolerance to the hepatitis B virus surface antigen in hepatitis B virus-transgenic mice. *J Immunol* 2001; **166**: 1389-1397
- 5 **Maini MK**, Bertoletti A. How can the cellular immune response control hepatitis B virus replication? *J Viral Hepat* 2000; **7**: 321-326
- 6 **Guidotti LG**, Chisari FV. Noncytolytic control of viral infections by the innate and adaptive immune response. *Annu Rev Immunol* 2001; **19**: 65-91
- 7 **Sing GK**, Ladhams A, Arnold S, Parmar H, Chen X, Cooper J, Butterworth L, Stuart K, D'Arcy D, Cooksley WG. A longitudinal analysis of cytotoxic T lymphocyte precursor frequencies to the hepatitis B virus in chronically infected patients. *J Viral Hepat* 2001; **8**: 19-29
- 8 **Thimme R**, Wieland S, Steiger C, Ghraeyeb J, Reimann KA, Purcell RH, Chisari FV. CD8(+) T cells mediate viral clearance and disease pathogenesis during acute hepatitis B virus infection. *J Virol* 2003; **77**: 68-76
- 9 **Cao T**, Desombere I, Vanlandschoot P, Sällberg M, Leroux-Roels G. Characterization of HLA DR13-restricted CD4⁺ T cell epitopes of hepatitis B core antigen associated with self-limited, acute hepatitis B. *J Gen Virol* 2002; **83**: 3023-3033
- 10 **Kimura K**, Kakimi K, Wieland S, Guidotti LG, Chisari FV. Activated intrahepatic antigen-presenting cells inhibit hepatitis B virus replication in the liver of transgenic mice. *J Immunol* 2002; **169**: 5188-5195
- 11 **Guidotti LG**. The role of cytotoxic T cells and cytokines in the control of hepatitis B virus infection. *Vaccine* 2002; **20**(Suppl 4): A80-82
- 12 **Kakimi K**, Isogawa M, Chung J, Sette A, Chisari FV. Immunogenicity and tolerogenicity of hepatitis B virus structural and nonstructural proteins: implications for immunotherapy of persistent viral infections. *J Virol* 2002; **76**: 8609-8620
- 13 **Maini MK**, Boni C, Lee CK, Larrubia JR, Reignat S, Ogg GS, King AS, Herberg J, Gilson R, Alisa A, Williams R, Vergani D, Naoumov NV, Ferrari C, Bertoletti A. The role of virus-specific CD8(+) cells in liver damage and viral control during persistent hepatitis B virus infection. *J Exp Med* 2000; **191**: 1269-1280
- 14 **Banchereau J**, Schuler-Thurner B, Palucka AK, Schuler G. Dendritic cells as vectors for therapy. *Cell* 2001; **106**: 271-274
- 15 **Guernonprez P**, Valladeau J, Zitvogel L, Thery C, Amigorena S. Antigen presentation and T cell stimulation by dendritic cells. *Annu Rev Immunol* 2002; **20**: 621-667
- 16 **Wen YM**, Qu D, Zhou SH. Antigen-antibody complex as therapeutic vaccine for viral hepatitis B. *Int Rev Immunol* 1999; **18**: 251-258
- 17 **Sallberg M**, Hughes J, Javadian A, Ronlov G, Hultgren C, Townsend K, Anderson CG, O' Dea J, Alfonso J, Eason R, Murthy KK, Jolly DJ, Chang SM, Mento SJ, Milich D, Lee WT. Genetic immunization of chimpanzees chronically infected with the hepatitis B virus, using a recombinant retroviral vector encoding the hepatitis B virus core antigen. *Hum Gene Ther* 1998; **9**: 1719-1729
- 18 **Huang ZH**, Zhuang H, Lu S, Guo RH, Xu GM, Cai J, Zhu WF. Humoral and cellular immunogenicity of DNA vaccine based on hepatitis B core gene in rhesus monkeys. *World J Gastroenterol* 2001; **7**: 102-106
- 19 **Thermet A**, Rollier C, Zoulim F, Trepo C, Cova L. Progress in DNA vaccine for prophylaxis and therapy of hepatitis B. *Vaccine* 2003; **21**: 659-662
- 20 **Michel ML**, Loirat D. DNA vaccines for prophylactic or therapeutic immunization against hepatitis B. *Intervirology* 2001; **44**: 78-87
- 21 **Guan XJ**, Guan XJ, Wu YZ, Jia ZC, Shi TD, Tang Y. Construction and characterization of an experimental ISCOMS-based hepatitis B polypeptide vaccine. *World J Gastroenterol* 2002; **8**: 294-297
- 22 **You Z**, Huang XF, Hester J, Rollins L, Rooney C, Chen SY. Induction of vigorous helper and cytotoxic T cell as well as B cell responses by dendritic cells expressing a modified antigen targeting receptor-mediated internalization pathway. *J Immunol* 2000; **165**: 4581-4591
- 23 **Stober D**, Trobonjaca Z, Reimann J, Schirmbeck R. Dendritic cells pulsed with exogenous hepatitis B surface antigen particles efficiently present epitopes to MHC class I-restricted cytotoxic T cells. *Eur J Immunol* 2002; **32**: 1099-1108
- 24 **Jenne L**, Schuler G, Steinkasserer A. Viral vectors for dendritic cell-based immunotherapy. *Trends Immunol* 2001; **22**: 102-107
- 25 **Nakamura Y**, Suda T, Nagata T, Aoshi T, Uchijima M, Yoshida A, Chida K, Koide Y, Nakamura H. Induction of protective immunity to listeria monocytogenes with dendritic cells retrovirally transduced with a cytotoxic T lymphocyte epitope minigene. *Infect Immun* 2003; **71**: 1748-1754
- 26 **Lapointe R**, Royal RE, Reeves ME, Altomare I, Robbins PF, Hwu P. Retrovirally transduced human dendritic cells can generate T cells recognizing multiple MHC class I and class II epitopes from the melanoma antigen glycoprotein 100. *J Immunol* 2001; **167**: 4758-4764
- 27 **Meyer zum Buschenfelde C**, Nicklisch N, Rose-John S, Peschel C, Bernhard H. Generation of tumor-reactive CTL against the tumor-associated antigen HER2 using retrovirally transduced dendritic cells derived from CD34⁺ hemopoietic progenitor cells. *J Immunol* 2000; **165**: 4133-4140
- 28 **Takayama T**, Kaneko K, Morelli AE, Li W, Tahara H, Thomson AW. Retroviral delivery of transforming growth factor-beta1 to myeloid dendritic cells: inhibition of T-cell priming ability and influence on allograft survival. *Transplantation* 2002; **74**: 112-119
- 29 **Akiyama Y**, Maruyama K, Watanabe M, Yamaguchi K. Retroviral-mediated IL-12 gene transduction into human CD34⁺ cell-derived dendritic cells. *Int J Oncol* 2002; **21**: 509-514
- 30 **Wang FS**, Xing LH, Liu MX, Zhu CL, Liu HG, Wang HF, Lei ZY. Dysfunction of peripheral blood dendritic cells from patients with chronic hepatitis B virus infection. *World J Gastroenterol* 2001; **7**: 537-541
- 31 **Livingston BD**, Alexander J, Crimi C, Oseroff C, Celis E, Daly K, Guidotti LG, Chisari FV, Fikes J, Chesnut RW, Sette A. Altered helper T lymphocyte function associated with chronic hepatitis B virus infection and its role in response to therapeutic vaccination in humans. *J Immunol* 1999; **162**: 3088-3095

A novel stop codon mutation in HBsAg gene identified in a hepatitis B virus strain associated with cryptogenic cirrhosis

Xu Yang, Xiao-Peng Tang, Jian-Hua Lei, Hong-Yu Luo, Yong-Hong Zhang

Xu Yang, Xiao-Peng Tang, Jian-Hua Lei, Hong-Yu Luo, Yong-Hong Zhang, Liver Disease Research Center, The Second Xiangya Hospital, Central South University, Changsha 410011, Hunan Province, China

Correspondence to: Dr Xu Yang, Liver Disease Research Center, The Second Xiangya Hospital, Central South University, 86 Ren Min Avenue, Changsha 410011, Hunan Province, China yangxu@vip.163.com

Telephone: +86-731-5524222-2263 **Fax:** +86-731-5533525

Received: 2003-03-04 **Accepted:** 2003-04-01

Abstract

AIM: HBsAg is the most important serological marker for acute or chronic hepatitis B. Nevertheless, there were reports of HBsAg-negative infection caused by hepatitis B virus in recent years. We had a patient with cryptogenic cirrhosis who was negative for HBsAg, positive for anti-HBs and HBeAg. This paper was to explore the pathogenic and molecular basis of the unusual serological pattern.

METHODS: HBV serologic markers were qualitatively and quantitatively determined. HBV DNA in serum was qualitatively tested using routine Polymerase chain reaction (PCR), and the viral level was determined with real-time fluorescence quantitative PCR. HBsAg gene was amplified and cloned. Four clones were sequenced. The new genomic sequences were compared with GenBank on the DNA level as well as the protein level.

RESULTS: The qualitative results of serological markers were HBsAg(-), anti-HBs(+), HBeAg(+), anti-HBe(-) and anti-HBc(+). The quantitative results of serological marker were HBsAg (S/N): 0.77 (cut off of S/N: ≥ 2.00), HBeAg (S/N): 56.43 (cut off S/N: ≥ 2.10), anti-HBc (S/C₀): 2.03 (cut off of S/C₀: ≤ 1.00). The viral level was as high as 1.54×10^9 copies/ml. Sequencing of the HBsAg gene clones revealed a unique point mutation at nucleotide 336 (C to A), which resulted in a novel stop codon at aa 61. The novel HBsAg gene stop mutation had not been described.

CONCLUSION: The lack of detection of HBsAg in the presence of high viral levels of replication may be caused by the existence of viral genomes harboring point mutations which resulted in stop codon upstream of the "a" determinant in HBsAg gene.

Yang X, Tang XP, Lei JH, Luo HY, Zhang YH. A novel stop codon mutation in HBsAg gene identified in a hepatitis B virus strain associated with cryptogenic cirrhosis. *World J Gastroenterol* 2003; 9(7): 1516-1520

<http://www.wjgnet.com/1007-9327/9/1516.asp>

INTRODUCTION

Hepatitis B virus (HBV) is a small DNA-containing virus with 4 overlapping open reading frames. The four genes are core, surface, X and polymerase. The surface antigen open reading

frame is divided into three regions, pre-S1, pre-S2 and S, which encode three envelope proteins respectively termed large, middle and major protein. All the three envelope proteins contain the major protein, HBsAg, which consists of 226 amino acids and is the predominant protein of the 20 nm small spherical particles representing circulation excess surface protein^[1,2].

Serological evidence for acute or chronic hepatitis B is provided most commonly by assays detecting the HBsAg. Its detection is believed to prove the presence of hepatitis B virus in the liver and the peripheral blood. Both the clearance of HBsAg from serum and the appearance of antibodies to HBsAg (anti-HBs) are associated with a resolution of hepatitis in acute or chronic hepatitis B infection^[3]. However, the development of polymerase chain reaction (PCR) technique has permitted the detection of very low levels of HBV in patients. There are a number of reports of HBsAg-negative virus carriers^[4,5]. Moreover, even cases of anti-HBs-positive carriers have been described although antibodies against the viral envelope usually neutralize the virus and confer protection from infection^[6]. China is a highly endemic area for HBV infection, some studies suggested that 30 % to 40 % of HBsAg-negative patients with cryptogenic cirrhosis, chronic active hepatitis, or chronic persistent hepatitis had HBV-DNA in serum or liver tissue^[7]. A well-characterized explanation for the latter pattern is surface mutation. Over the past decade many kinds of surface mutations have been described. We present here a patient with cirrhosis and active viral replication in the presence of anti-HBs. Sequencing of the HBV DNA from the patient revealed a point mutation at nucleotide 336 (C to A) in HBs-gene. This mutation led to a stop codon at 61 amino acids of HBsAg and a premature translation stop, which has not been described elsewhere up to now.

MATERIALS AND METHODS

Case report

The patient was a 56-year-old man. He was positive for HBsAg but asymptomatic in 1988. In 1990 his alanine aminotransferase (ALT) level was slightly elevated. In 1992 he developed a very severe disease which was diagnosed as severe type hepatitis B. He recovered 3 months later. He felt well from 1992 to 1998, no data about HBV serology and liver function were available during that period. However, he began to feel fatigue, weakness, abdominal distension from the beginning of 1999. His WBC and platelet were markedly decreased, but negative for HBsAg, and positive for anti-HBs. Abdominal ultrasound examination showed splenomegaly. Cryptogenic cirrhosis was diagnosed. Cirrhosis caused by HCV, alcohol, drugs, Wilson's disease and schistosomiasis was excluded. In order to find the cause of the cirrhosis, he came to our hospital in August 2000. Serum was collected at the time and stored at -70 °C until analysis.

HBV serological markers detection

HBsAg, anti-HBs, HBeAg, anti-Hbe, anti-HBc-IgG and anti-HBc-IgM were tested using commercially available standard enzyme immunoassay kit (Kehua Bio-Engineering Co. LTD, Shanghai, China). HBsAg, HbeAg and anti-HBc-IgG were

quantitatively determined using Abbott reagent with IMX automatic immunoassay analyzer (Abbott Laboratories, North Chicago, IL), according to the manufacturer's instructions.

Serum HBV DNA detection

HBV DNA detection was carried out using commercially available PCR kit (Liver Research Institute, Beijing Medical University, Beijing, China), according to the manufacturer's instructions. Serum samples (200 μ l) were digested with 1 g/L proteinase K and 0.5 % sodium dodecyl sulfate (at 37 °C for 2 hours), followed by phenol-chloroform extractions and ethanol precipitation. After centrifugation, the pellet was dissolved in 10 μ l distilled water. Five μ l elute was used for PCR. Thermal cycling conditions were as follows: 35 cycles of amplification were performed at 94 °C for 30 s and at 60 °C for 45 s. The PCR products were investigated by staining with ethidium bromide on ultraviolet transilluminator after electrophoresis in 1.5 % agarose gel.

HBV DNA quantification

HBV DNA in serum was quantified using a commercially available real-time fluorescence quantitative PCR (FQ-PCR) kit (Da An Gene Diagnostic Center, Sun Yet-Sen Medical University, Guangzhou, China), in accordance with the manufacturer's instructions. Briefly, 40 μ l of serum was mixed with 40 μ l of DNA-extracting solution (provided by the kit). The mixture was vortexed and placed in a 100 °C heating block for 10 min, then overnight at 4 °C. The mixture was centrifuged for 5 min at 10 000 rpm. Two μ l of supernatant was added to the tube containing FQ-PCR core reagent (provided by the kit). FQ-PCR was performed using a GeneAmp 5700 sequence detection system (Perkin Elmer, Foster City, CA). Thermal cycling conditions were as follows: at 93 °C for 2 min for initial denaturation, followed by 40 cycles of at 93 °C for 30 s, at 55 °C for 60 s. Analysis of raw data was done with the GeneAmp 5700 SDS Software (PE Biosystems). Data were collected at the annealing step of each cycle, and the threshold cycle (C_T) for each sample was calculated by determining the point at which the fluorescence exceeded the threshold limit. The standard curve was calculated automatically by plotting the C_T value against each standard of known concentration and calculation of the linear regression line of this curve. Calculation of the correlation coefficient was done for each run, and the minimal value was 0.98. Sample copy numbers were calculated by interpolation of the experimentally determined standard curve.

Amplification of HBsAg gene

The primers were designed by ourselves according to the sequences published^[8,10], which could amplify whole HBsAg gene (from nt 155 to 833). The procedures for HBV DNA extraction were the same as routine PCR described above. The reaction conditions were: the total volume was 30 μ l, containing 50 mmol/L KCl, 10 mmol/L tris-HCl (pH9.0), 0.1 % triton 100, 0.2 mmol/L dNTP, 1.5 mmol/L MgCl₂, 15 pmol primer 1 and primer 2, TaqDNA polymerase 2.5U, a drip of paraffin oil was added on the top of the solution. PCR conditions were as follows: at 94 °C for 5 min for initial denaturation, followed by 30 cycles at 94 °C for 1 min, at 56 °C for 50 s, at 72 °C for 10 s, at 72 °C for 10 min for extension. The PCR products were investigated by staining with ethidium bromide on ultraviolet transilluminator after electrophoresis in 1.5 % agarose gel or used for HBsAg gene cloning.

Forward primer: 5' GGGAAAGCTTATGGAGAACATCAGGATTC3'
Reverse primer: 5' CGCGGATCCTTAAATGTATACCCAGAGACAAAA3'.

Cloning and sequencing of HBsAg gene

The amplified products of HBsAg gene were cloned using pGEM-T easy vectors system kit (Promega Co., Madison, WI.),

according to the manufacture's instructions. To detect the vectors containing the PCR products, white/blue colony selection was used. The inserted products were analyzed by electrophoresis in 1 % agarose gel after EcoR 1 digestion and PCR (as amplification of HBsAg gene described above). Four clones were sequenced. The sequence of the complete HBsAg gene was obtained by forward and reverse reading of overlapping fragments using ABI PRISM BigDye terminator cycle sequencing ready reaction kit (Perkin Elmer, Foster City, CA). To identify mutations, the new genomic sequences were compared with GenBank on the DNA level as well as the protein level.

RESULTS

All HBV serologic markers were tested repeatedly. HBsAg, HBeAg and anti HBe were tested again using Abbott reagent. The results confirmed that the patient was HBsAg-negative, anti-HBs-positive and HBeAg-positive. It was estimated that the patient had cirrhosis caused by HBV. To confirm the diagnosis, the presence of HBV DNA in serum of the patient was tested using routine PCR and HBV DNA was detected. The quantity of HBV DNA in serum was determined using real-time fluorescent quantitative PCR, which was unexpectedly as high as 1.54 \times 10⁹/ml (Tables 1 and 2).

Table 1 Viral and clinical examination results of the patient

Item	Jan. 1999	Apr. 1999	Oct. 1999	Aug. 2000	Nov. 2000	Mar. 2001
HBsAg	-	-	-	-	-	-
Anti-HBs	+	+	+	+	+	+
HbeAg	+	+	+	+	+	+
Anti-Hbe	-	-	-	-	-	-
Anti-HBc-IgG	+	+	+	+	+	+
Anti-HBc-IgM	+	-	-	-	-	-
HBV DNA	Nd	Nd	Nd	Nd	+	+
HBV DNA copies/ml	Nd	Nd	Nd	Nd	1.02 \times 10 ⁸	1.54 \times 10 ⁹
ALT (U/L)	49.0	56.9	67.1	74.4	69.0	68.6
Albumin (g/L)	42.3	40.4	38.5	40.3	41.5	40.8
Globulin (g/L)	28.6	30.7	28.5	34.4	31.9	32.6
Bilirubin (μ mol/L)	18.9	23.2	28.6	25.8	27.7	28.4
Hemoglobin (g/L)	Nd	Nd	Nd	111	115	110
WBC (10 ⁹ /L)	Nd	Nd	Nd	2.1	2.8	2.6
Platelet (10 ⁹ /L)	Nd	Nd	Nd	26	58	40

Nd, not determined; +, positive; -, negative. ALT, alanine aminotransferase; WBC, white blood cell.

Table 2 HBsAg, HBeAg and anti-HBe level determined using Abbott reagent

Item	Results	Cut off
HBsAg	0.77	\geq 2.00(S/N)
HbeAg	56.433	\geq 2.10(S/N)
Anti-HBe	2.033	\leq 1.0(S/Co)

Due to the massive production of viral particles in the absence of HBsAg and presence of anti-HBs, HBsAg gene mutation, possibly in the "a" determinant, was suspected. Therefore, HBV DNA was extracted from the serum of the patient, HBsAg gene was amplified. After electrophoresis of the PCR products corresponding to the complete HBsAg gene amplified from serum and ethidium bromide staining of the gel, a PCR fragment about 700 bp was detected (the figure was not shown). Then the PCR products of HBsAg gene were cloned, 4 clones were sequenced. The complete sequence of

the HBsAg gene was obtained by forward and reverse reading of overlapping fragments (Table 3). All of the 4 clones had the same sequence. The nucleotide and amino acid sequences of the HBsAg gene were compared with GenBank. There were no nucleotide insertions or deletions in the HBsAg gene. Surprisingly, sequencing of the HBsAg gene clones revealed a unique point mutation at nucleotide 336 (C to A), which resulted in a novel stop codon at aa 61. Thus, only a truncated version of HBsAg containing 21 amino acids could be synthesized from this gene, which lacked the entire "a" determinant. The novel HBsAg gene stop codon caused by a point substitution mutation upstream of the "a" determinant of HBsAg gene has not been described up to now.

The isolate belonged to subtype adw2 according to the amino acid sequence deduced from the nucleotide sequence of the

HBsAg gene. The patient's nucleotide sequence and amino acid sequence were compared with a published sequence of the same subtype reported by Ono *et al*^[9] and a Chinese consensus sequence of the same subtype (China J Microbiol Immunol, 1999; 19: 197-200). A two by two analysis of the three nucleotide and amino acid sequences demonstrated a relatively high degree of homogeneity. The nucleotide and amino acid difference was 5.28 % and 8.37 % between the patient's and Ono's sequences, and was 4.84 % and 7.92 % between the patient's and the Chinese consensus sequences, respectively. The "a" determinant of the patient's sequence differed from the Ono's sequence by only 2 amino acids and differed from the Chinese consensus sequence by another 2 amino acids, which might reflect the genetic heterogeneity of the same subtype and could not be the mutation (Table 4).

Table 3 The complete nucleotide sequence of the HBsAg gene from the patient

nt																Codon
155	ATG	GAG	AAC	ATC	ACA	TCA	GGA	TTC	CCA	GGA	CCC	CTG	CTC	GTA	TTA	15
200	CAG	GCG	GGG	TTT	TTC	TTG	TTG	ACA	AAA	ATC	CTC	ACA	ATA	CCA	CAG	30
245	AGT	CTA	GAC	TCG	TGG	TGG	ACT	TCT	CTC	AAT	TTT	CTA	GGG	GGA	ACA	45
290	CCC	GTG	TGT	CTT	GGC	CAA	AAT	TCG	CAG	TCC	CAA	ATC	TCC	AGT	CAC	60
335	TAA	CCA	ACC	TGC	TGT	CCT	CCA	ATT	TGT	CCT	GGT	TAT	CGC	TGG	ATG	75
380	TGT	CTG	CGG	CGT	TTT	ATC	ATC	TGC	CTC	TGC	ATC	CTG	CTG	CTA	TGC	90
425	CTC	ATC	TTC	TTG	TTG	GTT	CTT	CTG	GAC	TAT	CAA	GGT	ATG	TTG	CCC	105
470	GTT	TGT	CCT	CTA	CTT	CCA	GGA	TCA	ACA	ACA	ACC	AGC	ACC	GGA	CCA	120
515	TGC	AAA	ACC	TGC	ACG	ACT	CCT	GCT	CAA	GGC	AAC	TCT	AAG	TTT	CCC	135
560	TCT	TGT	TGC	TGT	ACA	AAA	CCT	ACG	GAC	GGA	AAC	TGC	ACC	TGT	ATT	150
605	CCC	ATC	CCA	TCA	TCT	TGG	GCT	TTC	GCA	AAA	TAC	CTA	TGG	GAG	TGG	165
650	GCC	TCA	GTC	CGT	TTC	TCT	TGG	CTC	AGT	TTA	CTA	GTG	CCA	TTT	GTT	180
695	CAG	TGG	TTC	GTA	GGG	CTT	TCC	CCC	ACT	GTC	TGG	CTT	TCA	GTT	ATA	195
740	TGG	ATG	ATG	TGG	TTT	TGG	GGG	CCA	AGT	CTG	TAC	AAC	ATC	GTG	AGT	210
785	CCC	TTT	ATG	CCG	CTG	TTA	CCA	ATT	TTC	TTT	TGT	CTC	TGG	GTA	TAC	225
830	ATT	TAA														227

Table 4 Comparison of nucleotide sequences and amino acid sequences of HBsAg gene among the 3 adw subtypes

Codon	4	9	14	24	29	45	47
Sequence(1)	ATC Ile	CTA Leu	GTG Val	AGA Arg	CCG pro	TCA Ser	CTA Leu
Sequence(2)	ATC Ile	CCA Pro	GTA Val	AAA Lys	CCA Pro	TCA Ser	GTA Val
Sequence(3)	ACA Thr	CTA Leu	GTG Val	AGA Arg	CCA Pro	GCT Ala	GTA Val
Codon	49	56	57	59	61	64	71
Sequence(1)	CCT pro	CCA His	ACC Thr	AAT Asn	TCA Ser	TCC Ser	GGT Gly
Sequence(2)	CTT Leu	CAA Glu	ATC Ile	AGT Ser	TAA stop	TGT Cys	GGT Gly
Sequence(3)	CTT Leu	CCA His	ACC Thr	AAT Asn	TCA Ser	TCT Ser	GGC Gly
Codon	82	83	85	94	99	100	110
Sequence(1)	ATA Ile	TTC Phe	TTC Phe	TTA Leu	GAT Asp	TAT Tyr	ATT Ile
Sequence(2)	ATC Ile	TGC Cys	TGC Cys	TTG Leu	GAC Asp	TAT tyr	CTT Leu
Sequence(3)	ATA Ile	TTC Phe	TTC Phe	TTG Leu	GAC Asp	TAC Tyr	CTT Leu
Codon	113	114	115	117	118	122	126
Sequence(1)	TCA Ser	ACA Thr	ACA Thr	AGT Ser	ACG Thr	AAA Lys	ACT Thr
Sequence(2)	TCA ser	TCA Ser	ACA Thr	AGC Ser	ACC Thr	AAC Lys	ACT Thr
Sequence(3)	ACA Thr	TCA Ser	ACT Thr	AGC Ser	ACG Thr	AAG Lys	ATT Ile
Codon	130	131	132	136	143	144	146
Sequence(1)	GGC Gly	AAC Asn	AAG Lys	TCA Ser	ACG Thr	GAT Asp	AAT Asn
Sequence(2)	GGA gly	ACC Thr	ATG Met	TCA Ser	ACG Thr	GAC Asp	AAC Asn
Sequence(3)	GGA Gly	ACC Thr	ATG Met	TCT Ser	TCG Ser	GAC Asp	AAC Asn
Codon	148	154	155	160	161	171	190
Sequence(1)	ACC Thr	TCG Ser	TCC Ser	AAA Lys	TAC Thr	TCT Ser	GTT Val
Sequence(2)	ACC Thr	TCA Ser	TCT Ser	AAA Lys	TAC Thr	TCT Ser	GTC Val
Sequence(3)	ACT Thr	TCA Ser	TCT Ser	AGA Agr	TTC Phe	TCC ser	GTT val
Codon	194	200	207	209	213	214	215
Sequence(1)	GCT Ala	TAT Thr	AGC Ser	GTG Val	ATA Ile	CCG Pro	CTC Leu
Sequence(2)	GTT Val	TTT Phe	AAC Asn	TTG Leu	ATG met	CCG Pro	CTG Leu
Sequence(3)	GTT val	TAT Thr	AAC Asn	TTG Leu	TTA Leu	CCT Pro	CTA Leu
Codon	222						
Sequence(1)	CTC Leu						
Sequence(2)	CTC Leu						
Sequence(3)	CTT Leu						

Sequence (1): adw subtype reported by Ono *et al*. Sequence (2): The patient's sequence. Sequence (3): The Chinese consensus sequence of adw subtype.

DISCUSSION

Hepatitis B virus replicates via an RNA intermediate, using a reverse transcriptase that appears to lack a proofreading function. Therefore, HBV exhibits a mutation rate more than 10-fold higher than other DNA virus^[10-12]. Mutations in all 4 genes have been described. Surface gene mutation were initially noted as vaccine escape mutants, detected in 2-3 % of children in HBV endemic regions receiving HBV immunoprophylaxis at birth, and also observed in liver transplanted HBV carriers who received hepatitis B immunoglobulin to prevent re-infection of the graft^[13-17]. Similar mutations could also arise in the natural course of HBV infection. The prevalence and clinical significance of naturally occurring mutations in full-length surface and overlapping polymerase genes of hepatitis B virus were analyzed in 42 patients with chronic hepatitis, mutations were observed in 10 patients (24 %) in the “a” determinant region^[18,19].

The surface gene of HBV contains a dominant neutralizing epitope termed “a” determinant located between aa 121-149 of HBsAg. The production of antibodies to the “a” determinant after vaccination usually protects against HBV infection. The surface protein variants noted in most studies were clustered within the “a” determinant, especially the substitution of glycine for arginine at aa 145, which makes this epitope unlikely to bind to antibodies generated to wild-type HBsAg. However, other kinds of mutation outside of the “a” determinant have been described in recent years, including deleting and inserting mutations in the surface gene of HBV^[20-22].

In contrast to the mutations mentioned above, an uncommon point mutation at nucleotide 336 (C to A) of HBsAg-gene occurred in our isolates, which resulted in a novel stop codon at aa 61. This finding could not be a laboratory error, because all sequences of four clones were the same. Because of this new stop codon introduction, only truncated molecules of surface antigen could be expressed, which contained only 60 amino acid residues and was lack of the “a” determinant. This unique mutation could well explain the patient’s unusual serologic pattern: HBsAg-negative, but HBeAg-positive, anti-HBs-positive and HBV DNA-positive. The novel HBsAg gene stop codon caused by a point substitution mutation upstream of the “a” determinant has not been described up to now. Our finding is very similar to the deletion mutation of HBsAg gene described by Weinberger *et al.* The deletion mutation located at the nucleotide 31 of the HBsAg gene, which led to a frame-shift and introduced a stop-codon after 21 amino acids of HBsAg^[23].

To initiate infection, a virus must attach to a host cell receptor via one of its surface proteins. Hepatitis B virus has three related surface proteins, small S, middle S, and large S. It is not clear which of these three proteins serves as the HBV attachment protein. It has been thought that the pre-S region or S region determines viral binding^[24,25]. However, due to the lack of a susceptible cell line that could be used to test specific blocking reagents, which protein is involved in the initial stage of HBV infection is difficult to determine. The HBV DNA level in our patient was as high as 10⁹/ml in serum, indicating that isolates that bear such truncated molecules on their surface (the mutant HBsAg was only equal to one-fourth of HBsAg from wild type) can well finish their life cycle including viral binding and entry. Our finding presented here provides the evidence that sequences in the pre-S region determine viral binding.

However, our finding raises a theoretical question: Cells infected with hepatitis B virus produce both virions and 20nm subviral (surface antigen) particles. Although hepatitis B virus encodes three envelope proteins, all of the information required to produce 20 nm HBsAg particles resides within the S protein^[26]. The nucleotide sequence of the HBsAg gene

predicts the existence of three hydrophobic domains, located at residues 4 to 28 (signal I), 80 to 100 (signal II) and 164 to 221 (signal III). Studies on certain artificial deletion mutants suggested that deletion of signal II completely destabilized the chain, and deletion of the signal III resulted in a nonsecreted chain^[27]. How such a drastically shortened HBsAg which is lack of signal II and signal III, can be able to form morphologically correct viral and subviral particles? Because when co-expressed with wild type S protein, the mutant polypeptide can be incorporated into particles and secreted, therefore, it is assumed that the presence of a minor population of intact genomes helps in replication and formation of intact virions. All virus isolates consist of a mixture of viral strains. Multiple variants have been found in a single host. Advances in molecular biology technique have revealed significant diversities in sequence of HBV isolates. Sequencing results suggest that there were HBV quasispecies groups in chronically infected patients^[28-31]. Actually, electron microscopy of serum samples containing mutated DNA from the patient reported by Weinberger *et al.* revealed typical subviral particles with an average diameter of 17-20 nm, but did not reveal a single filamentous particle^[23]. Our results show that lack of detection of HBsAg in the presence of high viral levels of replication may be caused by the existence of viral genomes harboring point mutation which results in stop codon upstream of the “a” determinant of HBsAg gene.

REFERENCES

- 1 **Tiollais P**, Charnay P, Vyas GN. Biology of hepatitis B Virus. *Science* 1981; **213**: 406-411
- 2 **Michel ML**, Tiollais P. Structure and expression of the hepatitis B virus genome. *Hepatology* 1987; **7**(Suppl): 61s-63s
- 3 **Krugman S**, Overby LR, Mushahwar IK, Ling CM, Frosner GG, Deinhardt F. Viral hepatitis type B: Studies on natural history and prevention re-examined. *N Engl J Med* 1979; **300**: 101-106
- 4 **Brechot C**, Degos F, Lugassy C, Thiers V, Zafrani S, Franco D, Bismuth H, Trepo C, Benhamou JP, Wands J, Isselbacher KJ, Tiollais P, Berthelot P. Hepatitis B virus DNA in patients with chronic liver disease and negative tests for hepatitis B surface antigen. *N Engl J Med* 1985; **312**: 270-276
- 5 **Sanchez-Quijano A**, Jauregui JI, Leal M, Pineda JA, Castilla A, Abad MA, Civeira MP, Garcia de Pesquera F, Prieto J, Lissen E. Hepatitis B virus occult infection in subjects with persistent isolated anti-HBc reactivity. *J Hepatol* 1993; **17**: 288-293
- 6 **Rehermann B**, Ferrari C, Pasquinelli C, Chisari FV. The hepatitis B virus persists for decades after patients’ recovery from acute viral hepatitis despite active maintenance of a cytotoxic T-lymphocyte response. *Nat Med* 1996; **2**: 1104-1108
- 7 **Zhang YY**, Guo LS, Li L, Zhang YD, Hao LJ, Hansson BG, Nordenfelt E. Hepatitis B virus DNA detected by PCR in sera and liver tissues of Chinese patients with chronic liver diseases. *Chin Med J Engl* 1993; **106**: 7-12
- 8 **Galibert F**, Mandart E, Fitoussi F, Tiollais P, Charnay P. Nucleotide sequence of the hepatitis B virus genome (subtype ayw) cloned in *E. coli*. *Nature* 1979; **281**: 646-650
- 9 **Ono Y**, Onda H, Sasada R, Igarashi K, Sugino Y, Nishioka K. The complete nucleotide sequences of the cloned hepatitis B virus DNA: subtype adr and adw. *Nucleic Acids Res* 1983; **11**: 1747-1757
- 10 **Blum HE**. Variants of hepatitis B, C and D viruses: molecular biology and clinical significance. *Digestion* 1995; **56**: 85-95
- 11 **Carman WF**, Thomas HC. Genetic variation in hepatitis B virus. *Gastroenterology* 1992; **102**: 711-719
- 12 **Hasegawa K**, Huang J, Rogers SA, Blum HE, Liang TJ. Enhanced replication of a hepatitis B virus mutant associated with an epidemic of fulminant hepatitis. *J Virol* 1994; **68**: 1651-1659
- 13 **Karthigesu VD**, Allison LM, Ferguson M, Howard CR. A hepatitis B virus variant found in the sera of immunised children induces a conformational change in the HBsAg “a” determinant. *J Med Virol* 1999; **58**: 346-352
- 14 **He JW**, Lu Q, Zhu QR, Duan SC, Wen YM. Mutations in the “a” determinant of hepatitis B surface antigen among Chinese in-

- fants receiving active postexposure hepatitis B immunization. *Vaccine* 1998; **16**: 170-173
- 15 **Cooreman MP**, Leroux-Roels G, Paulij WP. Vaccine-and hepatitis B immune globulin-induced escape mutations of hepatitis B virus surface antigen. *J Biomed Sci* 2001; **8**: 237-247
- 16 **Carman WF**, Zanetti AR, Karayiannis P, Waters J, Manzillo G, Tanzi E, Zuckerman AJ, Thomas HC. Vaccine-induced escape mutant of hepatitis B virus. *Lancet* 1990; **336**: 325-329
- 17 **Chen WN**, Oon CJ. Hepatitis B virus surface antigen (HBsAg) mutants in Singapore adults and vaccinated children with high anti-hepatitis B virus antibody levels but negative for HBsAg. *J Clin Microbiol* 2000; **38**: 2793-2794
- 18 **Hou J**, Wang Z, Cheng J, Lin Y, Lau GK, Sun J, Zhou F, Waters J, Karayiannis P, Luo K. Prevalence of naturally occurring surface gene variants of hepatitis B virus in nonimmunized surface antigen-negative Chinese carriers. *Hepatology* 2001; **34**: 1027-1034
- 19 **Ghany MG**, Ayola B, Villamil FG, Gish RG, Rojter S, Vierling JM, Lok AS. Hepatitis B virus S mutants in liver transplant recipients who were re-infected despite hepatitis B immune globulin prophylaxis. *Hepatology* 1998; **27**: 213-222
- 20 **Ogura Y**, Kurosaki M, Asahinna Y, Enomoto N, Marumo F, Sato C. Prevalence and significance of naturally occurring mutations in the surface and polymerase genes of hepatitis B virus. *J Infect Dis* 1999; **180**: 1444-1451
- 21 **Hou J**, Karayiannis P, Waters J, Luo K, Liang C, Thomas HC. A unique insertion in the S gene of surface antigen-negative hepatitis B virus Chinese carriers. *Hepatology* 1995; **21**: 273-278
- 22 **Chen HB**, Fang DX, Li FQ, Jing HY, Tan WG, Li SQ. A novel hepatitis B virus mutant with A-to-G at nt551 in the surface antigen gene. *World J Gastroenterol* 2003; **9**: 304-308
- 23 **Weinberger KM**, Zoulek G, Bauer T, Bohm S, Jilg W. A novel deletion mutant of hepatitis B virus surface antigen. *J Med Virol* 1999; **58**: 105-110
- 24 **Mehdi H**, Yang X, Peeples ME. An altered form of apolipoprotein H binds hepatitis B virus surface antigen most efficiently. *Virology* 1996; **217**: 58-66
- 25 **Neurath AR**, Seto B, Strick N. Antibodies to synthetic peptides from the preS1 region of the hepatitis B virus (HBV) envelope (env) protein are virus-neutralizing and protective. *Vaccine* 1989; **7**: 234-236
- 26 **Laub O**, Rall LB, Truett M, Shaul Y, Standring DN, Valenzuela P, Rutter WJ. Synthesis of hepatitis B surface antigen in mammalian cells: expression of the entire gene and the coding region. *J Virol* 1983; **48**: 271-280
- 27 **Bruss V**, Ganem D. Mutational analysis of hepatitis B surface antigen particle assembly and secretion. *J Virol* 1991; **65**: 3813-3820
- 28 **Dong J**, Cheng J, Wang QH, Wang G, Shi SS, Liu Y, Xia XB, Li LI, Zhang GQ, Si CW. Quasispecies and variations of hepatitis B virus: core promoter region as an example. *Zhonghua Shiyan He Linchuangbing Duxue Zazhi* 2002; **16**: 264-266
- 29 **Mathet VL**, Feld M, Espinola L, Sanchez DO, Ruiz V, Mando O, Carballal G, Quarleri JF, D' Mello F, Howard CR, Oubina JR. Hepatitis B virus S gene mutants in a patient with chronic active hepatitis with circulating Anti-HBs antibodies. *J Med Virol* 2003; **69**: 18-26
- 30 **Ngui SL**, Teo CG. Hepatitis B virus genomic heterogeneity: variation between quasispecies may confound molecular epidemiological analyses of transmission incidents. *J Viral Hepat* 1997; **4**: 309-315
- 31 **Torresi J**. The virological and clinical significance of mutations in the overlapping envelope and polymerase genes of hepatitis B virus. *J Clin Virol* 2002; **25**: 97-106

Edited by Ma JY and Wang XL

Aggregate formation of hepatitis B virus X protein affects cell cycle and apoptosis

Chang-Zheng Song, Zeng-Liang Bai, Chang-Cheng Song, Qing-Wei Wang

Chang-Zheng Song, Zeng-Liang Bai, Laboratory of Immunobiology, College of Life Sciences, Shandong University, Jinan 250100, Shandong Province, China

Chang-Zheng Song, Shandong Research Center for Medical Biotechnology, Shandong Academy of Medical Sciences, Jinan 250062, Shandong Province, China

Chang-Cheng Song, Basic Research Laboratory, National Cancer Institute at Frederick, MD 21702, USA

Qing-Wei Wang, Cancer Research Center, Qilu Hospital of Shandong University, Jinan 250012, Shandong Province, China

Correspondence to: Dr. Chang-Zheng Song, Project of Viral Vaccine, Shandong Research Center for Medical Biotechnology, Shandong Academy of Medical Sciences, Jinan 250062, Shandong Province, China. songcz@life.sdu.edu.cn

Telephone: +86-531-2919611

Received: 2002-12-28 **Accepted:** 2003-02-18

Abstract

AIM: To investigate whether the formation of aggregated HBx has a potential linking with its cellular responses.

METHODS: Recombinant HBx was expressed in *Escherichia coli* and purified by Ni-NTA metal-affinity chromatography. Anti-HBx monoclonal antibody was developed for immunocytochemical detection. Bicistronic expression vector harboring full-length DNA of HBx was employed for transfection of human HepG2 cells. Immunocytochemical staining was used to examine the intracellular HBx aggregates in cells. The effects of HBx aggregation on cell cycle and apoptosis were assessed by flow cytometry.

RESULTS: Immunocytochemical staining revealed most of the HBx was formed intracellular aggregate in cytoplasm and frequently accumulated in large granules. Flow cytometry analysis showed that HepG2 cells transfected with vector harboring HBx significantly increased apoptosis and largely accumulated in the G0-G1 phase by maintenance in serum medium for 36 hours. Control cells without HBx aggregates in the presence of serum entered S phase and proliferated more rapidly at the same time. EGFP fluorescence in HBx expression cells was significantly decreased.

CONCLUSION: Our observations show that cells with HBx aggregate undergo growth arrest and apoptosis, whereas control cells without HBx remain in growth and progression into S phase. Our data may provide helpful information to understand the biological effects of HBx aggregates on cells.

Song CZ, Bai ZL, Song CC, Wang QW. Aggregate formation of hepatitis B virus X protein affects cell cycle and apoptosis. *World J Gastroenterol* 2003; 9(7): 1521-1524

<http://www.wjgnet.com/1007-9327/9/1521.asp>

INTRODUCTION

Hepatitis B virus (HBV) causes transient and chronic

infections of the liver. Transient infections may produce serious illness, and approximately 0.5 % terminates with fatal, fulminant hepatitis. Chronic infections may also have serious consequences: nearly 25 % terminate in untreatable liver cancer. Worldwide deaths from liver cancer caused by HBV infection probably exceed one million per year. X gene is a unique fourth open reading frame of HBV. X gene codes for a 16.5-kDa protein (X protein, HBx) and is well conserved among the mammalian hepadnaviruses^[1]. HBx is a multifunctional viral regulator that modulates transcription, cell responses to genotoxic stress, protein degradation, and signaling pathways^[2]. The ability of HBx to modulate cell survival is potentially relevant to viral pathogenicity in acute and chronic HBV infection as well as to the late development of hepatocellular carcinoma^[3]. HBx activates signal-transduction cascades such as the Ras/Raf mitogen-activated protein kinase, Src kinase, c-Jun NH2-terminal kinase and Janus family tyrosine kinases/signal transducer and activators of transcription^[4,5]. HBx targets mitochondrial calcium and activates cytosolic calcium-dependent proline-rich tyrosine kinase-2^[6,7]. HBx may directly interact with transcription factors^[8]. HBx is also known to play an important role in altering gene expression, sensitizing cells to apoptosis and affect cell cycle checkpoints^[2]. The fate of infected cells expressing HBx is likely to be determined by the balance between apoptotic and anti-apoptotic signals of viral, cellular, and environmental origin.

HBx expression in different cells results in distinct and opposing cellular function responses of cell cycle and apoptosis^[9,10]. Most of the investigations described the effects of HBx through cellular signal-transduction pathways. Some reports suggested that HBx could induce cell death when it was expressed at high levels^[11-13]. The nine residues of cysteine among 154 amino acids of HBX might involve in disulfide bridge formation and be in favor of aggregate formation^[14]. Protein aggregation leads to cell cycle arrest and initiates cell death^[15]. We propose that intracellular deposition of aggregated HBx may have a potential linking to its cellular responses. In this study, we reported the cytoplasmic aggregates of HBx and its effect on cell cycle and apoptosis.

MATERIALS AND METHODS

Biological and chemical materials

Restriction enzymes and T4 DNA ligase were obtained from TaKaRa Biotech (Japan). QIA express Kit including pQE-60 Vector, *E. coli* strain M15 [pREP4] and Ni-NTA Superflow was purchased from QIAGEN (USA). GeneJammer transfection reagent was from Stratagene (USA). The plasmid pSPX46, a gift of Dr. Curtis C. Harris (National Institutes of Health, USA), encodes full-length HBx of the adr subtype. The bicistronic expression vector pIRES-EGFP-HBx harboring X gene (subtype ayw) was kindly provided by Drs. Jingyu Diao and Christopher D. Richardson (University of Toronto, Canada). SABC immunocytochemical detection kit was from Wuhan Boster Biological Technology Co. (China). Other chemicals of analytical grade were from Sigma.

Construction of HBx expression vector

The coding DNA fragment was amplified by polymerase chain reaction (PCR) using the pSPX46 as a template and the 5' -PCR primer (5' -TTT CCA TGG CTG CTC GGG TGT GC-3') carrying the NcoI site before and the 3' -PCR primer (5' GCGAGATCTGGCAGAGGTTGAAAAGTTG-3') carrying the Bgl II site after the X reading frame. The PCR product was digested with NcoI and Bgl II and ligated into pQE-60. According to the cloning strategy, recombinant construct based on the pQE-60 vector was produced by placing the 6xHis tag at the carboxy-terminus of HBx with the protein beginning with its natural ATG start codon. pQE-60X was obtained as an expression system for biosynthesis of HBx.

Expression and purification of HBx

Recombinant pQE-60X was transformed into *E. coli* strain M15 [pREP4]. The culture was induced with 1 mM isopropyl β -D-thiogalactopyranoside for 4.5 hours at 37 °C. The bacteria were harvested and lysed in a buffer containing 6 mol/L guanidine hydrochloride. The purification procedure of QIAexpress Kit was optimized. Elution with 250 mmol/L imidazole could effectively separate HBx from nickel-nitrilotriacetic acid (Ni-NTA) resins. Recombinant HBx was analysed by sodium dodecyl sulfate -polyacrylamide gel electrophoresis (SDS-PAGE). Electrophoresis was performed on 15 % polyacrylamide gel. After electrophoresis, gels were fixed in 30 % ethanol, 10 % acetic acid, and stained with Coomassie brilliant blue.

Preparation of monoclonal antibody against HBx

Balb/c mice were immunized repeatedly. Spleen cells from the most responding mouse were fused with myeloma cells (Sp-2/0) according to the routine method described by Yang *et al*^[16]. Positive hybrids were selected on hypoxanthine, aminopterin and thymidine containing medium.

Cell culture and transfections

Human hepatoma cell line HepG2 was grown on coverslips or 60-mm dish and maintained in Dulbecco' s modified Eagle minimal medium containing penicillin (100 IU/ml) and streptomycin (100 mg/ml) and supplemented with 10 % fetal calf serum. Bicistronic expression vector pIRES-EGFP-HBx derived from pIRES-EGFP by adding the DNA fragments of HBx^[17]. Cells at 70 % confluence were respectively transfected with pIRES-EGFP-HBx and pIRES-EGFP using GeneJammer transfection reagent. DNA transfections were performed according to the protocols supplied with the reagents.

Immunocytochemical assay

After transfection for 36 hours, HepG2 cells were washed in phosphate-buffered saline (PBS) and fixed with 90 % ethanol. SABC detection kit was used for immunocytochemical analysis. Cells were incubated with HBx monoclonal antibody for 1 hour at 37 °C. After washed three times with PBS, cells were incubated with anti-mouse biotinylated secondary antibody. Following extensive washes with PBS, color development was demonstrated with diaminobenzidine tetrahydrochloride chromagen. Finally, the slides were counterstained with hematoxylin. Stained cells were examined using light microscopy and photographed.

Flow cytometric analysis

To assess the effect of HBx aggregation on cell cycle, apoptosis and fluorescence of enhanced green fluorescent protein (EGFP), we analyzed the transfected cells by flow cytometry for GFP fluorescence and DNA content^[18]. The efficiency of transfection was verified by fluorescent signal. Cells were

released by trypsinization, resuspended in PBS at a density of 2×10^6 cells/ml, and analyzed on a Becton Dickinson flow cytometer using CellQuest software.

RESULTS

Vector construction for encoding HBx

In order to develop an HBx: anti-HBx antibody system for immunocytochemical purposes, an efficient *E. coli* expression system to produce HBx in large quantity was established. HBx was expressed in *E. coli* cells harboring pQE-60X as HBx carboxy-terminally fused to six histidine residues. pQE-60X was confirmed by PCR, restriction enzymes analysis and DNA sequencing.

HBx antigen and anti-HBx monoclonal antibody

Recombinant HBx was expressed in *Escherichia coli*. Because of the high stability of HBx aggregates, the purification procedure was optimized. *E. coli* cells were lysed in a buffer containing 6 mol/L guanidine hydrochloride. Six consecutive histidine residues that placed at the carboxy-terminus of HBx facilitated Ni-NTA metal-affinity chromatography. Elution with 250 mmol/L imidazole could effectively separate HBx from Ni-NTA resins. HBx was eluted as a pure protein (Figure 1). Starting with 1L of culture, only one milligram of recombinant HBx was attained under our experimental conditions. An anti-HBx monoclonal antibody was established following the conventional approach. The anti-HBx monoclonal antibody recognized the recombinant antigen as proved by high optical density measured in a simple binding enzyme-linked immunosorbent assay. Monoclonal antibody secreted by hybridoma clone was alike optimal for immunocytochemistry.

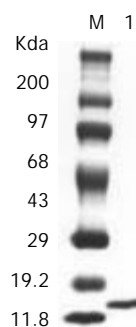


Figure 1 SDS-PAGE analyses of the purified HBx. SDS-PAGE showed a single band at the expected molecular weights (lane 1).

Immunohistochemical detection of HBx aggregates

HBx aggregate and its distribution were verified by immunocytochemistry. HBx-bearing cells exhibited positively staining by anti-HBx monoclonal antibody. Cytoplasmic HBx characteristically accumulated in large granules or strongly stained aggregates (Figure 2A, arrows). No immunoreactivity could be detected in a negative control stained by the same antibody under the same conditions (Figure 2B).

Flow cytometric analysis of HepG2 cells

A transient expression plasmid, pHbX-IRES-EGFP was used in this experiment. The vector contained HBx and EGFP reporter genes under control of a cytomegalovirus promoter and the element of internal ribosome entry site (IRES), respectively^[17]. More than 80 % of human HepG2 cells could be transfected with pIRES-EGFP-HBx and pIRES-EGFP respectively as shown by fluorescence flow cytometry. A representative flow cytometric profile at the 36th is shown in Figure 3A and 3B. Results were expressed as percentage of HepG2 cells in G0-G1, G2-M and S phases of the cell cycle

(Figure 3C). Apoptosis was also monitored by flow cytometry (Figure 3C). Each value corresponded to the mean \pm standard deviation of two independent experiments. Using Student's *t*-test, statistical analysis was performed. HepG2 cells transfected with vector harboring HBx were accumulated largely in the G0-G1 phase after maintenance in serum medium for 36 hours. Control cells that could not synthesize HBx protein in the presence of serum proliferated more rapidly and entered S phase at the same time.

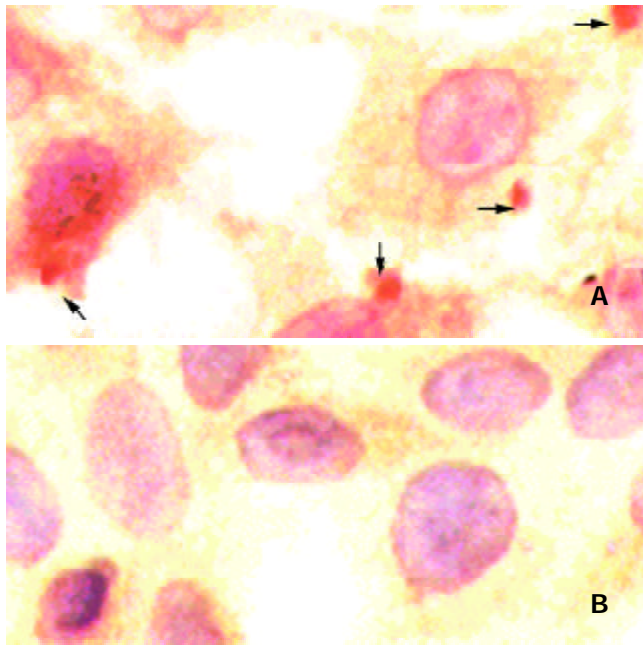


Figure 2 Immunocytochemical detection of HBx aggregates within HepG2 cells (magnification, $\times 400$). HBx aggregates were clearly visible as granules within the cytoplasm (A). HBx could not be detected within control cells transfected with pIRES-EGFP (B).

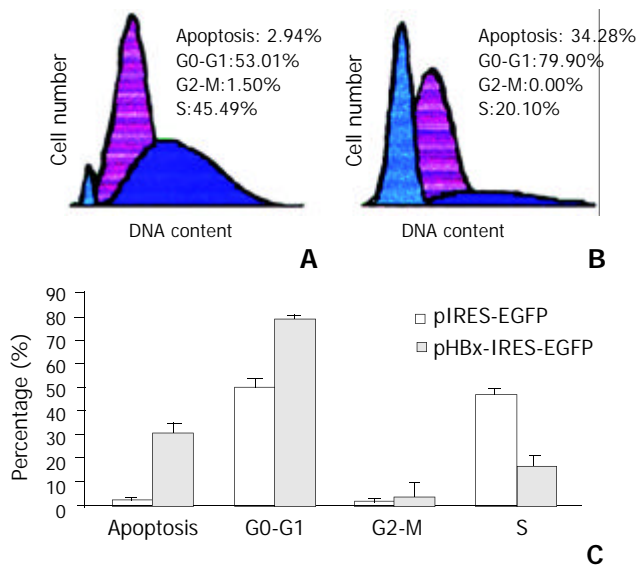


Figure 3 Flow cytometric analysis of apoptosis and cell cycle phases of HepG2 cells. (A) Control cells transfected with vector alone did not contain HBx. (B) Cells transiently transfected with the HBx expression plasmid. Apoptosis was significantly increased in HepG2 cells compared with control cells without HBx (C, $P < 0.02$). Cells displayed a marked decrease in S phase ($P < 0.02$) and demonstrated an evident increase in G0-G1 fraction ($P < 0.01$) with control expression vector that lacked the HBx gene (C).

EGFP fluorescence was decreased in HBx transfected cells

The mean fluorescence of 10^4 EGFP positive cells was measured by fluorescence cytometer. The EGFP fluorescence value was 4.43 ± 0.58 and 3.45 ± 0.15 of experiments in triplicate for HepG2 cells transfected with pIRES-EGFP and pIRES-EGFP-HBx, respectively. EGFP fluorescence in HBx expression cells was significantly decreased as compared with control pIRES-EGFP ($P < 0.05$).

DISCUSSION

The X open reading frame of HBV is highly conserved among all mammalian hepadnaviruses. HBx might regulate the expression of certain viral and cellular genes which are important for the creation of an environment suitable for viral propagation. HBx inhibits clonal outgrowth of cells and induces apoptosis by a p53-independent pathway. HBx expression can induce a late G1 cell cycle block prior to their counterselection by apoptosis. Furthermore, mutations in the HBx-gene evolving in hepatocellular carcinoma can abolish both HBx-induced growth arrest and apoptosis. Abrogation of the anti-proliferative and apoptotic effects of HBx by naturally occurring mutations might render the hepatocytes susceptible to uncontrolled growth and contribute to multistep hepatocarcinogenesis associated with HBV infection^[18]. HBx has been shown to be able to regulate cell cycle. HBx can activate the cyclin A promoter, induce cyclin A-cyclin-dependent kinase 2 complexes, and promote cycling of growth-arrested cells into G1 through a pathway involving activation of Src tyrosine kinases^[5]. HBx stimulation of Src kinases and cyclin gene expression was found to force growth-arrested cells to transit through G1 but to stall at the junction with S phase, which may be important for viral replication.

The structure feature of HBx may affect its biophysical properties including solubility, tendency toward aggregation with itself and with other proteins. Gupta *et al.*^[19] purified HBx from *E. coli*, subjected the protein to air oxidation, and analyzed intramolecular disulfide bonds. They found that eight of the nine cysteines were disulphide linked in a sequential manner. The disulphide linkages were between Cys7 and Cys78, Cys17 and Cys115, Cys61 and Cys137, Cys69 and Cys143 while Cys148 was free. The disulphide arrangement in HBx followed a pattern where each cysteine was joined to the fourth cysteine. HBx is able to form intramolecular disulfide bonds even under the reducing conditions of the cytosol. With analysis of purified HBx from eukaryotic sources by using electrospray ionization mass spectrometry, Urban *et al.*^[14] uncovered some components: the unmodified, monomeric, fully oxidized form with five intramolecular disulfide bridges, and its N-acetylated modification. It is not very clear whether the disulfide bridge formation is a prerequisite of HBx function, but a point mutation of Cys-69 to Ala abolishes its transactivation activity^[20]. Intracellular deposition of aggregated proteins is a prominent cytopathological feature of most neurodegenerative diseases^[21]. Protein aggregation is a central event in the initiation of cell death^[6]. Protein aggregation directly impairs the function of the ubiquitin-proteasome system and leads to cell cycle arrest and cell death.

In view of the investigations, we proposed apoptotic effects of HBx be related to its aggregate formation. Immunohistochemical examination revealed that only a minor immunological signal of HBx was detectable in a soluble form, whereas most of the protein formed intracellular aggregates in cytoplasm. HBx frequently accumulated in large granules. Our observation could suggest that HBx transfected cells underwent growth arrest and apoptosis, whereas control cells without HBx remained in growth and progression into S phase. In addition, we used the reporter molecule EGFP to reflect the situation of

HBx expression indirectly. By counting equal number of EGFP positive cells, pIRES-EGFP-HBx transfected cells showed a weak fluorescence as compared with pIRES-EGFP transfected cells. Diao *et al.*^[17] also reported that human primary hepatocytes transfected with pIRES-EGFP-HBx showed less intense fluorescent signal. HBx aggregates may affect the fluorescence intensity of EGFP in the same cell.

HBx were detected in aggregated structures and it was further showed that HBx aggregates mediated growth arrest and cell death. Our data may provide helpful information on the biological effects of HBx aggregates. The precise mechanism by which HBx aggregates could affect cell cycle and apoptosis remains to be established.

REFERENCES

- 1 **Seeger C**, Mason WS. Hepatitis B virus biology. *Microbiol Mol Biol Rev* 2000; **64**: 51-68
- 2 **Murakami S**. Hepatitis B virus X protein: a multifunctional viral regulator. *J Gastroenterol* 2001; **36**: 651-660
- 3 **Rui E**, de Moura PR, Kobarg J. Expression of deletion mutants of the hepatitis B virus protein HBx in *E. coli* and characterization of their RNA binding activities. *Virus Res* 2001; **74**: 59-73
- 4 **Arbuthnot P**, Capovilla A, Kew M. Putative role of hepatitis B virus X protein in hepatocarcinogenesis: effects on apoptosis, DNA repair, mitogen-activated protein kinase and JAK/STAT pathways. *J Gastroenterol Hepatol* 2000; **15**: 357-368
- 5 **Bouchard M**, Giannakopoulos S, Wang EH, Tanese N, Schneider RJ. Hepatitis B virus HBx protein activation of cyclin A-cyclin-dependent kinase 2 complexes and G1 transit via a Src kinase pathway. *J Virol* 2001; **75**: 4247-4257
- 6 **Bouchard MJ**, Wang LH, Schneider RJ. Calcium signaling by HBx protein in hepatitis B virus DNA replication. *Science* 2001; **294**: 2376-2378
- 7 **Diao J**, Garces R, Richardson CD. X protein of hepatitis B virus modulates cytokine and growth factor related signal transduction pathways during the course of viral infections and hepatocarcinogenesis. *Cytokine Growth Factor Rev* 2001; **12**: 189-205
- 8 **Wei W**, Dorjsuren D, Lin Y, Qin W, Nomura T, Hayashi N, Murakami S. Direct interaction between the subunit RAP30 of transcription factor IIF (TFIIF) and RNA polymerase subunit 5, which contributes to the association between TFIIF and RNA polymerase II. *J Biol Chem* 2001; **276**: 12266-12273
- 9 **Su F**, Schneider RJ. Hepatitis B virus HBx protein sensitizes cells to apoptotic killing by tumor necrosis factor alpha. *Proc Natl Acad Sci U S A* 1997; **94**: 8744-8749
- 10 **Lee S**, Tarn C, Wang WH, Chen S, Hullinger RL, Andrisani OM. Hepatitis B virus X protein differentially regulates cell cycle progression in X-transforming versus nontransforming hepatocyte (AML12) cell lines. *J Biol Chem* 2002; **277**: 8730-8740
- 11 **Chirillo P**, Pagano S, Natoli G, Puri PL, Burgio VL, Balsano C, Levrero M. The hepatitis B virus X gene induces p53-mediated programmed cell death. *Proc Natl Acad Sci U S A* 1997; **94**: 8162-8167
- 12 **Terradillos O**, Pollicino T, Lecoeur H, Tripodi M, Gougeon ML, Tiollais P, Buendia MA. p53-independent apoptotic effects of the hepatitis B virus HBx protein *in vivo* and *in vitro*. *Oncogene* 1998; **17**: 2115-2123
- 13 **Shintani Y**, Yotsuyanagi H, Moriya K, Fujie H, Tsutsumi T, Kanegae Y, Kimura S, Saito I, Koike K. Induction of apoptosis after switch-on of the hepatitis B virus X gene mediated by the Cre/loxP recombination system. *J Gen Virol* 1999; **80**: 3257-3265
- 14 **Urban S**, Hildt E, Eckerskorn C, Sirma H, Kekule A, Hofschneider PH. Isolation and molecular characterization of hepatitis B virus X-protein from a baculovirus expression system. *Hepatology* 1997; **26**: 1045-1053
- 15 **Bence NF**, Sampat RM, Kopito RR. Impairment of the ubiquitin-proteasome system by protein aggregation. *Science* 2001; **292**: 1552-1555
- 16 **Yang LJ**, Sui YF, Chen ZN. Preparation and activity of conjugate of monoclonal antibody HAB18 against hepatoma F(ab')₂ fragment and staphylococcal enterotoxin A. *World J Gastroenterol* 2001; **7**: 216-221
- 17 **Diao J**, Khine AA, Sarangi F, Hsu E, Iorio C, Tibbles LA, Woodgett JR, Penninger J, Richardson CD. X protein of hepatitis B virus inhibits Fas-mediated apoptosis and is associated with up-regulation of the SAPK/JNK pathway. *J Biol Chem* 2001; **276**: 8328-8340
- 18 **Sirma H**, Giannini C, Poussin K, Paterlini P, Kremsdorf D, Brechot C. Hepatitis B virus X mutants, present in hepatocellular carcinoma tissue abrogate both the antiproliferative and transactivation effects of HBx. *Oncogene* 1999; **18**: 4848-4859
- 19 **Gupta A**, Mal TK, Jayasuryan N, Chauhan VS. Assignment of disulphide bonds in the X protein (HBx) of hepatitis B virus. *Biochem Biophys Res Commun* 1995; **212**: 919-924
- 20 **Arii M**, Takada S, Koike K. Identification of three essential regions of hepatitis B virus X protein for trans-activation function. *Oncogene* 1992; **7**: 397-403
- 21 **Schulz JB**, Dichgans J. Molecular pathogenesis of movement disorders: are protein aggregates a common link in neuronal degeneration? *Curr Opin Neurol* 1999; **12**: 433-439

Anti-HBV effect of TAT- HBV targeted ribonuclease

Jin Ding, Jun Liu, Cai-fang Xue, Wei-dong Gong, Ying-hui Li, Ya Zhao

Jin Ding, Jun Liu, Cai-Fang Xue, Wei-Dong Gong, Ying-Hui Li, Ya Zhao, Department of Etiology, Fourth Military Medical University, Xi'an 710032, Shaanxi Province, China

Supported by National Natural Science Foundation of China, No. 30100157; Medical Research Fund of Chinese PLA, No.01MA184 and Innovation Project of FMMU, No.CX99005

Correspondence to: Professor Cai-Fang Xue or Dr. Jun Liu, Department of Etiology, Fourth Military Medical University, Xi'an 710032, Shaanxi Province, China. etiology@fmmu.edu.cn

Telephone: +86-029-3374536 **Fax:** +86-029-3374594

Received: 2003-03-05 **Accepted:** 2003-04-09

Abstract

AIM: To prepare and purify TAT-HBV targeted ribonuclease fusion protein, evaluate its transduction activity and investigate its effect on HBV replication in 2.2.15 cells.

METHODS: The prokaryotic expression vector pTAT containing TR gene was used in transforming *E.coli* BL21 (DE3) LysS and TR was expressed with the induction of IPTG. The TAT-TR fusion protein was purified using Ni-NTA-agrose and PD-10 desalting columns, and analyzed by SDS-PAGE. Transduction efficiency of TAT-TR was detected with immunofluorescence assay and the concentration of HBeAg in the supernatant of the 2.2.15 cells was determined via solid-phase radioimmunoassay (spRIA). MTT assay was used to detect the cytotoxicity of TAT-TR.

RESULTS: The SDS-PAGE showed that the TAT-TR fusion protein was purified successfully, and the purity of TAT-TR was 90 %. The visualization of TAT-TR by immunofluorescence assay indicated its high efficiency in transducing 2.2.15 cells. RIA result suggests that TAT-TR could inhibit the replication of HBV effectively, it didn't affect cell growth and had no cytotoxicity.

CONCLUSION: TAT-TR possesses a significant anti-HBV activity and the preparation of TAT-TR fusion protein has laid the foundation for the use of TR in the therapeutic trial of HBV infection.

Ding J, Liu J, Xue CF, Gong WD, Li YH, Zhao Y. Anti-HBV effect of TAT- HBV targeted ribonuclease. *World J Gastroenterol* 2003; 9(7): 1525-1528

<http://www.wjgnet.com/1007-9327/9/1525.asp>

INTRODUCTION

The introduction of proteins into mammalian cells has been achieved by transfection of expression vectors, microinjection, or infectious virus, *etc.* Although these approaches have been somewhat successful, the classical manipulation methods are not easily regulated and can be laborious. One approach to resolve these problems is the use of PTD-mediated protein transduction^[1, 2]. Linked covalently to proteins, peptides, nucleic acids, or as in-frame fusions with full-length proteins, PTD would let them enter any cell type in a receptor and transporter independent fashion^[3]. HIV-TAT is a member of

protein transduction domains and appears to possess high level of protein-transduction efficiency^[4,5]. TAT fusion proteins were shown to transduce into all cells and tissues present in mice^[6], including those present across the blood-brain barrier^[7,8]. And many, if not most, proteins may be transduced into cells by using this technology. Therefore, TAT PTD may let us address new questions in preclinical research work and even help in the treatment of human disease.

Hepatitis B is a major world-wide health problem^[9-13]. Chronic infection is associated with high risk of liver cirrhosis and primary liver carcinoma^[14-22]. Currently available therapies are of limited efficiency^[23-35]. HBV targeted ribonuclease (TR) gene, a fusion gene of HBVc and hEDN, was constructed by Liu *et al* in our lab^[36], according to the theory of capsid-targeted viral inactivation (CTVI) which is a promising strategy in anti-virus research. HBVc was used as the target molecule, which was the structure protein of HBV and was indispensable during the packaging of HBV particle. The effector molecule was hEDN, a kind of human ribonuclease that can degrade pgRNA of HBV. Transfection of 2.2.15 cells with the eukaryotic expression vector bearing TR gene suggested that TR inhibited the replication of HBV significantly^[37]. Therefore, linking HIV-TAT to TR would provide us a more efficient approach to deliver TR into hepatocytes, and greatly help us to utilize TR in the treatment of HBV infection. Reported here are the purification of TAT-TR fusion protein, the identification of its transduction and the anti-HBV effect on the 2.2.15 cells. To confirm its anti-HBV mechanism, we also prepared and purified TAT-TRmut, TAT-hEDN and TAT-HBVc proteins for use as negative controls.

MATERIALS AND METHODS

Materials

Ni-NTA-agrose was purchased from Qiagen Company. PD-10 desalting columns were purchased from Amersham Pharmacia Biotech. Anti-his mAb was from Santa Cruz Company. Protein molecular mass markers, IPTG and G418, imidazole and MTT were all from Sino-American Biotech. RIA HBVeAg assay kit was purchased from Beiming Dongya Biotechnology Institute. 2.2.15 cells was a kind gift of Prof. Cheng, 302 Hospital of Chinese PLA. hEDN was purified by Li *et al*^[36]. pTAT-HA/TR, TAT-HA/TRmut, pTAT-HA/hEDN and pTAT-HA/HBVc were all prepared in our Lab^[38]. PET-30a/TR, PET-30a/TRmut, PET-30a/HBVc and *E.coli* BL21 (DE3) LysS were maintained in our Lab.

Methods

Expression and purification of TAT fusion proteins pTAT-HA/TR, TAT-HA/TRmut, pTAT-HA/hEDN, pTAT-HA/HBVc and pTAT-HA were employed to transform *E.coli* BL21 (DE3) LysS by using CaCl₂ perforation. The transformants were separately cultured in 3 mL TB amp (100 µg/L) at 37 °C overnight. 100 µL culture was inoculated into 10 mL fresh TB amp, and incubated for up to 4 hours at 37 °C. Then IPTG was added to each tube to a final concentration of 100 µmol/L, and the culture was incubated for an additional 4 hours. The induced cells were harvested by centrifugation, and cell lysates were analyzed by 120 g/L SDS-PAGE. The his-tagged fusion

proteins were purified by using Ni-NTA-agarose and PD-10 desalting columns according to the manufacturer's recommendations (Qiagen and Amersham Pharmacia). The purified proteins were analyzed by 120 g/L SDS-PAGE.

Expression and purification of proteins without TAT PTD
 PET-30a/TR, pET-30a/TRmut, and pET-30a/HBVc transformed *E. coli* BL21 (DE3) LysS. After the analysis of expression levels, the three proteins were purified in the same way as for TAT fusion proteins.

Culture of 2.2.15 cells Cells were cultured in DMEM containing 150 mL/L fetal bovine serum at 37 °C in 50 mL/L CO₂ and 100 mg/L G418.

Identification of TAT fusion protein transduction 2.2.15 cells (2×10^8 /L) were plated into 6-well plates with coverslips, and allowed to adhere for 24 hours. TAT-TR, TAT-TRmut, TAT-hEDN, TAT-HBVc, TR, TRmut, hEDN and HBVc were added into the wells, respectively, at the final concentration of 100 nmol/L. Incubated for 30 min at 37 °C, all cells were immediately washed with sterile PBS (pH8.0), fixed in 20 g/L paraformaldehyde and 1 g/L TritonX-100 diluted in PBS and put on ice for 30 min. Cells were washed three times with cold PBS. Non-specific epitopes were blocked by using 10 g/L BSA for 10 min at 42 °C. Cells were washed three times with cold PBS, and then incubated with mouse anti-His mAb (1:500) for 15 min at 42 °C. After washing three times in cold PBS, the rabbit anti-mouse IgG labeled with FITC (1:1 000) was added to each well and incubated for 10 min at 42 °C. Rinsed with PBS for 1 hour and the coverslips were mounted on slides by using 500 mL/L glycerol. The cells were observed by fluorescence microscopy.

Determination of anti-HBV effect of TAT-TR 2.2.15 cells were plated at the density of 2×10^8 /L into 12-well plates. TAT-TR, TAT-TRmut, TAT-hEDN and TAT-HBVc were added into the wells, respectively, at the final concentration of 100 nmol/L. 20 μ L DMEM was added into wells as mock group. Four parallels were set up for each group. 24 hours later, HBVAg in the supernatant was determined by using sPRIA kit as described by the manufacturer.

MTT assay 2.2.15 cells were plated at the density of 2×10^8 /L into 96-well plates. After 24 hours, TAT-TR, TAT-TRmut, TAT-HEDN, TAT-HBVc were added into (A), (B), (C), (D) groups at the final concentration of 100 nmol/L. 20 μ L DMEM was added into well (E). 72 hours later, the morphology of cells was observed through inverted microscopy and MTT was applied in each well at the final concentration of 5 g/L. After another 4 hours' culturing, 150 μ L DMSO was added into all wells and the light absorbance at A₄₉₀ was detected.

Statistical analysis

All data obtained were processed by SPSS software. $P < 0.05$ was considered statistically significant.

RESULTS

Expression and purification of TAT fusion proteins

In order to obtain the fusion proteins, pTAT-HA/TR, pTAT-HA/TRmut, pTAT-HA/hEDN and pTAT-HA/HBVc were used to transform *E. coli* BL21 (DE3) LysS and expressed with the induction of IPTG. The same strain transformed by pTAT-HA was used as negative control. The expression levels were determined by 120 g/L SDS-PAGE. Four predicted new bands could be detected in the lysates of TAT fusion transformants, but not in the control. Then the proteins were purified by using Ni-NTA affinity columns and PD-10 desalting columns (Figure 1). The degrees of purity of the fusion proteins were 90 %, 88 %, 80 % and 85 % respectively.

Expression and purification of proteins without TAT PTD

In a similar fashion, pET-30a/TR, pET-30a/TRmut and pET-30a/HBVc were induced to express proteins without TAT PTD by IPTG in BL21 (DE3) LysS, and they produced proteins with predicted molecular masses (Figure 2). Then the proteins were purified by using Ni-NTA affinity columns and PD-10 desalting columns. The degrees of purity of the fusion proteins were 88 %, 76 % and 81 % respectively.

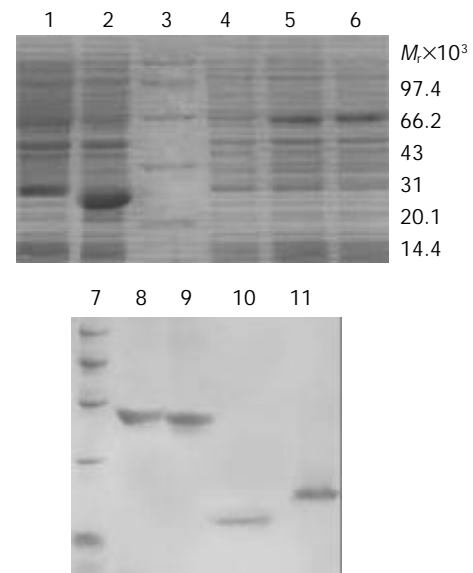


Figure 1 SDS-PAGE analysis of expression and purification for TAT fusion proteins. 1: Transformed by pTAT-HA /HBVc; 2: Transformed by pTAT-HA /hEDN; 3: Protein marker; 4: Transformed by pTAT-HA; 5: Transformed by pTAT-HA/TR; 6: Transformed by pTAT-HA/TRmut; 7: Protein marker; 8: Purified TAT-TN; 9: Purified TAT-TNmut; 10: Purified TAT-hEDN; 11: Purified TAT-HBVc.

Identification of protein transduction

To evaluate the fusion proteins' transduction ability in crossing the membrane of 2.2.15 cells. TAT-TR, TAT-TR mut, TAT-hEDN and TAT-HBVc were added in the culture media at the final concentration of 100 nmol/L. TR, TRmut, hEDN and HBVc without TAT PTD were used as negative controls. Under the fluorescence microscope, abundant fluorescence could be seen in cytoplasm of the cells transduced with TAT fusion proteins, but no fluorescence could be found in the control cells (Figure 3). This result clearly suggests that TAT fusion proteins could cross the membrane of 2.2.15 cells with high efficiency.

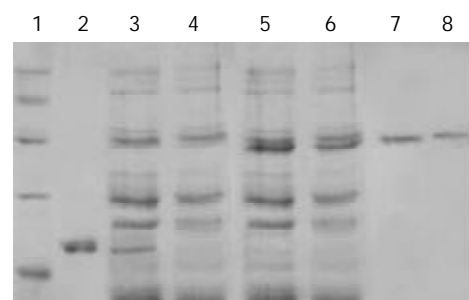


Figure 2 SDS-PAGE analysis of purified control proteins. 1: Protein marker; 2: Purified HBVc; 3: Expression product of BL21 transformed by pET30-a/HBVc; 4: Expression product of BL21 transformed by pET30-a; 5: Expression product of BL21 transformed by pET30-a /TR; 6: Expression product of BL21 transformed by pET30-a/TRmut; 7: Purified TR; 8: Purified TRmut.

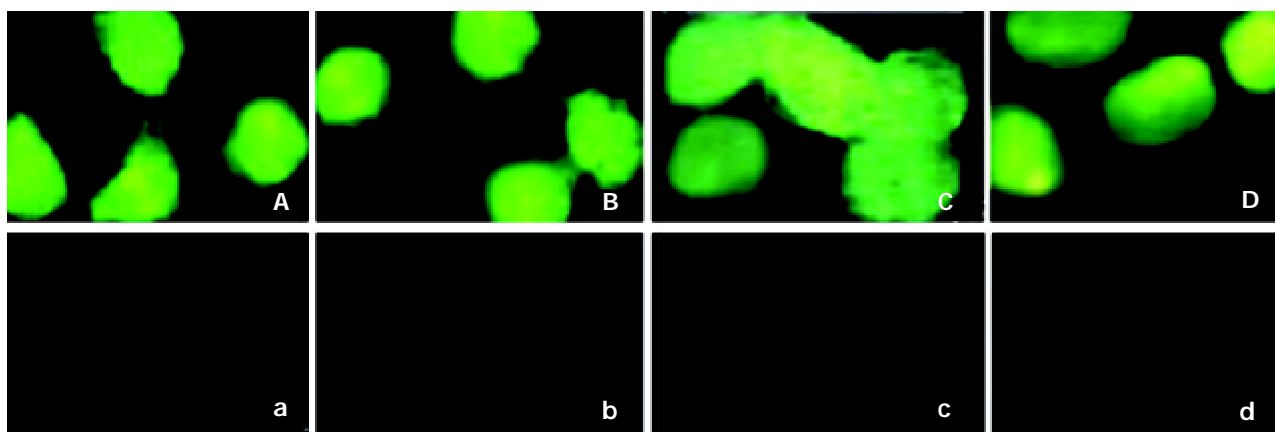


Figure 3 Detection of the transduction of the TAT fusion proteins in 2.2.15 cells. A: Added with TAT-TR; B: Added with TAT-hEDN; C: Added with TAT-HBVC; D: Added with TAT-TRmut; a: Added with TR; b: Added with hEDN; c: Added with HBVc; d: Added with TRmut.

Analysis of anti-HBV activity for TAT-TR

Statistical analysis with SPSS software showed that the mean HBeAg concentration of the TAT-TR group decreased significantly as compared with control groups (The mean difference is significant at the 0.05 level). In addition, there is no significant difference among the mean concentration of control groups ($P > 0.05$). The HBeAg concentration of TAT-TR group decreased by 60.3 % (Figure 4).

MTT assay

After 72 hours culture, the morphology of cells was observed under inverted microscope and it was found that there was no discernible difference among the four experiment groups and the DMEM control. MTT assay showed no significant difference among the five groups. Their A_{490} absorbance values ($\bar{x} \pm s$, $n=4$) were 0.4875 ± 0.018 , 0.4675 ± 0.022 , 0.4690 ± 0.028 , 0.4800 ± 0.029 and 0.4855 ± 0.050 , respectively, ($P > 0.05$).

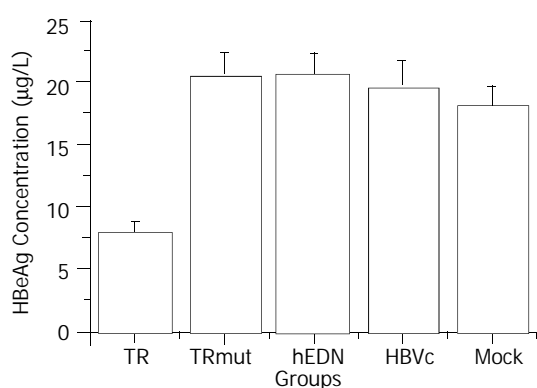


Figure 4 Comparison of HBeAg concentration between different groups.

DISCUSSION

The transduction of proteins into cells was first described in 1988 independently by Green *et al.*^[39] and Frankel *et al.*^[40]. In 1994, Fawcett *et al.*^[5] expanded these observations by demonstrating that heterologous proteins chemically cross-linked to a 36 amino acid domain of TAT were able to transduce into cells. Subsequent to the TAT discovery, other transduction domains were identified that resided in the Antennapedia (Antp) protein from *Drosophila*^[41] and HSV VP22 protein from HSV^[42]. Although the exact mechanism of protein transduction across the cellular membrane remains unclear, PTD's widespread application has been realized. TAT-mediated

transduction provides several advantages over DNA transfection, the current standard method of intracellular protein expression. Importantly, all eukaryotic cell types tested to date are susceptible to transduction, even osteoclasts, primary cells and peripheral-blood mononuclear cells, which are impervious to DNA transfection and retroviral infection, can be effectively transduced^[43,44]. Additionally, as transduction occurs so rapidly (15 min rather than 12 h in serum-free media for transfection), issues of timing can be addressed. The exact intracellular concentration can also be controlled precisely just by varying the amount added to the culture medium. Furthermore, every cell in the population appears to contain a near-identical intracellular protein level^[3]. Another dominant advantage of the system allows denatured fusion protein be directly applied without the laborious renature course, and thus it also provides much convenience for protein purification. Once transduced inside the cells, the denatured proteins can be correctly refolded by chaperones^[45], and are capable of binding their cognate intracellular targets and performing biochemical functions.

To explore the feasibility of using PTD in the anti-HBV research work and provide an alternative strategy for treatment of hepatitis B in this study, we prepared and purified the TAT-TR fusion protein, and also other control proteins. Transduction of TAT-fusion proteins was detected by immunofluorescence assay. Strong fluorescence appeared in the cytoplasm of the cells applied with four TAT fusion proteins, but not in the control groups. These results showed the high transduction efficiency of TAT fusion proteins. We also investigated TAT-TR's anti-HBV activity by radioimmunoassay and got an exciting result. As compared with the mock group, concentration of HBeAg in TAT-TR group decreased by 60.3 %, which indicated that the purified TAT-TR possessed a potent anti-HBV activity. There was no significant difference between any other group and the mock group, suggesting HBVc or hEDN alone had no effect on HBV replication, and TRmut, a fusion molecule of HBVc with an inactivated mutant hEDN, also had no inhibitory effect. These further confirmed the anti-HBV mechanism of the HBV targeted ribonuclease. While TR was transduced into 2.2.15 cells, it could be packaged into the HBV core particles by HBVc, and then hEDN, as a ribonuclease, could degrade the pgRNA packed in the core particles, thus inhibiting the replication of HBV. We performed MTT assay to reveal whether the TAT fusion proteins were harmful to 2.2.15 cells, and the results indicate that they did not affect the growth of 2.2.15 cells and the purified TAT-TR may be applied *in vivo*. Therefore, we conclude that the TAT-HBV targeted ribonuclease fusion protein obtained in this study has laid the foundation for using TR in the therapy of HBV infection.

REFERENCES

- 1 **Becker-Hapak M**, McAllister SS, Dowdy SF. TAT-mediated protein transduction into mammalian cells. *Methods* 2001; **24**: 247-256
- 2 **Schwarze SR**, Dowdy SF. *In vivo* protein transduction: intracellular delivery of biologically active proteins, compounds and DNA. *Trends Pharmacol Sci* 2000; **21**: 45-48
- 3 **Schwarze SR**, Hruska KA, Dowdy SF. Protein transduction: unrestricted delivery into all cells? *Trends Cell Biol* 2000; **10**: 290-295
- 4 **Vives E**, Brodin P, Lebieu B. A truncated HIV-1 Tat protein basic domain rapidly translocates through the plasma membrane and accumulates in the cell nucleus. *J Biol Chem* 1997; **272**: 16010-16017
- 5 **Fawell S**, Seery J, Daikh Y, Moore C, Chen LL, Pepinsky B, Barsoum J. Tat-mediated delivery of heterologous proteins into cells. *Proc Natl Acad Sci USA* 1994; **91**: 664-668
- 6 **Schwarze SR**, Ho A, Vocero-Akbani A, Dowdy SF. *In vivo* protein transduction: delivery of a biologically active protein into the mouse. *Science* 1999; **285**: 1569-1572
- 7 **Nagahara H**, Vocero-Akbani AM, Snyder EL, Ho A, Latham DG, Lissy NA, Becker-Hapak M, Ezhevsky SA, Dowdy SF. Transduction of full-length TAT fusion proteins into mammalian cells: TAT-p27kip1 induces cell migration. *Natl Med* 1998; **4**: 1449-1452
- 8 **Chellaiah MA**, Soga N, Swanson S, McAllister S, Alvarez U, Wang D, Dowdy SF, Hruska KA. Rho-A is critical for osteoclast podosome organization, motility and bone resorption. *Biol Chem* 2000; **275**: 11993-12002
- 9 **Shi H**, Wang FS. Host factors in chronicity of hepatitis B virus infection and their significances in clinic. *Shijie Huaren Xiaohua Zaizhi* 2001; **9**: 66-69
- 10 **Befeler AS**, Di Bisceglie AM. Hepatitis B. *Infect Dis Clin North Am* 2000; **14**: 617-632
- 11 **Maddrey WC**. Hepatitis B: an important public health issue. *J Med Virol* 2000; **61**: 362-366
- 12 **Lau GK**. Hepatitis B infection in China. *Clin Liver Dis* 2001; **5**: 361-379
- 13 **Merican I**, Guan R, Amarapuka D, Alexander MJ, Chutaputti A, Chien RN, Hasnian SS, Leung N, Lesmana L, Phiet PH, Sjalfoellah Noer HM, Sollano J, Sun HS, Xu DZ. Chronic hepatitis B virus infection in Asian countries. *J Gastroenterol Hepatol* 2000; **15**: 1356-1361
- 14 **Guo SP**, Wang WL, Zhai YQ, Zhao YL. Expression of nuclear factor-kappa B in hepatocellular carcinoma and its relation with the X protein of hepatitis B virus. *World J Gastroenterol* 2001; **7**: 340-344
- 15 **Shi DR**, Lu L, Wang JH, Dong CL, Cong WT. HBV DNA distribution of hepatitis B virus in pancreas and liver of patients with cirrhosis. *Shijie Huaren Xiaohua Zaizhi* 2000; **8**: 751-754
- 16 **Wu C**, Cheng ML, Ding YS, Liu RC, Li J, Wang WL, Hu L. A five-year follow up survey of risk factor of viral hepatic cirrhosis. *Shijie Huaren Xiaohua Zaizhi* 2000; **8**: 1365-1367
- 17 **Wang HY**, Yan RQ, Long JB, Wu QL. Cyclin D1 amplification is associated with HBV DNA intergration and pathology in human hepatocellular carcinoma. *Shijie Huaren Xiaohua Zaizhi* 1999; **7**: 98-100
- 18 **Fan ZR**, Yang DH, Qin HR, Huang CC, Xu C, Qiu QL. Expression of IGF-I, IGF-I receptor mRNA in hepatocellular carcinomas and adjacent nontumor tissue. *Shijie Huaren Xiaohua Zaizhi* 1999; **7**: 848-850
- 19 **Yan JC**, Ma Y, Chen WB, Shun XH. Pathological significance of expression of intrahepatic smooth muscle fiber in hepatitis B. *Shijie Huaren Xiaohua Zaizhi* 2000; **8**: 1242-1246
- 20 **Zhai SH**, Liu JB, Liu YM, Zhang LL, Du ZH. Expression of HBsAg, HCV-Ag and AFP in liver cirrhosis and hepatocarcinoma. *Shijie Huaren Xiaohua Zaizhi* 2000; **8**: 524-527
- 21 **Feitelson MA**. Hepatitis B virus in hepatocarcinogenesis. *J Cell Physiol* 1999; **181**: 188-202
- 22 **Arbuthnot P**, Kew M. Hepatitis B virus and hepatocellular carcinoma. *Int J Exp Pathol* 2001; **82**: 77-100
- 23 **Zhuang L**, You J, Tang BZ, Ding SY, Yan KH, Peng D, Zhang YM, Zhang L. Preliminary results of Thymosin-a1 versus interferon- α -treatment in patient with HBeAg negative and serum HBV DNA positive chronic hepatitis B. *World J Gastroenterol* 2001; **7**: 407-410
- 24 **Xie Q**, Guo Q, Zhou XQ, Gu RY. Effect of adenine arabinoside monophosphate coupled to lactosaminated human serum albumin on duck hepatitis B virus. *Shijie Huaren Xiaohua Zaizhi* 1999; **7**: 125-126
- 25 **Li J**, Tang B. Effect on replication of hepatitis B virus by Chinese traditional medicine. *Shijie Huaren Xiaohua Zaizhi* 2000; **8**: 945-946
- 26 **Zhu Y**, Wang YL, Shi L. Clinical analysis of the efficacy of interferon alpha treatment of hepatitis. *World J Gastroenterol* 1998; **4**: 85-86
- 27 **Xu KC**, Wei BH, Yao XX, Zhang WD. Recently therapy for chronic hepatitis B virus by combined traditional Chinese and Western medicine. *Shijie Huaren Xiaohua Zaizhi* 1999; **7**: 970-974
- 28 **Lau GK**. Use of immunomodulatory therapy (other than interferon) for the treatment of chronic hepatitis B virus infection. *J Gastroenterol Hepatol* 2000; **15**(Suppl): E46-52
- 29 **Guan R**. Interferon monotherapy in chronic hepatitis B. *J Gastroenterol Hepatol* 2000; **15** (Suppl): E34-40
- 30 **Torresi J**, Locarnini S. Antiviral chemotherapy for the treatment of hepatitis B virus infections. *Gastroenterology* 2000; **118** (Suppl): S83-103
- 31 **Schiff ER**. Lamivudine for hepatitis B in clinical practice. *J Med Virol* 2000; **61**: 386-391
- 32 **Jarvis B**, Faulds D. Lamivudine. A review of its therapeutic potential in chronic hepatitis B. *Drugs* 1999; **58**: 101-141
- 33 **Malik AH**, Lee WM. Chronic hepatitis B virus infection: treatment strategies for the next millennium. *Ann Intern Med* 2000; **132**: 723-731
- 34 **Farrell GC**. Clinical potential of emerging new agents in hepatitis B. *Drugs* 2000; **60**: 701-710
- 35 **Song YH**, Lin JS, Liu NZ, Kong XJ, Xie N, Wang NX, Jin YX, Liang KH. Anti-HBV hairpin ribozyme-mediated cleavage of target RNA *in vitro*. *World J Gastroenterol* 2002; **8**: 91-94
- 36 **Li YH**, Liu J, Xue CF. Construction of HBV targeted ribonuclease and its expression in 2.2.15 cell line. *Xibao Yu Fenzi Mianyixue Zaizhi* 2002; **18**: 217-220
- 37 **Liu J**, Li YH, Xue CF, Ding J, Gong WD, Zhao Y. HBV targeted ribonuclease can inhibit HBV replication. *World J Gastroenterol* 2003; **9**: 295-299
- 38 **Ding J**, Liu J, Xue CF, Li YH, Gong WD. Construction and expression of prokaryotic expression vector for pTAT-HBV targeted ribonuclease fusion protein. *Xibao Yu Fenzi Mianyixue Zaizhi* 2003; **19**: 49-51
- 39 **Green M**, Loewenstein PM. Autonomous functional domains of chemically synthesized human immunodeficiency virus tat trans-activator protein. *Cell* 1988; **55**: 1179-1188
- 40 **Frankel AD**, Pabo Co. Cellular uptake of the tat protein from human immunodeficiency virus. *Cell* 1988; **55**: 1189-1193
- 41 **Derossi D**, Joliet AH, Chassaing G, Prochiantz A. The third helix of the Antennapedia homeodomain translocates through biological membranes. *J Biol Chem* 1994; **269**: 10444-10450
- 42 **Elloit G**, O' Hare P. Intercellular trafficking and protein delivery by a herpesvirus structural protein. *Cell* 1997; **88**: 223-233
- 43 **Chellaiah MA**, Soga N, Swanson S, McAllister S, Alvarez U, Wang D, Dowdy SF, Hruska KA. Rho-A is critical for osteoclast podosome organization, motility, and bone resorption. *J Biol Chem* 2000; **275**: 11993-2002
- 44 **Schutze-Redelmeier MP**, Gournier H, Garcia-Pons F, Moussa M, Joliet AH, Volovitch M, Prochiantz A, Lemonnier FA. Introduction of exogenous antigens into the MHC class I processing and presentation pathway by Drosophila antennapedia homeodomain primes cytotoxic T cells *in vivo*. *J Immunol* 1996; **157**: 650-655
- 45 **Gottesman S**, Wickner S, Maurizi MR. Protein quality control: triage by chaperones and proteases. *Genes Dev* 1997; **11**: 815-823

Construction of hpaA gene from a clinical isolate of *Helicobacter pylori* and identification of fusion protein

Ya-Fei Mao, Jie Yan, Li-Wei Li, Shu-Ping Li

Ya-Fei Mao, Jie Yan, Li-Wei Li, Shu-Ping Li, Department of Medical Microbiology and Parasitology, College of Medical Sciences, Zhejiang University, Hangzhou 310031, Zhejiang Province, China
Supported by the Excellent Young Teacher Fund of Chinese Education Ministry and the General Research Plan of Science and Technology Department of Zhejiang Province, No. 001110438

Correspondence to: Dr. Jie Yan, Department of Medical Microbiology and Parasitology, College of Medical Sciences, Zhejiang University, 353 Yan an Road, Hangzhou 310031, Zhejiang Province, China. yanchen@mail.hz.zj.cn

Telephone: +86-571-87217385 **Fax:** +86-571-87217044

Received: 2003-03-02 **Accepted:** 2003-03-28

Abstract

AIM: To clone hpaA gene from a clinical strain of *Helicobacter pylori* and to construct the expression vector of the gene and to identify immunity of the fusion protein.

METHODS: The hpaA gene from a clinical isolate Y06 of *H. pylori* was amplified by high fidelity PCR. The nucleotide sequence of the target DNA amplification fragment was sequenced after T-A cloning. The recombinant expression vector inserted with hpaA gene was constructed. The expression of HpaA fusion protein in *E. coli* BL21DE3 induced by IPTG at different dosages was examined by SDS-PAGE. Western blot with commercial antibody against whole cell of *H. pylori* as well as immunodiffusion assay with self-prepared rabbit antiserum against HpaA fusion protein were applied to determine immunity of the fusion protein. ELISA was used to detect the antibody against HpaA in sera of 125 patients infected with *H. pylori* and to examine HpaA expression of 109 clinical isolates of *H. pylori*.

RESULTS: In comparison with the reported corresponding sequences, the homologies of nucleotide and putative amino acid sequences of the cloned hpaA gene were from 94.25-97.32 % and 95.38-98.46 %, respectively. The output of HpaA fusion protein in its expression system of pET32a-hpaA-BL21DE3 was approximately 40 % of the total bacterial proteins. HpaA fusion protein was able to combine with the commercial antibody against whole cell of *H. pylori* and to induce rabbit producing specific antiserum with 1:4 immunodiffusion titer after the animal was immunized with the fusion protein. 81.6 % of the serum samples from 125 patients infected with *H. pylori* (102/125) were positive for HpaA antibody and all of the tested isolates of *H. pylori* (109/109) were detectable for HpaA.

CONCLUSION: A prokaryotic expression system with high efficiency of *H. pylori* hpaA gene was successfully established. The HpaA expressing fusion protein showed satisfactory immunoreactivity and antigenicity. High frequencies of HpaA expression in different *H. pylori* clinical strains and specific antibody production in *H. pylori* infected patients indicate that HpaA is an excellent and ideal antigen for developing *H. pylori* vaccine.

Mao YF, Yan J, Li LW, Li SP. Construction of hpaA gene from a clinical isolate of *Helicobacter pylori* and identification of fusion protein. *World J Gastroenterol* 2003; 9(7): 1529-1536
<http://www.wjgnet.com/1007-9327/9/1529.asp>

INTRODUCTION

In China, chronic gastritis and peptic ulcer are the most prevalent gastric diseases and gastric cancer is one of the malignant tumors with high morbidities^[1-34]. *Helicobacter pylori*, a microaerophilic, spiral and gram-negative bacillus, is recognized as a human-specific gastric pathogen that colonizes the stomachs of at least half of the world's populations^[35]. Most infected individuals are asymptomatic. However, in some subjects, the infection causes acute, chronic gastritis or peptic ulceration, and plays an important role in the development of peptic ulcer and gastric adenocarcinoma, mucosa-associated lymphoid tissue (MALT) lymphoma and primary gastric non-Hodgkin's lymphoma^[36-43]. This organism is categorized as a class I carcinogen pronounced by the World Health Organization^[44], and direct evidence of carcinogenesis was recently demonstrated in an animal model^[45,46]. Immunization against the bacterium represents a cost-effective strategy to prevent *H. pylori*-associated peptic ulcer diseases and to reduce the incidence of global gastric cancers^[47]. The selection of antigenic targets is critical in the design of *H. pylori* vaccine. To date, this field is scarcely touched upon. The majority of studies focused on urease enzyme, heat shock protein, vacuolating cytotoxin, and so on^[35,48-50], but rarely on *H. pylori* adhesin (HpaA) which is a flagellar sheath protein with approximately 29KDa located in the bacterial outer membrane^[51]. So, in this study, a recombinant plasmid inserted with the gene (hpaA) responsible for encoding HpaA was constructed and the immunogenicity and immunoreactivity of its expression product were examined. Furthermore, the fusion protein of HpaA and its rabbit antiserum were also used to detect serum samples from *H. pylori* infected patients and *H. pylori* isolates, respectively. The results of this study will be helpful for determining whether the recombinant HpaA (rHpaA) becomes one of the good candidates as an antigen in *H. pylori* vaccine.

MATERIALS AND METHODS

Materials

A well-characterized clinical strain of *H. pylori*, provisionally named Y06, was provided by the Department of Medical Microbiology and Parasitology, College of Medical Sciences, Zhejiang University. Plasmid pET32a (Promega) and *E. coli* BL21 DE3 (Promega) were used as expression vector and host cell, respectively. The primers for amplification were synthesized by BioAsia (Shanghai, China). EX Taq high fidelity PCR kit and restriction endonucleases were purchased from TaKaRa (Dalian, China). T-A cloning kit and sequencing service were offered by BBST (Shanghai, China). Rabbit antibody against the whole cell of *H. pylori* and HRP-labeling sheep antibodies against rabbit IgG and human IgG were

purchased from DACO and Jackson ImmunoResearch, respectively. The agents used in isolation and identification of *H. pylori* were purchased from Sigma and bioMérieux, etc. 126 biopsy specimens from patients with positive *H. pylori* (86 males and 40 females; age range: 6-78 years; mean age: 40.5 years) for gastroduodenoscopy in four different hospitals in Hangzhou were collected during the period of the end of 2001 to the midyear of 2002. Each of the patients consented to be enrolled in this study and all of them agreed to offer their biopsy samples. Among the 126 patients, 68 suffered from chronic gastritis (CG) in cluding 48 with chronic superficial gastritis, 10 with chronic active gastritis and 10 with chronic atrophic gastritis, and 58 patients suffered from peptic ulcer (PU) in cluding 12 with gastric ulcer, 40 with duodenal ulcer and 6 with gastric and duodenal ulcer. None of the patients had received nonsteroidal anti-inflammatory drugs or antacid drugs and antibiotics within the previous two weeks before the study. At the same time, 126 serum specimens from these patients were also collected.

Methods

Isolation and identification of clinical *H. pylori* strains Each of the biopsy specimens was homogenized with a tissue grinder and then inoculated onto Columbia agar plates supplemented with 8.0 % (V/V) sheep blood, 0.2 % (W/V) cyclodextrin, 5 mg/L trimethoprim, 10 mg/L vancomycin, 2.5 mg/L amphotericin B and 2 500 U/L polymyxin B. The plates were incubated at 37 °C under microaerobic conditions (5 % O₂, 10 % CO₂ and 85 % N₂) for 3 to 5 days. Isolates were identified as *H. pylori* according to typical Gram stain morphology, positive biochemical tests for urease and oxidase, and agglutination with commercial rabbit antibody against whole cell of the microbe. All of *H. pylori* isolates were stored at -70 °C for ELISA.

Preparation of DNA template Genomic DNA of *H. pylori* strain Y06 was extracted by routine phenol-chloroform method, DNase-free RNase digestion and phenol-chloroform extraction. The DNA template was solved in TE buffer, and its concentration and purity were determined by ultraviolet spectrophotometry^[52].

Polymerase chain reaction Oligonucleotide primers were designed to amplify the whole sequence of hpaA gene from *H. pylori* strain Y06 based on the published corresponding genome sequence^[51,53]. The sequence of sense primer with an endonuclease site of *Bam*H I was: 5' -CCGGGATCCATGAGCAAATAATC-3'. The sequence of antisense primer with an endonuclease site of *Eco*R I was: 5' -CCGGAATTCTTCTTATGCGTTATTTG-3'. The total volume of PCR reaction mixture was 100 µL containing 2.5 mol·L⁻¹ each dNTP, 250 nmol·L⁻¹ each primer, 15 mol·L⁻¹ MgCl₂, 3.0 U EX Taq polymerase, 200 ng DNA template and 1×PCR buffer (pH8.3). The parameters for PCR were as follows: at 94 °C for 5 min, one cycle; at 94 °C for 30 sec, at 50 °C for 30 sec, at 72 °C for 60 sec, 10 cycle; at 94 °C for 30 sec, at 50 °C for 30 sec, at 72 °C for 70 sec (additional 10 sec for each of the following cycles), 20 cycle, at 72 °C for 10 min, 1 cycle. The results of PCR were observed under UV light after electrophoresis in 15 g·L⁻¹ agarose pre-stained with ethidium bromide. The expected size of target amplification fragment was 802 bp.

Cloning and sequencing The target amplification DNA fragment of hpaA gene was cloned into pUCm-T vector (pUCm-T-hpaA) by using the T-A cloning kit according to the manufacturer's instructions. The recombinant plasmid was amplified in *E. coli* strain DH5α and then extracted by Sambrook's method^[52]. A professional company (BBST) was responsible for nucleotide sequence analysis of the inserted fragments. Two different strains of *E. coli* DH5α containing pUCm-T-hpaA and expression vector pET32a were amplified respectively and the two plasmids were extracted^[52]. The

plasmids were digested with *Bam*H I and *Eco*R I. The target fragments of hpaA and pET32a were recovered and then ligated. The recombinant expression vector pET32a-hpaA was transformed into *E. coli* BL21DE3. pET32a-hpaA was prepared for sequencing again after the amplification in its host cell.

Expression and identification of the fusion protein The hpaA prokaryotic expression system pET32a-hpaA-BL21DE3 was rotationally cultured in LB medium at 37 °C under induction of isopropylthio-β-D-galactoside (IPTG) at different dosages of 1, 0.5 and 0.1 mmol·L⁻¹. The supernatant and precipitate were isolated by centrifugation after the engineering bacterium pellet was ultrasonically broken (300V, 5sec once for three times). The molecular weight, output and location of HpaA fusion protein were examined by SDS-PAGE. HpaA fusion protein was collected by Ni-NTA affinity chromatography. The immunoreactivity of HpaA fusion protein was determined by Western blot with commercial rabbit antibody against whole cell of *H. pylori* and HRP-labeling sheep antibody against rabbit IgG, respectively. Rabbits were immunized with HpaA fusion protein to obtain the antiserum. Immunodiffusion assay was applied to determine antigenicity of the fusion protein.

ELISA The antibodies against HpaA in sera of the patients infected with *H. pylori* were detected by ELISA with HpaA fusion protein at the concentration of 20 µg/mL as coated antigen, the patients' sera (1:200 dilution) as the first antibody, HRP-labeling sheep antibody against human IgG (1:4 000 dilution) as the second antibody and ortho-phenylene diamine as a substrate. The result of ELISA for a patient's serum sample was considered as positive if its OD₄₉₀ value was over the mean plus 3 SD of 6 cases of negative serum samples^[54]. HpaA expression of clinical isolates of *H. pylori* was detected by ELISA using ultrasonic supernatant at the protein concentration of 50 µg/mL of each *H. pylori* isolate as coated antigen, the self-prepared rabbit antiserum against HpaA fusion protein (1:2 000 dilution) as the first antibody, HRP-labeling sheep antibody against rabbit IgG (1:3 000 dilution) as the second antibody and ortho-phenylene diamine as a substrate. The result of ELISA for an *H. pylori* ultrasonic supernatant was considered as positive if its OD₄₉₀ value was over the mean plus 3 SD of 6 cases of ultrasonic supernatant at the same protein concentration of *E. coli* ATCC 25922 played as negative control^[54].

Data analysis The nucleotide sequences of the cloned hpaA gene inserted in the two recombinant plasmid vectors were compared for homologies with 6 published hpaA gene sequences (X92502, NC000915, X61574, NC000921, AF479028 and U35455)^[51,53,55-58] with a special molecular biological analysis soft ware.

RESULTS

PCR

Target fragment with expected size amplified from DNA template of *H. pylori* strain Y06 is shown in Figure 1.

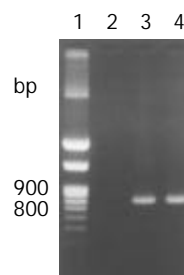


Figure 1 The target fragment of hpaA gene amplified from *H. pylori* strain Y06 (1: 100 bp DNA marker; 2: blank control; 3 and 4: the target fragment amplified from *H. pylori* strain Y06 DNA).

Nucleotide sequence analysis

The hpaA gene nucleotide sequences in the recombinant plasmid vectors of pUCm-T-hpaA and pET32a-hpaA were completely the same. The homologies of the nucleotide and

putative amino acid sequences in the pUCm-T-hpaA and pET32a-hpaA compared with the published hpaA gene sequences^[51,53,55-58] were from 94.25-97.32 % and 95.38-98.46 %, respectively (Figures 2, 3).

```
[1]1  ATGAGAGCAAATAATCATTTTTAAAGATTTTGCATGGAAAAAATGCCTTTTATAGCGCGAGC
[2]1  . . . . . A . . . . . T . . . . .
[3]1  . . . . . A . A . . . . . GG . . . . . G . . . . . A . . . . .
[4]1  . . . . . A . A . . . . . GG . . . . . G . . . . . T . . . . .
[5]1  . . . . . A . A . . . . . GG . . . . . G . . . . . T . . . . .
[6]1  . . . . . A . A . . . . . GG . . . . . G . . . . .
[7]1  . . . . .

[1]61  GTGGTGGCTTTATTAGTGGGATGCAGCCCGCATATTATTGAAACCAATGAAGTCGCTTTG
[2]61  . . . . . G . . . . .
[3]61  . . . . . G . . . . . G . . . . .
[4]61  . . . . . G . T . . . . . T . . . . .
[5]61  . . . . .
[6]61  . . . . . G . . . . .
[7]61  . . . . . G . G . . . . .

[1]121 AAATTGAATTACCATCCAGCTAGCGAGAAAGTTCAAGCGTTAGATGAAAAGATTTTGTCTT
[2]121 . . . . .
[3]121 . . . . . G . . . . .
[4]121 . . . . . A . . . . .
[5]121 . . . . .
[6]121 . . G . . . . .
[7]121 . . . . . C . . . . .

[1]181 TTAAGGCCAGCTTTCCAATATAGCGATAATATCGCTAAAGAGTATGAAAACAAATTCAAG
[2]181 . . . . . T . . . . . C . . . . . T . . . . .
[3]181 . . . . . A . . . . . C . . . . . C . T . . . . . T . . . . .
[4]181 . . . . . C . . . . . T . . . . .
[5]181 . . . . . C . . . . . T . . . . .
[6]181 . . . . . T . . . . . C . . . . . T . . . . .
[7]181 . . . . . T . . . . . C . . . . . T . . . . .

[1]241 AATCAAACCGCGCTCAAGGTTGAACAGATTTTGCAAAATCAAGGCTATAAGGTTATTAGC
[2]241 . . . . . G . . . . .
[3]241 . . . . . A . . . . . T . A . . . . . G . . . . . C . . . . . G . . . . . C . . . . . C . AT
[4]241 . . . . . A . . . . . T . A . . . . . G . . . . . C . . . . . G . . . . . AT
[5]241 . . . . . G . . . . . C . . . . . C . AT
[6]241 . . . . . T . . . . . G . . . . . AT
[7]241 . . . . . A . . . . . T . . . . . G . . . . . C . . . . .

[1]301 GTAGATAGCAGCGATAAAGACGATTTTTCTTTTGCACAAAAAAGAAGGGTATTTGGCG
[2]301 . . . . . C . . . . . T . G . . . . . T . . . . .
[3]301 . . G . . . . . G . . . . .
[4]301 . . G . . . . . G . . . . . T . . . . .
[5]301 . . G . . . . . T . . . . . G . . . . .
[6]301 . . G . . . . . G . . . . . T . . . . .
[7]301 . . . . . C . . . . . T . G . . . . . C . . . . .

[1]361 GTTGCTATGAATGGCGAAATTTGTTTTACGCCCGATCCTAAAAGGACCATACAGAAAAA
[2]361 . . . . .
[3]361 . . . . . T . . . . . A . . . . .
[4]361 . . C . . . . .
[5]361 . . . . .
[6]361 . . C . . . . . T . . . . .
[7]361 . . C . . . . .
```

```

[1]421 TCAGAACCCGGGTTATTATTCTCCACCGGTTTGGACAAAATGGAAGGGGTTTTAATCCCG
[2]421 .....G.....T.....T.....A
[3]421 .....T.....T.....C.....
[4]421 .....T.....T.....
[5]421 .....T.....T.....
[6]421 .....T.....T.....
[7]421 .....T.....

[1]481 GCTGGGTTTTATTAAAGGTTACCATACTAGAGCCTATGAGTGGGGAATCTTTGGATTCTTTT
[2]481 ..C.....G.C.....
[3]481 ..C..T..G.C.....A...C...
[4]481 .....G.C.....
[5]481 .....T.....A.....
[6]481 .....G.C.....T.....
[7]481 .....G.C.....A.....

[1]541 ACGATGGATTTGAGCGAGTTGGACATTCAAGAAAATTCTTAAAAACCACCCATTCAAGC
[2]541 .....
[3]541 .....T...A.....G.....
[4]541 .....
[5]541 .....C.....
[6]541 .....
[7]541 .....

[1]601 CATAGCGGGGGTTAGTTAGCACTATGGTTAAGGGAACGGATAATTCTAATGACGCGATC
[2]601 .....
[3]601 .....A.....T.....
[4]601 .....A.....G.....A..T
[5]601 .....
[6]601 .....
[7]601 .....

[1]661 AAGAGCGCTTTGAATAAGATTTTTGCAAATATCATGCAAGAAATAGACAAAAAACTCACT
[2]661 .....
[3]661 .....G.....G..T..G.....
[4]661 .....G.....G..T..G.....
[5]661 .....C.....
[6]661 .....G..G.....
[7]661 .....G.....

[1]721 CAAAAGAATTTAGAATCTTATCAAAAAGACGCCAAAGAATTAAAAGGCAAAAAGAAACCGA
[2]721 .....G.....
[3]721 ...G.....G...G...AA...G.....
[4]721 ...G.....G...AA...G.....
[5]721 .....G...G...AA...G.....
[6]721 .....
[7]721 .....G...G...AA...G.....

[1]781 TAAAAACAAATAACGCATAA
[2]781 ...
[3]781 ...G.....
[4]781 .....
[5]781 ...
[6]781 .....
[7]781 TAA.G.....GAA

```

Figure 2 Homology comparison of *H. pylori* hpaA gene nucleotide sequences ([1]-[6]: the reported sequence from GenBank (No. X92502, strain 11637; No. NC000915, strain 26695; No. X61574, strain 8826; No. NC_000921, strain J99; No. AF479028, strain CH-CTX1; No. U35455, strain CCUG 17874); [7]: the sequencing result of *H. pylori* strain Y06 hpaA gene. outline region: oligonucleotide primer sequences; square frame: start code and end code).

```

[1]1  MRANNHFKDFAWKKCLLGASVVALLVGCSPHIIETNEVALKLNYPASEKVQALDEKILL
[2]1  .K.....
[3]1  .KT.G.....T.....
[4]1  .KT.G.....F.....
[5]1  .KT.G.....
[6]1  .KT.G.....G.....
[7]1  .....

[1]61  LRPAFQYSDNIAKEYENKFKNQ TALKVEQILQNQGYKVISVDSSDKDDFSFAQKKEGYLA
[2]61  .....L.S.....
[3]61  .K.....T.E.....N.....
[4]61  .....T.E.....N.....
[5]61  .....N.....
[6]61  .....V.....N.....
[7]61  .....T.E.....L.S.....

[1]121 VAMNGEIVLRPDPKRTIQKKSEPGLLFSTGLDKMEGVLIIPAGFIKVTILEPMSGESLDSF
[2]121 .....V.....
[3]121 ...I.....V.....
[4]121 .....V.....
[5]121 .....
[6]121 .....V.....
[7]121 .....V.....

[1]181 TMDLSELDIQEKFLKTTHSSHSGGLVSTMVKGTDNSNDAIKSALNKIFANIMQEIDKKLT
[2]181 .....
[3]181 .....S.M.....
[4]181 .....S.M.....
[5]181 .....
[6]181 .....GS.....
[7]181 .....

[1]241 QKNLESYQKDAKELKGKRRN
[2]241 .....
[3]241 .....N.....
[4]241 .R.....N.....
[5]241 .....N.....
[6]241 .....
[7]241 .....N.....

```

Figure 3 Homology comparison of the putative amino acid sequences of hpaA gene ([1]-[6]: the reported sequence from GenBank (No. X92502, strain 11637; No. NC000915, strain 26695; No. X61574, strain 8826; No. NC_000921, strain J99; No. AF479028, strain CH-CTX1; No. U35455, strain CCUG 17874); [7]: the sequencing result of Hp strain Y06 hpaA gene).

Expression of target fusion protein

1, 0.5 and 0.1 mmol·L⁻¹ of IPTG were able to efficiently induce the expression of HpaA fusion protein in pET32a-hpaA-BL21DE3 system. The product of HpaA fusion protein was mainly presented in ultrasonic precipitate and the output was approximately 40 % of the total bacterial proteins (Figure 4).

Immunoreactivity and antigenicity of HpaA fusion protein

The commercial rabbit antibody against the whole cell of *H. pylori* could combine with HpaA fusion protein confirmed

by Western blot (Figure 5) and the titer demonstrated by immunodiffusion assay between HpaA fusion protein and rabbit antiserum against the fusion protein was 1:4.

ELISA

The mean \pm SD at OD₄₉₀ of the negative serum samples was 0.11 \pm 0.03 and the positive reference value was 0.20. The mean \pm SD at OD₄₉₀ of the negative bacterial control was 0.04 \pm 0.04 and the positive reference value was 0.16. According to the reference values, 81.6 % (102/125, another serum sample was

contaminated) of the tested patients' serum samples were positive for antibodies against HpaA fusion protein with a range of 0.54-1.84 and 100 % (109/109, other 17 isolates could not be revived from -70 °C) of the tested *H.pylori* isolates were detectable for HpaA with a range of 0.52-1.47.

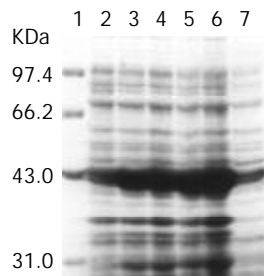


Figure 4 Expression of HpaA gene in pET32a-hpaA-BL21DE3 induced by IPTG with different dosages shown in SDS-PAGE (1: protein marker; 2: non-induced; 3-5: induced with 0.1, 0.5, 1 mmol·L⁻¹ of IPTG, respectively; 6: the bacterial precipitate induced with 1 mmol·L⁻¹ of IPTG; 7: the bacterial supernatant induced with 1 mmol·L⁻¹ of IPTG).

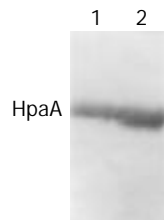


Figure 5 Western blot result of commercial rabbit antibody against whole cell of *H.pylori* and HpaA fusion protein (1 and 2: 20 µl and 40 µl of expressed HpaA product induced with 0.1 mmol·L⁻¹ of IPTG, respectively).

DISCUSSION

The outer membrane is a continuous structure on the surface of gram-negative bacteria. For outer membrane proteins in the outer monolayer of bacterial membrane, they have bilateral particular significance as a potential target for protective immunity and bacterial pathogens. Outer membrane vaccines have been used with considerable success to induce protection against a number of organisms, including heat shock protein, vacuolating cytotoxin, ureases A, B of *H.pylori* and so on^[59-65]. HpaA is one of the major structural outer membrane proteins of *H.pylori* and plays an important role in adhesion of the microbe^[51,53]. HpaA gene is located in genome DNA of *H.pylori* and considerably conservative for its nucleotide and amino acid sequences^[55,56]. Furthermore, antibody against HpaA could be found in approximately 86 % of *H.pylori* infected patients' sera and this proportion was obviously higher than that of heat shock protein (68 %) and vacuolating cytotoxin (68 %)^[57] and was similar to that of urease B^[64]. Therefore, HpaA is an ideal antigen candidate for *H.pylori* vaccine.

In this study, the homologies of the nucleotide and putative amino acid sequences in the cloned HpaA gene from *H.pylori* strain Y06 compared with the 6 published hpaA gene sequences^[51, 53, 55-58] were as high as 94.25-97.32 % and 95.38-98.46 %, respectively, whereas the nucleotide and putative amino acid homologies among the 6 HpaA gene sequences were 93.72-98.21 % and 95.00-98.78 %. These data indicate that the mutation level of the HpaA gene of *H.pylori* strain Y06 is within the range reported by the literatures.

The results of SDS-PAGE demonstrated that the constructed expression system pET32a-hpaA-BL21DE3 was able to

efficiently produce the target fusion protein presented with the form of inclusion body even if induced by IPTG at lower concentration of 0.1 mmol·L⁻¹ and the output was approximately 40 % of the total bacterial proteins.

The rabbit antibody against the whole cell of *H.pylori* could recognize and combine with HpaA fusion protein confirmed by Western blot, indicating that the fusion protein has an active and satisfactory immunoreactivity. The immunodiffusion assay performed in this study demonstrated that HpaA fusion protein could efficiently induce rabbit to produce specific antibody with a higher titer against the fusion protein, which indicates that HpaA fusion protein has favorable antigenicity. The results of ELISA showed that all of the tested clinical isolates of *H.pylori* would express HpaA and the majority of *H.pylori* infected patients' sera (81.6 %) were present for the specific antibody against the microbe.

All the evidences mentioned above suggest that HpaA is an excellent and ideal antigen for developing *H.pylori* vaccine and an HpaA expression system with high efficiency was successfully constructed in this study.

REFERENCES

- 1 **Ye GA**, Zhang WD, Liu LM, Shi L, Xu ZM, Chen Y, Zhou DY. *Helicobacter pylori* vacA gene polymorphism and chronic gastritis. *Shijie Huaren Xiaohua Zazhi* 2001; **9**: 593-595
- 2 **Lu SY**, Pan XZ, Peng XW, Shi ZL. Effect of *Hp* infection on gastric epithelial cell kinetics in stomach diseases. *Shijie Huaren Xiaohua Zazhi* 1999; **7**: 760-762
- 3 **Zhang Z**, Yuan Y, Gao H, Dong M, Wang L, Gong YH. Apoptosis, proliferation and p53 gene expression of *H.pylori* associated gastric epithelial lesions. *World J Gastroenterol* 2001; **7**: 779-782
- 4 **Lu XL**, Qian KD, Tang XQ, Zhu YL, Du Q. Detection of *H.pylori* DNA in gastric epithelial cells by in situ hybridization. *World J Gastroenterol* 2002; **8**: 305-307
- 5 **Yao YL**, Xu B, Song YG, Zhang WD. Overexpression of cyclin E in Mongolian gerbil with *Helicobacter pylori*-induced gastric precancerosis. *World J Gastroenterol* 2002; **8**: 60-63
- 6 **Guo DL**, Dong M, Wang L, Sun LP, Yuan Y. Expression of gastric cancer-associated MG7 antigen in gastric cancer, precancerous lesions and *H. pylori*-associated gastric diseases. *World J Gastroenterol* 2002; **8**: 1009-1013
- 7 **Peng ZS**, Liang ZC, Liu MC, Ouyang NT. Studies on gastric epithelial cell proliferation and apoptosis in *Hp* associated gastric ulcer. *Shijie Huaren Xiaohua Zazhi* 1999; **7**: 218-219
- 8 **Hiyama T**, Haruma K, Kitadai Y, Miyamoto M, Tanaka S, Yoshihara M, Sumii K, Shimamoto F, Kajiyama G. B-cell monoclonality in *Helicobacter pylori*-associated chronic atrophic gastritis. *Virchows Arch* 2001; **483**: 232-237
- 9 **Xia HHX**. Association between *Helicobacter pylori* and gastric cancer: current knowledge and future research. *World J Gastroenterol* 1998; **4**: 93-96
- 10 **Quan J**, Fan XG. Progress in experimental research of *Helicobacter pylori* infection and gastric carcinoma. *Shijie Huaren Xiaohua Zazhi* 1999; **7**: 1068-1069
- 11 **Liu HF**, Liu WW, Fang DC. Study of the relationship between apoptosis and proliferation in gastric carcinoma and its precancerous lesion. *Shijie Huaren Xiaohua Zazhi* 1999; **7**: 649-651
- 12 **Zhu ZH**, Xia ZS, He SG. The effects of ATRA and 5-Fu on telomerase activity and cell growth of gastric cancer cells *in vitro*. *Shijie Huaren Xiaohua Zazhi* 2000; **8**: 669-673
- 13 **Tu SP**, Zhong J, Tan JH, Jiang XH, Qiao MM, Wu YX, Jiang SH. Induction of apoptosis by arsenic trioxide and hydroxy camptothecin in gastric cancer cells *in vitro*. *World J Gastroenterol* 2000; **6**: 532-539
- 14 **Cai L**, Yu SZ, Zhang ZF. *Helicobacter pylori* infection and risk of gastric cancer in Changle County, Fujian Province, China. *World J Gastroenterol* 2000; **6**: 374-376
- 15 **Yao XX**, Yin L, Zhang JY, Bai WY, Li YM, Sun ZC. Htert expression and cellular immunity in gastric cancer and precancerosis. *Shijie Huaren Xiaohua Zazhi* 2001; **9**: 508-512
- 16 **Xu AG**, Li SG, Liu JH, Gan AH. Function of apoptosis and ex-

- pression of the proteins *Bcl-2*, *p53* and *C-myc* in the development of gastric cancer. *World J Gastroenterol* 2001; **7**: 403-406
- 17 **Wang X**, Lan M, Shi YQ, Lu J, Zhong YX, Wu HP, Zai HH, Ding J, Wu KC, Pan BR, Jin JP, Fan DM. Differential display of vincristine-resistance-related gene in gastric cancer SGC7901 cells. *World J Gastroenterol* 2002; **8**: 54-59
- 18 **Liu JR**, Li BX, Chen BQ, Han XH, Xue YB, Yang YM, Zheng YM, Liu RH. Effect of cis-9, trans-11-conjugated linoleic acid on cell cycle of gastric adenocarcinoma cell line (SGC-7901). *World J Gastroenterol* 2002; **8**: 224-229
- 19 **Cai L**, Yu SZ. A molecular epidemiologic study on gastric cancer in Changde, Fujian Province. *Shijie Huaren Xiaohua Zazhi* 1999; **7**: 652-655
- 20 **Gao GL**, Yang Y, Yang SF, Ren CW. Relationship between proliferation of vascular endothelial cells and gastric cancer. *Shijie Huaren Xiaohua Zazhi* 2000; **8**: 282-284
- 21 **Xue XC**, Fang GE, Hua JD. Gastric cancer and apoptosis. *Shijie Huaren Xiaohua Zazhi* 1999; **7**: 359-361
- 22 **Niu WX**, Qin XY, Liu H, Wang CP. Clinicopathological analysis of patients with gastric cancer in 1200 cases. *World J Gastroenterol* 2001; **7**: 281-284
- 23 **Li XY**, Wei PK. Diagnosis of stomach cancer by serum tumor markers. *Shijie Huaren Xiaohua Zazhi* 2001; **9**: 568-570
- 24 **Fang DC**, Yang SM, Zhou XD, Wang DX, Luo YH. Telomere erosion is independent of microsatellite instability but related to loss of heterozygosity in gastric cancer. *World J Gastroenterol* 2001; **7**: 522-526
- 25 **Morgner A**, Miehle S, Stolte M, Neubauer A, Alpen B, Thiede C, Klann H, Hierlmeier FX, Ell C, Ehninger G, Bayerdorffer E. Development of early gastric cancer 4 and 5 years after complete remission of *Helicobacter pylori* associated gastric low grade marginal zone B-cell lymphoma of MALT type. *World J Gastroenterol* 2001; **7**: 248-253
- 26 **Deng DJ**. Progress of gastric cancer etiology: N-nitrosamides in the 1990s. *World J Gastroenterol* 2000; **6**: 613-618
- 27 **Liu ZM**, Shou NH, Jiang XH. Expression of lung resistance protein in patients with gastric carcinoma and its clinical significance. *World J Gastroenterol* 2000; **6**: 433-434
- 28 **Guo CQ**, Wang YP, Liu GY, Ma SW, Ding GY, Li JC. Study on *Helicobacter pylori* infection and p53, c-erbB-2 gene expression in carcinogenesis of gastric mucosa. *Shijie Huaren Xiaohua Zazhi* 1999; **7**: 313-315
- 29 **Cai L**, Yu SZ, Ye WM, Yi YN. Fish sauce and gastric cancer: an ecological study in Fujian Province, China. *World J Gastroenterol* 2000; **6**: 671-675
- 30 **Xue FB**, Xu YY, Wan Y, Pan BR, Ren J, Fan DM. Association of *H. pylori* infection with gastric carcinoma: a Meta analysis. *World J Gastroenterol* 2001; **7**: 801-804
- 31 **Wang RT**, Wang T, Chen K, Wang JY, Zhang JP, Lin SR, Zhu YM, Zhang WM, Cao YX, Zhu CW, Yu H, Cong YJ, Zheng S, Wu BQ. *Helicobacter pylori* infection and gastric cancer: evidence from a retrospective cohort study and nested case-control study in China. *World J Gastroenterol* 2002; **8**: 1103-1107
- 32 **Hua JS**. Effect of Hp: cell proliferation and apoptosis on stomach cancer. *Shijie Huaren Xiaohua Zazhi* 1999; **7**: 647-648
- 33 **Liu DH**, Zhang XY, Fan DM, Huang YX, Zhang JS, Huang WQ, Zhang YQ, Huang QS, Ma WY, Chai YB, Jin M. Expression of vascular endothelial growth factor and its role in oncogenesis of human gastric carcinoma. *World J Gastroenterol* 2001; **7**: 500-505
- 34 **Cao WX**, Ou JM, Fei XF, Zhu ZG, Yin HR, Yan M, Lin YZ. Methionine-dependence and combination chemotherapy on human gastric cancer cells *in vitro*. *World J Gastroenterol* 2002; **8**: 230-232
- 35 **Michetti P**, Kreiss C, Kotloff KL, Porta N, Blanco JL, Bachmann D, Herranz M, Saldinger PF, Corthesy-Theulaz I, Losonsky G, Nichols R, Simon J, Stolte M, Acherman S, Monath TP, Blum AL. Oral immunization with urease and *Escherichia coli* heat-labile enterotoxin is safe and immunogenic in *Helicobacter pylori*-infected adults. *Gastroenterology* 1999; **116**: 804-812
- 36 **Suganuma M**, Kurusu M, Okabe S, Sueoka N, Yoshida M, Wakatsuki Y, Fujiki H. *Helicobacter pylori* membrane protein 1: a new carcinogenic factor of *Helicobacter pylori*. *Cancer Res* 2001; **61**: 6356-6359
- 37 **Nakamura S**, Matsumoto T, Suekane H, Takeshita M, Hizawa K, Kawasaki M, Yao T, Tsuneyoshi M, Iida M, Fujishima M. Predictive value of endoscopic ultrasonography for regression of gastric low grade and grade MALT lymphomas after eradication of *Helicobacter pylori*. *Gut* 2001; **48**: 454-460
- 38 **Uemura N**, Okamoto S, Yamamoto S, Matsumura N, Yamaguchi S, Yamakido M, Taniyama K, Sasaki N, Schlemper RJ. *Helicobacter pylori* infection and the development of gastric cancer. *N Engl J Med* 2001; **345**: 8298-8232
- 39 **Morgner A**, Miehle S, Fischbach W, Schmitt W, Muller-Hermelink H, Greiner A, Thiede C, Schetelig J, Neubauer A, Stolte M, Ehninger G, Bayerdorffer E. Complete remission of primary high-grade B-cell gastric lymphoma after cure of *Helicobacter pylori* infection. *J Clin Oncol* 2001; **19**: 2041-2048
- 40 **Kate V**, Ananthkrishnan N, Badrinath S. Effect of *Helicobacter pylori* eradication on the ulcer recurrence rate after simple closure of perforated duodenal ulcer: retrospective and prospective randomized controlled studies. *Br J Surg* 2001; **88**: 1054-1058
- 41 **Zhuang XQ**, Lin SR. Progress in research on the relationship between Hp and stomach cancer. *Shijie Huaren Xiaohua Zazhi* 2000; **8**: 206-207
- 42 **Gao HJ**, Yu LZ, Bai JF, Peng YS, Sun G, Zhao HL, Miu K, Lu XZ, Zhang XY, Zhao ZQ. Multiple genetic alterations and behavior of cellular biology in gastric cancer and other gastric mucosal lesions: *H. pylori* infection, histological types and staging. *World J Gastroenterol* 2000; **6**: 848-854
- 43 **Yao YL**, Zhang WD. Relation between *Helicobacter pylori* and gastric cancer. *Shijie Huaren Xiaohua Zazhi* 2001; **9**: 1045-1049
- 44 **Goto T**, Nishizono A, Fujioka T, Ikewaki J, Mifune K, Nasu M. Local secretory immunoglobulin A and postimmunization gastritis correlated with protection against *Helicobacter pylori* infection after oral vaccination of mice. *Infect Immun* 1999; **67**: 2531-2539
- 45 **Watanabe T**, Tada M, Nagai H, Sasaki S, Nakao M. *Helicobacter pylori* infection induces gastric cancer in mongolian gerbils. *Gastroenterology* 1998; **115**: 642-648
- 46 **Honda S**, Fujioka T, Tokieda M, Satoh R, Nishizono A, Nasu M. Development of *Helicobacter pylori*-induced gastric carcinoma in mongolian gerbils. *Cancer Res* 1998; **58**: 4255-4259
- 47 **Hatzifoti C**, Wren BW, Morrow JW. *Helicobacter pylori* vaccine strategies-triggering a gut reaction. *Immuno Today* 2000; **21**: 615-619
- 48 **Kotloff KL**, Sztein MB, Wasserman SS, Losonsky GA, DiLorenzo SC, Walker RI. Safety and immunogenicity of oral inactivated whole-cell *Helicobacter pylori* vaccine with adjuvant among volunteers with or without subclinical infection. *Infect Immun* 2001; **69**: 3581-3590
- 49 **Dubois A**, Lee CK, Fiala N, Kleantous H, Mehlman PT, Monath T. Immunization against natural *Helicobacter pylori* infection in nonhuman primates. *Infect Immunity* 1998; **66**: 4340-4346
- 50 **Ikewaki J**, Nishizono A, Goto T, Fujioka T, Mifune K. Therapeutic oral vaccination induces mucosal immune response sufficient to eliminate longterm *Helicobacter pylori* infection. *Microbiol Immunol* 2000; **44**: 29-39
- 51 **Evans DG**, Karjalainen TK, Evans DJ, Graham DY, Lee CH. Cloning, nucleotide sequence, and expression of a gene encoding an adhesin subunit protein of *Helicobacter pylori*. *J Bacteriol* 1993; **175**: 674-683
- 52 **Sambrook J**, Fritsch E F, Maniatis T. Molecular Cloning, A Laboratory Manual. 2nd edition. New York: Cold Spring Harbor Laboratory Press. 1989, 1.21-1.52, 2.60-2.80, 7.3-7.35, 9.14-9.22
- 53 **Jones AC**, Logan RP, Foyne S, Cockayne A, Wren BW, Penn CW. A flagellar sheath protein of *Helicobacter pylori* is identical to HpaA, a putative N-acetylneuraminylactose-binding hemagglutinin, but is not an adhesin for AGS cells. *J Bacteriol* 1997; **179**: 5643-5647
- 54 **Chen Y**, Wang J, Shi L. *In vitro* study of the biological activities and immunogenicity of recombinant adhesin of *Helicobacter pylori* rHpaA. *Zhonghua Yixue Zazhi* 2001; **81**: 276-279
- 55 **Tomb JF**, White O, Kerlavage AR, Clayton RA, Sutton GG, Fleischmann RD, Ketchum KA, Klenk HP, Gill S, Dougherty BA, Nelson K, Quackenbush J, Zhou L, Kirkness EF, Peterson S, Loftus B, Richardson D, Dodson R, Khalak HG, Glodek A, McKenney K, Fitzgerald LM, Lee N, Adams MD, Hickey EK, Berg DE, Gocayne JD, Utterback TR, Peterson JD, Kelley JM, Karp PD, Smith HO, Fraser CM, Venter JC. The complete genome sequence of the gastric pathogen *Helicobacter pylori*. *Nature* 1997; **388**: 539-547

- 56 **Alm RA**, Ling SL, Moir DT, King BL, Brown ED, Doig PC, Smith DR, Noonan B, Guild BC, Dejonge BL, Carmel G, Tummino PJ, Caruso A, Uria-Nickelsen M, Mills DM, Lves C, Gibson R, Merberg D, Mills SD, Jiang Q, Taylor DE, Vovis GF, Trust TJ. Genomic-sequence comparison of two unrelated isolates of the human gastric pathogen *Helicobacter pylori*. *Nature* 1999; **397**: 176-180
- 57 **Opazo P**, Muller I, Rollan A, Valenzuela P, Yudelevich A, Garcia-de la Guarda R, Urra S, Venegas A. Serological response to *Helicobacter pylori* recombinant antigens in Chilean infected patients with duodenal ulcer, non-ulcer dyspepsia and gastric cancer. *APMIS* 1999; **107**: 1069-1078
- 58 **Otoole PW**, Janzon L, Doig P, Huang J, Kostrzynska M, Trust TJ. The putative neuraminylactose-binding hemagglutinin hpaA of *Helicobacter pylori* CCUG 17874 is a lipoprotein. *J Bacteriol* 1995; **177**: 6049-6057
- 59 **Hocking D**, Webb E, Radcliff F, Rothel L, Taylor S, Pinczower G, Kapouleas C, Braley H, Lee A, Doidge C. Isolation of recombinant protective *Helicobacter pylori* antigens. *Infect and Immun* 1999; **67**: 4713-4719
- 60 **Sheng T**, Zhang JZ. Current situation on studies of *Hp* urease. *Shijie Huaren Xiaohua Zazhi* 1999; **7**: 881-884
- 61 **Huang XQ**. *Helicobacter pylori* infection and gastrointestinal hormones: a review. *World J Gastroenterol* 2000; **6**: 783-788
- 62 **Hou P**, Tu ZX, Xu GM, Gong YF, Ji XH, Li ZS. *Helicobacter pylori* vacA genotypes and cagA status and their relationship to associated diseases. *World J Gastroenterol* 2000; **6**: 605-607
- 63 **Jiang Z**, Tao XH, Huang AL, Wang PL. A study of recombinant protective *H. Pylori* antigens. *World J Gastroenterol* 2002; **8**: 308-311
- 64 **Wu C**, Zou QM, Guo H, Yuan XP, Zhang WJ, Lu DS, Mao XH. Expression, purification and immunocharacteristics of recombinant UreB protein of *H. pylori*. *World J Gastroenterol* 2001; **7**: 389-393
- 65 **Keenan J**, Oliaro J, Domigan N, Potter H, Aitken G, Allardyce R, Roake J. Immune response to an 18-Kilodalton outer membrane antigen identifies lipoprotein 20 as a *Helicobacter pylori* vaccine candidate. *Infect and Immun* 2000; **68**: 3337-3343

Edited by Xu XQ

Density of *Helicobacter pylori* may affect the efficacy of eradication therapy and ulcer healing in patients with active duodenal ulcers

Yung-Chih Lai, Teh-Hong Wang, Shih-Hung Huang, Sien-Sing Yang, Chi-Hwa Wu, Tzen-Kwan Chen, Chia-Long Lee

Yung-Chih Lai, Sien-Sing Yang, Chi-Hwa Wu, Tzen-Kwan Chen, Chia-Long Lee, Department of Internal Medicine, Cathay General Hospital, Taipei, Taiwan, China

Teh-Hong Wang, Department of Internal Medicine, National Taiwan University Hospital, Taipei, Taiwan, China

Shih-Hung Huang, Department of Pathology, Cathay General Hospital, Taipei, Taiwan, China

Supported by the grant from Cathay General Hospital, Taipei, Taiwan

Correspondence to: Dr. Yung-Chih Lai, Department of Internal Medicine, Cathay General Hospital, 280, Jen-Ai Road, Section 4, Taipei 106, Taiwan, China. yungchihlai@hotmail.com

Telephone: +86-2-27082121 Ext. 3120 **Fax:** +86-2-27074949

Received: 2003-03-12 **Accepted:** 2003-04-11

Abstract

AIM: To evaluate the association of pre-treatment *Helicobacter pylori* (*H. pylori*) density with bacterial eradication and ulcer healing rates in patients with active duodenal ulcer.

METHODS: One hundred and four consecutive duodenal ulcer outpatients with *H. pylori* infection ascertained by gastric histopathology and ¹³C-urea breath test (UBT) were enrolled in this study. *H. pylori* density was graded histologically according to the Sydney system (normal, mild, moderate, and marked). In each patient, lansoprazole (30 mg b.i.d.), clarithromycin (500 mg b.i.d.) and amoxicillin (1 g b.i.d.) were used for 1 week, then 30 mg lansoprazole once daily was continued for an additional 3 weeks. Follow-up endoscopy was performed at 4 weeks after completion of the therapy, and UBT was done at 4 and 8 weeks after completion of the therapy.

RESULTS: The *H. pylori* eradication rates were 88.9 %/100.0 %, 94.3 %/100.0 %, and 69.7 %/85.2 %; and the ulcer healing rates were 88.9 %/100.0 %, 94.3 %/100.0 %, and 63.6 %/77.8 % (intention-to-treat/per protocol analysis) in the mild, moderate, and marked *H. pylori* density groups, respectively. The association of pretreatment *H. pylori* density with the eradication rate and ulcer healing rate was both statistically significant ($P=0.013/0.006$ and $0.002/<0.001$, respectively; using results of intention-to-treat/per protocol analysis).

CONCLUSION: Intra-gastric bacterial load may affect both the outcome of eradication treatment and ulcer healing in patients with active duodenal ulcer disease.

Lai YC, Wang TH, Huang SH, Yang SS, Wu CH, Chen TK, Lee CL. Density of *Helicobacter pylori* may affect the efficacy of eradication therapy and ulcer healing in patients with active duodenal ulcers. *World J Gastroenterol* 2003; 9(7): 1537-1540 <http://www.wjgnet.com/1007-9327/9/1537.asp>

INTRODUCTION

Helicobacter pylori (*H. pylori*) has been considered as the main

cause of chronic gastritis and peptic ulcer^[1]. It has been identified in 90-95 % of patients with duodenal ulcer and 60-80 % of patients with gastric ulcer^[2]. Strong evidence has also shown an association between the eradication of *H. pylori* infection and the cure of peptic ulcer diseases^[3-5].

Recommendations and guidelines for *H. pylori* eradication therapy have been developed rapidly during recent years. The global trend of eradication therapy has now shifted to proton pump inhibitor (PPI)-based triple therapy (a PPI and two different anti-microbials)^[6], which can assure rapid symptom relief, improve ulcer healing, and reduce ulcer recurrence^[7,8]. However, some cases failed to heal with this advanced PPI-based triple therapy. Patient compliance and antibiotic resistance are currently regarded as the major causes of eradication failure^[9]. Several researchers have also revealed that high antral density of *H. pylori* may increase the rate of ulcer recurrence and be related with low eradication rate after triple therapy^[10-12]. Intra-gastric bacterial load might be another factor affecting the success of eradication therapy^[12]. Therefore, we conducted this study to investigate the association of *H. pylori* density in the stomach with the efficacy of eradication therapy and ulcer healing in patients with active duodenal ulcers.

MATERIALS AND METHODS

Patients

From January 2000 to June 2002, consecutive outpatients with endoscopically verified active duodenal ulcers (5 mm in diameter or larger) at Cathay General Hospital were enrolled in this study. All panendoscopic examinations were performed and interpreted by the same group of experienced endoscopists. We only enrolled patients with positive diagnosis of *H. pylori* infection proven by both histological examinations and ¹³C-urea breath tests (UBT). To avoid interference in evaluating the status of *H. pylori*, the following patients were initially excluded before endoscopy: those who had ingested bismuth, antibiotics, anti-secretory medication, or PPI during the 4 weeks prior to the beginning of the study; those who used non-steroidal anti-inflammatory drugs; those who were pregnant or immuno-compromised, and those who had a history of gastric surgery or a previous attempt to eradicate *H. pylori*. The patients with coexisting gastric ulcers or gastric cancer were also excluded. All procedures were performed after obtaining informed consent from the patients.

The patients enrolled were treated with the same regimen of 30 mg lansoprazole b.i.d. plus 500 mg clarithromycin b.i.d. and 1 g amoxicillin b.i.d. for 7 days. After 1 week of anti-*H. pylori* therapy, 30 mg lansoprazole once daily was continued for an additional 3 weeks. From then on, either PPI or anti-secretory H₂-blocker was avoided; only oral antacids were taken for symptomatic relief when necessary. The second endoscopic examination was performed 4 weeks after completion of the therapy.

Histology

During the first endoscopic examination, three biopsies were taken from the gastric antrum (one near the incisura and the

other two on the greater and lesser curvature, 2 cm within the pyloric ring)^[13]. On the follow-up endoscopic examination, two additional specimens were taken from the greater curvature of the gastric body due to the possibility of patchy distribution of *H. pylori* after eradication therapy. An "Olympus GIF-XQ 200" endoscope was used, the biopsy forceps were the "FB 25-K" type. The specimens were stained with hematoxylin-eosin and with a modified Giemsa stain. Then they were examined by experienced histopathologist who was unaware of the clinical diagnosis for the existence of *H. pylori* of the patients. The version of the visual analogue scale in the updated Sydney system was used to grade the density of *H. pylori* (4 grades: normal, no bacteria; mild, focal few bacteria; moderate, more bacteria in several areas; and marked, abundance of bacteria in most glands)^[14]. If the density varied, the highest grade of density in the specimens was selected.

Urea breath test

UBTs were performed before the start of therapy and on two separate occasions, at 4 and 8 weeks after the cessation of therapy, respectively. The ¹³C-urea used was 100 mg 99 % ¹³C-labelled urea produced by the Institute of Nuclear Energy Research, Taiwan. Patients drank 100 ml of fresh milk as the test meal. The procedure was modified from the European standard protocol for the detection of *H. pylori*^[15,16]. We chose 3 per mil for the cut-off level of the rise in the delta value of ¹³CO₂ at 15 min after the ingestion of ¹³C-urea. UBT was defined as positive when the excess $\delta^{13}\text{CO}_2$ was above this value. By using this cut-off, the sensitivity and specificity of UBT were 97 % and 95 %, respectively^[16].

Eradication of *H. pylori* infection was defined as negative results on UBT and histology tests at 4 weeks after the cessation of therapy or negative results on two UBTs at both 4 and 8 weeks after the cessation of therapy^[17]. Healing of ulcers was defined as complete disappearance of the ulcer and non-healing as persistence of ulcers, even if the size had decreased^[18].

To be included in the intention-to-treat analysis, the infection of *H. pylori* had to be confirmed using both UBT and histological examination results. When protocol violations which were likely to influence the response variable or its assessment occurred, patients were excluded from the per protocol analysis.

Statistical analysis

Chi-square or Fisher's exact test was used to evaluate the qualitative data. ANOVA test was applied for the quantitative data. The eradication rates of *H. pylori* and healing rates of duodenal ulcers in the three groups of different *H. pylori* densities were compared using chi-square test or Fisher's exact test and assessed on the basis of both intention-to-treat and per protocol analysis. The 95 % confidence intervals (95 % CI) were calculated. The relationship between *H. pylori* eradication and duodenal ulcer healing was evaluated by Fisher's exact test. *P* value less than 0.05 was considered significant.

RESULTS

Patients

One hundred and ten patients were initially included in the study, but 6 patients were later excluded due to their negative results of *H. pylori*. We enrolled 104 patients who fulfilled the inclusion criteria. Table 1 shows the demographic and other baseline characteristics of the patients divided by the grade of *H. pylori* density. None of differences in variables was statistically significant. Among them, 12 patients did not complete the study because of poor compliance of taking medications (3 cases) or refusal to receive the second

endoscopy (9 cases). Because we wanted to observe the results of both the eradication therapy and the ulcer healing, the patients who refused the second endoscopy were excluded. Therefore, 92 patients were included for per protocol analysis.

Table 1 Clinical characteristics of patients

	<i>H. pylori</i> density		
	Mild (n=36)	Moderate (n=35)	Marked (n=33)
Sex (male/female)	23/13	25/10	23/10
Age (years, Mean \pm S.D.)	45.6 \pm 10.3	44.1 \pm 12.7	47.2 \pm 13.4
Smoking(yes/no)	18/18	20/15	18/15
Ulcer size			
< 1 cm	32	32	30
1-2 cm	4	2	3
>2 cm	0	1	0
Ulcer number			
One	34	32	30
Two	2	3	3
Drop outs	4	2	6

Eradication rate and the density of *H. pylori*

The overall eradication rates were 84.6 % (95 % CI: 75.9-90.7 %) in the intention-to-treat analysis set and 95.7 % (95 % CI: 88.6-98.6 %) in the per protocol set. The eradication rates of the three grades of bacterial densities had a downward trend as the bacterial load became denser (Table 2). The association was statistically significant (*P*=0.013 and 0.006, by intention-to-treat and per protocol analysis).

Table 2 Eradication rates and the density of *H. pylori*

	Eradication rates	95% CI	<i>P</i> value
Intention-to-treat			
<i>H. pylori</i> density			
Mild	32/36 (88.9%)	73.0 – 96.4 %	
Moderate	33/35 (94.3%)	79.5 – 99.0 %	
Marked	23/33 (69.7%)	51.1 – 83.8 %	
Total	88/104 (84.6%)	75.9 – 90.7 %	0.013 ^a
Per protocol			
<i>H. pylori</i> density			
Mild	32/32 (100.0%)	86.7 – 100.0 %	
Moderate	33/33 (100.0%)	87.2 – 100.0 %	
Marked	23/27 (85.2%)	65.4 – 95.2 %	
Total	88/92 (95.7%)	88.6 – 98.6 %	0.006 ^b

Notes: ^aBased on Chi-square test; ^bBased on Fisher's exact test.

Healing rates of duodenal ulcer and the density of *H. pylori*

The healing rates of active duodenal ulcer are shown in Table 3. According to both of the intention-to-treat and per protocol analysis, the differences in the ulcer healing rates of the three grades of *H. pylori* densities were statistically significant (*P*=0.002 and <0.001, respectively). As the bacterial density increased in the stomach, the healing rate of duodenal ulcer decreased.

Relationship between *H. pylori* eradication and duodenal ulcer healing

Table 4 shows the positive impact of *H. pylori* eradication on duodenal ulcer healing. The association was statistically significant (*P*<0.001). Active ulcers of 97.7 % of the patients with successful *H. pylori* eradication had healed at the time of

the second endoscopic examination.

Table 3 Healing rates of duodenal ulcer and the density of *H. pylori*

	Healing rates	95% CI	P value
Intention-to-treat			
<i>H. pylori</i> density			
Mild	32/36 (88.9%)	73.0 – 96.4 %	
Moderate	33/35 (94.3%)	79.5 – 99.0 %	
Marked	21/33 (63.6%)	45.1 – 79.0 %	
Total	86/104 (82.7%)	73.8 – 89.2 %	0.002 ^a
Per Protocol			
<i>H. pylori</i> density			
Mild	32/32 (100.0%)	86.7 – 100.0 %	
Moderate	33/33 (100.0%)	87.2 – 100.0 %	
Marked	21/27 (77.8%)	57.3 – 90.6 %	
Total	86/92 (93.5%)	85.8 – 97.3 %	<0.001 ^b

Notes: ^aBased on Chi-square test; ^bBased on Fisher's exact test.

Table 4 Relationship between *H. pylori* eradication and duodenal ulcer healing

	<i>H. pylori</i>	
	Eradicated (n=88)	Not eradicated (n=4)
Duodenal ulcer		
Healed	86 (97.7%) ^a	0 (0.0%)
Not healed	2 (2.3%)	4 (100.0%)

^aP<0.001 vs not eradicated group, based on Fisher's exact test.

DISCUSSION

H. pylori is an important factor in the pathogenesis of duodenal ulcer. Researchers have shown the eradication of *H. pylori* not only prevents ulcer recurrence but also aids ulcer healing^[19]. Eradication of *H. pylori* has changed the natural history of duodenal ulcer and has become a standard therapy for duodenal ulcer patients^[3, 4, 10].

At present, short-term (7-day) triple therapies including a PPI and two antibiotics (clarithromycin, and amoxicillin or a nitroimidazole compound) are considered as the first line in anti-*H. pylori* regimens^[12]. However, despite of the high efficacy of different anti-*H. pylori* treatment schemes, a proportion of patients, varying from 10 % to 25 %, fails the first attempt to eradicate *H. pylori*^[9]. Patient compliance and antibiotic resistance are currently regarded as the key factors affecting the outcome of treatment^[9,12]. The evidence for other possible factors associated with lower eradication rates is somewhat sparse and equivocal. Nevertheless, several reports revealed that the patients with higher intragastric *H. pylori* load had reduced eradication rates. This association was found in both bismuth and PPI-based triple therapies^[9-12]. Therefore, pre-treatment bacterial density was used by some authors to predict the success of *H. pylori* eradication in patients with chronic duodenal ulcer^[10,11].

Our working hypothesis was that “the higher the intragastric *H. pylori* colonization, the less effective the short-term triple therapy”. In our study, an inverse relationship between successful eradication and intragastric bacterial load was found, which is compatible with the results of other studies^[9-12]. Increased bacterial density of *H. pylori* was associated with a significant reduction in the eradication rate after anti-*H. pylori* treatment. This correlation provides additional support for the importance of bacterial density as a factor in *H. pylori* eradication.

With more *H. pylori* inhabiting the antrum, the gastric mucosa will suffer greater damage by this bacteria^[20, 21]. The denser infection of *H. pylori* associated with greater antral inflammation may cause lower somatostatin expression, leading to higher levels of gastrin and acid production, which may therefore predispose the duodenum to ulceration^[22]. Alam et al^[21] have shown that the prevalence of duodenal ulcer increased with increasing *H. pylori* density, and a greater likelihood of ulceration was noted among patients with high concentrations of *H. pylori*. Effective *H. pylori* eradication was found to induce good responses in peptic ulcer healing^[18]. Treiber et al^[23] reported successful *H. pylori* eradication therapy accelerated peptic ulcer healing even without concomitant acid suppression. In several trials, *H. pylori* eradication not only did result in greater duodenal ulcer healing, but also dramatically decreased ulcer recurrence rate 12 months following treatment^[24]. The cure rates of *H. pylori* infection could be expected more than 90 % using standard triple therapy according to the Maastricht consensus guidelines, and the effective *H. pylori* eradication therapy could achieve rapid peptic ulcer healing in more than 90 % of subjects^[23,25].

In our study, 86/88 cases (97.7 %) in the *H. pylori* eradication group had complete healing of ulcers, which were proven by the results of follow-up endoscopy. The association between *H. pylori* eradication and ulcer healing was statistically significant. Therefore, a positive impact of *H. pylori* eradication on peptic ulcer healing is concluded.

Intragastric bacterial load can affect the success of *H. pylori* eradication therapy, and *H. pylori* eradication can influence the healing of duodenal ulcer. Thus, the healing of duodenal ulcer might be associated with the *H. pylori* density in the stomach. According to our results, *H. pylori* density was revealed to be inversely related to ulcer healing. We asked every patient enrolled to receive follow-up endoscopic examinations so that we could observe the healing process of duodenal ulcer directly. Although some patients refused the second endoscopic examination, our results were still able to confirm the assumed association mentioned above.

Identification of pre-treatment predictors of eradication therapy is important in clinical practice. Therapeutic regimens may be tailored to individual patients according to their particular conditions. Despite the fact that high *H. pylori* density might adversely influence the efficacy of eradication therapy, patients with high intragastric bacterial loads were found to benefit from an extension of eradication regimen from 1 to 2 weeks^[9]. Prolonging duration of the standard triple therapy was proposed as a way to overcome the unfavorable effects caused by high *H. pylori* density and proved to be effective^[9,12].

Most patients (101/104 cases, 97.1 %) included in this study had good drug compliance. Bacterial culture and drug sensitivity test to assess the effect of antibiotic resistance were not performed. Therefore, we could not demonstrate the influence of drug resistance on eradication therapy by our results. Although some authors mentioned the resistance to antimicrobials could be considered as a statistical event and estimated as a certain proportion of the *H. pylori* population in the stomach^[26], the relationship between antibiotic resistance and bacterial load of *H. pylori* has not been studied. Further investigation is warranted to elucidate this issue. The culture and susceptibility testing of *H. pylori* are time-consuming and expensive, and they are rarely performed in most developing countries^[27]. In Taiwan, they are not routinely performed either. Our study may thus provide a practical option to identify the pre-treatment predictors of eradication therapy and ulcer healing when information on drug sensitivity is not available.

In conclusion, our findings reveal that pre-treatment high bacterial density of *H. pylori* in the stomach adversely affects

the success of eradication therapy and influences the healing of ulcers in patients with active duodenal ulcers, and effective *H. pylori* eradication is also shown to be significantly associated with duodenal ulcer healing. Identifying patients with high bacterial loads before treatment and making adjustments of therapeutic regimens accordingly may further improve the efficacy of eradication therapy.

ACKNOWLEDGMENTS

We would like to thank Mr. Shui-Cheng Lee (Institute of Nuclear Energy Research) for his help in the assessment of urea breath test.

REFERENCES

- 1 **Wewer V**, Andersen LP, Parregaard A. Treatment of *Helicobacter pylori* in children with recurrent abdominal pain. *Helicobacter* 2001; **6**: 244-248
- 2 **Hunt RH**. Peptic ulcer disease: defining the treatment strategies in the era of *Helicobacter pylori*. *Am J Gastroenterol* 1997; **92**: 36S-43S
- 3 **Moss S**, Calam J. *Helicobacter pylori* and peptic ulcers: the present position. *Gut* 1992; **33**: 289-292
- 4 **Hunt RH**. pH and *Hp* – gastric acid secretion and *Helicobacter pylori*: implications for ulcer healing and eradication of the organism. *Am J Gastroenterol* 1993; **88**: 481-483
- 5 **Graham DY**, Lew GM, Klein PD. Effect of treatment of *Helicobacter pylori* infection on the long-term recurrence of gastric or duodenal ulcer: a randomized, controlled study. *Ann Intern Med* 1992; **116**: 705-708
- 6 **Asaka M**, Sugiyama T, Kato M. A multicenter, double-blind study on triple therapy with lansoprazole, amoxicillin and clarithromycin for eradication of *Helicobacter pylori* in Japanese peptic ulcer patients. *Helicobacter* 2001; **6**: 254-261
- 7 **Penston JG**. *Helicobacter pylori* eradication: understandable caution but no excuse for inertia. *Aliment Pharmacol Ther* 1994; **8**: 369-389
- 8 **Logan RP**, Bardhan KD, Celestin LR. Eradication of *Helicobacter pylori* and prevention of recurrence of duodenal ulcer: a randomized double-blind, multi-centre trial of omeprazole with or without clarithromycin. *Aliment Pharmacol Ther* 1995; **9**: 417-423
- 9 **Maconi G**, Parente F, Russo A, Vago L, Imbesi V, Porro GB. Do some patients with *Helicobacter pylori* infection benefit from an extension to 2 weeks of a proton pump inhibitor-based triple eradication therapy? *Am J Gastroenterol* 2001; **96**: 359-366
- 10 **Sheu BS**, Yang HB, Su IJ, Shiesh SC, Chi CH, Lin XZ. Bacterial density of *Helicobacter pylori* predicts the success of triple therapy in bleeding duodenal ulcer. *Gastrointest Endosc* 1996; **44**: 683-688
- 11 **Moshkowitz M**, Konikoff FM, Peled Y. High *Helicobacter pylori* numbers are associated with low eradication rate after triple therapy. *Gut* 1995; **36**: 845-847
- 12 **Perri F**, Clemente R, Festa V. Relationship between the results of pre-treatment urea breath test and efficacy of eradication of *Helicobacter pylori* infection. *Ital J Gastroenterol Hepatol* 1998; **30**: 146-150
- 13 **Genta RM**, Graham DY. Comparison of biopsy site for the histopathologic diagnosis of *Helicobacter pylori*: a topographic study of *H. pylori* density and distribution. *Gastrointest Endosc* 1994; **40**: 342-345
- 14 **Dixon MF**, Genta RM, Yardley JH, Correa P. Classification and grading of gastritis. The updated Sydney system. *Am J Surg Pathol* 1996; **20**: 1161-1181
- 15 **Logan RP**, Polson RJ, Misiewicz JJ, Rao G, Karim NQ, Newell D, Johnson P, Wadsworth J, Waiker MM, Baron JH. Simplified single sample ¹³Carbon urea breath test for *Helicobacter pylori*: comparison with histology, culture, and ELISA serology. *Gut* 1991; **32**: 1461-1464
- 16 **Wang WM**, Lee SC, Ding HJ. Quantification of *Helicobacter pylori* infection: simple and rapid ¹³C-urea breath test in Taiwan. *J Gastroenterol* 1998; **33**: 330-335
- 17 **Unge P**. The OAC and OMC options. *Eur J Gastroenterol Hepatol* 1999; **11**: S9-S17
- 18 **Ge ZZ**, Zhang DE, Xiao SD, Chen Y, Hu YB. Does eradication of *Helicobacter pylori* alone heal duodenal ulcers? *Aliment Pharmacol Ther* 2000; **14**: 53-58
- 19 **Hosking SW**, Ling TK, Chung SC. Duodenal ulcer healing by eradication of *Helicobacter pylori* without anti-acid treatment: randomized controlled trial. *Lancet* 1994; **343**: 508-510
- 20 **McCull KE**. Pathophysiology of duodenal ulcer disease. *Eur J Gastroenterol Hepatol* 1997; **9**: S9-S12
- 21 **Alam K**, Schubert TT, Bologna SD, Ma CK. Increased density of *Helicobacter pylori* on antral biopsy is associated with severity of acute and chronic inflammation and likelihood of duodenal ulceration. *Am J Gastroenterol* 1992; **87**: 424-428
- 22 **Atherton JC**, Tham KT, Peek RM, Cover TL, Blaser MJ. Density of *Helicobacter pylori* infection *in vivo* as assessed by quantitative culture and histology. *J Infect Dis* 1996; **174**: 552-556
- 23 **Treiber G**, Lambert JR. The impact of *Helicobacter pylori* eradication on peptic ulcer healing. *Am J Gastroenterol* 1998; **93**: 1080-1084
- 24 **Williams MP**, Pounder RE. What are appropriate end-points for *Helicobacter pylori* eradication in the treatment of duodenal ulcer? *Drugs* 1998; **56**: 1-10
- 25 **Working Party of the European Helicobacter pylori Study Group**. Guidelines for clinical trials in *Helicobacter pylori* infection. *Gut* 1997; **41**: S1- S9
- 26 **Graham DY**, de Boer WA, Tytgat GN. Choosing the best anti-*Helicobacter pylori* therapy: effect of antimicrobial resistance. *Am J Gastroenterol* 1996; **91**: 1072-1076
- 27 **Lam SK**, Talley NJ. *Helicobacter pylori* consensus: report of the 1997 asia pacific consensus conference on the management of *Helicobacter pylori* infection. *J Gastroenterol Hepatol* 1998; **13**: 1-12

Edited by Xu XQ and Wang XL

Polymorphism in transmembrane region of MICA gene and cholelithiasis

Shou-Chuan Shih, Yann-Jinn Lee, Hsin-Fu Liu, Ching-Wen Dang, Shih-Chuan Chang, Shee-Chan Lin, Chin-Roa Kao

Shou-Chuan Shih, Division of Gastroenterology, Department of Medicine, Mackay Memorial Hospital; Mackay Junior School of Nursing, Taipei, Taiwan

Yann-Jinn Lee, Department of Pediatrics and Medical Research, Mackay Memorial Hospital; College of Medicine, Taipei Medical University, Taipei, Taiwan

Hsin-Fu Liu, Ching-Wen Dang, Shih-Chuan Chang, Department of Medical Research, Mackay Memorial Hospital, Taipei, Taiwan

Shee-Chan Lin, Chin-Roa Kao, Division of Gastroenterology, Department of Medicine, Mackay Memorial Hospital, Taipei, Taiwan

Supported by MMH Grant 8844 from Mackay Memorial Hospital

Correspondence to: Dr. Yann-Jinn Lee, Departments of Pediatrics and Medical Research, Mackay Memorial Hospital, 92, Section 2, Chung-Shan North Road, Taipei, Taiwan. yannlee@ms2.mmh.org.tw

Telephone: +886-2-25433535 **Fax:** +886-2-25433642

Received: 2003-04-02 **Accepted:** 2003-04-24

Abstract

AIM: To study the significance of polymorphism of MHC class I chain-related gene A (MICA) gene in patients with cholelithiasis.

METHODS: Subjects included 170 unrelated adults (83 males) with cholelithiasis and 245 randomly selected unrelated adults (130 males) as controls. DNA was extracted from peripheral leukocytes and analyzed for polymorphism of 5 alleles (A4, A5, A5.1, A6 and A9) of the MICA gene.

RESULTS: There was no significant difference in phenotype, allele, and genotype frequencies of any of the 5 alleles between cholelithiasis patients and controls.

CONCLUSION: This study demonstrates that MICA alleles studied bear no relation to cholelithiasis.

Shih SC, Lee YJ, Liu HF, Dang CW, Chang SC, Lin SC, Kao CR. Polymorphism in transmembrane region of MICA gene and cholelithiasis. *World J Gastroenterol* 2003; 9(7): 1541-1544
<http://www.wjgnet.com/1007-9327/9/1541.asp>

INTRODUCTION

Molecular genetics has a substantial impact on our understanding of inherited susceptibility to many diseases. There is an increased familial frequency of cholelithiasis^[1], which is a prevalent disorder in Taiwan^[2]. HLA gene is associated with many human diseases. It is reasonable to speculate on whether there is a correlation between cholelithiasis and HLA gene.

MICA gene is located near HLA-B on chromosome 6, and is by far the most divergent mammalian MHC class I gene known^[3]. It lies 46.4 kb centromeric to HLA-B gene, and they are oriented head-to-head. It has a triplet repeat microsatellite polymorphism (GCT)_n in the transmembrane region. This polymorphism consists of five alleles, with 4, 5, 6, and 9 repetitions of GCT or 5 repetitions of GCT with 1 additional

nucleotide insertion (G), designated as A4, A5, A6, A9, and A5.1, respectively^[4]. The alleles vary among individuals, and hence this microsatellite can be used as an informative polymorphic marker for genetic mapping and for analysis of disease susceptibility.

To date, there have been no reports investigating an association between MICA gene and cholelithiasis. We designed this study to compare MICA polymorphism among Chinese with cholelithiasis, their family members, and unaffected controls.

MATERIALS AND METHODS

Patients with cholelithiasis and controls

One hundred and seventy unrelated adult patients (83 males) with cholelithiasis were enrolled. The average age at diagnosis was 50.5±3.1 years. Cholelithiasis was documented ultrasonographically and/or after operation (75 patients underwent cholecystectomy). The ultrasonographic criterion for diagnosis of cholelithiasis was echogenic material with a postural shift and/or casting an acoustic shadow in the gallbladder. According to their number and size, ultrasonographic patterns of gallbladder stones were divided into 3 types: single, particle (multiple, larger size) and sandy (multiple, sand-like appearance). Control subjects consisted of 245 unrelated subjects (130 males) from the same area where the patients resided. They came to the hospital for physical checkups, minor operations or injuries, or evaluation of fever or abdominal pain. Those with autoimmune disorders, liver diseases, or blood diseases were excluded from the study. In addition, a total of 144 family members of 75 patients with cholelithiasis were included for further comparison. Blood was drawn from all the subjects to extract genomic DNA. All the subjects were Chinese, and they all gave written consent. The study was approved by the local ethics committee.

DNA extraction

Genomic DNA was extracted from fresh or frozen peripheral blood leukocytes by standard techniques^[5, 6].

Determination of the polymorphism of (GCT)_n microsatellite

Primers for analysis of microsatellite polymorphism in the transmembrane region of MICA gene, PCR primers flanking the transmembrane region (MICA5F, 5' - CCTTTTTTTCAGGGAAAGTGC-3'; MICA5R, 5' - CCTTACCATCTCCAGAAACTGC-3') were designed according to the reported sequences^[3, 4]. The MICA5F primer corresponded to the intron 4 and exon 5 boundary region and MICA5R was located in intron 5^[4]. MICA5R was 5' end-labelled with fluorescent dye (Applied Biosystems)^[7, 8].

Polymerase chain reaction (PCR) The amplification reaction mixture (15 µl) contained 50 ng genomic DNA, 10 mM Tris-HCl (pH 9.0), 50 mM KCl, 1.5 mM MgCl₂, 0.01 % gelatin, 0.1 % Triton X-100, 0.2 mM of each dNTP, 0.5 mM of each primer and 0.5 unit Pro Taq DNA polymerase (Protech Technology Enterprise). PCR amplification was carried out in a GeneAmp PCR system (Applied Biosystems). The mixture

was subjected to denaturation at 95 °C for 5 min, followed by 10 cycles at 94 °C for 15 sec, at 55 °C for 15 sec, at 72 °C for 30 sec, then by an additional 20 cycles at 89 °C for 15 sec, at 55 °C for 15 sec, at 72 °C for 30 sec, and by a final extension at 72 °C for 10 min.

Analysis of triplet repeat polymorphism The amplified products were denatured at 100 °C for 5 min, mixed with formamide-containing stop buffer, and subjected to electrophoresis on 4 % polyacrylamide gels containing 8-M urea in an automated DNA sequencer (ABI Prism 377-18 DNA sequencer, Applied Biosystems). The number of microsatellite repeats was estimated automatically with Genescan 672 software (Applied Biosystems) by means of the local Southern method with a size standard marker of GS-350 TAMRA (Applied Biosystems)^[8]. Alleles were designated according to Mizuki *et al.*^[4] and Perez-Rodriguez *et al.*^[9], with amplified sizes of 179 bp (A4), 182 bp (A5), 183 bp (A5.1), 185 bp (A6), 194 bp (A9), and 197 bp (A10).

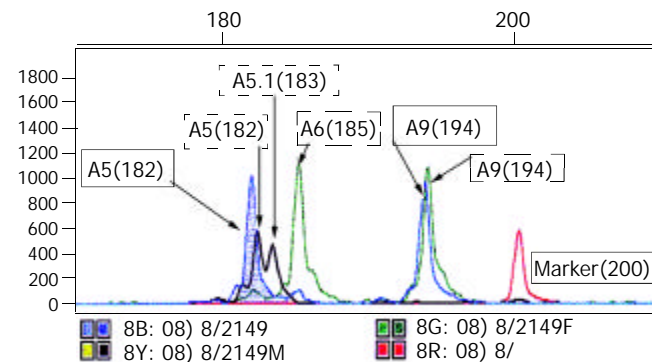
Statistical analysis

Evaluation of the Hardy-Weinberg equilibrium was performed by comparing observed and expected heterozygotes and homozygotes, as well as observed and expected genotypes, using the χ^2 test^[10]. Phenotype, allele, or genotype frequencies of patients and controls were compared by the χ^2 test with Yates' correction where appropriate (one expected number <5). Patients and controls positive for a factor were compared using a free statistical program on the internet^[11]. P values were corrected using the Bonferonni inequality method for the number of comparisons^[12]. Statistical significance was defined as $P < 0.05$.

RESULTS

Figure 1 shows the electrophoretograms of the PCR products of 3 subjects. We did not detect A10 in any of the patients or

controls. The distribution of MICA genotypes in the two groups was in Hardy-Weinberg equilibrium, i.e. observed and expected figures did not differ. No significant difference was found between patients with cholelithiasis and controls in phenotype, allele, or genotype frequencies. There were also no differences between male and female patients or between patients with different sonographic stone types. Age at diagnosis was also not correlated with allele frequency (Tables 1, 2 3). As the difference between patients and controls was not remarkable, it was not meaningful to compare the results between patients and their family members (data not shown).



Genotypes of a subject (2149), his father (2149F), and mother (2149M)

Subject	Line	Genotype
2149	solid	A5/A9
2149F	dash	A6/A9
2149M	dot	A5/A5.1

Figure 1 Electrophoretograms of the PCR products for three subjects. Amplified sizes of the alleles were 182 bp (A5), 183 bp (A5.1), 185 bp (A6), and 194 bp (A9).

Table 1 Phenotype frequencies of the polymorphism in transmembrane region of MICA gene in patients with cholelithiasis and controls

Phenotype	Patient ^a		Control ^a		Single ^b		Particle ^b		Sandy ^b		Male ^c		Female ^c	
	n	%	n	%	n	%	n	%	n	%	n	%	n	%
A4	49	28.8	69	28.2	10	35.7	24	30.0	15	24.2	30	36.1	19	21.9
A5	85	50.0	133	54.3	15	53.6	43	53.8	27	43.6	42	50.6	43	49.4
A5.1	72	42.4	113	46.1	9	32.1	32	40.0	31	50.0	33	39.8	39	44.8
A6	23	13.5	30	12.2	4	14.3	10	12.5	9	14.5	9	10.8	14	16.1
A9	64	37.7	79	32.2	11	39.3	31	38.8	22	35.5	30	36.1	34	39.1
Total	170	100	245	100	28	100	80	100	62	100	83	100	87	100

^aP=0.81, ^bP=0.441, ^cP=0.316.

Table 2 Allele frequencies of the polymorphism in transmembrane region of MICA gene in patients with cholelithiasis and controls

Allele	Patient ^a		Control ^a		Single ^b		Particle ^b		Sandy ^b		Age at Dx ≤ 50		Age at Dx ≤ 30		Age at Dx ≤ 40 ^d		Male ^c		Female ^c	
	n	%	n	%	n	%	n	%	n	%	n	%	n	%	n	%	n	%	n	%
A4	53	15.6	74	15.1	11	19.6	26	16.3	16	12.9	21	13.8	3	15.0	5	8.1	34	20.5	19	10.9
A5	105	30.9	162	33.1	18	32.1	56	35.0	31	25.0	49	32.2	6	30.0	19	30.6	51	30.7	54	31.0
A5.1	85	25.0	135	27.6	11	19.6	35	21.9	39	31.5	39	25.7	5	25.0	18	29.0	38	22.9	47	27.0
A6	24	7.1	32	6.5	4	7.1	10	6.3	10	8.1	13	8.6	2	10.0	6	9.7	10	6.0	14	8.0
A9	73	21.5	87	17.8	12	21.4	33	20.6	28	22.6	30	19.7	4	20.0	14	22.6	33	19.9	40	23.0
Total	340	100	490	100	56	100	160	100	124	100	152	100	20	100	62	100	166	100	174	100

^aP=0.71, ^bP=0.541, ^cP=0.415, ^dP=0.501 (age ≤ 40 vs. control), Dx=Diagnosis.

Table 3 Genotype frequencies of the polymorphism in transmembrane region of MICA gene in patients with cholelithiasis and controls

Genotype	Patient ^a		Control ^{a, b}		Single ^b		Particle ^b		Sandy ^b		Age at Dx ≤ 50		Male ^c		Female ^c	
	n	%	n	%	n	%	n	%	n	%	n	%	n	%	n	%
A4 / A4	4	2.4	5	2.0	1	3.6	2	2.5	1	1.6	2	2.6	4	4.8	0	0
A4 / A5	14	8.2	22	9.0	3	10.7	8	10.0	3	4.8	6	7.9	8	9.6	6	6.9
A4 / A5.1	13	7.6	23	9.4	2	7.1	6	7.5	5	8.1	6	7.9	7	8.4	6	6.9
A4 / A6	2	1.2	8	3.3	0	0	1	1.3	1	1.6	0	0	2	2.4	0	0
A4 / A9	16	9.4	11	4.5	4	14.3	7	8.8	5	8.1	5	6.6	9	10.8	7	8.0
A5 / A5	20	11.8	29	11.8	3	10.7	13	16.3	4	6.5	8	10.5	9	10.8	11	12.6
A5 / A5.1	21	12.4	37	15.1	2	7.1	8	10.0	11	17.7	10	13.2	11	13.3	10	11.5
A5 / A6	10	5.9	11	4.5	4	14.3	3	3.8	3	4.8	7	9.2	3	3.6	7	8.0
A5 / A9	20	11.8	34	13.9	3	10.7	11	13.8	6	9.7	10	13.2	11	13.3	9	10.3
A5.1 / A5.1	13	7.6	22	9.0	2	7.1	3	3.8	8	12.9	6	7.9	5	6.0	8	9.2
A5.1 / A6	8	4.7	7	2.9	0	0	5	6.3	3	4.8	3	3.9	3	3.6	5	5.7
A5.1 / A9	17	10.0	24	9.8	3	10.7	10	12.5	4	6.5	8	10.5	7	8.4	10	11.5
A6 / A6	1	0.6	2	0.8	0	0	0	0	1	1.6	1	1.3	1	1.2	0	0
A6 / A9	2	1.2	2	0.8	0	0	1	1.3	1	1.6	1	1.3	0	0	2	2.3
A9 / A9	9	5.3	8	3.3	1	3.6	2	2.5	6	9.7	3	3.9	3	3.6	6	6.9
Total	170	100	245	100	28	100	80	100	62	100	76	100	83	100	87	100

^aP=0.797, ^bP=0.063 (control vs. stone types), ^cP=0.337, Dx=Diagnosis.

DISCUSSION

Cholelithiasis is quite prevalent in Taiwan^[2] and is easily detected by ultrasonography, which has become a commonly used screening tool for health maintenance exams. There is as yet no well documented method to prevent cholelithiasis formation. However, it is now well known that detecting genetic defects may lead to better surveillance or even avoidance of certain diseases. Thus it seems worthwhile to search for gene disorders in a common disease like cholelithiasis.

MHC class I genes (HLA-A, -B and -C) encode single polypeptides organized into three domains: α_1 , α_2 and α_3 . Their surface expression on most nucleated cells of the body depends on the noncovalent association with a fourth domain, the non-MHC-encoded polypeptide β_2 -microglobulin^[13]. MHC class I molecules are important in the efferent limb of immunity, which is designed to destroy cells bearing foreign antigens. Foreign peptides presented within the cell are deposited in the binding groove of MHC class I molecules and expressed on the cell surface. Cytotoxic T cells recognize them and destroy the cell^[14]. Certain MHC class I molecules have been found to be associated with various diseases, including type 1 diabetes and cholelithiasis^[15-18]. An even stronger association has been found with MHC class II molecules^[18, 19]. The initial explanation of HLA class I associations is linkage disequilibrium between certain subtypes of MHC class I and class II molecules^[19, 20]. However, other studies have suggested that there may be other loci in the MHC gene complex that also play a role^[21, 22]. Further investigation of such loci nearby or within MHC class I genes, such as MICA gene, is necessary to clarify these discrepancies.

MICA gene has recently been found to be more significantly associated with disease susceptibility that had been previously reported to be associated with the HLA-B locus (HLA-B7, -B8, -B15, -B18 in Caucasians; -Bw22, and -Bw54 in Chinese; -B5, -Bw52, and -Bw54 in Japanese are reportedly associated with various diseases)^[4, 7, 8, 15, 16, 23-28]. This suggests that susceptibility associated with the HLA-B locus might be due to different genotypes of MICA gene.

MICA is specifically expressed by fibroblasts, epithelial cells, keratinocytes, endothelial cells, and monocytes^[3, 29]. The molecule is similar to MHC class I antigens. Thus MICA is thought to represent a second lineage of MHC antigens and

possibly to play a specialized or modified role in the immune response^[3]. The recruitment of $\gamma\delta$ T cells in skin and intestinal mucosa mirrors the pattern of expression of MICA and is consistent with the hypothesis that these molecules may play a role in inflammation and in the response to stress or damage in certain tissues^[29]. MICA expression is regulated by promoter heat shock elements similar to those of HSP70 genes^[30]. The high levels of MICA expression in epithelial cell lines together with the upregulation of MICA after heat shock may represent a molecular mechanism for exposing stressed epithelial cells to the immune system^[31]. Thus MICA may function as an indicator of cell stress and may be recognized by $\gamma\delta$ T cells in an unusual interaction. It is possible, therefore, that MICA regulates the immune response when cells are stressed and might be involved in the development of cholelithiasis.

However, our study showed that the polymorphic MICA alleles were not significantly associated with cholelithiasis, nor were there any differences when we looked at subgroups of patients, stratified according to sex, types of gallstone, or age. The latter factor is of interest in considering the contribution of heredity vs. environment. These results are perhaps not surprising, since the pathogenesis of cholelithiasis in Taiwan is multifactorial^[32]. Nevertheless, our demonstration of the absence of an association between MICA gene and cholelithiasis is useful in pointing future research in other directions. The fact of the increased familial frequency of cholelithiasis^[1] thus remains to be explained, perhaps by studying other loci on the human chromosome.

REFERENCES

- 1 **Gilat T**, Feldman C, Halpern Z, Dan M, Bar-Meir S. An increased familial frequency of gallstones. *Gastroenterol* 1983; **84**: 242-246
- 2 **Su CH**, Lui WY, P'eng FK. Relative prevalence of gallstone diseases in Taiwan. A nationwide cooperative study. *Dig Dis Sci* 1992; **37**: 764-768
- 3 **Bahram S**, Bresnahan M, Geraghty DE, Spies T. A second lineage of mammalian major histocompatibility complex class I genes. *Proc Natl Acad Sci USA* 1994; **91**: 6259-6263
- 4 **Mizuki N**, Ota M, Kimura M, Ohno S, Ando H, Katsuyama Y, Yamazaki M, Watanabe K, Goto K, Nakamura S, Bahram S, Inoko H. Triplet repeat polymorphism in the transmembrane region of

- the MICA gene: A strong association of six GCT repetitions with Behcet's disease. *Proc Natl Acad Sci USA* 1997; **94**: 1298-1303
- 5 **Buffone GJ**, Darlington GJ. Isolation of DNA from biological specimens without extraction with phenol. *Clin Chem* 1985; **31**: 164-165
- 6 **Lee HH**, Chao HT, Ng HT, Choo KB. Direct molecular diagnosis of CYP21 mutations in congenital adrenal hyperplasia. *J Med Genet* 1996; **33**: 371-375
- 7 **Goto K**, Ota M, Ohno S, Mizuki N, Ando H, Katsuyama Y, Maksymowych WP, Kimura M, Bahram S, Inoko H. MICA gene and ankylosing spondylitis: linkage analysis via a transmembrane-encoded triplet repeat polymorphism. *Tissue Antigens* 1997; **49**: 503-507
- 8 **Goto K**, Ota M, Maksymowych WP, Mizuki N, Yabuki K, Katsuyama Y, Kimura M, Inoko H, Ohno S. Association between MICA gene A4 allele and acute anterior uveitis in white patients with and without HLA-B27. *Am J Ophthalmol* 1998; **126**: 436-441
- 9 **Perez-Rodriguez M**, Corell A, Arguello JR, Cox ST, McWhinnie A, Marsh SG, Madrigal JA. A new MICA allele with ten alanine residues in the exon 5 microsatellite. *Tissue Antigens* 2000; **55**: 162-165
- 10 **Hedrick PW**. Genetics of Populations. 2nd ed. Sudbury, Massachusetts: Jones and Bartlett Publishers 2000: 1-553
- 11 **Lee YJ**, Chen MR, Chang WC, Lo FS, Huang FY. A freely available statistical program for testing association. *MD Comput* 1998; **15**: 327-330
- 12 **Svejgaard A**, Ryder LP. HLA and disease associations: detecting the strongest association. *Tissue Antigens* 1994; **43**: 18-27
- 13 **Todd JA**, Bell JI, McDevitt HO. A molecular basis for genetic susceptibility to insulin-dependent diabetes mellitus. *Trends Genet* 1988; **4**: 129-134
- 14 **Walker RH**. The HLA system. In: Walker RH, eds. Technical Manual. Bethesda: American Association of Blood Banks 1993: 287-307
- 15 **Singal DP**, Blajchman MA. Histocompatibility (HL-A) antigens, lymphocytotoxic antibodies and tissue antibodies in patients with diabetes mellitus. *Diabetes* 1973; **22**: 429-432
- 16 **Nerup J**, Platz P, Anderson OO, Christy M, Lyngsoe J, Poulsen JE, Ryder LP, Nielsen LS, Thomsen M, Svejgaard A. HL-A antigens and diabetes mellitus. *Lancet* 1974; **2**: 864-866
- 17 **Papasteriades C**, Al-Mahmoud I, Papageorgakis N, Romania ST, Katsas A, Ollier W, Economidou I. HLA antigen in Greek patients with cholelithiasis. *Dis Markers* 1990; **8**: 17-21
- 18 **Pokorny CS**, McCaughan GW, Gallagher ND, Selby WS. Sclerosing cholangitis and biliary tract calculi-primary or secondary. *Gut* 1992; **33**: 1376-1380
- 19 **Solow H**, Hidalgo R, Singal DP. Juvenile-onset diabetes HLA-A, -B, -C, and-DR alloantigens. *Diabetes* 1979; **28**: 1-4
- 20 **Farid NR**, Sampson L, Noel P, Barnard JM, Davis AJ, Hillman DA. HLA-D-related (DRw) antigens in juvenile diabetes mellitus. *Diabetes* 1979; **28**: 552-557
- 21 **Raum D**, Awdeh Z, Yunis EJ, Alper CA, Gabbay KH. Extended major histocompatibility complex haplotypes in type 1 diabetes mellitus. *J Clin Invest* 1984; **74**: 449-454
- 22 **Robinson WP**, Barbosa J, Rich SS, Thomson G. Homozygous parent affected sib pair method for detecting disease predisposing variants: Application to insulin dependent diabetes mellitus. *Genet Epidemiol* 1993; **10**: 273-288
- 23 **Ota M**, Katsuyama Y, Mizuki N, Ando H, Furihata K, Ono S, Pivetti-Pezzi P, Tabbara KF, Palimeris GD, Nikbin B, Davatchi F, Chams H, Geng Z, Bahram S, Inoko H. Trinucleotide repeat polymorphism within exon 5 of the MICA gene (MHC class I chain-related gene A): allele frequency data in the nine population groups Japanese, Northern Han, Uygur, Kazakhstan, Iranian, Saudi Arabian, Greek and Italian. *Tissue Antigens* 1997; **49**: 448-454
- 24 **Goto K**, Ota M, Ando H, Mizuki N, Nakamura S, Inoue K, Yabuki K, Kotake S, Katsuyama Y, Kimura M, Inoko H, Ohno S. MICA gene polymorphisms and HLA-B27 subtypes in Japanese patients with HLA-B27-associated acute anterior uveitis. *Invest Ophthalmol Vis Sci* 1998; **39**: 634-637
- 25 **Fukuda K**, Sugawa K, Wakisaka A, Moriuchi J, Matsuura N, Sato Y. Statistical detection of HLA and disease association. *Tissue Antigens* 1985; **26**: 81-86
- 26 **Thomson G**. HLA disease associations: Models for the study of complex human genetic disorders. *Crit Rev Clin Lab Sci* 1995; **32**: 183-219
- 27 **Hawkins BR**. Human leukocyte antigens in chinese. Hong-Kong: Hong-Kong University Press 1987: 1-122
- 28 **Kobayashi T**, Tamemoto K, Nakanishi K, Kato N, Okubo M. Immunogenetic and clinical characterization of slowly progressive IDDM. *Diabetes Care* 1993; **16**: 780-788
- 29 **Zwimer NW**, Fernandez-Vina MA, Stastny P. MICA, a new polymorphic HLA-related antigen, is expressed mainly by keratinocytes, endothelial cells, and monocytes. *Immunogenetics* 1998; **47**: 139-148
- 30 **Groh V**, Bahram S, Bauer S, Herman A, Beauchamp M, Spies T. Cell stress-regulated human major histocompatibility complex class I gene expressed in gastrointestinal epithelium. *Proc Natl Acad Sci USA* 1996; **93**: 12445-12450
- 31 **Bahram S**, Mizuki N, Inoko H, Spies T. Nucleotide sequence of the human MHC class I MICA gene. *Immunogenetics* 1996; **44**: 80-81
- 32 **Ho KJ**, Lin XZ, Yu SC, Chen JS, Wu CZ. Cholelithiasis in Taiwan. Gallstones characteristics, surgical incidence, bile lipid composition and role of β -glucuronidase. *Dig Dis Sci* 1995; **40**: 1963-1973

Improvements of postburn renal function by early enteral feeding and their possible mechanisms in rats

Li Zhu, Zong-Cheng Yang, De-Chang Chen

Li Zhu, Department of Anesthesiology, Naval General Hospital, Beijing 100037, China

Zong-Cheng Yang, Institute of Burn Research, Southwest Hospital, Third Military Medical University, Chongqing 400038, China

De-Chang Chen, Department of Critical Care Medicine, Peking Union Medical College Hospital, Chinese Academy of Medical Sciences, Beijing 100730, China

Supported by National Natural Science Foundation of China, No. 30290700

Correspondence to: Dr. Zhu Li, Department of Anesthesiology, Naval General Hospital, Beijing 100037, China. zlicu@mail.china.com

Telephone: +86-10-68589503

Received: 2003-04-02 **Accepted:** 2003-05-19

Abstract

AIM: To investigate the protective effects of early enteral feeding (EEF) on postburn impairments of renal function and their possible mechanisms.

METHODS: Wistar rats with 30 % of total body surface area (TBSA) full-thickness burn were adopted as the experimental model. The effects of EEF on the postburn changes of gastric intramucosal pH (pHi), endotoxin levels in portal vein, water contents of renal tissue, and blood concentrations of tumor necrosis factor (TNF- α), urea nitrogen (BUN), creatinine (Cr), as well as the changes of clearance of creatinine (CCr) were dynamically observed within 48 h postburn.

RESULTS: EEF could significantly improve gastric mucosal acidosis, reduce portal vein endotoxin levels and water contents of renal tissue, as well as blood concentrations of TNF- α after severe burns ($P < 0.01$). The postburn elevations of BUN and BCr were not found to be recovered by EEF. However, the CCr in EEF group was greatly increased by 4.67-fold compared with that of the non-feeding burned control (16.43 ± 2.90 vs. 3.52 ± 0.79 , $P < 0.01$).

CONCLUSION: EEF has beneficial effects on the improvement of renal function in severely burned rats, which may be related to its increase of splanchnic blood flow, decrease of the translocation of gut-origin endotoxin and the release of inflammatory mediators.

Zhu L, Yang ZC, Chen DC. Improvements of postburn renal function by early enteral feeding and their possible mechanisms in rats. *World J Gastroenterol* 2003; 9(7): 1545-1549

<http://www.wjgnet.com/1007-9327/9/1545.asp>

INTRODUCTION

Acute renal failure (ARF) is one of the well-known complications after severe burns with an extremely high incidence of death^[1-4]. In most circumstances, it manifests as a part of multiorgan dysfunction syndrome^[5, 6] and the kidney-oriented supportive therapy so far has not achieved satisfactory

results^[6, 7]. In recent years, abundant researches have suggested that the translocation of gut-origin endotoxin in certain pathological conditions may lead to remote organ injury^[8, 9], which may also be the major contributor to renal dysfunction^[10-13]. Meanwhile, it has become increasingly apparent that early enteral feeding (EEF) in various groups of patients could produce multiple beneficial effects, including increase of blood flow to the splanchnic organs, maintenance of gut mucosal integrity, prevention of intramucosal acidosis and permeability disturbances, and alleviation of the translocation of gut-origin bacteria and endotoxin^[14-19]. We therefore presume that EEF might be possible to improve renal function injured by severe burns, which up to now has been seldom documented. Thus, the present study was designed to demonstrate this hypothesis, in attempt to seek ways to improve the treatment of severely injured patients, which would be no doubt of both theoretical and practical importance.

MATERIALS AND METHODS

Animals

Healthy adult Wistar rats of both sexes, weighing 220 ± 30 g, were employed in the study. They were housed in individual metabolic cages in a temperature conditioned room ($22-24$ °C) with a 12 h light-dark circle, allowed access to standard rat chow (provided by experimental animal center, Third Military Medical University) and water ad libitum, and acclimatized to the surroundings for 7 days prior to the experiments.

Operative procedure

All animals were weighed and anesthetized with 1 % pentobarbitale sodium (30 mg/kg, ip). After laparotomy, a polyethylene catheter (1.5 mm in diameter) was inserted into duodenum on the anterior wall 1.5 cm from pylorus via a puncture hole made by a metal needle for enteral feeding. The catheter was appropriately fixed, tunneled under the skin and exited through the nape skin. The animals were housed and fed as described above after operation.

Burn injury and resuscitation

After a recovery period of 24 h, the animals inserted with a feeding tube were anesthetized, having their dorsal hair shaved and placed in a wooden template designed to expose 30 % of the total body surface area (TBSA), and then immersed in water at 92 °C for 20 seconds, which resulted in a clearly demarcated full-thickness burn. One hour after burn injury, the animals were resuscitated with 10 ml of warm 0.9 % NaCl (normal saline solution, 37 °C) given by intraperitoneal injection. Control animals were similarly anesthetized, shaved, resuscitated but not burned.

Feeding and experimental protocol

Nutrient feeding liquid was prepared as one with a caloric of 2.1 KJ/ml before use by mixing nutritional powder (ENSURE, USA) with an appropriate amount of warm boiled water. According to different feeding regimens, the animals were randomly divided into three groups: (1) EEF group. Enteral

feeding was initiated 1 h postburn in burned animals via a feeding tube with a total caloric of 202 KJ·Kg⁻¹·24 h⁻¹. The feeding nutrient liquid required for 24 hours was administered evenly at 6 time points. (2) Burn group. The animals were treated exactly the same as EEF group, except that the nutrient feeding liquid was substituted for the same amount of saline. (3) Control group. Only the feeding tube was inserted, whereas no tube feeding and burn were conducted. The animals in this group were allowed access to standard rat chow, nutrition liquid and water ad libitum. Time points for different measurements and assays in all groups were made at 3, 6, 12, 24 and 48 h postburn, except for the determination of renal tissue water content, which was performed at 12 h after thermal injury. 24-hr urine was collected for the detection of urea nitrogen and creatinine that were used to calculate CCr. For plasma assays, rats were sacrificed by decapitation at each time point and heparinised blood was collected in a separator tube spun at 3 000 g for 10 min, decanted and frozen at -20 °C until analysis.

Measurements

The gastric intramucosal pH was determined with an indirect method as previously described^[20] with minor modifications. Briefly, the animals were anesthetized and injected cimetidine (15 mg) intraperitoneally 1 h prior to each time point, a polyethylene catheter was inserted into gastric lumen through pylorus via a puncture hole on the anterior wall of duodenum made by a metal needle after a midline laparotomy. A 2.5-ml of normal saline was injected into gastric lumen through the catheter and removed in order to get rid of intragastric residues, then 1.5-ml of normal saline was injected and retained in the gastric lumen. After an equilibration interval of 60 min, 1 ml of saline solution was aspirated and PCO₂ was determined using the blood gas analyzer. A simultaneously obtained arterial blood sample was used to determine the [HCO₃⁻]. pHi was then calculated as:

$$\text{pHi} = 6.1 + \log \left(\frac{[\text{HCO}_3^-]}{[\text{PCO}_2 \times 0.03]} \right)$$

The multifunction-biochemical analyzer Beckman Synchron CX-7 was employed to detect urea nitrogen and creatinine in both blood and urine.

Portal plasma endotoxin levels were assayed with the limulus-amoebocyte-lysate test (LAL)^[21]. Briefly, plasma samples were diluted tenfold with pyrogen-free water and heated to 75 °C for 5 min to overcome assay inhibition by plasma. The samples were incubated with LAL for 33 min at 37 °C. Then the chromogenic substrate was added and the samples were incubated for another 3 min. After the reaction

was stopped with acetic acid, sample optical density was read at 545 nm and the endotoxin concentration was finally expressed as Eu/ml.

Radioimmunoassay of TNF-α levels in systemic circulation was conducted according to the instructions with kits from Dong-Ya Research Institute of Immunotechnology.

Renal tissue water contents were determined with a method as reported in a previous study^[22] with minor modifications. Eight renal tissue samples for each group were harvested at 12 h postburn, weighed and put in an oven at 90 °C for 24 h, then weighed again. The renal tissue water contents were calculated as: Renal tissue water contents=(wet weight - dry weight / wet weight)×100 %

Statistical analysis

Experimental results were analyzed by analysis of variance and *t*-tests for multiple comparisons. Data were expressed as mean ± standard error of the mean. Statistical significance was determined at *P*<0.05.

RESULTS

BUN and BCr in both EEF and Burn groups were significantly increased postburn with the peak value at 6 h. Though gradually decreased thereafter, they were still significantly higher than those of the control at 24 and 48 h time points (*P*<0.01). The beneficial effects of EEF on the renal function manifested as the improvement of CCr, in which a 4.67-fold increase was observed in EEF group as compared with burn group and the CCr value in EEF group tended to be close to that in the control (Table 1).

Gastric mucosal acidosis was significantly improved in EEF group as indicated by the elevation of gastric pHi at most of the postburn time points, however, gastric pHi in burn group was sustained in lower levels until 48 h postburn (Table 2).

Table 3 displays the changes in portal endotoxin levels after severe burns. Three hours postburn, endotoxin concentration was significantly increased in burn group and peaked at 6 h, another increase appeared at 24 h and persisted until 48 h postburn. However, the portal endotoxin levels in animals that received EEF markedly decreased at almost all time points as compared with that of the burn group.

The data for plasma TNF-α levels are shown in Table 4. In accordance with other observations, EEF could also significantly reduce TNF-α levels in systemic circulation at most postburn time points as compared with that of burnt animals.

Table 1 Effects of EEF on postburn changes of BUN, BCr and CCr ($\bar{x} \pm s$)

Group	Samples	Postburn hours (h)				
		3	6	12	24	48
EEF	40					
BUN (mmol/L)		10.30±0.67 ^{a d}	17.67±1.52 ^{b d}	13.73±1.43 ^d	8.73±2.10 ^d	7.50±1.16 ^d
BCr (mmol /L)		53.77±3.20 ^d	89.60±6.54 ^{b d}	55.44±3.57 ^d	46.95±2.66 ^d	42.90±2.23 ^d
CCr (ml/h/100g)					16.43±2.90 ^b	
Burn	40					
BUN (mmol/L)		11.76±1.72 ^d	15.42±1.74 ^d	13.48±1.56 ^d	9.27±1.75 ^d	7.68±1.63 ^d
BCr (mmol /L)		51.80±2.83 ^d	71.23±2.63 ^d	57.70±4.93 ^d	44.75±1.69 ^d	41.76±1.26 ^d
CCr (ml/h/100g)					3.52 ±0.79 ^d	
Control	40					
BUN (mmol/L)		4.67±0.85	4.49±0.58	4.74±0.80	4.31±0.69	4.52±0.93
BCr (mmol /L)		37.43±3.64	37.67±3.26	37.28±4.42	36.94±3.71	37.69±3.47
CCr (ml/h/100g)					19.45±2.21	

^a*P*<0.05, ^b*P*<0.01 vs Burn group; ^c*P*<0.05, ^d*P*<0.01 vs Control.

Table 2 Effects of EEF on postburn changes of gastric intramucosal pH ($\bar{x}\pm s$)

Group	Samples	Postburn hours (h)				
		3	6	12	24	48
EEF	50	7.119±0.078 ^{ab}	6.943±0.089 ^{ab}	7.074±0.037 ^{ab}	7.285±0.098 ^a	7.257±0.077 ^{ab}
Burn	50	7.017±0.037 ^b	6.826±0.049 ^b	6.802±0.080 ^b	6.949±0.082 ^b	7.074±0.041 ^b
Control	50	7.321±0.054	7.296±0.067	7.343±0.045	7.306±0.069	7.348±0.074

^a $P<0.01$ vs Burn group; ^b $P<0.01$ vs Control.

Table 3 Effects of EEF on postburn changes of portal endotoxin level (Eu/ml, $\bar{x}\pm s$)

Group	Samples	Postburn hours (h)				
		3	6	12	24	48
EEF	40	0.683±0.072 ^{ab}	0.797±0.085 ^{ab}	0.542±0.078 ^{ab}	0.725±0.061 ^{ab}	0.461±0.049 ^{ab}
Burn	40	1.394±0.126 ^b	1.518±0.173 ^b	1.124±0.133 ^b	1.627±0.215 ^b	1.168±0.188 ^b
Control	40	0.206±0.032	0.195±0.043	0.189±0.049	0.204±0.037	0.215±0.051

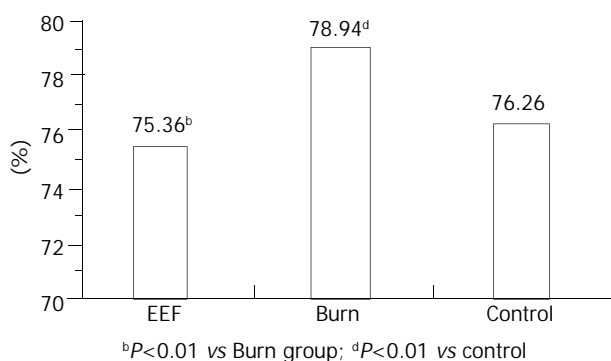
^a $P<0.01$ vs Burn group; ^b $P<0.01$ vs Control.

Table 4 Effects of EEF on postburn changes of plasma TNF- α level (ng/ml, $\bar{x}\pm s$)

Group	Samples	Postburn hours (h)				
		3	6	12	24	48
EEF	40	1.48±0.38 ^{ab}	2.57±0.45 ^{ab}	2.36±0.47 ^{ab}	1.92±0.26 ^{ab}	1.68±0.45 ^{ab}
Burn	40	1.92±0.19 ^b	4.49±0.47 ^b	3.51±0.45 ^b	4.07±0.71 ^b	3.24±0.61 ^b
Control	40	0.83±0.08	0.78±0.11	0.83±0.12	0.81±0.09	0.85±0.10

^a $P<0.01$ vs Burn group; ^b $P<0.01$ vs Control.

For EEF, burn and control groups of animals, the renal tissue water contents reached 75.36±0.99 %, 78.94±1.56 % and 76.26±1.25 % respectively (Figure 1). It was evident that a significant decrease of renal tissue water content was seen in EEF group compared with that in burn group at 12 h postburn ($P<0.01$).

**Figure 1** Effects of EEF on water content of renal tissue 12 h postburn.

DISCUSSION

Nutritional support plays an important role in the management of critically ill patients to prevent and treat multiple organ dysfunction syndrome (MODS)^[23]. Numerous clinical and animal studies have demonstrated that early enteral feeding could preserve the gut barrier function, diminish hypermetabolic

response, maintain caloric intake, reduce the chance of gut origin infection and significantly shorten hospital stay following injury^[14-19]. Unfortunately, the protective effects of EEF on the splanchnic function after severe traumas were relatively neglected in most of these investigations.

In a previous study, Roberts and his associates^[24] observed that acute impairment of renal function inflicted by rhabdomyolysis was improved with EEF. Through 72 h dynamic observation, they found both BUN and BCr in EEF rats decreased by 65.7 % and 60 % respectively and the mortality reduced by 43 % compared with that of the animals fed with water. In contrast, in present animal model of severely thermal injury, BUN and BCr in both EEF and burn groups were significantly elevated, and no effect of EEF on the postburn changes of these variables was noted. We conjecture the phenomenon might be attributed to the more severity of the injury, difference in feeding components and blood condensation postburn. It has been reported that CCr could correlate well with the inulin clearance and exhibit renal function more accurately in the presence of acute renal failure^[25]. In an animal study on renal dysfunction caused by ischemia, Mouser and his colleagues^[25] demonstrated that the percentage of CCr increment in enterally fed animals was 2.5-fold higher than that in animals fed intravenously, whereas no significant changes of BUN and BCr were observed, showing that the improvement of renal function would not be always in accordance with BUN and BCr changes. In the present study, CCr in EEF animals increased by 4.67-fold compared with that in burn group, indicating that EEF could exert protective effects on the postburn renal impairment, and that abortive

attention should be paid to the selection of proper variables to perform such investigations.

The mechanisms of EEF to improve posttrauma renal function so far have not been clarified yet. It was once considered that the enhanced feeding of certain nutrients such as proteins or amino acids might increase the glomerular filtration rate (GFR). However, Mouser *et al.*^[25] have shown that even with the same kind of nutrients, CCr in intravenously fed animals with renal ischemia was significantly lower than that in enterally fed animals, suggesting that the enteric factors beyond nutrients play a role in the improvement of impaired renal function. In fact, in severe traumas including burn, loss of large amount body fluids and release of stress hormones caused a sharp reduce of blood flow to many organs, especially the gastrointestinal tract and the kidney. Reduced intestinal blood flow then led to translocation of bacteria and/or their toxic products through the gut mucosa. Subsequent bacteria-and/or toxin-induced persistent and excessive release of cytokines (i.e. tumor necrosis factor, interleukins) and complement activation initiated progressive multiple organ failure and even caused death^[26, 27]. In accordance with this theory, numerous studies have proposed that the renal ischemia and endotoxemia occurred in various pathological conditions be the major contributors to the renal dysfunction^[10-13, 28-30].

Postprandial gut hyperemia is a locally mediated vascular response to the presence of foodstuff in the lumen, an important physiological phenomenon for food digestion and absorption. Even though in some pathological conditions, this phenomenon still exists. In burned guinea pigs, Inoue *et al.*^[31] using radiolabeled microspheres demonstrated that blood flow to the jejunum and cecum was higher in the diet group than in the control during initial 24 h of enteral feeding. In a dog model of splanchnic ischemia induced with endotoxin, Eleftheriadis *et al.*^[32] reported that portal vein, hepatic and superior mesenteric artery blood flow, hepatic and intestinal microcirculation, hepatic tissue PO₂ and energy charge, and intestinal intramucosal pH were significantly increased after early enteral feeding, which were all reduced in the early septic condition. In the present study, we showed that postburn EEF could effectively restore reduced gastric intramucosal pH, decrease endotoxin concentrations in portal vein and TNF- α levels in systemic circulation, as well as alleviate renal tissue edema compared with burn controls. All the above indicate that in addition to provision of nutritional substrates, posttrauma EEF is most likely via a mechanism of postprandial hyperemia, to improve gut low flow and splanchnic ischemic status, to maintain gut mucosal integrity, and to block the vicious circle of mutual activation between the translocation of gut origin bacteria and their toxic products, and the release of inflammatory mediators^[33], thereby reducing hypoxic and inflammatory tissue damage. However, detailed mechanisms are needed to be further studied.

The facts that EEF could improve postburn renal function are of both theoretical and practical importance. The present study revealed that EEF should not be taken merely as a method or a route for nutritional support. Its clinical value has exceeded the range of nutrition and is not limited to the locally enteric benefits as well. Although the results from the animal study can not be extrapolated directly to humans, a better understanding of the postburn EEF might lead to new ways for the further improvement in prevention and treatment of MODS posttrauma.

REFERENCES

- 1 **Holm C**, Horbrand F, von Donnersmarck GH, Muhlbauer W. Acute renal failure in severely burned patients. *Burns* 1999; **25**: 171-178
- 2 **Anlatici R**, Ozerdem OR, Dalay C, Kesiktas E, Acarturk S, Seydaoglu G. A retrospective analysis of 1083 Turkish patients with serious burns. Part 2: burn care, survival and mortality. *Burns* 2002; **28**: 239-243
- 3 **Kim GH**, Oh KH, Yoon JW, Koo JW, Kim HJ, Chae DW, Noh JW, Kim JH, Park YK. Impact of burn size and initial serum albumin level on acute renal failure occurring in major burn. *Am J Nephrol* 2003; **23**: 55-60
- 4 **Chrysopoulo MT**, Jeschke MG, Dziewulski P, Barrow RE, Herndon DN. Acute renal dysfunction in severely burned adults. *J Trauma* 1999; **46**: 141-144
- 5 **Davies MP**, Evans J, McGonigle RJ. The dialysis debate: acute renal failure in burns patients. *Burns* 1994; **20**: 71-73
- 6 **Triolo G**, Mariano F, Stella M, Salomone M, Magliacani G. Dialytic therapy in severely burnt patients with acute renal failure. *G Ital Nefrol* 2002; **19**: 155-159
- 7 **Tremblay R**, Ethier J, Querin S, Beroniade V, Falardeau P, Leblanc M. Veno-venous continuous renal replacement therapy for burned patients with acute renal failure. *Burns* 2000; **26**: 638-643
- 8 **Turnage RH**, Guice KS, Oldham KT. Endotoxemia and remote organ injury following intestinal reperfusion. *J Surg Res* 1994; **56**: 571-578
- 9 **LaNoue JL Jr**, Turnage RH, Kadesky KM, Guice KS, Oldham KT, Myers SI. The effect of intestinal reperfusion on renal function and perfusion. *J Surg Res* 1996; **64**: 19-25
- 10 **Yamaguchi H**, Kita T, Sato H, Tanaka N. Escherichia coli endotoxin enhances acute renal failure in rats after thermal injury. *Burns* 2003; **29**: 133-138
- 11 **Yokota M**, Kambayashi J, Tahara H, Kawasaki T, Shiba E, Sakon M, Mori T. Renal insufficiency induced by locally administered endotoxin in rabbits. *Methods Find Exp Clin Pharmacol* 1990; **12**: 487-491
- 12 **Heyman SN**, Rosen S, Darmon D, Goldfarb M, Bitz H, Shina A, Brezis M. Endotoxin-induced renal failure. II. A role for tubular hypoxic damage. *Exp Nephrol* 2000; **8**: 275-282
- 13 **Zager RA**. Escherichia coli endotoxin injections potentiate experimental ischemic renal injury. *Am J Physiol* 1986; **251**: F988-994
- 14 **Yamaguchi H**, Kita T, Sato H, Tanaka N. Escherichia coli endotoxin enhances acute renal failure in rats after thermal injury. *Burns* 2003; **29**: 133-138
- 15 **Hanna MK**, Kudsk KA. Nutritional and pharmacological enhancement of gut-associated lymphoid tissue. *Can J Gastroenterol* 2000; **14**(Suppl): 145D-151D
- 16 **Fukatsu K**, Zarzaur BL, Johnson CD, Lundberg AH, Wilcox HG, Kudsk KA. Enteral nutrition prevents remote organ injury and death after a gut ischemic insult. *Ann Surg* 2001; **233**: 660-668
- 17 **Alexander JW**. Is early enteral feeding of benefit? *Intensive Care Med* 1999; **25**: 129-130
- 18 **Kompan L**, Kremzar B, Gadzijev E, Prosek M. Effects of early enteral nutrition on intestinal permeability and the development of multiple organ failure after multiple injury. *Intensive Care Med* 1999; **25**: 157-161
- 19 **Eleftheriadis E**. Role of enteral nutrition-induced splanchnic hyperemia in ameliorating splanchnic ischemia. *Nutrition* 1999; **15**: 247-248
- 20 **Noc M**, Weil MH, Sun S, Gazmuri RJ, Tang W, Pakula JL. Comparison of gastric luminal and gastric wall PCO₂ during hemorrhagic shock. *Circ Shock* 1993; **40**: 194-199
- 21 **Buttenschoen K**, Berger D, Hiki N, Strecker W, Seidelmann M, Beger HG. Plasma concentrations of endotoxin and antiendotoxin antibodies in patients with multiple injuries: a prospective clinical study. *Eur J Surg* 1996; **162**: 853-860
- 22 **Jiang DJ**, Tao JY, Xu SY. Inhibitory effects of clonidine on edema formation after thermal injury in mice and rats. *Zhongguo Yaoli Xuebao* 1989; **10**: 540-542
- 23 **Bengmark S**, Gianotti L. Nutritional support to prevent and treat multiple organ failure. *World J Surg* 1996; **20**: 474-481
- 24 **Roberts PR**, Black KW, Zaloga GD. Enteral feeding improves outcome and protects against glycerol-induced acute renal failure in the rat. *Am J Respir Crit Care Med* 1997; **156**: 1265-1269
- 25 **Mouser JF**, Hak EB, Kuhl DA, Dickerson RN, Gaber LW, Hak LJ.

- Recovery from ischemic acute renal failure is improved with enteral compared with parenteral nutrition. *Crit Care Med* 1997; **25**: 1748-1754
- 26 **Vincent JL**. Prevention and therapy of multiple organ failure. *World J Surg* 1996; **20**: 465-470
- 27 **Pastores SM**, Katz DP, Kvetan V. Splanchnic ischemia and gut mucosal injury in sepsis and the multiple organ dysfunction syndrome. *Am J Gastroenterol* 1996; **91**: 1697-1710
- 28 **Lugon JR**, Boim MA, Ramos OL, Ajzen H, Schor N. Renal function and glomerular hemodynamics in male endotoxemic rats. *Kidney Int* 1989; **36**: 570-575
- 29 **Van Lambalgen AA**, Van Kraats AA, Van den Bos GC, Stel HV, Straub J, Donker AJ, Thijs LG. Renal function and metabolism during endotoxemia in rats: role of hypotension. *Circ Shock* 1991; **35**: 164-173
- 30 **Begany DP**, Carcillo JA, Herzer WA, Mi Z, Jackson EK. Inhibition of type IV phosphodiesterase by Ro 20-1724 attenuates endotoxin-induced acute renal failure. *J Pharmacol Exp Ther* 1996; **278**: 37-41
- 31 **Inoue S**, Lukes S, Alexander JW, Trocki O, Silberstein EB. Increased gut blood flow with early enteral feeding in burned guinea pigs. *J Burn Care Rehabil* 1989; **10**: 300-308
- 32 Eleftheriadis E, **Kazamias P**, Kotzampassi K, Koufogiannis D. Influence of enteral nutrition-induced splanchnic hyperemia on the septic origin of splanchnic ischemia. *World J Surg* 1998; **22**: 6-11
- 33 **Gianotti L**, Alexander JW, Nelson JL, Fukushima R, Pyles T, Chalk CL. Role of early enteral feeding and acute starvation on postburn bacterial translocation and host defense: prospective, randomized trials. *Crit Care Med* 1994; **22**: 265-272

Edited by Zhang JZ and Wang XL

Application of modified two-cuff technique and multiglycosides tripterygium wilfordii in hamster-to-rat liver xenotransplant model

Hua Guo, Yi-Jun Wu, Shu-Sen Zheng, Wei-Lin Wang, Jun Yu

Hua Guo, Yi-Jun Wu, Shu-Sen Zheng, Wei-Lin Wang, Jun Yu,
Department of Hepatobiliary Surgery, First Affiliated Hospital,
Medical College Zhejiang University, Hangzhou 310003, Zhejiang
Province, China

Supported by Chinese Traditional Medicine Administration of
Zhejiang Province Foundation, No.2000C55

Correspondence to: Dr. Hua Guo, Department of Hepatobiliary
Surgery, First Affiliated Hospital, Medical College of Zhejiang
University, 79 Qingchun Lu, Hangzhou 310003, Zhejiang Province,
China. ggghua@mail.hz.zj.cn

Telephone: +86-571-87236857 **Fax:** +86-571-87236618

Received: 2003-01-11 **Accepted:** 2003-03-10

Abstract

AIM: To modify the hamster-to-rat liver xenotransplant technique to prevent postoperative complications, and to study the inhibiting effect of multiglycosides tripterygium wilfordii (T_{II}) on immune rejection.

METHODS: Female golden hamsters and inbred male Wistar rats were used as donors and recipients, respectively. One hundred and twelve orthotopic liver xenotransplants were performed by Kamada's cuff technique with modifications. Over 72 hour survival of the animal after operation was considered as a successful operation. When the established surgical model became stable, 30 of the latest 42 cases were divided into untreated control group ($n=15$) and T_{II} group ($n=15$) at random. Survival of recipients was observed. Liver specimens were collected at 2 and 72 h from the operated animals and postmortem, respectively, for histological study.

RESULTS: The successfully operative rate of the 30 operations was 80 %, and the survival of the control and T_{II} group was 7.1 ± 0.35 was days and 7.2 ± 0.52 days, respectively ($t=0.087, P=0.931$). The rate of conjunctival hyperemia in control group (100 %) differed significantly from that (31 %) in T_{II} group ($P=0.001$). Rejection did not occur in both groups within 2 h postoperatively, but became obvious in control group at 72 h after surgery and mild in T_{II} group. Although rejections were obvious in both groups at death of recipients, it was less severe in T_{II} group than in control group.

CONCLUSION: This modified Kamada's technique can be used to establish a stable hamster-to-rat liver xenotransplant model. Monotherapy with multiglycosides tripterygium wilfordii ($30 \text{ mg} \cdot \text{kg}^{-1} \cdot \text{d}^{-1}$) suppresses the rejection mildly, but fails to prolong survival of recipients.

Guo H, Wu YJ, Zheng SS, Wang WL, Yu J. Application of modified two-cuff technique and multiglycosides tripterygium wilfordii in hamster-to-rat liver xenotransplant model. *World J Gastroenterol* 2003; 9(7): 1550-1553

<http://www.wjgnet.com/1007-9327/9/1550.asp>

INTRODUCTION

The hamster-to-rat liver transplant model is useful to study

immunology and physiology of liver xenotransplantation (XT)^[1-11], especially for the extended host response to long-surviving xenografts^[12]. As it is very difficult to establish this surgical model^[13], we summarized our surgical experience in producing for performing this model.

The model could serve as a tool to evaluate immunosuppressive drugs^[14,15]. Tripterygium wilfordii hook F (TWHF) has been used for more than two thousand years as a traditional Chinese herb. T_{II} is extracted and refined from the root of TWHF. In recent years, T_{II} and other extracts of TWHF have been applied to allotransplantation and cardiac XT as immunosuppressive drugs with successful results^[16-27]. However, the effects of T_{II} in liver XT are unknown and deserve study.

MATERIALS AND METHODS

Animals and liver xenotransplantation

Female golden hamsters (weighing 80-130 g) and inbred male Wistar rats (weighing 130-180 g) were used as donors and recipients, respectively. One hundred and twelve orthotopic liver xenotransplants were performed by Kamada's cuff technique^[28] with modifications, which were outlined as follows.

Donor operation Ligaments and vessels around the liver were partially dissected while the liver was protected by wrapping film. The common bile duct was entered from anterior wall and a Teflon catheter was inserted into the lumen proximally. The proper hepatic artery was dissected but not ligated. The infrahepatic vena cava (VC) was clamped at the level of left renal vein. The liver was perfused through the abdominal aorta with 10-20 ml of cold (4 °C) lactated Ringer's solution containing 5 U/ml of heparin. Meanwhile the thoracic cavity was opened with the thoracic aorta clamped, and the thoracic inferior VC was opened to release the perfusate. Then, the infrahepatic VC was transected at the upper part of the clamp. So the perfusate could escape from the two ends of VC. Deep ligaments around the liver were dissected while perfusing and the right suprarenal vein was ligated. At the end of perfusion, the proper hepatic artery and portal vein (PV) at the level of splenic vein were ligated and transected. The free liver was stored in lactated Ringer's solution at 0-4 °C.

Preparation of donor liver Preparation of the donor liver was done in lactated Ringer's solution at 0-4 °C. Two cuffs with different diameters were mounted on the PV and infrahepatic VC, respectively. The cystic duct near the common bile duct was ligated and followed by removal of the gallbladder. The suprahepatic VC was trimmed and a stitch was left on each side for suture.

Recipient operation Vessels, the common bile duct and ligaments around the recipient liver were divided, respectively. The right suprarenal vein behind the papilla lobe was ligated, the recipient liver was removed and covered with fresh film orthotopically. The suprahepatic VC was sutured, the PV was anastomosed with cuff method. The infrahepatic VC was anastomosed as the method for suprahepatic VC. Finally, the distal part of Teflon catheter in donor bile duct was inserted into the recipient bile duct and secured by a silk suture. The greater omentum was wrapped around the bile duct. The abdominal incision was closed with continuous suture.

Treatment of the animal with T_{II}

When the model became stable, 30 recipients of the latest 42 cases were divided into untreated controls ($n=15$) and treatment group with T_{II} $30 \text{ mg} \cdot \text{kg}^{-1} \cdot \text{d}^{-1}$ ($n=15$) at random by gavages three days prior to operation till the end of experiment.

Liver specimens were collected at 2 and 72 h after operation or at death of the recipients, respectively, fixed in 10 % formalin, embedded in paraffin, sectioned and stained with hematoxylin and eosin for light microscopy to determine the grade of rejection.

Statistical methods

The results were analyzed by *t* test and Fisher's exact test, respectively. Statistical significance was defined as a *P* value less than 0.05.

RESULTS**Liver xenotransplantation**

One hundred and twelve operations were performed from October 2000 to March 2001. The successful rate of the latest 30 operations was 80 % (24/30). The causes of death were

anesthesia accident in one case, chronic hemorrhage from the surface of donor liver in 3 cases, thrombosis in infrahepatic VC in one case and suppurate peritonitis in one case. The 6 recipients died within 72 h after operation were excluded from the experiment^[14]. The average survival of 24 cases was 7.2 ± 0.44 days.

Effects of T_{II} on survival of recipients

The average survival of the untreated controls and T_{II} group was 7.1 ± 0.35 days and 7.2 ± 0.52 days, respectively ($t=0.087$, $P=0.931$). Four cases in controls and 2 in T_{II} group died within 72 h after operation were eliminated from statistic study.

Effects of T_{II} on conjunctival hyperemia of recipients

The morbidity of conjunctival hyperemia was 100 % (11/11) in controls and 31 % (4/13) in T_{II} group ($P=0.001$). The commence time of conjunctival hyperemia in controls and T_{II} group were 4.73 ± 0.47 days and 5.75 ± 0.5 days, respectively ($t=3.688$, $P=0.003$).

Pus in conjunctiva was obvious in controls with conjunctival hyperemia, and three cases had ablepsia. However, no pus and ablepsia were observed in T_{II} group.

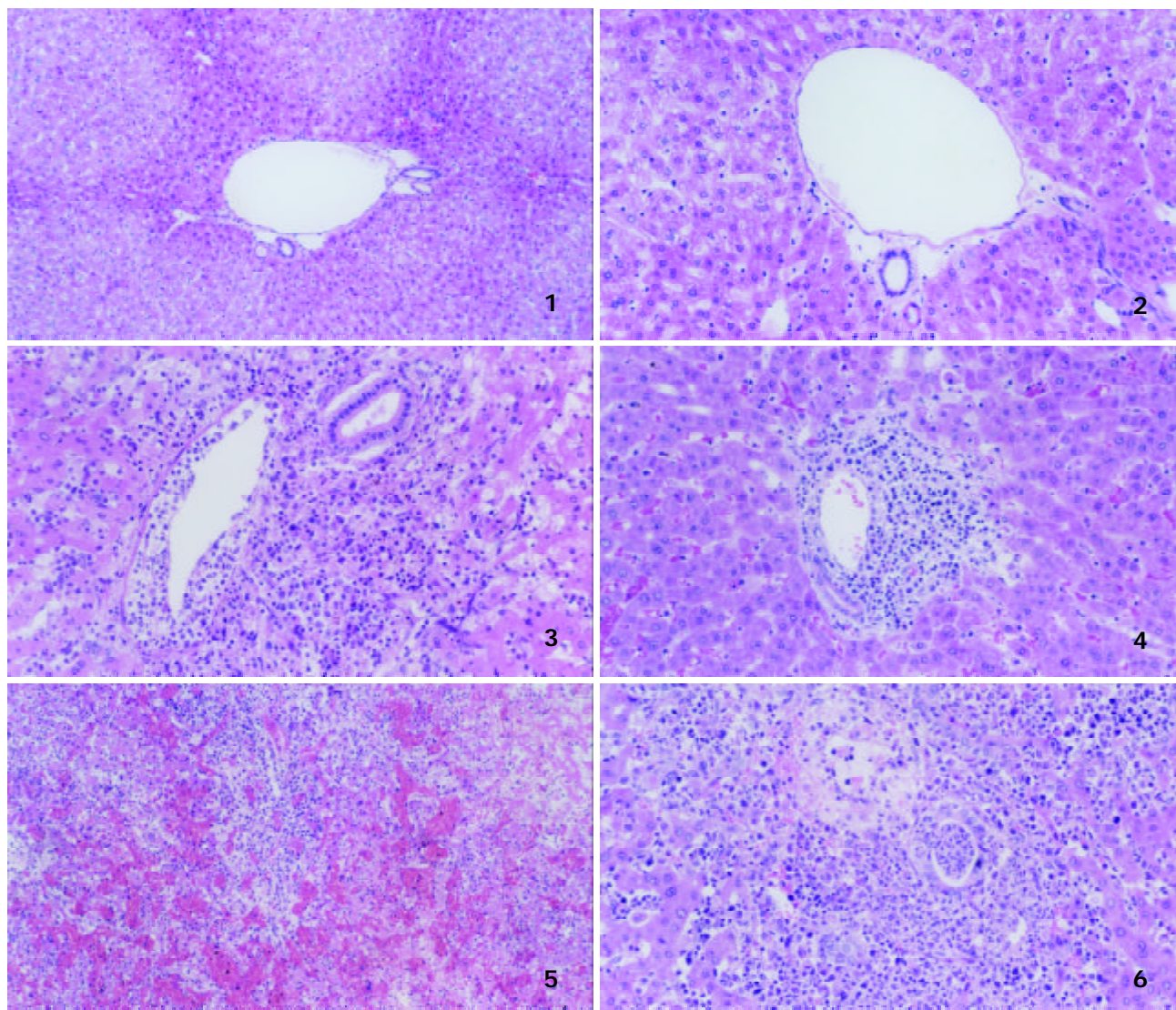


Figure 1 Histological changes of the liver in controls (HE, $\times 100$).
Figure 2 Histological changes of the liver in T_{II} group (HE, $\times 200$).
Figure 3 Histological changes of the liver in controls (HE, $\times 200$).
Figure 4 Histological changes of the liver in T_{II} group (HE, $\times 200$).
Figure 5 Histological changes of the liver in controls (HE, $\times 100$).
Figure 6 Histological changes of the liver in T_{II} group (HE, $\times 200$).

Histopathology

Two hours after operation The structures of hepatic lobule were normal and no inflammatory cells in portal area in both groups were observed (Figures 1 and 2).

Seventy-two hours after operation In controls, hepatic lobules were normal, numerous inflammatory cells consisting mainly of mononuclear cells and neutrophilic granulocytes infiltrated in portal area, edema could be seen in the tunica intima of interlobular veins and inflammatory cells infiltrated into subintima. However, epithelia of interlobular bile ducts were not injured (Figure 3).

In T_{II} group, the structures of hepatic lobules and interlobular veins were normal, moderate amounts of inflammatory cells were found in portal area, and epithelium of interlobular bile ducts was intact (Figure 4).

Postmortem specimens on day 7 postoperation In controls, hepatic lobules were damaged severely, inflammatory cells consisting mainly of mononuclear cells and neutrophilic granulocytes in portal area as well as massive hemorrhage were observed, interlobular vessels were disappeared and damaged epithelia of interlobular bile ducts were observed (Figure 5).

In T_{II} group, many mixed cells could also be seen in portal area, but most of the interlobular vessels and bile ducts were existed with inflammatory intima, and variable injured epithelia, hepatocytes around portal area were swollen, degenerated and partially necrotic and some liver plates were destroyed (Figure 6).

DISCUSSION

Sun *et al.*^[29] firstly advocated that perfusate should enter the liver via dual vascular systems of the hepatic artery and the PV, then the liver and its structures around were divided. The authors performed 300 liver transplantations in rats, and the successful rate of operation and survival rate in one week were 92.7 % and 88.4 %, respectively. So we adopted this dual perfusion except for perfusion by PV in initial trials of 20 cases. We found that perfusion by PV could often result in incomplete perfusion in some small areas and undesirable pressure. Incomplete perfusion did not occur with dual perfusion, and due to the invariant pressure of intestinal circulation, the liver was not mechanically injured by fluctuant pressure and warm ischemia and mechanical injuries were avoided. If the donor liver was dissected at the end of complete perfusion, the vessels became pale and were difficult to be identified and were easily injured accidentally. After modification of the technique, the quality of the liver in donor was excellent in the trials and the survival time of recipient animals was similar to that in the literature^[14,30,31].

We used to ligate the cystic duct, and then to remove the gallbladder and electrocauterize the bed of the gallbladder. However, it usually rendered slow hemorrhage in the bed of the gallbladder and the recipients died in hours after transplantation. So we modified the method as follows: ligating cystic duct near the common bile duct, then ligating cervix of the gallbladder and cutting gallbladder at the distal side of the ligation. No postoperative hemorrhage was observed after the modifications.

For the sake of exposing and ligating suprahepatic VC of the donor and the recipient, papilla lobe and right lobe of the liver were turned over frequently and thus were injured easily, and the recipient could die from mild hemorrhage from the surface of the graft. Sometimes, ligation of the infra-branch of suprarenal vein was mistaken for main stem with left supra-branch unligated, which rendered hemorrhage at recipient liver's cutting and posttransplantation. Therefore, we ligated the right suprarenal vein at the end of perfusion, the structures around the donor liver were divided completely and the right

suprarenal vein was exposed easily, so that liver injury and false ligation were reduced. Loop-ligation behind papilla lobe method was used to ligate the suprarenal vein of the recipient. The right suprarenal vein and part of ligaments behind the recipient liver were ligated with 5-0 silk sutures behind the papilla lobe and near the infrahepatic VC. This ligation was reliable, simple, and shortened the anhepatic phase directly.

Hamster's liver is more fragile than that of rat. Slight press or attrition on its surface could result in contuse and chronic hemorrhage. Moreover, it has poor coagulating mechanism. Thus, fresh film has been used to protect the donor liver in operation, and the pressure on donor liver could be dispersed, the accident stab to the donor liver by instruments could be relieved to some extent and the donor liver could be kept from drying and crisping. Moreover, careful and delicate operation should not be ignored. Nevertheless, in our 30 trials, 3 of 6 failed cases died due to chronic hemorrhage on the surface of the donor liver.

We found that T_{II} at a dosage of 30 mg·kg⁻¹·d⁻¹ could not prolong the survival of the operated animal. But the rejection in T_{II} group was less severe in comparison with that of controls. We speculated that this dosage of T_{II} had certain limited immunosuppressive effect. Li *et al.*^[32] found that the extracts of TWHF could inhibit human peripheral blood mononuclear cells (PBMC) in a concentration-dependent manner and the best inhibitory rate could be achieved at 72 h. Another research suggested that T_{II} at a dosage of 30 mg·kg⁻¹·d⁻¹ had no effects on the liver, kidney, heart and the total number of WBC in rat, but could inhibit the transforming of spleen lymphocytes significantly. T_{II} at this dosage could prolong the survival time of renal allotransplantation in Wistar-to-SD combination significantly. When it was combined with CsA, the survival time could be further prolonged^[19]. Nevertheless, in other organ transplantations such as small intestine transplantation, whose rejection was relatively strong, and the monotherapy with T_{II} was demonstrated to have limited effects^[21]. Wang *et al.*^[16] applied PG27 (extract of TWHF) combined with a low dosage of CsA to hamster-to-rat cardiac xenotransplantation and all xenografts survived more than 100 days. However, they found that either PG27 or CsA had no such effects. Therefore, although a high dosage of T_{II} was given to the recipient 3 days before operation in our trials as monotherapy, the survival time of the recipient was not prolonged due to the strong rejection in this model.

In this study, conjunctival hyperemia occurred in all untreated control recipients on day 4-5 after operation, and deteriorated rapidly, even resulted in ablepsia. However, in the recipients treated with T_{II} , the sign occurred only in 31 % rats (on day 5-6 after transplantation) and ablepsia did not occur. The differences between the two groups were highly significant and the similar report has not been found in literature. We speculated that conjunctival hyperemia could be a local representation of rejection in this model. Relieving the sign with T_{II} treatment supported the hypothesis, but the exact mechanism of the sign needs to be further studied.

REFERENCES

- 1 **Tandin A**, Goller AL, Miki T, Lee YH, Kovscek AM, Fung JJ, Starzl TE, Valdivia LA. Concordant hamster-to-rat liver xenotransplantation leads to hyperlipidemia. *Transplant Proc* 2000; **32**: 1109
- 2 **Celli S**, Marto JA, Falchetto R, Shabanowitz J, Valdivia LA, Fung JJ, Hunt DF, Kelly RH. Serum protein immunogenicity: implications for liver xenografting. *Electrophoresis* 2000; **21**: 965-975
- 3 **Molleivi DG**, Jaurrieta E, Ribas Y, Hurtado I, Serrano T, Gomez N, de-Oca J, Fiol C, Figueras J. Liver xenotransplantation: changes in lipid and lipoprotein concentration after long-term graft survival. *J Hepatol* 2000; **32**: 655-660

- 4 **Tan JW**, Zhang SG, Jiang Y, Yang JM, Qian GX, Wu MC. Apoptosis in acute rejection of hamster-to-rat liver transplantation. *HBPD Int* 2002; **1**: 340-344
- 5 **Tan JW**, Yao HX, Yang JM, Qian GX, Wu MC. The role of spleen in rejection of concordant liver xenograft. *Zhonghua Qiguan Yizhi Zazhi* 2000; **21**: 83-85
- 6 **Valdivia LA**, Fung JJ, Demetris AJ, Celli S, Pan F, Tsugita M, Starzl TE. Donor species complement after liver xenotransplantation. *Transplantation* 1994; **57**: 918-922
- 7 **Schraa EO**, Stockmann HB, Broekhuizen AJ, Scheringa M, Schnurman HJ, Marquet RL, Ijzermans JN. IgG, but IgM, mediates hyperacute rejection in hepatic xenografting. *Xenotransplantation* 1999; **6**: 110-116
- 8 **Diao TJ**, Yuan TY, Li YL. Immunologic role of nitric oxide in acute rejection of golden hamster to rat liver xenotransplantation. *World J Gastroenterol* 2002; **8**: 746-751
- 9 **Zhang SG**, Wu MC, Tan JW, Chen H, Yang JM, Qian QJ. Expression of perforin and granzyme B mRNA in judgement of immunosuppressive effect in rat liver transplantation. *World J Gastroenterol* 1999; **5**: 217-220
- 10 **Valdivia LA**, Demetris AJ, Fung JJ, Celli S, Murase N, Starzl TE. Successful hamster-to-rat liver xenotransplantation under FK506 immunosuppression induces unresponsiveness to hamster heart and skin. *Transplantation* 1993; **55**: 659-661
- 11 **Celli S**, Valdivia LA, Fung JJ, Kelly RH. Early recipient-donor switch of the complement type after liver xenotransplantation. *Immunol Invest* 1997; **26**: 589-600
- 12 **Molleivi DG**, Ribas Y, Ginesta MM, Serrano T, Mestre M, Vidal A, Figueras J, Jaurrieta E. Heart and liver xenotransplantation under low-dose tacrolimus: graft survival after withdrawal of immunosuppression. *Transplantation* 2001; **71**: 217-223
- 13 **Tan JW**, Zhang SG, Qian GX, Wu MC. The modified orthotopic liver transplantation model in hamster-to-rat. *Zhongguo Puwai Jichu Yu Linchuang Zazhi* 1999; **6**: 201-203
- 14 **Murase N**, Starzl TE, Demetris AJ, Valdivia L, Tanabe M, Cramer D, Makowka L. Hamster-to-rat heart and liver xenotransplantation with FK506 plus antiproliferative drugs. *Transplantation* 1993; **55**: 701-708
- 15 **Murase N**, Demetris AJ, Tanabe M, Miyazawa H, Valdivia LA, Nakamura K, Starzl TE. Effect of FK506 and antiproliferative agents for heart and liver xenotransplantation from hamster to rat. *Transplant Proc* 1993; **25**: 425-426
- 16 **Wang J**, Xu R, Jin R, Chen Z, Fidler JM. Immunosuppressive activity of the Chinese medicinal plant *Tripterygium wilfordii*. II. Prolongation of hamster-to-rat cardiac xenograft survival by combination therapy with the PG27 extract and cyclosporine. *Transplantation* 2000; **70**: 456-464
- 17 **He X**, Verran D, Hu C, Wang C, Li L, Wang L, Huang J, Sun J, Sheil AG. Synergistic effect of *Tripterygium Wilfordii* Hook F [TWHF] and cyclosporine A in rat liver transplantation. *Transplant Proc* 2000; **32**: 2054
- 18 **Qian YY**, Shi BY, Liang CQ, Li N, Shi YC, Xia JM. Effects of total glucosides of *Tripterygium wilfordii* (T_{II}) on the reproductive organs of transplant recipients. *Zhonghua Miniao Waiké Zazhi* 2002; **23**: 209-211
- 19 **Zhang LL**, Sun JH. Synergistic effect of *Tripterygium wilfordii* hook f and cyclosporine A on heterotopic rat cardiac allograft survival. *Zhonghua Shiyān Waiké Zazhi* 2001; **18**: 407-408
- 20 **Qian YY**, Shi BY, Liang CQ, Kang XJ, Shi YC, Li N, Xia JM. Total glucosides of *Tripterygium wilfordii* in the management of rats with renal allograft. *Zhonghua Miniao Waiké Zazhi* 1996; **17**: 338-340
- 21 **Li YX**, Li N, Wu B, Li JS. The effect of *Tripterygium wilfordii* on acute rejection in small bowel transplantation in rats. *Zhonghua Xiaoe Waiké Zazhi* 2000; **21**: 49-51
- 22 **Wang DH**, Wang JP, Wang L. Role of *Tripterygium wilfordii* hook f (T_{co}) on pancreaticoduodenal allograft in rats. *Zhonghua Qiguan Yizhi Zazhi* 2000; **21**: 220-222
- 23 **Shao QX**, Yin L, Xu HX, Li LJ, Liu GZ, Cao YQ, Chen M. Using DcsMcAb and tripterygll multi-glycosidorum to prevent the rejection of heart-lung allogeneic transplantation in rats. *Zhongguo Mianyixue Zazhi* 1998; **14**: 356-359
- 24 **Li N**, Li JS, Li YS, Jiang ZW, Yin L, Zhao YZ. Experimental and clinical studies of small bowel allotransplantation. *Zhonghua Waiké Zazhi* 1995; **33**: 11-14
- 25 **Qian YY**, Shi BY, Liang CQ. Total glucosides of *Tripterygium wilfordii* (T_{II}) as an immuno-suppressant in kidney transplantation. *Zhonghua Miniao Waiké Zazhi* 1995; **16**: 268-269
- 26 **Chen BJ**. Triptolide, a novel immunosuppressive and anti-inflammatory agent purified from a Chinese herb *Tripterygium wilfordii* Hook F. *Leuk Lymphoma* 2001; **42**: 253-265
- 27 **Ramgolam V**, Ang SG, Lai YH, Loh CS, Yap HK. Traditional Chinese medicines as immunosuppressive agents. *Ann Acad Med Singapore* 2000; **29**: 11-16
- 28 **Kamada N**, Calne RY. A surgical experience with five hundred thirty liver transplants in the rat. *Surgery* 1983; **93**: 64-69
- 29 **Sun JH**, Zeng QH, Wu MC. Experience with orthotopic rat liver transplantation. *Chin Med J Engl* 1990; **103**: 142-145
- 30 **Valdivia LA**, Monden M, Gotoh M, Hasuike Y, Kubota N, Endoh W, Okamura J, Mori T. Hepatic xenografts from hamster to rat. *Transplant Proc* 1987; **XIX**: 1158-1159
- 31 **Sankary HN**, Yin DP, Chong ASF, Ma LL, Blinder L, Shen JK, Foster P, Williams JW. FK506 treatment in combination with leflunomide in hamster-to-rat heart and liver xenograft transplantation. *Transplantation* 1998; **66**: 832-837
- 32 **Li XW**, Weir MR. Radix *Tripterygium Wilfordii*-a Chinese herbal medicine with potent immunosuppressive properties. *Transplantation* 1990; **50**: 82-86

Edited by Ren SY and Wang XL

Expression of metallothionein gene at different time in testicular interstitial cells and liver of rats treated with cadmium

Xu-Yi Ren, Yong Zhou, Jian-Peng Zhang, Wei-Hua Feng, Bing-Hua Jiao

Xu-Yi Ren, Yong Zhou, Jian-Peng Zhang, Wei-Hua Feng, Bing-Hua Jiao, Department of Biochemistry and Molecular Biology, Second Military Medical University, Shanghai 200433, China
Supported by the National Natural Science Foundation of China, No. 39970631

Correspondence to: Dr. Xu-Yi Ren, Department of Biochemistry and Molecular Biology, Second Military Medical University, Shanghai 200433, China. renxuyi2003@163.com
Telephone: +86-21-25070306-8008 **Fax:** +86-21-65334344
Received: 2002-12-30 **Accepted:** 2003-03-04

Abstract

AIM: Rodent testes are generally more susceptible to cadmium (Cd)-induced toxicity than liver. To clarify the molecular mechanism of Cd-induced toxicity in testes, we compared metallothionein (MT) gene expression, MT protein accumulation, and Cd retention at different time in freshly isolated testicular interstitial cells and liver of rats treated with Cd.

METHODS: Adult male Sprague-Dawley rats weighing 250-280 g received a s.c injection of 4.0 μmol Cd/kg and were euthanized by CO₂ asphyxiation 1 h, 3 h, 6 h, or 24 h later. Tissue was sampled and testicular interstitial cells were isolated. There were three replicates per treatment and 3 animals per replicate for RNA analyses, others, three replicates per treatment and one animal per replicate. MT1 and MT2 mRNA levels were determined by semi-quantitative RT-PCR analysis followed by densitometry scanning, and MT was estimated by the enzyme-linked immunosorbent assay (ELISA) method. Cadmium content was determined by atomic absorption spectrophotometry. The same parameters were also analyzed in the liver, since this tissue unquestionably accumulate MT.

RESULTS: The rat testis expressed MT1 and MT2, the major isoforms. We also found that untreated animals contained relatively high basal levels of both isoform mRNA, which were increased after Cd treatment in liver and peaked at 3 h, followed by a decline. In contrast, the mRNA levels in interstitial cells peaked at 6 h. Interestingly, the induction of MT1 mRNA was lower than MT2 mRNA in liver of rat treated with Cd, but it was opposite to interstitial cells. Cd exposure substantially increased hepatic MT (3.9-fold increase), but did not increase MT translation in interstitial cells.

CONCLUSION: Cd-induced expression of MT isoforms is not only tissue dependent but also time-dependent. The inability to induce the metal-detoxifying MT-protein in response to Cd, may account for a higher susceptibility of testes to Cd toxicity and carcinogenesis compared to liver.

Ren XY, Zhou Y, Zhang JP, Feng WH, Jiao BH. Expression of metallothionein gene at different time in testicular interstitial cells and liver of rats treated with cadmium. *World J Gastroenterol* 2003; 9(7): 1554-1558
<http://www.wjgnet.com/1007-9327/9/1554.asp>

INTRODUCTION

Metallothionein (MT) gene expression appears to be not only tissue specific but also cell specific^[1,2]. In rodents, the testes and ventral prostate have been shown to have a higher sensitivity to cadmium (Cd)-induced carcinogenesis than many other tissues^[3]. These tissues have also been shown to have either no induction or a reduced expression of MT gene when animals were exposed to Cd or some other MT inducer agents^[4,5]. It has been reported that testicular Cd is bound to a protein different from MT. The testicular Cd-binding protein contains less cysteine and more glutamate than MT^[6]. However, some other studies have shown that MT is constitutively expressed in the whole testes or specific testicular cells at levels higher than that in some other organs, e.g. the liver, and that *in vivo* or *in vitro* Cd exposure increases MT gene expression in the testes^[7-9].

Therefore, the published data are inconclusive as to whether MT exists in the testes under physiological conditions and whether this protein plays an important role in the detoxification of testicular Cd. Some of the controversies may derive from analyzing the whole testicular tissue instead of individual cell types, since MT gene expression appears to be not only tissue specific but also cell specific^[1,2]. On the other hand, MT might affect testicular Cd accumulation toxicokinetically by sequestering the metal in the liver, thus diverting it from target tissues, such as the testes. It has been well established that Cd significantly enhances hepatic MT gene expression and MT synthesis. Such enhancement of liver MT might lead to lower testicular Cd uptake and toxicity.

In rodents testicular Cd appears to be localized in the interstitial tissue and a high incidence of interstitial cell (Leydig cell) tumors can occur following Cd exposure. However, testicular lesions as a result of Cd exposure have not been reported in men^[10]. A single s.c. dose $\geq 5 \mu\text{mol}$ Cd/kg could result in a high incidence of testicular interstitial cell tumors. An elevated incidence of testicular tumors in rats was also found after chronic oral exposure to Cd. Within the interstitial tissue, Leydig cells appeared to be highly sensitive to Cd cytotoxicity^[11]. However, most of the studies on MT gene expression and synthesis have been focused on the whole testes, which might mask the results on MT activity in these specific cells, since they only contributed to 11 % of parenchymal volume. Some authors investigated Cd-induction of MT expression in cultured Leydig cell lines established from Leydig cell tumors^[12], but their findings gave little insight into MT synthesis in normal testicular interstitial cells or purified Leydig cells isolated from animals exposed to Cd.

Furthermore, MT gene expression is time-dependent. It was reported that both MT isoform mRNA levels in rat livers were substantially increased 4-6 h after Cd treatment, followed by a reduction and chromatography demonstrated a significant time-related increase in MT protein level. *In vitro* studies showed that MT induction was dose- and time-dependent in both Leydig and Sertoli cells^[13]. Therefore some of the controversies may derive from the different study time.

In general, the studies on Cd-induced MT gene expression and MT synthesis in the testis, have been carried out under acute exposure to toxic Cd levels. It is also conceivable that

the biochemical changes occurring in the testes under such conditions of Cd toxicity might mask the molecular processes of MT gene expression at a lower Cd exposure dose.

Although there is a wealth of published information regarding MT gene expression and MT synthesis following induction by Cd^[14-16], little systematic information is available on MT gene expression at different time in testes, particularly in testicular interstitial cells. The aim of this study therefore was to clone MT gene and to investigate MT gene expression, MT accumulation, and Cd retention at different time in testicular interstitial cells isolated by collagenase dispersion and density gradient centrifugation from rats treated with a non-toxic Cd dose. The same parameters in the liver were also analyzed, since this tissue unquestionably accumulated MT.

MATERIALS AND METHODS

Animals and treatments

Adult male Sprague-Dawley rats weighing 250-280 g were obtained from the Animal Center of Second Military Medical University. Rats received a single s.c. injection of 4 µmol Cd/kg and were euthanized by CO₂ asphyxiation 1 h, 3 h, 6 h, or 24 h later for RNA, total Cd, and MT analyses in interstitial cells and liver. Untreated rats (0 h) were also treated as described above. There were three replicates per treatment and 3 animals per replicate for RNA analyses, others, three replicates per treatment and one animal per replicate. Testes and liver were weighed and processed as described below.

Preparation and purification of testicular interstitial cells

Immediately after the testes were removed, these cells were decapsulated, deveined and incubated in a solution of 2 mg/ml collagenase (334 µg/mg, Type IA, Worthington Biochemical Co.) with minimum essential medium (MEM) (6 ml/2 testes) at 37 °C in a shaking water bath at 90 oscillations/min for 15 min. DNase (Sigma Chemical Co.) was added as needed (5-10 drops of 0.1 %) to reduce the clumping of cells to the DNA released from damaged cells. After collagenase dispersion, the digestion media were diluted with 12 ml prewarmed MEM and the tubules were allowed to settle. The resultant supernatant was centrifuged at 80×g for 10 min at 4 °C. Crude interstitial cells from 2 testes were resuspended in ≤3 ml cold MEM and layered on the top of a linear (0-50 %) Percoll density gradient. The gradient was prepared in a LKB gradient mixer with 4 ml of a solution containing 50 % Percoll, 0.15 M NaCl, and 0.07 % bovine serum albumin (BSA) in the diluting chamber and 4 ml of an aqueous solution with 0.15 M NaCl, and 0.07 % BSA in the mixing chamber. Crude interstitial cells were then separated from other cell types by centrifugation at 800×g for 20 min in tubes (8×1.5 cm, 3 tubes for one type of cells from one sample) at 4 °C. Purified interstitial cells formed a distinct band at 41-42 mm from the gradient bottom. Cell band was aspirated, diluted three times its volume with cold MEM to remove Percoll and centrifuged at 80×g for 10 min. Testicular interstitial cells were then suspended in a minimal volume of MEM and processed for RNA, total Cd, or MT protein analysis after aliquots was taken for cell count. Morphological observations by light microscopy showed that the purity ranged from 80 % to 85 %.

Cadmium content

Interstitial cells and liver tissue were wet-ashed in HNO₃ (u. p.)-H₂O₂ and Cd was determined by atomic absorption spectrophotometry (detection limit: 0.001ppm). Precautions were taken to avoid Cd contamination by acid-washing all glasswares and blanks were run along with the samples.

RNA extraction

Total ribonucleic acids were extracted from freshly isolated interstitial cells and liver tissue using RNazol (GibcoBRL). Total RNA was determined by UV absorbance at 260 nm and its purity was estimated by the absorbance ratio A₂₆₀/A₂₈₀ nm. In addition, RNA integrity was confirmed by ethidium bromide staining of ribosomal RNA following gel electrophoresis.

Polymerase chain reaction(PCR) primers

Oligonucleotide primers were synthesized using a DNA synthesizer (Worthington Biochemical Co.). The sequences of sense and antisense primers for rat MT-1 were 5' -ACTGCCTTCTTGTGCGCTTA-3' and 5' -TGGAGGTGTA-CGGCAAGACT-3' respectively. They spanned a 310bp fragment. The sequences of sense and antisense primers for rat MT-2 were 5' -CCAAGTCCGCCTCCATTTCG-3' and 5' -GAAAAAGTGTGGAGAACCG-3' respectively, spanning a 300bp fragment. The sequences of sense and antisense primers for β-actin were 5' -CCCATTGAACACGG-CATTG-3' and 5' -GGTACGACCAGAGGCATACA-3' respectively, spanning a 236bp fragment.

Reverse transcription-PCR (RT-PCR) and products analysis

First-strand cDNA was synthesized with 1 µg total RNA, 50 pmol oligo (dT)₁₈, 10U avian myeloblastosis virus (AMV) reverse transcriptase and 20U RNase inhibitor in a final 20 µl reaction mixture containing 1× reverse transcriptase buffer, 8 mM MgCl₂, 0.5 mM of each dNTP. The reaction mixture was incubated at 42 °C for 60 min. The cDNA products were stored at -20 °C until use.

PCR was carried out in a 25 µl reaction mixture containing 0.2 mM of each dNTP, 1 pmol of each sense and antisense primer and 0.625 unit of Taq DNA polymerase (TaKaRa), including 4 µl of cDNA products. After an initial denaturation at 95 °C for 5 min, amplification was carried out for approximately 27 cycles comprising 1 min at 95 °C for denaturation, 1 min at 55 °C for annealing, 1 min at 72 °C for extension with a final extension step at 72 °C for 5 min. The PCR products were applied to electrophoresis using a 2.0 % (w/v) agarose gel, which was stained with ethidium bromide and visualized under UV light. In order to confirm that there was no significant contamination in the total RNA preparation, we synthesized the first-strand DNA and performed control reactions in the absence of reverse transcriptase, and did not find any band on further PCR. In order to guarantee amplification in phase of exponential increase, we minimize the cycles of PCR in condition that the strap of gel electrophoresis could be detected. MT1 and MT2 mRNA levels were determined by RT-PCR analysis followed by densitometry scanning. All MT1 and MT2 RT-PCR products were normalized to the corresponding β-actin RT-PCR results that served as an internal control to ensure an approximate ratio of MTs mRNA.

Cloning of PCR products

PCR products were cloned using pUCm-T vector, The constructed plasmids were transfected into JM109, positive colonies were selected and the DNA sequence was analysed using a DNA sequencer (Worthington Biochemical Co.).

MT content analysis

Testicular interstitial cells were suspended in 500 µl of 10 mM Tris-HCL, pH 7.4, and lysed by sonication (3×10 s) on ice. Cytosol was then obtained by centrifugation at 18 000×g for 20 min at 4 °C. Liver tissue was homogenated in 10 mM Tris-HCL, pH 7.4, with a glass homogenizer and a Teflon pestle. MT content analysis was performed by the enzyme-linked

immunosorbent assay (ELISA) method. The test procedure was similar to that described by Ruitenber *et al*^[17] and affinity-purified sheep anti-(rat MT) IgG was provided by Environmental Health Sciences Division, National Institute for Environmental Studies, Japan.

Statistical analysis

Data were represented as means ±S.E. of three replicates per Cd treatment or untreated. Differences between Cd-treated (1 h, 3 h, 6 h, 24 h) and untreated rats were evaluated by Student's *t*-test with *P*<0.05 as the limit of significance.

RESULTS

DNA sequences of RT-PCR products

After cloning the RT-PCR products described above into a pUCm-T vector, we examined their DNA sequences (Figure 1) and compared with rat liver MT1 and MT2 cDNAs. These data clearly indicate that the MT1 and MT2 genes are constitutively expressed in the rat testis.

MT1

ACTGCCCTTCTTGTCGCTTACACCGTTGCTCCAGATTCACCAGATCTCGGAAT
GGACCCCAACTGCTCCTGCTCCACCGGGCTCCTGCACCTGCTCCAGCTC
CTGCGGCTGCAAGAAGTCAAATGCACCTCCTGCAAGAAGAGCTGCTGCT
CCTGCTGCCCCGTTGGGCTGCTCCAAATGTGCCAGGGCTGTGCTGCAAAG
GTGCTCGGACAAGTGCACGTGCTGTGCCTGAAGTGACGAACAGTGTGC
TGCCCTCAGGTGTAATAAATTTCCGGACCAACTCAGAGTCTTCCGTACAC
CTCCA

MT2

CCAAGTCCGCTCCATTCGCCATGGACCCCAACTGCTCCTGTGCCACAGA
TGGATCCTGCTCCTGCGCTGGCTCCTGCAAATGCAAACAATGCAAATGCAC
CTCCTGCAAGAAAAGCTGCTGTTCCTGCTGCCCCGTTGGGCTGTGCGAAGT
GCTCCAGGGCTGCATCTGCAAAGAGGCTTCGGACAAGTGCAGCTGCTGC
GCCTGAAGTGGGGGCTCCTCACAATGGTGTAAATAAAACAACGTAAGGA
ACCTAGCCTTTTTTTGTACAACCCTGACCGGTTCTCCACACTTTTTTC

Figure 1 DNA sequences of RT-PCR products from rat testis.

Cadmium content

Cadmium accumulated in the liver rapidly after its administration, but then leveled off. 24 h after Cd content in the liver increased about 10 000-fold whereas interstitial cell Cd was not detected (Figure 2). This indicated that the Cd content in interstitial cells might be below atomic absorption spectrophotometry detection limit (<1 ng/10⁷ cells).

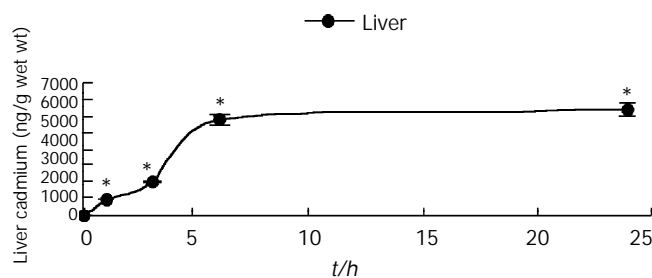


Figure 2 Time course of Cd accumulation in liver after a single subcutaneous injection of 4 μmol Cd/kg. The values were the mean ± S.E. (n=3). An asterisk indicated a significant difference (**P*<0.05 vs control) from the untreated.

Effects of cadmium on transcription of MTs in interstitial and cells liver

To assess gene expression of both MT1 and MT2 genes, semi-quantitative RT-PCR was used. Results from the semi-quantitative RT-PCR (Figure 3) showed that untreated animals contained relatively high basal levels of both isoform mRNA, which were substantially increased after Cd treatment in the liver and peaked at 3 h, followed by a decline. In contrast, the mRNA levels in interstitial cells peaked at 6 h (Figure 3). Interestingly, the induction of MT1 mRNA was lower than MT2 mRNA in the liver of rats treated with Cd, but it was opposite to interstitial cells.

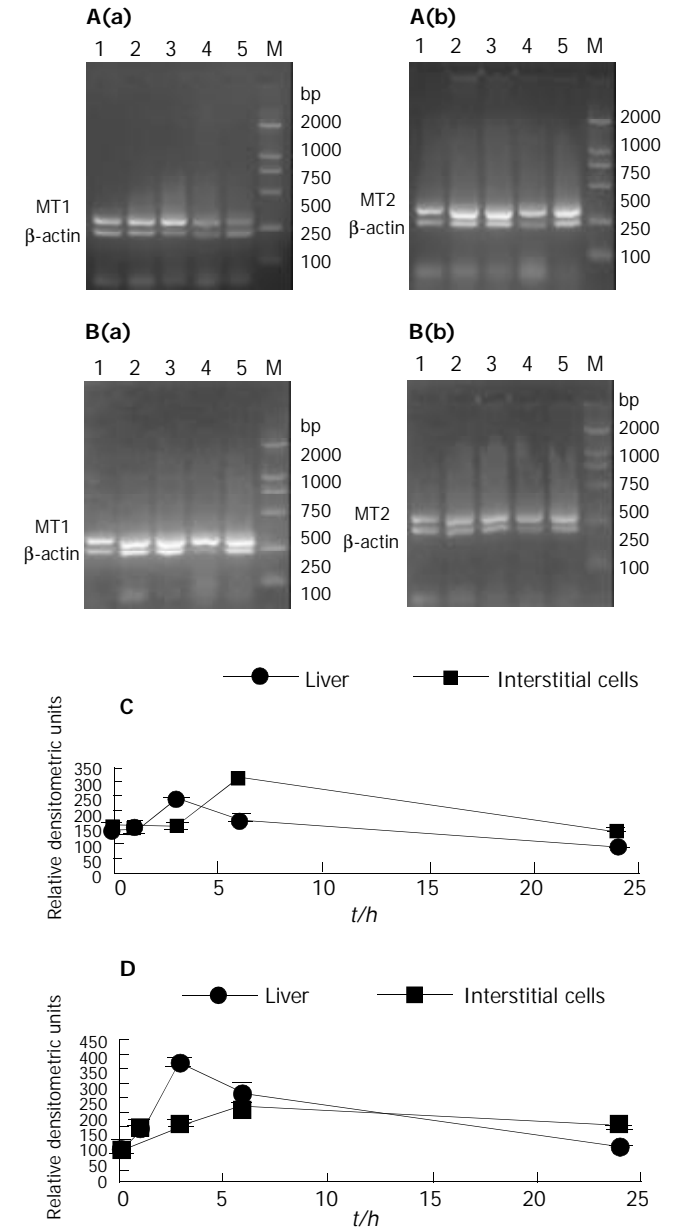


Figure 3 Effect of cadmium treatment on MT1(a) and MT2(b) mRNA levels in testicular interstitial cells (B) and the liver (A) of untreated rats (0h) and Cd-treated rats after 1 h, 3 h, 6 h, or 24 h (lanes 1-5). Values were obtained by RT-PCR analysis followed by densitometry scanning and expressed as MT1(C) or MT2(D) mRNA RT-PCR products to β-actin mRNA RT-PCR products ratio. Data represented the mean ± SE (n=9, three treatment replicates with three analyses per replicate).

Effects of cadmium on translation of MT in testicular interstitial cells and liver

In parallel to the elevation of liver Cd, the level of hepatic MT

increased significantly (3.9 fold increase) 24 h after Cd injection (Figure 4). In sharp contrast to the 3.9-fold elevation of hepatic MT, the MT in testicular interstitial cells of rats treated with Cd slightly declined as compared to untreated animals.

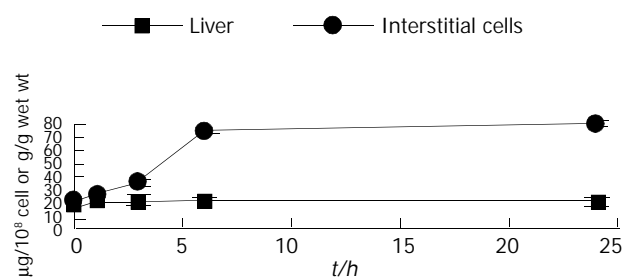


Figure 4 Metallothionein protein in testicular interstitial cells and liver of untreated and Cd-treated rats. Experimental conditions are shown in Figure 3. The values were the mean \pm S.E. ($n=3$).

DISCUSSION

MTs exist not only in tissues from various animal species, but also in bacteria and plants, and are thought to play essential, but as yet unknown roles in cellular processes^[18-22]. MTs are known to detoxify heavy metals. However, male genital organs, particularly testis, are extremely susceptible to Cd. Thus, it has been a long-standing issue as to whether MTs are present in male genital organs or not. We have previously summarized the major points of dispute arising from earlier studies that advocated either the presence or the absence of MTs in the testis, since these earlier studies utilized indirect experimental methods to characterize testicular Cd-binding proteins. Therefore, we considered it essential to analyse directly the cDNA sequence. It has been demonstrated by RT-PCR analysis and DNA sequence analysis of the cloned PCR products that MT1 and MT2 genes are transcribed as their respective mRNA in the rat testis. The present results have clearly shown that the rat testis contains MT1 and MT2, the major isoforms of MT, thus supporting the results of earlier studies, not only in terms of the amounts of MT(-like) proteins estimated by the Cd-binding method in the rat testis, but also in regard to the localization of MT in male genital tissues.

Our observations demonstrated that MT1 and MT2 mRNAs were expressed in interstitial cells under normal physiological conditions, which confirmed the results of others in the whole testes of rats and mice. Furthermore, our results showed that both MT1 and MT2 mRNA increased, but did not translate into any higher protein in interstitial cells in response to Cd treatment. Cd-inducibility of MT1 and MT2 mRNA that we observed in freshly isolated interstitial cells, corroborated the findings of others using cultured mouse interstitial tumor cell lines exposed to Cd *in vitro*. In contrast, other reports indicated decrease, no changes, or little increases of MTs mRNA levels in the whole testes of Cd-treated rats and mice^[16,23]. The discrepancy in the results among the various studies might be due to analysis of whole testicular tissue rather than isolated interstitial cells, or species and strain differences in Cd-induced MT. MT expression in male reproductive tissue might also depend on doses, time course between Cd administration and tissue sampling, age and reproductive states of the animals^[24]. The present data showed that untreated animals contained relatively high basal levels of both isoforms of mRNA, which were substantially increased after Cd treatment in the liver and peaked at 3 h, followed by a decline. In contrast, the mRNA levels in interstitial cells peaked at 6 h (Figure 3). Interestingly,

the induction of MT1 mRNA was lower than MT2 mRNA in the liver of rats treated with Cd, but it was opposite to interstitial cells. This indicates that Cd-induced transcription of MT gene is not only tissue-dependent, but also time-dependent. Therefore, the time selected to analyse mRNA levels might be another source of discrepancy. Furthermore, both isoforms were different from Cd-induction in different tissues or cells. The cause is unclear, and might be related to methylation status of the MT gene, since DNA methylation controls MT gene expression in murine lymphoid cells.

We also found that interstitial cells isolated from untreated animals contained relatively high basal levels of MT protein, thus supporting the results of earlier studies that MT were constitutively present in the testes at levels higher than that in many other tissues, such as the liver and kidney^[25].

MT might not have any significant role in the detoxification of Cd in the testes, since 20 μ mol Cd/kg destroyed the testicular endothelium of both normal mice and mice with inactivated MT1 and MT2 genes. Furthermore, mouse strain differences in Cd-induced testicular toxicity have not been reported to be correlated with testicular MT levels. In fact, resistance to Cd-induced testicular necrosis is linked to the *cdm* gene, which is located in a different chromosome from the genes for MT1 and MT2.

One hypothesis, which may explain why Cd-induced MT mRNA in interstitial cells was not accompanied by an increase of MT synthesis, is that MT mRNA increases were not translated into the corresponding protein. The existence of nonfunctional MT translations in interstitial cells could explain the higher susceptibility of testes than the liver to Cd toxicity. On the other hand, the absence of an increase in the MT gene translation product in interstitial cells accompanied by a significant increase in the liver of Cd-treated animals, could also be due to kinetic differences between interstitial cells and liver on the rate at which MT mRNA molecules were translated into MT or the rate of MT degradation^[1]. The discrepancy between MT mRNA and MT protein in interstitial cells suggested that MT synthesis was regulated at the level of post-transcription^[26], since an increase of mRNA should not result in decreased protein if regulation was only through transcription. While it is well known that MT gene expression is specifically induced by metals through metal response elements and the heavy metal induction of MT is mediated through the transcription factor MTF-1^[27-29]. We not determine whether the effect of these metals on MT mRNA translation and/or protein degradation was specific to MT. Therefore it is possible that the metals have a more widespread effect on translation of genes^[30-32]. However, it is clear that metals do not have a widespread effect on gene transcription through stress or nonspecific events. For example, housekeeping genes, such as β -actin or dihydrofolate reductase, in the liver and kidney of CD-1 mice were unaffected when treated with 0.6 mg cadmium/kg.

In summary, our observations clearly demonstrate that both MT mRNA and MT are constitutively expressed in isolated interstitial cells and Cd-induced expression of MT isoforms are not only tissue dependent but also time-dependent. Our findings of Cd-induced MT mRNA without increases in MT protein in interstitial cells deserve further investigation. The inability to induce metal-detoxifying MT-protein, in response to Cd, might account for the higher susceptibility of testes to Cd toxicity and carcinogenesis compared to the liver.

ACKNOWLEDGEMENTS

We thank for Prof. Chiharu Tohyama for kindly providing affinity-purified sheep anti-(rat MT) IgG and Dr. Xu Qin-Hua for invaluable assistance with analysis of cadmium content.

REFERENCES

- 1 **Vasconcelos MH**, Tam SC, Hesketh JE, Reid M, Beattie JH. Metal and tissue-dependent relationship between metallothionein mRNA and protein. *Toxicol Appl Pharmacol* 2002; **182**: 91-97
- 2 **Ren XY**, Zhou Y, Zhang JP, Feng WH, Jiao BH. Metallothionein gene expression under different time in testicular Sertoli and spermatogenic cells of rats treated with cadmium. *Reprod Toxicol* 2003; **17**: 219-227
- 3 **Abe T**, Yamamoto O, Gotoh S, Yan Y, Todaka N, Higashi K. Cadmium-induced mRNA expression of Hsp32 is augmented in metallothionein-I and -II knock-out mice. *Arch Biochem Biophys* 2000; **382**: 81-88
- 4 **Xu G**, Zhou G, Jin T, Zhou T, Hammarstrom S, Bergh A, Nordberg G. Apoptosis and p53 gene expression in male reproductive tissues of cadmium exposed rats. *Biometals* 1999; **12**: 131-139
- 5 **Coogan TP**, Shiraishi N, Waalkes MP. Minimal basal activity and lack of metal-induced activation of the metallothionein gene correlates with lobe-specific sensitivity to the carcinogenic effects of cadmium in the rat prostate. *Toxicol Appl Pharmacol* 1995; **132**: 164-173
- 6 **Mullins JE**, Fredrickson RA, Fuentealba IC, Markham RJ. Purification and partial characterization of a cadmium-binding protein from the liver of rainbow trout (*Onchorynchus mykiss*). *Can J Vet Res* 1999; **63**: 225-229
- 7 **Suzuki JS**, Kodama N, Molotkov A, Aoki E, Tohyama C. Isolation and identification of metallothionein isoforms (MT-1 and MT-2) in the rat testis. *Biochem J* 1998; **334**: 695-701
- 8 **Lee KF**, Lau KM, Ho SM. Effects of cadmium on metallothionein-I and metallothionein-II mRNA expression in rat ventral, lateral, and dorsal prostatic lobes: quantification by competitive RT-PCR. *Toxicol Appl Pharmacol* 1999; **154**: 20-27
- 9 **Katakura M**, Sugawara N. Preventive effect of selenium against the testicular injury by cadmium. *Nippon Eiseigaku Zasshi* 1999; **54**: 481-489
- 10 **Cook JC**, Klinefelter GR, Hardisty JF, Sharpe RM, Foster PM. Rodent Leydig cell tumorigenesis: a review of the physiology, pathology, mechanisms, and relevance to humans. *Crit Rev Toxicol* 1999; **29**: 169-261
- 11 **McKenna IM**, Bare RM, Waalkes MP. Metallothionein gene expression in testicular interstitial cells and liver of rats treated with cadmium. *Toxicology* 1996; **107**: 121-130
- 12 **Shiraishi N**, Hochadel JF, Coogan TP, Koropatnick J, Waalkes MP. Sensitivity to cadmium-induced genotoxicity in rat testicular cells is associated with minimal expression of the metallothionein gene. *Toxicol Appl Pharmacol* 1995; **130**: 229-236
- 13 **Wang SH**, Chen JH, Lin LY. Functional integrity of metallothionein genes in testicular cell lines. *J Cell Biochem* 1994; **55**: 486-495
- 14 **Liu J**, Corton C, Dix DJ, Liu Y, Waalkes MP, Klaassen CD. Genetic background but not metallothionein phenotype dictates sensitivity to cadmium-induced testicular injury in mice. *Toxicol Appl Pharmacol* 2001; **176**: 1-9
- 15 **Valverde M**, Fortoul TI, Diaz-Barriga F, Mejia J, Castillo ER. Induction of genotoxicity by cadmium chloride inhalation in several organs of CD-1 mice. *Mutagenesis* 2000; **15**: 109-114
- 16 **Zhou T**, Zhou G., Song W, Eguchi N, Lu W, Lundin E, Jin T, Nordberg G. Cadmium-induced apoptosis and changes in expression of p53, c-jun and MT-I genes in testes and ventral prostate of rats. *Toxicology* 1999; **142**: 1-13
- 17 **Ruitenbergh EJ**, Steerenberg PA, Brosi BJM, Buys J. Reliability of the enzyme-linked immunosorbent assay (ELISA) for the serodiagnosis of *Trichinella spiralis* infections in conventionally raised pigs. *Tijdschr Diergeneesk* 1976; **101**: 57-70
- 18 **Cai L**, Deng DX, Jiang J, Chen S, Zhong R, Cherian MG, Chakrabarti S. Induction of metallothionein synthesis with preservation of testicular function in rats following long term renal transplantation. *Urol Res* 2000; **28**: 97-103
- 19 **Waalkes MP**, Rehm S, Cherian MG. Repeated cadmium exposures enhance the malignant progression of ensuing tumors in rats. *Toxicol Sci* 2000; **54**: 110-120
- 20 **Klaassen CD**, Liu J. Metallothionein transgenic and knock-out mouse models in the study of cadmium toxicity. *J Toxicol Sci* 1998; **23**: 97-102
- 21 **Eid H**, Gecci L, Magori A, Bodrogi I, Institoris E, Bak M. Drug resistance and sensitivity of germ cell testicular tumors: evaluation of clinical relevance of MDR1/Pgp, p53, and metallothionein (MT) proteins. *Anticancer Res* 1998; **18**: 3059-3064
- 22 **Satoh M**, Kaji T, Tohyama C. Low dose exposure to cadmium and its health effects. (3) Toxicity in laboratory animals and cultured cells. *Nippon Eiseigaku Zasshi* 2003; **57**: 615-623
- 23 **Shiraishi N**, Waalkes MP. Enhancement of metallothionein gene expression in male Wistar(WF/NCr) rats by treatment with calmodulin inhibitors: potential role of calcium regulatory pathways in metallothionein induction. *Toxicol Appl Pharmacol* 1994; **125**: 97-103
- 24 **Betka M**, Callard GV. Stage-dependent accumulation of cadmium and induction of metallothionein-like binding activity in the testis of the Dogfish shark, *Squalus acanthias*. *Biol Reprod* 1999; **60**: 14-22
- 25 **Cyr DG**, Dufresne J, Pillet S, Alfieri TJ, Hermo L. Expression and regulation of metallothioneins in the rat epididymis. *J Androl* 2001; **22**: 124-135
- 26 **Vasconcelos MH**, Tam SC, Beattie JH, Hesketh JE. Evidence for differences in the post-transcriptional regulation of rat metallothionein isoforms. *Biochem J* 1996; **315**: 665-671
- 27 **Dufresne J**, Cyr DG. Effects of short-term methylmercury exposure on metallothionein mRNA levels in the testis and epididymis of the rat. *J Androl* 1999; **20**: 769-778
- 28 **Radtke F**, Heuchel R, Georgiev O, Hergersberg M, Gariglio M, Dembic Z, Schaffner W. Cloned transcription factor MTF-1 activates the mouse metallothionein I promoter. *EMBO J* 1993; **12**: 1355-1362
- 29 **Saydam N**, Georgiev O, Nakano MY, Greber UF, Schaffner W. Nucleo-cytoplasmic trafficking of metal-regulatory transcription factor1 is regulated by diverse stress signals. *J Biol Chem* 2001; **276**: 25487-25495
- 30 **Min KS**, Kim H, Fujii M, Tetsuchikawahara N, Onosaka S. Glucocorticoids suppress the inflammation-mediated tolerance to acute toxicity of cadmium in mice. *Toxicol Appl Pharmacol* 2002; **178**: 1-7
- 31 **Ozawa N**, Goda N, Makino N, Yamaguchi T, Yoshimura Y, Suematsu M. Leydig cell-derived heme oxygenase-1 regulates apoptosis of premeiotic germ cells in response to stress. *J Clin Invest* 2002; **109**: 457-467
- 32 **Matsuura T**, Kawasaki Y, Miwa K, Sutou S, Ohinata Y, Yoshida F, Mitsui Y. Germ cell-specific nucleocytoplasmic shuttling protein, tesmin, responsive to heavy metal stress in mouse testes. *J Inorg Biochem* 2002; **88**: 183-191

Edited by Zhang JZ and Wang XL

Effect of compound rhodiola sachalinensis A Bor on CCl₄-induced liver fibrosis in rats and its probable molecular mechanisms

Xiao-Ling Wu, Wei-Zheng Zeng, Pi-Long Wang, Chun-Tao Lei, Ming-De Jiang, Xiao-Bin Chen, Yong Zhang, Hui Xu, Zhao Wang

Xiao-Ling Wu, Pi-Long Wang, Chun-Tao Lei, Department of Gastroenterology, First Affiliated Hospital, Chongqing University of Medical Sciences, Chongqing 400016, China

Wei-Zheng Zeng, Ming-De Jiang, Xiao-Bin Chen, Yong Zhang, Hui Xu, Zhao Wang, Department of Digestion, General Hospital of Chengdu Military Command, Chengdu 610083, Sichuan Province, China

Supported by the Tenth-Five Year Plan of Medical Science Foundation of Chengdu Military Command, No. 01A009

Correspondence to: Professor Wei-Zheng Zeng, Department of Digestion, General Hospital of Chengdu Military Command, Chengdu 610083, Sichuan Province, China. zengweizheng@163.com

Telephone: +86-28-86570347

Received: 2002-11-06 **Accepted:** 2002-12-30

Abstract

AIM: To explore the anti-fibrotic effect of a traditional Chinese medicine, compound rhodiola sachalinensis A Bor on CCl₄-induced liver fibrosis in rats and its probable molecular mechanisms.

METHODS: Ninety healthy male SD rats were randomly divided into three groups: normal group ($n=10$), treatment group of compound rhodiola sachalinensis A Bor ($n=40$) and CCl₄-induced model group ($n=40$). The liver fibrosis was induced by CCl₄ subcutaneous injection. Treatment group was administered with compound rhodiola sachalinensis A Bor (0.5 g/kg) once a day at the same time. Then the activities of several serum fibrosis-associated enzymes: alanine aminotransferase (ALT), aspartate aminotransferase (AST), N-acetyl-beta-D-glucosaminidase (β -NAG) and the levels of serum procollagen III (PCIII), collagen IV (CIV), hyaluronic acid (HA) were assayed. The histopathological changes were observed with HE, VG and Masson stain. The expression of TGF- β 1 mRNA, α 1(I) mRNA and Na⁺/Ca²⁺ exchanger (NCX) mRNA was detected by reverse transcription polymerase chain reaction (RT-PCR) *in situ*.

RESULTS: Compound rhodiola sachalinensis A Bor significantly reduced serum activities of ALT, AST, β -NAG and decreased the levels of PCIII, CIV, HA, improved the liver histopathological changes, inhibited the expression of TGF- β 1 mRNA, α 1(I) mRNA and Na⁺/Ca²⁺ exchanger mRNA in rats.

CONCLUSION: Compound rhodiola sachalinensis A Bor can intervene in CCl₄-induced liver fibrosis in rats, in which potential mechanisms may be decreasing the production of TGF- β 1, reducing the production of collagen, preventing the activation of hepatic stellate cell (HSC) and inhibiting the expression of TGF- β 1 mRNA, α 1(I) mRNA and Na⁺/Ca²⁺ exchanger mRNA.

Wu XL, Zeng WZ, Wang PL, Lei CT, Jiang MD, Chen XB, Zhang Y, Xu H, Wang Z. Effect of compound rhodiola sachalinensis A Bor on CCl₄-induced liver fibrosis in rats and its probable molecular mechanisms. *World J Gastroenterol* 2003; 9(7): 1559-1562
<http://www.wjgnet.com/1007-9327/9/1559.asp>

INTRODUCTION

Transforming growth factor beta 1 (TGF- β 1) is the most potent profibrogenic mediator in liver fibrosis and cirrhosis as shown in animal models and human chronic hepatic injury^[1-4]. It plays critical roles in the activation of hepatic stellate cell (HSC) and the regulation of the production, degradation, and accumulation of extracellular matrix (ECM) proteins^[5-7]. Recent studies have identified that TGF-beta 1 mRNA transcription is significantly increased during chronic liver injury. Thus the TGF-beta signal transduction pathway has become a new effective target for the prevention or treatment of liver fibrosis^[8-11]. Several traditional Chinese herbs have been shown to have the ability of intervention in liver fibrosis^[12-20], however, most of them were limited in morphological and serum studies, lacking of deep research in their molecular biological mechanisms. Our previous study has shown another Chinese medicine, compound rhodiola sachalinensis A Bor, can effectively prevent CCl₄-induced liver fibrosis in rats^[21-23]. In this study, the probable biological mechanism of it, especially in the expression of TGF-beta 1 mRNA, α 1(I) mRNA and Na⁺/Ca²⁺ exchanger mRNA was explored.

MATERIALS AND METHODS

Animals

Male SD rats (weighing 140-160 g) were obtained from the Experimental Animal Center of Sichuan University (Chengdu, Sichuan Province, China). The rats were housed in a room with controlled temperature (15-20 °C) and lighting (10 h light, 14 h dark). Free access to water and food was allowed during the experimental period. All the rats were randomly divided into three groups: normal group ($n=10$), treatment group ($n=40$) and model group ($n=40$). For model group, 300 mL/L CCl₄ in liquid paraffin was injected subcutaneously at a dose of 3 mL/kg twice weekly. The treatment group, apart from the administration of CCl₄, was fed with compound rhodiola sachalinensis A Bor 0.5 g/kg once per day. The model group was given normal food and water, received injection of liquid paraffin with the same dosage and duration as CCl₄.

At the end of the 15-week experimental period, all the rats were anesthetized with intramuscular injection of sodium pentobarbital (30 mg/kg) before sacrificed. Blood was collected from the heart and the serum obtained through centrifugation. The liver was removed rapidly, part of it was conserved in 100 mL/L neutral formalin, and the rest was frozen in a refrigerator at -20 °C.

Serum parameters of hepatic fibrosis

Parameters of hepatic fibrosis were determined by levels of type III procollagen (PCIII), type IV collagen (CIV) and hyaluronic acid (HA), using radioimmunoassay (commercial kit obtained from Shanghai Navy Medical Institute, China). Serum activities of alanine aminotransferase (ALT) and aspartate aminotransferase (AST) were assayed by a automatic analyzer. Another serum enzyme N-acetyl-beta-D-glucosaminidase (β -NAG) was assayed with spectrophotometric method.

Table 1 Primer sequences of $\alpha 1(I)$, TGF- $\beta 1$ and Na⁺/Ca²⁺ exchanger mRNA

mRNA	Upstream (5' → 3')	Downstream (5' → 3')
$\alpha 1(I)$	CAC CCT CAA GAG CCT GAG TC	GTT CGG GCT GAT GTA CCA GT
TGF- $\beta 1$	CTT TGT ACA ACA GCA CCC GC	GTC AAA AGA CAG CCA CTC AGG
NCX	TAT TGC CGA ACC GGT TTA TGT	CTC GTC TCT CCA TCT GGG AC

Table 2 Liver fibrosis-associated enzymes and fibrosis markers in serum ($\bar{x} \pm s$)

Group	ALT (IU/L)	AST (IU/L)	β -NAG (μ mol/L)	PCIII (μ g/L)	CIV (μ g/L)	HA (μ g/L)
Normal	87.93 \pm 18.61 ^a	104.3 \pm 32.40 ^a	189.00 \pm 26.70 ^a	89.99 \pm 10.85 ^a	35.69 \pm 9.68 ^a	112.41 \pm 45.62 ^a
Model	198.64 \pm 71.02	514.59 \pm 180.22	415.77 \pm 133.37	265.54 \pm 98.21	159.67 \pm 29.64	455.79 \pm 113.55
Treatment	114.17 \pm 47.89 ^a	291.62 \pm 141.75 ^a	244.67 \pm 46.8 ^a	164.25 \pm 45.68 ^a	96.73 \pm 16.48 ^a	289.35 \pm 75.68 ^a

^a $P < 0.01$ vs model group.

Histopathological grading

Liver samples from each rat were embedded in paraffin, stained with hematoxylin-eosin (HE), Van Gieson (VG) and Masson trichrome collagen stain, and then examined under an optical microscope. Fibrosis-degree of liver sections was graded numerically based on the criteria described below: 0, no fibrosis; +, slight fibrosis, fibrosis located in the central liver lobule; +2, moderate fibrosis, widen central fibrosis; +3, severe fibrosis, fibrosis extended to the edge of liver lobule; +4, liver cirrhosis.

Molecular biological detection: RT-PCR in situ

Each liver sample embedded in paraffin was sectioned and fixed onto a poly-L-lysine covered glass. The expression of $\alpha 1(I)$ mRNA, TGF- $\beta 1$ mRNA and Na⁺/Ca²⁺ exchanger (NCX) mRNA was detected with RT-PCR *in situ*. (primers obtained from Shanghai Sangon Biotechnology Co. Ltd.) (Table 1).

Statistical analysis

Data were analyzed using *t*-test and Microsoft Excel 2000.

RESULTS

Changes of serum fibrosis-associated markers

In model group, the serum activities of ALT, AST and β -NAG were significantly increased ($P < 0.01$), the serum levels of PCIII, CIV and HA were also elevated ($P < 0.01$). With administration of compound *Rhodiola Sachalinensis* A Bor (RSC), serum activities of ALT, AST, β -NAG and levels of PCIII, CIV, HA were decreased obviously ($P < 0.01$), although they were still higher than those in normal group ($P < 0.05$) (Table 2).

Histopathological changes of the liver

The control livers showed a normal lobular architecture with central veins and radiating hepatic cords. The staging score was 0. Subcutaneous injection of CCl₄ caused severe liver pathological damages such as: inflammation, necrosis and excessive collagen deposition. The semiquantitative staging score of hepatic fibrosis was raised to 3.53 \pm 0.68 in model group. The livers in treatment group showed less inflammation, necrosis, collagen deposition and a significantly decreased staging score of 2.43 \pm 0.47 ($P < 0.05$) (Table 3, Figures 1, 2).

Molecular biological changes

Scoring method: according to the number of positive cells within one visual field on average. (-), no positive cells, scoring 0; (+), positive cells $< 1/3$, scoring 1; (++) , positive cells $< 2/3$, scoring 2; (+++) , positive cells $> 2/3$, scoring 3. There were less positive signals of $\alpha 1(I)$ mRNA, TGF- $\beta 1$ mRNA and Na⁺/Ca²⁺ exchanger mRNA detected with RT-PCR *in situ* in normal

group, in which scores were 1.11, 0.75, 0.10 and the ratio of positive samples was 77.8 %, 62.5 %, 10.0 % respectively (Tables 4-6). In model group, the positive signals of RT-PCR *in situ* for $\alpha 1(I)$ mRNA, TGF- $\beta 1$ mRNA and Na⁺/Ca²⁺ exchanger mRNA were significantly enhanced. The semiquantitative scores of them were increased to 2.80, 2.40, 2.30 and the ratio of positive samples rised to 100.0 %, 90.0 %, 100.0 % respectively ($P < 0.01$). Treatment with RSC made the scores reduced to 1.63, 1.20, 1.50, and positive ratio lowered to 87.5 %, 80.0 %, 80.0 % respectively in comparison with model group ($P < 0.05$) (Tables 4-6, Figures 3-6).

Table 3 Histopathological semiquantitative scores in the liver

Group	<i>n</i>	0	+1	+2	+3	+4	Staging scores
Normal	10	10	0	0	0	0	0 ^a
Model	30	0	0	3	8	19	3.53 \pm 0.68
Treatment	35	0	2	18	13	2	2.43 \pm 0.47 ^b

^a $P < 0.01$, ^b $P < 0.05$ vs model group.

Table 4 Expression of $\alpha 1(I)$ mRNA (semiquantitative scores and positive ratio)

Group	<i>n</i>	-	+	++	+++	Scores	Positive ratio (%)
Normal	9	2	4	3	0	1.11 ^a	77.8 ^b
Model	10	0	0	2	8	2.80	100.0
Treatment	8	1	2	4	1	1.63 ^b	87.5 ^b

^a $P < 0.01$, ^b $P < 0.05$ vs model group.

Table 5 Expression of TGF- $\beta 1$ mRNA (semiquantitative scores and positive ratio)

Group	<i>n</i>	-	+	++	+++	Scores	Positive ratio (%)
Normal	8	3	4	1	0	0.75 ^a	62.5 ^a
Model	10	1	1	1	7	2.40	90.0
Treatment	10	2	5	2	1	1.20 ^b	80.0 ^b

^a $P < 0.01$, ^b $P < 0.05$ vs model group.

Table 6 Expression of Na⁺/Ca²⁺ exchanger mRNA (semiquantitative scores and positive ratio)

Group	<i>n</i>	-	+	++	+++	Scores	Positive ratio (%)
Normal	10	9	1	0	0	0.10 ^a	10.0 ^a
Model	10	0	2	3	5	2.30	100.0
Treatment	10	2	3	3	2	1.50 ^b	80.0 ^b

^a $P < 0.01$, ^b $P < 0.05$ vs model group.

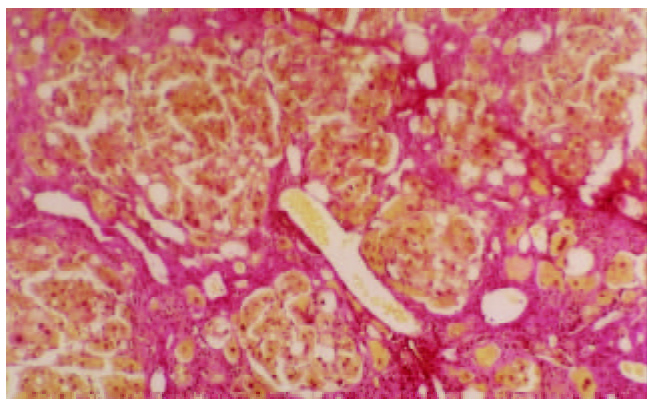


Figure 1 Liver VG staining in model rats (10×40).

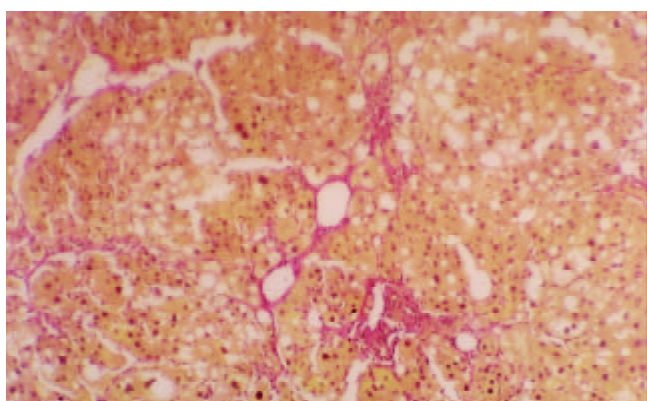


Figure 2 Liver VG staining in treatment rats (10×40).

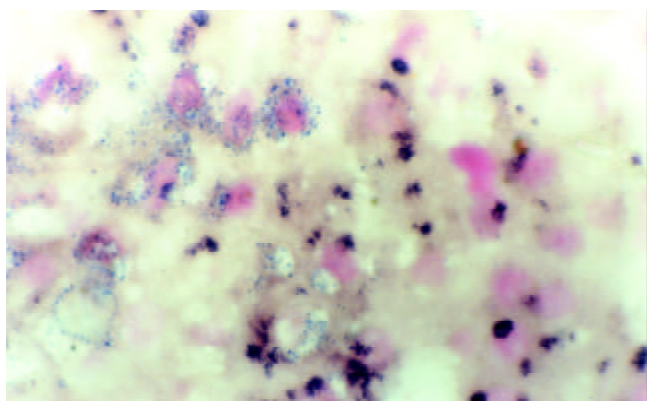


Figure 3 Expression of TGF-β1 mRNA in liver of model rats (10×40).

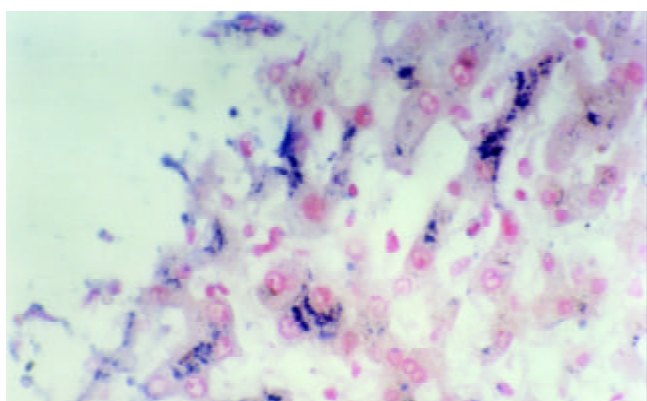


Figure 4 Expression of TGF-β1 mRNA in liver of treatment rats (10×40).

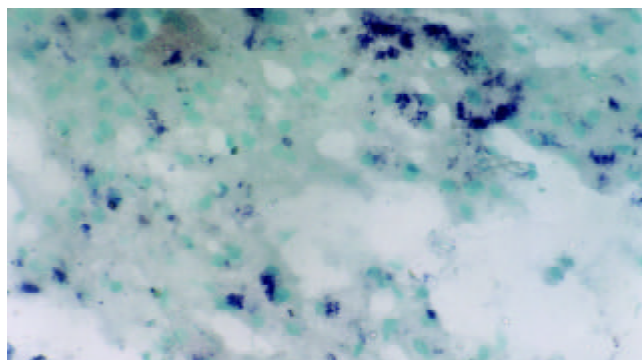


Figure 5 Expression of NCX mRNA in liver of model rats (10×40).

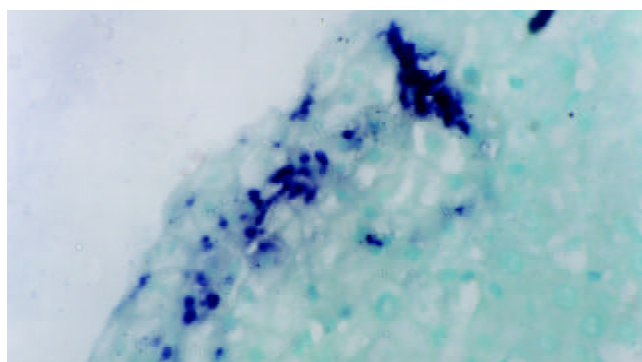


Figure 6 Expression of NCX mRNA in liver of treatment rats (10×40).

DISCUSSION

Liver fibrosis is generally preceded by chronic liver injury despite of its primary causes, including alcohol, hepatic virus, oxidant stress and other persistent damages. The activation of hepatic stellate cells (HSC) is considered to be of great importance during the long period of liver fibrosis, which is induced by some critical cytokines and then becomes the main source of most collagen proteins^[24]. Among the cytokine mediating factors, transforming growth factor beta 1 (TGF-β1) has been considered as the essential profibrogenesis factor and the main target of treatment^[25-31]. Additionally, Na⁺/Ca²⁺ exchanger was a newly noticed factor whose expression increased along with the activation of HSC, and its real role in liver fibrosis has not been interpreted^[32]. Thus, detection of the expression of TGF-β1 and Na⁺/Ca²⁺ exchanger mRNA is useful in exploring the probable mechanisms of anti-fibrotic drugs.

Several drugs, including cytokines, antioxidant, chemical drugs, soluble type II receptor of TGF-β1^[9,33], antibody of TGF-β1 have been used to block liver fibrosis. But their effects are not as prosperous as we expected^[1]. Besides, some traditional Chinese drugs have been found to be effective on preventing fibrogenesis and other chronic liver injury, which develop a more hopeful future in controlling liver fibrosis and cirrhosis. The present study aimed at exploring the effects of a traditional Chinese herb, compound rhodiola sachalinensis A Bor, which consists of rhodiola sachalinensis A Bor, sophora flavescens Ait and other herbs, on the prevention of CCl₄ induced liver fibrosis in rats. The potential mechanisms of RSC was explained at the same time.

In this study, chronic administration of CCl₄ caused liver fibrosis and cirrhosis as indicated by the changes of serum markers, histopathological changes, and molecular biological changes. The activities of serum fibrosis-associated enzymes, namely ALT, AST, β-NAG and contents of extracellular matrix (ECM) components (PCIII, CIV, HA) were significantly

increased along with increased expression of $\alpha 1(I)$ mRNA, TGF- $\beta 1$ mRNA and Na^+/Ca^{2+} exchanger mRNA. Under the light microscope, the liver fibrosis/cirrhosis was verified by the typical liver structure: inflammation, necrosis and excessive collagen deposition, some of the samples even had pseudolobules. With the therapy of compound rhodiola sachalinensis A Bor, serum parameters of liver fibrosis (ALT, AST, β -NAG, PCIII, CIV, HA) were significantly decreased ($P < 0.01$). HE, VG and Masson stained histopathological sections showed mild inflammation, necrosis and fewer collagen deposition. The semiquantitative fibrosis staging scores were also decreased obviously ($P < 0.01$). The expression of $\alpha 1(I)$ mRNA, TGF- $\beta 1$ mRNA and Na^+/Ca^{2+} exchanger mRNA was significantly inhibited using RT-PCR *in situ* ($P < 0.01$). These results suggest that compound rhodiola sachalinensis A Bor may prevent experimental liver fibrosis by modulating the synthesis and releasing of critical cytokines, such as TGF- $\beta 1$, thus inhibiting the activation of HSC and its production of collagen proteins. The inhibition of Na^+/Ca^{2+} exchanger mRNA may partly relate to its anti-fibrotic effects. In conclusion, traditional Chinese medicine compound rhodiola sachalinensis A Bor has significant anti-fibrogenesis effects on CCl_4 -induced liver fibrosis in rats. The probable molecular mechanisms may include blocking the synthesis of TGF- $\beta 1$, interfering with the activation of HSC, preventing production and deposition of collagen, and inhibiting the expression of Na^+/Ca^{2+} exchanger mRNA. The exact molecular mechanisms remain to be explored.

REFERENCES

- Bissell DM, Roulot D, George J. Transforming growth factor β and the liver. *Hepatology* 2001; **34**: 859-867
- Liu F, Liu JX. The role of transforming growth factor b1 in liver fibrosis. *Shijie Huaren Xiaohua Zazhi* 2000; **8**: 86-88
- Schuppan D, Porov Y. Hepatic fibrosis: From bench to bedside. *J Gastroenterol Hepatol* 2002; **7**(Suppl 3): S300-S305
- Cui DL, Yao XX. The serum detection of liver fibrosis. *Shijie Huaren Xiaohua Zazhi* 2000; **8**: 683-684
- Qin JP, Jiang MD. The phenotype and regulation of hepatic stellate cell and liver fibrosis. *Shijie Huaren Xiaohua Zazhi* 2001; **9**: 801-804
- Wu JX, Meng XJ, Chen YW, Li DG, Lu HM. Message molecular of Smads and the activation of hepatic stellate cells. *Weichangbingxue He Ganbingxue Zazhi* 2002; **11**: 197-199
- Shi YJ, Tian ZB, Zhao QX. The current research of Smads protein family. *Zhonghua Fubu Jibing Zazhi* 2002; **2**: 497-500
- Li D, Friedman SL. Liver fibrogenesis and the role of hepatic stellate cells: New insights and prospects for therapy. *J Gastroenterol Hepatol* 1999; **14**: 618-633
- George J, Roulot D, Kotelninsky VE, Bissell DM. *In vivo* inhibition of rat stellate cell activation by soluble transforming growth factor β type II receptor: A potential new therapy for hepatic fibrosis. *Proc Natl Acad Sci USA* 1999; **96**: 12719-12724
- Yoshiji H, Kuriyama S, Yoshii J, Ikenaka Y, Noguchi R, Nakatani T, Tsujinoue H, Fukui H. Angiotensin-II type 1 receptor interaction is a major regulator for liver fibrosis development in rats. *Hepatology* 2001; **34**(4Pt 1): 745-750
- Jiang SL, Yao XX, Sun YF. The treatment of liver fibrosis. *Shijie Huaren Xiaohua Zazhi* 2000; **8**: 684-686
- Sun YF, Yao XX, Jiang SL. The traditional Chinese medicine treatment of liver fibrosis. *Shijie Huaren Xiaohua Zazhi* 2000; **8**: 686-687
- Du WD, Zhang YE, Zhai WR, Zhou XM. Dynamic changes of type I, III and IV collagen synthesis and distribution of collagen-producing cells in carbon tetrachloride-induced rat liver fibrosis. *World J Gastroenterol* 1999; **5**: 397-403
- Liu P, Liu C, Xu LM, Xue HM, Liu CH, Zhang ZQ. Effects of Fuzheng Huayu 319 recipe on liver fibrosis in chronic hepatitis B. *World J Gastroenterol* 1998; **4**: 348-353
- Liu CH, Hu YY, Wang XL, Liu P, Xu LM. Effects of salvianolic acid-A on NIH/3T3 fibroblast proliferation, collagen synthesis and gene expression. *World J Gastroenterol* 2000; **6**: 361-364
- Cai DY, Zhao G, Chen JC, Ye GM, Bing FH, Fan BW. Therapeutic effect of Zijin capsule in liver fibrosis in rats. *World J Gastroenterol* 1998; **4**: 260-263
- Shimizu I. Sho-saiko-to: Japanese herbal medicine for protection against hepatic fibrosis and carcinoma. *J Gastroenterol Hepatol* 2000; **15**(Suppl): d84-90
- Yang W, Zeng M, Fan Z, Mao Y, Song Y, Jia Y, Lu L, Chen CW, Peng YS, Zhu HY. Prophylactic and therapeutic effect of oxymatrine on D-galactosamine-induced rat liver fibrosis. *Zhonghua Ganzangbing Zazhi* 2002; **10**: 193-196
- Li CX, Li L, Lou J, Yang XW, Lei TW, Li YH, Liu J, Cheng ML, Huang LH. The protective effects of traditional Chinese medicine prescription, Han-Dan-Gan-Le, on CCl_4 -induced liver fibrosis in rats. *Am J Chin Med* 1998; **16**: 325-332
- Liu P, Hu YY, Liu C, Zhu DY, Xue HM, Xu ZQ, Xu LM, Liu CH, Gu HT, Zhang ZQ. Clinical observation of salvianolic acid B in treatment of liver fibrosis in chronic hepatitis B. *World J Gastroenterol* 2002; **8**: 679-685
- Zeng WZ, Wu XL, Jiang MD, Chen XB, Xu H, Wang Z, Xiong BJ. The effect of rhodiola sachalinensis compound on the expression of TGF- $\beta 1$ mRNA in rats of CCl_4 -induced liver fibrosis. *Zhongguo Zhongxiyi Jiehe Xiaohua Zazhi* 2002; **10**: 138-141
- Jiang MD, Gan XY, Xie FW, Zeng WZ, Wu XL. Effect of salidroside on the proliferation and collagen mRNA transcription in rat hepatic stellate cells stimulated by acetaldehyde. *Yaoxue Xuebao* 2002; **37**: 841-844
- Wu XL, Zene WZ, Chen XB, Jiang MD, Xiong BJ, Zhang Y, Xu H. The effects of rhodiola sachalinensis A Bor on the activities of fibrosis-associated enzymes in serum and tissue in rats of CCl_4 -induced liver fibrosis. *Huaxi Yaoxue Zazhi* 2002; **17**: 416-418
- Schuppan D, Koda M, Bauer M, Hahn EG. Fibrosis of liver, pancreas and intestine: common mechanisms and clear targets? *Acta Gastroenterol Belg* 2000; **63**: 366-370
- Gressner AM, Weiskirchen R, Breitkopf K, Dooley S. Roles of TGF-beta in hepatic fibrosis. *Front Biosci* 2002; **7**: d793-807
- Neuman MG, Benhamou JP, Bourliere M, Ibrahim A, Malkiewicz I, Asselah T, Martinot-Peignoux M, Shear NH, Katz GG, Akremi R, Benali S, Boyer N, Lecomte L, Le Breton V, Le Guludec G, Marcellin P. Serum tumour necrosis factor-alpha and transforming growth factor-beta levels in chronic hepatitis C patients are immunomodulated by therapy. *Cytokine* 2002; **17**: 108-117
- Bissell DM. Chronic liver injury, TGF-beta, and cancer. *Exp Mol Med* 2001; **33**: 179-190
- Kanzler S, Baumann M, Schirmacher P, Dries V, Bayer E, Gerken G, Dienes HP, Lohse AW. Prediction of progressive liver fibrosis in hepatitis C infection by serum and tissue levels of transforming growth factor-beta. *J Viral Hepat* 2001; **8**: 430-437
- Paizis G, Gilbert RE, Cooper ME, Murthi P, Schembri JM, Wu LL, Rumble JR, Kelly DJ, Tikellis C, Cox A, Smallwood RA, Angus PW. Effect of angiotensin II type 1 receptor blockade on experimental hepatic fibrogenesis. *J Hepatol* 2001; **35**: 376-385
- Deng L, Zhou Y, Peng X, Deng H, Deng Y, Yao J. Serum markers and pathological evaluation in hepatitis fibrosis of chronic hepatitis B treated with interferon alpha. *Zhonghua Ganzangbing Zazhi* 2001; **9**: 66-67
- Jiang W, Wang J, Yang C, Wang Y, Liu W, He B. Effects of antisense transforming growth factor beta receptor-I expressing plasmid on pig serum-induced rat liver fibrosis. *Zhonghua Yixue Zazhi* 2002; **82**: 1160-1164
- Toshio N, Shigeki A, Kazunobu M, Masaharu F, Yoshihisa T, Masayuki I, Makoto T, Yasunobu O. Expression of the Na^+/Ca^{2+} exchanger emerges in hepatic stellate cells after activation in association with liver fibrosis. *Physiology* 1998; **95**: 5389-5394
- Ueno H, Sakamoto T, Nakamura T, Qi Z, Astuchi N, Takeshita A, Shimizu K, Ohashi H. A soluble transforming growth factor beta receptor expressed in muscle prevents liver fibrogenesis and dysfunction in rats. *Hum Gene Ther* 2000; **11**: 33-42

Effect of tetramethylpyrazine on P-selectin and hepatic/renal ischemia and reperfusion injury in rats

Jin-Lian Chen, Tong Zhou, Wei-Xiong Chen, Jin-Shui Zhu, Ni-Wei Chen, Ming-Jun Zhang, Yun-Lin Wu

Jin-Lian Chen, Wei-Xiong Chen, Jin-Shui Zhu, Ni-Wei Chen, Department of Gastroenterology, Shanghai Sixth People's Hospital, Shanghai Jiao-Tong University, Shanghai 200233, China

Tong Zhou, Department of Nephrology, Ruijin Hospital, Shanghai Second Medical University, Shanghai 200025, China

Ming-Jun Zhang, Animal Laboratory, Ruijin Hospital, Shanghai Second Medical University, Shanghai 200025, China

Yun-Lin Wu, Department of Gastroenterology, Ruijin Hospital, Shanghai Second Medical University, Shanghai 200025, China

Supported by the National Natural Science Foundation of China (No. 39970340) and the Scientific Foundation of Ministry of Public Health

Correspondence to: Jin-Lian Chen, Department of Gastroenterology, Shanghai Sixth People's Hospital, Shanghai Jiao-Tong University, Shanghai 200233, China. cqinqin@fm365.com

Telephone: +86-21-64369181

Received: 2002-12-30 **Accepted:** 2003-02-19

Abstract

AIM: To investigate the effect of tetramethylpyrazine on hepatic/renal ischemia and reperfusion injury in rats.

METHODS: Hepatic/renal function, histopathological changes, and hepatic/renal P-selectin expression were studied with biochemical measurement and immunohistochemistry in hepatic/renal ischemia and reperfusion injury in rat models.

RESULTS: Hepatic/renal insufficiency and histopathological damage were much less in the tetramethylpyrazine-treated group than those in the saline-treated groups. Hepatic/renal P-selectin expression was down regulated in the tetramethylpyrazine-treated group.

CONCLUSION: P-selectin might mediate neutrophil infiltration and contribute to hepatic/renal ischemia and reperfusion injury. Tetramethylpyrazine might prevent hepatic/renal damage induced by ischemia and reperfusion injury through inhibition of P-selectin.

Chen JL, Zhou T, Chen WX, Zhu JS, Chen NW, Zhang MJ, Wu YL. Effect of tetramethylpyrazine on P-selectin and hepatic/renal ischemia and reperfusion injury in rats. *World J Gastroenterol* 2003; 9(7): 1563-1566

<http://www.wjgnet.com/1007-9327/9/1563.htm>

INTRODUCTION

Hepatic/renal ischemia-reperfusion injury is common clinically. Up to now, there has been no effective treatment for this pathological injury. Cell adhesion molecules have been found to play an important role in hepatic/renal ischemia-reperfusion injury by mediating interactions of polymorphonuclear neutrophils with endothelium. P-selectin monoclonal antibody has been demonstrated to prevent effectively reperfusion-induced hepatic/renal tissue damage^[1-23]. Tetramethylpyrazine (TMP), a traditional Chinese herb, has been widely used especially in the treatment of patients with cerebral and cardiac ischemic diseases in China. Experimental study has found that

TMP could protect vascular endothelial cells, and inhibit respiratory explosion and free radicals of polymorphonuclear neutrophils^[24-28]. In the present study, we investigated the effect of TMP and P-selectin on hepatic ischemia and reperfusion injury in rats.

MATERIALS AND METHODS

Animal model

Ninety male Wistar rats (Shanghai Experimental Animal Center of Chinese Academy of Sciences), weighing 200±10 g, were given free access to food and water for three days before the experiments. The rats were anesthetized with 2.5 % sodium pentobarbital intraperitoneally, and randomly divided into 2 groups. In one group of rats, the ligament linking liver, diaphragm and abdominal wall were separated, the portal vein and liver artery that drain blood to left hepatic lobe were freed by blunt dissection and then blocked with a microvascular clamp for 60 minutes, then the clamp was removed, and reperfusion was performed. While in the other group, the left renal artery was freed, and blocked with a microvascular clamp for 60 minutes, then the clamp was removed and reperfusion was performed, simultaneously, the right kidney was cut off. The two groups of rats were randomly divided into TMP-treated group ($n=20$) and non-treated group ($n=20$). They were divided into subgroups according to the indicated time 1,3,6,24 hours after reperfusion. TMP or saline was intravenously injected five minutes before the reperfusion. A sham-operated group ($n=5$, anesthesia and opening celiac cavity, no blocking of hepatic or renal blood flow) served as control.

Collection and measurement methods of specimens

Blood and hepatic and renal tissues were harvested at the indicated time. Serum levels of aspartate aminotransferase (AST) and alanine aminotransferase (ALT), and blood urea nitrogen (BUN) and creatinine (Cr) were measured with a 747 automatic analyzer (Hitachi Boehringer Mannheim, Mannheim, Germany). Hepatic and renal tissue samples were fixed in 10 % formalin and embedded in paraffin. 5 μ m thick sections were cut into and stained with hematoxylin and eosin for light microscope examination. Expression of P-selectin in hepatic/renal tissue was detected by immunohistochemistry method with a labeled streptavidin biotin (LSAB) kit (Fujian Maixin Biotechnology Co., products of Biotechnology Co. CA, USA).

Statistical analysis

Data were presented as $\bar{x}\pm s$, and Student's t test was used to determine changes between different groups. $P<0.05$ was considered significant.

RESULTS

Histopathologic evaluation

One hour after reperfusion, visual observation revealed that the left hepatic lobe was more swollen than the right lobe, and was dark in color. Under the light microscope, interstitial congestion and infiltration of inflammatory cells were

observed. One hour after reperfusion, the renal cortex was macroscopically pale, the renal medulla displayed blood stagnation and was dark in color. Under the light microscope, edema, denaturation with different extent and necrosis of renal tubular epithelial cells were observed. Simultaneously, interstitial congestion, edema and infiltration of inflammatory cells were also observed. However, in the TMP-treated group, the outward appearance of the liver and kidney was similar to that of normal. Hepatic cells and tubular cells showed less swelling and no denaturation or necrosis, and interstitial changes were not obvious.

Hepatic and renal function evaluation

Twenty four hours after hepatic reperfusion, the serum levels of ALT (628 ± 91 u/L) and AST ($1\ 608 \pm 199$ u/L) in the saline-treated group were much higher than those in the sham-operated group (52 ± 11 u/L and 80 ± 17 u/L respectively, $P < 0.01$). The TMP-treated group revealed significantly lower levels of ALT (190 ± 21 u/L) and AST (386 ± 62 u/L) than those in the saline-treated group ($P < 0.01$).

Twenty four hours after renal reperfusion, the serum levels of BUN (14.54 ± 0.67 mmol/L) and Cr (102.2 ± 4.67 μ mol/L) were much higher in the TMP-treated group than those in the sham-operated group (7.88 ± 0.57 mmol/L and 39.00 ± 4.47 μ mol/L, respectively, $P < 0.01$). The TMP-treated group presented with significantly lower levels of BUN (11.21 ± 0.56 mmol/L) and Cr (70.61 ± 4.95 μ mol/L) than those in the saline-treated group ($P < 0.01$).

P-selectin expression in hepatic and renal tissues

P-selectin was expressed widely within hepatic and renal tissues 1 hour after reperfusion, which was mainly distributed on small vessels of left hepatic lobe and kidney. In addition, it was also expressed on part of hepatic cellular membrane, glomerulomesangium, capillary loops, and interstitium. After treatment with TMP, there were no obvious yellow-brown positive granules in the hepatic and renal tissues, suggesting that P-selectin expression was not displayed.

DISCUSSION

Recently, the role of cell adhesion molecules and neutrophils in ischemia and reperfusion injury has aroused attention^[29-50]. Ischemia reperfusion liver injury is characterized by microvascular leukocyte accumulation and massive infiltration of postischemic tissues. Primary leukocyte endothelial cell interaction (rolling) is mediated by selectins, whereas firm adherence and transendothelial migration involve immunoglobulin superfamily (intercellular adhesion molecule-1, ICAM-1) with leukocyte β_2 -integrins (CD11/CD18)^[51]. As a potential member of the selectin family, P-selectin has been found in both Weibel-Palade body of epithelial cells of middle and small blood vessels and α -granule of platelets. It is expressed rapidly on the surface of these cells in seconds after their activation. Furthermore, P-selectin can be up-regulated by *de novo* synthesis in the ischemia-reperfusion injury in hours. P-selectin plays an important role in inflammation by initiating neutrophil rolling, adhesion and recruitment to injured tissue^[15]. Blockade of P-selectin expression or interaction with its ligands can attenuate leukocyte adherence and infiltration during ischemia and reperfusion injury. And P-selectin monoclonal antibody has been found to have protective effects on the injury^[21].

Tetramethylpyrazine (TMP) is an active ingredient of Ligustium Wallich Franch. It has been shown in animal models and clinical investigations that TMP is effective on ischemic diseases such as heart, brain and lung. TMP could block the calcium channel, reduce the bioactivity of platelets and platelet

aggregation, and inhibit free radicals, and has inhibitory roles in platelets and arterial thrombus formation in dogs^[52]. However, the roles and mechanisms of TMP in treatment of digestive diseases have not been extensively studied.

The effect of TMP on ischemia and reperfusion injury was observed in this study based on the established rat model of hepatic/renal ischemia-reperfusion.

Hepatic and renal tissues displayed significantly histopathologic damages after hepatic/renal ischemia-reperfusion while the serum levels of ALT and AST as well as BUN and Cr were increased. It was showed that hepatic/renal injury induced by ischemia-reperfusion was remarkably attenuated when TMP was given 5 minutes before reperfusion as shown by improved hepatic/renal function and less pathologic damage. The results suggest that TMP has a protective effect on hepatic/renal reperfusion injury by inhibiting the interaction of neutrophils and endothelium.

After ischemia and reperfusion, P-selectin expression was up-regulated in hepatic and renal tissues, suggesting that P-selectin is related to hepatic/renal reperfusion injury. It was found that leukocyte rolling and recruitment were delayed when deficient mice are infected, suggesting that P-selectin is involved in the early events of inflammation mediated by leukocytes^[53]. Results from this study showed that P-selectin expression in hepatic and renal tissues was inhibited in TMP-treated group. This is consistent with down-regulated expression of sialyl Lewis X, a ligand for P-selectin located mainly in neutrophils, as with anti-P-selectin therapy (unpublished data). These suggest that P-selectin might mediate neutrophil infiltration within the liver and kidney in the early stage of hepatic/renal reperfusion injury. Furthermore, blockade of P-selectin can attenuate inflammatory cell infiltration and pathological damage. Wu found that TMP could reduce significantly the number of α -granule membrane protein (GMP140) of platelets and had inhibitory effects on platelets and arterial thrombus formation in dogs. TMP can play a protective role in hepatic and renal injury caused by ischemia-reperfusion by inhibiting the adhesion and activation of neutrophils mediated by P-selectin.

In an animal model of thioacetamide (TAA) induced acute hepatotoxicity, increase of serum SGOT and SGPT produced by TAA was decreased by TMP, and increase of malondialdehyde (MDA) produced by TAA was also prevented by *in vitro* addition of TMP to liver homogenates. A rise of serum interleukin-2 was similarly prevented. The results suggest that part of hepatocellular injury induced by TAA is mediated by oxidative stress caused by the action of cytokines through lipid peroxidation, TMP may act by preventing lipid peroxidation^[54]. Another study showed that the hepatoprotective effect of TMP might be in part due to its inhibitory ability on membrane lipid peroxidation and free radical formation and its free radical scavenging ability^[55]. Therefore, TMP might be effective on the treatment of on reperfusion injury.

REFERENCES

- 1 **Funaki H**, Shimizu K, Harada S, Tsuyama H, Fushida S, Tani T, Miwa K. Essential role for nuclear factor kappaB in ischemic preconditioning for ischemia-reperfusion injury of the mouse liver. *Transplantation* 2002; **74**: 551-556
- 2 **Khandoga A**, Biberthaler P, Enders G, Axmann S, Hutter J, Messmer K, Krombach F. Platelet adhesion mediated by fibrinogen-intercellular adhesion molecule-1 binding induces tissue injury in the postischemic liver *in vivo*. *Transplantation* 2002; **74**: 681-688
- 3 **Satoh S**, Suzuki A, Asari Y, Sato M, Kojima N, Sato T, Tsuchiya N, Sato K, Senoo H, Kato T. Glomerular endothelium exhibits enhanced expression of costimulatory adhesion molecules, CD80 and CD86, by warm ischemia/reperfusion injury in rats. *Lab In-*

- vest 2002; **82**: 1209-1217
- 4 **de Rossi LW**, Horn NA, Buhre W, Gass F, Hutschenreuter G, Rossaint R. The effect of isoflurane on neutrophil selectin and beta(2)-integrin activation *in vitro*. *Anesth Analg* 2002; **95**: 583-587
 - 5 **Burne MJ**, Rabb H. Pathophysiological contributions of fucosyltransferases in renal ischemia reperfusion injury. *J Immunol* 2002; **169**: 2648-2652
 - 6 **Faure JP**, Hauet T, Han Z, Goujon JM, Petit I, Mauco G, Eugene M, Carretier M, Papadopoulos V. Polyethylene glycol reduces early and long-term cold ischemia-reperfusion and renal medulla injury. *J Pharmacol Exp Ther* 2002; **302**: 861-870
 - 7 **Khandoga A**, Enders G, Biberthaler P, Krombach F. Poly(ADP-ribose) polymerase triggers the microvascular mechanisms of hepatic ischemia-reperfusion injury. *Am J Physiol Gastrointest Liver Physiol* 2002; **283**: G553-560
 - 8 **Horie Y**, Yamagishi Y, Kato S, Kajihara M, Tamai H, Granger DN, Ishii H. Role of ICAM-1 in chronic ethanol consumption-enhanced liver injury after gut ischemia-reperfusion in rats. *Am J Physiol Gastrointest Liver Physiol* 2002; **283**: G537-543
 - 9 **Olanders K**, Sun Z, Borjesson A, Dib M, Andersson E, Lasson A, Ohlsson T, Andersson R. The effect of intestinal ischemia and reperfusion injury on ICAM-1 expression, endothelial barrier function, neutrophil tissue influx, and protease inhibitor levels in rats. *Shock* 2002; **18**: 86-92
 - 10 **Kubes P**, Payne D, Woodman RC. Molecular mechanisms of leukocyte recruitment in postischemic liver microcirculation. *Am J Physiol Gastrointest Liver Physiol* 2002; **283**: G139-147
 - 11 **Leonard MO**, Hannan K, Burne MJ, Lappin DW, Doran P, Coleman P, Stenson C, Taylor CT, Daniels F, Godson C, Petasis NA, Rabb H, Brady HR. 15-Epi-16-(para-fluorophenoxy)-lipoxin A(4)-methyl ester, a synthetic analogue of 15-epi-lipoxin A(4), is protective in experimental ischemic acute renal failure. *J Am Soc Nephrol* 2002; **13**: 1657-1662
 - 12 **Farmer DG**, Amersi F, Shen XD, Gao F, Anselmo D, Ma J, Dry S, McDiarmid SV, Shaw G, Busuttill RW, Kupiec-Weglinski J. Improved survival through the reduction of ischemia-reperfusion injury after rat intestinal transplantation using selective P-selectin blockade with P-selectin glycoprotein ligand-Ig. *Transplant Proc* 2002; **34**: 985
 - 13 **Oktar BK**, Gulpinar MA, Bozkurt A, Ghandour S, Cetinel S, Moini H, Yegen BC, Bilsel S, Granger DN, Kurtel H. Endothelin receptor blockers reduce I/R-induced intestinal mucosal injury: role of blood flow. *Am J Physiol Gastrointest Liver Physiol* 2002; **282**: G647-655
 - 14 **Kuzu MA**, Koksoy C, Kuzu I, Gurhan I, Ergun H, Demirpence E. Role of integrins and intracellular adhesion molecule-1 in lung injury after intestinal ischemia-reperfusion. *Am J Surg* 2002; **183**: 70-74
 - 15 **Zhou T**, Li X, Wu P, Zhang D, Zhang M, Chen N, Dong D. Effect of anti-P-selectin monoclonal antibody on renal ischemia/reperfusion injury in rats. *Chin Med J* 2000; **113**: 790-793
 - 16 **Stepkowski SM**, Chen W, Bennett CF, Condon TP, Stecker K, Tian L, Kahan BD. Phosphorothioate/methoxyethyl-modified ICAM-1 antisense oligonucleotides improves prevention of ischemic/reperfusion injury. *Transplant Proc* 2001; **33**: 3705-3706
 - 17 **Deng J**, Kohda Y, Chiao H, Wang Y, Hu X, Hewitt SM, Miyaji T, McLeroy P, Nibhanupudya B, Li S, Star RA. Interleukin-10 inhibits ischemic and cisplatin-induced acute renal injury. *Kidney Int* 2001; **60**: 2118-2128
 - 18 **Redlin M**, Werner J, Habazettl H, Griethe W, Kuppe H, Pries AR. Cariporide (HOE 642) attenuates leukocyte activation in ischemia and reperfusion. *Anesth Analg* 2001; **93**: 1472-1479
 - 19 **Salter JW**, Krieglstein CF, Issekutz AC, Granger DN. Platelets modulate ischemia/reperfusion-induced leukocyte recruitment in the mesenteric circulation. *Am J Physiol Gastrointest Liver Physiol* 2001; **281**: G1432-1439
 - 20 **Lindner JR**, Song J, Christiansen J, Klivanov AL, Xu F, Ley K. Ultrasound assessment of inflammation and renal tissue injury with microbubbles targeted to P-selectin. *Circulation* 2001; **104**: 2107-2112
 - 21 **Wu P**, Li X, Zhou T, Zhang MJ, Chen JL, Wang WM, Chen N, Dong DC. Role of P-selectin and anti-P-selectin monoclonal antibody in apoptosis during hepatic/renal ischemia reperfusion injury. *World J Gastroenterol* 2000; **6**: 244-247
 - 22 **Kojima N**, Sato M, Suzuki A, Sato T, Satoh S, Kato T, Senoo H. Enhanced expression of B7-1, B7-2, and intercellular adhesion molecule 1 in sinusoidal endothelial cells by warm ischemia/reperfusion injury in rat liver. *Hepatology* 2001; **34**: 751-757
 - 23 **Weigand MA**, Plachky J, Thies JC, Spies-Martin D, Otto G, Martin E, Bardenheuer HJ. N-acetylcysteine attenuates the increase in alpha-glutathione S-transferase and circulating ICAM-1 and VCAM-1 after reperfusion in humans undergoing liver transplantation. *Transplantation* 2001; **72**: 694-698
 - 24 **Huang X**, Ren P, Wen AD, Wang LL, Zhang L, Gao F. Pharmacokinetics of traditional Chinese syndrome and recipe: a hypothesis and its verification (I). *World J Gastroenterol* 2000; **6**: 384-391
 - 25 **Zhou S**, Shao W, Zhang W. Clinical study of Astragalus injection plus ligustrazine in protecting myocardial ischemia reperfusion injury. *Zhongguo Zhongxiyi Jiehe Zazhi* 2000; **20**: 504-507
 - 26 **Liu CF**, Lin CC, Ng LT, Lin SC. Protection by tetramethylpyrazine in acute absolute ethanol-induced gastric lesions. *J Biomed Sci* 2002; **9**: 395-400
 - 27 **Liu CF**, Lin MH, Lin CC, Chang HW, Lin SC. Protective effect of tetramethylpyrazine on absolute ethanol-induced renal toxicity in mice. *J Biomed Sci* 2002; **9**: 299-302
 - 28 **Li M**, Handa S, Ikeda Y, Goto S. Specific inhibiting characteristics of tetramethylpyrazine, one of the active ingredients of the Chinese herbal medicine 'Chuanxiong,' on platelet thrombus formation under high shear rates. *Thromb Res* 2001; **104**: 15-28
 - 29 **Dragun D**, Hoff U, Park JK, Qun Y, Schneider W, Luft FC, Haller H. Prolonged cold preservation augments vascular injury independent of renal transplant immunogenicity and function. *Kidney Int* 2001; **60**: 1173-1181
 - 30 **Young CS**, Palma JM, Mosher BD, Harkema J, Naylor DF, Dean RE, Crockett E. Hepatic ischemia/reperfusion injury in P-selectin and intercellular adhesion molecule-1 double-mutant mice. *Am Surg* 2001; **67**: 737-744
 - 31 **Yabe Y**, Kobayashi N, Nishihashi T, Takahashi R, Nishikawa M, Takakura Y, Hashida M. Prevention of neutrophil-mediated hepatic ischemia/reperfusion injury by superoxide dismutase and catalase derivatives. *J Pharmacol Exp Ther* 2001; **298**: 894-899
 - 32 **Maroszynska I**, Fiedor P. Leukocytes and endothelium interaction as rate limiting step in the inflammatory response and a key factor in the ischemia-reperfusion injury. *Ann Transplant* 2000; **5**: 5-11
 - 33 **Laskowski I**, Pratschke J, Wilhelm MJ, Gasser M, Tilney NL. Molecular and cellular events associated with ischemia/reperfusion injury. *Ann Transplant* 2000; **5**: 29-35
 - 34 **Burne MJ**, Elghandour A, Haq M, Saba SR, Norman J, Condon T, Bennett F, Rabb H. IL-1 and TNF independent pathways mediate ICAM-1/VCAM-1 up-regulation in ischemia reperfusion injury. *J Leukoc Biol* 2001; **70**: 192-198
 - 35 **Fuller TF**, Sattler B, Binder L, Vetterlein F, Ringe B, Lorf T. Reduction of severe ischemia reperfusion injury in rat kidney grafts by a soluble P-selectin glycoprotein ligand. *Transplantation* 2001; **72**: 216-222
 - 36 **Oe S**, Hirotsu T, Fujii H, Yasuchika K, Nishio T, Limuro Y, Morimoto T, Nagao M, Yamaoka Y. Continuous intravenous infusion of deleted form of hepatocyte growth factor attenuates hepatic ischemia-reperfusion injury in rats. *J Hepatol* 2001; **34**: 832-839
 - 37 **Kobayashi A**, Imamura H, Isobe M, Matsuyama Y, Soeda J, Matsunaga K, Kawasaki S. Mac-1 (CD11b/CD18) and intercellular adhesion molecule-1 in ischemia-reperfusion injury of rat liver. *Am J Physiol Gastrointest Liver Physiol* 2001; **281**: G577-585
 - 38 **Cabrera PV**, Blanco G, Argibay P, Hajos SE. Isoforms modulation of CD44 adhesion molecule in a murine model of ischemia and intestinal reperfusion. *Medicina* 2000; **60**: 940-946
 - 39 **Serracino-Inglott F**, Habib NA, Mathie RT. Hepatic ischemia-reperfusion injury. *Am J Surg* 2001; **181**: 160-166
 - 40 **Taut FJ**, Schmidt H, Zapletal CM, Thies JC, Grube C, Motsch J, Klar E, Martin E. N-acetylcysteine induces shedding of selectins from liver and intestine during orthotopic liver transplantation. *Clin Exp Immunol* 2001; **124**: 337-341
 - 41 **Bojakowski K**, Abramczyk P, Bojakowska M, Zwolinska A, Przybylski J, Gaciong Z. Fucoidan improves the renal blood flow in the early stage of renal ischemia/reperfusion injury in the rat. *J Physiol Pharmacol* 2001; **52**: 137-143

- 42 **Opal SM**, Sypek JP, Keith JC Jr, Schaub RG, Palardy JE, Parejo NA. Evaluation of the safety of recombinant P-selectin glycoprotein ligand-immunoglobulin G fusion protein in experimental models of localized and systemic infection. *Shock* 2001; **15**: 285-290
- 43 **Zingarelli B**, Yang Z, Hake PW, Denenberg A, Wong HR. Absence of endogenous interleukin 10 enhances early stress response during post-ischaemic injury in mice intestine. *Gut* 2001; **48**: 610-622
- 44 **Rivera-Chavez FA**, Toledo-Pereyra LH, Martinez-Mier G, Nora DT, Harkema J, Bachulis BL, Dean RE. L-selectin blockade and liver function in rats after uncontrolled hemorrhagic shock. *J Invest Surg* 2001; **14**: 7-12
- 45 **Chen W**, Bennett CF, Condon TP, Stecker K, Tian L, Kahan BD, Stepkowski SM. Methoxyethyl modification of phosphorothioate ICAM-1 antisense oligonucleotides improves prevention of ischemic/reperfusion injury. *Transplant Proc* 2001; **33**: 854
- 46 **Ghobrial R**, Amersi F, Stecker K, Kato H, Melinek J, Singer J, Mhoyan A, Busuttil RW, Kupiec-Weglinski JW, Stepkowski SM. Amelioration of hepatic ischemia/reperfusion injury with intercellular adhesion molecule-1 antisense oligodeoxynucleotides. *Transplant Proc* 2001; **33**: 538
- 47 **Koksoy C**, Kuzu MA, Kuzu I, Ergun H, Gurhan I. Role of tumour necrosis factor in lung injury caused by intestinal ischaemia-reperfusion. *Br J Surg* 2001; **88**: 464-468
- 48 **Sun Z**, Wang X, Lasson A, Bojesson A, Annborn M, Andersson R. Effects of inhibition of PAF, ICAM-1 and PECAM-1 on gut barrier failure caused by intestinal ischemia and reperfusion. *Scand J Gastroenterol* 2001; **36**: 55-65
- 49 **Amersi F**, Dulkanchainun T, Nelson SK, Farmer DG, Kato H, Zaky J, Melinek J, Shaw GD, Kupiec-Weglinski JW, Horwitz LD, Horwitz MA, Busuttil RW. A novel iron chelator in combination with a P-selectin antagonist prevents ischemia/reperfusion injury in a rat liver model. *Transplantation* 2001; **71**: 112-118
- 50 **Wada K**, Montalto MC, Stahl GL. Inhibition of complement C5 reduces local and remote organ injury after intestinal ischemia/reperfusion in the rat. *Gastroenterology* 2001; **120**: 126-133
- 51 **Chen JL**, Zhou T, Chu YD, Xu HM, Li X, Zhang MJ, Zhang DH, Wu YL. Study on intercellular adhesion-1 and P-selectin in liver ischemia and reperfusion injury. *J SSMU* 1998; **10**: 63-65
- 52 **Zou LY**, Hao XM, Zhang GQ, Zhang M, Guo JH, Liu TF. Effect of tetramethyl pyrazine on L-type calcium channel in rat ventricular myocytes. *Can J Physiol Pharmacol* 2001; **79**: 621-626
- 53 **Frenette PS**, Mayadas TN, Rayburn H, Hynes RO, Wagner DD. Susceptibility to infection and altered hematopoiesis in mice deficient in both P- and E-selectins. *Cell* 1996; **84**: 563-574
- 54 **So EC**, Wong KL, Huang TC, Tasi SC, Liu CF. Tetramethylpyrazine protects mice against thioacetamide-induced acute hepatotoxicity. *J Biomed Sci* 2002; **9**: 410-414
- 55 **Liu CF**, Lin CC, Ng LT, Lin SC. Hepatoprotective and therapeutic effects of tetramethylpyrazine on acute econazole-induced liver injury. *Planta Med* 2002; **68**: 510-514

Edited by Xu XQ and Wang XL

Role of NF- κ B and cytokine in experimental cancer cachexia

Wei Zhou, Zhi-Wei Jiang, Jie Tian, Jun Jiang, Ning Li, Jie-Shou Li

Wei Zhou, Zhi-Wei Jiang, Jun Jiang, Ning Li, Jie-Shou Li, Department of Surgery, School of Medicine, Nanjing University, Nanjing 210002, Jiangsu Province, China

Jie Tian, Department of Anaesthesiology, School of Life Sciences, Nanjing University, Nanjing 210002, Jiangsu Province, China

Correspondence to: Dr. Wei Zhou, Department of Surgery, Jinling Hospital, 305 East Zhongshan Road, Nanjing 210002, Jiangsu Province, China. nuzw@sohu.com

Telephone: +86-25-3685194 **Fax:** +86-25-4803956

Received: 2003-03-02 **Accepted:** 2003-03-29

Abstract

AIM: To assess the putative involvement of NF- κ B and pro-inflammatory cytokines in the pathogenesis of cancer cachexia and the therapeutic efficacy of indomethacin (IND) on cachexia.

METHODS: Thirty young male BABL/c mice were divided randomly into five groups: (a) control, (b) tumor-bearing plus saline, (c) tumor-bearing plus IND (0.25 mg·kg⁻¹), (d) tumor-bearing plus IND (0.5 mg·kg⁻¹), and (e) tumor-bearing plus IND (2 mg·kg⁻¹). Colon 26 adenocarcinoma cells of murine were inoculated subcutaneously to induce cachexia. Saline and IND were given intraperitoneally daily for 7 days from the onset of cachexia to sacrifice. Food intake and body composition were documented, serum levels of TNF- α and IL-6 and activity of NF- κ B in the spleen were investigated in all animals.

RESULTS: Weight loss was observed in all tumor-bearing mice. By day 16, body weights of non-tumor mice were about 72 % of healthy controls ($P < 0.01$), and the weight of gastrocnemius was decreased by 28.7 % ($P < 0.01$). No difference was found between groups in food intake ($P > 0.05$). Gastrocnemius weight was increased markedly ($P < 0.01$) after treatment of IND (0.5 mg·kg⁻¹), while the non-tumor body weights were not significantly elevated. Tumor-bearing caused a 2-3 fold increase in serum levels of both TNF- α and IL-6 ($P < 0.01$). The concentration of TNF- α ($P < 0.05$) and IL-6 ($P < 0.01$) in tumor-bearing mice was reduced after administration of 0.5 mg·kg⁻¹ IND for 7 days. But the level of IL-6 was slightly elevated following treatment of IND 2.0 mg·kg⁻¹. NF- κ B activation in the spleen was increased in tumor-bearing mice in comparison with controls in electrophoretic mobility shift assay (EMSA). NF- κ B activity was reduced in mice treated with 0.5 mg·kg⁻¹ of IND, whereas a higher NF- κ B activity was observed in mice treated with 2.0 mg·kg⁻¹ of IND.

CONCLUSION: Colon 26 adenocarcinoma cells can induce severe cancer cachexia experimentally, and the mechanism may be partially due to the enhanced TNF- α and IL-6 in tumor-bearing animals, which is controlled by NF- κ B. Low dose of indomethacin alleviates the cachexia, decreases the activation of NF- κ B and the serum levels of TNF- α and IL-6, and prevents body weight loss and muscle atrophy, while no further effect is gained by a higher dosage.

Zhou W, Jiang ZW, Tian J, Jiang J, Li N, Li JS. Role of NF- κ B and cytokine in experimental cancer cachexia. *World J Gastroenterol* 2003; 9(7): 1567-1570

<http://www.wjgnet.com/1007-9327/9/1567.asp>

INTRODUCTION

Cancer cachexia is characterized by significant weight loss even at an early course of malignancy, and reduces the quality of life of patients as well as responsiveness to chemotherapy. It is the most debilitating and life-threatening aspect of cancer and is associated with psychological distress and a lower quality of life. Thus, it is necessary to clarify the cellular and molecular biological mechanisms of cancer cachexia for the improvement of cancer treatment.

It has been well established that pro-inflammatory cytokines are important in inducing and promoting the development of experimental cancer cachexia. Most research efforts have focused on the role of cytokines of tumor necrosis factor α (TNF- α), interleukin 6 (IL-6) and interleukin 1 (IL-1)^[1-4]. Many of these cytokines are responsible for weight loss, an acute phase of protein response, fat and skeletal muscle protein breakdown and elevated energy expenditure in animals and patients^[5]. The nuclear factor-kappaB proteins are ubiquitous transcription factors that mediate cellular responses to a diverse array of stimuli, including lipopolysaccharide, reactive oxygen species (ROS) and several cytokines. Over the past decade, significant advances have been made in elucidation of the molecular signals leading to NF- κ B activation, as well as in identification of gene regulation by NF- κ B. The role of NF- κ B proteins in regulating genes associated with immune system and inflammation has been extensively studied. Activation of NF- κ B in immune cells upregulates the expression of cytokines, and growth factors that are essential to immune response contribute to inflammation. An autoregulatory feedback loop has been generated with production of cytokines TNF- α and IL-1. NF- κ B represents an upstream element of a common pathway that produces catabolic cytokines^[6-8]. Such a pathway has an obvious clinical importance in providing potential targets for therapeutic intervention to inhibit or reverse cancer cachexia.

In the present study, a cachectic model was established in mouse bearing colon 26 adenocarcinoma cells for studying the mechanism and therapies of cancer cachexia. As with human cachexia, there was a significant loss of body weight in this model, and the animals had substantial hypoglycemia and an increase of circulating pro-inflammatory cytokines that were thought to be correlative to the onset of cancer cachexia^[9-12]. Early researches showed that indomethacin (IND) could prolong the mean survival time of patients with advanced solid cancer^[13]. In this study, we chose IND as an anti-inflammatory agent to study its effect on peripheral blood cytokine levels and NF- κ B activation in spleen. The purpose of this study was to assess the relationship of NF- κ B and cancer cachexia and the role of IND in the treatment of cachexia.

MATERIALS AND METHODS

Animals and tumor implantation

BABL/c male mice aged 6-8 weeks (weighing 19-22 g) were

purchased from the Animal Center of Chinese Academy of Sciences, Shanghai, China. They had free access to standard laboratory chow and tap water, and were maintained in a temperature-controlled room (22 ± 1 °C) on a 12-h light-dark cycle. Thirty animals were evenly divided into five groups randomly: (a) control, (b) tumor-bearing plus saline, (c) tumor-bearing plus IND (0.25 mg·kg⁻¹, ICN, Biomedicals Inc. Ohio, USA), (d) tumor-bearing plus IND (0.5 mg·kg⁻¹), and (e) tumor-bearing plus IND (2 mg·kg⁻¹). The mice were allowed to adjust to new environment and diet for at least 1 week before experiment.

Colon 26 adenocarcinoma is appropriate for investigating cancer cachexia. This murine tumor is responsible for inducing weakness, abnormal carbohydrate metabolism, hypercorticism, and elevated levels of pro-inflammatory cytokines. Colon 26 adenocarcinoma cells were kindly supplied by Institute Materia Medica, Chinese Academy of Medical Sciences. Stock cells were passed on the BABL/c mice. Mice of passages three or four were used in the study. On day 0, a homogenate of murine colon 26 adenocarcinoma (50 mg of solid tumor tissue in 0.1 ml of sterile 0.9 % NaCl) was injected s.c. into armpits of the tumor-bearing groups. All procedures in the study were approved by the Institutional Animal Care Committee.

Experimental procedures

After inoculation of tumor cells, physical activity, fur condition, and other signs of general well being of the animals were registered. The tumor inoculation site and the tumor size were inspected. The tumor volume was estimated by using the equation $ab^2/2$, where a and b are length and width (cm) of the tumor. Body weight was monitored and food intake was measured at 10 a.m. everyday.

Significant loss of body weight was observed in tumor-bearing groups beginning on day 9 to day 16, 0.1 ml saline and variable dosages of indomethacin were given intraperitoneally to groups b, c, d and e daily for 7 days, respectively. On day 16, carcass weight was measured after removing the entire tumor. Blood samples were collected from orbital veins by removal of one side eyeballs of the animals and stored at -20 °C for determination of TNF- α and IL-6 by ELISA kit (Bender Medsystems, Vienna, Austria). Weight of the gastrocnemius of left hind leg was measured. The spleens were frozen in liquid nitrogen, and stored at -70 °C for nuclear protein extraction and electrophoretic mobility shift assay.

Nuclear protein extraction and electrophoretic mobility shift assay (EMSA)

Nuclear extracts of spleen tissues were prepared by hypotonic

lyses followed by high salt extraction as references^[14,15]. EMSA was performed using a commercial kit (Gel Shift Assay System; Promega, Madison, WI) as previously described. The NF- κ B oligonucleotide probe, (5' -AGTTGAGGGACTTTCCCAGGC-3'), was end-labeled with [γ -³²P] ATP (Free Biotech, Beijing, China) with T4-polynucleotide kinase. Nuclear protein (20 μ l) was preincubated in 9 μ l of a binding buffer, consisting of 10 mM Tris -Cl, pH 7.5, 1 mM MgCl₂, 50 mM NaCl, 0.5 mM EDTA, 0.5 mM DTT, 4 % glycerol, and 0.05 g·L⁻¹ of poly-(deoxyinosinic deoxycytidylic acid) for 15 min at room temperature. After addition of 1 μ l ³²P-labeled oligonucleotide probe, the incubation was continued for 30 min at room temperature. Reaction was stopped by adding 1 μ l of gel loading buffer, and the mixture was subjected to non-denaturing 4 % polyacrylamide gel electrophoresis in 0.5×TBE buffer. The gel was vacuum-dried and exposed to X-ray film (Fuji Hyperfilm) at -70 °C with an intensifying screen. NF- κ B was quantitated with densitometry.

Statistical analysis

Data were expressed as means \pm SE. Statistical significance was determined by one-way ANOVA using SPSS 10.0. $P < 0.05$ was considered statistically significant.

RESULTS

Tumors were palpable in mice initially on day 5 after inoculation of tumor cells, symptoms of cachexia began 3-4 days later. Weight loss began once a tumor grew to 1 cm³ and a rapid loss of body weight occurred. Initial body weights of mice before experiment had no difference. By day 16, non-tumor body weights of tumor-bearing mice were about 72 % of healthy controls ($P < 0.01$), and the weights of gastrocnemius were lowered by 28.7 % ($P < 0.01$), though the final whole body weights were elevated because of tumor growth. Food intake between groups was not different ($P > 0.05$, Table 1).

After administration of indomethacin for 1 week, the non-tumor body weights of tumor-bearing mice were increased, but had no significant difference from that in group b. The gastrocnemius weights in animals treated with 0.5 mg·kg⁻¹ of IND increased significantly ($P < 0.01$). But no weight gain of gastrocnemius in animals treated with IND 2.0 mg·kg⁻¹ was observed. On the contrary, the tumor weight of this group was increased compared with that in saline group ($P < 0.01$, data not shown). There was no evidence that IND had additional effects on appetite because quantity of food intake of mice treated with IND did not increase.

Table 1 Clinical features of tumor-bearing and non-tumor-bearing mice

Group	Initial body wt (g)	Final body wt (g)	Nontumor body wt (g)	Gastrocnemius muscle wt (mg)	Dry food intake (g·day ⁻¹)
Control	20.93 \pm 1.40	25.50 \pm 1.71	25.50 \pm 1.71	136.8 \pm 6.11	6.65 \pm 0.24
Tumor + saline	20.91 \pm 1.29	25.95 \pm 1.61	20.92 \pm 1.52 ^a	97.5 \pm 8.32 ^a	6.53 \pm 0.31
Tumor +IND(0.25 mg·kg ⁻¹)	20.98 \pm 1.42	27.75 \pm 2.20	21.75 \pm 1.64	95.65 \pm 13.5	6.56 \pm 0.27
Tumor +IND(0.5 mg·kg ⁻¹)	20.92 \pm 1.14	27.83 \pm 1.88	22.48 \pm 1.57	115.82 \pm 9.63 ^b	6.70 \pm 0.32
Tumor +IND(2.0 mg·kg ⁻¹)	21.38 \pm 1.00	28.00 \pm 1.24	21.90 \pm 1.38	93.15 \pm 10.83	6.53 \pm 0.19

^a $P < 0.01$, vs control; ^b $P < 0.01$, vs tumor + saline.

Table 2 Serum levels of TNF- α and IL-6 in mice

Parameter	Control	Tumor + saline	Tumor+IND (0.25mg·kg ⁻¹)	Tumor + IND (0.5mg·kg ⁻¹)	Tumor +IND (2.0mg·kg ⁻¹)
TNF- α (pg/ml)	43.24 \pm 13.37	113.83 \pm 16.91 ^a	89.9 \pm 4.5	71.68 \pm 16.70 ^b	110.96 \pm 20.93
IL-6 (pg/ml)	1445.82 \pm 244.20	2646.05 \pm 93.39 ^a	2527.78 \pm 266.43	1983.07 \pm 219.19 ^c	2733.33 \pm 201.84

^a $P < 0.01$, vs control; ^b $P < 0.05$, vs tumor + saline; ^c $P < 0.01$, vs tumor + saline.

Tumor-bearing caused a 2-3 fold increase in serum levels of both TNF- α and IL-6 ($P < 0.01$). Administration of IND 0.5 mg·kg⁻¹ for 7 days reduced the concentrations of TNF- α ($P < 0.05$) and IL-6 ($P < 0.01$) in tumor-bearing mice (Table 2). But level of IL-6 slightly increased after administration of 2.0 mg·kg⁻¹ of IND.

EMSA experiments were performed to examine the effect of indomethacin on the activation of NF- κ B induced by tumor bearing. As shown in Figure 1, NF- κ B activation in spleen was increased in tumor-bearing mice, compared to controls. The tumor-bearing mice treated with 0.5 mg·kg⁻¹ of indomethacin had a lower level of NF- κ B than the cachectic mice without treatment. No dose-dependent response of NF- κ B activity to different dose of IND treatment was observed. Instead, a higher NF- κ B activity was found in the mice treated with IND 2.0 mg·kg⁻¹.

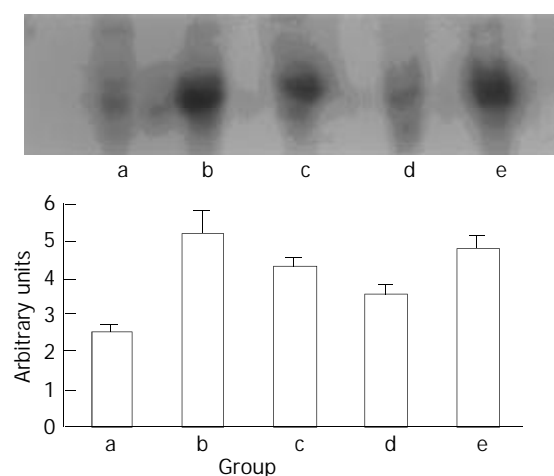


Figure 1 Activation of NF- κ B in spleen. Lane a represents the control group, Lane b, c, d, e represents the group of tumor-bearing plus saline, indomethacin 0.25 mg·kg⁻¹, 0.5 mg·kg⁻¹, 2 mg·kg⁻¹, respectively.

DISCUSSION

The syndrome of cancer cachexia including progressive weight loss, particularly in skeletal muscle and adipose tissue, weakness, anemia, and often accompanied by anorexia is an important problem in the management of cancer patients. Nearly all cancer patients have significant weight loss by the time of death. Progressive wasting is an acknowledged clinical problem, it contributes to cancer mortality and may reduce the ability of patients to tolerate aggressive chemotherapy and radiotherapy. Although cachexia is frequently accompanied by anorexia, the decrease of food intake alone may be insufficient to account for cachexia because the body composition change in cachexia differs from that of starvation. Loss of skeletal muscle is more prominent in cachectic patients, leading to weakness and immobility of cancer patients eventually to death due to dysfunction of respiratory muscle. The fact that calories provided by total parenteral nutrition cannot maintain body weight of cancer patients suggests that weight loss is resulted from complex metabolic events rather than simple nutrition insufficiency^[16].

Some possible mechanisms can be considered for the wasting in cachexia. It has been reported that weight loss is associated with anorexia in some tumor cachexia model^[17]. But it is unlikely that the cachexia in our model was due to anorexia, because food intake was not significantly reduced while the mice were losing weight. Several cytokines are suggested to be involved in the development of cancer cachexia. The last decade has witnessed the discovery of multiple actions of cytokines on the regulation of metabolism

in normal and pathophysiological conditions. Some of them are clearly involved in the wasting process that is often accompanied by chronic infection or cancer. We found that TNF- α and IL-6 levels in peripheral blood of animals were elevated while body and muscle weight decreased, which suggested the two cytokines were involved in our cachectic model. TNF- α levels were detectable in serum of pancreatic cancer patients, particularly in those with advanced disease, and these levels correlated with poor nutritional status^[18]. Muscle wasting during tumor growth may be associated with the activation of non-lysosomal ubiquitin-dependent proteases associated with enhanced skeletal muscle proteolysis. This activation seems to be mediated by these cytokines, especially TNF- α , IL-6 and some other catabolic factors produced by tumors and hosts^[19-22]. It was previously reported that TNF- α was partially mediated DNA fragmentation in skeletal muscle, suggesting an apoptotic phenomenon during experimental cancer-associated cachexia^[23]. Production of pro-inflammatory cytokines also induces production of corresponding anti-inflammatory cytokines such as IL-15, IL-1 and IL-6 receptor antagonist, which may significantly reduce the severity of key parameters of cachexia^[24-26]. Clearly the balance between pro-inflammatory and anti-inflammatory mediators may be crucial in determining the net clinical effects.

Several experiments suggested that cytokines (IL-1, IL-6, and TNF- α) induced anorexia in tumor-bearing and infected animals, and the appetite was improved in indomethacin-treated animals^[17]. However, tumor-bearing mice in our experiments had no significant appetite change, and indomethacin had no obvious effect on diet consumption. So, the wasting condition in this model may have no relation with food consumption, but may be attributed to metabolic disorders. The present study confirmed previous reports demonstrating that a low dose of NASID, particularly indomethacin could inhibit cancer cachexia, whereas a high dose might be toxic^[17, 27, 28]. We found a low dose of indomethacin treatment could decrease TNF- α and IL-6 productions which were very important in the process of immune regulation and inflammation in this experimental model. Indomethacin also protected the host from deterioration in body composition, particularly lean body mass. It is likely that the inhibition was confined to host cell, since indomethacin caused no growth inhibition of tumors. However, contrary evidence also exists. Other reports suggested that IND appeared to suppress the growth of colon 26 as long as the tumor burden was small, whereas it facilitated the tumor growth when the tumor burden was large^[29].

NF- κ B is normally sequestered in the cytoplasm of nonstimulated cells and must translocate into nuclei to regulate effector gene expression. A family of inhibitory proteins, I κ Bs, binds to NF- κ B and masks its nuclear localization signal domain and therefore controls the translocation of NF- κ B. Exposure of cells to extracellular stimuli that perturb redox balance results in rapid phosphorylation, ubiquitination, and proteolytic degradation of I κ Bs. This process frees NF- κ B from the NF- κ B/I κ Bs complexes and enables NF- κ B to translocate to the nuclei where they regulate gene transcription. Many effector genes such as those encoding cytokines and adhesion molecules are in turn regulated by NF- κ B^[6]. Some anti-inflammatory agents (e.g. salicylates, dexamethasone) can inhibit NF- κ B, which also indicates that NF- κ B is an important molecular target for modulation of inflammatory disease^[30-33]. However, the identity of NF- κ B, and its role in cancer cachexia still remain to be investigated. In the present study, a low baseline activity of spleen NF- κ B was observed in controls, while tumor bearing increased NF- κ B activities markedly. A low dose of indomethacin decreased NF- κ B activities variably.

In summary, colon 26 adenocarcinoma cells could produce severe cancer cachexia, including loss of non-tumor whole

body and gastrocnemius muscle weight. The wasting condition may be partially due to the enhanced TNF- α and IL-6 production in the tumor-bearing animals, which is controlled by NF- κ B. A low dose of indomethacin alleviates the wasting, decreases the activation of NF- κ B, and serum level of TNF- α and IL-6, delays body weight loss and muscle atrophy. These results suggest that activation of NF- κ B may play a critical role in inflammatory response of cancer cachexia. However, other possible mechanisms cannot be excluded. Indomethacin can suppress activation of NF- κ B, and can be used as a reagent to improve the catabolic status in cancer cachexia. Although the present study could not clarify the definite mode of the anticachectic action of IND, the ability of IND to reverse cachexia should be considered as one of the various actions of this drug. Further studies are required to evaluate its clinical effects and mechanism in patients with cancer cachexia.

ACKNOWLEDGEMENT

We thank Dr. Genbao Feng for his technical assistance.

REFERENCES

- Kurzrock R.** The role of cytokines in cancer-related fatigue. *Cancer* 2001; **92**(Suppl): 1684-1688
- Tisdale MJ.** Wasting in cancer. *J Nutr* 1999; **129**(Suppl): 243S-246S
- Barton BE, Murphy TF.** Cancer cachexia is mediated in part by the induction of IL-6-like cytokines from the spleen. *Cytokine* 2001; **16**: 251-257
- Barton BE.** IL-6-like cytokines and cancer cachexia: consequences of chronic inflammation. *Immunol Res* 2001; **23**: 41-58
- O' Riordain MG, Falconer JS, Maingay J, Fearon KC, Ross JA.** Peripheral blood cells from weight-losing cancer patients control the hepatic acute phase response by a primarily interleukin-6 dependent mechanism. *Int J Oncol* 1999; **15**: 823-827
- Baeuerle PA, Baltimore D.** NF-kappa B: ten years after. *Cell* 1996; **87**: 13-20
- Schwartz SA, Hernandez A, Mark Evers B.** The role of NF-kappaB/IkappaB proteins in cancer: implications for novel treatment strategies. *Surg Oncol* 1999; **8**: 143-153
- Wang T, Zhang X, Li JJ.** The role of NF-kappaB in the regulation of cell stress responses. *Int Immunopharmacol* 2002; **2**: 1509-1520
- Strassmann G, Jacob CO, Fong M, Bertolini DR.** Mechanisms of paraneoplastic syndromes of colon-26: involvement of interleukin 6 in hypercalcemia. *Cytokine* 1993; **5**: 463-468
- Tanaka M, Miyazaki H, Takeda Y, Takeo S.** Detection of serum cytokine levels in experimental cancer cachexia of colon 26 adenocarcinoma-bearing mice. *Cancer Lett* 1993; **72**: 65-70
- Strassmann G, Fong M, Kenney JS, Jacob CO.** Evidence for the involvement of interleukin 6 in experimental cancer cachexia. *J Clin Invest* 1992; **89**: 1681-1684
- Tanaka Y, Eda H, Tanaka T, Udagawa T, Ishikawa T, Horii I, Ishitsuka H, Kataoka T, Taguchi T.** Experimental cancer cachexia induced by transplantable colon 26 adenocarcinoma in mice. *Cancer Res* 1990; **50**: 2290-2295
- Lundholm K, Gelin J, Hyltander A, Lonroth C, Sandstrom R, Svaninger G, Korner U, Gulich M, Karrefors I, Norli B.** Anti-inflammatory treatment may prolong survival in undernourished patients with metastatic solid tumors. *Cancer Res* 1994; **54**: 5602-5606
- Gong JP, Liu CA, Wu CX, Li SW, Shi YJ, Li XH.** Nuclear factor kB activity in patients with acute severe cholangitis. *World J Gastroenterol* 2002; **8**: 346-349
- Liu Z, Yu Y, Jiang Y, Li J.** Growth hormone increases lung NF-kappaB activation and lung microvascular injury induced by lipopolysaccharide in rats. *Ann Clin Lab Sci* 2002; **32**: 164-170
- Tisdale MJ.** Cancer anorexia and cachexia. *Nutrition* 2001; **17**: 438-442
- Cahlin C, Korner A, Axelsson H, Wang W, Lundholm K, Svanberg E.** Experimental cancer cachexia: The role of host-derived cytokines interleukin (IL)-6, IL-12, interferon-gamma, and tumor necrosis factor alpha evaluated in gene knockout, tumor-bearing mice on C57 Bl background and eicosanoid-dependent cachexia. *Cancer Res* 2000; **60**: 5488-5493
- Karayiannakis AJ, Syrigos KN, Polychronidis A, Pitiakoudis M, Bounovas A, Simopoulos K.** Serum levels of tumor necrosis factor-alpha and nutritional status in pancreatic cancer patients. *Anticancer Res* 2001; **21**: 1355-1358
- Llovera M, Carbo N, Lopez-Soriano J, Garcia-Martinez C, Busquets S, Alvarez B, Agell N, Costelli P, Lopez-Soriano FJ, Celada A, Argiles JM.** Different cytokines modulate ubiquitin gene expression in rat skeletal muscle. *Cancer Lett* 1998; **133**: 83-87
- Costelli P, Bossola M, Muscaritoli M, Grieco G, Bonelli G, Bellantone R, Doglietto GB, Baccino FM, Fanelli FR.** Anticytokine treatment prevents the increase in the activity of ATP-ubiquitin- and Ca(2+)-dependent proteolytic systems in the muscle of tumour-bearing rats. *Cytokine* 2002; **19**: 1-5
- Tisdale MJ.** The 'cancer cachectic factor'. *Support Care Cancer* 2003; **11**: 73-78
- Llovera M, Garcia-Martinez C, Agell N, Lopez-Soriano FJ, Argiles JM.** TNF can directly induce the expression of ubiquitin-dependent proteolytic system in rat soleus muscles. *Biochem Biophys Res Commun* 1997; **230**: 238-241
- Carbo N, Busquets S, van Royen M, Alvarez B, Lopez-Soriano FJ, Argiles JM.** TNF-alpha is involved in activating DNA fragmentation in skeletal muscle. *Br J Cancer* 2002; **86**: 1012-1016
- Strassmann G, Kambayashi T.** Inhibition of experimental cancer cachexia by anti-cytokine and anti-cytokine-receptor therapy. *Cytokines Mol Ther* 1995; **1**: 107-113
- Carbo N, Lopez-Soriano J, Costelli P, Busquets S, Alvarez B, Baccino FM, Quinn LS, Lopez-Soriano FJ, Argiles JM.** Interleukin-15 antagonizes muscle protein waste in tumour-bearing rats. *Br J Cancer* 2000; **83**: 526-531
- Strassmann G, Masui Y, Chizzonite R, Fong M.** Mechanisms of experimental cancer cachexia. Local involvement of IL-1 in colon-26 tumor. *J Immunol* 1993; **150**: 2341-2345
- Gelin J, Andersson C, Lundholm K.** Effects of indomethacin, cytokines, and cyclosporin A on tumor growth and the subsequent development of cancer cachexia. *Cancer Res* 1991; **51**: 880-885
- Niu Q, Li T, Liu A.** Cytokines in experimental cancer cachexia. *Zhonghua Zhongliu Zazhi* 2001; **23**: 382-384
- Tanaka Y, Tanaka T, Ishitsuka H.** Antitumor activity of indomethacin in mice bearing advanced colon 26 carcinoma compared with those with early transplants. *Cancer Res* 1989; **49**: 5935-5939
- Cai E, Chen Z, Wu W.** The effects of lipopolysaccharide and anti-inflammatory drugs on nuclear factor-kappa B in pulmonary intravascular macrophage. *Zhonghua Jiehe He Huxi Zazhi* 1999; **22**: 283-286
- Crinelli R, Antonelli A, Bianchi M, Gentilini L, Scaramucci S, Magnani M.** Selective inhibition of NF-kB activation and TNF-alpha production in macrophages by red blood cell-mediated delivery of dexamethasone. *Blood Cells Mol Dis* 2000; **26**: 211-222
- Chang CK, Llanes S, Schumer W.** Effect of dexamethasone on NF-kB activation, tumor necrosis factor formation, and glucose dyshomeostasis in septic rats. *J Surg Res* 1997; **72**: 141-145
- Amann R, Peskar BA.** Anti-inflammatory effects of aspirin and sodium salicylate. *Eur J Pharmacol* 2002; **447**: 1-9

Edited by Ren SY and Wang XL

Maxizyme-mediated specific inhibition on mutant-type p53 *in vitro*

Xin-Juan Kong, Yu-Hu Song, Ju-Sheng Lin, Huan-Jun Huang, Nan-Xia Wang, Nan-Zhi Liu, Bin Li, You-Xin Jin

Xin-Juan Kong, Yu-Hu Song, Ju-Sheng Lin, Huan-Jun Huang, Nan-Xia Wang, Nan-Zhi Liu, Institute of Liver Disease, Tongji Hospital, Tongji Medical College, Huazhong University of Science and Technology, Wuhan 430030, Hubei Province, China

Xin-Juan Kong, Bin Li, You-Xin Jin, State Key Laboratory of Molecular Biology, Shanghai Institute of Biochemistry, Chinese Academy of Sciences, Shanghai 200031, China

Supported by the National Natural Science Foundation of China, No.30171061

Correspondence to: Professor You-Xin Jin, State Key Laboratory of Molecular Biology, Shanghai Institute of Biochemistry, Chinese Academy of Sciences, 320 Yueyang Road, Shanghai 200031, China. yxjin@sunm.shnc.ac.cn

Telephone: +86-21-64315030-5221 **Fax:** +86-21-64338357

Received: 2002-11-26 **Accepted:** 2003-02-19

Abstract

AIM: To evaluate the specific inhibition of maxizyme directing against mutant-type p53 gene (mtp53) at codon 249 in exon 7 (AGG→AGT) *in vitro*.

METHODS: Two different monomers of anti-mtp53 maxizyme (maxizyme right MzR, maxizyme left MzL) and control mutant maxizyme (G⁵→A⁵) were designed by computer and cloned into vector pBSKU6 (pBSKU6MzR, pBSKU6MzL). After being sequenced, the restrictive endonuclease site in pBSKU6MzR was changed by PCR and then U6MzR was inserted into pBSKU6MzL, the recombinant vector was named pU6Mz and pU6asMz (mutant maxizyme). Mtp53 and wild-type p53 (wtp53) gene fragments were cloned into pGEM-T vector under the T7 promoter control. The ³²p-labeled mtp53 transcript was the target mRNA. Cold maxizyme transcripts were incubated with ³²p-labeled target RNA *in vitro* and radioautographed after denaturing polyacrylamide gel electrophoresis.

RESULTS: In cell-free systems, pU6Mz showed a specific cleavage activity against target mRNA at 37 °C and 25 mM MgCL₂. The cleavage efficiency of pU6Mz was 42 %, while pU6asMz had no inhibitory effect. Wtp53 was not cleaved by pU6Mz either.

CONCLUSION: pU6Mz had a specific catalytic activity against mtp53 in cell-free system. These lay a good foundation for studying the effects of anti-mtp53 maxizyme in HCC cell lines. The results suggest that maxizyme may be a promising alternative approach for treating hepatocellular carcinoma containing mtp53.

Kong XJ, Song YH, Lin JS, Huang HJ, Wang NX, Liu NZ, Li B, Jin YX. Maxizyme-mediated specific inhibition on mutant-type p53 *in vitro*. *World J Gastroenterol* 2003; 9(7): 1571-1575

<http://www.wjgnet.com/1007-9327/9/1571.asp>

INTRODUCTION

Hepatocellular carcinoma (HCC) is one of the major causes of

mortality worldwide^[1,2]. Several risk factors are associated with the development of HCC including chronic infection with hepatitis B virus (HBV) and hepatitis C virus (HCV), exposure to genotoxic environmental agents such as aflatoxins. The high incidence of HCC has been observed in areas such as sub-saharan Africa, Thailand and the Southern region of China (Qidong) where concomitant infection occurs with HBV and high intake of aflatoxins^[3-5]. Mutational inactivation of tumor suppressor gene p53 is very common in hepatocellular carcinoma. Indeed, p53 gene mutations, deletions or loss is a very important step during carcinogenesis and might participate in all stages of HCC development^[6-9]. AGG to AGT transversion in codon 249 (the third base of codon 249) of exon 7 of p53 gene occurs in over 50 % of HCC from endemic regions, where both chronic infection with HBV and exposure to carcinogens such as aflatoxin B1 (AFB1) prevail^[10-13]. The p53 tumor suppressor gene product plays a crucial physiological role as a "cellular gatekeeper" by exerting a variety of effects following DNA damage^[14,15]. Study of p53 as a tumor suppressor gene has attracted a large number of top scientists worldwide. But mutant p53 has drawn much less attention. Mutant p53 may not be an inactivated tumor suppressor gene, it appears to be one of the most prominent members of a new family of oncogenes^[16,17]. Inactivation of p53 contributes not only to tumor progression but also to resistance of cancer cells to chemotherapy. Mutant p53 protein may possess transforming ability and can cooperate with other oncogenes in the transformation of normal cells. Mutant p53 protein has a prolonged halflife of 2 to 12 hours, resulting in higher intracellular concentrations than the wild-type protein^[18,19]. Loss of ability to suppress transformation and gain of transforming potential and tumorigenicity are the properties of mutant p53 gene product.

Ribozyme is a kind of catalytic RNA which can catalyze the cleavage of sequence-specific RNA^[20]. Among different types of ribozymes discovered, hammerhead ribozyme has been studied extensively for the treatment of disorders ranging from cancer to infectious disease^[21-29]. However, because the limited number of cleavable sequences on target RNA, in some cases conventional ribozyme does not have precise cleavage specificity. This shortcoming may greatly limit the utility of hammerhead ribozyme^[30,31]. A minizyme (minimised ribozyme) is a hammerhead ribozyme with short oligonucleotide linker instead of stem II. It has lower cleavage activity compared with that of wild-type parental hammerhead ribozyme^[32,33]. Two minizymes could form an active dimeric structure. The dimers can be homodimeric (with two identical binding sequences) or heterodimer (with two different binding sequences). In order to distinguish monomeric forms of conventional minizymes that have extremely low activity from novel heterodimer with high-level activity, the latter was designated as "maxizyme"^[34-36]. Maxizyme stands for minimized, active, heterodimeric, and intelligent ribozyme. Some study showed that maxizyme could cleave chimeric genes, such as BCR-ABL mRNA, which causes chronic myelogenous leukemia (CML)^[37]. In this study, we designed maxizyme targeting mtp53 mRNA by computer and examined its cleavage activity *in vitro*.

MATERIALS AND METHODS

Materials

In vitro transcription kit and pGEM-T vector were purchased from Promega Company. Restriction endonucleases, T4 DNA ligase, RNase inhibition and DNA marker were purchased from TaKaRa Company. [α - 32 P] dUTP was purchased from Beijing Yuhui Company. *E. coli* DH5 α was maintained in our laboratory. pBSKU6 vector was a generous gift from Dr. You-Xin Jin. pCMV-mtp53 (or wtp53) plasmid was kindly provided by Pro. Bert Vogelstein (Howard Hughes Medical Institute). Materials used were of analytical purity.

Maxizyme design

Maxizyme targeting mutant-type p53 (249 codon) was designed. Only after binding mutant-type p53 in codon 249 (the third base of 249 codon, AGG \rightarrow AGT) can the maxizyme cleave mtp53 in 201bp site. The oligonucleotide sequences included Xba I and BamH I linker sites and were as follows: *MzL*: 5' CTA GAG AGG ATG GCT GAT GAG CGA AAG GTC TGG 3'; 5' GAT CCC AGA CCT TTC GCT CAT CAG CCA TCC TCT 3'. *MzR*: 5' CTA GAA GTT TCC ACT GAT GAG CGA AAC TCC GGG 3'; 5' GAT CCC CGG AGT TTC GCT CAT CAG TGG AAA CTT 3'. A mutant maxizyme was designed with a sequence almost identical to that of the maxizyme except for G⁵ to A⁵ mutation within the catalytic core. This mutant maxizyme was expected to have no cleavage activity. They were chemically synthesized in Beckman Oligo 1000-DNA synthesizer. The structure of maxizyme against mtp53 is shown in Figure 1.

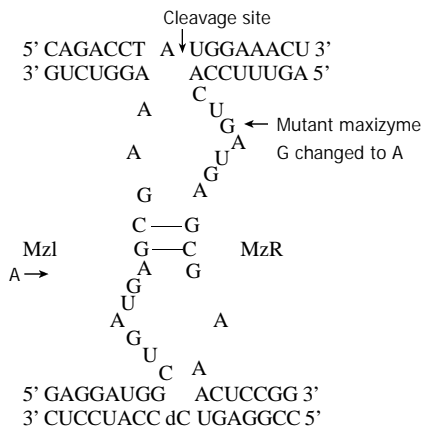


Figure 1 Structure of maxizyme against mtp53.

Methods

Construction of cell-free transcription plasmid for target RNA Mtp53 and wtp53 gene containing a cDNA fragment with 986 bases was amplified by PCR from pCMV-p53mt249 and pCMV-wtp53 vector. The PCR products were analyzed and purified by 2 % agarose gel and cloned into the transcription vector pGEM-T downstream of the T7 bacteriophage RNA promoter. The reconstructed plasmids were named as pmtp53 and pwtp53. The primers used were: upstream primer 5' GAT TCT CTT CCT CTG TGC 3' and downstream primer 5' CTT TCC ACG ACG GTG ACA 3'.

Construction of cell-free transcription plasmid for maxizyme Maxizyme targeting mtp53 was designed according to the computer software from professor Chen Nong-An (Shanghai Institute of Biochemistry of Chinese Academy of Sciences). The homologous possibility with the gene of human being was excluded by consulting with RNA sequences of human cell from NCBI Genebank. The *in vitro* transcription vector pBSKU6 was digested with *Xba* I and *Bam*HI restriction enzymes. The linearized vector pBSKU6 was purified by 1 %

agarose gel electrophoresis. After annealed, oligonucleotides of MzL and MzR were cloned into pBSKU6. The reconstructed plasmids were named as pBSKU6MzL and pBSKU6MzR. After being sequenced, the restrictive endonuclease site in pBSKU6MzR was changed by PCR and then U6MzR was inserted into pBSKU6MzL, the recombinant was named as pU6Mz. pBSKU6 vector contained the T7 RNA polymerase promoter for driving transcription of Mz *in vitro*. The steps of pU6Mz construction was shown in Figure 2.

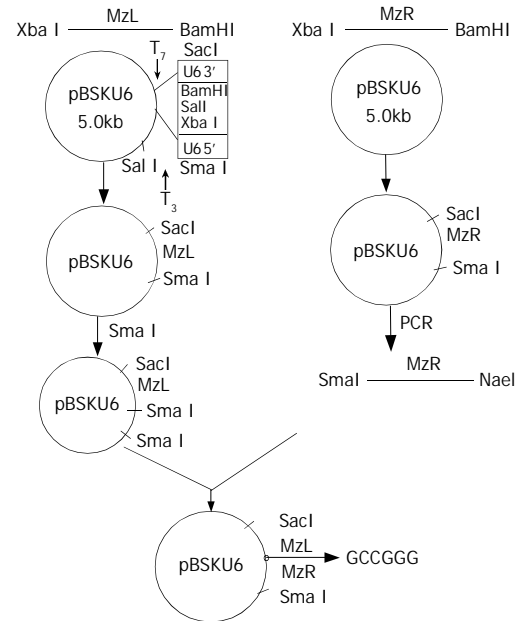


Figure 2 Steps of pU6Mz construction.

***In vitro* transcription of target RNA and maxizyme** Templates pmtp53 and pwtp53 were linearized with Sal, while pU6Mz was linearized with Sma I. The linearized templates were transcribed in the presence of [α - 32 P]dUTP (10 μ l) using T7 RNA polymerase according to the manufacturer's protocol. Transcription was performed for three hours at 37 $^{\circ}$ C in a 50 μ l final volume. The samples were purified by cutting off the autoradiograph bands after running on 8 % polyacrylamide (8 mol/l urea) gel and soaking in NES (0.5 M NH₄Ac, 0.1M EDTA, 0.1 % SDS pH 5.4) at 42 $^{\circ}$ C overnight. The products were precipitated by ethanol, washed once by 70 % ethanol, dissolved in DEPC-treated water and kept at -20 $^{\circ}$ C.

***In vitro* cleavage reaction** The products of maxizyme and target RNA were quantified by measuring their radioactive cpm in 1 μ l solution. The cleavage reaction was performed for 90 minutes at 37 $^{\circ}$ C in 25 mmol/l Tris-Cl (pH7.5) and 25 mmol/l MgCl₂ with cold maxizyme to [α - 32 P] dUTP-labeled substrate ratio of 4:1 and stopped by adding 1 μ l RNA loading buffer (0.25 % bromophenol blue, 0.25 % xylene cyanol FF, 20 mmol/l EDTA and saturated urea) and heated for 3 minutes at 95 $^{\circ}$ C. The cleaved products were separated by 8 % polyacrylamide gel electrophoresis(PAGE) with 8M urea. The cleavage efficiency was calculated from cpm values of the bands of substrates (S) and products (P): cleavage efficiency=[P/(S+P)] \times 100 %.

RESULTS

Construction of cloning vector pU6Mz

Mz gene was successfully cloned into the vector pBSKU6. The gene complex was treated with restriction endonuclease *Sma* I and *Sac* I and analyzed by 2 % agarose gel (Figure 3). The DNA sequence analysis showed that chimeric U6 maxizyme was correct.

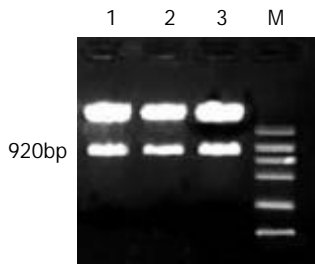


Figure 3 Restrictive enzyme analysis of recombinant plasmid pU6Mz by Sma I and Sac I. M was DNA Marker (DL2000). 1, 2, 3 were selected clones.

Identification of transcripts of pU6Mz and target RNA

The lengths of RNA transcribed from Sal I-linearized templates of pmtp53 and pwt53 should be 1002nt (Figure 4A). The transcription of pU6Mz from Sma I-linearized templates including U6 and Mz bases should be 910nt (Figure 4B). The results showed that our design was correct.

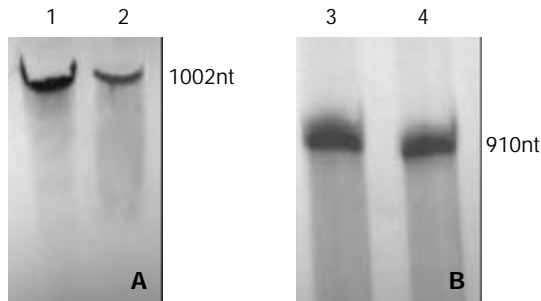


Figure 4 *In vitro* transcripts. (A) *In vitro* transcripts of wtp53 and mtp53 (1002nt). (B) *In vitro* transcripts of maxizyme and control maxizyme (910nt). lane 1: mtp53; lane 2: wtp53; lane 3: maxizyme; lane 4: control maxizyme.

In vitro cleavage reaction of Mz

Target RNA was ³²p-labeled. The cleavage results showed that the designed maxizyme had correct structure, it cleaved mtp53 mRNA efficiently, giving cleavage products with the expected size of 874nt and 128nt under conditions at 37 °C and high Mg concentration (25 mM), the cleavage efficiency was 42 %. More encouraging was that no cleavage was found with mutant maxizyme under the same conditions, and wtp53 was not cleaved by maxizyme (Figure 5).

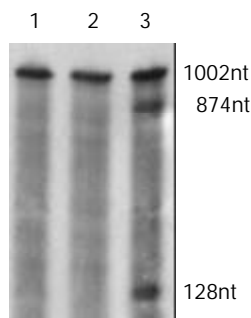


Figure 5 *In vitro* cleavage reaction. lane 1: cleavage of wtp53 by cold maxizyme; lane 2: cleavage of mtp53 by inactive cold maxizyme; lane 3: cleavage of mtp53 by cold maxizyme.

DISCUSSION

Ribozyme is a class of small catalytic RNA molecules that recognize specific substrate RNA by their complementary

nucleotide sequence, and cleave the substrate RNA as an endoribonuclease at enzymatic rate. It has been demonstrated that potential utility in attenuating eukaryotic gene expression was studied in preclinical gene therapy models. Among different types of ribozymes discovered, the hammerhead ribozyme has received a great deal of attention in recent years because of its application in treatment of malignant and infectious diseases^[38,39]. Many different hammerhead ribozymes targeting oncogene and HIV, HBV have been developed. The hammerhead ribozyme could cleave almost any RNA molecules containing the 3 base target recognition sequence NUX (N=any base, X is any nucleotide except G). The basic structure of a hammerhead ribozyme is composed of a catalytic core of 24 conserved bases containing helix II and two self-associating helices, I and III which are antisense to the substrate and position of ribozyme to catalyze cleavage. However, because the limited number of cleavable sequences on target RNA, in some cases conventional hammerhead ribozyme does not have precise cleavage specificity. Some scientists found that the stem II (loop II) region of hammerhead ribozyme did not appear to be directly involved in catalysis. For development of chemically synthesized ribozyme as potential therapeutic agent, it would certainly be advantageous to remove surplus nucleotides. This consideration led to the production of minizymes, which are conventional hammerhead ribozyme with a deleted stem II region. But the activities of minizyme are two or three orders of magnitude lower than those of the parental hammerhead ribozyme, suggesting that minizymes might not be suitable as gene inactivating reagents. But Kinetic and NMR analysis indicated that the minizyme was essentially inactive as a monomer but exhibited strong catalytic activity as a dimer. This dimeric structure is called maxizyme^[40-42]. The maxizyme is also a metalloenzyme, its activity depends on the presence or absence of the correct formation of Mg ion-binding pocket. The maxizyme could bind to two different substrate-binding sites, one substrate-binding site functions as the “eye” that identifies the specific mRNA, whereas the other serves as the “scissors” and cleaves the target mRNA. Some studies showed that only after binding to the target gene can the maxizyme form a cavity that captures the Mg ions.

As a novel class of ribozyme, maxizyme that targets different chimeric genes has been studied^[43,45]. The chimeric gene is generated as a result of reciprocal chromosomal translocation. A well known chimeric gene is BCR-ABL gene which causes chronic myelogenous leukemia(CML). In the design of ribozyme that might cleave chimeric mRNA, it is necessary to avoid the cleavage of normal mRNA. There have been many attempts to specifically cleave chimeric BCR-ABL gene using ribozymes, but it is very difficult to cleave only chimeric gene without affecting the normal genes, such as BCR or ABL gene. Kuwabara *et al.*^[44] designed a maxizyme directly against BCR-ABL mRNA. The results showed that the maxizyme had extremely high specificity and high level activity not only *in vitro* but also in cultured cells. p53 mutation in 249 codon was observed in 50 % of hepatocellular carcinoma. Some studies have suggested that p53 has a gain of transforming function after mutation in addition to loss of tumor suppressor activity. Several groups have attempted to develop gene therapy methods to treat HCC via introduction of wild-type p53 cDNA into cancer cells. Unfortunately, these approaches did not result in regulated expression of p53 gene and did not reduce the expression of mutant p53 that was overexpressed in HCC cells. These shortcomings may greatly limit the utility of this gene replacement approach.

We designed a maxizyme directing against mutant-type p53 (249 codon). The cleavage results showed that the maxizyme cleaved mtp53 target mRNA efficiently. More encouraging

was that no cleavage was found in wild-type p53 under the same conditions. The activity of maxizyme must have originated from the formation of active heterodimers. So control of inactive maxizyme was also made by the mutation of a functionally indispensable ($G^5 \rightarrow A^5$) in the catalytic core. The *in vitro* cleavage reaction showed that the inactive maxizyme had no effects on target mRNA. This suggests that the cleavage effects of active maxizyme are clearly originated from the chemical cleavage. For the application of maxizyme to gene therapy, they must be expressed *in vivo* under the control of a strong promoter. Development of an efficient system for the expression of a small piece of RNA in the cell, such as antisense RNA and ribozyme, is a major challenge in nonviral gene therapy. Recently, U6 RNA has been explored to drive the expression of antisense RNA and oligonucleotide. It is much efficient than the CMV promoter which is used often^[46,47]. In our study, the U6 expression system was explored for the construction of maxizyme plasmid. These lay a good foundation for the study in HCC cell lines.

In conclusion, the results of the present study showed that chimeric U6 maxizyme could cleave mtp53 mRNA *in vitro* with high efficiency. Anti-mtp53 maxizyme may be a promising tool for the treatment of hepatocellular carcinoma with an oncogenic mutation in codon 249 of p53 gene.

ACKNOWLEDGEMENTS

We would like to thank Dr Bert Vogelstein for his generous gift of plasmid p53. We also thank Mr.F Xu, Mr.XL Chen and Miss W Li for their kind help.

REFERENCES

- Tang ZY.** Hepatocellular carcinoma-cause,treatment and metastasis. *World J Gastroenterol* 2001; **7**: 445-454
- Tang ZY.** Advances in clinical research of hepatocellular carcinoma in China. *Huaren Xiaohua Zazhi* 1998; **6**: 1013-1016
- Lin NF, Tang J, Ismael HS.** Study on environmental etiology of high incidence areas of liver cancer in China. *World J Gastroenterol* 2000; **6**: 572-576
- Zhai SH, Liu JB, Liu YM, Zhang LL, Du ZH.** Expression of HBsAg, HCV-Ag and AFP in liver cirrhosis and hepatocarcinoma. *Shijie Huaren Xiaohua Zazhi* 2000; **8**: 524-527
- Li Y, Tang ZY, Ye SL, Lin YK, Chen J, Xue Q, Chen J, Gao DM, Bao WH.** Establishment of cell clones with different metastatic potential from the metastatic hepatocellular carcinoma cell line MHCC97. *World J Gastroenterol* 2001; **7**: 630-636
- Qin LL, Su JJ, Li Y, Yang C, Ban KC, Yian RQ.** Expression of IGF-II, p53, p21 and HBxAg in precancerous events of hepatocarcinogenesis induced by AFB1 and/or HBV in tree shrews. *World J Gastroenterol* 2000; **6**: 138-139
- Blandino G, Levine AJ, Oren M.** Mutant p53 gain of function: differential effects of different p53 mutants on resistance of cultured cells to chemotherapy. *Oncogene* 1999; **18**: 477-485
- Sohn S, Jaitovitch-Groisman I, Benlimame N, Galipeau J, Batist G, Alaoui-Jamali MA.** Retroviral expression of the hepatitis B virus x gene promotes liver cell susceptibility to carcinogen-induced site specific mutagenesis. *Mutation Res* 2000; **460**: 17-28
- Ghebranious N, Sell S.** Hepatitis B injury, male gender, aflatoxin, and p53 expression each contribute to hepatocarcinogenesis in transgenic mice. *Hepatology* 1998; **27**: 383-391
- Bressac B, Kew M, Wands J, Ozturk M.** Selective G to T mutations of p53 gene in hepatocellular carcinoma from southern Africa. *Nature* 1991; **350**: 429-431
- Prost S, Ford JM, Taylor C, Doig J, Harrison DJ.** Hepatitis B x protein inhibits p53-dependent DNA repair in primary mouse hepatocytes. *J Bio Chem* 1998; **273**: 33327-33332
- Liu H, Wang Y, Zhou Q, Gui SY, Li X.** The point mutation of p53 gene exon 7 in hepatocellular carcinoma from Anhui Province, a non HCC prevalent area in China. *World J Gastroenterol* 2002; **8**: 480-482
- Niu ZS, Li BK, Wang M.** Expression of p53 and C-myc genes and its clinical relevance in the hepatocellular carcinomatous and pericarcinomatous tissues. *World J Gastroenterol* 2002; **8**: 822-826
- Levine AJ.** P53, the cellular gatekeeper for growth and division. *Cell* 1997; **88**: 323-331
- Qin LX, Tang ZY, Ma ZC, Wu ZQ, Zhou XD, Ye QH, Ji Y, Huang LW, Jia H L, Sun HC, Wang L.** p53 immunohistochemical scoring: an independent prognostic marker for patients after hepatocellular carcinoma resection. *World J Gastroenterol* 2002; **8**: 459-463
- Doppert W, Gohler T, Koga H, Kom E.** Mutant p53: "gain of function" through perturbation of nuclear structure and function? *J Cell Biochem Suppl* 2000; **35**(Suppl): 115-122
- Lee YI, Lee S, Das GC, Park US, Park SM, Lee YI.** Activation of the insulin-like growth factor II transcription by aflatoxin B1 induced p53 mutant 249 is caused by activation of transcription complexes; implications for a gain-of-function during the formation of hepatocellular carcinoma. *Oncogene* 2000; **19**: 3717-3726
- Koga H, Deppert W.** Identification of genomic DNA sequences bound by mutant p53 protein(Gly245->Ser) *in vivo*. *Oncogene* 2000; **19**: 4178-4183
- Zheng SX, Liu LJ, Shao YS, Zheng QP, Ruan YB, Wu ZB.** Relationship between ras p53 gene RNA and protein expression and HCC metastasis. *Huaren Xiaohua Zazhi* 1998; **6**: 104-105
- Phylactou LA.** Ribozyme and peptide-nucleic acid-based gene therapy. *Adv Drug Deliv Rev* 2000; **44**: 97-108
- Song YH, Lin JS, Liu NZ, Kong XJ, Xie N, Wang NX, Jin YX, Liang KH.** Anti-HBV hairpin ribozyme-mediated cleavage of target RNA *in vitro*. *World J Gastroenterol* 2002; **8**: 91-94
- Tanaka M, Kijima H, Itoh J, Matsuda T, Tanaka T.** Impaired expression of a human septin family gene Bradeion inhibits the growth and tumorigenesis of colorectal cancer *in vitro* and *in vivo*. *Cancer Gene Ther* 2002; **9**: 483-488
- Tokunaga T, Abe Y, Tsuchide T, Hatanaka H, Oshika Y, Tomisawa M, Yoshimura M, Ohnishi Y, Kijima H, Yamazaki H, Ueyama Y, Nakamura M.** Ribozyme mediated cleavage of cell-associated isoform of vascular endothelial growth factor inhibits liver metastasis of a pancreatic cancer cell line. *Int J Oncol* 2002; **21**: 1027-1032
- Qu Y, Liu S, Liu B.** Attenuation of telomerase activity by hammerhead ribozyme targeting the 5' -end of hTERT mRNA. *Zhonghua Yixue Yichuanxue Zazhi* 2002; **19**: 389-392
- Blount KF, Grover NL, Mokler V, Beigelman L, Uhlenbeck OC.** Steric interference modification of the hammerhead ribozyme. *Chem Biol* 2002; **9**: 1009-1016
- Huesker M, Folmer Y, Schneider M, Fulda C, Blum HE, Hafkemeyer P.** Reversal of drug resistance of hepatocellular carcinoma cells by adenoviral delivery of anti-MDR1 ribozymes. *Hepatology* 2002; **36**: 874-884
- Sullenger BA, Gilboa E.** Emerging clinical applications of RNA. *Nature* 2002; **418**: 252-258
- Xu R, Lin J, Zhou X, Xie Q, Jin Y, Yu H, Liao D.** Activity identification of anti-caspase-3 mRNA hammerhead ribozyme in both cell-free condition and BRL-3A cells. *Chinese Medical Journal(Engl)* 2001; **114**: 606-611
- Yu YC, Mao Q, Gu CH, Li QF, Wang YM.** Activity of HDV ribozymes to trans-cleave HCV RNA. *World J Gastroenterol* 2002; **8**: 694-698
- Zhang YA, Nemunaitis J, Tong AW.** Generation of a ribozyme-adenoviral vector against k-ras mutant human lung cancer cells. *Mol Biotechnol* 2000; **15**: 39-49
- Hammann C, Lilley DM.** Folding and activity of the hammerhead ribozyme. *ChemBiochem* 2002; **3**: 690-700
- Sioud M, Opstad A, Hendry P, Lockett TJ, Jennings PA, McCall MJ.** A minimised hammerhead ribozyme with activity against interleukin-2 in human cells. *Biochem Biophys Res Commun* 1997; **231**: 397-402
- Amontov S, Nishikawa S, Taira K.** Dependence on Mg²⁺ ions of the activities of dimeric hammerhead minizymes. *FEBS Lett* 1996; **386**: 99-102
- Iyo M, Kawasaki H, Taira K.** Allosterically controllable maxizymes for molecular gene therapy. *Curr Opin Mol Ther* 2002; **4**: 154-165
- Tani K.** Target therapy for CML-applying maxizyme. *Nippon Rinsho* 2001; **59**: 2439-2444

- 36 **Kuwabara T**, Hamada M, Warashina M, Taia K. Allosterically controlled single-chained maxizymes with extremely high and specific activity. *Biomacromolecules* 2001; **2**: 788-799
- 37 **Kuwabara T**, Tanabe T, Warashina M, Xiong KX, Tani K, Taira K, Asano S. Allosterically controllable maxizyme-mediated suppression of progression of leukemia in mice. *Biomacromolecules* 2001; **2**: 1220-1228
- 38 **Morino F**, Tokunaga T, Tsuchida T, Handa A, Nagata J, Tomii Y, Kijima H, Yamazaki H, Watanabe N, Matsuzaki S, Ueyama Y, Nakamura M. Hammerhead ribozyme specifically inhibits vascular endothelial growth factor gene expression in a human hepatocellular carcinoma cell line. *Int J Oncol* 2000; **17**: 495-499
- 39 **Ozaki I**, Zern MA, Liu S, Wei DL, Pomerantz RJ, Duan L. Ribozyme-mediated specific gene replacement of the alpha1-antitrypsin gene in human hepatoma cells. *J Hepatol* 1999; **31**: 53-60
- 40 **Kuwabara T**, Warashina M, Taira K. Cleavage of an inaccessible site by the maxizyme with two independent binding arms: an alternative approach to the recruitment of RNA helicases. *J Biochem (Tokyo)* 2002; **132**: 149-155
- 41 **Kuwabara T**, Warashina M, Taira K. Allosterically controllable maxizymes cleave mRNA with high efficiency and specificity. *Trends Biotechnol* 2000; **18**: 462-468
- 42 **Nakayama A**, Warashina M, Kuwabara T, Taira K. Effects of cetyltrimethylammonium bromide on reactions catalyzed by maxizymes, a novel class of metalloenzymes. *J Inorg Biochem* 2000; **78**: 69-77
- 43 **Hamada M**, Kuwabara T, Warashina M, Nakayama A, Taira K. Specificity of novel allosterically trans- and cis-activated connected maxizymes that are designed to suppress BCR-ABL expression. *FEBS Lett* 1999; **461**: 77-85
- 44 **Kuwabara T**, Warashina M, Tanabe T, Tani K, Asano S, Taira K. A novel allosterically trans-activated ribozyme, the maxizyme, with exceptional specificity in vitro and in vivo. *Mol Cell* 1998; **2**: 617-627
- 45 **Suwanai H**, Matsushita H, Kobayashi H, Ikeda Y, Kizaki M. A novel therapeutic technology of specific RNA inhibition for acute promyelocytic leukemia: improved design of maxizymes against PML/RARalpha mRNA. *Int J Oncol* 2002; **20**: 127-130
- 46 **Kuwabara T**, Warashina M, Orita M, Koseki S, Ohkawa J, Taira K. Formation of a catalytically active dimer by tRNA(Val)-driven short ribozymes. *Nat Biotechnol* 1998; **16**: 961-965
- 47 **Lui VW**, He Y, Huang L. Specific down-regulation of HER-2/neu mediated by a chimeric U6 hammerhead ribozyme results in growth inhibition of human ovarian carcinoma. *Mol Ther* 2001; **3**: 169-177

Edited by Yuan HT and Wang XL

High level of deoxycholic acid in human bile does not promote cholesterol gallstone formation

Ulf Gustafsson, Staffan Sahlin, Curt Einarsson

Ulf Gustafsson, Staffan Sahlin, Department of Surgery, Danderyd Hospital, Stockholm, Sweden

Curt Einarsson, Division of Gastroenterology and Hepatology, Department of Medicine, Huddinge University Hospital, Karolinska Institutet, Stockholm, Sweden

Supported by the grants from the Swedish Science Council

Correspondence to: Dr. Curt Einarsson, Division of Gastroenterology and Hepatology, Department of Medicine, K63, Huddinge University Hospital, SE-141 86 Stockholm, Sweden. curt.einarsson@medhs.ki.se

Telephone: +46-8-58582328 **Fax:** +46-8-58582335

Received: 2002-12-07 **Accepted:** 2002-12-22

Abstract

AIM: To study whether patients with excess deoxycholic acid (DCA) differ from those with normal percentage of DCA with respect to biliary lipid composition and cholesterol saturation of gallbladder bile.

METHODS: Bile was collected during operation through puncturing into the gallbladder from 122 cholesterol gallstone patients and 46 gallstone-free subjects undergoing cholecystectomy. Clinical data, biliary lipids, bile acid composition, presence of crystals and nucleation time were analyzed.

RESULTS: A subgroup of gallstone patients displayed a higher proportion of DCA in bile than gallstone free subjects. By choosing a cut-off level of the 90th percentile, a group of 13 gallstone patients with high DCA levels (mean 50 percent of total bile acids) and a large group of 109 patients with normal DCA levels (mean 21 percent of total bile acids) were obtained. The mean age of the patients with high DCA levels was higher than that of the group with normal levels (mean age: 62 years vs 45 years) and so was the mean BMI (28.3 vs. 24.7). Plasma levels of cholesterol and triglycerides were slightly higher in the DCA excess groups compared with those in the normal DCA group. There was no difference in biliary lipid composition, cholesterol saturation, nucleation time or occurrence of cholesterol crystals in bile between patients with high and normal levels of DCA.

CONCLUSION: Gallstone patients with excess DCA were of older age and had higher BMI than patients with normal DCA. The two groups of patients did not differ with respect to biliary lipid composition, cholesterol saturation, nucleation time or occurrence of cholesterol crystals. It is concluded that DCA in bile does not seem to contribute to gallstone formation in cholesterol gallstone patients.

Gustafsson U, Sahlin S, Einarsson C. High level of deoxycholic acid in human bile does not promote cholesterol gallstone formation. *World J Gastroenterol* 2003; 9(7): 1576-1579
<http://www.wjgnet.com/1007-9327/9/1576.asp>

INTRODUCTION

The two major primary bile acids formed in human liver are

cholic acid (CA) and chenodeoxycholic acid (CDCA). During the enterohepatic circulation, CA and CDCA are partly 7 α -dehydroxylated by microbial enzymes, yielding deoxycholic acid (DCA) and lithocholic acid, respectively^[1]. Only a small amount of lithocholic acid is absorbed from the intestine, whereas DCA is efficiently reabsorbed mainly via active transport in the distal part of ileum but also by passive diffusion along the small intestine and probably also from the proximal part of colon. DCA constitutes usually 10-35 % of bile acids in the bile. However, individuals may vary widely in the proportion of DCA in bile from 0 to more than 50 % of biliary bile acids. These wide inter-individual variations in DCA probably reflect the difference in colonic flora.

According to some previous studies, the proportion of DCA in bile of patients with cholesterol gallstone is higher than that of stone-free subjects and it has been suggested that DCA may play a role in cholesterol gallstone formation^[2-8]. Other authors have found a normal percentage of DCA in patients with cholesterol gallstones^[9-13]. An increased proportion of DCA in the bile acid pool of gallstone patients has been associated with higher levels of 7 α -dehydroxylating faecal bacteria^[6,14]. In a recent study, Thomas *et al*^[8] found an increased 7 α -hydroxylating activity in the caecal aspirates of patients with cholesterol gallstones, which was associated with slower colonic transit time and increased percentage of DCA in fasting serum. Berr *et al*^[6] have reported about a subgroup of cholesterol gallstone patients with DCA excess and increased 7 α -dehydroxylating activity and levels of faecal 7 α -dehydroxylating bacteria which may trigger cholesterol gallstone disease.

In a recent study including large series of gallstone patients and gallstone free subjects, we could not find a significantly higher proportion of biliary DCA in cholesterol gallstone patients compared to pigment stone patients or gallstone-free subjects^[13]. No correlation was found between the percentage of DCA and cholesterol saturation in gallbladder bile. However, a subgroup of the patients with cholesterol gallstones had a high percentage of DCA.

The purpose of this study was to study whether patients with excess DCA differed from patients with a normal percentage of DCA with respect to biliary lipid composition, cholesterol saturation, nucleation time and occurrence of cholesterol crystals in gallbladder bile.

MATERIALS AND METHODS

Patients

The patients in the present study were included in a recent report from our group dealing with lipid composition of gallbladder bile in large series of patients with cholesterol gallstones and pigment stones and gallstone free subjects undergoing elective cholecystectomy^[13]. In this study, only cholesterol gallstone patients ($n=122$) and gallstone-free subjects ($n=46$) in which data on biliary bile acid composition were available were included. Data on the patients are shown in Table 1. None of the patients had clinical or laboratory evidence of diabetes mellitus, alcohol abuse or other diseases that affect the function of the kidney or the liver. The patients

Table 1 Clinical data of patients with cholesterol gallstones and gallstone free subjects

Group	<i>n</i>	Female/male ratio(% Female)	Median age years (range)	Body mass index kg/m ² (<i>n</i>)	Plasma cholesterol mmol/l (<i>n</i>)	Plasma triglycerides mmol/l (<i>n</i>)
Total gallstone	122	96/26 (79)	49 (18-83)	25.0±0.3 (111)	5.7±0.1 (81)	1.5±0.1 (82)
High DCA	13	10/3 (77)	62 ^b (37-74)	28.3±1.3 ^b (10)	6.4±0.3 ^a (11)	2.2±0.4 ^a (10)
Low DCA	109	86/23 (79)	45 (18-83)	24.7±0.4 (101)	5.6±0.1 (70)	1.5±0.1 (72)
Gallstone free	46	38/18 (83)	45 (20-71)	23.2±0.5 ^c (45)	5.8±0.2 (36)	1.4±0.1 (36)

Notes: Mean values ± Standard Error of the Mean. *n*=number. ^a*P*<0.05 vs Low DCA, ^b*P*<0.005 vs Low DCA, ^c*P*<0.01 vs Total gallstone.

were not on any medications known to affect lipid metabolism. None of the patients received or had been treated with antibiotics prior to or during cholecystectomy. The gallstone-free patients were cholecystectomized either because of polyps, cholesterosis or adenomyomatosis or because of frequent, recurrent right upper biliary colic and other symptoms suggestive of gallbladder dysfunction.

Informed consent was obtained from each patient before operation. The ethical aspects of the study were approved by the Ethical Committee at Karolinska Institutet, Stockholm.

Experimental procedure

All patients were hospitalized in the surgical ward. The operations were done after an overnight fasting. After opening the abdomen or in the case of a laparoscopic procedure following application of pneumoperitoneum and establishing four laparoscopic ports, the gall bladder was completely emptied of bile with a sterile needle and syringe to avoid possible stratification of bile^[15]. Indicative of a functioning gallbladder was the presence of dark concentrated bile in the gallbladder and no evidence of impacted stones in the neck of the cystic duct at operation. The gall bladder was then removed. The gallstones were classified as cholesterol stones by visual inspection and when necessary by analysis in the laboratory^[16,17]. All gall bladders were routinely examined by a pathologist.

Analysis of biliary lipids and calculation of cholesterol saturation

Gallbladder bile was extracted with chloroform-methanol (2/1, w/w) for measurement of cholesterol and phospholipids. Cholesterol was measured by an enzymatic method^[18] and phospholipids by the method of Rouser *et al*^[19]. The total bile acid concentration in one aliquot of the bile sample was measured using a 3- α -hydroxysteroid dehydrogenase assay^[20]. Cholesterol saturation was calculated as a percentage of the predicted cholesterol solubility at the respective biliary lipid concentration and composition as described by Carey^[21].

Measurement of bile acid composition

Aliquots of bile were hydrolyzed in 1 mol/L potassium hydroxide at 110 °C for 12 h. The conjugated bile acids were extracted with diethyl ether after acidification to pH 1 with hydrochloric acid. After preparation of trimethylsilyl ethers, the bile acids were analyzed by gas-liquid chromatography using 1 % Hi-Eff BP 8 as the stationary phase. A Pye Unicam gas chromatograph (Pye Unicam Ltd, Cambridge, UK) equipped with a 1.5 m×4 mm column was used^[22].

Analysis of cholesterol crystals and nucleation time

Bile samples were examined for typical rhomboid monohydrate cholesterol crystals by polarising light microscopy on pre-warmed slides. Nucleation time (NT) was determined by the method of Holan *et al*^[23] with minor modifications^[24].

Statistical analysis

Data were presented as mean ± SEM. The statistical significance of differences was evaluated with Student's *t*-test. Nucleation time was evaluated by Wilcoxon's sum of rank test.

RESULTS

Age, body mass index and plasma lipids

As can be seen in Figure 1, a subgroup of gallstone patients displayed a higher proportion of DCA in bile than gallstone-free subjects. Choosing a cut-off level of the 90th percentile, a group of 13 gallstone patients with high DCA-levels was obtained. The proportion of DCA in the high DCA-group averaged 50 % compared with 21 % in the normal DCA-group.

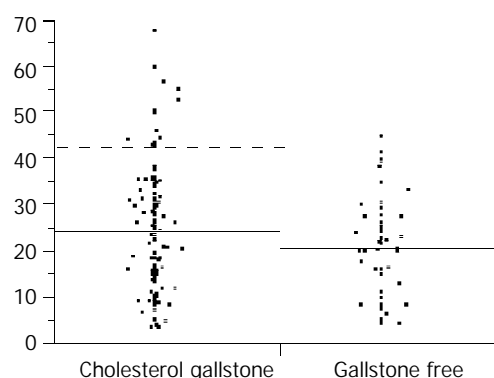


Figure 1 Deoxycholic acid levels in 122 gallstone patients and 46 gallstone free patients (Dotted line represented the 90th percentile in the gallstone patients).

The mean age of the patients with high DCA-levels was significantly higher than that of the patients with normal DCA-levels (mean ages: 62 years vs 45 years, Table 1). The mean body mass index (BMI) was also higher in the high DCA-group, 28.3, compared to 24.7 in the normal DCA-group (*P*<0.005). Plasma levels of cholesterol and triglycerides were slightly higher in the high DCA-group.

Lipid composition, cholesterol saturation, nucleation time and occurrence of crystals in gallbladder bile

The results are summarized in Table 2. There was no difference in biliary lipid composition, total lipid concentration or cholesterol saturation of bile between patients with high and normal levels of DCA. The molar percentage of cholesterol in cholesterol gallstone patients was significantly higher (7.8 mol %), compared to gallstone-free subjects (5.8 mol %). The total biliary lipid concentration was significantly lower in cholesterol gallstone patients compared to gallstone-free patients. Also the mean cholesterol saturation was significantly higher in gallstone patients (112 %) compared to gallstone-free subjects (79 %), (*P*<0.0001).

Table 2 Occurrence of crystals and lipid composition in gallbladder bile of patients with cholesterol gallstones and gallstone free subjects

Group (n)	Single stone % (n)	Crystals positive % (n)	Median nucleation time days, (range) (n)	Cholesterol mol %	Bile acid mol %	Phospholipids mol %	Total lipid concentration g/dl	Cholesterol saturation %
Total gallstone (122)	29 (116)	79 (112)	6 (1-56) (46)	7.8±0.3	68.6±0.6	23.6±0.4	9.4±0.4	112±4
High DCA (13)	42 (12)	73 (11)	14 (2-28) (4)	8.1±0.6	68.1±1.6	23.8±1.2	8.2±1.0	116±10
Low DCA (109)	28 (104)	79 (101)	3 (1-56) (42)	7.8±0.3	68.7±0.6	23.6±0.5	9.6±0.5	112±5
Gallstone free (46)	-	11 ^a (45)	17 ^a (1-35) (24)	5.8±0.3 ^a	71.3±0.8	22.9±0.7	13.1±0.6 ^a	79±3 ^a

Notes: Mean values ± Standard Error of the Mean. n=Number of observations. ^aP<0.0001 vs Total gallstone.

Table 3 Bile acid composition in patients with cholesterol gallstones and gallstone free subjects

Group	n	Cholic acid %	Deoxycholic acid %	Chenodeoxy-cholic acid %	Lithocholic acid %	Ursodeoxy-cholic acid %
Total gallstone	122	38.9±1.0	24.2±1.2	34.5±0.9	1.0±0.1	1.3±0.2
High DCA	13	22.7±1.7	50.0±2.1	24.5±1.7	1.4±0.4	1.3±0.9
Low DCA	109	40.8±1.0	21.1±0.9	35.7±0.9	0.9±0.1	1.3±0.2
Gallstone free	46	46.1±1.6 ^b	20.7±1.6	30.6±1.0 ^a	0.6±1.6	1.7±0.4

Notes: Mean values ± Standard Error of the Mean. n=Number of observations, ^aP<0.05 vs Total gallstone, ^bP<0.001 vs Total gallstone.

There was a tendency to shorter nucleation time in patients with normal DCA-levels compared to those with high DCA-levels, but the difference did not reach statistical significance. The proportion of patients with crystals in their bile was the same between patients with high and normal levels of DCA. Nucleation time was significantly shorter in cholesterol gallstone patients compared to that in gallstone-free patients, 6 days vs. 17 days ($P<0.0001$). The proportion of patients with bile positive for cholesterol crystals was significantly higher among gallstone patients (79 %) compared to gallstone-free subjects (11 %), ($P<0.0001$).

Bile acid composition

The bile acid composition is summarized in Table 3. The proportion of cholic acid was significantly lower and that of chenodeoxycholic acid was higher in the gallstone patients compared to the gallstone-free patients. There was no significant difference in the proportion of deoxycholic acid, lithocholic acid or ursodeoxycholic acid between gallstone patients and gallstone-free subjects.

DISCUSSION

In the present study, a subgroup of cholesterol gallstone patients with a high proportion of DCA in the gallbladder bile, mean 50 %, was compared to gallstone patients with a normal proportion of DCA, mean 21 %. The high DCA-level was not associated with either higher cholesterol content or cholesterol saturation of bile. The proportion of patients with cholesterol crystals in the bile did not differ between patients with high and normal levels of DCA. Nor was the nucleation time shortened in patients with high DCA content. If anything, there was a tendency to longer nucleation time in patients with high DCA-levels although the difference was not significant. These results were in agreement with some previous studies, showing that a high proportion of DCA in human gallbladder bile was not associated with a higher risk for formation of cholesterol gallstones^[9-13].

The gallstone patients with a high level of DCA were of older age than those with a normal level of DCA. The reason why old age is associated with a high percentage of DCA in bile is not quite apparent. Slow colonic transit has been reported to lead to high biliary proportions of DCA, probably by increasing the intestinal residence time of bile salts^[2]. Recently,

Thomas *et al*^[8] reported that slow colonic transit in combination with increased number of colonic gram-positive anaerobes and greater 7 α -dehydroxylating activity favours enhanced DCA-formation in gallstone patients. Berr *et al*^[6] also found that a group of gallstone patients with DCA-excess had higher 7 α -dehydroxylating activity and increased counts of 7 α -dehydroxylating bacteria in feces compared with a group of patients with normal DCA, but this difference was not due to a slow intestinal transit time. In agreement with that, van der Werf *et al*^[25] have previously shown that elderly persons (55-75 years old) have a higher fractional turnover of cholic acid and a higher deoxycholic acid input rate from the large bowel than young adults (20-30 years old) and this is not due to any difference in gut transit time.

Another finding of this study was that high level of DCA was also associated with high BMI. This could indicate a potential role of BMI as a confounder when analysing biliary DCA levels in studies on cholesterol gallstone patients.

To conclude, gallstone patients with excess DCA are of older age and have higher BMI than patients with normal DCA. The two groups of patients do not differ with respect to biliary lipid composition, cholesterol saturation, nucleation time or occurrence of cholesterol crystals. These findings further underline that DCA in bile does not significantly contribute to cholesterol gallstone formation.

ACKNOWLEDGMENTS

We greatly appreciate the skilful technical assistance by Ms Ingela Arvidsson and Ms Lisbet Benthin.

REFERENCES

- Carey MC, Duane WC. Enterohepatic circulation. In: Arias IM, Boyer JL, Fausto N, Jakoby WB, Schachter D, Shafritz DA, eds. The liver: biology and pathobiology. New York: Raven Press 1994: 719-767
- Marcus NS, Heaton KW. Intestinal transit, deoxycholic acid and the cholesterol saturation of bile - three inter-related factors. *Gut* 1986; **27**: 550-558
- Berr F, Schreiber E, Frick U. Interrelationships of bile acid and phospholipid fatty acid species with cholesterol saturation of duodenal bile in health and gallstone disease. *Hepatology* 1992; **16**: 71-81
- Hussaini SH, Pereira SP, Murphy GM, Dowling RH. Deoxycholic acid influences cholesterol solubilization and microcrystal nucle-

- ation time in gallbladder bile. *Hepatology* 1995; **22**: 1735-1744
- 5 **Shoda J**, He BF, Tanaka N, Matsuzaki Y, Osuga T, Yamamori S, Miyazaki H, Sjövall J. Increase of deoxycholate in supersaturated bile of patients with cholesterol gallstone disease and its correlation with de novo syntheses of cholesterol and bile acids in liver, gallbladder emptying and small intestinal transit. *Hepatology* 1995; **21**: 1291-1302
 - 6 **Berr F**, Kullak-Ublick GA, Paumgartner G, Munzing W, Hylemon PB. 7 α -dehydroxylating bacteria enhance deoxycholic acid input and cholesterol saturation of bile in patients with gallstones. *Gastroenterology* 1996; **111**: 1611-1620
 - 7 **Azzaroli FG**, Mazzella G, Mazzeo C, Simoni P, Festi D, Colecchia A, Montagnani M, Martino C, Villanova N, Roda A, Roda E. Sluggish small bowel motility is involved in determining increased biliary deoxycholic acid in cholesterol gallstone patients. *Am J Gastroenterol* 1999; **94**: 2453-2459
 - 8 **Thomas LA**, Veysey MJ, Bathgate T, King A, French G, Smeeton NC, Murphy GM, Dowling RH. Mechanism for the transit-induced increase in colonic deoxycholic acid formation in cholesterol cholelithiasis. *Gastroenterology* 2000; **119**: 806-815
 - 9 **Van Erpecum KJ**, Portincasa P, Stolk MFJ, Van de Heijning BJM, Van der Zaag ES, Van den Broek AMWC, Van Berge Henegouwen GP, Renooij W. Effects of bile salt and phospholipid hydrophobicity on lithogenicity of human gallbladder bile. *Eur J Clin Invest* 1994; **24**: 744-750
 - 10 **Noshiro H**, Chijiwa K, Makino I, Nakano K, Hirota I. Deoxycholic acid in gall bladder bile does not account for the shortened nucleation time in patients with cholesterol gall stones. *Gut* 1995; **36**: 121-125
 - 11 **Miguel JF**, Nunez L, Amigo L, Gonzalez S, Raddatz A, Rigotti A, Nervi F. Cholesterol saturation, not proteins or cholecystitis, is critical for crystal formation in human gallbladder bile. *Gastroenterology* 1998; **114**: 1016-1023
 - 12 **Jungst D**, Muller I, Kullak-Ublick GA, Meyer G, Frimberger E, Fischer S. Deoxycholic acid is not related to lithogenic factors in gallbladder bile. *J Lab Clin Med* 1999; **133**: 370-377
 - 13 **Gustafsson U**, Sahlin S, Einarsson C. Biliary lipid composition in patients with cholesterol and pigment gallstones and gallstone-free subjects: deoxycholic acid does not contribute to formation of cholesterol gallstones. *Eur J Clin Invest* 2000; **30**: 1099-1106
 - 14 **Wells JE**, Berr F, Thomas LA, Dowling RH, Hylemon PB. Isolation and characterization of cholic acid 7 α -dehydroxylating fecal bacteria from cholesterol gallstone patients. *J Hepatol* 2000; **32**: 4-10
 - 15 **Tera H**. Stratification of human gallbladder bile *in vivo*. *Acta Chir Scand Supplement* 1960; **256**: 4-65
 - 16 **Trotman BW**, Ostrow JD, Soloway RD. Pigment vs cholesterol cholelithiasis: comparison of stone and bile composition. *Am J Dig Dis* 1974; **19**: 585-590
 - 17 **Whiting MJ**, Down RH, Watts JMCK. Biliary crystals and granules, the cholesterol saturation index, and the prediction of gallstone type. *Surg Gastroenterol* 1982; **1**: 17-21
 - 18 **Roda A**, Festi D, Sama C, Mazzella G, Aldini T, Roda E, Barbara L. Enzymatic determination of cholesterol in bile. *Clin Chim Acta* 1975; **64**: 337-341
 - 19 **Rouser G**, Fleischer S, Yamamoto A. Two dimensional thin layer chromatography separation of polar lipids and determination of phospholipids by phosphorous analysis of spots. *Lipids* 1970; **5**: 494-496
 - 20 **Fausa O**, Skallehegg BA. Quantitative determination of bile acids and their conjugates using thin-layer chromatography and a purified 3 α -hydroxysteroid dehydrogenase. *Scand J Gastroenterol* 1974; **9**: 249-254
 - 21 **Carey MC**. Critical tables for calculating the cholesterol saturation of native bile. *J Lipid Res* 1978; **19**: 945-955
 - 22 **Angelin B**, Einarsson K, Leijd B. Biliary lipid composition during treatment with different hypolipidaemic drugs. *Eur J Clin Invest* 1979; **9**: 185-190
 - 23 **Holan KR**, Holzbach RT, Hermann RE, Cooperman AM, Claffey WJ. Nucleation time; a key factor in the pathogenesis of cholesterol gallstone disease. *Gastroenterology* 1979; **77**: 611-617
 - 24 **Sahlin S**, Ahlberg J, Angelin B, Reihner E, Einarsson K. Nucleation time of gall bladder bile in gallstone patients: influence of bile acid treatment. *Gut* 1991; **32**: 1554-1557
 - 25 **Van der Werf SDJ**, Huijbregts AWM, Lamers HLM, van Berge Henegouwen GP, van Tongeren JHM. Age dependent differences in human bile acid metabolism and 7 α -dehydroxylation. *Eur J Clin Invest* 1981; **11**: 425-431

Edited by Xu XQ

Association of *CagA* and *VacA* presence with ulcer and non-ulcer dyspepsia in a Turkish population

Kantarceken Bulent, Aladag Murat, Atik Esin, Koksal Fatih, Harputluoglu MMMurat, Harputluoglu Hakan, Karıncaoglu Melih, Ates Mehmet, Yildirim Bulent, Hilmioglu Fatih

Kantarceken Bulent, Aladag Murat, Karıncaoglu Melih, Hilmioglu Fatih, Division of Gastroenterology, Medical Faculty, Inonu University, Malatya, Turkey
Atik Esin, Mustafa Kemal University, Department of Pathology, Medical Faculty, Hatay, Turkey
Koksal Fatih, Department of Microbiology, Medical Faculty, Cukurova University, Adana, Turkey
Harputluoglu MMMurat, Ates Mehmet, Division of Gastroenterology, Medical Faculty, Inonu University, Malatya, Turkey
Harputluoglu Hakan, Department of Internal Medicine, Medical Faculty, Inonu University, Malatya, Turkey
Yildirim Bulent, Division of Gastroenterology, Medical Faculty, Inonu University, Malatya, Turkey
Correspondence to: Bulent Kantarceken, Zafer Mah. Mehmet Buyruk Cad. 2.Ordu karsýsý Hapimbey Apt. Dai. No: 19, 44300/Malatya, Turkey. bkantarceken@inonu.edu.tr, bulentkc@lycos.com
Telephone: +90-422-3411199 **Fax:** +90-422-3410729(28)
Received: 2003-01-14 **Accepted:** 2003-02-25

Abstract

AIM: The mostly known genotypic virulence features, of *H. pylori* are cytotoxin associated gene A (*cagA*) and Vacuolating cytotoxin gene A (*VacA*). We investigated the association of these major virulence factors with ulcer and non-ulcer dyspepsia in our region.

METHODS: One hundred and forty two dyspeptic patients were studied (average age 44.8±15.9 years, range 15-87 years, 64 males and 78 females). Antral and corpus biopsies were taken for detecting and genotyping of *H. pylori*. 107 patients who were *H. pylori* positive by histological assessment were divided into three groups according to endoscopic findings: Duodenal ulcer (DU), gastric ulcer (GU) and non-ulcer dyspepsia (NUD). The polymerase chain reaction (PCR) was used to detect *CagA* and *VacA* genes of *H. pylori* using specific primers.

RESULTS: *H. pylori* was isolated from 75.4 % (107/142) of the patients. Of the 107 patients, 66 (61.7 %) were *cagA*-positive and 82 (76.6 %) were *VacA*-positive. *CagA* gene was positively associated with DU and GU ($P<0.01$, $P<0.02$), but not with NUD ($P>0.05$). Although *VacA* positivity in ulcer patients was higher than that in NUD group, the difference was not statistically significant ($P>0.05$).

CONCLUSION: There is a significantly positive association between *CagA* genes and DU and GU. The presence of *VacA* is not a predictive marker for DU, GU, and NUD in our patients.

Bulent K, Murat A, Esin A, Fatih K, MMMurat H, Hakan H, Melih K, Mehmet A, Bulent Y, Fatih H. Association of *CagA* and *VacA* presence with ulcer and non-ulcer dyspepsia in a Turkish population. *World J Gastroenterol* 2003; 9(7): 1580-1583
<http://www.wjgnet.com/1007-9327/9/1580.asp>

INTRODUCTION

Helicobacter pylori (*H. pylori*) is a gram-negative, spiral shaped microaerophilic bacterium that colonizes in the gastric mucosa in humans^[1]. In the majority of individuals, infection causes asymptomatic histological chronic gastritis. A significant minority subsequently develop peptic ulcer disease (PUD), and infection with *H. pylori* is a significant risk factor for gastric carcinoma and mucosa-associated lymphoid tissue (MALT) lymphoma^[2-4]. The process by which different disease patterns develop has not been fully elucidated. But two putative virulence determinants of *H. pylori* have been identified as markers of ulcerogenic strains, the cytotoxin associated gene A (*CagA*) and the vacuolating cytotoxin gene A (*VacA*) (Phenotype 1, ulcerogenic; *CagA* & *VacA*-positive, phenotype 2, non-ulcerogenic; *CagA* & *VacA*-negative). The *CagA* gene encodes a 120-140 kDa protein of unknown function in about 60-70 % of *H. pylori* strains. This gene is part of the *cag* pathogenicity island (PAI), a 40-kbp segment with several genes involved in cytokine production^[5, 6]. Strains that do not produce the *CagA* protein generally lack the entire *cag* PAI. *H. pylori* strains produced by *CagA* have been detected in patients with PUD more frequently than in patients with chronic gastritis alone^[7- 9]. Another virulence factor that injures epithelial cells is encoded by *VacA*. *VacA* is present nearly in all *H. pylori* strains and contains at least two variable parts^[10,12]. The s-region (encoding the signal peptide) exists as s1 or s2 allelic types. Among type s1 strains, subtypes s1a, s1b, and s1c have been identified. The m-region (middle) occurs as m1 or m2 allelic types. Among type m2, two subtypes have been identified, and designated as m2a and m2b^[11]. Production of the vacuolating cytotoxin is related to the mosaic structure of *VacA*. The *VacA* signal sequence type s1, but not type s2 is closely associated with *in vitro* cytotoxin activity, PUD, and the presence of *CagA* gene^[9, 10, 12]. The m1 allele is associated with higher levels of toxin activity and more severe gastric epithelial damage than the m2 allele^[10, 12].

MATERIALS AND METHODS

Materials

Patients and classification of endoscopic findings One hundred forty two dyspeptic patients (excluding those taking proton pump inhibitors [PPIs] and/or NSAIDs in the past month, and/or had previous *H. pylori* eradication) were studied (average age 44.8±15.9 years, range 15-87 years, 64 males and 78 females) and referred for routine endoscopy at the Department of Gastroenterology in the Turgut Özal Medical Center, Malatya, Turkey. Endoscopic findings were recorded and according to endoscopic findings, *H. pylori* positive patients were divided into three groups: Group 1: Patients with duodenal ulcer (DU); Group 2: Patients with gastric ulcer (GU); Group 3: Patients with non-ulcer dyspepsia (NUD). All the patients gave informed consent to participate in the study.

Methods

Endoscopy and detection of *H. pylori* by histological assessment During each endoscopic procedure (by Olympus

GIF XQ 240 videoendoscope), two antral and two corpus mucosal biopsy specimens were obtained by using biopsy forceps (FB-25 k; Olympus, Japan) which were cleaned with a detergent and disinfected after each examination. Two biopsy samples were transported to pathology laboratory and fixed in 10 % formalin overnight. Tissue processing was undertaken with graded ethanol solutions and clearing was made with xylene. Paraffin tissue blocks were cut into 4-5 µm sections with a rotary microtome. The sections were stained with hematoxylin-eosin and tissue Giemsa and assessed for the presence of *H.pylori* microorganisms. 107 (75.4 %) patients (average age 45.8±15.7 years, range 17-87 years, 50 males and 57 females) were found to be *H. pylori* positive and the other two biopsy specimens of those patients were transported to the microbiology laboratory for PCR examination to determine *CagA* and *VacA* status.

PCR examination Biopsy samples obtained from 107 patients with positive *H. pylori* were put into 20 % dextrose solution and stored at -20 °C until a sufficient number was reached for PCR assay. The transport media contained the tissue samples were discarded and the tissue samples were resuspended with 100-200 µg/ml of lysis buffer (10 mM Tris-HCL, 0.1 M EDTA, 5 % SDS, 100-200 µg/ml proteinase K). The mixture was incubated at 52 °C for 2 hours in a thermal cycler. 100 µl phenol-chloroform-isoamyl alcohol (25:24:1) was added into the mixture. The mixture was then vortexed and centrifuged at 5 000×g for 5 minutes. The supernatant was discarded and isoamyl alcohol (24:1) was added as much as the taken volume. The mixture was vortexed and centrifuged as described above. The supernatant was discarded and 2.5 volume of cold ethanol (70 %) was added and stored at -20 °C overnight. On the following day, the mixture was centrifuged at 13 000×g for 13 minutes. The supernatant was discarded and the pellet was resuspended with TE buffer and used for PCR assay. The reaction mixture (50 µl) was prepared for *CagA* as described below. 2 µl dNTP mix (200 µM/ µl of each deoxynucleotide), 1 µl primer I (0.5 µM/1 µl of each oligonucleotide), 1 µl primer II, 1 µl taq polymerase (2.5U/ µl), 4.5 µl 10×PCR buffer, 0.5 µl MgCl₂ (5 µM/ µl), 35 µl distilled water, 5 µl sample DNA. PCR reaction was performed in the thermal cycler (M.J. research) with the following incubation steps: at 94 °C for 4 min (Pre-heating), 35 cycles at 94 °C for 1 min (denaturation), at 57 °C 1.30 min (annealing) and at 74 °C for 2 min (elongation), 1 cycle at 74 °C for 5 min post elongation. *CagA* primers: 5' -GAT AAC AGG CAA GCT TTT GAG G-3', 5' - CTG CAA AAG ATT ATT TGG CAA GA-3' targeting 349 bp fragment. The reaction mixture was prepared for *VacA* as described below. 2 µl dNTP mix, 1 µl primer I, 1 µl primer II, 1 µl taq polymerase, 4.5 µl 10×PCR buffer, 0.5 µl MgCl₂, 35 µl distilled water, 5 µl sample DNA. Then at 94 °C for 1 min (denaturation), at 63 °C for 1.30 min (annealing), at 72 °C for 1 min (elongation), 30 cycles, and at 74 °C for 5 min 1 cycle for post elongation. *VacA* primers: 5' - CCG AAG AAG CCA ATA AAA CCC CAG-3', 5' - CAA AGT CAA AAC CGT AGA GCT GGC-3' targeting 467 bp fragment. The PCR products were analysed by 2 % agarose gel with 0.5 % ethidium bromide via electrophoresis.

Statistical analysis

Normal χ^2 analysis and Fisher's exact χ^2 method were used for statistical evaluation of data derived from the results of the procedures mentioned above.

RESULTS

Prevalence of *H. pylori* infection

H. pylori infection was found in 107 of 142 patients (75.4 %).

Endoscopic findings

35 of the 107 patients had DU (32.7 %), 24 (22.4 %) GU and 48 NUD (44.9 %).

Prevalence of *CagA* and *VacA* among *H. pylori* positive patients

While 66 of 107 *H. pylori* strains were *CagA* positive (61.7 %), 82 of the patients were *VacA* positive (76.6 %), and 62 of the patients were both *CagA* and *VacA* positive (57.9 %).

Relation between *CagA-VacA* status and DU, GU, and NUD

28 of 35 patients with DU (80 %), 20 of 24 patients with gastric ulcers (83.3 %) and 18 of 48 patients with NUD (37.5 %) were *CagA* positive. The presence of *CagA* in the patients with DU and GU was significantly higher than that in the patients with NUD, respectively ($P=0.007$, $P=0.013$). *CagA* positivity was statistically lower in patients with NUD ($P<0.001$). 29 of 35 patients with DU (82.9 %), 21 of 24 patients with gastric ulcer (87.5 %), and 32 of 48 patients with NUD (66.7 %) were *VacA* positive. *VacA* positivity was both higher in the patients with DU and GU than that in the patients with NUD, but this difference between the groups was not statistically significant ($P>0.05$). We detected phenotype 1 *H. pylori*, characterized by the expression of both *CagA* and *VacA*, in 57.9 % (62 of 107) of the patients (71.4 % DU, 79.2 % GU, 37.5 % NUD patients). The prevalence of phenotype 1 was significantly higher in patients with duodenal or gastric ulcer, than that in the patients with NUD ($P<0.0004$, $P<0.0002$). Phenotype 2 *H. pylori* characterized by a lack of expression of either *CagA* or *VacA*, was found in 19.6 % of the patients (21 of 107) in our study (8.6 % DU, 8.3 % GU, 33.3 % NUD). The prevalence of phenotype 2 in the patients with NUD was significantly higher than that in patients with duodenal or gastric ulcer ($P<0.01$, $P<0.04$). The remaining 22.4 % of the total number of patients studied (24 of 107) had an intermediate phenotype, which expressed either *CagA* independent of the presence of *VacA* (*CagA*-positive and *VacA*-negative, 3.7 %) or vice versa (*CagA*-negative and *VacA* positive, 18.7 %). There was not any significant difference between the groups according to intermediate phenotypes ($P>0.05$) (Table 1).

DISCUSSION

The most common interaction between *H. pylori* and human is asymptomatic bacterial colonisation in the gastric mucosa, which can be continued lifelong. However, the presence of this bacterium in an individual increases the risk of serious

Table 1 Distribution of endoscopic findings according to *CagA* and *VacA* status

	<i>CagA</i> +	<i>VacA</i> +	<i>CagA</i> + <i>VacA</i> + (Phenotype 1)	<i>CagA</i> + <i>VacA</i> -	<i>CagA</i> - <i>VacA</i> +	<i>CagA</i> - <i>VacA</i> - (Phenotype 2)
DU(35)	28(80%)	29(82.8%)	25(71.4%)	3(8.6%)	4(11.4%)	3(8.6%)
GU(24)	20(83.3%)	21(87.5%)	19(79.2%)	1(4.2%)	2(8.3%)	2(8.3%)
NUD(48)	18(37.5%)	32(66.6%)	18(37.5%)	0(0.0%)	14(29.2%)	16(33.3%)
Total(107)	66(61.6%)	82(76.6%)	62(57.9%)	4(3.7%)	20(18.6%)	21(19.6%)

gastroduodenal diseases such as gastritis, GU, DU, gastric cancer and MALT lymphoma^[3, 4, 13, 14]. It has been suggested that *H. pylori* may induce more or less severe gastroduodenal diseases according to the strain virulence. Two major markers of virulence, *CagA* and *VacA*, have been described in *H. pylori*. The association between putative virulence markers with ulcer and NUD was investigated in a Turkish population.

In our study, the presence of *CagA*, and both *CagA* and *VacA* was significantly more prevalent in patients with DU and GU, than those in patients with NUD ($P < 0.05$). The positivity of *VacA* was higher in the patients with DU and GU than that in the patients with NUD, but difference was not statistically significant ($P > 0.05$). Previous studies from different countries showed that *CagA*-positive strains were more common in patients with ulcer disease. *CagA*-positive strains were found in 79 % to 100 % of DU patients^[7, 8, 15, 18-31], 71 % to 100 % of GU patients^[7-9, 19, 20, 27, 28], as compared with 37 % to 89.7 % of NUD patients^[8, 18-24, 26-31]. In the present study, we found a significantly higher prevalence of *CagA*-positive strains in DU and GU than that in NUD patients (80 %, 83.3 %, and 37.5 %, respectively). It was reported from different centers that in patients with duodenal ulcer, the positivity rates of *cagA*, *VacA*, and both *CagA* and *VacA* were 79-100 %, 47.5-92 %, 37-75 %, respectively^[7, 8, 15, 18-31]. The positivity rates of *CagA*, *VacA*, and both *CagA* and *VacA* in the patients with gastric ulcer, have been reported to be 71-100 %, 40.8-75 %, and 38.8-56.6 %, respectively^[7-9, 19-30]. In all of these studies, the positivity of *CagA* and *VacA* was higher in the patients with DU or GU, however some was statistically significant^[7-10, 12, 15-18, 24-26, 28-31] and some not^[19-21, 23, 32, 33, 35-37, 39, 42, 43] when it was compared to patients without ulcer.

In patients with NUD, the positivity rates of *CagA* and *VacA* were reported to be 37-89.7 %^[8, 18, 19, 21-24, 26, 28, 29] and 33.3-73 %^[8, 19, 21-23, 28-30], respectively. Nearly in all of these studies, *CagA* and *VacA* positivity rate in the patients with NUD was found to be low compared to that in the patients with ulcer, however, this difference was statistically significant in some studies^[7-9, 15-18, 24-26, 28-30], but not in some others^[19-21, 23, 27, 33, 35-38, 41, 42]. In our study, the *CagA* positivity in the patients with NUD was significantly lower than that in the ulcer patients ($P < 0.01$). This supported the results of DU and GU mentioned above. Although *VacA* positivity was higher in the patients with ulcer than that in the patients with NUD, this was not statistically significant and did not seem to be an important risk factor for the development of ulcer in our patients. However, determination the *VacA* genotypes and the presence of *CagA* gene together may contribute to potential clinic determination of patients who have different levels of risk. It has been shown that *VacA* type s1/m1 strains produce more cytotoxins than type s1/m2, and that type s2/m2 strains do not produce active cytotoxins^[10]. Many studies have confirmed these findings^[9, 12, 24, 25, 31, 38]. In this study, we couldn't detect the *VacA* subtypes for not having their primers. Also, we had no information on the *in vitro* cytotoxin production of our strains, so we could not compare our results directly with those from other studies. If we could have determined these factors, perhaps we would find an association between *VacA* and ulcer disease. It was reported that the presence of *CagA* and *VacA* genes in *H. pylori* isolates increased the risk of gastric cancer^[22, 40] but some studies refused this^[37, 41, 42]. In two studies, no statistically significant difference between the presence of *CagA* or *VacA* in patients with MALT lymphoma and NUD was found^[8]. In another study which interrogated the importance of the presence of *CagA* for developing resistance to metronidazole, which was used in eradication therapies of *H. pylori*, an association between resistance and the presence of *CagA* was not shown. It was investigated that if the patients could be selected for gastroscopy adequately only by looking

for anti *H. pylori* and anti-*CagA* serologically, and it was observed that the method was not adequate for screening, since many serious pathology and malignancy could not have been noticed by just a selection of this method^[43].

Gastroduodenal lesions developed in the patients infected with *H. pylori* isolates that had *CagA* and *VacA* gene and showed differences according to regions, countries and ethnic groups. In the literature, it has been controversial that *CagA* and *VacA* positive isolates cause more serious gastroduodenal lesions^[7-42]. In our study, it was seen that gastric and duodenal ulcer incidence increased in the patients with *CagA*, and both *CagA* and *VacA* positive. Recently, it was reported similar results for *CagA* in ulcer patients from Turkey obtained by using an ELISA method^[46]. Many risk factors have been determined for *H. pylori* infection (*CagA*, *VacA*, *IceA* etc.), but none of them is specific for disease. It has been put forward that *CagA* plays a partial role in increased mucosal inflammation, increased density of *H. pylori* in antrum, and causes more profound inhibition of mucin synthesis, DU, GU and gastric cancer^[7-9, 39, 44], and has a protective role in Barrett's esophagitis^[16, 17]. However direct association was found only with IL-8 induction^[32, 34, 45]. The *IceA* gene, considered as a virulence factor for *H. pylori* infection recently, has no disease specific features, and there is no biologic and epidemiologic evidences that *IceA* gene is a virulence factor associated with *H. pylori*^[33, 34]. The opinion that *VacA* genotyping may be useful clinically (for example, predicting the presence of DU) is controversial from now on^[19, 32, 34].

As a result, the association between, the virulence factors in *H. pylori* positive patients, clinical course and gastroduodenal lesions that develop subsequently has not been understood yet. For determining these interactions, it needs great scale and multicenter studies which examine the structural features of *H. pylori* (virulence factors), host features and environmental features together. To have definite results, study must be large enough and include different diseases and ethnic groups. Also, in our country, multicenter and large scale studies would reveal the virulence differences between different regions.

REFERENCES

- 1 Warren JR, Marshall BJ. Unidentified curved bacilli on gastric epithelium in active chronic gastritis. *Lancet* 1983; **1**: 1273-1275
- 2 Parsonnet J, Friedman GD, Vandersteen DP, Chang Y, Vogelstein JH, Orentreich N, Sibley RK. *Helicobacter pylori* infection and the risk of gastric carcinoma. *N Engl J Med* 1991; **325**: 1127-1131
- 3 Wotherspoon AC, Dogliani C, Diss TC, Pan L, Moschini A, de Boni M, Isaacson PG. Regression of primary low-grade B-cell gastric lymphoma of mucosa-associated lymphoid tissue type after eradication of *Helicobacter pylori*. *Lancet* 1993; **342**: 575-577
- 4 An international association between *Helicobacter pylori* infection and gastric cancer. The EUROGAST Study Group. *Lancet* 1993; **341**: 1359-1362
- 5 Censini S, Lange C, Xiang Z, Crabtree JE, Ghiara P, Borodovsky M, Rappuoli R, Covacci A. *cagA*, a pathogenicity island of *Helicobacter pylori*, encodes type I-specific and disease-associated virulence factors. *Proc Natl Acad Sci U S A* 1996; **93**: 14648-14653
- 6 Covacci A, Falkow S, Berg DE, Rappuoli R. Did the inheritance of a pathogenicity island modify the virulence of *Helicobacter pylori*? *Trends Microbiol* 1997; **5**: 205-208
- 7 Martin Guerrero JM, Hergueta Delgado P, Esteban Carretero J, Romero Castro R, Pellicer Bautista FJ, Herrerias Gutierrez JM. Clinical relevance of *Helicobacter pylori* *CagA*-positive strains: gastroduodenal peptic lesions marker. *Rev Esp Enferm Dig* 2000; **92**: 160-173
- 8 Lamarque D, Gilbert T, Roudot-Thoraval F, Deforges L, Chaumette MT, Delchier JC. Seroprevalence of eight *Helicobacter pylori* antigens among 182 patients with peptic ulcer, MALT gastric lymphoma or non-ulcer dyspepsia. Higher rate of seroreactivity against *CagA* and 35-kDa antigens in patients with peptic ulcer originating from Europe and Africa. *Eur J Gastroenterol Hepatol* 1999; **11**: 721-726
- 9 Rudi J, Rudy A, Maiwald M, Kuck D, Stieg A, Stremmel W. Di-

- rect determination of *Helicobacter pylori* vacA genotypes and cagA gene in gastric biopsies and relationship to gastrointestinal diseases. *Am J Gastroenterol* 1999; **94**: 1525-1531
- 10 **Atherton JC**, Cao P, Peek RM Jr, Tummuru MK, Blaser MJ, Cover TL. Mosaicism in vacuolating cytotoxin alleles of *Helicobacter pylori*. Association of specific vacA types with cytotoxin production and peptic ulceration. *J Biol Chem* 1995; **270**: 17771-17777
 - 11 **van Doorn LJ**, Figueiredo C, Sanna R, Pena S, Midolo P, Ng EK, Atherton JC, Blaser MJ, Quint WG. Expanding allelic diversity of *Helicobacter pylori* vacA. *J Clin Microbiol* 1998; **36**: 2597-2603
 - 12 **Atherton JC**, Peek RM Jr, Tham KT, Cover TL, Blaser MJ. Clinical and pathological importance of heterogeneity in vacA, the vacuolating cytotoxin gene of *Helicobacter pylori*. *Gastroenterology* 1997; **112**: 92-99
 - 13 **Sipponen P**, Hyvarinen H. Role of *Helicobacter pylori* in the pathogenesis of gastritis, peptic ulcer and gastric cancer. *Scand J Gastroenterol Suppl* 1993; **196**: 3-6
 - 14 **Cullen DJE**, Collins BJ, Christiansen KJ. Long term risk of peptic ulcer disease in people with *Helicobacter pylori* infection. A community based study. *Gut* 1993; **34**: F284
 - 15 **Lin CW**, Wu SC, Lee SC, Cheng KS. Genetic analysis and clinical evaluation of vacuolating cytotoxin gene A and cytotoxin-associated gene A in Taiwanese *Helicobacter pylori* isolates from peptic ulcer patients. *Scand J Infect Dis* 2000; **32**: 51-57
 - 16 **Vaezi MF**, Falk GW, Peek RM, Vicari JJ, Goldblum JR, Perez-Perez GI, Rice TW, Blaser MJ, Richter JE. CagA-positive strains of *Helicobacter pylori* may protect against Barrett's esophagus. *Am J Gastroenterol* 2000; **95**: 2206-2211
 - 17 **Loffeld RJ**, Werdmuller BF, Kuster JG, Perez-Perez GI, Blaser MJ, Kuipers EJ. Colonization with cagA-positive *Helicobacter pylori* strains inversely associated with reflux esophagitis and Barrett's esophagus. *Digestion* 2000; **62**: 95-99
 - 18 **Hennig EE**, Trzeciak L, Regula J, Butruk E, Ostrowski J. VacA genotyping directly from gastric biopsy specimens and estimation of mixed *Helicobacter pylori* infections in patients with duodenal ulcer and gastritis. *Scand J Gastroenterol* 1999; **34**: 743-749
 - 19 **Mahachai V**, Tangkijvanich P, Wannachai N, Sumpathanukul P, Kullavanijaya P. CagA and VacA: virulence factors of *Helicobacter pylori* in Thai patients with gastroduodenal diseases. *Helicobacter* 1999; **4**: 143-147
 - 20 **Tokumaru K**, Kimura K, Saifuku K, Kojima T, Satoh K, Kihira K, Ido K. CagA and cytotoxicity of *Helicobacter pylori* are not markers of peptic ulcer in Japanese patients. *Helicobacter* 1999; **4**: 1-6
 - 21 **Marshall DG**, Hynes SO, Coleman DC, O' Morain CA, Smyth CJ, Moran AP. Lack of a relationship between Lewis antigen expression and cagA, CagA, vacA and VacA status of Irish *Helicobacter pylori* isolates. *FEMS Immunol Med Microbiol* 1999; **24**: 79-90
 - 22 **Basso D**, Navaglia F, Brigato L, Piva MG, Toma A, Greco E, Di Mario F, Galeotti F, Roveroni G, Corsini A, Plebani M. Analysis of *Helicobacter pylori* vacA and cagA genotypes and serum antibody profile in benign and malignant gastroduodenal diseases. *Gut* 1998; **43**: 182-186
 - 23 **Holtmann G**, Talley NJ, Mitchell H, Hazell S. Antibody response to specific *H. pylori* antigens in functional dyspepsia, duodenal ulcer disease, and health. *Am J Gastroenterol* 1998; **93**: 1222-1227
 - 24 **Evans DG**, Queiroz DM, Mendes EN, Evans DJ Jr. *Helicobacter pylori* cagA status and s and m alleles of vacA in isolates from individuals with a variety of *H. pylori*-associated gastric diseases. *J Clin Microbiol* 1998; **36**: 3435-3437
 - 25 **Stephens JC**, Stewart JA, Folwell AM, Rathbone BJ. *Helicobacter pylori* cagA status, vacA genotypes and ulcer disease. *Eur J Gastroenterol Hepatol* 1998; **10**: 381-384
 - 26 **Warburton VJ**, Everett S, Mapstone NP, Axon AT, Hawkey P, Dixon MF. Clinical and histological associations of cagA and vacA genotypes in *Helicobacter pylori* gastritis. *J Clin Pathol* 1998; **51**: 55-61
 - 27 **Takata T**, Fujimoto S, Anzai K, Shirohara T, Okada M, Sawae Y, Ono J. Analysis of the expression of CagA and VacA and the vacuolating activity in 167 isolates from patients with either peptic ulcers or non-ulcer dyspepsia. *Am J Gastroenterol* 1998; **93**: 30-34
 - 28 **Ito A**, Fujioka T, Kodama K, Nishizono A, Nasu M. Virulence-associated genes as markers of strain diversity in *Helicobacter pylori* infection. *J Gastroenterol Hepatol* 1997; **12**: 666-669
 - 29 **Donati M**, Moreno S, Storni E, Tucci A, Poli L, Mazzoni C, Varoli O, Sambri V, Farencena A, Cevenini R. Detection of serum antibodies to CagA and VacA and of serum neutralizing activity for vacuolating cytotoxin in patients with *Helicobacter pylori*-induced gastritis. *Clin Diagn Lab Immunol* 1997; **4**: 478-482
 - 30 **Weel JF**, van der Hulst RW, Gerrits Y, Roorda P, Feller M, Dankert J, Tytgat GN, van der Ende A. The interrelationship between cytotoxin-associated gene A, vacuolating cytotoxin, and *Helicobacter pylori*-related diseases. *J Infect Dis* 1996; **173**: 1171-1175
 - 31 **Kidd M**, Lastovica AJ, Atherton JC, Louw JA. Heterogeneity in the *Helicobacter pylori* vacA and cagA genes: association with gastroduodenal disease in South Africa? *Gut* 1999; **45**: 499-502
 - 32 **Audibert C**, Janvier B, Grignon B, Salaun L, Burucoa C, Lecron JC, Fauchere JL. Correlation between IL-8 induction, cagA status and vacA genotypes in 153 French *Helicobacter pylori* isolates. *Res Microbiol* 2000; **151**: 191-200
 - 33 **Zheng PY**, Hua J, Yeoh KG, Ho B. Association of peptic ulcer with increased expression of Lewis antigens but not cagA, iceA, and vacA in *Helicobacter pylori* isolates in an Asian population. *Gut* 2000; **47**: 18-22
 - 34 **Graham DY**, Yamaoka Y. Disease-specific *Helicobacter pylori* virulence factors: the unfulfilled promise. *Helicobacter* 2000; **5**: S27-31
 - 35 **Mukhopadhyay AK**, Kersulyte D, Jeong JY, Datta S, Ito Y, Chowdhury A, Chowdhury S, Santra A, Bhattacharya SK, Azuma T, Nair GB, Berg DE. Distinctiveness of genotypes of *Helicobacter pylori* in Calcutta. *India J Bacteriol* 2000; **182**: 3219-3227
 - 36 **Opazo P**, Muller I, Rollan A, Valenzuela P, Yudelevich A, Garcia-de la Guarda R, Urrea S, Venegas A. Serological response to *Helicobacter pylori* recombinant antigens in Chilean infected patients with duodenal ulcer, non-ulcer dyspepsia and gastric cancer. *APMIS* 1999; **107**: 1069-1078
 - 37 **Kodama K**, Ito A, Nishizono A, Fujioka T, Nasu M, Yahiro K, Hirayama T, Uemura N. Divergence of virulence factors of *Helicobacter pylori* among clinical isolates does not correlate with disease specificity. *J Gastroenterol* 1999; **34**(Suppl 11): 6-9
 - 38 **Pan ZJ**, van der Hulst RW, Tytgat GN, Dankert J, van der Ende A. Relation between vacA subtypes, cytotoxin activity, and disease in *Helicobacter pylori*-infected patients from The Netherlands. *Am J Gastroenterol* 1999; **94**: 1517-1521
 - 39 **Beil W**, Enns ML, Muller S, Obst B, Sewing KF, Wagner S. Role of vacA and cagA in *Helicobacter pylori* inhibition of mucin synthesis in gastric mucous cells. *J Clin Microbiol* 2000; **38**: 2215-2218
 - 40 **Rudi J**, Kolb C, Maiwald M, Zuna I, von Herbay A, Galle PR, Stremmel W. Serum antibodies against *Helicobacter pylori* proteins VacA and CagA are associated with increased risk for gastric adenocarcinoma. *Dig Dis Sci* 1997; **42**: 1652-1659
 - 41 **Matsukura N**, Onda M, Kato S, Hasegawa H, Okawa K, Shirakawa T, Tokunaga A, Yamashita K, Hayashi A. Cytotoxin genes of *Helicobacter pylori* in chronic gastritis, gastroduodenal ulcer and gastric cancer: an age and gender matched case-control study. *Jpn J Cancer Res* 1997; **88**: 532-536
 - 42 **Mitchell HM**, Hazell SL, Li YY, Hu PJ. Serological response to specific *Helicobacter pylori* antigens: antibody against CagA antigen is not predictive of gastric cancer in a developing country. *Am J Gastroenterol* 1996; **91**: 1785-1788
 - 43 **Heikkinen M**, Janatuinen E, Mayo K, Megraud F, Julkunen R, Pikkarainen P. Usefulness of anti-*Helicobacter pylori* and anti-CagA antibodies in the selection of patients for gastroscopy. *Am J Gastroenterol* 1997; **92**: 2225-2229
 - 44 **McGee DJ**, Mobley HL. Mechanisms of *Helicobacter pylori* infection: bacterial factors. *Curr Top Microbiol Immunol* 1999; **241**: 155-180
 - 45 **Yamaoka Y**, Kodama T, Graham DY, Kashima K. Search for putative virulence factors of *Helicobacter pylori*: the low-molecular-weight (33-35 K) antigen. *Dig Dis Sci* 1998; **43**: 1482-1487
 - 46 **Demirturk L**, Ozel AM, Yazgan Y, Solmazgul E, Yildirim S, Gultepe M, Gurbuz AK. CagA status in dyspeptic patients with and without peptic ulcer disease in Turkey: association with histopathologic findings. *Helicobacter* 2001; **6**: 163-168

Expression of local renin and angiotensinogen mRNA in cirrhotic portal hypertensive patient

Li Zhang, Zhen Yang, Bao-Min Shi, Da-Peng Li, Chong-Yun Fang, Fa-Zu Qiu

Li Zhang, Bao-Min Shi, Department of General Surgery, Shandong Provincial Hospital, Jinan 250021, Shandong Province, China

Zhen Yang, Fa-Zu Qiu, Department of General Surgery, Tongji Hospital, Tongji Medical College, Huazhong Science and Technology University, Wuhan 430030, Hubei Province, China

Da-Peng Li, Department of General Surgery, Shanghai First People's Hospital, Shanghai, 200080, China

Chong-Yun Fang, Immunology Institute of Tongji Medical College, Huazhong Science and Technology University, Wuhan 430030, Hubei Province, China

Supported by the National Natural Science Foundation of China, No 30170920

Correspondence to: Li Zhang, Department of General Surgery, Shandong Provincial Hospital, Jinan 250021, Shandong Province, China. pzzi@sina.com

Telephone: 0531-5266692

Received: 2002-11-29 **Accepted:** 2003-01-13

Abstract

AIM: To investigate the expression of local renin and angiotensinogen mRNA in cirrhotic portal hypertensive patients.

METHODS: The expression of local renin and angiotensinogen mRNA in the liver, splenic artery and vein of PH patients was detected by RT-PCR analysis.

RESULTS: Expression of local renin mRNA in the liver of control group was (0.19 ± 0.11) , significantly lower than that in splenic artery (0.45 ± 0.17) or splenic vein (0.39 ± 0.12) respectively, ($P < 0.05$). Expression of local angiotensinogen mRNA in the liver was (0.64 ± 0.21) , significantly higher than that in splenic artery (0.41 ± 0.15) or in splenic vein (0.35 ± 0.18) respectively, ($P < 0.05$). Expression of local renin mRNA in the liver, splenic artery and vein of PH group was (0.78 ± 0.28) , (0.86 ± 0.35) and (0.81 ± 0.22) respectively, significantly higher than that in the control group, ($P < 0.05$). Expression of local angiotensinogen mRNA in the liver, splenic artery and vein of PH group was (0.96 ± 0.25) , (0.83 ± 0.18) and (0.79 ± 0.23) respectively, significantly higher than that in the control group, ($P < 0.05$). There was no significant difference between the liver, splenic artery and vein in the expression of local renin or local angiotensinogen mRNA in PH group, ($P < 0.05$).

CONCLUSION: In normal subjects the expression of local renin and angiotensinogen mRNA was organ specific, but with increase of the expression of LRAS, the organ-specificity became lost in cirrhotic patients. LRAS may contribute to increased resistance of portal vein with liver and formation of splanchnic vasculopathy.

Zhang L, Yang Z, Shi BM, Li DP, Fang CY, Qiu FZ. Expression of local renin and angiotensinogen mRNA in cirrhotic portal hypertensive patient. *World J Gastroenterol* 2003; 9(7): 1584-1588
<http://www.wjgnet.com/1007-9327/9/1584.asp>

INTRODUCTION

The initial clues to the presence of an extrarenal or tissue RAS

were suggested in the studies of hypertension. Biochemical and histologic evidences have been established for the existence of a tissue-based RAS within a variety of tissues such as blood vessels, liver, kidney, spleen. Many researchers documented that this RAS system was functionally independent of the endocrine system^[1-3] and called tissue or local RAS (LRAS). Its activation includes both short and long-term regulatory roles in cardiovascular homeostasis and secondary structural changes, instead of short-term regulatory profile for endocrine RAS. Locally generated AngII plays a significant role not only in controlling the growth of vascular smooth muscle cells (VSMC), hepatocytes and hepatic satellite cells (HSC was one of the most important cells in liver fibrosis^[4-6]), but also in regulating local vascular tone including hepatic microcirculation. Hyperdynamic circulation and splanchnic vasculopathy were the common pathological process and changes in cirrhotic portal hypertension^[7-9], vascular and hepatic RAS may have great contribution to it. Through detection of expression of the two components of LRAS, the relationship between local renin and angiotensinogen and cirrhotic portal hypertension was investigated.

MATERIALS AND METHODS

Materials

The liver tissues and a section of splenic artery and vein were obtained during the operation of esophagogastric devascularization and splenectomy in 20 cirrhotic portal hypertensive patients. The same samples were obtained during splenectomy and partial hepatectomy in 24 controls.

13 male and 7 female patients were included in this study with mean age of 49 ± 21 , mild or severe gastroesophageal varices and splenomegaly were found in all patients.

16 male and 8 female subjects with mean age of 39 ± 17 served as control, 12 of them underwent partial hepatectomy for hepatic trauma and 12 underwent splenectomy for splenic injury. Those with hepatitis or hypertension were excluded.

A portion of the resected tissues was routinely fixed with 10 % formalin and embedded in paraffin and cut into sections, another portion of tissues was stored in liquid nitrogens at -80°C for use.

Methods

Immunohistochemical analysis To investigate splanchnic vascular changes in these patients, we took the splenic veins by using monoclonal anti-vascular smooth muscle cell α -cm-actin antibody, PCNA, and the splenic veins were stained with HE. Immunohistochemical analysis was performed according to routine methods as suggested by the manufacturer.

Preparation of specimens for electron microscopic observation Fresh vascular tissues were made into cubes of 1 mm^3 and prefixed for 2 h in 2.5 % glutaraldehyde, and then postfixed at 4°C for 2 h in 1 % osmic acid. Alcohol of increasing concentrations and acetone were used for dehydration. The specimens were then embedded in epoxy resin EPON 812 and cut into ultrathin sections. Plumbum-double-staining was used to prepare the samples for ultrastructural observation under transmission electron

microscope (Opton EM 10C Model).

Reverse-transcription polymerase chain reaction (RT-PCR)

Messenger RNA (mRNA) levels of local renin and angiotensinogen were assessed by RT-PCR analysis using β -actin as the house keeping gene. Total RNA was prepared from frozen tissues of the liver, splenic artery and vein. Diluted complementary DNA was cloned in a total volume of 50 μ l containing DEPC 31.5 μ l, buffer solution 5 μ l, dNTP 4 μ l, 2.5 mmol/l $MgCl_2$ 3 μ l, primers 20 μ mol*4 μ l, cDNA 2.5 μ l, and TAG 0.25 μ l. The PCR conditions were at 94 °C for 4 min followed by 35 cycles at 90 °C for 30 sec, at 54 °C for 30 sec, and at 72 °C for 1 min. Total RNA was also analyzed for β -actin transcript expression and PCR for 28 cycles for β -actin.

Table 1 Primer sequences

MRNA		Sequence	Size of products
Renin	sense	5' -TCT CAG CCA GGA CAT CAT CA-3'	288bp
	antisense	5' -AGT GGA AAT TCC CTT CGT AA-3'	
Angiotensinogen	sense	5' -TGT TGC TGC TGA GAA GAT TG-3'	256bp
	antisense	5' -CCG AGA AGT TGT CCT GGA TG -3'	

RT-PCR products were visualized under ultraviolet and analyzed by computer which provided the data for analysis. Study values were normalized as a ratio to the β -actin signal in each sample, and each value was analyzed as a transcriptional index (transcript of the interest mRNA expression in samples of interest/ β -actin mRNA expression in samples of interest).

Statistical analysis

P value <0.05 was considered statistically significant, and all variable data were summarized in terms of mean \pm SD and analyzed by Student *t* test using SAS software.

RESULTS

Immunohistochemical staining

In these patients, such typical cirrhotic changes as hepatocyte degeneration, necrosis, pseudolobule formation and fibrosis were seen, and splenic vein wall was thickened and VSMC in media tunica was disorderly arranged (Figures 1,2). With α -cm-actin antibody staining method, VSMC could be seen in the intima of splenic vein, suggesting migration of VSMC from media to intima. Hyperplasia of VSMC could be seen in both splenic artery and vein by PCNA staining (Figures 3,4), there was no obviously positive staining in the control group.

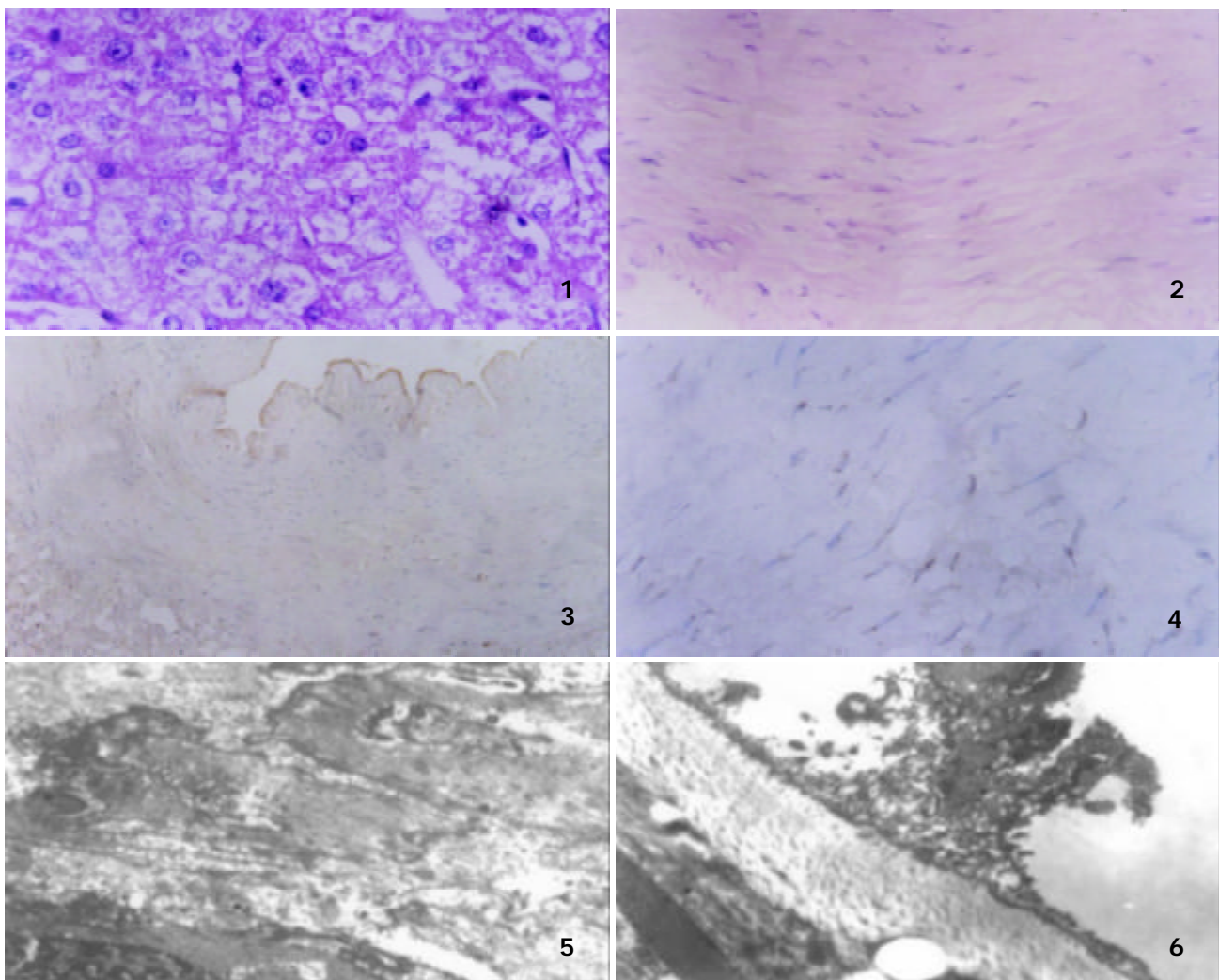


Figure 1 The liver tissue in portal hypertensive patients with HE staining \times (400).

Figure 2 Splenic vein in portal hypertensive patients with HE staining method (\times 400).

Figure 3 Splenic vein in portal hypertensive patients by immunohistochemical staining with α -cm-actin antibody (\times 400).

Figure 4 Splenic vein in portal hypertensive patients by immunohistochemical staining with PCNA (\times 400).

Figure 5 Splenic vein of portal hypertensive patients under transmission electron microscope (\times 4000).

Figure 6 Splenic vein of portal hypertensive patients under transmission electron microscope (\times 6000).

Electron microscopic observation

In the splenic vein of these patients, endothelium was damaged with adhered thrombus, VSMC of media migrated into the subintima under transmission electron microscopy (Figures 5,6).

RT-PCR analysis

In the control group, the expression of local renin mRNA in the liver was significantly lower than that in the splenic artery or vein, $P < 0.05$. Expression of local angiotensinogen mRNA in the liver was significantly higher than that in the splenic artery and vein, $P < 0.05$. There was no significant difference in the expression of local renin or angiotensinogen mRNA between splenic artery and vein. ($P > 0.05$, Figures 7,8,9).

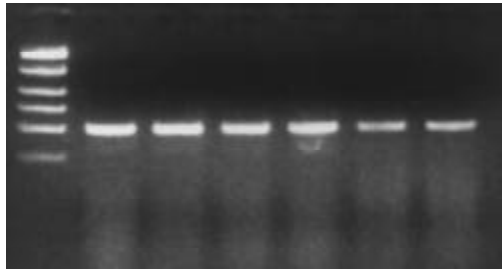


Figure 7 Expression of human β -actin mRNA (Note: from left to right there was PCR marker and lanes 1-6, figures 8,9 were the same).

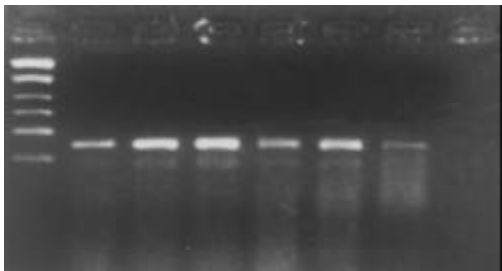


Figure 8 Expression of local renin mRNA in the liver, splenic artery and vein from the controls and cirrhotic portal hypertensive patients. Lanes 1,3,5 were splenic vein, artery and liver from controls, Lanes 2,4,6 were from patients.

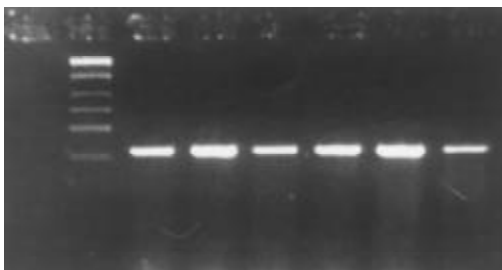


Figure 9 Expression of local angiotensinogen mRNA in the liver, splenic artery and vein from controls and portal hypertensive patients. Lanes 1,2,3 were splenic vein, artery and liver from controls, Lanes 4,5,6 were from portal hypertensive patients.

In cirrhotic portal hypertensive patient group, expression of local renin and angiotensinogen in liver, splenic artery and vein were all significantly higher than those in the controls respectively, $P < 0.05$. Expression of local renin and angiotensinogen mRNA in the liver was not significantly different from those in the splenic artery or vein in PH group, $P > 0.05$. The concrete data are listed in Table 2.

Table 2 Expression of local renin (Lr) and angiotensinogen (Lan) mRNA in the patient and control groups

	Control group (n=12)			Patient group (n=20)		
	Liver	Splenic artery	Splenic vein	Liver	Splenic artery	Splenic vein
Lr	0.19±0.11 ^a	0.45±0.17	0.39±0.12	0.78±0.28 ^b	0.86±0.35 ^b	0.81±0.22 ^b
Lan	0.64±0.21 ^a	0.41±0.15	0.35±0.18	0.96±0.25 ^b	0.83±0.18 ^b	0.79±0.23 ^b

The data were expressed as mean \pm SD. Lr and Lan mRNA in the patient group versus those in the control group, ^b $P < 0.05$. Within the same group, Lr and Lan mRNA in the liver versus those in splenic artery or vein respectively, ^a $P < 0.05$.

DISCUSSION

The results demonstrated that expression of hepatic renin and angiotensinogen mRNA in cirrhotic portal hypertensive patients was significantly higher than that of the controls. Therefore the end product of LRAS, the synthesized local AngII increased and exerted a strong effect on hepatic microcirculation via its paracrine pathway.

Firstly, local AngII constricted blood vessels as well as sinusoids leading to increase of intrahepatic portal venous pressure through an increase in intracellular calcium in VSMC. Although VSMC was absent in the hepatic sinusoid, hepatic stellate cells (HSCs) expressed receptors for AngII, could also contract and increase the intrahepatic resistance^[10-12].

Secondly, AngII has been shown to induce cell proliferation in various cell types, including hepatocytes and HSCs and was considered as a mediator of hepatic fibrogenesis^[3,13]. Local angiotensinogen also induced increase of TGF- β mRNA expression which was an important growth promoting factor for HSC^[14,15]. It was demonstrated that AngII could be a mitogenic factor for activated human HSCs through MAPK-dependent pathway^[3,16]. Significant relationship was seen between high TGF- β and AngII production and the development of progressive hepatic fibrosis caused by hepatitis C virus^[17,18]. AngII was also involved in the development of fibrosis in the heart and kidney through enhancement of TGF- β production^[19]. *In vitro* study found that AngII could increase mRNA levels for collagen types I and III, procollagen α (I) and fibronectin in cardiac fibrosis^[20]. Therefore it is possible that hepatic RAS plays an important role in the collagen synthesis, hepatic fibrosis and cirrhosis. In this study, the cirrhotic portal hypertension induced hepatic RAS activity which increased and accelerated the cirrhotic process and portal hypertension. By interrupting the vicious cycle, it was possible for medical treatment to prevent further progression of the disease. It has already been confirmed that catoprilil could reduce the expression of procollagenI significantly and prevent liver fibrogenesis in a rat model of hepatic fibrosis^[21-23].

The experimental data illustrated that expression of local renin and angiotensinogen mRNA in the splenic artery and vein of cirrhotic portal hypertensive patients was significantly higher than that of the controls and suggested that portal hypertension led to activation of LRAS of splenic vessels. The mechanism probably might be as follows: (1) Endothelial injury was caused by splanchnic hyperdynamic circulation and high blood flow shear, and the endothelial cells were the key site of LRAS metabolism^[2]. (2) The splenic vessel wall was stretched by the increment of splanchnic blood flow. (3) Influence of other vasoactive substance.

When the expression of LRAS increased in splenic vessel, it could participate in many pathologic processes. Firstly, vascular RAS induced VSMC proliferation and enhanced progression of vascular remodeling. AngII induced hypertrophy, proliferation and migration of VSMC^[24-26] with

modulation of expression of C-fos^[22], C-jun, C-myc and synthesis of cytokines such as PDGF, b-FGF^[23] etc. In this study, changes of VSMC in splenic vein of PH patients could be seen by HE stain, immunohistochemistry and electron microscopy. These suggested that vascular RAS was closely related with the structural alterations of the splenic vein. Response of VSMC to hypertension and injury of blood flow shear included: hypertrophy, proliferation and remodeling. As a result, the vascular RAS played an even more important role than endocrine RAS^[27-30]. In addition, the matrix modulation was another key event in remodeling and vasculopathy^[7,8]. Other studies reported that vascular RAS modulated the synthesis of vessel matrix via its effect on expression of PDGF and TGF- β etc^[31,32]. Therefore, LRAS plays an important role in vascular remodeling and vasculopathy in portal hypertension.

Secondly, LRAS has vasoconstrictive functions. The response of splanchnic blood vessel to AngII decreased in advanced portal hypertension^[33], it was due to decrease of AngII receptor on the blood vessel wall or due to the existence of post receptor dysfunction^[34,35]. Furthermore, glucagon and other vasoactive substances could influence the effect of AngII on splanchnic vessel^[36,37].

Thirdly, the imbalance of vasoconstrictors and vasodilators was existed in portal hypertension. Studies on vasculature showed that vascular RAS could change the response of blood vessel to other vasoactive substances^[29] and *vice versa*^[38]. For example, in the rabbit model of portal hypertension, the response degree of splanchnic vessel to AngII was improved by CO^[33], the presence of ET could induce the local renin activity and increase synthesis of AngII in rat mesentery artery^[39], and LRAS could decrease the degradation of endogenous bradykin^[30]. All the changes mentioned above could result in imbalance of vasodilators and vasoconstrictors. In this study, local renin and angiotensinogen mRNA expression in the liver was not significantly different from that in the splenic artery and vein in portal hypertensive patients, suggesting that the loss of expression of organ-specificity of LRAS components might be due to disordered metabolism of vasoactive substances.

In conclusion, increased LRAS activity in the hepatic and splenic vessels is due to cirrhotic portal hypertension, and the synthesis of local AngII increases, which contract the hepatic sinusoid, stimulate hyperplasia of HSC and proliferation of VSMC, and also interfere with the metabolism of other vasoactive substances. All these enhance the degree of cirrhosis and portal hypertension. By interruption of this vicious cycle, medical treatment may be able to improve the hemodynamic disturbance and ameliorate the splanchnic vasculopathy and to offer a new way for preventing the complications of portal hypertension^[40].

REFERENCES

- Gricndling KK**, Murphy TJ, Alexander RW. Molecular biology of the renin-angiotensin system. *Circulation* 1993; **87**: 1816-1828
- Kelly MP**, Kahr O, Aalkjaer C, Cumin F, Samani NJ. Tissue expression of components of the renin-angiotensin system in experimental post-infarction heart failure in rats: effects of heart failure and angiotensin-converting enzyme inhibitor treatment. *Clin Sci* 1997; **92**: 455-465
- Bataller R**, Gines P, Nicolas JM, Gorbis MN, Garcia-Ramallo E, Gasull X, Bosch J, Arroyo V, Rodes J. AngiotensinII induces contraction and proliferation of human hepatic stellate cells. *Gastroenterology* 2000; **118**: 1149-1156
- Yao XX**, Tang YW, Yao DM, Xiu HM. Effects of Yigan Decoction on proliferation and apoptosis of hepatic stellate cells. *World J Gastroenterol* 2002; **8**: 511-514
- Liu XJ**, Yang L, Mao YQ, Wang Q, Huang MH, Wang YP, Wu HB. Effects of the tyrosine protein kinase inhibitor genistein on the proliferation, activation of cultured rat hepatic stellate cells. *World J Gastroenterol* 2002; **8**: 739-745
- Du WD**, Zhang YE, Zhai WR, Zhou XM. Dynamic changes of type I, III and IV collagen synthesis and distribution of collagen-producing cells in carbon tetrachloride-induced rat liver fibrosis. *World J Gastroenterol* 1999; **5**: 397-403
- Yang Z**, Zhang L, Li D, Qiu F. Pathological morphology alteration of the splanchnic vascular wall in portal hypertensive patients. *Chin Med J* 2002; **115**: 559-562
- Yang Z**, Liu RZ, Yang RG, Qui FZ. Pathology of endothelium, extracellular matrix and smooth muscle in gastric coronary vein of cirrhotic patients. *Zhonghua Waike Zazhi* 1996; **34**: 138-140
- Shi BM**, Yang Z. Vascular lesion and its mechanisms in spleen under statement of portal hypertension. *Zhonghua Yixue Zazhi* 2000; **80**: 196-198
- Bataller R**, Nicolas JM, Gines P, Esteve A, Nieves GM, Garcia RE, Pinzani M, Ros J, Jimenez W, Thomas AP, Arroyo V, Rodes J. Arginine vasopressin induces contraction and stimulates growth of cultured human hepatic stellate cells. *Gastroenterology* 1997; **113**: 615-624
- Pinzani M**, Failli P, Ruocco C, Casini A, Milani S, Baldi E, Giotti A, Gentilini P. Fat-storing cells as liver-specific pericytes. Spatial dynamics of agonist-stimulated intracellular calcium transients. *J Clin Invest* 1992; **90**: 642-646
- Don R**. The cellular pathogenesis of portal hypertension: stellate cell contractility, endothelin, and nitric oxide. *Hepatology* 1997; **25**: 2-5
- Wei HS**, Lu HM, Li DG, Zhan YT, Wang ZR, Huang X, Cheng JL, Xu QF. The regulatory role of AT1 receptor on activated HSCs in hepatic fibrogenesis: effects of RAS inhibitors on hepatic fibrosis induced by CCL(4). *World J Gastroenterol* 2000; **6**: 824-828
- Powell EE**, Edwards CJ, Hay JL, Andrew DC, Darrell HC, Claudia S, David MP, Julie RJ. Host genetic factors influence disease progression in chronic hepatitis C. *Hepatology* 2000; **31**: 828-833
- Dai WJ**, Jiang HC. Advances in gene therapy of liver cirrhosis: a review. *World J Gastroenterol* 2001; **7**: 1-8
- Marra F**, Grandaliano G, Valente AJ, Abboud HE. Thrombin stimulates proliferation of liver fat-storing cells and expression of monocyte chemotactic protein-1: potential role in liver injury. *Hepatology* 1995; **22**: 780-787
- Arved WS**, Johann F K, Christian P K. Effect of Losartan, an angiotensin II receptor antagonist, on portal pressure in cirrhosis. *Hepatology* 1999; **29**: 334-339
- Powell EE**, Edwards-Smith CJ, Hay JL, Clouston AD, Crawford DH, Shorthouse C, Purdie DM, Jonsson JR. Host genetic factors influence disease progression in chronic hepatitis C. *Hepatology* 2000; **31**: 828-833
- Lee LK**, Meyer TW, Pollock AS, Lovett DH. Endothelial cell injury initiates glomerular sclerosis in the rat remnant kidney. *J Clin Invest* 1995; **96**: 953-964
- Lijnen P**, Petrov V. Renin-angiotensin system, hypertrophy and gene expression in cardiac myocytes. *J Mol Cell Cardiol* 1999; **31**: 949-970
- Julie RJ**, Andrew DC, Yuichi A, Livia IK, Murray JH, Michael DA, David MP, Elizabeth EP. Angiotensin-converting enzyme inhibition attenuates the progression of rat hepatic fibrosis. *Gastroenterology* 2001; **121**: 148-155
- Wei HS**, Li DG, Lu HM, Zhan YT, Wang ZR, Huang X, Zhang J, Cheng JL, Xu QF. Effects of AT1 receptor antagonist, losartan, on rat hepatic fibrosis induced by CCL(4). *World J Gastroenterol* 2000; **6**: 540-545
- Yang YY**, Lin HC, Huang YT, Lee TY, Hou MC, Lee FY, Liu RS, Chang FY, Lee SD. Effect of 1-week losartan administration on bile duct-ligated cirrhotic rats with portal hypertension. *J Hepatol* 2002; **36**: 600-606
- Dzau VJ**. Local expression and pathophysiological role of renin-angiotensin in the blood vessels and heart. *Basic Res Cardiol* 1993; **88** (Suppl 1): 1-14
- Naftilan AJ**, Pratt RE, Dzau VJ. Induction of platelet-derived growth factor A-chain and c-myc gene expressions by angiotensin II in cultured rat vascular smooth muscle cells. *J Clin Invest* 1989; **83**: 1419-1423
- Ferns GA**, Raines EW, Sprugel KH, Motani AS, Reidy MA, Ross

- R. Inhibition of neointimal smooth muscle accumulation after angioplasty by an antibody to PDGF. *Science* 1991; **253**: 1129-1132
- 27 **Taubman MB**, Berk BC, Izumo S, Tsuda T, Alexander RW, Nadal GB. Angiotensin II induces c-fos mRNA in aortic smooth muscle. Role of Ca²⁺ mobilization and protein kinase C activation. *J Biol Chem* 1989; **264**: 526-530
- 28 **Hiroshi I**, Masashi M, Richard EP, Gary HG, Victor JD. Multiple autocrine growth factors modulate vascular smooth muscle cell growth response to angiotensin II. *J Clin Invest* 1993; **91**: 2268-2274
- 29 **Holtz J**, Goetz RM. Vascular renin-angiotensin-system, endothelial function and atherosclerosis. *Basic Res cardiol* 1994; **89** (Suppl 1): 71-86
- 30 **Falkenhahn M**, Gohlke P, Paul M, Stoll M, Unger T. The renin-angiotensin system in the heart and vascular wall: new therapeutic aspects. *J Cardiovasc Pharmacol* 1994; **24** (Suppl 2):S6-13
- 31 **Hahn AW**, Resink TJ, Kern F, Buhler FR. Peptide vasoconstrictors, vessel structure, and vascular smooth-muscle proliferation. *J Cardiovasc Pharmacol* 1993; **22**(Suppl): S37-43
- 32 **Kato H**, Suzuki H, Tajima S, Ogata Y, Tominaga T, Sato A, Saruta T. Angiotensin II stimulates collagen synthesis in cultured vascular smooth muscle cells. *J Hypertens* 1991; **9**: 17-22
- 33 **Sitzmann JV**, Li SS, Wu YP, Groszmann R, Bulkley GB. Decreased mesenteric vascular response to angiotensin II in portal hypertension. *J Surg Res* 1990; **48**: 341-344
- 34 **James VS**, Yuping Wu, Greti A, Paul AC, R Cartland B. Loss of angiotensin-II receptors in portal hypertensive rabbits. *Hepatology* 1995; **22**: 559-564
- 35 **Castro A**, Jimenez W, Claria J, Ros J, Martinez JM, Bosch M, Arroyo V, Piulats J, Rivera F, Rodes J. Impaired responsiveness to angiotensin II in experimental cirrhosis: role of nitric oxide. *Hepatology* 1993; **18**: 367-372
- 36 **Sitzmann JV**, Bulkley GB, Mitchell MC, Campbell K. Role of prostacyclin in the splanchnic hyperemia contributing to portal hypertension. *Ann Surg* 1989; **209**: 322-327
- 37 **Benoit JN**, Barrowman JA, Harper SL, Kvietys PR, Granger DN. Role of humoral factors in the intestinal hyperemia associated with chronic portal hypertension. *Am J Physiol* 1984; **247**: G486-493
- 38 **Moller S**, Bendtsen F, Henriksen JH. Splanchnic and systemic hemodynamic derangement in decompensated cirrhosis. *Can J Gastroenterol* 2001; **15**: 94-106
- 39 **Rakugi H**, Tabuchi Y, Nakamaru M, Nagano M, Higashimori K, Mikami H, Ogihara T. Endothelin activates the vascular renin-angiotensin system in rat mesenteric arteries. *Biochem Int* 1990; **21**: 867-872
- 40 **Hulagu S**, Senturk O, Erdem A, Ozgur O, Celebi A, Karakaya AT, Seyhogullari M, Demirci A. Effects of losartan, somatostatin and losartan plus somatostatin on portal hemodynamics and renal functions in cirrhosis. *Hepatogastroenterology* 2002; **49**: 783-787

Edited by Wu XN and Zhu LH

Biliary carcinoembryonic antigen levels in diagnosis of occult hepatic metastases from colorectal carcinoma

Jaques Waisberg, Rogério T. Palma, Luís Contim Neto, Lourdes C. Martins, Maurício S. L. Oliveira, Carlos A. Nagashima, Antonio C. Godoy, Fabio S. Goffi

Jaques Waisberg, Rogério T. Palma, Luís Contim Neto, Lourdes C. Martins, Maurício S. L. Oliveira, Antonio C. Godoy, Fabio S. Goffi, Surgical Gastroenterology Department, Hospital do Servidor Público Estadual, São Paulo, Brazil

Carlos A. Nagashima, Clinical Laboratory Department, Hospital do Servidor Público Estadual, São Paulo, Brazil

Correspondence to: Jaques Waisberg, M.D., Rua das Figueiras, 550 apto. 134 Bairro Jardim, 09080-300 Santo André - São Paulo - Brazil. jaqueswaisberg@uol.com.br

Telephone: +55-11-44362461 **Fax:** +55-11-44362160

Received: 2003-02-26 **Accepted:** 2003-03-16

Abstract

AIM: To prospectively explore the role of carcinoembryonic antigen (CEA) in gallbladder bile in patients with colorectal carcinoma and the morphological and clinical features of neoplasia and the occurrence of hepatic metastases.

METHODS: CEA levels in the gallbladder and peripheral blood were studied in 44 patients with colorectal carcinoma and 10 patients with uncomplicated cholelithiasis. CEA samples were collected from the gallbladder bile and peripheral blood during the operation, immediately before extirpating the colorectal neoplasia or cholecystectomy. Values of up to 5 ng/ml were considered normal for bile and serum CEA.

RESULTS: In the 44 patients with colorectal carcinoma who underwent operation with curative intent, the average level of serum CEA was 8.5 ng/ml (range: 0.1 to 111.0 ng/ml) and for bile CEA it was 74.5 ng/ml (range: 0.2 to 571.0 ng/ml). In the patients with uncomplicated cholelithiasis who underwent cholecystectomy, the average level of serum CEA was 1.9 ng/ml (range: 1.0 to 3.5 ng/ml) and for bile CEA it was 1.2 ng/ml (range: 0.3 to 2.9 ng/ml). The average duration of follow-up time was 16.5 months (range: 6 to 48 months). Four patients who underwent extirpation of the colorectal carcinoma without evidence of hepatic metastasis and with an average bile CEA value of 213.2 ng/ml presented hepatic metastases between three and seventeen months after removal of the primary colorectal neoplasia. Three of them successfully underwent extirpation of the hepatic lesions.

CONCLUSION: High CEA levels in gallbladders of patients undergoing curative operation for colorectal carcinoma may indicate the presence of hepatic metastases. Such patients must be followed up with special attention to the diagnosis of such lesions.

Waisberg J, Palma RT, Neto LC, Martins LC, Oliveira MSL, Nagashima CA, Godoy AC, Goffi FS. Biliary carcinoembryonic antigen levels in diagnosis of occult hepatic metastases from colorectal carcinoma. *World J Gastroenterol* 2003; 9(7): 1589-1593

<http://www.wjgnet.com/1007-9327/9/1589.asp>

INTRODUCTION

Colorectal carcinoma is the second most common cancer type in the Western world and the liver is the organ most affected by its distant metastases^[1,2]. At the time when primary tumor is extirpated, hepatic metastases are encountered in 20 to 25 % of the patients. Approximately half of the patients who have had colorectal lesions extirpated in an apparently curative manner will develop hepatic metastases postoperatively^[1,3,4].

The majority of relapse monitoring programs for operated colorectal carcinoma include determinations at regular intervals of the serum concentration of carcinoembryonic antigen (CEA) and hepatic imaging via abdominal ultrasonography, tomography and/or magnetic resonance^[3,5]. Nonetheless, even with such investigations, around 10 to 30 % of hepatic metastases will remain undiagnosed^[4]. When lesions are present in the liver, extirpation is the treatment of choice. However, this is only possible in 20 % of such patients and only 25 % of these will achieve survival of more than 5 years^[1,3,4].

In 1965, Gold and Freedman^[6] described the presence of CEA in extracts from malignant tumors and fetal intestinal tissue. Today, assaying of blood CEA is utilized preoperatively and postoperatively among colorectal carcinoma patients for the detection of disease relapse^[7-10].

In 1989, Yeatman *et al*^[11] suggested that CEA concentration in bile could constitute a marker for detecting hepatic metastases at an earlier stage. Their hypothesis was based on the observation that CEA derived from hepatic metastases could be excreted both in bile and in blood. Since the bile volume is less than the plasma volume, rises in the detectable CEA concentration occur earlier in the gallbladder than in peripheral blood^[11-13]. Yeatman and Paul *et al*^[11-14] found elevated CEA concentrations in bile among patients with colorectal carcinoma and proven hepatic metastases and among patients who underwent curative extirpation without any hepatic involvement could be detected via imaging methods.

The role of CEA level in gallbladder bile remains controversial with regard to its contribution towards early detection of hepatic metastases in patients undergoing curative operation for colorectal carcinoma^[15-23].

The aim of this study was to prospectively analyze the results of CEA determinations in peripheral blood and gallbladder bile among a series of patients treated by curative operation for colorectal carcinoma, relating them to morphological features of the neoplasia and hepatic relapse.

MATERIALS AND METHODS

Patients

Between 1998 and 2001, 44 patients experienced extirpation of colorectal carcinoma with curative intent. The term curative was utilized to designate an absence of macroscopic disease at the termination of the surgical procedure, verified in the report on the anatomopathological examination of the extirpated neoplastic lesions and associated structures. Samples of gallbladder bile and peripheral blood were collected during the operation, immediately before the start of excision of the neoplasia, for all patients.

This investigation was made in accordance with the ethical standards accepted by the Helsinki Declaration of the World Medical Association, adopted in 1964 and amended in 1996. The patients were aware of the study protocol and signed a statement of free and informed consent upon entering the present study.

The following were considered to be inclusion criteria: achievement of curative operation, absence of distant metastases and presence of adenocarcinoma of the large intestine confirmed by means of histopathological study of the extirpated lesion. Patients submitted to operations that were evaluated as non-curative were not included in this sample.

The clinical and morphological data were obtained by consulting the hospital records of the patients included in the study, or by interviewing the patients or their relatives at return outpatient visits.

Thirty-nine patients (88.6 %) were white, three were oriental (6.8 %) and two were black (4.5 %). Twenty-one patients (47.7 %) were male and 23 (52.3 %) were female. The average age was 63 ± 14.7 years (range: 29 to 90 years). All patients had their preoperative diagnosis of colorectal carcinoma confirmed by biopsy specimens obtained via colonoscopy. For this, the thin sections were stained using the hematoxylin-eosin (HE) method and analyzed by a pathologist.

Neoplasia was considered to be Dukes A when it did not reach the external muscle tunica of the intestinal wall, Dukes B when it extended throughout the wall and also reached the adventitious adipose tissue, and Dukes C when lymph nodes were compromised, independent of the depth of parietal invasion.

Preoperative investigation of the presence of an extra-intestinal lesion was made via abdominal ultrasonography, abdominal tomography and chest radiography, and did not reveal metastases in any of these patients.

In ten patients with uncomplicated cholecystolithiasis who underwent elective cholecystectomy via laparotomy, blood and gallbladder bile samples were collected under the same conditions as for the patients with colorectal carcinoma. These served to furnish CEA levels in gallbladder bile for comparison purposes. All these patients were white, of whom seven (70 %) were female and three (30 %) were male. The average age was 50.8 ± 20.1 years (range: 23 to 74 years old).

Sample collection

Blood and bile sample collection was performed during the operation. After making an inventory of the abdominal cavity, 5 ml samples of gallbladder bile were obtained via puncture of the fundic region of the gallbladder using a caliber 23 needle coupled to a plastic syringe of capacity 10 ml. Then, using another syringe of capacity 20 ml, the remainder gallbladder bile was evacuated, followed by occlusion of the location of the puncture by a pouch suture using thin atraumatic absorbable thread made of polyglycolic acid. At the start of the operation, prior to removing the colorectal neoplasia, 5 ml blood samples were collected via peripheral venous puncture in the non-dominant upper limb, divested of intravenous infusion of any solution, using a caliber 37 needle coupled to a plastic syringe of capacity 10 ml.

CEA assay

The serum and bile samples were stored in a freezer at -70°C until the CEA analyses were done. A solid-phase fluoroimmuno-metric assay system was utilized (Delfia CEA Kit, Pharmacia, Turku, Finland) for assaying the serum and bile CEA. The precision of the method was estimated via the coefficient of variation (c.v.), with intra-assay c.v. of 3.4 % and 2.4 % for low and high values, respectively, and inter-assay c.v. of 4.6 % and 2.8 % for the same parameters. The sensitivity of this CEA

assay was 0.2 ng/ml and the upper limit on the recognition curve was 500 ng/ml. Whenever this value was exceeded, dilutions were needed for adjustment of the reactions.

The limit of normality adopted for bile CEA was 5 ng/ml which was based on the analysis of the values obtained in the group of patients who underwent cholecystectomy.

Statistical analysis

Considering the nature of the samples, non-parametric statistical tests were utilized in the evaluation of the results. Quantitative variables were represented by absolute frequency (n) and relative frequency (%). The statistical models utilized were arithmetic mean, standard deviation, Mann-Whitney test, Wilcoxon test and Kruskal-Wallis test. The normality of the data were tested using the Kolmogorov-Smirnov test and the homogeneity of the variance was verified using the Levene test.

In all tests, the level for the rejection of the null hypothesis was set at 0.05 % (significance level of 95 %), in accordance with the current standards in biological studies.

RESULTS

In the group of patients with colorectal carcinoma, there was a single lesion in 43 patients (97.7 %) and multiple lesions in one of them (2.3 %). The neoplasia was located in the rectum in 24 patients (54.5 %), in the cecum-ascending colon in 6 (13.7 %), in the transverse colon in 6 (13.6 %), in the sigmoid in 4 (9.1 %), in the descending colon in 2 (4.5 %), in the left flexure in 1 (2.3 %), and the lesion involved the cecum and rectum simultaneously in 1 patient (2.3 %). With regard to the degree of histopathological differentiation of the neoplasia, all the lesions were considered to be moderately differentiated. All the patients operated for colorectal carcinoma evolved without notable interurrences and were discharged from hospital. The average duration of follow-up for the patients was 16.5 months (range: 6 to 48 months).

Concerning the Dukes classification, 2 patients (4.6 %) were classified as class A, 21 (47.7 %) as class B, and 21 (47.7 %) as class C.

Thirteen patients (29.5 %) classified as Dukes C were submitted to adjuvant chemotherapy using intravenous 5-fluorouracil over seven sessions.

In the patients with colorectal carcinoma, the average value was 8.5 ± 18.7 ng/ml (range: 0.1 to 111.0 ng/ml) for serum CEA, and was 74.5 ± 130.3 ng/ml for bile CEA (0.2 to 571 ng/ml) (Table 1).

In the group of patients with uncomplicated cholelithiasis, the average value was 1.94 ± 0.8 ng/ml (range: 1.0 to 3.5 ng/ml) for serum CEA, and was 1.24 ± 0.9 ng/ml for bile CEA (range: 0.3 to 2.9 ng/ml) (Table 2). The patients in this group were discharged from hospital with uneventful recovery.

Seventeen patients (38.6 %) presented a serum CEA value of more than 5.0 ng/ml, while 27 patients (61.4 %) exhibited a blood CEA level less than or equal to 5.0 ng/ml. With regard to bile CEA, 29 patients (65.9 %) exhibited values of more than 5.0 ng/ml, whereas 15 patients (34.1 %) had determinations of less than or equal to 5.0 ng/ml. In 35 patients (79.5 %), the bile CEA level was greater than the serum CEA level, and in nine patients (20.5 %), the serum CEA level was higher than the bile CEA level. Thirteen patients (29.5 %) simultaneously presented serum CEA and bile CEA values of more than 5 ng/ml. In 11 patients (25.0 %), the determinations obtained for serum CEA and bile CEA were less than or equal to 5.0 ng/ml.

The bile CEA values in the patients operated for colorectal carcinoma were significantly greater than those determined in the blood ($P < 0.0001$) (Table 1). On the other hand, in the group of patients who underwent cholecystectomy, the bile CEA

values were significantly less than those of serum CEA ($P=0.46$) (Table 2). The bile CEA levels in patients with colorectal carcinoma were significantly greater ($P<0.0001$) than those that underwent cholecystectomy. Comparison of the bile CEA/serum CEA ratios for the colorectal carcinoma and cholecystectomy patients showed significantly greater values in the group with neoplasia of the large intestine than in those with cholecystectomy ($P<0.0001$) (Table 3).

Table 1 Average values for serum and bile CEA obtained from patients operated for colorectal carcinoma

Variables	Average (ng/ml)	S.D.	Minimum (ng/ml)	Maximum (ng/ml)	n
Serum CEA	8.5	18.7	0.1	111.0	44
Bile CEA	74.5	130.26	0.2	571.0	44

Wilcoxon (Z)=-4.614, $P<0.0001$ (Serum CEA vs Bile CEA), Notes: S.D.=standard deviation.

Table 2 Average values for serum and bile CEA obtained from patients operated for uncomplicated cholelithiasis

Variables	Average (ng/ml)	S.D.	Minimum (ng/ml)	Maximum (ng/ml)	n
Serum CEA	1.9	0.8	1.0 ng/ml	3.5 ng/ml	10
Bile CEA	1.2	0.9	0.3 ng/ml	2.9 ng/ml	10

Wilcoxon (Z)=-1.992, $P<0.46$ (Serum CEA vs Bile CEA), Notes: S.D.=standard deviation.

Table 3 Average values of the bile CEA/serum CEA ratio obtained from patients operated for colorectal carcinoma and cholelithiasis

Group	Variables	Average	S.D.	Minimum	Maximum	n
Colorectal carcinoma	Bile CEA/serum CEA	22.1	48.5	0.02	287.0	44
Cholelithiasis	Bile CEA/serum CEA	0.6	0.3	0.3	1.9	10

Mann-Whitney (U)=63.5, $P<0.0001$ (colorectal carcinoma group vs cholelithiasis group), Notes: S.D.=standard deviation.

In this study, there was no significant relationship between Dukes classification and serum CEA values ($P=0.60$) or bile CEA values ($P=0.78$). Besides, the bile and serum CEA values showed a non-significant relationship with the localization of the neoplastic lesions in the right colon, left colon or rectum ($P=0.93$ and $P=0.53$, respectively).

Four patients (9.1 %) with colorectal carcinoma showing elevated bile CEA levels who were operated on with curative intent presented evolution to hepatic metastases. They were initially diagnosed due to a rise in postoperative serum CEA levels, with an average of 8.6 ng/ml (range: 0.3 to 22.8 ng/ml). Only two of them presented increased serum CEA levels at the time of operation, although all four presented elevated bile CEA levels, with an average of 228.4 ng/ml (range: 6.6 to 571 ng/ml). They corresponded to 13.8 % of the 29 patients with elevated bile CEA. In these four patients, hepatic metastases developed on average around 9.7 months (range: 3 to 17 months) after removal of the primary colorectal lesion. Three of them were staged as Dukes C and one as Dukes B (Table 4). With the exception of the single Dukes B patient, who presented disease relapse with hepatic metastases disseminated in both lobes, the other three patients were submitted to hepatectomy for the removal of their metastases. Two of them died after removal of the hepatic lesions: one around nine

months afterwards and the other 21 months afterwards. Although no necropsy was performed on these patients, there was no evidence of neoplasia recurrence up to the time of death. The third of these patients is still alive, without active disease, around eight months after extirpation of the hepatic metastases. The remaining 40 patients are alive, without signs of disease relapse, six to 48 months after removal of the primary colorectal lesion.

Table 4 Location of the lesion, Dukes staging and serum and bile CEA values, obtained from the patients operated for colorectal carcinoma with hepatic metastases during the follow-up

Case	Location	Dukes	Serum CEA (ng/ml)	Bile CEA (ng/ml)
1	Transverse colon	B	22.8	510.0
2	Rectum	C	2.1	292.0
3	Rectum	C	9.4	44.1
4	Sigmoid	C	6.6	6.6
Average			10.2	213.2

DISCUSSION

An ability to predict the appearance of hepatic metastases in patients operated on for colorectal carcinoma with curative intent could influence the use of adjuvant chemotherapy and intensify the follow-up of patients with indications for surgical treatment for lesions that could be extirpated^[18,20,24-26].

Determination of bile CEA levels may be a potentially sensitive method for diagnosing hepatic metastases of colorectal carcinoma, since hepatic lesions smaller than 1 cm³ are able to produce elevations of CEA concentrations in bile^[11,16,22,26].

Huang and Tang^[17] studied serum and bile CEA obtained by drainage using a preoperative duodenal tube in patients with benign affections and colorectal carcinoma, with and without hepatic metastases. These authors verified that the difference between bile CEA values in patients operated upon for colorectal carcinoma with and without hepatic metastases was significant, thus showing that the bile CEA level assisted in confirming the existence of hepatic lesions. Novell and Moura *et al*^[19, 22] studied the levels of serum and bile CEA in patients with colorectal carcinoma and suggested that a determination of the bile CEA level might be useful in diagnosing concealed hepatic metastases. In the four patients of the present study who evolved with hepatic metastases, and in 29 other patients (65.9 %) who did not present metastases, the bile CEA values were also significantly greater than those for serum CEA. The average follow-up duration of 16.5 months was not yet sufficient for a conclusive evaluation of bile CEA determination as a predictive parameter for the appearance of hepatic metastases in these patients. An average follow-up for at least 60 months would increase the possibility of finding hepatic relapse of the disease and would furnish more consistent support for an assessment of the usefulness of bile CEA.

In patients with hepatic metastases of colorectal carcinoma, the concentrating capacity of the gallbladder has been singled out as the mechanism responsible for the elevated bile CEA levels in comparison with serum CEA levels^[18,27-29]. The finding of elevated bile CEA values in the absence of hepatic metastases may also be credited to the fact that bile CEA is derived not only from the hepatic metastases but also from the primary tumor^[29]. This situation is thought to contribute to the existence of a direct relationship between serum and bile CEA levels^[13]. That is, when serum CEA levels are significantly elevated, bile CEA levels will also be, and consequently the serum CEA levels produced by the primary tumor may elevate the bile levels, even in the absence of hepatic metastases. These events could justify the findings in the present sample, in which 25 patients (86.2 %) with elevated bile CEA levels had not

presented hepatic metastases at the time of last follow-up consultation. Nonetheless, other studies^[13,14,17,30] have suggested that increased CEA levels in bile in the presence of hepatic metastases are exclusively produced by neof ormation in the liver, without originating in the portal circulation, indicating that patients with elevated bile CEA have silent hepatic metastatic disease. Paul *et al*^[14] suggested that the bile CEA predicted hepatic disease only when collected after the removal of the primary tumor, which would avoid any significant contribution of serum CEA to bile CEA levels. It remains to be proven whether the finding of elevated serum and bile CEA levels during the extirpation of colorectal carcinoma, as occurred in 27 patients (61.4 %) of this study would constitute a selecting criterion for monitoring bile CEA levels after operation.

Yeatman *et al*^[11] found elevated bile CEA levels in 70 % of their patients with colorectal carcinoma extirpated in a curative manner that had normal intraoperative hepatic ultrasonography. Over the average follow-up of 30 months for this group of patients, 13 % of them presented hepatic metastases. The result was close to that found in the present study, which observed that 9.1 % of patients had hepatic metastases over an average follow-up of 16.5 months. Li Destri *et al*^[23] found a diagnostic accuracy for bile CEA of 91 % among patients operated for colorectal carcinoma with or without hepatic metastases, and 89.5 % among patients who evolved with hepatic metastases. Ishida *et al*^[21] analyzed the relationship of CEA values in gallbladder bile collected during operation and in peripheral blood, with the appearance of metachronic hepatic metastases of colorectal carcinoma. In 49 patients without evidence of hepatic metastases at the time of operation, the elevated levels of bile CEA were predictive of the appearance of metachronic hepatic metastases with a 75 % sensitivity rate, 85 % specificity and 84 % accuracy. In another study, Ishida *et al*^[15] showed that patients with elevated bile CEA or elevated bile CEA / serum CEA ratio could be candidates for hepatic relapse.

In the present study, four patients (9.1 %) operated for colorectal carcinoma with curative intent developed hepatic metastases after removal of the neoplastic lesion. Since the average follow-up duration for the patients was 16.5 months, it was possible that the number of patients affected by hepatic metastases and elevated bile CEA increased with the prolongation of the follow-up. This could make the determination of bile CEA levels a predictive parameter for the development of hepatic lesions.

However, other studies did not share the idea that bile CEA had a predictive value in relation to the development of hepatic metastases. Dorrance *et al*^[20] determined serum and bile CEA levels in 26 patients submitted to curative surgery and followed up for an average of 63.5 months. Twelve patients (46.1 %) survived without relapse and 14 (53.8 %) died because of recurrence of neoplasia. The average value of serum CEA in the group free of disease was significantly greater than that in the group with relapse. The accuracy of serum CEA as a predictive indicator for concealed hepatic metastases was 77 %, in comparison with 72 % for bile CEA, without significant difference. The authors concluded that determination of intraoperative bile CEA levels was not more accurate than serum CEA as a predictive indicator for the occurrence of metastases among patients undergoing potentially curative surgery for colorectal carcinoma. Panaguzzi *et al*^[16] studied the follow-up of patients operated for colorectal carcinoma without hepatic metastases although with elevated bile CEA levels. They concluded that, although the bile CEA levels were elevated in patients with hepatic metastases, these levels did not represent a predictive parameter for their presence in colorectal carcinoma. Garcia *et al*^[18] determined the concentration of bile CEA in 24 patients with colorectal carcinoma, all of them exhibited elevated bile CEA, of whom

21 did not present evidence of hepatic metastases, while three had such lesions in the liver. These authors followed up their patients for an average of 32.3 months. Three of them developed hepatic metastases. The authors stressed that there was no clear relationship between the bile CEA values and the appearance of hepatic metastases, although they recognized that their sample was not large enough for definitive conclusions.

In our sample, nine patients (20.5 %) presented bile CEA values less than the respective values for serum CEA. One possible explanation for this fact is that the liver purification mechanisms for CEA produced by primary colorectal neoplasia might not be saturated and consequently the levels excreted into the bile would be less than into blood.

Bile CEA has apparently emerged as a promising tool for identifying patients with undiagnosed hepatic metastases. In patients with verified recurrence of neoplasia, the sensitivity of CEA determination in bile is greater than that for values found in the blood. Consequently, there could be a broadening of the indication for hepatectomy or radiofrequency ablation^[31] due to hepatic metastases. Local or systemic chemotherapy procedures^[32] could be introduced earlier, as could radioimmunoguided surgery or also treatments using anti-CEA monoclonal antibodies. To prove the real value of bile CEA for detecting hepatic relapses at an earlier stage, prospective studies with an adequate length of follow-up time, and standardized intervals between extirpation of colorectal neoplastic lesion and withdrawal of the bile samples, are needed.

REFERENCES

- 1 **Adson MA.** Resection of liver metastases: when is it worthwhile? *World J Surg* 1987; **11**: 511-520
- 2 **Kievit J, Bruinvels JD.** Detection of recurrence after surgery for colorectal cancer. *Eur J Cancer* 1995; **31A**: 1222-1225
- 3 **Fantini GA, DeCosse JJ.** Surveillance strategies after resection of carcinoma of the colon and rectum. *Surg Gynecol Obstet* 1990; **171**: 267-273
- 4 **Finlay IG, McArdle CS.** Occult hepatic metastases in colorectal carcinoma. *Br J Surg* 1986; **73**: 732-735
- 5 **Stone MD, Kane R, Bothe A Jr, Jessup JM, Cady B, Steele GD Jr.** Intraoperative ultrasound imaging of the liver at the time of colorectal cancer resection. *Arch Surg* 1994; **129**: 431-436
- 6 **Gold P, Freedman SO.** Demonstration of tumor-specific antigens in human colonic carcinomata by immunological tolerance and absorption techniques. *J Exp Med* 1965; **121**: 439-462
- 7 **Fletcher RH.** Carcinoembryonic antigen. *Ann Intern Med* 1986; **104**: 66-73
- 8 **Hohenberger P, Schlag PM, Gerneth T, Herfarth C.** Pre- and post-operative carcinoembryonic antigen determinations in hepatic resection for colorectal metastases. Predictive value and implication for adjuvant treatment based on multivariate analysis. *Ann Surg* 1994; **219**: 135-143
- 9 **King J, Caplehorn JR, Ross WB, Morris DL.** High serum carcinoembryonic antigen concentration in patients with colorectal liver metastases is associated with poor cell-mediated immunity, which is predictive of survival. *Br J Surg* 1997; **84**: 1382-1385
- 10 **Bakalakov EA, Burak WE Jr, Young DC, Martin EW Jr.** Is carcinoembryonic antigen useful in the follow-up management of patients with colorectal liver metastases? *Am J Surg* 1999; **177**: 2-6
- 11 **Yeatman TJ, Bland KI, Copeland EM 3rd, Hollenbeck JI, Souba WW, Vogel SB, Kimura AK.** Relationship between colorectal liver metastases and CEA levels in gallbladder bile. *Ann Surg* 1989; **210**: 505-512
- 12 **Yeatman TJ, Kimura AK, Copeland EM 3rd, Bland KI.** Rapid analysis of carcinoembryonic antigen levels in gallbladder bile. Identification of patients at high risk of colorectal liver metastasis. *Ann Surg* 1991; **213**: 113-117
- 13 **Paul MA, Visser JJ, Mulder C, Blomjous JG, van Kamp GJ, Cuesta MA, Meijer S.** Detection of occult liver metastases by measurement of biliary carcinoembryonic antigen concentrations. *Eur J Surg* 1996; **162**: 483-488

- 14 **Paul MA**, Visser JJ, Mulder C, van Kamp GJ, Cuesta MA, Meijer S. The use of biliary CEA measurements in the diagnosis of recurrent colorectal cancer. *Eur J Surg Oncol* 1997; **23**: 419-423
- 15 **Ishida H**, Hojo I, Gonda T, Nakajima H, Hirukawa H, Itoh M, Satoh K, Higuchi T, Toyooka M, Yoshinaga K. Measurement of bile CEA levels in patients with colorectal cancer: is it of value for diagnosis of occult liver metastases aiming at prophylactic regional hepatic chemotherapy? *Gan To Kagaku Ryoho* 1993; **20**: 1551-1554
- 16 **Paganuzzi M**, Onetto M, de Paoli M, Castagnola M, de Salvo L, Civalleri D, Grossi CE. Carcinoembryonic antigen (CEA) in serum and bile of colorectal cancer patients with or without detectable liver metastases. *Anticancer Res* 1994; **14**: 1409-1412
- 17 **Huang M**, Tang D, Li B. Evaluation of biliary CEA in the diagnosis of colorectal cancer with liver metastases. *Zhonghua Zhongliu Zazhi* 1999; **21**: 45-47
- 18 **Garcia BA**, Madrona AP, Ayalla MP, Paricio PP. The usefulness of determining carcinoembryonic antigen in the bile for the prognosis of the development of hepatic metastases following the resection of colorectal cancer. *Med Clin (Barc)* 1997; **108**: 396
- 19 **Novell F**, Trias M, Molina R, Filella X. Detection of occult liver metastases in colorectal cancer by measurement of biliary carcinoembryonic antigen. *Anticancer Res* 1997; **17**: 2743-2746
- 20 **Dorrance HR**, McGregor JR, McAllister EJ, O'Dwyer PJ. Bile carcinoembryonic antigen levels and occult hepatic metastases from colorectal cancer. *Dis Colon Rectum* 2000; **43**: 1292-1296
- 21 **Ishida H**, Yoshinaga K, Gonda T, Ando M, Hojo I, Fukunari H, Iwama T, Mishima Y. Biliary carcinoembryonic antigen levels can predict metachronous liver metastasis of colorectal cancer. *Anticancer Res* 2000; **20**: 523-526
- 22 **Moura RM**, Matos D, Galvão Filho MM, D'Ippolito G, Sjenfeld J, Giuliano LM. Value of CEA level determination in gallbladder bile in the diagnosis of liver metastases secondary to colorectal adenocarcinoma. *Sao Paulo Med J* 2001; **119**: 110-113
- 23 **Li Destri G**, Curreri R, Lanteri R, Gagliano G, Rodolico M, Di Cataldo A, Puleo S. Biliary carcinoembryonic antigen in the diagnosis of occult hepatic metastases from colorectal cancer. *J Surg Oncol* 2002; **81**: 8-11
- 24 **Wang JY**, Chiang JM, Jeng LB, Changchien CR, Chen JS, Hsu KC. Resection of liver metastases from colorectal cancer: are there any truly significant clinical prognosticators? *Dis Colon Rectum* 1996; **39**: 847-851
- 25 **Gervaz P**, Blanchard A, Pampallona S, Mach JP, Fontollet C, Gillet M. Prognostic value of postoperative carcinoembryonic antigen concentration and extent of invasion of resection margins after hepatic resection for colorectal metastases. *Eur J Surg* 2000; **166**: 557-561
- 26 **Uchino R**, Kanemitsu K, Obayashi H, Hiraoka T, Miyauchi Y. Carcinoembryonic antigen (CEA) and CEA-related substances in the bile of patients with biliary diseases. *Am J Surg* 1994; **167**: 306-308
- 27 **Frikart L**, Fournier K, Mach JP, Givel JC. Potential value of biliary CEA assay in early detection of colorectal adenocarcinoma liver metastases. *Eur J Surg Oncol* 1995; **21**: 276-279
- 28 **Svenberg T**, Hammarstrom S, Hedin A. Purification and properties of biliary glycoprotein I (BGP I). Immunochemical relationship to carcinoembryonic antigen. *Mol Immunol* 1979; **16**: 245-252
- 29 **Thomas P**. Studies on the mechanisms of biliary excretion of circulating glycoproteins. The carcinoembryonic antigen. *Biochem J* 1980; **192**: 837-843
- 30 **Tabuchi Y**, Deguchi H, Imanishi K, Saitoh Y. Comparison of carcinoembryonic antigen levels between portal and peripheral blood in patients with colorectal cancer. Correlation with histopathologic variables. *Cancer* 1987; **59**: 1283-1288
- 31 **Liu LX**, Jiang HC, Piao DX. Radiofrequency ablation of liver cancers. *World J Gastroenterol* 2002; **8**: 393-399
- 32 **Liu LX**, Zhang WH, Jiang HC. Current treatment for liver metastases from colorectal cancer. *World J Gastroenterol* 2003; **9**: 193-200

Edited by Xu XQ and Wang XL

Effects of carbon dioxide and nitrogen on adhesive growth and expressions of E-cadherin and VEGF of human colon cancer cell CCL-228

Kai-Lin Cai, Guo-Bing Wang, Li-Juan Xiong

Kai-Lin Cai, Guo-Bing Wang, General Surgery Department, Union Hospital, Tongji Medical College, Huazhong University of Science and Technology, Wuhan 430022, Hubei Province, China

Li-Juan Xiong, Infectious Disease Department, Union Hospital, Tongji Medical College, Huazhong University of Science and Technology, Wuhan 430022, Hubei Province, China

Supported by the Natural Science Foundation of Hubei Province, No. 2000J062

Correspondence to: Dr. Kai-Lin Cai, General Surgery Department, Union Hospital, Tongji Medical College, Huazhong University of Science and Technology, Wuhan 430022, Hubei Province, China. caikailin@yahoo.com.cn

Telephone: +86-27-85726405 **Fax:** +86-27-85776343

Received: 2003-03-03 **Accepted:** 2003-04-05

Abstract

AIM: To study the effects of carbon dioxide on the metastatic capability of cancer cells, and to compare them with that of nitrogen.

METHODS: The colon cancer cell CCL-228 was treated with 100 % carbon dioxide or nitrogen at different time points and then cultured under normal condition. Twelve hours after the treatment, the survival rates of suspension cells and the expressions of e-cadherin and VEGF were examined.

RESULTS: After 60 min of carbon dioxide and longer time of nitrogen treatment, the suspended cells increased and the expression of e-cadherin decreased while the expression of VEGF was enhanced significantly. And the effects of nitrogen were similar to, but weaker than, those of carbon dioxide.

CONCLUSION: Carbon dioxide may improve the metastatic capability of cancer cells and its effects are significantly stronger than that of nitrogen. A sequential use of carbon dioxide and nitrogen in pneumoperitoneum may take the advantage of both gases.

Cai KL, Wang GB, Xiong LJ. Effects of carbon dioxide and nitrogen on adhesive growth and expressions of E-cadherin and VEGF of human colon cancer cell CCL-228. *World J Gastroenterol* 2003; 9(7): 1594-1597
<http://www.wjgnet.com/1007-9327/9/1594.asp>

INTRODUCTION

The indications for laparoscopic surgery have expanded significantly thanks to the improved expertise and equipment. The main method to expose the operative field is carbon dioxide pneumoperitoneum. A large number of laparoscopic surgeries for gastrointestinal malignant diseases, especially rectum or colon resections, have been performed. But there is a dispute on whether laparoscopic surgery is suitable for

malignant diseases^[1-6]. To investigate if carbon dioxide influences the metastatic capability of gastrointestinal cancer cells, we studied the effects of carbon dioxide on the adhesive growth and the expression of cadherin and VEGF of a colon cancer cell line CCL-228 propagated *in vitro*. And the effects of carbon dioxide were compared with those of nitrogen. We found that, the metastatic ability of CCL-228 cells might elevate after carbon dioxide treatment and the influence of nitrogen was significantly milder than that of carbon dioxide. Based on these results, we proposed a sequential pneumoperitoneum method to reduce the side-effect but remain the safe-guardness of carbon dioxide, *i.e.*, to establish the pneumoperitoneum with carbon dioxide and to maintain it with nitrogen, and before the end of the surgery, insufflating carbon dioxide to remove the unabsorbable nitrogen. In the present study, we evaluated the influence of the sequential gas treatment on the expression of E-cadherin and VEGF in CCL-228 cells.

MATERIALS AND METHODS

Cell culture

Human colon cancer cell line CCL-228, supplied by the Type Culture Collection Center, Wuhan University, was maintained in RPMI 1640 medium supplemented with 10 % fetal bovine serum. The cell cultures were maintained as monolayer in a plastic flask and incubated in 5 % CO₂, 95 % air at 37 °C. The cultures were free of mycoplasma.

Carbon dioxide or nitrogen treatment

The CCL-228 cells were seeded onto 6-well plates (1×10⁶ cells per well). When the button was 80 % covered, the cells were divided into two groups. Three parallel wells of cells in each group were incubated either in 100 % CO₂ (CO₂ group) or in 95 % N₂+5 % CO₂ (N₂ group) for 30, 60, 120, 180 min, respectively. To evaluate the effect of sequential pneumoperitoneum on the metastatic ability of colon cancer cells, 3 wells of CCL-228 cells were treated with CO₂ for 15 min, with nitrogen for 90 min or 150 min, and then with CO₂ again for 15 min. After the gas treatment, all cells were incubated again in 5 % CO₂, 95 % air for 12 h.

Histology

The supernate was collected and stained with typan blue, and the survival rate of the supernatant cells was estimated.

Immunohistochemistry

The adhesive growth cells were collected and stained for immunohistochemical studies on the expressions of VEGF and E-cadherin. The cell smear was fixed with cold acetone for 10 min at room temperature and rinsed with phosphate-buffered saline (PBS). The endogenous peroxidase was blocked using 3 % hydrogen peroxide for 10 min and the unspecific combined site was blocked with normal goat serum. Excessive blocking serum was drained and the samples were incubated at 40 °C for 18 h with the appropriate dilution of monoclonal mouse anti-human

VEGF or E-cadherin (Santa Cruz). Each sample was then rinsed with PBS and incubated for 10 min at room temperature with 50 μ l of biotin-labeled goat anti-mouse IgG. The samples were then rinsed with PBS and incubated for 10 min at room temperature with 50 μ l peroxidase conjugated avidin. The smears were rinsed with PBS and incubated for 5 min with diaminobenzidine. They were then washed with water and counterstained with Mayer's hematoxylin and fixed with neutral resin. The smears were examined under microscope and positive reaction was indicated by brownish precipitate in cytoplasm.

Analysis of results

The smears were analyzed with MPZAS-500 multimedia color pathological graph analyzing system. The average integral light density (ILD) of positive staining in each sample was obtained and presented as $\bar{x} \pm s$. Results were then analyzed with Student's *t* test.

RESULTS

Effects of CO₂ and N₂ on adhesive growth of CCL-228

Sixty min of CO₂ treatment or 120 min of N₂ treatment was sufficient to increase the rate of suspending growth cells very significantly (Table 1). The difference of rates of alive suspending cells between CO₂ and N₂ treatments was very significant after 60 min of treatment ($P < 0.01$).

Table 1 Counts and survival rate of suspension CCL-228 cells after CO₂ or N₂ treatment

Duration	Counts of suspension cells ($\times 1000$ /ml)		Survival rate of suspension cells	
	CO ₂ group	N ₂ group	CO ₂ group	N ₂ group
0 min	4.2 \pm 0.1		0.884 \pm 0.011	
30 min	7.5 \pm 2.9	4.9 \pm 2.5	0.912 \pm 0.018	0.852 \pm 0.022
60 min	16.7 \pm 5.4 ^{ab}	5.2 \pm 0.7	0.914 \pm 0.041	0.897 \pm 0.021
120 min	23.2 \pm 10.7 ^{ac}	8.5 \pm 1.4 ^d	0.904 \pm 0.034	0.912 \pm 0.023
180 min	32.1 \pm 5.5 ^{ac}	9.7 \pm 3.3 ^d	0.845 \pm 0.028	0.912 \pm 0.032

^a $P < 0.01$, vs the 0 min in same group; ^b $P < 0.05$, vs N₂ group at same time; ^c $P < 0.01$, vs N₂ group at same time; ^d $P < 0.05$, vs 0 min in same group.

Effects of CO₂ and N₂ on expression of E-cadherin in CCL-228 cell

Both CO₂ and N₂ treatment depressed the expression of E-cadherin in CCL-228 cell (Figure 1). The expression of E-cadherin after 60 min or longer time of CO₂ treatment was significantly different from that after the same time periods of N₂ treatment. Comparing with the expression of E-cadherin before any gas treatment, 120 min or longer time of CO₂ treatment produced a very significant depression ($P < 0.01$) and the same periods of N₂ treatment caused a significant depression ($P < 0.05$).

Effects of CO₂ and N₂ on expression of VEGF in CCL-228 cell

Both CO₂ and N₂ treatment improved the expression of VEGF in CCL-228 cell (Figure 2). Thirty min to 120 min of CO₂ treatment caused significantly higher expression of VEGF comparing with the normal control and the same periods of N₂ treatment ($P < 0.05$). CO₂ treatment for 180 min resulted in a VEGF expression significantly lower than CO₂ treatment for 120 min, but still significantly higher than normal control. As for N₂, 30 min to 180 min of treatment resulted in a continuous increase of VEGF expression.

Effects of sequential treatment with CO₂ and N₂ on expression of E-cadherin and VEGF in CCL-228 cell

The effects of sequential gas treatment for 120 min or 180 min on expression of E-cadherin and VEGF in CCL-228 cell were

not significantly different from those of continuous nitrogen treatment but significantly milder than those of continuous carbon dioxide treatment (Figures 1 and 2).

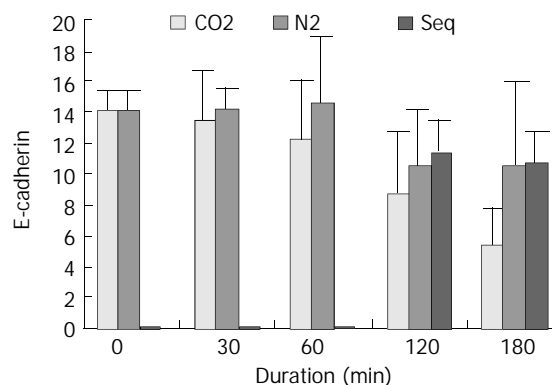


Figure 1 The expression of E-Cadherin in CCL-228 cells after gas treatment.

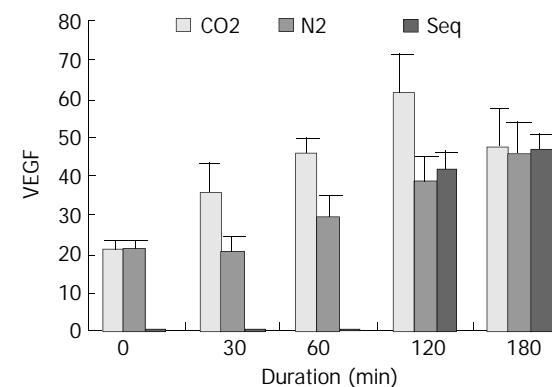


Figure 2 The expression of VEGF in CCL-228 cells after gas treatment.

DISCUSSION

It has been verified that laparoscopic surgery has many virtues such as minimal injury, less pain, sooner rehabilitation and less intervention in the immune function^[7-11]. Now many gastroenteric surgeries including cancer resection could be fulfilled under laparoscope. Clinical trials have proved that laparoscopic surgery is feasible for gastroenteric malignant diseases. However, cancer metastasis in trocar site has been reported and has aroused a debate about whether laparoscopic surgery is suitable for malignant diseases. There is no consensus on if the incidence of metastasis in trocar site was accurately higher than that in the wound after open surgery^[6], because the cases were few in each paper and there has been a decline in incidence of trocar site metastasis in recent reports, due to more attention paid to the wound protection during extraction of the specimen. Moreover, open surgery has been reported to increase cancer metastasis^[12-15], and had more intervention in immunity. Therefore, whether laparoscopic surgery is suitable to early malignant diseases needs to be clarified by more clinical trials and further laboratory studies. In the present experiment, we studied the effect of carbon dioxide on the adhesive ness of colon cancer cells to the culture plate and the expressions of E-cadherin and VEGF. It should be noted that, the duration of carbon dioxide treatment was much longer than others because a laparoscopic surgery for gastroenteric cancer resection often lasts 2-3 hours.

We found that both carbon dioxide and nitrogen influenced the adhesive growth of CCL-228 cells. The cells in supernate increased after CO₂ or N₂ treatment. The rate of living cells in

supernate had no significant change confirmed by typan blue staining. Therefore, increase of cells in the supernate was a result of detachment of cells from the culture plate, but not the result of apoptosis or necrosis after gas treatment. It is suggested that CO₂ or N₂ could influence the adhesive ness of CCL-228 to matrix, resulting in easier metastasis by improving the detachment of cancer cells from the original lesion. We found that 30 min of CO₂ treatment caused an obvious increase of suspensive growth but the increase was not statistically significant, while 60 min and longer time produced very significant results. There were several laboratory reports on the effect of CO₂ on liver metastasis of intestinal cancer but the conclusions were controversial. We suppose that the controversy might result from a relatively short duration of pneumoperitoneum. Considering that laparoscopic surgery for malignant diseases usually needs several hours, the pneumoperitoneum time in experiments should be long enough to produce a practical result.

E-cadherin is one of the key adhesive molecules to mediate intercellular adhesion. It has been proved that, E-cadherin expression is depressed in metastatic tissues, which is helpful for the detachment of cancer cells from original lesions^[16-20]. We examined the expression of E-cadherin in CCL-228 to explore if it plays a role in the influence of carbon dioxide on the adhesive growth of CCL-228. The results showed that, carbon dioxide treatment depressed E-cadherin expression and the effect was positively related to the duration of carbon dioxide treatment. Because cancer metastasis course includes the detachment of cells from the original lesion and also the settlement in the new environment, depression of adhesion has a two-edged effect on the metastasis of cancer. It is helpful for cancer cell dissemination but unfavorable to the settlement of circulating cancer cells.

The expression of VEGF is essential for cancer metastasis because it is a vital factor in tumor angiogenesis. A great deal of researches have indicated that cancer cells with higher VEGF expression results in much more persistently growing metastatic lesions, and inhibition of VEGF expression or function could interrupt the metastasis^[21-25]. Therefore, we studied further the effect of carbon dioxide on VEGF expression in CCL-228 and found that it promoted VEGF expression. The promotion of VEGF expression suggests that decrease of E-cadherin expression in CCL-228 cells was not due to a general inhibition of protein synthesis by carbon dioxide, and the results implicate that carbon dioxide pneumoperitoneum was favorable for not only the detachment of cancer cells from the primary lesion but also for the growth of micrometastatic cells and their aggregation into a mass.

Many factors are supposed to be associated with the favorable effect on cancer growth and metastasis by carbon dioxide. The topical acidosis might be the main reason, and the less absorbable gases such as nitrogen and helium have less influence on metastasis^[1,26,27]. In this experiment, we found that, comparing with carbon dioxide, nitrogen had a similar but much more mild effects on cancer cells. Since carbon dioxide had a significant duration-effect relationship with the expression of E-cadherin and VEGF, reduced carbon dioxide insufflation duration might be less harmful to patients with malignant diseases. Here we propose a sequential pneumoperitoneum, namely, establishing the pneumoperitoneum with carbon dioxide and maintaining it with nitrogen, and then, before the end of surgery, insufflating carbon dioxide to remove the unabsorbable nitrogen. We found that, during the 120 min or 180 min of gas treatment, when carbon dioxide was applied in the first and last 15 min but replaced with nitrogen in the time between E-cadherin and VEGF expressions were significantly different from that by persistent carbon dioxide treatment. Therefore, we think that in laparoscopic surgery

for malignant diseases, the sequential pneumoperitoneum method may take the advantages of both nitrogen and carbon dioxide, as the effect of carbon dioxide on metastasis is reduced by nitrogen replacement during the operation, and the safe guard ness of carbon dioxide to prevent from gas embolism, usually happening during the establishment of pneumoperitoneum, is remained. And the remaining gas in abdomen after surgery is also carbon dioxide, which is ready to be absorbed.

REFERENCES

- 1 **Neuhaus SJ**, Watson DI, Ellis T, Rowland R, Rofe AM, Pike GK, Mathew G, Jamieson GG. Wound metastasis after laparoscopy with different insufflation gases. *Surgery* 1998; **123**: 579-583
- 2 **Schaeff B**, Paolucci V, Thomopoulus J. Port site recurrences after laparoscopic surgery. *Dig Surg* 1998; **15**: 124-134
- 3 **Wexner S**, Cohen SM. Port site metastases after laparoscopic colorectal surgery for cure of malignancy. *Br J Surg* 1995; **82**: 295-298
- 4 **Lacy AM**, Delgado S, Garcia-Valdecasas JC, Castells A, Pique JM, Grande L, Fuster J, Targarona EM, Pera M, Visa J. Port site metastases and recurrence after laparoscopic colectomy. *Surg Endosc* 1998; **12**: 1039-1042
- 5 **Mathew G**, Watson DI, Rofe AM, Baigrie CF, Ellis T, Jamieson GG. Wound metastases following laparoscopic and open surgery for abdominal cancer in a rat model. *Br J Surg* 1996; **83**: 1087-1090
- 6 **Gibson M**, Byrd C, Pierce C, Wright F, Norwood W, Gibson T, Zibari GB. Laparoscopic colon resections: a five-year retrospective review. *Am Surg* 2000; **66**: 245-248
- 7 **Trokkel MJ**, Bessler M, Treat MR, Whelan RL, Nowygrod R. Preservation of immune response after laparoscopy. *Surg Endosc* 1994; **8**: 1385-1387
- 8 **Allendorf JD**, Bessler M, Whelan RL, Trokkel M, Laird DA, Terry MB, Treat MR. Postoperative immune function varies inversely with the degree of surgical trauma in a murine model. *Surg Endosc* 1997; **11**: 427-430
- 9 **Cho JM**, LaPorta AJ, Clark JR, Schofield MJ, Hammond SL, Mallory PL 2nd. Response of serum cytokines in patients undergoing laparoscopic cholecystectomy. *Surg Endosc* 1994; **8**: 1380-1383
- 10 **Wexner SD**, Cohen SM, Johansen OB, Noguera JJ, Jagelman DG. Laparoscopic colorectal surgery: a prospective assessment and current perspective. *Br J Surg* 1993; **80**: 1602-1605
- 11 **Evrard S**, Falkenrodt A, Park A, Tassetti V, Mutter D, Marescaux J. Influence of CO₂ pneumoperitoneum on systemic and intra-abdominal cell-mediated immunity. *World J Surg* 1997; **21**: 353-356
- 12 **Murthy SM**, Goldschmidt RA, Rao LN, Ammirati M, Buchmann T, Scanlon EF. The influence of surgical trauma on experimental metastasis. *Cancer* 1989; **64**: 2035-2044
- 13 **Da Costa ML**, Redmond P, Bouchier-Hayes DJ. The effect of laparotomy and laparoscopy on the establishment of spontaneous tumor metastases. *Surgery* 1998; **124**: 516-525
- 14 **Paik PS**, Misawa T, Chiang M, Towson J, Im S, Ortega A, Beart RW Jr. Abdominal incision tumor implantation following pneumoperitoneum laparoscopic procedure vs. standard open incision in a syngeneic rat model. *Dis Colon Rectum* 1998; **41**: 419-422
- 15 **Ishida H**, Murata N, Yamada H, Nakada H, Takeuchi I, Shimomura K, Fujioka M, Idezuki Y. Pneumoperitoneum with carbon dioxide enhances liver metastases of cancer cells implanted into the portal vein in rabbits. *Surg Endosc* 2000; **14**: 239-242
- 16 **Dorudi S**, Hanby AM, Poulosom R, Northover J, Hart IR. Level of expression of E-cadherin mRNA in colorectal cancer correlates with clinical outcome. *Br J Cancer* 1995; **71**: 614-616
- 17 **Jiang WG**. E-cadherin and its associated protein catenins, cancer invasion and metastasis. *Br J Surg* 1996; **83**: 437-446
- 18 **Kinsella AR**, Green B, Lepts GC, Hill CL, Bowie G, Taylor BA. The role of the cell-cell adhesion molecule E-cadherin in large bowel tumour cell invasion and metastasis. *Br J Cancer* 1993; **67**: 904-909

- 19 **Jiang WG.** Cell adhesion molecules in the formation of liver metastasis. *J Hepatobiliary Pancreat Surg* 1998; **5**: 375-382
- 20 **Zhou YN,** Xu CP, Han B, Li M, Qiao L, Fang DC, Yang JM. Expression of E-cadherin and beta-catenin in gastric carcinoma and its correlation with the clinicopathological features and patient survival. *World J Gastroenterol* 2002; **8**: 987-993
- 21 **Bruns CJ,** Liu W, Davis DW, Shaheen RM, McConkey DJ, Wilson MR, Bucana CD, Hicklin DJ, Ellis LM. Vascular endothelial growth factor is an in vivo survival factor for tumor endothelium in a murine model of colorectal carcinoma liver metastases. *Cancer* 2000; **89**: 488-499
- 22 **Ellis LM,** Takahashi Y, Liu W, Shaheen RM. Vascular endothelial growth factor in human colon cancer: biology and therapeutic implications. *Oncologist* 2000; **5**(Suppl 1): 11-15
- 23 **Kondo Y,** Arii S, Mori A, Furutani M, Chiba T, Imamura M. Enhancement of angiogenesis, tumor growth, and metastasis by transfection of vascular endothelial growth factor into LoVo human colon cancer cell line. *Clin Cancer Res* 2000; **6**: 622-630
- 24 **Liu DH,** Zhang XY, Fan DM, Huang YX, Zhang JS, Huang WQ, Zhang YQ, Huang QS, Ma WY, Chai YB, Jin M. Expression of vascular endothelial growth factor and its role in oncogenesis of human gastric carcinoma. *World J Gastroenterol* 2001; **7**: 500-505
- 25 **Tao HQ,** Lin YZ, Wang RN. Significance of vascular endothelial growth factor messenger RNA expression in gastric cancer. *World J Gastroenterol* 1998; **4**: 10-13
- 26 **Jacobi CA,** Sabat R, Bohm B, Zieren HU, Volk HD, Müller JM. Pneumoperitoneum with carbon dioxide stimulates growth of malignant colonic cells. *Surgery* 1997; **121**: 72-78
- 27 **Jacobi CA,** Wenger F, Sabat R, Volk T, Ordemann J, Muller JM. The impact of laparoscopy with carbon dioxide versus helium on immunologic function and tumor growth in a rat model. *Dig Surg* 1998; **15**: 110-116

Edited by Ma JY

Meta analysis of risk factors for colorectal cancer

Kun Chen, Jiong-Liang Qiu, Yang Zhang, Yu-Wan Zhao

Kun Chen, Jiong-Liang Qiu, Yang Zhang, Yu-Wan Zhao,
Department of Epidemiology, School of Medicine, Zhejiang
University, Hangzhou 310031, Zhejiang Province, China
Supported by the National Natural Science Foundation of China,
No.30170828

Correspondence to: Kun Chen, Department of Epidemiology, School
of Medicine, Zhejiang University, Hangzhou 310031, Zhejiang
Province, China. ck@zjuem.zju.edu.cn

Telephone: +86-571-87217190

Received: 2003-03-02 **Accepted:** 2003-04-01

Abstract

AIM: To study the risk factors for colorectal cancer in China.

METHODS: A meta-analysis of the risk factors of colorectal
cancer was conducted for 14 case-control studies, and
reviewed 14 reports within 13 years which included 5034
cases and 5205 controls. Dersimonian and Laird random
effective models were used to process the results.

RESULTS: Meta analysis of the 14 studies demonstrated that
proper physical activities and dietary fibers were protective
factors (pooled OR<0.8), while fecal mucohemorrhage,
chronic diarrhea and polyposis were highly associated with
colorectal cancer (all pooled OR>4). The stratified results
showed that different OR values of some factors were due to
geographic factors or different resources.

CONCLUSION: Risks of colorectal cancer are significantly
associated with the histories of intestinal diseases or relative
symptoms, high lipid diet, emotional trauma and family
history of cancers. The suitable physical activities and dietary
fibers are protective factors.

Chen K, Qiu JL, Zhang Y, Zhao YW. Meta analysis of risk
factors for colorectal cancer. *World J Gastroenterol* 2003; 9
(7): 1598-1600

<http://www.wjgnet.com/1007-9327/9/1598.asp>

INTRODUCTION

Meta-analysis named by Glass, is generally defined as a
quantitative summary of studies in a particular area, which
has addressed the same research question, and an overall
summary obtained by statistically aggregating the results of
the reviewed studies. It is used to improve the statistical
efficiency, to evaluate the disadvantages of formulated
researches, and hypothesis and to reach reliable conclusions
from the mixed assortment of the potentially relevant studies
to determine the most promising directions for future
researches. It has been gradually applied in medicine since it
was adopted in 1970s.

Colorectal cancer is one of the most malignant cancers in
China and has been steadily increasing in frequency in large
or middle cities^[1]. Thus, in order to provide the overall
information on colorectal cancer risk factors, we performed
a meta analysis of the results of 14 case-control studies in
China.

MATERIALS AND METHODS

Materials

The published Chinese literatures of case-control studies related
to colorectal cancer risk factors from 1988 to 2000 were
collected by bibliographic searches through Index of Chinese
Science and Technology Data. The selection criteria of
literature were as follows: The independent case-control studies
were published in Chinese magazines from 1988 to 2000, each
study should have the synthetic statistical index: odds ratio
(OR), the similar research goal with the identical study method.
The overall results of literature should be presented with the
corresponding statistical index, the latest articles were chosen
among several ones with the same sample size. Duplicated,
poor quality reports or those with little information on colon
cancer were discarded. Thus, 14 papers were chosen by
screening, and 5 034 cases and 5 205 controls were accumulated.

Methods

Different stratified studies were performed, including studies
on prevalence/death cases (CD) versus incidence cases (ND)
according to different cases, studies on general population (PB)
and on patients in hospital (HB). The studies were classified
in rural or urban areas in the north (NOR) and those in the
south (SOU) separated by the Yangtze River as the boundary.
Studies were divided into colon cancer (Jca) and rectal cancer
(Zca) according to the sites of cancer.

Statistical treatment

Test of equal variance was conducted before statistical analysis,
and the index odds ratio (OR) was performed using the model
established by Dersimonian and Laird. The fundamental
principle was as follows: $y_i = \ln OR_i$, with its variance: $S_i = [P_{1i}$
 $(1 - P_{1i})/y_i n_{1i}] + [P_{2i}(1 - P_{2i})/n_{2i}]$, (P_{1i} and n_{1i} are the exposing rate
of the case group and the sample size, respectively; P_{2i} and n_{2i}
are the corresponding parameters in control group). OR could
be calculated with the confidence limit, standard error or Chi-
squared value in some way if the basic data could not be
acquired. If the total comprehensive effect was \bar{y}^* , then $\bar{y}^* = \sum$
 $(W_i^* \cdot y_i) / \sum W_i^*$, with 95 % confidence interval $\bar{y}^* \pm 1.96 \cdot SE(\bar{y}^*)$.

$$SE(\bar{y}^*) = 1 / \sum W_i^*$$

$$W_i^* = (W_i^{-1} + \Delta^2)^{-1}$$

$$W_i = S_i^{-1}$$

$$\Delta^2 = \max\{0, Q - (k-1) / \sum W_i - (\sum W_i^2 / \sum W_i)\}$$

$$Q = \sum [W_i (y_i - \bar{y})^2]$$

$$\bar{y} = \sum (W_i \cdot y_i) / \sum W_i$$

RESULTS

The papers used in the studies are shown in Table 1. The
number of literature in Zhejiang accounted for a half of the
total in this country since Zhejiang had a high incidence of
colorectal cancer.

Meta analysis showed that all the risk factors of colorectal
cancer except alcohol drinking were significant ($P < 0.05$),
(Table 2), while proper physical activities and dietary fibers
were protective factors (pooled OR was 0.6-0.8). Histories of
fecal mucohemorrhage and bowel polyps were more

significantly associated with colorectal cancer (pooled OR>4) than other ones (pooled OR was 1-4).

Results of the stratified meta analysis including index cases, study area, location of cancer and origins of the controls are shown in Table 3. The pooled OR of family history of cancers differed significantly between prevalence/death cases (CD) and

incidence cases (ND), which in the latter (pooled OR=3.73 [95 % confidence interval (CI) 3.14-4.44]) was one-fold more than that in the former (1.76 [1.71-1.81]). History of chronic diarrhea was more frequently significant among rectum cancers (pooled OR=4.02, $P<0.05$). However, no significant association was observed with colon cancer ($P>0.05$).

Table 1 Case-control studies on risk factors of colorectal cancer

No	Author	Area	Number of cases	Number of factors	Sources of references
1	JIAO Den-Ao	Jiashan	160	9	Zhonghua Liuxingbingxue Zazhi, 1988, 9(6): 354-357
2	WU Den-Ren	Jiashan	114	5	Shiyong Zhongliu Zazhi, 1990, 5(2): 95-99
3	YANG Gong	Shanghai	850	2	Zhonghua Liuxingbingxue Zazhi, 1992, 13(1): 30-33
4	ZHANG Cao	Beijing	250	5	Zhonghua Liuxingbingxue Zazhi, 1992, 13(6): 321-323
5	ZOU Run	Jiashan	41	10	Zhongguo Manxingbing Yufang Yu Kongzhi, 1993, 1(5): 213-215
6	MEN Fan-He	Guangdong	100	3	Diyi Junyi Daxue Xuebao, 1994, 14(4): 281-283
9	LIU Xi-Yong	Shanghai	286	6	Zhongguo Manxingbing Yufang Yu Kongzhi, 1994, 2(3): 122-124
7	YANG Gong	Shanghai	1328	4	Zhonghua Liuxingbingxue Zazhi, 1994, 15(5): 299-303
8	YANG Gong			3	Zhongguo Zhongliu Linchuang, 1995, 22(6): 403-408
10	LAI Kuang-De	Dalian	129	3	Zhongguo Manxingbing Yufang Yu Kongzhi, 1995, 3(3): 106-109
11	HE Xi-Zhen	Shenyang	390	2	Shiyong Zhongliu Xuebao, 1996, 10(2): 64-65
12	YANG Gong	Shanghai	3166	3	Zhongliu, 1996, 16(2): 74-78
13	ZOU Run	Hangzhou	245	5	Zhejiang Yike Daxue Xuebao, 1996, 25(5): 204-206
4	LIU Ai-Zong	Hunan	153	7	Zhongguo Gonggong Weisheng, 1997, 13(4): 206-207

Table 2 Results from meta-analysis of risk factors of colorectal cancer

Factors	Number of references	Pooled OR and 95 % C.I.	Factors	Number of references	Pooled OR and 95% C.I.
(1) History of chronic diarrhea	7	4.80 (4.30~5.37)	(8) Pickled vegetables	3	1.86 (1.67~2.07)
(2) History of fecal mucohemorrhage	5	7.18 (5.06~10.21)	(9) High lipid food	3	3.16 (2.22~4.51)
(3) History of bowel polyps	5	12.69 (7.49~21.48)	(10) Proper physical activities	4	0.74 (0.72~0.77)
(4) History of constipation	4	2.23 (1.95~2.54)	(11) Alcohol drinking	5	1.06 (0.91~1.24)
(5) History of appendicitis	3	1.98 (1.71~2.28)	(12) Cigarette smoking	5	1.40 (1.10~1.77)
(6) Dietary fibers	5	0.79 (0.59~0.99)	(13) Emotional trauma	4	2.95 (2.81~3.09)
(7) Fish fry-cooked with soybean sauce	4	2.99 (2.69~3.35)	(14) Family history of cancers	7	2.27 (2.12~2.44)
(1) references: 1,2,5,7,9,13, 14		(2) references: 1,5,7,9,13	(3) references: 1,2,5,7,12		
(4) references: 1,5,7,9		(5) references: 1,2,5	(6) references: 4,6,10,11,14		
(7) references: 1,5,6, 7		(8) references: 2,6,14	(9) references: 4,5,14		
(10) references: 4,10,13,14		(11) references: 2,5,8,13,14	(12) references: 2,5,6,8,14		
(13) references: 1,4,5,7		(14) references: 1,3,4,5,6,7,14			

Table 3 Results from stratified meta-analysis of risk factors of colorectal cancer

Factors	Strata	Pooled OR and 95% C.I.	Factors	Strata	Pooled OR and 95% C.I.
History of chronic diarrhea	CD ^a	6.04 (5.45~6.70)	Pickled vegetables	CD	1.58 (1.20~2.07)
	ND ^a	3.99 (2.81~5.66)		ND	2.30 (1.30~4.20)
	Jca ^b	7.01 (0.48~10.12)		Jca	1.70 (1.10~2.50)
	Zca ^b	4.02 (1.13~14.21)		Zca	1.50 (1.01~2.30)
	HB	6.60 (2.46~11.21)		HB	2.30 (1.30~4.20)
Fecal mucohemorrhage	PB	4.50 (3.90~5.17)	Alcohol drinking	PB	1.58 (1.20~2.07)
	CD ^b	9.81 (4.55~21.17)		CD ^b	0.91 (0.71~1.17)
	ND ^b	3.60 (2.80~4.80)		ND ^b	1.65 (1.03~2.63)
	Jca ^b	2.80 (0.75~10.46)		HB ^b	1.65 (1.03~2.63)
	Zca ^b	4.56 (2.12~9.81)		PB ^b	0.91 (0.71~1.17)
History of bowel polyps	CD ^a	7.40 (4.13~13.28)	Cigarette smoking	CD ^b	0.74 (0.43~1.27)
	ND ^a	22.30 (12.40~40.01)		ND ^b	1.92 (1.49~2.47)
	Jca	17.42 (14.54~20.85)		HB ^b	1.92 (1.49~2.47)
	Zca	12.14 (3.07~28.00)		PB ^b	0.74 (0.43~1.27)
History of constipation	CD	2.53 (1.55~4.11)	Emotional trauma	Jca ^b	2.80 (1.51~3.28)
	ND	1.90 (1.50~2.40)		Zca ^b	1.63 (0.39~6.85)
	Jca ^b	3.4 (1.02~11.39)		NOR	3.36 (2.21~5.12)
	Zca ^b	0.89 (0.09~8.53)		SOU	2.53 (2.28~2.81)
	HB ^b	0.86 (0.58~0.96)		Proper physical activities	CD
PB ^b	0.37 (0.06~2.13)	ND	0.57 (0.35~0.90)		
Dietary fibers	CD	2.84 (2.31~3.48)	NOR ^a		0.69 (0.67~0.71)
	ND	1.02 (0.40~2.57)	SOU ^a		0.77 (0.70~0.85)
	NOR ^b	0.43 (0.18~0.97)	HB		0.57 (0.35~0.90)
	SOU ^b	1.02 (0.40~2.57)	PB	0.79 (0.77~0.81)	
	HB ^b	0.86 (0.58~0.96)	Family history of cancers	CD ^a	1.76 (1.71~1.81)
PB ^b	0.37 (0.06~2.13)	ND ^a		3.73 (3.14~4.44)	
CD	2.84 (2.31~3.48)	Jca ^a		2.84 (2.58~3.13)	
ND	3.20 (1.60~6.30)	Zca ^a		1.52 (1.34~1.72)	
Jca ^b	7.01 (1.10~12.01)	HB ^a		3.73 (3.14~4.44)	
Fish fry-cooked with soybean	Zca ^b	1.18 (0.30~8.01)	PB ^a	1.76 (1.71~1.81)	
	HB	3.20 (1.60~6.30)			
	PB	2.84 (2.31~3.48)			

^a: No mutual involvement of OR by correspondent two ranges of 95 % CI was found. ^b: At least one 95 % CI of pooled OR was found including 1.00.

DISCUSSION

Environmental factors are the predominant contributors to colorectal cancer, and genetic factors show significant effects^[1,3-5]. Meta analysis indicated that a variety of factors could contribute to colorectal cancer as follows.

1. Intestinal disorders and colorectal cancer Precancerous syndromes or diseases based on the review of Chinese literature included chronic diarrhea, fecal mucohemorrhage, polyposis, constipation, etc. Therefore, colorectal cancer should be suspected if chronic diarrhea, fecal mucohemorrhage or constipation of unknown cause occur in patients with a history of bowel polyps^[2]. In addition, whether appendicitis is a risk factor of colorectal cancer remains plausible. However, it is considered as one of the risk factors since its pooled OR was 1.98 ($P<0.05$) demonstrated in this study. Because appendicitis weakens the immunological function of appendix and thus causes colorectal cancer.

2. Diet High fat diet was the highest risk factor of colon cancer ($OR=3.16$), followed by fish fry-cooked with soybean sauce ($OR=2.99$) and pickled vegetables ($OR=1.86$). In contrast, dietary fibers played a protective role in colorectal cancer (pooled $OR=0.79$, $P<0.05$). Fried fish with soybean sauce may generate mutagenic heterocyclic amines as red meats^[6,7]. The dietary fiber may shorten the transporting time of excrement in intestines, decrease the time of carcinogens affecting intestinal mucus and reduce the growth of bacterial strains that produce carcinogens in the colonic lumen. However, no evidence was reported to suggest that high dietary fiber could reduce the incidence or recurrence of adenomatous polyps during a two to four year period^[8]. In addition, many experimental findings indicated an association between diet with high calcium and vitamin D and low risk for colorectal cancer, which deserve further study^[9].

3. Physical activity, cigarette smoking and alcohol The relationship between physical activities and colorectal cancer has been noticed recently. Studies showed that people with proper physical activities had low incidence of colorectal cancer since appropriate physical activities could decrease the random segmentation without propulsion of the intestine, and increase effective vermiculation, thus shortening the transit time of excrement in the intestine and reducing the contact between intestinal mucosa and carcinogen. No significant association was found between alcohol and colorectal cancer in meta analysis, though other studies reported that significantly lower levels of serum cholesterol and triglycerides were found in daily alcohol drinkers with colorectal adenomas^[10], while cigarette smoking was regarded as a risk factor since its OR exceeded 1 ($P<0.05$) although it is plausible whether smoking causes colorectal cancer.

Moreover, it was suggested that long-term emotional trauma and family history of cancers were related to the increased risk of colorectal cancer. However, further work is needed to clarify the mechanism.

Bias and confounding factors can also be found in meta analysis, and so we conducted the stratified analysis as follows: (1) Since studies on the prevalence or death cases could lead to bias due to selection and exposure misclassification, stratified analysis for the index cases was performed, which showed that there was a difference between studies on the prevalence or death cases and those on the incidence cases (Table 3). (2) The results of different strata suggested that studies on incidence cases based on the population should be conducted strictly in the future. (3) Risk factors of colorectal cancer in south and in the north may be different. (4) The cause of colon cancer may not be completely the same as that of cancer in the rectum. In this study, chronic diarrhea and fecal mucohemorrhage were more frequent in cancers of rectum, while complaint of constipation, fish fry-cooked with soybean sauce and emotional trauma were more frequently seen in colon cancer.

Meta means "more comprehensive, transcending"^[11]. Meta analysis has extended quickly from social sciences to medical sciences. Incidence of colorectal cancer has increased over the last decade in China, and it is necessary to study its causes. Thus, synthetic analysis was performed on the etiology of colorectal cancer in China in 12 years with meta analysis. However, the potential confounding factors may not be well controlled due to the limited literature and therefore the result may be affected. Thus, further study is required.

REFERENCES

- Zhang ZS**, Zhang YL. Development of research on colorectal cancer in China. *Shijie Huaren Xiaohua Zazhi* 2001; **9**: 489-494
- Li SR**. Strategy for the early diagnosis of colorectal cancer. *Shijie Huaren Xiaohua Zazhi* 2001; **9**: 780-782
- Lai MD**. Related genes of generation and development of colorectal cancer in China. *Shijie Huaren Xiaohua Zazhi* 2001; **9**: 1227-1232
- Sheng JQ**, Chen ZM. Screening of colorectal cancer with the related genes. *Shijie Huaren Xiaohua Zazhi* 2001; **9**: 783-785
- Johns LE**, Houlston RS. A systematic review and meta-analysis of familial colorectal cancer risks. *Am J Gastroenterol* 2001; **96**: 2992-3003
- Sweeney C**, Coles BE, Nowell S, Lang NP, Kadlubar FF. Novel marker of susceptibility to carcinogens in diet: Associations with colorectal cancer. *Toxicology* 2002; **181-182**: 83-87
- Norat T**, Lukanova A, Ferrari P, Riboli E. Meat consumption and colorectal cancer risk: dose-response meta-analysis of epidemiological studies. *Int J Cancer* 2002; **98**: 241-256
- Asano T**, Mcleod RS. Dietary fiber for the prevention of colorectal adenomas and carcinomas. *Cochrane Database Syst Rev* 2002; **2**: CD003430
- Lipkin M**. Update of preclinical and human studies of calcium and colon cancer prevention. *World J Gastroenterol* 1999; **5**: 461-464
- Fujimori S**, Kishida T, Mitsui K, Yonezawa M, Nagata K, Shibata Y, Tanaka S, Tatsuguchi A, Sato J, Yokoi K, Tanaka N, Ohaki Y, Sakamoto C, Kobayashi M. Influence of alcohol consumption on the association between serum lipids and colorectal adenomas. *Scand J Gastroenterol* 2002; **37**: 1309-1312
- Bailar JC**, Mosteller F. Medical uses of statistics. 2nd edition. *Waltham Mass: Nejm Books* 1992: 422-427

Edited by Ren SY and Wang XL

Expressions of PCNA, p53, p21^{WAF-1} and cell proliferation in fetal esophageal epithelia: Comparative study with adult esophageal lesions from subjects at high-incidence area for esophageal cancer in Henan, North China

Ying Xing, Yu Ning, Li-Qiang Ru, Li-Dong Wang

Ying Xing, Li-Qiang Ru, Department of Neurobiology, Tongji Medical College, Huazhong University of Science and Technology, Wuhan, 430030, Hubei Province, China

Yu Ning, Department of Physiology, College of Medicine, Zhengzhou University, Zhengzhou, 450052, Henan Province, China

Li-Dong Wang, Laboratory for Cancer Research, College of Medicine, Zhengzhou University, Zhengzhou, 450052, Henan Province, China
Supported by National Distinguished Young Scientist Foundation of China, No.30025016

Correspondence to: Dr. Li-Dong Wang, Professor of Pathology and Oncology and Ying Xing, Professor of Physiology, Laboratory for Cancer Research, College of Medicine, Zhengzhou University, Zhengzhou 450052, Henan Province, China. lidong0823@sina.com
Telephone: +86-371-6970165 **Fax:** +86-371-6970165

Received: 2003-03-02 **Accepted:** 2003-03-25

Abstract

AIM: To characterize the expression of p53, p21^{WAF-1} and proliferation-cell-nuclear-antigen (PCNA) in fetal esophageal epithelia and to determine the role of these genes in proliferation of fetal and adult esophageal epithelial cells.

METHODS: Immunohistochemical avidin-biotin peroxidase complex (ABC) method was applied to 31 cases of fetal esophageal specimens and 194 cases of adult esophageal specimens to detect the expression of p53, p21^{WAF-1} and PCNA in fetal and adult esophageal epithelia.

RESULTS: Both the PCNA positive immunostaining cell number and PCNA positive immunostaining rate in fetal esophageal epithelia (506±239) were significantly higher than those in adults, including normal epithelia (200±113) and epithelia with basal cell hyperplasia (BCH) (286±150) ($P<0.05$, t test). However, the number of PCNA positive immunostaining cells in adult esophageal dysplasia (719±389) and squamous cell carcinoma (SCC) (1261±545) was apparently higher than that in fetal esophageal epithelia (506±239) ($P<0.05$, t test). The positive immunostaining rate of P53 was 10 % (3/31) in fetal esophageal epithelia, which was significantly lower than that in adult normal esophageal epithelia (50 %), adult epithelia with basal cell hyperplasia (62 %), dysplasia (73 %) and squamous cell carcinoma (86 %) ($P<0.05$, Fisher's exact test). No p21^{WAF-1} positive immunostaining cells were observed in fetal esophageal epithelia. However, p21^{WAF-1} positive immunostaining cells were observed in adult esophagus with 39 % (11/28) in normal, 38 % (14/37) in BCH, 27 % (3/11) in DYS and 14 % (1/7) in SCC.

CONCLUSION: PCNA could act as an indicator accurately reflecting the high proliferation status of fetal esophageal epithelium. p53 may play an important role in growth and differentiation of fetal esophageal epithelium. p21^{WAF-1} may have no physiological function in development of fetal esophageal epithelium.

Xing Y, Ning Y, Ru LQ, Wang LD. Expressions of PCNA, p53, p21^{WAF-1} and cell proliferation in fetal esophageal epithelia: Comparative study with adult esophageal lesions from subjects at high-incidence area for esophageal cancer in Henan, North China. *World J Gastroenterol* 2003; 9(7): 1601-1603
<http://www.wjgnet.com/1007-9327/9/1601.asp>

INTRODUCTION

Fetal esophageal epithelium is characterized by cellular hyperproliferation. Tumor suppressor genes have been known to suppress malignant cell proliferation through encoding corresponding proteins that inhibit cell cycle. But it is still not clear whether this inhibition effect of tumor suppressor genes is also involved in the proliferative activity of fetal epithelium.

Tumor suppressor proteins p53 and p21^{WAF-1} play important roles in regulating G1 phase progression, which is the key modulation point in the cell cycle^[1-8]. Proliferating cell nuclear antigen (PCNA) acts as a good marker for cell proliferation and can reflect the status of epithelium growth^[9,10]. To detect the expression of these proteins would help to explore fetal esophageal epithelium proliferation status and characteristics, and to further understand the role of tumor suppressor genes in fetal esophageal epithelium growth control.

Most previous studies about fetal esophagus development focused on the influences of certain chemical factors, such as nitrosamine^[11,12], and biological factors, such as alternariol^[13]. There are, however, few reports about the proliferation characteristics and control of cell cycle in growth of fetal esophageal epithelium.

In this study, immunohistochemical avidin-biotin peroxidase complex (ABC) method was applied to investigate the expression of PCNA, p53 and p21^{WAF-1} in fetal esophageal epithelium and adult esophageal epithelium with different histopathological subtypes. Comparison between the expression of the above proteins in fetal and adult esophageal epithelium would provide important evidences for characteristics of fetal esophageal epithelium proliferation and the mechanisms of its cell cycle control.

MATERIALS AND METHODS

Tissue collection and processing

Thirty-one cases of fetal esophageal specimens were collected from Runan County, Taikang County, Lankao County and Zhengzhou City. The ages of the fetuses ranged from 4 months to 10 months (Table 1). No history of drug using and family history of tumor were found among all the parents of these fetuses. 194 cases of adult esophageal specimens were collected in the same areas for control of PCNA expression, among which 83 adult esophageal specimens were used for the control of p53 and p21^{WAF-1} expression. All specimens were fixed in 85 % ethanol, embedded with paraffin and serially sectioned at

5 μ m. The sections were mounted onto the histostick-coated slides. Four or five adjacent ribbons were collected for histopathological diagnosis (hematoxylin and eosin stain) and immunohistochemical staining.

Table 1 Distribution of fetus sex and age

Sex	Age (months)						Mean age (months)
	4	5	6	7	8	>9	
Male	0	2	4	3	0	0	6.11±0.78
Female	2	5	4	7	3	1	6.36±1.47 ^a
Total	2	7	8	10	3	1	6.29±1.30

^a $P>0.05$, t -test, no significant difference was detected in the distribution of age between male and female fetuses.

Histopathologic diagnosis

Histopathological diagnosis and categorization for esophageal epithelium were based on the changes in cellular morphology and tissue architecture in reference to previous reports^[14-17], and the adult esophageal epithelium was correspondingly classified as normal, basal cell hyperplasia (BCH), dysplasia (DYS) and squamous cell carcinoma (SCC).

Immunohistochemical staining (IHC)

Anti-p53 antibody is a monoclonal mouse anti-serum against p53 of human origin, and recognizes both wild and mutant type p53 (Ab-6, Oncogene Science, Manhasset, NY). Anti-PCNA antibody is a monoclonal mouse anti-serum against PCNA of human origin (Mab, DAKO, Carpinteria, CA). Anti-p21^{WAF-1} antibody is a monoclonal mouse anti-serum against p21^{WAF-1} of human origin, and recognizes both wild and mutant type p21 (Ab-6, Oncogene Science, Manhasset, NY). The avidin-biotin-peroxidase complex method was used for the immunostaining of p53, PCNA and p21^{WAF-1} as previously reported. In brief, after dewaxing, inactivating endogenous peroxidase activity and blocking cross-reactivity with normal serum (Vectastain Elite Kit; Vector, Burlingame, CA), the sections were incubated overnight at 4 °C with a diluted solution of the primary antibodies (1:500 for p53, 1:200 for PCNA and 1:20 for p21^{WAF-1}). Location of the primary antibodies was achieved by subsequent application of a biotinylated anti-primary antibody, an avidin-biotin complex conjugated to horseradish peroxidase, and diaminobenzidine (Vectastain Elite Kit, Vector, Burlingame, CA). The slides were counter-stained by hematoxylin. Negative controls were established by replacing the primary antibody with PBS and normal mouse serum. Known immunostaining-positive slides were used as positive controls.

The criteria of positive staining for p53 and p21^{WAF-1} were as previously reported^[6-8, 14-16]. Quantitative analysis of PCNA immunostaining results was recorded as the number of positive staining cells per mm² of the tissue section^[17,18]. All the immunostaining slides were observed by two pathologists independently and the final concordant results were adopted.

Statistic analysis

Fisher's exact χ^2 test and t -test were applied for the statistical analysis and two-sided P value of less than 0.05 was considered statistically significant.

RESULTS

Histopathological results

Among the cases of fetal esophageal epithelium, the number of basal cell layers ranged from 2 to 6. Five cases contained more than 10 basal cell layers and showed a high proliferation

activity. As for the cases of adult esophageal epithelium, the results of histopathological diagnosis were 31 normal cases, 106 cases with BCH, 31 cases with DYS and 26 cases with SCC.

Comparison of PCNA protein expression between fetal and subtypes of adult esophageal epithelium

PCNA positive immunostaining cells were located mainly in the basal cell layer. And the positive immunoreaction occurred mainly in the nucleolus in dark brown. The mean number of PCNA positive immunostaining cells was 506±239 per mm² in fetal esophageal epithelia, which was significantly higher than that in adult esophageal epithelia of normal and BCH ($P<0.05$, t -test), but significantly lower than that in adult esophageal epithelia with DYS and SCC ($P<0.05$, t -test) (Table 2).

Table 2 Quantitative comparison of PCNA expression between fetal and subtypes of adult esophageal epithelia

Histopathological subtypes	Case (n)	Number of immunostaining positive cells/mm ²
Adult normal	31	200±113
Adult BCH	106	286±150
Fetal	31	506±239 ^a
Adult DYS	31	719±389
Adult SCC	26	1261±545

^a $P<0.05$ vs t -test.

Comparison of P53 protein expression between fetal and subtypes of adult esophageal epithelia

p53 positive immunostaining cells were located mainly in the basal cell layer and the positive immunoreaction occurred mainly in the nucleoli in brown.

The positive immunostaining rate of p53 was 10 % (3/31) in fetal esophageal epithelia, which was significantly lower than that of adult normal esophageal epithelia (50 %, 14/28), adult epithelia with BCH (62 %, 23/37), DYS (73 %, 8/11) and SCC (86 %, 6/7) ($P<0.05$, Fisher's exact test) (Table 3).

Table 3 Comparison of p53 expression between fetal and subtypes of adult esophageal epithelia

Histopathological subtypes	Case (n)	Positive immunostaining	
		Number	Percentage (%)
Fetal	31	3	10 ^a
Adult normal	28	14	50
Adult BCH	37	23	62
Adult DYS	11	8	73
Adult SCC	7	6	86

^a $P<0.05$ vs Fisher's exact test.

Expression of p21^{WAF-1} protein in fetal esophageal epithelia

No positive immunoreaction of p21^{WAF-1} was detected in all the fetal esophageal epithelia. However, p21^{WAF-1} positive immunostaining cells were observed in adult esophagus with 39 % (11/28) in normal, 38 % (14/37) in BCH, 27 % (3/11) in DYS and 14 % (1/7) in SCC.

DISCUSSION

To our knowledge, this is the first report about the role of PCNA as an indicator of proliferation status of fetal esophageal epithelium. In our study, we observed that most PCNA immunostaining positive cells were located in the basal layer

of fetal esophageal epithelium. PCNA is an important index of cell proliferation kinetics. Qian *et al*^[18] found that according to the proliferation status, most cell nuclei were in the G1 phase to S phase of cell cycle in the cell clones with high proliferative activity. And the positive rate of PCNA expression increased gradually in cell nuclei with the progress of G1 phase and reached a peak when entering S phase. Our research found that all fetal esophageal epithelia showed a positive immunoreaction of PCNA and possessed high level of positive immunostaining cells per mm², which was much higher than that in normal adult esophageal epithelium and BCH. This result is concordant with previous theory and suggests that PCNA may act as a good marker for fetal esophageal epithelium proliferation status.

In our study, we also observed that malignant adult esophageal epithelia possessed much more PCNA positive immunostaining cells than fetal esophageal epithelia. This phenomenon is plausible. It was reported that PCNA played a role in DNA damage repair (DDR). With the presence of nucleotide excision, PCNA binds replication protein A (RPA) and constitutes a subunit of DNA polymerase δ ^[19,20]. Kieczkowska *et al*^[21] also supposed that PCNA could combine with hMSH6 and hMSH3, the subunits of hMutSalpha and hMutSbeta that acted as cofactors in DNA mismatch repair system. Malignant tissue was characterized by high frequencies of DNA mismatch, breakages and mutations, which would in turn induce more expression of PCNA for its repair function. As for fetal esophageal epithelia, there were few opportunities of contacting external environmental carcinogens and incurring much DNA damages and mutations. As a result, adult malignant esophageal epithelia had much more PCNA positive immunostaining cells, which implied that PCNA could potentially act as an indicator of malignant proliferation.

For the expression of p53, the positive immunostaining rate was 10 % in fetal esophageal epithelia, which was much lower than that in adult esophageal epithelia of each histopathological subtype. These differences were due to lack of induced p53 expression by external environmental factors in fetal esophageal epithelia. But in our study, there were some cases that were observed with expression of p53. Guo *et al*^[11] reported that no expression of p53 was detected in fetal esophageal epithelia that had been cultured by NMBzA for up to 3 weeks. p53 supervised cell cycle through G1 phase checkpoint^[21]. Then we supposed that stable expression of p53 might be required for normal cell cycle in the highly proliferative fetal esophageal epithelia. Lowe *et al*^[21] found that disfigurement was not detected during development of rat fetus, which showed strong p53 expression. It was suggested that p53 possessed a protective function in fetal tissue development. Although this mechanism should be studied further, our study confirmed its existence in fetal esophageal epithelium development and maybe this function of p53 worked in a special stage of fetal esophageal epithelium proliferation and differentiation.

No positive expression of p21^{WAF-1} was observed in fetal esophageal epithelia. This protein has been reported to be trans-activated by p53 and could repair genomic DNA damages^[7, 8]. Fetal esophageal epithelium encountered few outer carcinogens and few DNA damages occurred in this tissue. We hypothesize that there may not be a large number of p21^{WAF-1} required for DNA damage repair in development of fetal esophageal epithelium.

In conclusion, PCNA can reflect the proliferation status of fetal esophageal epithelium, and p53 may contribute to its development. But p21^{WAF-1} may not play a role in the process of its development. Further studies to explore the molecular mechanisms of these proteins in esophageal development should be performed to provide more pronounced evidences.

REFERENCES

- 1 **Wang LD**, Chen H. Alterations of tumor suppressor gene p53-Rb system and human esophageal carcinogenesis. *Shijie Huaren Xiaohua Zazhi* 2002; **9**: 367-371
- 2 **Shi ST**, Yang GY, Wang LD, Xue Z, Feng B, Ding W, Xing EP, Yang CS. Role of P53 gene mutations in human esophageal carcinogenesis: results from immunohistochemical and mutation analysis of carcinomas and nearby non-cancerous lesions. *Carcinogenesis* 1999; **20**: 591-597
- 3 **Sidransky D**, Hollstein M. Clinical implications of the p53 gene. *Annu Rev Med* 1996; **47**: 285-301
- 4 **Gao H**, Wang LD, Zhou Q, Hong JY, Huang TY, Yang CS. p53 tumor suppressor gene mutation in early esophageal precancerous lesions and carcinoma among high-risk populations in Henan, China. *Cancer Res* 1994; **54**: 4342-4346
- 5 **Bennett WP**, Hollstein MC, He A, Zhu SM, Resau JH, Trump BF, Metcalf RA, Welsh JA, Midgley C, Lane DP. Archival analysis of p53 genetic and protein alterations in Chinese esophageal Cancer. *Oncogene* 1991; **6**: 1779-1784
- 6 **Ohbu M**, Kobayashi N, Okayasu I. Expression of cell cycle regulatory proteins in the multistep process of oesophageal carcinogenesis: stepwise over-expression of cyclin E and p53, reduction of p21(WAF1/CIP1) and dysregulation of cyclin D1 and p27(KIP1). *Histopathology* 2001; **39**: 589-596
- 7 **Shirakawa Y**, Naomoto Y, Kimura M, Kawashima R, Yamatsuji T, Tamaki T, Hamada M, Haisa M, Tanaka N. Topological analysis of p21WAF1/CIP1 expression in esophageal squamous dysplasia. *Clin Cancer Res* 2000; **6**: 541-550
- 8 **Wang LD**, Yang WC, Zhou Q, Xing Y, Jia YY, Zhao X. Changes of p53 and Waf1p21 and cell proliferation in esophageal carcinogenesis. *China Natl J New Gastroenterol* 1997; **3**: 87-89
- 9 **Lohr F**, Wenz F, Haas S, Flentje M. Comparison of proliferating cell nuclear antigen (PCNA) staining and BrdUrd-labelling index under different proliferative conditions in vitro by flow cytometry. *Cell Prolif* 1995; **28**: 93-104
- 10 **Gillen P**, McDermott M, Grehan D, Hourihane DO, Hennessy TP. Proliferating cell nuclear antigen in the assessment of Barrett's mucosa. *Br J Surg* 1994; **81**: 1766-1768
- 11 **Guo YJ**, Lu SX, Liang YY. Alterations of oncogenes in human fetal esophageal epithelium induced by N-methylbenzyl nitrosamine (NMBzA). *Zhonghua Zhongliu Zazhi* 1994; **16**: 407-410
- 12 **Lu SX**. Esophageal carcinoma in human fetus induced by N-methyl-N-benzyl nitrosamine (NMBzA). *Zhonghua Zhongliu Zazhi* 1989; **11**: 401-403
- 13 **Zhang P**. Studies on the activation of oncogenes by alternariol monomethyl ether in human fetal esophageal epithelium. *Zhonghua Binglixue Zazhi* 1991; **20**: 14-17
- 14 **Chen H**, Wang LD, Guo M, Gao SG. Alterations of p53 and PCNA in cancer and adjacent tissues from concurrent carcinomas of the esophagus and gastric cardia in the same patient in Linzhou, a high incidence area for esophageal cancer in northern China. *World J Gastroenterol* 2003; **9**: 16-21
- 15 **Wang LD**, Shi ST, Zhou Q, Goldstein S, Hong JY, Shao P, Qiu SL, Yang CS. Changes in P53 and cyclin D1 protein level and cell proliferation in different stages of Henan esophageal and gastric-cardia carcinogenesis. *Int J Cancer* 1994; **59**: 514-519
- 16 **Wang LD**, Hong JY, Qiu SL, Gao HG, Yang CS. Accumulation of p53 protein in human esophageal precancerous lesions: a possible early biomarker for carcinogenesis. *Cancer Res* 1993; **53**: 1783-1787
- 17 **Koide N**, Yamanda T, Iida F, Usuda N, Nagata T. Immunohistochemical studies of vascular volume and proliferative activity in squamous cell carcinoma of the esophagus. *Surg Today* 1997; **27**: 99-106
- 18 **Qian LF**, Zhang DX, Cheng AM. Cytophotometric determination of DNA content of esophageal mucosa cells of human fetus with different monthly age and analysis of proliferation of cells in tissues. *Xi'an Yike Daxue Zazhi* 1991; **12**: 49-53
- 19 **Mitkova AV**, Biswas EE, Biswas SB. Cell cycle specific plasmid DNA replication in the nuclear extract of *Saccharomyces cerevisiae*: modulation by replication protein A and proliferating cell nuclear antigen. *Biochemistry* 2002; **41**: 5255-5265

Vascular endothelial growth factor and microvascular density in esophageal and gastric carcinomas

Jin-Rong Du, Ying Jiang, Yan-Mei Zhang, Hong Fu

Jin-Rong Du, Ying Jiang, Yan-Mei Zhang, Hong Fu, Department of Pathology, the Second Affiliated Hospital, Harbin Medical University, Harbin 150086, Heilongjiang Province, China

Correspondence to: Dr. Jin-Rong Du, Department of Pathology, the Second Affiliated Hospital, Harbin Medical University, Harbin 150086, Heilongjiang Province, China. jying1972@yahoo.com
Telephone: +86-451-6605803

Received: 2002-11-19 **Accepted:** 2003-01-16

Abstract

AIM: To observe the relationship between the expression of vascular endothelial growth factor (VEGF), microvascular density (MVD) and the pathological characteristics of esophageal and gastric carcinomas.

METHODS: S-P immunohistochemical staining was used to investigate the expression of VEGF in all the specimens. The antibody against factor VIII-related antigen was used to display vascular endothelial cells, and MVD was examined by counting the factor VIII-positive vascular endothelial cells.

RESULTS: The positive rates of VEGF expression in esophageal carcinoma and gastric carcinoma were 81.36 % and 67.5 % respectively, and the MVD averaged 41.81 ± 8.44 and 34.36 ± 9.67 respectively, which were higher than those in benign diseases. The expression of VEGF and MVD were closely correlated with the degree of differentiation, lymphatic metastasis, but not related to depth of cancer invasion. In early stage gastric carcinoma, the rate of expression of VEGF and MVD was lower than that in progressive gastric carcinomas.

CONCLUSION: The expression of VEGF is correlated with tumor angiogenesis, and VEGF plays an important role in new blood vessels formation, the expression of VEGF and MVD play an important role in tumor growth and metastasis. MVD and the expression of VEGF may be two important indexes for patients' prognosis.

Du JR, Jiang Y, Zhang YM, Fu H. Vascular endothelial growth factor and microvascular density in esophageal and gastric carcinomas. *World J Gastroenterol* 2003; 9(7): 1604-1606
<http://www.wjgnet.com/1007-9327/9/1604.asp>

INTRODUCTION

The growth and metastasis of solid tumor, a complex biological event, are affected by many factors. Recent research found that the growth and metastasis of tumors needed constant angiogenesis, which could provide a way for tumor metastasis through vessels, and could affect the prognosis of patients^[1]. Angiogenesis is not an active process by itself, and it is controlled by some angiogenic factors and some angiogenic inhibitors^[2]. Of all the angiogenic factors, vascular endothelial growth factor (VEGF) is a potent, multifunctional cytokine that exerts several important and possibly independent actions on vascular

endothelium. That is its property and capacity to induce angiogenesis, which has excited the greatest interest in VEGF^[3].

In this study, we used immunohistochemical method to detect VEGF expression and MVD in 59 cases of esophageal carcinoma and 80 cases of gastric carcinoma. We studied the relationship between VEGF expression and MVD and pathological features, which will help to understand the role of VEGF and angiogenesis in the growth of esophageal and gastric cancers.

MATERIALS AND METHODS

Materials

The resected specimens from 59 cases of esophageal cancer and 80 cases of gastric cancer were obtained from our hospital from January 2000 to June 2002. Of 59 cases of esophageal carcinoma, 57 were male and 2 were female, with a mean age of 57 (38 to 79). Of 80 cases of gastric carcinoma, 55 were male, 25 were female, with a mean age of 59 (35 to 69). All these specimens were clearly classified by experienced pathologists based on the depth of invasion, metastasis of lymph nodes and degree of differentiation. We collected specimens of 20 normal esophageal tissues and 20 gastric tissues as control. All of them had not received any radiotherapy or chemotherapy.

Reagents and methods

Rabbit anti-human VEGF polyclonal antibodies (RAB-0243), rabbit anti-human VIII polyclonal antibodies (RAB-0070) and ready-to-use SP immunohistochemical reagent box were purchased from Fujian Maxin Co. Ltd. Formalin-fixed, paraffin-embedded specimens were available and sectioned sequentially with a thickness of 4 μ m. The sections carrying the detected antigen were stained with SP immunohistochemical method.

In this study we used lung cancer specimen that was known as positive of VEGF expression to be positive control, and with the first antibody substituted by PBS as negative control.

Results

Criteria of positive staining VEGF According to the criteria proposed by Volms *et al*^[4], brown granules in the cytoplasm of tumor cells or vascular endothelial cells were identified to be positive VEGF. The sections were graded respectively according to the density (1) and the percentage (2) of positively stained tumor cells into score 0, 1, 2 and 3. If the sum of two scores (1) and (2) were 0-2, the section was considered as negative, whereas 3-6 was considered as positive VEGF.

MVD According to the criteria proposed by Weidners *et al*^[5], when the cytoplasm of vascular endothelial cells was stained brown or brownish yellow, it was positive. The microvessels were counted according to the number of single endothelial cell or endothelial cell cluster showing brownish yellow granules in the cytoplasm. The sections were observed first under the low power ($\times 40$), then the most dense area of microvessel sections was selected under the high power ($\times 200$, the surface area of every vision field being 0.785 mm²). The number of microvessel in three vision fields were counted and averaged as MVD of this specimen.

Statistical methods

Statistic analysis was performed by using the χ^2 test to dispose the expression of VEGF and the pathological features. *t* test was used to detect the relationships between the expression of VEGF and MVD, and between MVD and pathological characteristics.

RESULTS

The relationship between the expression of VEGF and pathological features of esophageal carcinoma

Of 59 cases of esophageal carcinoma, 11 cases were negative and 48 cases were positive, and the positive rate was 81.36 % (48/59). Of 20 normal esophageal tissues, 4 cases were positive, and the positive rate was 20 %. The rate of expression of VEGF in esophageal carcinoma was higher than that in normal esophageal tissue ($\chi^2=24.99, P<0.001$). The expression of VEGF was closely related to pathological grade, that is, the poorer differentiation of the tumor, the higher expression of VEGF ($\chi^2=7.08, P<0.05$). The cases having lymph node metastasis had significantly higher VEGF expression than those having no lymph node metastasis ($\chi^2=5.59, P<0.05$). The VEGF expression was not related to invasion depth of tumor (Table 1).

Table 1 Relationship between expression of VEGF and MVD and pathological features of esophageal carcinoma

Pathological characteristics	n	VEGF				MVD	
		-	+++	χ^2	P	$\bar{x}\pm s$	P(t)
Degree of differentiation							
Well differentiated	27	9	18	7.08	<0.05	38.52±9.22	<0.05
Poorly differentiated	32	2	30			43.43±7.61	(t=2.07)
Depth of invasion							
Invading muscularis	37	7	30	0.01	>0.05	40.38±8.31	>0.05
Invading serosa	22	4	18			42.53±9.24	(t=0.88)
LN metastasis							
-	35	10	25	5.59	<0.05	38.22±8.54	<0.05
+	24	1	24			45.5±7.04	(t=3.23)

The relationship between the expression of VEGF and pathological features of gastric carcinoma

Of 80 cases of gastric carcinomas, 26 cases were negative and 54 cases were positive, and the positive rate was 67.5 % (54/80). There was no positive stain in 20 cases of gastric tissues. The expression of VEGF was closely related to degree of differentiation ($\chi^2=11.31, P<0.01$) and lymph node metastasis ($\chi^2=9.32, P<0.01$). As in esophageal carcinoma, the expression of VEGF had no significant difference between the different depths of invasion ($\chi^2=0.40, P<0.05$). The expression of VEGF in early stage carcinoma was significantly lower than that in progressive stage cancer ($\chi^2=19.67, P<0.001$) (Table 2).

The relationship between MVD and pathological features in esophageal carcinoma and gastric carcinoma

In the two carcinomas, MVD was higher than that in normal tissue, and MVD was closely related to differentiation degree of tumor and metastasis of lymph nodes, but not related to depth of invasion. In gastric carcinoma, MVD was significantly different between the different stages of carcinoma. (Table 1 and Table 2).

The relationship between VEGF expression and MVD in the two cancers

In this study, MVD was closely related to the expression of

VEGF in gastric carcinoma and esophageal carcinoma, that is, the stronger the expression of VEGF, the higher the MVD. This suggested that VEGF be related to MVD and angiogenesis. VEGF and MVD were closely related to tumor growth (Table 3).

Table 2 Relationship between expression of VEGF and MVD and pathological features of gastric carcinoma

Pathological characteristics	n	VEGF				MVD	
		-	+++	χ^2	P	$\bar{x}\pm s$	P(t)
Degree of differentiation							
Well differentiated	43	21	22	11.31	<0.001	32.85±6.14	<0.01
Poorly differentiated	37	5	32			38.63±5.10	(t=4.53)
Depth of invasion							
Not invading serosa	39	14	25	0.40	>0.05	34.94±9.26	>0.05
Invading serosa	41	12	29			33.68±9.12	(t=0.30)
Tumor stage							
Early stage	21	15	6	19.67	<0.001	32.14±5.89	<0.05
Progressive stage	59	11	48			35.46±6.58	(t=2.04)
LN metastasis							
-	52	23	29	9.32	<0.01	33.06±5.33	<0.05
+	28	3	25			35.74±7.58	(t=2.07)

Table 3 Relationship between VEGF expression and MVD in the two cancers

Pathological characteristics	n	MVD	
		$\bar{x}\pm s$	P(t)
VEGF expression in esophageal carcinoma			
-	11	43.45±6.98	<0.05
+++	48	31.30±8.74	(t=4.33)
VEGF expression in esophageal carcinoma			
-	26	31.08±9.54	<0.05
+++	54	36.83±8.87	(t=2.65)

DISCUSSION

The importance of tumor angiogenesis in the growth and infiltration of tumor has been well known since J Folkman first proposed the hypothesis “Growth of solid tumor and the formation of metastasis are dependent on the formation of new blood vessels” in 1971. Growth of solid tumors is dependent on the induction of new blood vessels^[6]. In order to maintain the unlimited growth of tumor, tumor tissue must depend on the constant and wide formation of new blood vessels, which is essential for tumors to grow beyond minimal size, providing oxygenation and nutrient perfusion as well as removal of waste products^[7]. In normal organism, angiogenesis is strictly controlled, but in tumors, angiogenesis is uncontrolled and immature^[8]. Controlled by angiogenic factors and angiogenic inhibitors, tumor cells, endothelial cells and other cells can produce and release VEGF protein if the local microenvironment is changed by hypoxia, *etc*^[9]. Some researches proved that in tumors with foci of relative hypoxia, VEGF mRNA may be expressed not only by malignant cells but also by stromal cells^[10,11]. Different tumor needs different angiogenesis factors, such as bFGF, which is a very important angiogenesis factor in fibrosarcoma. In gastroenteric tumors VEGF proved to play a key role.

VEGF, also known as VPF (vascular permeability factor), is secreted by some tumor cells. It combines with its receptors on endothelial cells. It can render venules and small veins hyperpermeable to circulatory macromolecules, and induce angiogenesis, which can induce tumor growth^[12].

The human VEGF gene has been assigned to chromosome 6p21.3. Its coding region spans approximately 14kb. Native VEGF is a basic, heparin-binding homodimeric glycoprotein^[13,14]. VEGF target cell is endothelial cell. On the one hand it renders microvascular hyperpermeable, so that plasma proteins and fibrinogen leak, can stimulate angiogenesis and new stroma formation. On the other hand, VEGF stimulates the endothelial cell of microvessels to proliferate, migrate and alters their pattern of gene expression^[15].

More and more researches proved the important role of VEGF in tumor growth. Recently, Meada *et al*^[16] found that VEGF expression was consistent with MVD, that is, MVD of gastric carcinoma with positive expression of VEGF was higher than that with negative expression of VEGF, and MVD was higher in the area where VEGF expression was positive. Toi *et al*^[17] found that the positive expression of VEGF and factor VIII were detected in the samples of breast carcinoma which were poorly differentiated, with invasive growth and lymph node metastasis. So strong expression of VEGF and factor VIII may indicate a poor prognosis.

In our study, a strong correlation was found between VEGF expression and increased tumor microvasculature, malignancy and metastasis in esophageal carcinoma and gastric carcinoma. These results indicate that VEGF and angiogenesis promoted by VEGF play important roles in cancer growth, infiltration and metastasis in esophageal and gastric carcinoma. It also implied that VEGF expression and MVD have prognostic significance. We also found that there was an obvious heterogeneity in VEGF expression and new vessel formation in cancer tissue. New tumor vessels were deficient in constant basement membrane. This proved that the new vessels were hyperpermeable. This may facilitate the tumor cells to penetrate through the blood vessels and metastasis. VEGF expression manifested that positive cells located at the center of tumor or at the edge of the necrosis area, this may be explained by the hypoxia, which can stimulate VEGF expression and its biological activity.

In the study of the correlation of VEGF expression and MVD, we proved that VEGF was closely related with MVD in the cancer tissues of both esophageal and gastric carcinoma, this result proved VEGF could induce formation of new blood vessels. Thus VEGF expression and MVD may play important roles in tumor biological behaviors, progression and prognosis.

In conclusion, VEGF overexpression and active angiogenesis exist in esophageal carcinoma and gastric carcinoma. VEGF and MVD are closely relevant to lymph node metastasis, tumor differentiation and clinical stage. VEGF and MVD may act as two valuable indexes of tumor prognosis. These conclusions may provide an important theoretical evidence for cancer therapy through antiangiogenesis.

REFERENCES

- 1 **Folkman J**, Shing Y. Angiogenesis. *J Biol Chem* 1992; **267**: 10931-10934
- 2 **Klagsbrun M**, D' Amore PA. Regulators of angiogenesis. *Annu Rev Physiol* 1991; **53**: 217-239
- 3 **Dvorak HF**, Brown LF, Detmer M, Dvorak AM. Vascular permeability factor/vascular endothelial growth factor, microvascular hyperpermeability and angiogenesis. *Am J Pathol* 1995; **146**: 1029-1039
- 4 **Volm M**, Koomagi R, Mattern J. Prognostic value of vascular endothelial growth factor and its receptor Flt-1 in squamous cell lung cancer. *Int J Cancer* 1997; **74**: 64-68
- 5 **Weidner N**, Folkman J, Pozza F, Bevilacqua P, Allred EN, Moore DH, Meli S, Gasparini G. Tumor angiogenesis: a new significant and independent prognostic indicator in early-stage breast carcinoma. *J Natl cancer Inst* 1992; **84**: 1875-1887
- 6 **Folkman J**. Angiogenesis and Angiogenesis inhibition: an overview. *EXS* 1997; **79**: 1-8
- 7 **Hanahan D**, Folkman J. Patterns and emerging mechanisms of the angiogenic switch during tumorigenesis. *Cell* 1996; **86**: 353-364
- 8 **Saaristo A**, Karpanen T, Alitalo K. Mechanism of angiogenesis and their use in the inhibition of tumor growth and metastasis. *Oncogene* 2000; **19**: 6122-6129
- 9 **Goldberg MA**, Schneider TJ. Similarities between the oxygen sensing mechanisms regulating the expression of vascular endothelial growth factor and erythropoietin. *J Biol Chem* 1994; **269**: 4355-4359
- 10 **Brown LF**, Berse B, Jackman RW, Tognazzi K, Manseau EJ, Senger DR, Dvorak HF. Expression of vascular permeability factor (vascular endothelial growth factor) and its receptors in adenocarcinomas of the gastrointestinal tract. *Cancer Res* 1993; **53**: 4727-4735
- 11 **Brown LF**, Berse B, Jackman RW, Tognazzi K, Manseau EJ, Dvorak HF, Senger DR. Increased expression of vascular permeability factor (vascular endothelial growth factor) and its receptors in kidney and bladder carcinoma. *Am J Pathol* 1993; **143**: 1255-1262
- 12 **Ferrara N**, Davis-Smyth T. The biology of vascular endothelial growth factor. *Endocr Rev* 1997; **18**: 4-25
- 13 **Tischer E**, Mitchell R, Hartman T, Silva M, Gospodarowicz D, Fiddes JC, Abraham JA. The human gene for vascular endothelial growth factor. Multiple protein forms are encoded through alternative exon splicing. *J Biol Chem* 1991; **266**: 11947-11954
- 14 **Vincenti V**, Cassano C, Rocchi M, Persico G. Assignment of the vascular endothelial growth factor gene to human chromosome 6p21.3. *Circulation* 1996; **93**: 1493-1495
- 15 **Detmar M**, Velasco P, Richard L, Claffey KP, Streit M, Riccardi L, Skobe M, Brown LF. Expression of vascular endothelial growth factor induces an invasive phenotype in human squamous cell carcinomas. *Am J Pathol* 2000; **156**: 159-167
- 16 **Maeda K**, Chung YS, Ogawa Y, Takatsuka S, Kang SM, Ogawa M, Sawada T, Sowa M. Prognostic value of vascular endothelial growth factor expression in gastric carcinoma. *Cancer* 1996; **77**: 858-863
- 17 **Toi M**, Inada K, Hoshina S, Suzuki H, Kondo S, Tominaga T. Vascular endothelial growth factor and platelet-derived endothelial cell growth factor are frequently coexpressed in highly vascularized human breast cancer. *Clin Cancer Res* 1995; **1**: 961-964

Edited by Zhang JZ and Zhu LH

Effect of P-selectin monoclonal antibody on metastasis of gastric cancer and immune function

Jin-Lian Chen, Wei-Xiong Chen, Jin-Shui Zhu, Ni-Wei Chen, Tong Zhou, Ming Yao, Dong-Qing Zhang, Yun-Lin Wu

Jin-Lian Chen, Wei-Xiong Chen, Jin-Shui Zhu, Ni-Wei Chen,
Department of Gastroenterology, Shanghai Jiao-Tong University
affiliated Sixth People's Hospital, Shanghai 200233, China

Tong Zhou, Yun-Lin Wu, Ruijin Hospital, Shanghai Second Medical
University, Shanghai 200025, China

Ming Yao, Shanghai Cancer Institute, Shanghai 200233, China

Dong-Qing Zhang, Shanghai Institute of Immunology, Shanghai
200025, China

Supported by the Youth Science Foundation of Shanghai Public
Administration No.131984Y15

Correspondence to: Jin-Lian Chen, Department of Gastroenterology,
Shanghai Sixth People's Hospital, Shanghai Jiao-Tong University
affiliated Sixth People's Hospital, Shanghai 200233, China.
wjg_021002@163.com

Telephone: +86-21-64369181

Received: 2003-03-02 **Accepted:** 2003-03-29

Abstract

AIM: To investigate the effect of cell adhesion molecule P-selectin monoclonal antibody (Mab) on metastasis and immune function of mice orthotopically implanted with human gastric cancer tissue.

METHODS: SCID mice were implanted orthotopically with SGC-7901 human gastric carcinoma tissue. Starting from day 3 after operation, animals were given intravenously PBS or P-selectin Mab (100 µg/injection) (for both normal mice and tumor-implanted mice with tumors), twice weekly for 3 weeks. Two animals in each group were sacrificed randomly at the 1st, 2nd, 4th week and 6th week. While T cell and B cell transformation indices were determined with the ³H TdR infiltration method, the NK cell activity was detected by the LDH release method.

RESULTS: The metastatic rate in the P-selectin Mab treated group was lower than that in the PBS treated group (with tumors). The NK activity of normal mice increased over time. The immune functions (T, B cell function, NK activity) of the tumor group in the 6th week were significantly lower than those in the 4th week, but the change was attenuated by P-selectin Mab.

CONCLUSION: P-selectin Mab could suppress the metastasis of gastric cancer with no adverse effect on host immune function.

Chen JL, Chen WX, Zhu JS, Chen NW, Zhou T, Yao M, Zhang DQ, Wu YL. Effect of P-selectin monoclonal antibody on metastasis of gastric cancer and immune function. *World J Gastroenterol* 2003; 9(7): 1607-1610

<http://www.wjgnet.com/1007-9327/9/1607.asp>

INTRODUCTION

Gastric carcinoma is one of the most frequent tumors in China. Tumor metastasis is very common clinically. Cell adhesion molecules have been implicated to be crucial elements in the

process of metastasis^[1-28]. P-selectin is an adhesion molecules that mediates the cell to cell interaction of platelets and endothelial cells with neutrophils and monocytes as well as tumor cells^[29]. Our previous study indicates that P-selectin expression is related to aggressive behavior, dissemination and poor prognosis of human gastric carcinomas, and P-selectin monoclonal antibody can inhibit gastric carcinoma metastasis^[30-32]. The present study was performed to investigate effects of P-selectin monoclonal antibody on metastasis and immune function in SCID mouse metastatic models of human gastric cancer constructed by orthotopic implantation of histologically intact tumor tissue.

MATERIALS AND METHODS

Animal model

Forty-eight male SCID mice obtained from Shanghai Cancer Institute were 7-8 weeks old with weight of 20-25 g. Human gastric cancer SGC-7901, a poorly-differentiated adenocarcinoma line, was originally derived from a primary tumor and maintained by passage in nude mice subcutaneously.

SCID mice were randomly divided into experimental group ($n=24$) and normal group ($n=24$). Animal models in experimental group were made using orthotopic implantation of histologically intact tissue of human gastric carcinoma^[33]. Tumors were resected aseptically. Necrotic tumor tissues were removed and the remaining non-necrotic tumor tissues were minced into pieces about 5-7 mm in diameter in Hank's balanced salt solution. Each of the tumor pieces was weighed and adjusted to be 150 mg with scissors. Mice were anesthetized with 4.3 % trichloraldehyde hydrate and an incision was made through the left upper abdominal pararectal line and peritoneal cavity was carefully exposed and a part of the serosal membrane in the middle of the greater curvature of the glandular stomach was mechanically injured by using scissors. A tumor piece of 150 mg was fixed on each injured site of the serosal surface. The stomach was then returned to the peritoneal cavity, and the abdominal wall and skin were closed. 3 d later, all animals implanted with intact tumor tissues received i.v. injection of PBS (group3, $n=12$) or P-selectin antibody (Suzhou Medical College; 100 µg/injection; group4, $n=12$) twice weekly for 3 weeks. Animals in normal group received i.v. injections of PBS (group1, $n=12$) or P-selectin antibody (100 µg/injection; group2, $n=12$).

Sample collection and pathological examination

Two mice in each group were sacrificed randomly on weeks 1, 2, and 4. The remaining animals were sacrificed at 6th week and the tumors growing on the stomach wall were removed and examined histologically. Tissues from all organs were examined for metastasis after careful macroscopic examination. The spleen of mice was harvested for detection of immune function.

Lymphocyte transformation test

Using ³H TdR infiltration method, T cell transformation function was detected with Con A (5 µg/ml, Sigma), B cell function with LPS (50 µg/ml, Sigma). The spleen was made

into suspension and mononuclear cells were acquired with lymphocyte-separating fluid. The cell suspension was adjusted to 2×10^6 /ml with RPMI 1640 liquid containing 10 % calf serum (GIBCO). Then 200 μ l of the cell suspension was put into each well in 96-well plates. One plate was for Con A group, and another plate for LPS group. There were negative control group and experimental group for Con A or LPS group respectively, and each test had 5 repetitive wells and was cultivated under 5 % CO_2 at 37 °C. The cell suspension in Con A group was cultivated for 3 d, while it was done for 5 d in Con A group. All wells were added up ^3H TdR 16 h before the end of cultivation. They were collected in filtration paper, and given 0.5 ml of scintillating liquid to detect cpm value with β -scintillator, which was presented with SI. SI amounts to cpm of experimental group/cpm of empty group.

NK activity

NK activity was detected by the 4 h LDH release method. NK cell activity (%) =

$$\frac{\text{Experimental group's OD} - \text{Natural release group's OD}}{\text{Max release group's OD} - \text{Natural release group's OD}}$$

Statistical methods

Comparisons among groups were performed by the student's t test and χ^2 test. A value of $P < 0.05$ was considered significant.

RESULTS

Effects of P-selectin antibody on metastasis

All animals in each group were sacrificed randomly at the 1st, 2nd, 4th week and 6th week. Tumors grew in the implanted site. Under microscopy, the tumors demonstrated lower differentiated adenocarcinoma invading mucosal layer, submucosal layer and muscle layer. Tumor metastasis was observed most frequently in the regional lymph nodes and liver. It could be seen in lung, spleen and other organs.

In tumor group (Group 3), no metastasis was found at the 1st and 2nd week, but metastasis was found in 1 of 2 cases at the 4th week, in 5 of 6 cases at 6th week. However, in P-selectin antibody treated tumor group (Group 4), tumor metastasis was remarkably inhibited. No metastasis was found at 1st, 2nd, and 4th week, while it was found only in 1 of 6 mice at 6th week.

Table 1 Immune functions of mice in various groups ($\bar{x} \pm s$)

Group	Week 1	Week 2	Week 4	Week 6
T cell transformation indices (SI)				
Group 1	1.95 \pm 0.16	2.19 \pm 0.18	2.28 \pm 0.19	2.35 \pm 0.20
Group 2	2.10 \pm 0.19	2.13 \pm 0.21	2.42 \pm 0.23	2.27 \pm 0.22
Group 3	1.83 \pm 0.17	1.77 \pm 0.18	1.58 \pm 0.15	1.01 \pm 0.10 ^d
Group 4	1.92 \pm 0.19	1.82 \pm 0.16	1.63 \pm 0.17	1.43 \pm 0.13 ^a
B cell transformation indices (SI)				
Group 1	2.57 \pm 0.22	2.35 \pm 0.23	2.76 \pm 0.24	2.87 \pm 0.26
Group 2	2.49 \pm 0.24	2.33 \pm 0.26	2.82 \pm 0.28	2.59 \pm 0.29
Group 3	2.54 \pm 0.23	2.48 \pm 0.24	2.20 \pm 0.22	1.49 \pm 0.12 ^d
Group 4	2.60 \pm 0.22	2.51 \pm 0.21	2.43 \pm 0.26	2.11 \pm 0.20 ^a
NK activity (90)				
Group 1	8.66 \pm 0.78	11.21 \pm 0.99	14.22 \pm 1.22 ^b	18.62 \pm 1.14 ^c
Group 2	8.96 \pm 0.91	11.39 \pm 1.12	13.75 \pm 1.03	17.99 \pm 1.36
Group 3	8.12 \pm 0.81	7.63 \pm 0.74	6.75 \pm 0.62	4.17 \pm 0.52 ^d
Group 4	8.00 \pm 0.73	7.61 \pm 0.83	6.97 \pm 0.62	6.24 \pm 0.63 ^a

^a $P < 0.05$ vs group3; ^b $P < 0.05$, ^c $P < 0.01$ vs week1; ^d $P < 0.05$ vs week4.

Effect of P-selectin antibody on immune function

The NK activity of normal mice increased over time, but no significant difference of the immune functions of T cell and B cell was found in all the groups. Over time, the immune functions (T, B cell function, NK activity) of SCID mice orthotopically implanted with tumor tissue were significantly lower in the 6th week than those in the 4th week, but the change was attenuated by P-selectin antibody ($P < 0.05$) (Table 1).

DISCUSSION

Research on cell adhesion molecules and metastasis has aroused a lot of attention recently^[34-50]. P-selectin (GMP140, CD62, or PADGEM) is located in alpha granules of platelets and Weibel-Palade bodies of endothelial cells. Once platelet or endothelial cell is activated by mediators such as thrombin, alpha granule and weibel-palade body membranes fuse rapidly with the plasma membrane, leading to the expression of P-selectin on the cell surface^[29]. P-selectin contributes to interaction of tumor cell to cell adhesion by mediating endothelial cells and platelets with tumor cells.

We have immunohistochemically studied P-selectin expression in 60 cases of human gastric carcinomas. The study showed that P-selectin was expressed in human gastric cancer, which was detected not only on intratumoral endothelium but also on cancer cells. P-selectin expression was found higher in patients with lymph node metastasis than those without metastasis. The survival time and five-year survival rate were lower in P-selectin positive cases than those in negative cases^[30-32]. Recently, our study indicated that P-selectin mRNA expression is related to tumor metastasis, and the metastasis may be inhibited by the monoclonal antibody. This finding is in accordance with Stone's results^[22]. These results suggest that selectins play an important role in metastasis by mediating the interaction of endothelial cells and platelets with cancer cells, and the metastasis can be inhibited by the monoclonal antibody.

Recently, study on anti-adhesion therapy with adhesion molecule monoclonal antibodies exhibits good clinical prospective^[51-53]. However, there existed some problems. Antibody against intercellular adhesion molecule-1 (ICAM-1) might block inflammation while it inhibits the immune function of the body so that it increases the risk for infection^[54,55]. The present study investigated the effects of P-selectin monoclonal antibody on tumor metastasis and immune function of SCID mice orthotopically implanted with gastric cancer tissue to lay foundation for clinical application of anti-adhesion therapy. The result indicated that P-selectin antibody could inhibit the metastasis. This is consistent with our previous study.

Results obtained in this study showed that NK activity of normal mice got higher with the passage of time. It was higher at 6th week than between 1st week and 4th week. But there had no significant change in both T cell and B cell function. The experiment suggested that mice used for metastasis models should not be too old, otherwise the metastasis rate of the mice implanted with tumor would be low. Our experiment discovered that the immune functions (T, B cell function, NK activity) of the tumor group were significantly lower in the 6th week than in the 4th week, but the change was remarkably attenuated by P-selectin antibody. No difference of the immune functions between the two groups at 1st, 2nd, 4th week was found. This result suggested that the immune functions of mice was suppressed with the development of tumor metastasis. On the other hand, the metastatic rates of tumor group were 50 % (1/2) at 4th week and 83.3 % (5/6) at 6th week, whereas it was 16.7 % (1/6) at 6th week in P-selectin antibody treated tumor group. Therefore, the improved immune function in the

antibody treated tumor group might result from the inhibition of metastasis by the P-selectin monoclonal antibody. Sharar discovered that P-selectin could not inhibit functions of neutrophils. The results suggest that P-selectin monoclonal antibody could inhibit the metastatic tendency with no harmful effect on host immune function.

REFERENCES

- Xin Y**, Li XL, Wang YP, Zhang SM, Zheng HC, Wu DY, Zhang YC. Relationship between phenotypes of cell-function differentiation and pathobiological behavior of gastric carcinomas. *World J Gastroenterol* 2001; **7**: 53-59
- Ikonen T**, Matikainen M, Mononen N, Hyytinen ER, Helin HJ, Tommola S, Tammela TL, Pukkala E, Schleutker J, Kallioniemi OP, Koivisto PA. Association of E-cadherin germ-line alterations with prostate cancer. *Clin Cancer Res* 2001; **7**: 3465-3471
- Tsujitani S**, Kaibara N. Clinical significance of molecular biological detection of micrometastases in gastric carcinoma. *Nippon Geka Gakkai Zasshi* 2001; **102**: 741-744
- Murahashi K**, Yashiro M, Takenaka C, Matsuoka T, Ohira M, Chung KH. Establishment of a new scirrhous gastric cancer cell line with loss of heterozygosity at E-cadherin locus. *Int J Oncol* 2001; **19**: 1029-1033
- Okada Y**, Fujiwara Y, Yamamoto H, Sugita Y, Yasuda T, Doki Y, Tamura S, Yano M, Shiozaki H, Matsuura N, Monden M. Genetic detection of lymph node micrometastases in patients with gastric carcinoma by multiple-marker reverse transcriptase-polymerase chain reaction assay. *Cancer* 2001; **92**: 2056-2064
- Yanagimoto K**, Sato Y, Shimoyama Y, Tsuchiya B, Kuwao S, Kameya T. Co-expression of N-cadherin and alpha-fetoprotein in stomach cancer. *Pathol Int* 2001; **51**: 612-618
- Chun YS**, Lindor NM, Smyrk TC, Petersen BT, Burgart LJ, Guilford PJ, Donohue JH. Germline E-cadherin gene mutations: is prophylactic total gastrectomy indicated? *Cancer* 2001; **92**: 181-187
- Shun CT**, Wu MS, Lin MT, Chang MC, Lin JT, Chuang SM. Immunohistochemical evaluation of cadherin and catenin expression in early gastric carcinomas: correlation with clinicopathologic characteristics and Helicobacter pylori infection. *Oncology* 2001; **60**: 339-345
- Xin Y**, Grace A, Gallagher MM, Curran BT, Leader MB, Kay EW. CD44V6 in gastric carcinoma: a marker of tumor progression. *Appl Immunohistochem Mol Morphol* 2001; **9**: 138-142
- Chan AO**, Lam SK, Chu KM, Lam CM, Kwok E, Leung SY, Yuen ST, Law SY, Hui WM, Lai KC, Wong CY, Hu HC, Lai CL, Wong J. Soluble E-cadherin is a valid prognostic marker in gastric carcinoma. *Gut* 2001; **48**: 808-811
- Chan JK**, Wong CS. Loss of E-cadherin is the fundamental defect in diffuse-type gastric carcinoma and infiltrating lobular carcinoma of the breast. *Adv Anat Pathol* 2001; **8**: 165-172
- Werner M**, Becker KF, Keller G, Hofler H. Gastric adenocarcinoma: pathomorphology and molecular pathology. *J Cancer Res Clin Oncol* 2001; **127**: 207-216
- Machado JC**, Oliveira C, Carvalho R, Soares P, Bex G, Caldas C, Seruca R, Carneiro F, Sobrinho-Simoes M. E-cadherin gene (CDH1) promoter methylation as the second hit in sporadic diffuse gastric carcinoma. *Oncogene* 2001; **20**: 1525-1528
- Tamura G**, Sato K, Akiyama S, Tsuchiya T, Endoh Y, Usuba O, Kimura W, Nishizuka S, Motoyama T. Molecular characterization of undifferentiated-type gastric carcinoma. *Lab Invest* 2001; **81**: 593-598
- Futamura N**, Nakamura S, Tatematsu M, Yamamura Y, Kannagi R, Hirose H. Clinicopathologic significance of sialyl Le(x) expression in advanced gastric carcinoma. *Br J Cancer* 2000; **83**: 1681-1687
- Lynch HT**, Grady W, Lynch JF, Tsuchiya KD, Wiesner G, Markowitz SD. E-cadherin mutation-based genetic counseling and hereditary diffuse gastric carcinoma. *Cancer Genet Cytogenet* 2000; **122**: 1-6
- Fukudome Y**, Yanagihara K, Takeichi M, Ito F, Shibamoto S. Characterization of a mutant E-cadherin protein encoded by a mutant gene frequently seen in diffuse-type human gastric carcinoma. *Int J Cancer* 2000; **88**: 579-583
- Maehara Y**, Kabashima A, Koga T, Tokunaga E, Takeuchi H, Kakeji Y, Sugimachi K. Vascular invasion and potential for tumor angiogenesis and metastasis in gastric carcinoma. *Surgery* 2000; **128**: 408-416
- Koseki K**, Takizawa T, Koike M, Ito M, Nihei Z, Sugihara K. Distinction of differentiated type early gastric carcinoma with gastric type mucin expression. *Cancer* 2000; **89**: 724-732
- Uchiyama K**, Yamamoto Y, Taniuchi K, Matsui C, Fushida Y, Shirao Y. Remission of anti-pilgrin (laminin-5) cicatricial pemphigoid after excision of gastric carcinoma. *Cornea* 2000; **19**: 564-566
- Machado J**, Carneiro F, Sobrinho-Simoes M. E-cadherin mutations in gastric carcinoma. *J Pathol* 2000; **191**: 466-468
- Chen J**, Zhang Y, Chu Y. Inhibition of human stomach cancer metastasis in vivo by anti-P-selectin monoclonal antibody. *Zhonghua Yixue Zazhi* 1998; **78**: 437-439
- Luber B**, Candidus S, Handschuh G, Mentele E, Hutzler P, Feller S, Voss J, Hofler H, Becker KF. Tumor-derived mutated E-cadherin influences beta-catenin localization and increases susceptibility to actin cytoskeletal changes induced by pervanadate. *Cell Adhes Commun* 2000; **7**: 391-408
- Tamura G**, Yin J, Wang S, Fleisher AS, Zou T, Abraham JM, Kong D, Smolinski KN, Wilson KT, James SP, Silverberg SG, Nishizuka S, Terashima M, Motoyama T, Meltzer SJ. E-Cadherin gene promoter hypermethylation in primary human gastric carcinomas. *J Natl Cancer Inst* 2000; **92**: 569-573
- Hofler H**. Diffuse stomach carcinoma: from H&E diagnosis and molecular pathology to specific therapy. *Verh Dtsch Ges Pathol* 1999; **83**: 148-154
- Debruyne P**, Vermeulen S, Mareel M. The role of the E-cadherin/catenin complex in gastrointestinal cancer. *Acta Gastroenterol Belg* 1999; **62**: 393-402
- Park CK**, Shin YK, Kim TJ, Park SH, Ahn GH. High CD99 expression in memory T and B cells in reactive lymph nodes. *J Korean Med Sci* 1999; **14**: 600-606
- Stachura J**, Krzeszowiak A, Popiela T, Urbanczyk K, Pituch-Noworolska A, Wieckiewicz J, Zembala M. Preferential overexpression of CD44v5 in advanced gastric carcinoma Gosekigrades I and III. *Pol J Pathol* 1999; **50**: 155-161
- Chen JL**, Wu YL. Selectins and tumor metastasis. *Tumor* 1996; **16**: 43-44
- Chen JL**, Wu YL, Zhou T, Wang RN. Expression of P-selectin in human gastric cancer. *Shanghai Dier Yike Daxue Xuebao* 1996; **16**: 328-332
- Chen JL**, Wu YL, Zhou T, Wang RN, Chu YD, Xu HM. Prognostic significance of P-selectin expression in Chinese patients with gastric carcinoma. *J SMMU* 1999; **11**: 66-70
- Chen JL**, Zhang YX, Chu YD, Zhon T, Xu HM, Li ML. Inhibition of human stomach carcinoma metastasis in vivo by anti-P-selectin monoclonal antibody. *Shanghai Dier Yike Daxue Xuebao* 1998; **18**: 30-32
- Chen JL**, Chu YD, Zhang YX, Xu HM, Li ML. Metastatic models of human gastric carcinoma established by orthotopic implantation of histologically intact specimens in SCID mice. *Shanghai Shiyuan Dongwu Kexue* 1997; **17**: 207-209
- Koshikawa N**, Moriyama K, Takamura H, Mizushima H, Nagashima Y, Yanoma S, Miyazaki K. Overexpression of laminin gamma2 chain monomer in invading gastric carcinoma cells. *Cancer Res* 1999; **59**: 5596-5601
- Becker KF**, Kremmer E, Eulitz M, Becker I, Handschuh G, Schuhmacher C, Muller W, Gabbert HE, Ochiai A, Hirohashi S, Hofler H. Analysis of E-cadherin in diffuse-type gastric cancer using a mutation-specific monoclonal antibody. *Am J Pathol* 1999; **155**: 1803-1809
- Jawhari AU**, Noda M, Pignatelli M, Farthing M. Up-regulated cytoplasmic expression, with reduced membranous distribution of the src substrate p120(ctn) in gastric carcinoma. *J Pathol* 1999; **189**: 180-185
- Nollet F**, Bex G, van Roy F. The role of the E-cadherin/catenin adhesion complex in the development and progression of cancer. *Mol Cell Biol Res Commun* 1999; **2**: 77-85
- Schuhmacher C**, Becker KF, Reich U, Schenk U, Mueller J, Siewert JR, Hofler H. Rapid detection of mutated E-cadherin in perito-

- neal lavage specimens from patients with diffuse-type gastric carcinoma. *Diagn Mol Pathol* 1999; **8**: 66-70
- 39 **Hsieh HF**, Yu JC, Ho LI, Chiu SC, Harn HJ. Molecular studies into the role of CD44 variants in metastasis in gastric cancer. *Mol Pathol* 1999; **52**: 25-28
- 40 **Jawhari AU**, Noda M, Farthing MJ, Pignatelli M. Abnormal expression and function of the E-cadherin-catenin complex in gastric carcinoma cell lines. *Br J Cancer* 1999; **80**: 322-330
- 41 **Sato S**, Yokozaki H, Yasui W, Nikai H, Tahara E. Silencing of the CD44 gene by CpG methylation in a human gastric carcinoma cell line. *Jpn J Cancer Res* 1999; **90**: 485-489
- 42 **Yoo CH**, Noh SH, Kim H, Lee HY, Min JS. Prognostic significance of CD44 and nm23 expression in patients with stage II and stage IIIA gastric carcinoma. *J Surg Oncol* 1999; **71**: 22-28
- 43 **Nakanishi H**, Kodera Y, Yamamura Y, Kuzuya K, Nakanishi T, Ezaki T, Tatematsu M. Molecular diagnostic detection of free cancer cells in the peritoneal cavity of patients with gastrointestinal and gynecologic malignancies. *Cancer Chemother Pharmacol* 1999; **43**(Suppl): S32-36
- 44 **Taniuchi K**, Takata M, Matsui C, Fushida Y, Uchiyama K, Mori T, Kawara S, Yancey KB, Takehara K. Antiepileptin (laminin 5) cicatricial pemphigoid associated with an underlying gastric carcinoma producing laminin 5. *Br J Dermatol* 1999; **140**: 696-700
- 45 **Koyama S**, Maruyama T, Adachi S. Expression of epidermal growth factor receptor and CD44 splicing variants sharing exons 6 and 9 on gastric and esophageal carcinomas: a two-color flow-cytometric analysis. *J Cancer Res Clin Oncol* 1999; **125**: 47-54
- 46 **Isozaki H**, Ohyama T, Mabuchi H. Expression of cell adhesion molecule CD44 and sialyl Lewis A in gastric carcinoma and colorectal carcinoma in association with hepatic metastasis. *Int J Oncol* 1998; **13**: 935-942
- 47 **Saito H**, Tsujitani S, Katano K, Ikeguchi M, Maeta M, Kaibara N. Serum concentration of CD44 variant 6 and its relation to prognosis in patients with gastric carcinoma. *Cancer* 1998; **83**: 1094-1010
- 48 **Ham HJ**, Shen KL, Liu CA, Ho LI, Yang LS, Yueh KC. Hyaluronate binding assay study of transfected CD44 V4-V7 isoforms into the human gastric carcinoma cell line SC-M1. *J Pathol* 1998; **184**: 291-296
- 49 **Yasui W**, Kudo Y, Naka K, Fujimoto J, Ue T, Yokozaki H, Tahara E. Expression of CD44 containing variant exon 9 (CD44v9) in gastric adenomas and adenocarcinomas: relation to the proliferation and progression. *Int J Oncol* 1998; **12**: 1253-1258
- 50 **Castella EM**, Ariza A, Pellicer I, Fernandez-Vasalo A, Ojanguren I. Differential expression of CD44v6 in metastases of intestinal and diffuse types of gastric carcinoma. *J Clin Pathol* 1998; **51**: 134-137
- 51 **Chen JL**, Zhou T, Chu YD, Xu HM, Li X, Zhang MJ, Zhang DH, Wu YL. The significance of intercellular adhesion molecule-1 and P-selectin in hepatic ischemia-reperfusion injury. *Zhongguo Weizhongbing Jijiuyixue* 1998; **10**: 670-672
- 52 **Chen JL**, Chu YD, Zhou T, Xu HM, Li X, Zhang MJ. Effects of P-selectin and anti-P-selectin antibody on apoptosis during liver ischemia-reperfusion injury. *Shanghai Dier Yike Daxue Xuebao* 2000; **20**: 239-241
- 53 **Wu P**, Li X, Zhou T, Zhang MJ, Chen JL, Wang WM, Chen N, Dong DC. Role of P-selectin and anti-P-selectin monoclonal antibody in apoptosis during hepatic/renal ischemia reperfusion injury. *World J Gastroenterol* 2000; **6**: 244-247
- 54 **Sandborn WJ**, Targan SR. Biologic therapy of inflammatory bowel disease. *Gastroenterology* 2002; **123**: 1592-1608
- 55 **Burns RC**, Rivera-Nieves J, Moskaluk CA, Matsumoto S, Cominelli F, Ley K. Antibody blockade of ICAM-1 and VCAM-1 ameliorates inflammation in the SAMP-1/Yit adoptive transfer model of Crohn's disease in mice. *Gastroenterology* 2001; **121**: 1428-1436

Edited by Ren SY

Effects of heparin on liver fibrosis in patients with chronic hepatitis B

Jun Shi, Jing-Hua Hao, Wan-Hua Ren, Ju-Ren Zhu

Jun Shi, Jing-Hua Hao, Wan-Hua Ren, Ju-Ren Zhu, Center for Liver Diseases, Shandong Provincial Hospital, Jinan 250021, Shandong Province, China

Supported by Research Grant of Shandong Provincial Health Committee. No. 2001CA2CKA2

Correspondence to: Dr. Jun Shi, Center for Liver Diseases, Shandong Provincial Hospital, 342 Jing Wu Wei Qi Road, Jinan 250021, Shandong Province, China. sdshij@yahoo.com.cn

Telephone: +86-531-7938911-2450

Received: 2002-11-29 **Accepted:** 2003-03-02

Abstract

AIM: To evaluate the effects of heparin on liver fibrosis in patients with chronic hepatitis B.

METHODS: Fifty-two cases under study were divided into two groups, group A and group B. The two groups were given regular treatment and heparin/low molecular weight heparin (LMWH) treatment respectively. Hepatic functions, serum hyaluronic acid (HA) and type IV collagen levels were measured before and after the treatment, and six cases were taken liver biopsy twice.

RESULTS: After treatment, hepatic functions became significantly better in both groups. Serum HA and type IV collagen levels in group B compared with group A, decreased significantly after treatment. Collagen proliferation also decreased in group B after treatment.

CONCLUSION: Heparin/LMWH can inhibit collagen proliferation in liver tissues with hepatitis B.

Shi J, Hao JH, Ren WH, Zhu JR. Effects of heparin on liver fibrosis in patients with chronic hepatitis B. *World J Gastroenterol* 2003; 9(7): 1611-1614

<http://www.wjgnet.com/1007-9327/9/1611.asp>

INTRODUCTION

The treatment of liver cirrhosis is always a problem in the clinical practice. To control and stop liver fibrosis towards liver cirrhosis is of utmost importance. A recent trial indicated that heparin could inhibit the growth of Ito cells effectively *in vitro*^[1], which suggested that heparin might act as an antifibrosis drug. In this study, we aimed to seek a safe and effective antifibrosis drug in 52 patients with chronic hepatitis B.

MATERIALS AND METHODS

Materials

Fifty-two patients were treated in Shandong Provincial Hospital from 1999 to 2002. There were 39 males and 13 females, age ranged from 14 to 70 years, diagnosis was made by clinical manifestations and serum hepatitis B viral markers.

Experimental design

These 52 cases were divided into two groups randomly. The treatment regime of each group is listed in Table 1.

Table 1 Treatment regimes in group A and B

Group	n	Treatment regime
A	18	regular treatment(GIK,diammonium glycyrrhizinate injection,potassium magnesium aspartate,et al)
B	34	regular treatment and heparin(25mg,iv,bid) or low molecular weight heparin(6400IU,iH,qd)

Note: In group B, 18 cases were treated with heparin and 16 with low molecular weight heparin (LMWH). The LMWH was FLUX manufactured by ALFA WASSERMANN S.P.A (Italy).

All cases were treated for a course of 3 weeks. Serum alanine transaminase (ALT), prothrombin time (PT), total bilirubin (TBIL), hyaluronic acid (HA) and type IV collagen (IV-C) were measured before and after treatment. The liver tissue specimens were obtained by percutaneous needle biopsy. Ten cases in group A and sixteen in group B had liver biopsies before treatment. Six cases in group B had a second biopsy at 30-60 days after treatment.

Determination of serum HA and IV-C level

Serum HA and IV-C level was determined with radioimmunoassay. The procedures were strictly in accordance with the instructions.

Light microscopic examination

Part of the liver tissues were fixed in 10 % formalin, embedded in paraffin, and then cut into slices. The sections were stained with hematoxylin and eosin for histological study and Masson trichrome for collagen stained green.

Electron microscopic examination

Small liver blocks were fixed in 2.5 % glutaraldehyde, postfixed in 1 % OsO₄, dehydrated with ethanol, and embedded in epoxy resin. Ultrathin sections were stained with uranyl acetate and lead citrate and examined with H-800 transmitted electron microscope (Tokyo, Japan).

RESULTS

Changes of serum/plasma indexes before and after treatment

As shown in Table 2, the levels of ALT and TBIL decreased significantly after treatment, while the level of PT changed slightly only. The level of HA and IV-C in group B decreased markedly, while those in group A were elevated.

Table 2 Changes of the serum/plasma indexes before and after treatment in group A and B ($\bar{x}\pm s$)

	A		B	
	Before	After	Before	After
ALT	136.45±103.46	69.88±43.58 ^a	185.58±138.54	84.93±57.14 ^a
PT	17.84±3.22	15.98±2.67	18.45±4.25	18.62±3.67
TBIL	64.65±21.35	38.42±14.38 ^a	69.54±26.53	31.25±17.84 ^a
HA	254.43±116.37	309.48±214.03	579.59±191.45	286.45±136.54 ^a
IV-C	237.5±104.44	259.3±137.65	349.56±112.43	189.8±79.63 ^a

^aP<0.05, vs before treatment.

Histologic changes before and after treatment with heparin/LMWH

Hematoxylin and eosin staining Hepatocytes swelled and appeared balloon-like before treatment. Inflammatory cells penetrated into the interstitium. Red blood cells congregated in the sinusoids. After treatment with heparin/LMWH, the swollen hepatocytes alleviated, and the sinusoids became clearly seen (Figure 1,2).

Masson trichrome staining Collagens could be seen evidently before treatment. Some sinusoids had been compressed by collagens. After treatment with heparin/LMWH, the collagen fibers decreased significantly (Figure 3,4).

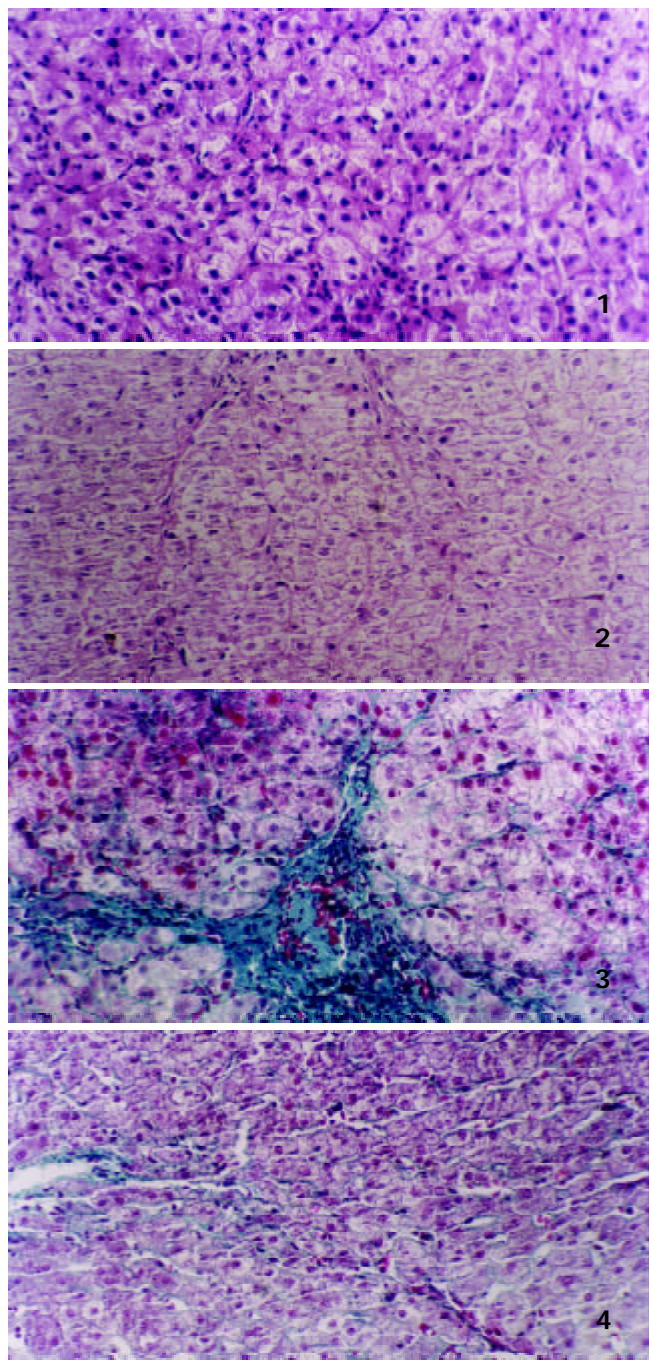


Figure 1 The liver tissue before treatment with heparin. H&E staining. $\times 200$.

Figure 2 The liver tissue after treatment with heparin. H&E staining. $\times 200$.

Figure 3 The liver tissue before treatment with heparin. Masson staining. $\times 200$.

Figure 4 The liver tissue after treatment with heparin. Masson staining. $\times 200$.

Electron microscopic observation Before treatment, hepatocytes were enlarged and cytoplasm appeared dissolved with swollen mitochondria. Base membrane was seen under the hepatic sinusoidal endothelial cells with collagen deposited in the Disse's space. The Ito cells simulated fibroblasts. The edge of membrane looked uneven, saw-like in severe cases. The number of fat drops decreased markedly. There was microfilament-like structure in the cytoplasm, fibrils were seen around the Ito cells. After treatment, the swollen hepatocytes decreased, so did the base membrane and the depositing collagen in the Disse's space. The edge of Ito cells turned smooth. Several fat drops could be seen in the cytoplasm of Ito cells (Figure 5-8).

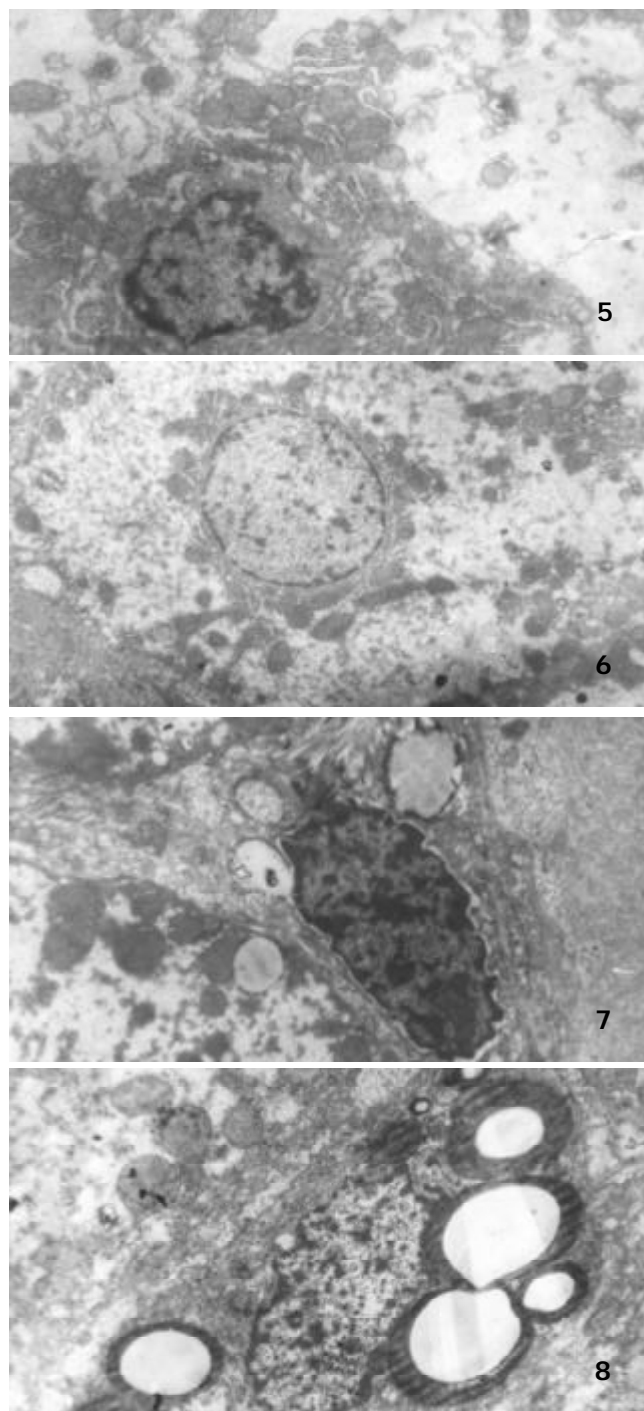


Figure 5 The hepatocyte before treatment heparin. $\times 6000$.

Figure 6 The hepatocyte after treatment with with heparin. $\times 3500$.

Figure 7 The Ito cell before treatment with heparin. $\times 5000$.

Figure 8 The Ito cell after treatment with with heparin. $\times 5000$.

DISCUSSION

Liver fibrosis is caused by the deposition of extracellular matrix (ECM)^[2-3]. All cells in the liver can synthesize and secrete ECM, which regulates the proliferation, differentiation and metabolism of liver cells. The abnormal metabolism and deposition of ECM lead to liver fibrosis. It has been recognized that Ito cells have intimate relationships with liver fibrosis^[4], which have been postulated to play critical roles in the development of fibrosis of the liver from viral infection, alcohol and many drugs^[5,6]. Ito cells are relatively inactive fibroblasts in the liver lobules. During liver fibrogenesis, cytokines such as TGF- β_1 , PDGF can activate Ito cells^[7-9] to acquire a myofibroblast-like phenotype characterized by increased proliferation and synthesis of ECM component^[10-27].

It has been proved in animal studies that heparin can inhibit the growth of Ito cells and the expression of α -actin, types I and IV procollagen *in vitro*^[1]. Our studies showed that heparin/LMWH could decrease serum HA and IV-C levels in patients with chronic hepatitis B. After treatment, the collagen fibrils in the liver tissues decreased significantly and Ito cells turned oval and fatty drops reappeared in the cytoplasm. The above results indicate that heparin/LMWH act on Ito cells.

The liver functions were improved in both group A and B after treatment. HA and IV-C levels decreased significantly in group B, in contrast, they were elevated in group A. These results suggest that the routine liver function tests could not reflect the fibrosis completely. Kopke-Aguiar *et al.*^[28] also proved that serum hyaluronic acid was a good marker for hepatic fibrosis at the initial phase.

Wanless *et al.*^[29] have studied hepatic veins of medium size (0.2 to 3 mm in diameter) in 61 cirrhotic livers. Intimal fibrosis with at least 10 % luminal narrowing was found in 70 % of cirrhotic livers. They considered that multiple layers of intimal fibrosis in some livers suggested the presence of recurrent thrombosis. In other words, thrombosis was related to intimal fibrosis and even caused obstruction of the veins. Our previous studies^[30] also showed that as an anticoagulant agent, heparin could improve hepatic microcirculation significantly and lessen sinusoidal capillarization. IV-C is considered an important marker of the development of hepatic sinusoidal capillarization and may appear basal-like membrane^[31,32]. Therefore, decrease of the IV-C concentration can not only reflect the improvement of hepatic microcirculation, but also inhibit the fibrosis. It can be used as antifibrosis drug together with antiviral drugs.

Heparin is cheap and safe. LMWH has a weaker effect on thrombin than heparin, but has stronger effect on Xa. 90 % of LMWH can be absorbed hypodermically and its anti-Xa effect can last for 24 hours and therefore, LMWH can be used once a day. One needs not measure the activated coagulation time (ACT) during the procedure^[33]. As to the mechanisms of its antifibrosis effect, further studies are necessary.

REFERENCES

- 1 **Yuan TX**, Zhang JS, Zhang YE, Chen Q. Culture of rat liver Ito cells and the observation of inhibitory effect of heparin on Ito cells. *Shanghai Yike Daxue Xuebao* 1996; **23**: 90-93
- 2 **Bissell DM**, Friedman SL, Maher JJ, Roll FJ. Connective tissue biology and hepatic fibrosis: report of a conference. *Hepatology* 1990; **11**: 488-498
- 3 **Schuppan D**. Structure of the extracellular matrix in normal and fibrotic liver: collagens and glycoproteins. *Semin Liver Dis* 1990; **10**: 1-10
- 4 **Friedman SL**. Cellular source of collagen and regulation of collagen production in liver. *Semin Liver Dis* 1990; **10**: 20-29
- 5 **Battaller R**, Brenner DA. Hepatic stellate cells as a target for the treatment of liver fibrosis. *Semin Liver Dis* 2001; **21**: 437-451
- 6 **Dai WJ**, Jiang HC. Advances in gene therapy of liver cirrhosis, a review. *World J Gastroenterol* 2001; **7**: 1-8
- 7 **Kinnman N**, Gorla O, Wendum D, Gendron MC, Rey C, Poupon R, Housset C. Hepatic stellate cell proliferation is an early platelet-derived growth factor-mediated cellular event in rat cholestatic liver injury. *Lab Invest* 2001; **81**: 1709-1716
- 8 **Gandhi CR**, Kuddus RH, Uemura T, Rao AS. Endothelin stimulates transforming growth factor- β_1 and collagen synthesis in stellate cells from control but not cirrhotic rat liver. *Eur J Pharmacol* 2000; **406**: 311-318
- 9 **Gabriel A**, Kuddus RH, Rao AS, Gandhi CR. Down-regulation of endothelin receptor by transforming growth factor β_1 in hepatic stellate cells. *Hepatology* 1999; **30**: 440-450
- 10 **Huang GC**, Zhang JS, Zhang YE. Effects of retinoic acid on proliferation, phenotype and expression of cyclin-dependent kinase inhibitors in TGF- β_1 stimulated rat hepatic stellate cells. *World J Gastroenterol* 2000; **6**: 819-823
- 11 **Chen PS**, Zhai WR, Zhou XM, Zhang JS, Zhang YE, Ling YQ, Gu YH. Effects of hypoxia, hyperoxia on the regulation of expression and activity of matrix metalloproteinase-2 in hepatic stellate cells. *World J Gastroenterol* 2001; **7**: 647-651
- 12 **Wang JY**, Zhang QS, Guo JS, Hu MY. Effects of glycyrrhetic acid on collagen metabolism of hepatic stellate cells at different stages of liver fibrosis in rats. *World J Gastroenterol* 2001; **7**: 115-119
- 13 **Eng FJ**, Friedman SL. Fibrogenesis I. New insight into hepatic stellate cell activation: the simple becomes complex. *Am J Physiol* 2000; **279**: G7-G11
- 14 **Friedman SL**. Molecular regulation of hepatic fibrosis, an integrated cellular response to tissue injury. *J Biol Chem* 2000; **275**: 2247-2250
- 15 **Albanis E**, Friedman SL. Hepatic fibrosis. Pathogenesis and principles of therapy. *Clin Liver Dis* 2001; **5**: 315-334
- 16 **Paradis V**, Perlemuter G, Bonvoust F, Dargere D, Parfait B, Vidaud M, Conti M, Huet S, Ba N, Buffet C, Bedossa P. High glucose and hyperinsulinemia stimulate connective tissue growth factor expression: a potential mechanism involved in progression to fibrosis in nonalcoholic steatohepatitis. *Hepatology* 2001; **34**: 738-744
- 17 **Schneiderhan W**, Schmid-Kotsas A, Zhao J, Grunert A, Nussler A, Weidenbach H, Menke A, Schmid RM, Adler G, Bachem MG. Oxidized low-density lipoproteins bind to the scavenger receptor, CD36, of hepatic stellate cells and stimulate extracellular matrix synthesis. *Hepatology* 2001; **34**: 729-737
- 18 **Benyon RC**, Arthur MJ. Extracellular matrix degradation and the role of hepatic stellate cells. *Semin Liver Dis* 2001; **21**: 373-384
- 19 **Vaillant B**, Chiramonte MG, Cheever AW, Soloway PD, Wynn TA. Regulation of hepatic fibrosis and extracellular matrix genes by the Th response: new insight into the role of tissue inhibitors of matrix metalloproteinases. *J Immunol* 2001; **167**: 7017-7026
- 20 **Breitkopf K**, Lahme B, Tag CG, Gressner AM. Expression and matrix deposition of latent transforming growth factor beta binding proteins in normal and fibrotic rat liver and transdifferentiating hepatic stellate cells in culture. *Hepatology* 2001; **33**: 387-396
- 21 **Bruck R**, Genina O, Aeed H, Alexiev R, Nagler A, Avni Y, Pines M. Halofuginone to prevent and treat thioacetamide-induced liver fibrosis in rats. *Hepatology* 2001; **33**: 379-386
- 22 **Watanabe T**, Niioka M, Hozawa S, Kameyama K, Hayashi T, Arai M, Ishikawa A, Maruyama K, Okazaki I. Gene expression of interstitial collagenase in both progressive and recovery phase of rat liver fibrosis induced by carbon tetrachloride. *J Hepatol* 2000; **33**: 224-235
- 23 **Nakamura T**, Sakata R, Ueno T, Sata M, Ueno H. Inhibition of transforming growth factor beta prevents progression of liver fibrosis and enhances hepatocyte regeneration in dimethylnitrosamine-treated rats. *Hepatology* 2000; **32**: 247-255
- 24 **Castera L**, Hartmann DJ, Chapel F, Guettier C, Mall F, Lons T, Richardet JP, Grimbert S, Morassi O, Beaugrand M, Trinchet JC. Serum laminin and type IV collagen are accurate markers of histologically severe alcoholic hepatitis in patients with cirrhosis. *J Hepatol* 2000; **32**: 412-418
- 25 **Brenner DA**, Waterboer T, Choi SK, Lindquist JN, Stefanovic B, Burchard E, Yamauchi M, Gillan A, Rippe RA. New aspects of hepatic fibrosis. *J Hepatol* 2000; **32**(Suppl 1): 32-38
- 26 **Benyon RC**, Iredale JP. Is liver fibrosis reversible? *Gut* 2000; **46**: 443-446

- 27 **Friedman SL**. Molecular regulation of hepatic fibrosis, an integrated cellular response to tissue injury. *J Biol Chem* 2000; **275**: 2247-2250
- 28 **Kopke-Aguiar LA**, Martins JR, Passerotti CC, Toledo CF, Nader HB, Borges DR. Serum hyaluronic acid as a comprehensive marker to assess severity of liver disease in schistosomiasis. *Acta Trop* 2002; **84**: 117-126
- 29 **Wanless IR**, Wong F, Blendis LM, Greig P, Heathcote EJ, Levy G. Hepatic and portal vein thrombosis in cirrhosis: possible role in development of parenchymal extinction and portal hypertension. *Hepatology* 1995; **21**: 1238-1247
- 30 **Hao JH**, Shi J, Ren WH, Han GQ, Wang WZ, Zhu JR, Wang SY, Xie YB. Usage of heparin in the patients with chronic hepatitis B. *Wei Xunhuan Xue Zazhi* 2001; **11**: 9-11
- 31 **Matsumoto S**, Yamamoto K, Nagano T, Okamoto R, Ibuki N, Tagashira M, Tsuji T. Immunohistochemical study on phenotypical changes of hepatocytes in liver disease with reference to extracellular matrix composition. *Liver* 1999; **19**: 32-38
- 32 **Marcato PS**, Bettini G, Della Salda L, Galeotti M. Pretelangiectasis and telangiectasis of the bovine liver: a morphological immunohistochemical and ultrastructural study. *J comp Pathol* 1998; **119**: 95-110
- 33 **Khosla S**, Kunjummen B, Guerrero M, Manda R, Razminia M, Trivedi A, Vidyarthi V, Elbazour M, Ahmed A, Lubell D. Safety and efficacy of combined use of low molecular weight heparin (enoxaparin, lovenox) and glycoprotein IIb/IIIa receptor antagonist (eptifibatide, integrilin) during nonemergent coronary and peripheral vascular intervention. *Am J Ther* 2002; **9**: 488-491

Edited by Wu XN

Effect of Sea buckthorn on liver fibrosis: A clinical study

Ze-Li Gao, Xiao-Hong Gu, Feng-Tao Cheng, Fo-Hu Jiang

Ze-Li Gao, Fo-Hu Jiang, Department of Gastroenterology, Baogang Hospital, Shanghai Second Medical University, Shanghai 201900, China
Xiao-Hong Gu, Feng-Tao Cheng, Department of Gastroenterology, Yangpu District Hospital, Shanghai 200090, China

Correspondence to: Dr. Ze-Li Gao, Department of Gastroenterology, Baogang Hospital, Shanghai Second Medical University, Shanghai 201900, China. gzeli@sina.com

Telephone: +86-21-56691101-6260

Received: 2002-12-28 **Accepted:** 2003-02-18

Abstract

AIM: To appraise the effect of sea buckthorn (*Hippophae rhamnoides*) on cirrhotic patients.

METHODS: Fifty cirrhotic patients of Child-Pugh grade A and B were randomly divided into two groups: Group A as the treated group ($n=30$), taking orally the sea buckthorn extract, 15 g 3 times a day for 6 months. Group B as the control group ($n=18$), taking vitamin B complex one tablet, 3 times a day for 6 months. The following tests were performed before and after the treatment in both groups to determine LN, HA, collagens types III and IV, cytokines IL-6 and TNF α , liver serum albumin, total bile acid, ALT, AST and prothrombin time.

RESULTS: The serum levels of TNF α , IL-6, laminin and type IV collagen in group A were significantly higher than those in the control group. After a course of sea buckthorn treatment, the serum levels of LN, HA, collagen types III and IV, total bile acid (TBA) decreased significantly as compared with those before and after treatment in the control group. The sea buckthorn notably shortened the duration for normalization of aminotransferases.

CONCLUSION: Sea buckthorn may be a hopeful drug for prevention and treatment of liver fibrosis.

Gao ZL, Gu XH, Cheng FT, Jiang FH. Effect of Sea buckthorn on liver fibrosis: A clinical study. *World J Gastroenterol* 2003; 9 (7): 1615-1617

<http://www.wjgnet.com/1007-9327/9/1615.asp>

INTRODUCTION

Liver cirrhosis is a common chronic hepatic injury caused by chronic hepatitis B, ethanol consumption and metabolic disorders, etc. The patients often die of hepatic failure due to portal hypertension, bleeding of esophageal and gastric varices. Recent studies have shown that fat storing cells now called hepatic stellate cells (HSCs) are the main collagen producing cells in fibrotic liver. Under the influence of inflammatory cytokines, vitamin A- rich cells are activated, proliferating and transforming into myofibroblasts, producing extracellular matrix (ECM)^[1,2]. Retinoic acid droplets and retinoic acid receptors (RAR) diminish. Recent studies have also shown that when retinyl esters and RAR contents are restored in HSC, HSCs would remain in the inactivated state. Hence HSCs are regarded as the therapeutic targets for prevention and treatment

of hepatic fibrosis^[3]. In this study, sea buckthorn (*Hippophae rhamnoides*,) was used in cirrhotic patients to determine its effect on the changes of fibrotic parameters, improvement of liver function and whether it could be used as a therapeutic antifibrotic agent.

MATERIALS AND METHODS

Subjects

Fifty patients aged 20-70 years were enrolled in this study with at least an elevation of two items of the following parameters, e.g, serum collagen types III and IV, laminin (LN), hyaluronic acid (HA). These patients were divided into treated group (group A, $n=30$, 25 hepatitis B cirrhosis and 5 alcoholic) and control group (group B $n=20$, 17 hepatitis B cirrhosis and 3 alcoholic). These two groups had similar demographic characteristics. All these patients had not taken any antifibrotic drug or immunomodulator or antiviral herbs in the past 6 months. Group A received sea buckthorn extract in fine granules (manufactured by Sichuan Pharmaceutical Co.LTD, China), 15 g, three times a day for 6 months. Group B received vitamin-B complex, 2 tablets once, 3 times a day for 6 months.

Measurement of cytokines, parameters of liver fibrosis and liver function tests

Cytokine: IL6 and TNF α were measured by enzyme-linked immunosorbent assay (ELISA). LN, HA, collagen types III and IV were measured by radioimmunoassay (RIA). Serum albumin (Alb), total bilirubin, aspartate aminotransferase (AST), alanine aminotransferase (ALT), alkaline phosphatase (ALP), conjugates, total bile acid (TBA), prothrombin time (PT) were measured by a biochemical autoanalyzer.

Statistical analysis

All data were analyzed with SAS software. The results were expressed as mean \pm standard deviation, the rate of normalization of AST, ALT was analyzed by Chi-square test. LN, HA, Alb, TBA, PT, collagen types III and IV were analyzed by signed rank test (both pre-and posttreatment in the same group) and Wilcoxon rank test (between the two groups, pre-and post treatment for comparison). P value <0.05 was considered statistically significant.

RESULTS

Determination of TNF α , IL-6, LN, HA

The levels of TNF α , IL-6, LN, collagen type IV in the 50 cirrhotic patients were significantly higher than those in the controls ($P<0.05$). There were positive correlations between TNF α , IL-6 and LN, collagen type IV (Table 1).

Table 1 Measurements of TNF α , IL-6, LN, type IV collagen ($\bar{x}\pm s$)

Group	<i>n</i>	TNF α (ng/L)	IL-6 (ng/L)	LN (μ g/L)	Type IV (ng/L)
A	30	19.6 \pm 3.2	15.1 \pm 2.8	374.1 \pm 31.2	250.9 \pm 22.6
B	20	6.7 \pm 1.2	3.8 \pm 1.1	99.4 \pm 6.8	51.8 \pm 4.6
<i>t</i> value		2.419	2.961	2.618	2.997
<i>P</i> value		<0.05	<0.05	<0.05	<0.05

Table 2 Normalization rates of AST,ALT ($\bar{x}\pm s$)

Group	AST (IU/L)		Normalization rate (%)	ALT (IU/L)		Normalization rate (%)
	Before treatment	After treatment		Before treatment	After treatment	
A	59.87±26.70	49.03±18.99	24/30(80) ^a	50.57±32.47	44.12±26.05	24/30(80) ^a
B	154.75±20.21	47.85±23.53	10/18(56)	41.65±23.54	39.15±16.68	10/18(56)

^a $P<0.05$ vs controls.

Table 3 Parameters of liver fibrosis ($\bar{x}\pm s$)

Parameters	Group	Before treatment	After treatment	Comparison of two groups	
				Stat Z	P value
III (ng/l)	A	428.43±196.02	149.43±75.91	0.0403	0.0394
	B	423.56±251.41	169.80±138.94		
IV (ng/l)	A	123.98±81.22	70.00±34.45	0.0393	0.0384
	B	178.32±89.45	139.85±98.15		
LN (μg/l)	A	210.91±165.12	136.51±105.56	0.0073	0.0070
	B	211.56±188.91	156.00±100.00		
HA (μg/l)	A	516.74±338.75	240.56±169.78	0.0148	0.0144
	B	494.74±272.26	387.16±196.28		

Wilcoxon rank test.

Table 4 Changes of TBA, PT, Alb ($\bar{x}\pm s$)

Parameters	Group	Before treatment	After treatment	Before treatment		Before/after treatment		Comparison of two groups before/after treatment	
				Stat(Z)	P value	Stat(t)	P value	Stat(S)	P value
TBA (ng/l)	A	38.70±27.50	22.83±12.28	0.751	0.743	189.32	0.0001	545.0	0.0003
	B	40.50±34.02	38.55±22.60						
PT (sec)	A	14.57±0.97	13.50±0.73	4.35	0.048	7.443	0.0001	2.21	0.1415
	B	15.15±0.93	14.40±0.74						
Alb (g/l)	A	34.07±9.35	35.13±7.13	7.02	0.010	1.205	0.238	0.48	0.4887
	B	27.45±7.41	27.40±6.25						

Signed rank test and Wilcoxon rank test.

ECM parameters and liver function tests

Remarkable changes were found in AST and ALT after sea buckthorn treatment. The rate of normalization was 80 % in the treated group and 56 % in the control group ($P<0.05$). No difference was found in serum albumin and prothrombin time. In group A, serum LN, HA, total bile acid (TBA), collagen types III and IV were decreased after treatment as compared with group B. There was a significant difference between the two groups ($P<0.05$). (Tables 2-4).

DISCUSSION

Sea buckthorn is a plant growing in severely cold region of South-west China, its fruit juice has been taken as a tonic by the local Mongolians and Tibetans. It contains a great deal of vitamins, amino acids and trace elements, which are beneficial to human health^[4]. Recent studies have shown that sea buckthorn contains lots of vitamin A precursors including β carotene and unsaturated fatty acids. Zhao *et al*^[5] reported that sea buckthorn could protect the liver from damage by CCl_4 . A combination of an antiviral drug and sea buckthorn in treating patients with chronic hepatitis B could shorten the duration for the normalization of serum ALT. The rate of turning negative of HBeAg and HBsAg was 52.16 % and 16.67 %, respectively^[6].

In the normal liver, HSCs are mainly involved in the storage

of vitamin A. In addition, they synthesize extracellular matrix components, matrix degrading metalloproteinases, cytokines, and growth factors^[7,8]. Following acute or chronic liver injury, HSCs are activated and undergo a process of transdifferentiation, leading to a myofibroblastic phenotype. The activated HSCs are characterized by a loss of vitamin A droplets, increase of proliferation, release of proinflammatory, profibrogenic, and prometogenic cytokines and migration to the sites of injury with increased production of extracellular matrix components and alterations in matrix protease activity and provision for the fundamental needs of tissue repair^[9]. In acute or self-limited liver damage, these changes are transient, whereas in case of persistent injury, they lead to chronic inflammation with an accumulation of extracellular matrix, resulting in liver fibrosis and ultimately cirrhosis. Several growth factors and cytokines are involved in HSCs activation and proliferation, of which transforming growth factor β (TGF β), platelet derived growth factor (PDGF), TNF α and IL-6 are probably the most important ones^[10].

TNF α is not only an anticancer factor, but also participates in the process of immunologic reaction and inflammation. The synthesis of collagen and some extracellular matrices were elevated 3 fold and 2.6 fold, respectively when rat HSCs were incubated with TNF α (5.0 nmol/l) for 24 hours^[11]. IL-6 is a cytokine which has many biologic functions, such as promoting cell proliferation and differentiation, regulating immune

function. Wang *et al.*^[12,13] reported IL-6 increased in the peripheral blood of an early animal model of liver fibrosis, and the peripheral blood level of IL-6 in cirrhotic patients was remarkably higher than that in those without^[14].

HSCs represent 5-8 % of all human liver cells. They have long cytoplasmic processes which run parallel to the sinusoidal endothelial wall. The second order branches sprout out from the processes, and embrace the sinusoids. Some HSCs are in close contact with nerve endings, some of which contain neuropeptides such as substance P, neuropeptide Y, somatostatin, and calcitonin gene-related peptide^[15,16].

Our previous study showed^[17] that retinoic acid receptor (RAR) and cAMP of primarily cultured HSCs were reduced, as compared with those in freshly isolated HSCs. The contents of RAR and cAMP of cultured HSCs were increased after treated with all-transretinoic acid (10^{-5} Mol/L).

Based on the recent articles and our results, we may deduce that the resting HSCs are activated by TNF α and IL-6 released by Kupffer cells during the process of acute or chronic inflammation, then TNF α and IL-6 in turn stimulate Kupffer cells to release TGF β and PDGF. Eventually, HSCs proliferation and synthesis of ECM, along with the loss of vitamin A droplets, will transform themselves into myofibroblast producing liver fibrosis^[18,19].

The present study showed that sea buckthorn could reduce the serum levels of laminin, hyaluronic acid, TBA, collagen types III and IV in patients with liver cirrhosis, indicating that it may restrain the synthesis of collagen and other components of ECM. We are attempting to restore vitamin A and RAR contents of HSCs, so as to keep HSCs in a quiescent status and to prevent progression of liver fibrosis. Sea buckthorn may be a hopeful drug for prevention and treatment of liver fibrosis, but further well controlled clinical trials are required.

REFERENCES

- 1 **Norifumi K**, Shuichi S, Masayasu I, Tetsuo K. Effect of antioxidants, resveratrol, quercetin, and N-Acetylcysteine on the function of cultured rat hepatic stellate cells and kupffer cells. *Hepatology* 1998; **27**: 1265-1274
- 2 **Giuliano R**, Thomas A. Cytokines in the liver. *Eur J Gastroenterol Hepatol* 2001; **13**: 777-784
- 3 **Reynaert H**, Thompson MG, Thomas T, Geerts A. Hepatic stellate cells: role in microcirculation and pathophysiology of portal hypertension. *Gut* 2002; **50**: 571-581
- 4 **Oomah BD**, Sery C, Godfrey DV, Beveridge TH. Rheology of sea buckthorn (*Hippophae rhamnoides* L) juice. *J Agric Chem* 1999; **47**: 3546-3550
- 5 **Zao TD**, Cheng ZX, Liu XY, Shao JY, Ren LJ, Zhang L, Chen WC. Protective effect of the sea buckthorn oil for liver injury induced by CCl₄. *Zhongcaoyao* 1987; **18**: 22-24
- 6 **Huang DL**, Chang XZ, Gui HN, Tian YD, Chen LX, Li ZP, Xing L. Analysis of 156 cases of chronic hepatitis treated with sea buckthorn. *Zhongxiyi Jiehe Zazhi* 1991; **11**: 697-6980
- 7 **Greerts A**. History, heterogeneity, developmental biology and functions of quiescent hepatic stellate cells. *Semin Liver Dis* 2001; **21**: 311-315
- 8 **Schumann J**, Tieggs G. Pathophysiological mechanisms of TNF during intoxication with natural or man-made toxins. *Toxicology* 1999; **138**: 103-126
- 9 **Lissoos TW**, Davis BH. Pathogenesis of hepatic fibrosis and the role of cytokines. *J Clin Gastroenterol* 1992; **15**: 63-67
- 10 **Friedman SL**. Molecular regulation of hepatic fibrosis, an integrated cellular response to tissue injury. *J Biol Chem* 2000; **275**: 2247-2250
- 11 **Knittel T**, Muller L, Saile B, Ramadori G. Effect of tumor necrosis factor -alpha on proliferation, activation and protein synthesis of rat hepatic stellate cells. *J Hepatol* 1997; **27**:1067-1080
- 12 **Weiner FR**, Giambone MA, Czaja MJ, Shah A, Annoni G, Takahashi S, Eghbali M, Zern MA. Ito-cell gene expression and collagen regulation. *Hepatology* 1990; **11**: 111-117
- 13 **Wang Q**, Xia HS, Jiang HY, Ma XX, Zhu F, Zuo LQ. The Immunologic regulation of liver in the process of rat liver fibrosis. *Zhonghua Yixue Zazhi* 1995; **75**:594-598
- 14 **Tili H**, Lissoos TW. Pathogenesis of hepatic fibrosis and the role of the cytokine. *Gastroenterology* 1992; **103**: 264-271
- 15 **Burt AD**, Le Bail B, Balabaud C, Bioulac-Sage P. Morphologic investigation of sinusoidal cells. *Semin Liver Dis* 1993; **13**: 21-38
- 16 **Stoyanova II**, Gulubova MV. Immunocytochemical study on the liver innervation in patients with cirrhosis. *Acta Histochem* 2000; **102**: 391-402
- 17 **Gao ZL**, Li DG, Lu HM. The effect of retinoic acid receptor and cAMP of HSC cell. *Weichangbingxue He Ganbingxue Zazhi* 1995; **4**: 20-22
- 18 **Rebecca G**, Wells. Fibrogenesis V. TGF- β signaling pathways. *Am J Physiol Gastrointest Liver Physiol* 2000; **279**: G845-G850
- 19 **Gangopadhyay A**, Bajanova O, Kelly TM, Thomas P. Carcinoembryonic antigen induces cytokine expression in Kupffer cells: implications for hepatic metastasis from colorectal cancer. *Cancer Res* 1996; **56**: 4805-4810

Edited by Wu XN and Wang XL

Fatty metamorphosis of the liver in patients with breast cancer: Possible associated factors

Cheng-Hsin Chu, Shee-Chan Lin, Shou-Chuan Shih, Chin-Roa Kao, Sun-Yen Chou

Cheng-Hsin Chu, Shee-Chan Lin, Shou-Chuan Shih, Chin-Roa Kao, Sun-Yen Chou, Division of Gastroenterology, Department of Internal Medicine, Mackay Memorial Hospital, Taipei, Taiwan, China
Correspondence to: Dr. Cheng-Hsin Chu, Department of Hepatology and Gastroenterology, Mackay Memorial Hospital, Address: No. 92, Sec. 2, Chung-Shan N. Road, Taipei, Taiwan, China. suyu5288@ms14.hinet.net
Telephone: +86-2-88661107 **Fax:** +86-2-25433642
Received: 2003-02-25 **Accepted:** 2003-03-16

Abstract

AIM: To investigate the relationship between breast cancer and fatty liver in Chinese patients.

METHODS: The study group consisted of 217 patients with newly diagnosed breast cancers and the control group of 182 subjects undergoing routine health examination in the same hospital. All subjects were female and the groups were matched for date of study. Ultrasound scanning was performed by the same operator using a 3.5 MHz transducer. Steatosis of the liver was diagnosed based on the criteria of Saverymuttu *et al.* Clinical variables were statistically analyzed.

RESULTS: Fatty liver was diagnosed in 98 patients of the study group and 37 patients of the control group, a significant difference was found in incidence (98/217, 45.2 % and 37/182, 20.3 %; $P < 0.0001$). On univariate analysis, fatty liver in breast cancer patients was associated with overweight, hyperlipidemia, and hepatitis. On multivariate analysis in the same patients, obesity and hyperlipidemia were significantly associated with fatty liver.

CONCLUSION: The cause of fatty liver in women with breast cancer may be multifactorial. The present study confirms its link with overweight and hyperlipidemia.

Chu CH, Lin SC, Shih SC, Kao CR, Chou SY. Fatty metamorphosis of the liver in patients with breast cancer: Possible associated factors. *World J Gastroenterol* 2003; 9(7): 1618-1620
<http://www.wjgnet.com/1007-9327/9/1618.htm>

INTRODUCTION

Breast cancer is a common cancer in the developed countries such as Western Europe and North America where women tend to be well-nourished. In 1973, the reported crude annual incidence rate of new breast cancer was 71.5 per 100 000 in Canada^[1]. This contrasts with the incidence in Taiwanese women of 6.11 per 100 000 published in 1971^[2]. However, more recent epidemiological studies revealed an increasing incidence of breast cancer with 12.46 per 100 000 in Taiwan^[3]. The development of breast cancer is multifactorial. Genetic, dietary, environmental, menstrual, endocrine and ethnic factors all influence it^[4]. In the course of using ultrasonography to assess liver metastases from breast cancer, we have noted a fair

number of women with breast cancer who also have fatty liver. The aim of this study was to investigate the incidence and clinicopathological factors associated with fatty liver in patients with breast carcinoma.

MATERIALS AND METHODS

A hospital-based prospective study was conducted to investigate the relationship between fatty liver and breast cancer. From May 1994 to August 1997, 217 consecutive, newly diagnosed women with breast cancer were enrolled as the study group. 182 subjects presenting to the same hospital for routine health examination was served as the control group of the same period. All subjects underwent abdominal ultrasonography performed by the same operator using a 3.5 MHz transducer (Toshiba SSA-340A). Fatty liver was diagnosed in the presence of at least two of the following sonographic features: (1) increase in liver echoes, (2) loss of echoes from the wall of the portal veins, (3) exaggeration of liver and kidney echo discrepancy, and (4) ultrasonic attenuation of the liver parenchyma. Overweight was defined as a BMI > 25 [body mass index = weight (kg)/height (m²)]. Subjects were excluded if they were pregnant, on a weight reduction diet in the 6 months preceding the study, or taking cholesterol-lowering therapy or steroids. Data collected included age, the presence of hepatitis C virus antibodies with elevation of alanine aminotransferase (GPT) and aspartate aminotransferase (GOT), BMI, a history of diabetes or hyperlipidemia, drug use (contraceptives, steroids, tamoxifen, alcohol), and chemotherapy.

Statistical analysis

The chi-square test was used for univariate analysis of these factors. Statistically significant variables on univariate analysis were subsequently subjected to multivariate analysis with logistic regression. A P value less than 0.05 was considered to be statistically significant.

RESULTS

The mean age of the breast cancer patients was slightly higher than that of the controls (48.6 \pm 10.5 vs 46.8 \pm 12.0; $P = 0.029$). None of the subjects in either group drank alcohol. Fatty liver was found in 98/217 (45.2 %) of the study group and in 37/182 (20.3 %) of the control group, with a statistically significant difference ($P < 0.0001$). The breast cancer subjects were also significantly more likely to be obese than controls (124/217, 57.1 % vs. 45/182, 24.7 %, $P < 0.0001$). There were no significant differences in the presence of hyperlipidemia or hepatitis C (Table 1).

On univariate analysis, fatty liver in subjects with breast cancer was significantly associated with overweight, hyperlipidemia, and hepatitis C but not with diabetes mellitus, tamoxifen, contraceptives, or chemotherapy (Table 2). Using logistic regression, the odds of fatty liver were increased in the breast cancer subjects in the presence of overweight (OR 1.406, $P < 0.0001$) and hyperlipidemia (OR 1.206, $P = 0.0473$) (Table 3).

Table 1 Clinical variables in patients with breast cancer and controls

Variables	Cases (n=217) Number (%)	Controls (n=182) Number (%)	P
Fatty liver			
No	119 (54.8)	145 (79.7)	<0.0001
Yes	98 (45.2)	37 (20.3)	
Overweight			
No	93 (42.9)	137 (75.3)	<0.0001
Yes	124 (57.1)	45 (24.7)	
Hyperlipidemia			
No	177 (81.6)	154 (84.6)	0.432
Yes	40 (18.4)	28 (15.4)	
Hepatitis C			
No	204 (94.0)	165 (90.6)	0.144
Yes	13 (6.0)	17 (9.4)	
Age			
Mean ± SD	48.6±10.5	46.8±12.0	0.029

Table 2 Clinical factors associated with fatty liver in patients with breast cancer (n=217)

Variables	Number of cases		P
	Fatty Liver (-)	Fatty Liver (+)	
Contraceptives			
No	117	94	0.28
Yes	2	4	
Tamoxifen			
No	25	13	0.14
Yes	94	85	
Chemotherapy			
No	52	49	0.59
Yes	58	47	
Hepatitis C			
No	116	88	0.031
Yes	10	3	
Diabetes			
No	113	92	0.73
Yes	6	6	
Overweight			
No	71	21	<0.0001
Yes	48	77	
Hyperlipidemia			
No	106	71	0.017
Yes	13	27	

Table 3 Significant variables on multivariate analysis for patients with breast cancer

Variables	Coefficient estimates and significant test			
	Coefficient	SD	P	Odds ratio
Overweight	0.3410	0.0474	0.0000	1.4064
Hyperlipidemia	0.0263	0.0132	0.0473	1.2066

DISCUSSION

Fatty liver is associated with alcohol abuse, obesity, malnutrition, diabetes mellitus, toxic agents, corticosteroids and endocrine imbalance. However, there had been little investigation of this disorder in relation to malignancy until Lanza reported in 1968 that a fair number of patients with

known cancer had steatosis on percutaneous liver biopsy^[5]. The diagnostic criteria and high accuracy of ultrasound in the detection of fatty liver were documented by Foster and Saverymuttu *et al*^[6,7]. In a similar manner, an unusually high proportion of fatty liver in patients with carcinoma of breast was observed in the present study (Table 1). In this study, fatty liver was observed in 37 out of 182 (20.3 %) asymptomatic control subjects, significantly less than the 45.2 % of breast cancer subjects. Fatty liver was related to BMI, dietary fat intake, and ethnic differences. The actual incidence in the general population was varied.

The results of numerous epidemiological studies have demonstrated that the risk for breast cancer is related to a variety of factors, including age at menarche and at first childbirth, parity, level of education, previous benign breast tumor, family history of breast cancer, young age at menopause, environmental factors, ethnicity, BMI, dietary fat intake, and high central adiposity^[2,8-10]. A significantly higher proportion of the breast cancer subjects were obese compared with controls (57.1 % vs. 15.4 %). With increasing weight, long chain fatty acid synthesis also increases, which in turn leads to lipid accumulation in the liver. It is likely that the higher incidence of fatty liver in our breast cancer subjects is related at least in part to their higher BMI.

The excess estrogen and insulin-like growth factor (IGF-1) produced by obese women have been suggested to be the key factor in promoting proliferation of mammary epithelial cells^[11-14]. Furthermore, obesity may lead to delay in diagnosis, and it appears to be a poor prognostic factor^[15,16].

Tamoxifen is an anti-estrogenic drug utilized in adjuvant therapy for breast cancer. Ogawa and colleagues suggested in 1998 that tamoxifen induced fatty liver in patients with breast cancer^[17]. Nguyen published a study in 2001 demonstrating an increase in fatty liver and accumulation of visceral adipose tissue in breast cancer patients receiving tamoxifen^[18]. Fatty liver can occur because of increased delivery of free fatty acids to the liver, increased synthesis of fatty acids in the liver, decreased β-oxidation of free fatty acids, and decreased synthesis or secretion of very low density lipoprotein^[19]. Tamoxifen must therefore disarrange some of the steps in lipid metabolism^[20].

There are a few reports of tamoxifen-associated steatohepatitis and multi-focal fatty infiltration of the liver^[21,22]. Generally speaking, patients with fatty liver are usually symptom-free, but severe steatohepatitis may lead to liver cirrhosis in some cases. Therefore, careful attention should be paid to functional and morphological changes of the liver during tamoxifen treatment^[21]. We have not yet found a significant relationship between tamoxifen and fatty liver in our subjects. This may be resulted from the insufficient length of tamoxifen treatment. Our subjects who took tamoxifen did for a mean of 12 months (range: 2-38 months), compared with a mean of 30 months (range: 4-84 months) in Nguyen's series^[18].

The clinical appearance of hepatic fatty changes may be diffuse, focal, multi-focal, the latter findings possibly mimic or harbor either primary or metastatic cancer^[17,22]. Because of the possibility of liver metastases as well as the possibility of fatty liver (including the chance of progression to steatohepatitis or cirrhosis) with or without tamoxifen, it would be wise to monitor liver function and imaging in patients with breast cancer.

REFERENCES

- 1 **Canada S.** New primary sites of malignant neoplasms in Canada. *Publication No 82-107*, 1976
- 2 **Lin TM,** Chen KP, MacMahon B. Epidemiologic characteristics of cancer of the breast in Taiwan. *Cancer* 1971; **27**: 1497-1504

- 3 **Cheng CJ**, You SL, Lin LH, Hsu WL, Yang YW. Cancer epidemiology and control in Taiwan: a brief review. *Jpn J Clin Oncol* 2002; **32**: S66-81
- 4 **Boring CC**, Squires BA, Tong T. Cancer statistics, 1991. *CA Cancer J Clin* 1991; **41**: 19-36
- 5 **Lanza FL**, Nelson RS. Fatty metamorphosis of the liver in malignant neoplasia. Special reference to carcinoma of the breast. *Cancer* 1968; **21**: 699-705
- 6 **Foster KJ**, Dewbury KC, Griffith AH, Wright R. The accuracy of ultrasound in the detection of fatty infiltration of the liver. *Br J Radiol* 1980; **53**: 440-442
- 7 **Saverymuttu SH**, Joseph AEA, Maxell JD. Ultrasound scanning in the detection of hepatic fibrosis and steatosis. *Br Med J* 1986; **292**: 13-15
- 8 **Gary GE**, Pike MC, Henderson BE. Breast cancer incidence and mortality rate in different countries in relation to known risk factors and dietary practices. *Br J Cancer* 1979; **39**: 1-7
- 9 **Choi NW**, Howe GR, Miller AB. An epidemiologic study of breast cancer. *Am J Epidemiol* 1978; **107**: 510-521
- 10 **Hirayama T**. Epidemiology of breast cancer with special reference to the role of diet. *Prev Med* 1978; **7**: 173-195
- 11 **Kirschner MA**, Ertel N, Schneider G. Obesity, hormones, and cancer. *Cancer Res* 1981; **41**: 3711-3717
- 12 **Schapira DV**, Kumar NB, Lyman GH, Cox CE. Abdominal obesity and breast cancer risk. *Ann Intern Med* 1990; **112**: 182-186
- 13 **Peyrat JP**, Bonneterre R, Dijane J, Demaille A. IGF1 receptors in human breast cancer and their relation to estradiol and progesterone receptors. *Cancer Res* 1988; **48**: 6429-6433
- 14 **Kern WH**, Hegar AH, Payne JH, DeWind LT. Fatty metamorphosis of the liver in morbid obesity. *Arch Pathol* 1973; **96**: 342-346
- 15 **Boyd NF**, Campbell JE, Germanson T. Body weight and prognosis in breast cancer. *J Natl Cancer Inst* 1981; **67**: 785-789
- 16 **Senie RT**, Rosen PP, Rhodes P. Obesity at diagnosis of breast carcinoma influences duration of disease-free survival. *Ann Intern Med* 1992; **51**: 25-32
- 17 **Ogawa Y**, Murata Y, Nishioka A, Inomata T, Yoshida S. Tamoxifen-induced fatty liver in patients with breast cancer. *Lancet* 1998; **351**: 725
- 18 **Nguyen MC**, Steward RB, Banerji MA. Relationships between tamoxifen use, liver fat and body fat distribution in women with breast cancer. *Int J Obesity* 2001; **25**: 296-298
- 19 **Lombardi B**. Consideration on the pathogenesis of fatty liver. *Lab Invest* 1966; **15**: 1-20
- 20 **Louis DB**, Claude G, Côme R. Severe lipemia induced by tamoxifen. *Cancer* 1986; **57**: 2123-2126
- 21 **Pino HC**, Baptista A, Camilo ME, de Costa EB, Valente A, de Moura MC. Tamoxifen-associated steatohepatitis-Report of three cases. *J Hepatol* 1995; **23**: 95-97
- 22 **Cai Q**, Bensen M, Greene R, Kirchner J. Tamoxifen-induced transient multifocal hepatic fatty infiltration. *Am J Gastroenterol* 2000; **95**: 277-279

Edited by Xu XQ and Zhu LH

Diarrhea and acaroid mites: A clinical study

Chao-Pin Li, Yu-Bao Cui, Jian Wang, Qing-Gui Yang, Ye Tian

Chao-Pin Li, Yu-Bao Cui, Jian Wang, Qing-Gui Yang, Ye Tian, Department of Etiology and Immunology, School of Medicine, Anhui University of Science & Technology, Huainan 232001, Anhui Province, China

Correspondence to: Dr. Chao-Pin Li, Department of Etiology and Immunology, School of Medicine, Anhui University of Science & Technology, Huainan 232001, Anhui Province, China. cpli@aust.edu.cn
Telephone: +86-554-6658770 **Fax:** +86-554-6662469

Received: 2002-12-28 **Accepted:** 2003-02-05

Abstract

AIM: To explore the characteristics of diarrhea caused by acaroid mites.

METHODS: Acaroid mites in fresh stools of 241 patients with diarrhea were separated by flotation in saturated saline. Meanwhile, skin prick test, total IgE and mite-specific IgE were detected in all patients.

RESULTS: The total positive rate of mites in stool samples of the patients was 17.01 % (41/241), the positive rates of mites in male and female patients were 15.86 % (23/145) and 18.75 % (18/96), respectively, without significant difference ($P > 0.05$). The percentage of skin prick test as "+++", "++", "+", "±" and "-" was 9.13 % (22/241), 7.47 % (18/241), 5.81 % (14/241), 4.98 % (12/241) and 72.61 % (175/241), respectively. The serum levels of total IgE, mite-specific IgE in patients with and without mites in stool samples were (165.72±78.55) IU/ml, (132.44±26.80) IU/ml and (145.22±82.47) IU/ml, (67.35±45.28) IU/ml, respectively, with significant difference ($P < 0.01$). The positive rate of mites in stool samples in staffs working in traditional Chinese medicine storehouses or rice storehouses (experimental group) was 26.74 % (23/86), which was significantly higher than that (11.61 %, 18/155) in people engaged in other professions ($\chi^2 = 8.97$, $P < 0.01$).

CONCLUSION: Acaroid mites cause diarrhea and increase serum levels of total IgE and mite-specific IgE of patients, and the prevalence of diarrhea caused by acaroid mites is associated with occupations rather than the gender of patients.

Li CP, Cui YB, Wang J, Yang QG, Tian Y. Diarrhea and acaroid mites: A clinical study. *World J Gastroenterol* 2003; 9(7): 1621-1624

<http://www.wjgnet.com/1007-9327/9/1621.asp>

INTRODUCTION

Grain or flour mite is a serious and widespread pest of stored foodstuffs, particularly grain and grain products^[1-10]. Further studies have shown that some mites with strong vitality not only live freely, feeding on a wide variety of food, but also exist in animals or human intestines. After ingesting contaminated food by mites, like grain and grain products, individuals might have diarrhea, abdominal pain, burning sensation around anus and other symptoms of gastrointestinal

tract^[11]. The characteristics of diarrhea caused by acaroid mites were investigated in 241 patients with diarrhea in this study.

MATERIALS AND METHODS

Patients

Two hundred and forty-one patients with diarrhea (male 145 and female 96, aged from 6 to 58 years) were divided into experimental group ($n=86$) including staffs working in traditional Chinese medicine storehouses ($n=47$) and staffs working in rice storehouses or mills ($n=39$), and control group ($n=155$) including miners ($n=36$), staffs of railway system ($n=34$), pupils ($n=62$) and others ($n=23$).

Reagents

Horse anti-human IgE and standard working solution for IgE (17 000 IU/ml) were provided by Beijing Institute of Biological Products, and horse anti-human horseradish peroxidase-IgE was provided by Third Affiliated Hospital, Shanghai Second Medical University.

Methods

History-taking, separation of mites from stool samples, skin prick test and detection of total IgE and mite-specific IgE were carried out in all 241 subjects.

History-taking Detailed information of each subject was collected via telephone and personal interview, including age, gender, present history, anamnesis, symptoms (i.e. abdominal pain, cramps, diarrhea, urodynia, cloudy urine, and urination frequency), onset and duration of symptoms, personal hygienic habits, living conditions and the date of stool samples collected.

Stool examination The stool samples were collected, the mites were separated by flotation in saturated saline and identified under microscope. Stool examination was performed three times for each person, positive specimens were labeled once either adult or larval mite, egg, or hypopus was found.

Skin prick test Skin prick test was performed with the concentration of 1:100 (W/V). After skin was disinfected, a little of extract (about 0.01 ml) was dripped on skin of the right forearm flexor, then a sterile needle was pricked into the skin through the drop of the extract for about 0.5-1 mm in depth without bloodshed. About 5 cm distal and proximal of the prick site, normal saline and histamine were used as negative and positive control, respectively. The mean diameter of the wheals or areolae was measured 15~20 min after the test. The reactions of skin prick test with the mean diameter 1.5 mm, 2 mm, 3 mm, 5 mm and 10 mm were regarded as ±, +, ++, +++ and +++++, respectively. Otherwise, the reaction was judged as negative^[12,13].

The test extract was prepared according to WHO approved document NIBSC 82/518 in 1984. The purified fraction was prepared as follows: the mites cultured in initial medium for several months were frozen and thawed several times. A 48-h maceration in borate buffer at pH 8.5 was centrifuged. The supernatant was neutralized and submitted to acetone precipitation at gradually increasing concentrations. The fraction precipitated in 80 % acetone was isolated, washed and dried. The purified extract was lyophilized or stocked in

50 % glycerol and 5 % phenol^[14-16].

Detection of total IgE and mite-specific IgE To investigate humoral immune function in individuals with diarrhea caused by acaroid mites, the levels of total IgE and mite-specific IgE in peripheral blood of mite-positive individuals were tested with ELISA. Peripheral venous blood of the subjects was withdrawn and saved in eppendorf tubes, then the optical density (OD) value was tested on enzyme labeling meters. Positive and negative control tubes were included each time. When the OD value in the tested sample was 2.1 times that or more in negative control, it was regarded as positive.

Mites separated from environment Directcopy, waterenacopy and tullgren were used to separate mites from mill floor dust, stores of traditional Chinese medicine, and traditional Chinese herbs of wolfberry fruit, ophiopogon root liquorice, boat-fruited sterculia seed and safflower, etc.

Statistical analysis

The positive rates were expressed as percentage, and *t* and χ^2 tests were used in statistical analysis. A probability value of less than 0.05 was considered statistically significant.

RESULTS

Stool examination

The positive rate of mites in stool samples in all the individuals was 17.01 % (41/241), and was 15.86 % (23/145) and 18.75 % (18/96), respectively in samples from male and female subjects, without significant difference ($\chi^2=0.34$, $P>0.05$). The mites separated from stool samples were confirmed to be *Acarus siro*, *TyroPhagus putrescentiae*, *Dermatophagoides farinae*, *D. pteronyssinus*, *Glycyphagus domesticus*, *G.ornatus*, *Carpoglyphus lactis* and *Tarsonemus granaries*. Among 41 cases with mites in stools, adult mites, larval mites, both adult and larval mites, adult mites and eggs, adult and larval mites and eggs, larval mites and eggs, and both hypopus and eggs were found in 15, 6, 11, 3, 2, 2 and 2 cases, and the constituent ratios of them were 36.59 %, 14.63 %, 26.83 %, 7.32 %, 4.88 %, 4.88 % and 4.88 %, respectively. In addition, the statistics of this investigation showed that the case number with concentration of mites of 1-2/cm³, 2-4/cm³ and >5/cm³ was 6, 12 and 23, respectively. Among the 41 mite-positive cases, 3 cases had other intestinal parasites, 6 cases had pathogenic bacteria. The remaining 32 cases had mites in stool samples only.

Skin prick test

The percentages of cases with “+++”, “++”, “+”, “±” and “-” were 9.13 % (22/241), 7.47 % (18/241), 5.81 % (14/241), 4.98 % (12/241) and 72.61 % (175/241), respectively. The positive number of skin prick test was 54, of which, 41 subjects with mites in stools were all included. In other words, all the 22 subjects with “+++” reaction were confirmed to be mite-positive, and 14 subjects with mites in stools were found in the 18 subjects with “++” reactions, 5 subjects with mites in stools were found in the 14 subjects with “+” reaction. However, all the 41 subjects with mites in stools were positive in skin prick test.

Detection of total IgE and specific IgE

The levels of total IgE and mite-specific IgE in 41 cases with mites were higher than those in individuals without mites ($P<0.01$) (Table 1).

Relationship between diarrhea caused by acaroid mites and occupation

Among the 241 patients with diarrhea, the positive rate of mites

in experimental group was 26.74 % (23/86), which was higher than that in control group ($\chi^2=8.97$, $P<0.01$) (Table 2).

Table 1 Serum total IgE and mite-specific IgE in patients with diarrhea (IU/ml, $\bar{x}\pm s$)

Group	<i>n</i>	Total IgE (IU/ml)	Specific IgE (IU/ml)
Mite-positive cases	41	165.72±78.55 ^a	145.22±82.47 ^b
Mite-negative cases	200	132.44±26.80	67.35±45.28
Total	241	138.10±35.37	80.59±53.62

^a $P<0.01$, $t=4.81$; ^b $P<0.01$, $t=8.52$ vs mite-negative cases.

Table 2 Mites in stool samples in patients with different occupations (*n*, %)

Groups	Cases	Positive number	Positive rate
Experimental group	86	23 ^c	26.74
Staffs working in traditional Chinese medicine storehouses	47	14	29.79
Staffs working in rice storehouses or mills	39	9	23.08
Control group	155	18	11.61
Miners	36	4	11.11
Staffs of railway system	34	3	8.82
Pupils	62	8	12.90
Others	23	3	13.04
Total	241	41	17.01

^c $P<0.01$, $\chi^2=8.97$ vs control group.

Mites separated from work environment

Samples of mill floor dust (30 shares), stores of traditional Chinese medicine, and traditional Chinese herbs (146 species) of wolfberry fruit, ophiopogon root liquorice, boat-fruited sterculia seed, safflower and other work environment and foodstuffs were collected and separated for mites. The results showed that the number of breeding mites per gram was 91-1862, 21-186, 0-483, 10-348, 51-712, and 311-1193, in mill floor dust, traditional Chinese medicine stores, traditional Chinese herbs such as candied fruit, dry fruit, brown sugar, and expired cake. Twenty-two species of mites were separated and identified belonging to nine families, i.e. *Acaridae*, *Lardoglyphidae*, *Glycyphagidae*, *Chortoglyphidae*, *Carpoglyphidae*, *Histiostomidae*, *Pyroglyphidae*, *Tarsonemus*, *Cheyletus*. The results of this study showed that the mites separated from work environment were identical to those from stored food.

DISCUSSION

In this study, *Acarus siro*, *TyroPhagus putrescentiae*, *Dermatophagoides farinae*, *D. pteronyssinus*, *Glycyphagus domesticus*, *G.ornatus*, *Carpoglyphus lactis* and *Tarsonemus granaries* were separated from stool of patients with diarrhea. This confirmed that acaroid mites were able to parasitize in human intestines, which might play an important role in diarrhea. Like other intestinal parasites, the mites living in intestinal tract may stimulate mechanically and damage intestinal tissues with its gnathosoma, chelicera and feet^[17-25]. Certainly they may also intrude into mucous and deep tissues, and cause inflammation and necrosis.

The results of this study support the idea that the patients with mites in stool samples are allergic to acaroid mites. Skin

prick test is one of the specific methods for clinical diagnosis of allergic disease. After superficial layer of skin is pierced by a special needle, interaction occurs between the test extract and mastocytes in the skin, which causes mastocytes degranulation and inflammation-media release like histamine that is able to increase capillary telangiectasia and permeability. Thereby wheal and flush appear on the surface of skin tested^[26,27]. Among the 241 patients tested with skin prick test, 54 subjects had positive reactions. This demonstrated that some of the patients with diarrhea were allergic to acaroid mites. Moreover, the results of skin prick test on 41 patients with mites in their stools were all positive. It provided the evidence that acaroid mites in intestine might lead to the allergy of patients to acaroid mites. The reason why there were no mites found in stools taken from 13 patients with positive reaction of skin prick test is that mites live in other locus besides intestines, and that mites may be missed in detection with saturated saline flotation methods.

Although the serum level of total IgE is a marker of human sensitization to extrinsic allergen, the level of specific IgE is a sensitive index for allergic reaction to acaroid mites^[28-34]. In this study, the levels of specific IgE in 41 patients with mites were higher than those without mites. This provides another evidence that acaroid mites can cause allergy. The dejecta, products of metabolism, and cleaved pieces of dead mites in intestine may stimulate lymphocytes and reticuloendothelial system, and produce specific antibodies, such as IgE.

This study confirms that the prevalence of diarrhea caused by acaroid mites was associated with the patients' occupation. The positive rates of mites in stools of staffs working in traditional Chinese medicine storehouses and rice storehouses or mills were 29.79 % (14/47) and 23.08 % (9/39), respectively, which were higher than those of patients with other occupations. However, no significant association was observed between diarrheas caused by the organism with the gender of patients. The positive rates of mites in male and female patients were 15.86 % (23/145) and 18.75 % (18/96), respectively.

Eight species of acaroid mites separated from stool samples could be found in the house dust collected from traditional Chinese medicine storehouses, rice storehouses and flourmills, suggesting that the source of diarrhea caused by acaroid mites is mites in our living environment and stored food. Generally speaking, the path of the mites invading human is related to ingestion of stored food. However, some mites in dust or in air might invade intestine through mouth, or nasal cavity, gorge^[35-37]. We have set up eight sampling sites in traditional Chinese medicine storehouses by dust sampler, and separated thirteen mites from dust samples collected from 640 L of air in work environment of the storehouses.

In conclusion, acaroid mites in our living and working environments may invade human intestines and cause diarrhea. The levels of total IgE, mite-specific IgE of the patients with diarrhea caused by acaroid mites increased, the prevalence was associated with the patient's occupation rather than gender. It is suggested that separation of mites from stool samples, skin prick test and detection of total IgE and mite-specific IgE should be used in the diagnosis of diarrhea caused by acaroid mites.

REFERENCES

- 1 Sun HL, Lue KH. Household distribution of house dust mite in central Taiwan. *J Microbiol Immunol Infect* 2000; **33**: 233-236
- 2 Cadman A, Prescott R, Potter PC. Year-round house dust mite levels on the Highveld. *S Afr Med J* 1998; **88**: 1580-1582
- 3 Croce M, Costa-Manso E, Baggio D, Croce J. House dust mites in the city of Lima, Peru. *Investig Allergol Clin Immunol* 2000; **10**: 286-288
- 4 Arlian LG, Neal JS, Vyszynski-Moher DL. Reducing relative humidity to control the house dust mite *Dermatophagoides farinae*. *J Allergy Clin Immunol* 1999; **104**: 852-856
- 5 Mumcuoglu KY, Gat Z, Horowitz T, Miller J, Bar-Tana R, Ben-Zvi A, Naparstek Y. Abundance of house dust mites in relation to climate in contrasting agricultural settlements in Israel. *Med Vet Entomol* 1999; **13**: 252-258
- 6 Arlian LG, Neal JS, Vyszynski-Moher DL. Fluctuating hydrating and dehydrating relative humidities effects on the life cycle of *Dermatophagoides farinae* (Acari: Pyroglyphidae). *J Med Entomol* 1999; **36**: 457-461
- 7 Racewicz M. House dust mites (Acari: Pyroglyphidae) in the cities of Gdansk and Gdynia (northern Poland). *Ann Agric Environ Med* 2001; **8**: 33-38
- 8 Solarz K. Risk of exposure to house dust pyroglyphid mites in Poland. *Ann Agric Environ Med* 2001; **8**: 11-24
- 9 Sadaka HA, Allam SR, Rezk HA, Abo-el-Nazar SY, Shola AY. Isolation of dust mites from houses of Egyptian allergic patients and induction of experimental sensitivity by *Dermatophagoides pteronyssinus*. *J Egypt Soc Parasitol* 2000; **30**: 263-276
- 10 Boquete M, Carballada F, Armisen M, Nieto A, Martin S, Polo F, Carreira J. Factors influencing the clinical picture and the differential sensitization to house dust mites and storage mites. *J Investig Allergol Clin Immunol* 2000; **10**: 229-234
- 11 Li CP, Wang J. Intestinal acariasis in Anhui Province. *World J Gastroenterol* 2000; **6**: 597-600
- 12 Baratawidjaja IR, Baratawidjaja PP, Darwis A, Soo-Hwee L, Fook-Tim C, Bee-Wah L, Baratawidjaja KG. Prevalence of allergic sensitization to regional inhalants among allergic patients in Jakarta, Indonesia. *Asian Pac J Allergy Immunol* 1999; **17**: 9-12
- 13 Yun YY, KO SH, Park JW, Lee IY, Ree HI, Hong CS. Comparison of allergenic components between German cockroach whole body and fecal extracts. *Ann Allergy Asthma Immunol* 2001; **86**: 551-556
- 14 Nuttall TJ, Lamb JR, Hill PB. Characterization of major and minor *Dermatophagoides* allergens in canine atopic dermatitis. *Res Vet Sci* 2001; **71**: 51-57
- 15 Basomba A, Tabar AI, de Rojas DH, Garcia BE, Alamar R, Olaguibel JM, del Prado JM, Martin S, Rico P. Allergen vaccination with a liposome-encapsulated extract of *Dermatophagoides pteronyssinus*: a randomized, double-blind, placebo-controlled trial in asthmatic patients. *J Allergy Clin Immunol* 2002; **109**: 943-948
- 16 Akcakaya N, Hassanzadeh A, Camcioglu Y, Cokugras H. Local and systemic reactions during immunotherapy with adsorbed extracts of house dust mite in children. *Ann Allergy Asthma Immunol* 2000; **85**: 317-321
- 17 Van der Geest LP, Elliot SL, Breeuwer JA, Beerling EA. Diseases of mites. *Exp Appl Acarol* 2000; **24**: 497-560
- 18 Zhou X, Li N, Li JS. Growth hormone stimulates remnant small bowel epithelial cell proliferation. *World J Gastroenterol* 2000; **6**: 909-913
- 19 Fryauff DJ, Prodjodipuro P, Basri H, Jones TR, Mouzin E, Widjaja H, Subianto B. Intestinal parasite infections after extended use of chloroquine or primaquine for malaria prevention. *J Parasitol* 1998; **84**: 626-629
- 20 Zhou JL, Xu CH. The method of treatment on protozoon diarrhea. *Shijie Huaren Xiaohua Zazhi* 2000; **8**: 93-95
- 21 Herwaldt BL, de Arroyave KR, Wahlquist SP, de Merida AM, Lopez AS, Juranek DD. Multiyear prospective study of intestinal parasitism in a cohort of Peace Corps volunteers in Guatemala. *J Clin Microbiol* 2001; **39**: 34-42
- 22 Fan WG, Long YH. Diarrhea in travelers. *Shijie Huaren Xiaohua Zazhi* 2000; **8**: 937-938
- 23 Feng ZH. Application of gene vaccine and vegetable gene in infective diarrhea. *Shijie Huaren Xiaohua Zazhi* 2000; **8**: 934-936
- 24 Xiao YH. Treatment of infective Diarrhea with antibiotic. *Shijie Huaren Xiaohua Zazhi* 2000; **8**: 930-932
- 25 Komatsu S, Nimura Y, Granger DN. Intestinal stasis associated bowel inflammation. *World J Gastroenterol* 1999; **5**: 518-521
- 26 Davis MD, Richardson DM, Ahmed DD. Rate of patch test reactions to a dermatophagoides mix currently on the market: a mite too sensitive? *Am J Contact Dermat* 2002; **13**: 71-73
- 27 Obase Y, Shimoda T, Tomari SY, Mitsuta K, Kawano T, Matsuse H, Kohno S. Effects of pranlukast on chemical mediators in induced sputum on provocation tests in atopic and aspirin-intolerant asthmatic patients. *Chest* 2002; **121**: 143-150

- 28 **Silva DA**, Gervasio AM, Sopelete MC, Arruda-Chaves E, Arruda LK, Chapman MD, Sung SS, Taketomi EA. A sensitive reverse ELISA for the measurement of specific IgE to Der p 2, a major Dermatophagoides pteronyssinus allergen. *Ann Allergy Asthma Immunol* 2001; **86**: 545-550
- 29 **Pumhirun P**, Jane-Trakoonroj S, Wasuwat P. Comparison of *in vitro* assay for specific IgE and skin prick test with intradermal test in patients with allergic rhinitis. *Asian Pac J Allergy Immunol* 2000; **18**: 157-160
- 30 **Nahm DH**, Kim HY, Park HS. House dust mite-specific IgE antibodies in induced sputum are associated with sputum eosinophilia in mite-sensitive asthmatics. *Ann Allergy Asthma Immunol* 2000; **85**: 129-133
- 31 **Walusiak J**, Palczynski C, Wyszynska-Puzanska C, Mierzwa L, Pawlukiewicz M, Ruta U, Krakowiak A, Gorski P. Problems in diagnosing occupational allergy to flour: results of allergologic screening in apprentice bakers. *Int J Occup Med Environ Health* 2000; **13**: 15-22
- 32 **Kanceljak-Macan B**, Macan J, Buneta L, Milkovic-Kraus S. Sensitization to non-pyroglyphid mites in urban population of Croatia. *Croat Med J* 2000; **41**: 54-57
- 33 **Morsy TA**, Saleh WA, Farrag AM, Rifaat MM. Chironomid potent allergens causing respiratory allergy in children. *J Egypt Soc Parasitol* 2000; **30**: 83-92
- 34 **Chew FT**, Lim SH, Goh DY, Lee BW. Sensitization to local dust-mite fauna in Singapore. *Allergy* 1999; **54**: 1150-1159
- 35 **Paufler P**, Gebel T, Dunkelberg H. Quantification of house dust mite allergens in ambient air. *Rev Environ Health* 2001; **16**: 65-80
- 36 **Roux E**, Hyvelin JM, Savineau JP, Marthan R. Human isolated airway contraction: interaction between air pollutants and passive sensitization. *Am J Respir Crit Care Med* 1999; **160**: 439-445
- 37 **Ponsonby AL**, Kemp A, Dwyer T, Carmichael A, Couper D, Cochrane J. Feather bedding and house dust mite sensitization and airway disease in childhood. *J Clin Epidemiol* 2002; **55**: 556-562

Edited by Ren SY and Wang XL

Modified technique for combined liver-small bowel transplantation in pigs

Zhen-Yu Yin, Xiao-Dong Ni, Feng Jiang, Ning Li, You-Sheng Li, Jie-Shou Li

Zhen-Yu Yin, Xiao-Dong Li, Feng Jiang, Research Institute of General Surgery, School of Medicine, Nanjing University, Nanjing, 210093, Jiangsu Province, China

Zhen-Yu Yin, Ning Li, You-Sheng Li, Jie-Shou Li, Research Institute of General Surgery, Nanjing PLA General Hospital, Nanjing, 210002, Jiangsu Province, China

Correspondence to: Zhen-Yu Yin, Research Institute of General Surgery, Nanjing PLA General Hospital, 305 East Zhongshan Road, Nanjing 210002, Jiangsu Province, China. davidmd@sohu.com

Telephone: +86-25-3685194 **Fax:** +86-25-4803956

Received: 2002-12-30 **Accepted:** 2003-02-08

Abstract

AIM: As the conventional combined liver-small bowel transplantation is complicated with many postoperative complications, the aim of this study was to describe a modified technique for the combined liver-small bowel transplantation with preservation of the duodenum, partial head of pancreas and hepatic biliary system in pigs.

METHODS: Composite liver/small bowel allotransplantations were undertaken in 30 long-white pigs. The graft included liver, about 3 to 4 m proximal jejunum, duodenum and partial pancreatic head. Vessels reconstructions included subhepatic vena cava-vena cava anastomosis, aorta-aorta anastomosis and portal-splenic vein anastomosis.

RESULTS: Without immunosuppressive treatment, the median survival time of the animals was 6 days (2 to 12 days), and about 76.9 % (20/26) of the animals survived for more than 4 days after operation.

CONCLUSION: The modified technique is feasible and safe for the composite liver/small bowel transplantation with duodenum and pancreas preserved in pigs. And also this technique can simplify the operation and decrease possible postoperative complications.

Yin ZY, Ni XD, Jiang F, Li N, Li YS, Li JS. Modified technique for combined liver-small bowel transplantation in pigs. *World J Gastroenterol* 2003; 9(7): 1625-1628

<http://www.wjgnet.com/1007-9327/9/1625.asp>

INTRODUCTION

As a result of total parenteral nutrition (TPN) induced end-stage liver disease, 60 % to 70 % of recipients of intestinal transplant procedures require simultaneous liver allografts^[1,2]. Although many clinical liver/small bowel transplantations (LSBT) were reported from different medical centers^[3-5], it remains an experimental procedure^[6]. Compared to the widely used rat LSBT model^[7,8], large animal models such as LSBT in pigs were rarely reported.

As a conventional composite liver-small bowel graft requires a loop of defunctionalized (Roux) allograft small bowel for biliary drainage^[9], its posttransplant biliary complications

include anastomotic leaks and obstruction in 12 % of the cases, with significantly associated morbidity and mortality in clinical reports^[1]. In the present study, we modified the technique for LSBT by preserving the duodenum, partial head of pancreas and hepatic biliary system, and also we modified the conventional vena cava and the portal drainage anastomotic methods. Experience with this technique for the LSBT in pigs has not been described previously.

MATERIALS AND METHODS

Donor preparation 60 long-white pigs weighing 20-40 Kg with random sex were undertaken 30 LSBTs. The weight of the donor was generally lower than that of the corresponding recipient. No immunosuppressive treatment was given in the group.

Preoperative treatment The animals were not allowed to eat for 24 hours and drink for 4 hours before operation respectively. The gut decontamination was attempted in all donors with an oral antibiotic preparation 3 days before surgery.

After anesthesia with 25 mg/kg of intravenous pentobarbital sodium, the animal was intubated and mechanically ventilated with a mixture of oxygen, nitrous oxide and isoflurane. In addition, the standard intravenous antibiotic prophylaxis was instituted with cefotaxime at the time of surgery.

Donor surgical technique

Initial exposure and isolation of the abdominal organs The procurement varied in details but followed the standard techniques for human multiorgan retrieval^[10-12]. Briefly, the donor operation was performed through a midline laparotomy. Cares should be taken not to damage the urethra of male pigs when opening the abdomen. The liver was mobilized by dividing its suspensory attachments. The right gastric and right gastroepiploic vessels were divided, and the pylorus was transected, which allowed the stomach to be reflected cranially. The proximal 3 to 4 m of jejunum (the total porcine small bowel is about 15 m) together with the liver was procured as the graft. After the redundant small bowel was dissected, its supply vessels were ligated. Then the intestinal tract was transected at the beginning of the descending colon, and then the redundant small bowel and the colon were removed from the operative field. Thus the duodenum, proximal jejunum and the aorta could be well exposed. The left gastric artery was ligated at the celiac axis.

Dissection of the vessels The suprahepatic vena cava was firstly dissected and encircled. An extensive Kocher maneuver allowed visualization of the inferior vena cava and its branch. The subhepatic vena cava was dissected and encircled. The left and right renal veins were ligated respectively.

With division of the left retroperitoneal artery, the superior mesenteric and celiac arteries were identified by extending dissection of the aorta. The right and left renal arteries were then isolated and ligated. The subrenal aorta was isolated and encircled distally for the eventual insertion of an infusion cannula. The abdominal aorta was also encircled above the celiac axis for later crossclamping when cold fluid was infused through the distal aortic cannula^[13]. It should be mentioned

that dissection of the celiac trunk would always open the diaphragm and result in pneumothorax.

The splenic vein was then freed and prepared for portal perfusion cannulation after division of the splenic artery. The splenic vein should be well protected when dividing the splenic artery^[14].

In situ cooling and removal of the organs Unlike the clinical transplantation, it was imperative to collect the donor's blood for the recipient operation. Before the infusion with cold solution, the donor's blood was collected from the iliac artery. After completion of the preliminary dissections and collection of the donor's blood, the liver and small bowel connected by the portal vein and the aortic segment were lavaged *in situ* with UW solution. Briefly, the donor was fully heparinized and the previously encircled proximal aorta was crossclamped, and the distal donor aorta was cannulated with infusion of cold UW solution. For the simultaneous portal venous infusion, a venous cannula was placed into the splenic vein and infused with the UW solution. The intrapericardial inferior vena cava and the subhepatic vena cava were transected to decompress the infused solution as in other reports^[15,16]. The amount of infusion was variable (between 50 mL/Kg and 100 mL/Kg), guided by blanching the organs and estimated by palpation of the degree of cooling. If the intestine did not feel cold after limited perfusion, there was no reason for concern, providing it was blanched, further surface cooling after immersion in cold fluid was rapid as the intestine is a hollow organ^[11]. It is important to avoid both venous hypertension and overperfusion of the intestine and pancreas, as overperfusion might result in duodenopancreatic and small bowel edema^[13,17]. Some solution was injected into the gallbladder to lavage the bile tract.

After infusion, the graft containing liver, hepatic hilus, pancreatic-duodeno complex, spleen together with the splenic vein, and small bowel was achieved with preservation of a segment of aorta containing the superior mesenteric artery and celiac trunk in continuity. The intestine was entrapped by stapling its two ends and carried with the specimen throughout the preservation. Thus the graft was *en bloc* removed and stored in UW solution at 0 to 4 °C.

Back table procedure Back table procedure was performed in the cold UW solution. It included suturing the orifice of suprahepatic vena cava and the proximal end of the aorta. The spleen was removed and the splenic vein was well preserved. The body and tail of the pancreas along the portal vein were isolated and transected, leaving partial pancreatic head attached to the allograft duodenum. This preserved the superior and inferior pancreatic duodenal arcades. The stump of the pancreas was stapled and then oversewn with a running suture using 4-0 polypropylene. The gallbladder was removed and a catheter was placed into the cystic duct stump for the early decompression and study of the donor biliary system during the early postoperative period.

Recipient operation

After anesthesia, a monitor was placed on the recipient. Two venous catheters were inserted for transfusion and central venous pressure monitoring. The arterial blood pressure was monitored through a thigh artery catheter.

Intestinal resection When the abdomen was opened, the small bowel and its mesentery were dissected. Most of the intestine was removed for an artificial short bowel with only about 30 cm left at each end.

Vascular preparation The subrenal aorta was exposed and encircled 2 cm under the renal artery. Small arterial and lymphatic vessels along the aorta were ligated to avoid later bleeding or lymphorrhea. Subhepatic vena cava was also dissected and encircled. The place just above the left renal vein was routinely used for the donor out-flow anastomosis.

The hilar of the recipient liver was dissected. The common bile duct and the liver artery were transected while the portal vein was crossclamped with a bulldog after transection.

Hepatectomy The resection of the recipient liver was another major step. The total vascular exclusive technique for hepatectomy in human being was not suitable to the pig, so the liver was removed lobe by lobe. Since the retrohepatic vena cava in the pig was passing through the liver with numerous small hepatic veins draining to this segment besides the major hepatic veins, it was hard to be skeletonized. In order to avoid massive bleeding when dissecting the retrohepatic vena cava, a small part of the liver around the retrohepatic vena cava was always saved and oversewn.

Graft implantation and revascularization The transplantation methods varied in details but followed the principles as described previously^[11]. The typical reconstruction is shown in Figure 1.

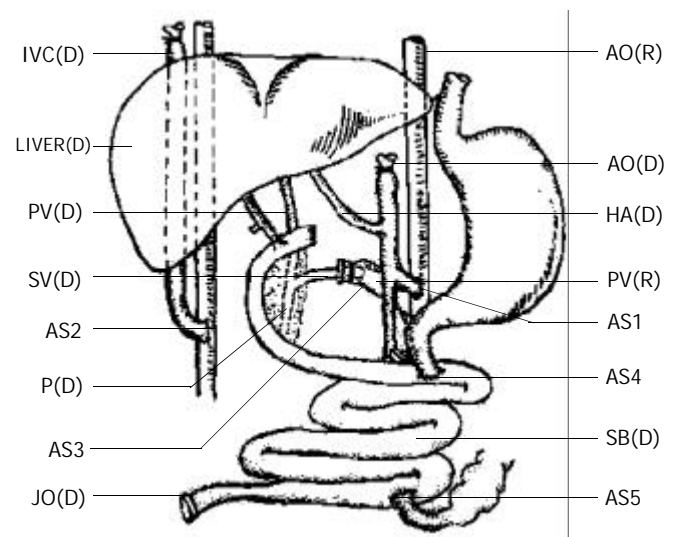


Figure 1 Composite liver/small bowel transplantation (D=donor, R=recipient, AO=aorta, HA=hepatic artery, PV=portal vein, SB=small bowel, IVC=inferior vena cava, SV=splenic vein, P=pancreas, JO=jejunum ostomy, AS1=aorta-aorta anastomosis, AS2=subhepatic vena cava- vena cava anastomosis, AS3=portal-splenic vein anastomosis, AS4=proximal jejunum-jejuno-jejunal anastomosis, AS5=distal jejunum-ileal anastomosis).

The graft was placed in an orthotopic position. The arterial inflow was created via an end-to-side anastomosis of the graft aorta to the subrenal native aorta with a running polypropylene suture. Donor and recipient vena cava were anastomosed end to side. The venous outflow was a modification of the piggyback fashion with the end of the graft subhepatic vena cava anastomosed to the side of the native subhepatic vena cava.

Before reperfusion, unclamping and perfusion of the allograft liver were achieved after a lavage of 300 to 500 ml donor blood or Ringer's solution through the splenic vein.

Anastomosis of the donor splenic vein to the recipient portal vein By using the graft splenic venous stump, a branch point left could be clamped separately and anastomosed to the recipient portal vein to allow outflow of the retained recipient viscera (stomach, pancreas, and spleen as well as the remaining native intestine). Since the splenic vein was smaller than the recipient portal vein, the cuff technique was always used for this anastomosis.

Gastrointestinal reconstruction The proximal duodenum was closed. The intestinal continuity was established proximally by end-to-side recipient-to-donor jejunum-jejunal anastomosis. The end of the recipient's distal ileum was anastomosed to the side of the donor distal jejunum including a donor distal

intestinal vent for the early decompression and surveillance endoscopies as described in some clinical reports^[18,19]. The bile was drained with a catheter in the donor's cystic tract.

Postoperative management After operation, the animal was returned to the monitor room, where hemodynamic monitoring and mechanical ventilation were performed as needed 24 hours after operation. Due to the high rate of inflammatory complications, broad-spectrum antibacterial prophylaxis was administered once for 5 days. Lactated Ringer's solution and parenteral nutrition were given daily until the animal was able to eat and drink.

The appearance of the allograft ostomy and the amount of ostomy output were useful clinical signs of graft dysfunction. Ostomy losses up to 100 cc/kg per day were acceptable and could be compensated by supplementary intravenous fluids.

RESULTS

After reperfusion, the liver was soft and pink with prompt bile production, evidenced through the cystic duct catheter. If the liver was harder than normal, the outflow of the liver might be obstructed and the vena cava anastomosis was required to be checked. The small bowel would be perfused well, with good mesenteric arterial inflow and venous outflow. The peristalsis and intraluminal mucous production were evident within 15 minutes after reperfusion.

Animals died suddenly after reperfusion were ruled out from the statistic series. 4 recipients died because of post reperfusion syndrome and operative techniques. The other 26 LSBT pigs had a median survival time of 6 days (from 2 to 12 days). The surgical records are shown in Table 1, and the values were expressed as median (range).

Table 1 Surgical records

Parameters	Values
Weight of the donor (KG)	22.5 (19-25)
Weight of the recipient (KG)	25 (22-38)
Length of the graft small bowel (m)	3.4 (2.8-4.2)
Weight of the graft liver (g)	760 (620-960)
Collection of the donor blood (ml)	800 (400-1200)
Cooling solution (ml)	1400 (1200-2000)
Donor operative time (hr)	3.3 (2.8-3.6)
Back table time (hr)	0.8 (0.5-1.1)
Preservation time (hr)	3.8 (3.0-4.5)
Total cold ischemia time (hr)	5.6 (3.8-6.6)
Total operative time (hr)	8.2 (7.0-11.4)
Postoperative survival time (day)	6 (2-12)
Survival rate (more than 4 days)	76.9%(20/26)

During the first three days, the intestinal graft stoma appeared healthy, and the mucosa was pink, moist, and well vascularized. No intestinal edema was found in most cases with stomal output averaging 500 ml/day and characterized by bile-stained stool. The high stomal output would decrease with time.

All liver grafts functioned immediately after serum bilirubin and transaminase levels peaked on the first postoperative day and fell rapidly thereafter.

Neither the duodenal allografts experienced signs of ischemia or stump leakage, nor experienced any biliary complication. Abdominal drains were monitored serially for amylase and lipase. Chemical pancreatitis was observed during the early postoperative period with lipase-rich fluid drainage. The biopsies of the dead animals indicated mild pancreatitis in the remained pancreas.

Histopathologic studies of the grafts showed no significant preservation injury. None of the biopsies obtained in the first

postoperative week had histological evidence of submucosal bacterial invasion. The frequent cause of death was postoperative rejection convinced by the graft biopsies when the animal was dead.

DISCUSSION

Specialties of porcine anatomy and LSBT model Firstly, the porcine liver is divided into 4 relatively independent lobes. There are obvious borderlines between lobes. This is the reason why we can remove the liver lobe by lobe when total vascular exclusive technique can not be used in hepatectomy. Secondly, the porcine retrohepatic vena cava is passing through the liver parenchyma with numerous small hepatic veins outflow to this segment besides the major hepatic veins. It is dangerous to remove the liver parenchyma when dissecting the retrohepatic vena cava. This is the reason why the classic piggyback liver transplantation is not suitable to the pig. The vena cava anastomosis was modified by replacing the major hepatic vein (or suprahepatic vena cava) anastomosis in classical piggyback transplantation with the subhepatic vena cava anastomosis (Figure 1). This modification has at least three advantages in porcine LSBT: (1). It is safe to remove the liver, for the whole recipient liver is not moved to expose the retrohepatic vena cava. (2). The subhepatic vena cava anastomosis can be easily performed. (3). The subhepatic vena cava anastomosis can adjust a flexible anastomotic interval to make the aorta-aorta and the portal-splenic vein anastomosis easier.

The third difference of porcine anatomy is that the interval between the celiac axis and superior mesenteric artery is longer than that of human being. It is about 2 to 2.5 cm in general, so the Carrel patch with celiac axis and superior mesenteric artery in human LSBT is not suitable to the pig. The long segment of aorta with celiac axis and superior mesenteric artery was used in porcine LSBT. (Figure 1).

Feasibility and safety of the porcine LSBT with pancreatic head and duodenum In clinical practice, Abu-Elmagd suggested that LSBT with pancreatic head and duodenum had some advantages including avoidance of biliary complications and simplification of the operative procedure^[20]. These possible advantages might exist in the animal LSBT.

The LSBT transplant procedure is a much more arduous surgical endeavor. The technique retaining the duodenum and the head of pancreas would simplify the back table preparation and avoid risks associated with dissection of the donor hepatic hilus.

Retrieval for composite grafts using the standard technique involves an obligatory reconstruction of the biliary system with a defunctionalized loop of proximal allograft jejunum^[3]. In this porcine LSBT model, no biliary reconstruction is required to eliminate the source of complications such as bile leakage, bile tract stricture or even the death of recipient. Liver transplantation related biliary complication rate is about 12 %, which would result in about 19 % of death of them^[21,22]. The LSBT with partial pancreas and duodenum would remarkably decrease such complications.

Without donor or recipient bowel for Roux-en-Y biliary reconstruction would enhance the potential benefits of any intestinal segment in freeing the pig for TPN, as it is directly kept in continuity with the alimentary tract.

The advantage of the composite technique is to maintain the hepatic hilus. The use of liver artery and superior mesenteric artery with a large arterial conduit would minimize the risk of hepatic artery thrombosis compared to isolated graft^[18,23].

In the experiments, we found that the graft with duodenum and partial pancreas was also convenient to be implanted as compared to the standard LSBT. Only three vascular anastomoses were required, including aorta-aorta anastomosis,

vena cava-vena cava anastomosis and portal-splenic vein anastomosis. The liver artery anastomosis and biliary reconstruction are not necessary when this method is used. Since the aorta and vena cava are end-to-side anastomosed with the recipient's aorta and vena cava partially excluded during the anastomosis. This method would avoid not only hemodynamic damages, but also possible kidney injuries, postoperative thrombus and lower limb ischemia.

Inclusion of the duodenum and pancreatic head to maintain continuity of the biliary system was associated with early postoperative allograft pancreatitis, and no significant morbidity was reported^[17]. This complication was also found in our study. It could be detected by measuring pancreatic enzymes in peritoneal fluid from abdominal drains and serum pancreatic enzymes^[20]. Early diagnosis and aggressive surgical management of the native pancreatitis have eliminated the need for repeated transplantation^[18]. At present, the following possible ways are considered to protect the allografted pancreas from postoperative pancreatitis. (1). To limit the cold solution and the pressure of perfusion^[13]. (2). To procure the pancreas entirely with the graft and avoid over-dissection of the tissue and vessels around the duodenum and pancreas^[24]. (3). To ligate the pancreatic tract and suture the pancreatic interface definitely. (4). To use somatostatin after operation.

Some reports suggested that LSBT with duodenum and pancreas head preserved would neither increase the possibility of rejection nor require more immunosuppressive treatment than that of the standard LSBT without pancreas and duodenum^[18,23]. The presence of allograft pancreas in the multivisceral allograft was not an important risk factor for mortality, and the incidence of rejection of the pancreas was only 12 % in some report^[18]. So the technique with preservation of the pancreas is safe in composite LSBT.

In summary, the modified technique is feasible and safe for composite liver/small bowel transplantation with duodenum and pancreas preserved. This technique can simplify the operation procedure and decrease possible postoperative complications. The immunosuppressive treatment in this large animal LSBT model needs to be further studied.

REFERENCES

- 1 **Reyes J**, Bueno J, Kocoshis S, Green M, Abu-Elmagd K, Furukawa H, Barksdale EM, Strom S, Fung JJ, Todo S, Irish W, Starzl TE. Current status of intestinal transplantation in children. *J Pediatr Surg* 1998; **33**: 243-254
- 2 **Grant D**. Intestinal transplantation: 1997 report of the international registry intestinal transplant. *Transplantation* 1999; **67**: 1061-1067
- 3 **Grant D**, Wall W, Mimeault R, Zhong R, Ghent C, Garcia B, Stilier C, Duff J. Successful small bowel/liver transplantation. *Lancet* 1990; **335**: 181-184
- 4 **Todo S**, Reyes J, Furukawa H, Abu-Elmagd K, Lee RG, Tzakis A, Rao AS, Starzl TE. Outcome analysis of 71 clinical intestinal transplantations. *Ann Surg* 1995; **222**: 270-280
- 5 **Goulet O**, Jan D, Sarnacki S, Brousse N, Colomb V, Salomon R, Cuenod B, Piloquet H, Ricour C, Revillon Y. Isolated and combined liver-small bowel transplantation in Paris: 1987-1995. *Transplant-Proc* 1996; **28**: 2750
- 6 **Muiesan P**, Dhawan A, Novelli M, Mieli-Vergani G, Rela M, Haton ND. Isolated liver transplant and sequential small bowel transplantation for intestinal failure and related liver disease in children. *Transplantation* 2000; **69**: 2323-2326
- 7 **Zhong R**, He G, Sakai Y, Zhang Z, Garcia B, Li XC, Jevnikar A, Grant D. The effect of donor-recipient strain combination on rejection and graft-versus-host disease after small bowel/liver transplantation in the rat. *Transplantation* 1993; **56**: 381-385
- 8 **Li XC**, Zhong R, He G, Sakai Y, Garcia B, Jevnikar A, Grant D. Host immune suppression after small bowel/liver transplantation in rats. *Transplant Int* 1994; **7**: 131-135
- 9 **Furukawa H**, Kaubu-Elmagd K, Reyes JL. Technical aspects of intestinal transplantation In: Braverman MH, Tawas RL, eds. *Surgical Technology International II*, San Francisco CA. *TF Laszlo* 1994: 165-170
- 10 **Starzl TE**, Todo S, Tzakis A, Alessiani M, Casavilla A, Abu-Elmagd K, Fung JJ. The many faces of multivisceral transplantation. *Surg Gynecol Obstet* 1991; **172**: 335-344
- 11 **Casavilla A**, Selby R, Abu-Elmagd K, Tzakis A, Todo S, Retes J, Fung J, Starzl TE. Logistics and technique for combined hepatic-intestinal retrieval. *Ann Surg* 1992; **216**: 605-609
- 12 **Williams JW**, Sankary HN, Foster PF. Technique for splanchnic transplantation. *J Pediatr Surg* 1991; **26**: 79-81
- 13 **Abu-Elmagd K**, Fung J, Bueno J, Martin D, Madariaga JR, Mazariegos G, Bond G, Molmenti E, Corry RJ, Starzl TE, Reyes J. Logistics and technique for procurement of intestinal, pancreatic, and hepatic grafts from the same donor. *Ann Surg* 2000; **232**: 680-687
- 14 **Goyet JdVd**, Mitchell A, Mayer AD, Beath SV, McKiernan PJ, Kelly DA, Mirza D, Buckles JA. En bloc combined reduced-liver and small bowel transplants: from large donors to small children. *Transplantation* 2000; **69**: 555-559
- 15 **Starzl TE**, Hakala TR, Shaw BW Jr, Hardesty RL, Rosenthal TJ, Griffith BP, Iwatsuki S, Bahnson HT. A flexible procedure for multiple cadaveric organ procurement. *Surg Gynecol Obstet* 1984; **158**: 223-230
- 16 **Starzl TE**, Miller C, Bronznick B, Makowka L. An improved technique for multiple organ harvesting. *Surg Gynecol Obstet* 1987; **165**: 343-348
- 17 **Casavilla A**, Selby R, Abu-Elmagd K, Tzakis A, Todo S, Starzl TE. Donor selection and surgical technique for en bloc liver-small bowel graft procurement. *Trans Spant Proc* 1993; **25**: 2622-2623
- 18 **Reyes J**, Fishbein J, Bueno J, Mazariegos G, Abu-Elmagd K. Reduced-size orthotopic composite liver-intestinal allograft. *Transplantation* 1998; **66**: 489-492
- 19 **Todo S**, Tzakis AG, Abu-Elmagd K, Reyes J, Fung JJ, Casavilla A, Nakamura K, Yagihashi A, Jain A, Murase N. Cadaveric small bowel and small bowel-liver transplantation in humans. *Transplantation* 1992; **53**: 369-376
- 20 **Abu-Elmagd K**, Reyes J, Todo S, Rao A, Lee R, Irish W, Furukawa H, Bueno J, McMichael J, Fawzy AT, Murase N, Demetris J, Rakela J, Fung JJ, Starzl TE. Clinical intestinal transplantation: New perspectives and immunologic considerations. *J Am Coll Surg* 1998; **186**: 512-527
- 21 **Lopez RR**, Benner KG, Ivancev K, Keeffe EB, Deveney CW, Pinson CW. Management of biliary complication after liver transplantation. *Am J Surg* 1992; **163**: 519-524
- 22 **Greif F**, Bronsther OL, Van Thiel DH, Casavilla A, Iwatsuki S, Tzakis A, Todo S, Fung JJ, Starzl TE. The incidence, timing and management of biliary tract complications after orthotopic liver transplantation. *Ann Surg* 1994; **219**: 40-45
- 23 **Bueno J**, Abu-Elmagd K, Mazariegos G, Madariaga J, Fung J, Reyes J. Composite liver-small bowel allografts with preservation of donor duodenum and hepatic biliary system in children. *J Pediatr Surg* 2000; **35**: 291-296
- 24 **Kato T**, Romero R, Verzaro R, Misiakos E, Khan FA, Pinna AD, Nery JR, Ruiz P, Tzakis AG. Inclusion of entire pancreas in the composite liver and intestinal graft in pediatric intestinal transplantation. *Pediatr Transplant* 1999; **3**: 210-214

Edited by Yuan HT, Zhu LH and Wang XL

In vitro assay for HCV serine proteinase expressed in insect cells

Li-Hua Hou, Gui-Xin Du, Rong-Bin Guan, Yi-Gang Tong, Hai-Tao Wang

Li-Hua Hou, Gui-Xin Du, Rong-Bin Guan, Yi-Gang Tong, Hai-Tao Wang, Department of Applied Molecular Biology, Institute of Microbiology and Epidemiology, Beijing 100071, China
Supported by the National Natural Science Foundation of China, No. 39630020

Correspondence to: Dr. Li-Hua Hou, Department of Applied Molecular Biology, Institute of Microbiology and Epidemiology, Beijing 100071, China. houlihua@sina.com

Telephone: +86-10-66948580 **Fax:** +86-10-63869835

Received: 2003-03-20 **Accepted:** 2003-04-11

Abstract

AIM: To produce the recombinant NS3 protease of hepatitis C virus with enzymatic activity in insect cells.

METHODS: The gene of HCV serine proteinase domain which encodes 181 amino acids was inserted into pFastBacHTc and the recombinant plasmid pFBCNS3N was transformed into DH10Bac competent cells for transposition. After the recombinant bacmids had been determined to be correct by both blue-white colonies and PCR analysis, the isolated bacmid DNAs were transfected into Sf9 insect cells. The bacmids DNA was verified to replicate in insect cells and packaged into baculovirus particles via PCR and electronic microscopic analysis. The insect cells infected with recombinant baculovirus were determined by SDS-PAGE and Western-blot assays. The recombinant protein was soluted in N-lauryl sarcosine sodium (NLS) and purified by metal-chelated-affinity chromatography, then the antigenicity of recombinant protease was determined by enzyme-linked immunoabsorbant assay and its enzymatic activity was detected.

RESULTS: The HCV NS3 protease domain was expressed in insect cells at high level and it was partially solved in NLS. Totally 0.2 mg recombinant serine proteinase domain with high purity was obtained by metal-chelated-affinity chromatography from 5×10^7 cells, and both antigenicity and specificity of the protein were evaluated to be high when used as antigen to detect hepatitis C patients' sera in indirect ELISA format. *In vitro* cleavage assay corroborated its enzymatic activity.

CONCLUSION: The recombinant HCV NS3 proteinase expressed by insect cells is a membrane-binding protein with good antigenicity and enzymatic activity.

Hou LH, Du GX, Guan RB, Tong YG, Wang HT. *In vitro* assay for HCV serine proteinase expressed in insect cells. *World J Gastroenterol* 2003; 9(7): 1629-1632
<http://www.wjgnet.com/1007-9327/9/1629.asp>

INTRODUCTION

Hepatitis C virus, the major etiological agent of post-transfusion non-A, non-B hepatitis, is an enveloped virus obtaining a single-stranded RNA genome of approximately 9.5kb^[1-3]. A single polyprotein of 3 010-3 030 amino acids is translated from

this genome in the order of NH₂-C-E1-E2-p7-NS2-NS3-NS4A-NS4B-NS5A-NS5B-COOH. Proteolytic procession of the viral precursor protein is required for replication and is mediated by either viral or host cell proteinases^[4-7]. HCV uses a serine proteinase located at the N-terminus of NS3, to process the cleavage of four sites (3/4A, 4A/4B, 4B/5A and 5A/5B). Since the NS3 protein is very important for releasing functional proteins from the polyprotein, it has been currently targeted in the development of drugs and diagnostics^[8-11].

In the absence of satisfactory cell culture, protein expression is the primary technological methods for HCV^[12-14]. In this report, we described the construction of the recombinant baculovirus, designed to express the NS3 proteinase in insects. The activity of the expressed enzyme has been demonstrated by *in vitro* assay.

MATERIALS AND METHODS

Cells, vectors and strains

Spodoptera frugiperda Sf9 cells were a gift from Professor Gu Shu-Yan, Institute of Virology, CDC, China. The vector pGEX-3X-NS3N containing the gene serine proteinase located at N-terminus of HCV NS3, was constructed in our lab before^[15]. The expression vector pFastBacHTc and *E.coli* DH10Bac were purchased from Invitrogen Inc.

Primers

The primers flanking the vector transfer pFastBacHTc MCS were WB538P (5' -TATTC CCGAT TATTC ATACC-3') and WHT62P (5' -TGGTA TGGCT GATTA TGAT-3'). The primers for bacmid were pUC/M13-R (5' -CAGGA AACAG CTATG AC) and pUC/M13-F (5' -GTTTT CCCAG TCACG AC-3').

Construction of recombinant transfer vector

The gene HCV NS3N serine proteinase was excised from pGEX-3X-NS3N with restriction enzyme *Bam*HI and *Eco*RI, and ligated with vector pFastBacHTc. The recombinant plasmids were transformed into *E.coli* DH5 α . The positive recombinants were identified with PCR and restriction enzyme digestion, then termed as pFBCNS3N.

Transposition

The recombinant transfer vector pFBCNS3N was transformed into the competent DH10Bac cells. After growth in the shaking incubator at 37 °C for 6 h, the cells were placed on the plates (containing 50 mg/L kanamycin, 7 mg/L gentamicin, 10 mg/L tetracycline, 40 mg/L IPTG and 100 mg/L X-gal) with serial dilution, then incubated at 37 °C for 48 h. The white colonies containing the recombinant bacmid, therefore, were selected for the isolation of recombinant bacmid DNA. The bacmid, termed as bacmid-NS3N, was analyzed by 0.5 % agarose gel electrophoresis to confirm the presence of high molecular weight DNA.

Production and analysis of recombinant baculovirus

9×10^5 of Sf9 cells were seeded to each well of a 6-well plate in TNM-FH medium and incubated at 27 °C. Bacmic-NS3N was transfected into Sf9 cells using Lipofectamine reagent (Gibco

BRL) after cells attached to the wells. The supernatant was collected as virus stock when cytopathic effect appeared. At the same time, virus particles in the supernatant were precipitated using PEG8000 to extract viral genome for PCR amplification with the primers WB538P, WHT62P and pUC/M13-R, F to confirm the recombinant virus containing the interested gene. The morpha of recombinant baculovirus was observed under transmission electron microscope.

Expression and purification of serine proteinase in insect cells

Monolayer insect cells were transfected by the recombinant baculovirus at a multiplicity of infection (MOI) of 10. The cells were harvested after incubation for 72 h at 27 °C, resuspended in lysis buffer (0.5 % NP-40, 20 mmol/L Tris-HCl pH 7.4, 150 mmol/L NaCl, 100 mg/L PMSF), and disrupted by ultrasonic. The supernatant and precipitation of the mixture were collected for SDS-PAGE and Western blotting. 5×10^7 of Sf9 cells were collected by centrifugation after transfection for 72 h to purify the recombinant serine proteinase. The cell pellet was resuspended in TNG buffer (50 mmol/L Tris-HCl pH 7.4, 0.2 % NLS (N-Lauryl Sarcosine Sodium), 10 % glycerol, 150 mmol/L NaCl, 100 mg/L PMSF), and disrupted by ultrasonic. The interested protein was purified from the supernatant by means of affinity chromatography on Ni-NTA columns (Qiagen).

In vitro assay of HCV NS3 proteinase activity

Fifteen μ g recombinant serine proteinase was mixed with 15 μ g substrate HCV NS5ab in 100 μ l of 25 mmol/L Tris-HCl pH 7.4, 10 % glycerol, 0.5 mol/L NaCl, 10 mmol/L DTT, 0.5 % NP-40. The incubation was carried out at room temperature for different time periods and the result was read through SDS-PAGE.

Antigenicity of recombinant HCV serine proteinase

The identity of recombinant proteins was confirmed by 50 HCV-positive and 10 HCV-negative sera. Microtitre cells were coated by overnight incubation at 4 °C with 100 μ l recombinant protein solution (10 mg/L proteins in 0.1 mol/L sodium carbonate buffer, pH 9.6). Serum samples diluted at 1:20 in PBSTM (PBS+0.3 % Tween-20+3 % fat-free milk) were added, and incubated at 37 °C for 1 hour after blocking. The specific binding was revealed using HRP anti-human IgG detection system (Sigma, USA).

RESULTS

Construction of recombinant transfer vector

A 540 bp fragment was excised from the plasmid pFBCNS3N with restriction endonuclease enzymes *HindIII* and *EcoRI* (Figure 1). The result showed that the construction of recombinant transfer vector was successful.

Generation of recombinant baculovirus

The recombinant baculoviruses were generated after the site-specific transposition of transfer plasmids in *E. coli*, transfection and packaging in insect cells. Large amounts of baculoviruses were observed in the nuclei of cells under transmission electron microscope (Figure 2). In PCR detection, genome DNA of the recombinant baculoviruses as template, 800 bp and 3 000 bp fragments appeared respectively with primers WB538P, WHT62P and pUC/M13-R, F. The result conformed to our previous expectation and revealed HCV serine proteinase gene existed in the genome of recombinant baculoviruses.

Efficient expression of HCV serine proteinase by recombinant baculovirus

Sf9 cells were transfected with the recombinant baculovirus

at a MOI of 10, and serious CPE appeared after 72 h. The total cell extracts were separated by 15 % SDS-PAGE and stained with Coomassie blue. A predominant band at 23 kDa (approximately 20 % of total proteins) was detected in the cell extracts from bacmic-NS3N infected cells but not in the uninfected cell extracts (Figure 3A). Immunoblot analysis with the HCV-positive sera (Figure 3B) revealed that the 23 kDa protein was clearly detected in cells infected with the recombinant baculovirus.

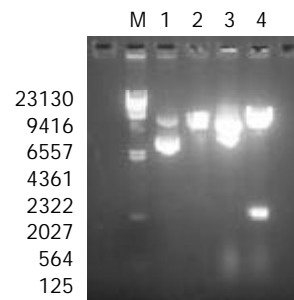


Figure 1 Restriction endonuclease enzyme analysis for recombinant bacmid. Lane M. λ /*HindIII* standard DNA molecular weight marker, Lane 1. pFastBacHTc plasmid, Lane 2. pFastBacHTc plasmid digested with *HindIII* and *EcoRI*, Lane 3. pFBCNS3N plasmid, Lane 4. pFBCNS3N plasmid digested with *HindIII* and *EcoRI*.

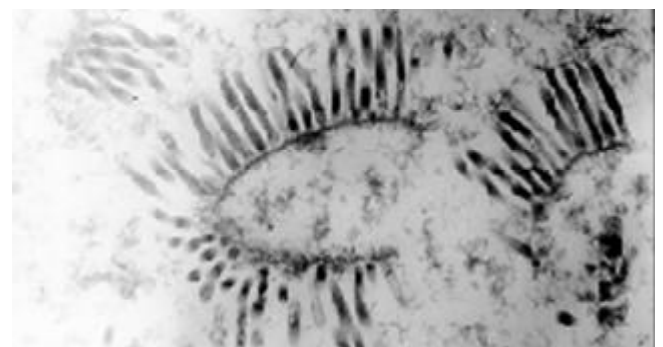


Figure 2 Recombinant baculovirus in insect cells under transmission electron microscope ($\times 36\ 000$).

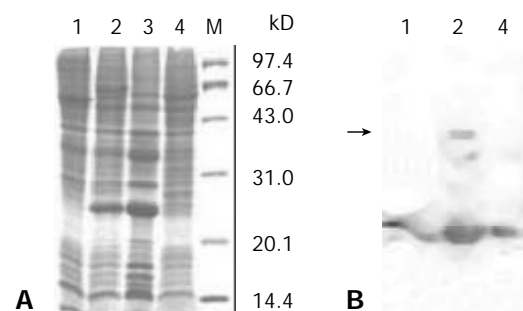


Figure 3 SDS-PAGE analysis (3A) and Western blotting analysis (3B) for the recombinant HCV serine proteinase expressed in insect cells. 3A. lane 1. untransfected Sf9 cells, lane 2. Sf9 cells transfected with rvBacNS3N, lane 3. the pellet of the cell lysate transfected with rvBacNS3N, lane 4. the supernatant of the cell lysate transfected with rvBacNS3N, Lane M. low molecular weight markers. 3B lanes 1,2,4 corresponded to Figure 3A.

Analysis of solubility of recombinant HCV serine proteinase

Though HCV serine proteinase was expressed efficiently in insect cells, a little was laid in the supernatant of the cell lysate.

Only by immunoblot analysis was the protein in the supernatant detected. Did the protein's misfolding or binding with endomembrane system in cells lead to insoluble protein? This question was analyzed by changing the composition of the lysis buffer. When the cell lysates were dissolved in TNG buffer containing N-lauryl sarcosine sodium, more interested protein was soluble because TNG as a detergent could dissolve proteins binding with membrane. Therefore, it was presumed that the recombinant HCV serine proteinase binding with membrane resulted in its insolubility. The HCV serine proteinase was extensively purified from 5×10^7 Sf9 cells and demonstrated a single protein band of 23kDa (more than 90 % of the total proteins by densitometric analysis) by using Ni-NTA columns. The total yield of the purified protein was about 0.2 mg.

Activity of baculovirus-expressing HCV serine proteinase *in trans*

In order to determine whether the baculovirus-expressing cleavage N-terminus of HCV NS3 has a proteinase activity, an *in vitro* proteolytic assay with HCV NS5ab protein (235aa) as a substrate containing the cleavage site of HCV NS5a and NS5b was designed. Figure 4 shows that the baculovirus-expressing HCV serine proteinase could cleave the substrate HCV NS5ab (about 35kDa) into bands of 24kDa and 11kDa (Figure 4). This means that the baculovirus-expressing HCV serine proteinase has a high proteolytic activity.

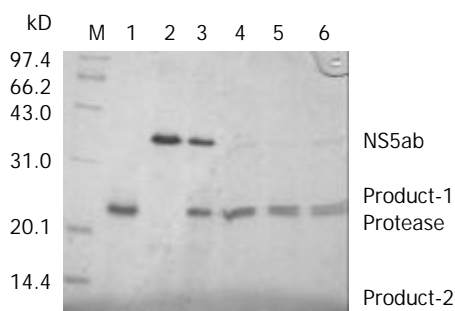


Figure 4 *In vitro* trans-cleavage at the NS5A/5B site of the recombinant HCV serine proteinase. Lane M. low molecular weight markers, lane 1. the purified HCV serine proteinase, lane 2. the substrate HCV NS5ab protein, lanes 3-6. cleavage reaction after 0, 10, 20 and 30 min.

Antigenicity of recombinant HCV serine proteinase

Fifty HCV positive sera and 10 HCV negative sera were evaluated for their reactivities against the purified HCV serine proteinase. A high degree of immunoreactivity was observed in 30 HCV positive sera, showing good antigenicity of HCV serine proteinase.

DISCUSSION

It has been proved that HCV NS3 protein with 631 amino acids possesses both serine proteinase in its N-terminus and NTP/RNA helicase activity in its C-terminus^[16]. Both *in vitro* translation and transient mammalian cells have shown that NS3 is a serine proteinase and is responsible for proteolytic processing of the non-structural region (NS3, NS4A, NS4B, NS5A and NS5B) of HCV polyprotein. Since the maturation of these non-structural proteins is the prerequisites for replication, and packaging of HCV, NS3 serine proteinase plays an important role in the life cycle of HCV and is an attractive target for antiviral therapy. We expressed only 181 amino acids in HCV NS3 N-terminus because previous experiments had corroborated it with good enzyme activity^[17].

Baculovirus-insect cell expression system has two advantages over others: first, in most cases the recombinant

protein in insect cells is processed, modified, and targeted to its appropriate cellular location, where it is functionally similar to its authentic counterparts. Second, high levels of heterogenous gene expression, up to 20 % of total cellular proteins, are often achieved compared with other eukaryotic expression systems^[18-20]. Here we chose the Bac-to-Bac expression system which is based on site-specific transposition of an expression cassette into a baculovirus shuttle vector (bacmid) propagated in *E. coli*^[21,22]. Colonies containing the recombinant bacmid are white in a background of blue colonies that harbor the unaltered bacmid. Recombinant bacmid DNA can be rapidly isolated from small scale cultures and then is used to transfect insect cells, eliminating the need for multiple rounds of plaque purification.

In our experiment, the interested gene was efficiently expressed in insect cells through the recombinant virus BacNS3N containing HCV NS3 serine proteinase gene, and the identity of the protein was validated by use of immunoblot. But the recombinant protein predominantly lay in the insoluble part, and the solubility could not be improved even by adding 1 % NP-40 into the lysate. Overton *et al* illuminated that HCV NS3 serine proteinase expressed in insect cells was a membrane-associated protein through discontinuous sucrose density gradients and only by adding some detergents did part of the protein gain the enzyme activity^[23]. Suzuki *et al* discovered that HCV serine proteinase from insect cells was soluble and active with 0.5 % NLS^[24]. Therefore, the TNG buffer including NLS and glycerol was used to dissolve the pellet. The results showed that part of the recombinant protein became soluble and more proteins were soluble when enhancing the percentage of NLS and adding EDTA both. The recombinant protein fused with 6 His tag at its N- terminus could be purified through metal-chelating chromatography. Finally, 0.2 mg purified recombinant protein was obtained from 5×10^7 insect cells. An *in vitro* detection system with SDS-PAGE and staining was developed with the recombinant HCV NS5ab as a substrate. The system eliminates the need of expensive instrument and reagent, heavy work, as compared with other cleavage systems^[25-27] and provides a simple and clear strategy for the screening of inhibitors against the HCV proteinase.

REFERENCES

- 1 **Choo QL**, Kuo G, Weiner AJ, Overby LR, Bradley DW, Houghton M. Isolation of a cDNA clone derived from a blood-borne non-A, non-B viral hepatitis genome. *Science* 1989; **244**: 359-362
- 2 **Kuo G**, Choo QL, Alter HJ, Gitnick GL, Redeker AG, Purcell RH, Miyamura T, Dienstag JL, Alter MJ, Stevens CE. An assay for circulating antibodies to a major etiologic virus of human non-A, non-B hepatitis. *Science* 1989; **244**: 362-364
- 3 **Alter MJ**, Margolis HS, Krawczynski K, Judson FN, Mares A, Alexander WJ, Hu PY, Miller JK, Gerber MA, Sampliner RE. The natural history of community-acquired hepatitis C in the United States. The Sentinel Counties Chronic non-A, non-B Hepatitis Study Team. *N Engl J Med* 1992; **327**: 1899-1905
- 4 **Okamoto H**, Okada S, Sugiyama Y, Kurai K, Iizuka H, Machida A, Miyakawa Y, Mayumi M. Nucleotide sequence of the genomic RNA of hepatitis C virus isolated from a human carrier: comparison with reported isolates for conserved and divergent regions. *J Gen Virol* 1991; **72**: 2697-2704
- 5 **Takamizawa A**, Mori C, Fuke I, Manabe S, Murakami S, Fujita J, Onishi E, Andoh T, Yoshida I, Okayama H. Structure and organization of the hepatitis C virus genome isolated from human carriers. *J Virol* 1991; **65**: 1105-1113
- 6 **Grakoui A**, Wychowski C, Lin C, Feinstone SM, Rice CM. Expression and identification of hepatitis C virus polyprotein cleavage products. *J Virol* 1993; **67**: 1385-1395
- 7 **Shimotohno K**, Tanji Y, Hirowatari Y, Komoda Y, Kato N, Hijikata M. Processing of the hepatitis C virus precursor protein. *J Hepatol* 1995; **22**(Suppl): 87-92

- 8 **Yan Y**, Li Y, Munshi S, Sardana V, Cole JL, Sardana M, Steinkuehler C, Tomei L, De Francesco R, Kuo LC, Chen Z. Complex of NS3 protease and NS4A peptide of BK strain hepatitis C virus: a 2.2 Å resolution structure in a hexagonal crystal form. *Protein Sci* 1998; **7**: 837-847
- 9 **Dymock BW**, Jones PS, Wilson FX. Novel approaches to the treatment of hepatitis C virus infection. *Antivir Chem Chemother* 2000; **11**: 79-96
- 10 **Llinas-Brunet M**, Bailey M, Fazal G, Ghire E, Gorys V, Goulet S, Halmos T, Maurice R, Poirier M, Poupart MA, Rancourt J, Thibeault D, Wernic D, Lamarre D. Highly potent and selective peptide-based inhibitors of the hepatitis C virus serine protease: towards smaller inhibitors. *Bioorg Med Chem Lett* 2000; **10**: 2267-2270
- 11 **Bartenschlager R**. The NS3/4A proteinase of the hepatitis C virus: unravelling structure and function of an unusual enzyme and a prime target for antiviral therapy. *J Viral Hepat* 1999; **6**: 165-181
- 12 **Takehara T**, Hayashi N, Miyamoto Y, Yamamoto M, Mita E, Fusamoto H, Kamada T. Expression of the hepatitis C virus genome in rat liver after cationic liposome-mediated *in vivo* gene transfer. *Hepatology* 1995; **21**: 746-751
- 13 **Bartenschlager R**, Lohmann V. Replication of hepatitis C virus. *J Gen Virol* 2000; **81**: 1631-1648
- 14 **Gale M Jr**, Beard MR. Molecular clones of hepatitis C virus: applications to animal models. *ILAR J* 2001; **42**: 139-151
- 15 **Du GX**, Hou LH, Guan RB, Tong YG, Wang HT. Establishment of a simple assay *in vitro* for hepatitis C virus NS3 serine protease based on recombinant substrate and single-chain protease. *World J Gastroenterol* 2002; **8**: 1088-1093
- 16 **Grakoui A**, McCourt DW, Wychowski C, Feinstone SM, Rice CM. Characterization of the hepatitis C virus-encoded serine proteinase: determination of proteinase-dependent polyprotein cleavage sites. *J Virol* 1993; **67**: 2832-2843
- 17 **Tanji Y**, Hijikata M, Hirowatari Y, Shimotohno K. Identification of the domain required for trans-cleavage activity of hepatitis C viral serine proteinase. *Gene* 1994; **145**: 215-219
- 18 **Luckow VA**. Baculovirus systems for the expression of human gene products. *Curr Opin Biotechnol* 1993; **4**: 564-572
- 19 **Patterson RM**, Selkirk JK, Merrick BA. Baculovirus and insect cell gene expression: review of baculovirus biotechnology. *Environ Health Perspect* 1995; **103**: 756-759
- 20 **Marchal I**, Jarvis DL, Cacan R, Verbert A. Glycoproteins from insect cells: sialylated or not? *Biol Chem* 2001; **382**: 151-159
- 21 **Luckow VA**, Lee SC, Barry GF, Olins PO. Efficient generation of infectious recombinant baculoviruses by site-specific transposon-mediated insertion of foreign genes into a baculovirus genome propagated in *Escherichia coli*. *J Virol* 1993; **67**: 4566-4579
- 22 **Joubert AM**, Louw AI, Joubert F, Neitz AW. Cloning nucleotide sequence and expression of the gene encoding factor Xa inhibitor from the salivary glands of the tick, *Ornithodoros savignyi*. *Exp Appl Acarol* 1998; **22**: 603-619
- 23 **Overton H**, McMillan D, Gillespie F, Mills J. Recombinant baculovirus-expressed NS3 proteinase of hepatitis C virus shows activity in cell-based and *in vitro* assays. *J Gen Virol* 1995; **76**: 3009-3019
- 24 **Suzuki T**, Sato M, Chieda S, Shoji I, Harada T, Yamakawa Y, Watabe S, Matsuura Y, Miyamura T. *In vivo* and *In vitro* trans-cleavage activity of hepatitis C virus serine proteinase expressed by recombinant baculoviruses. *J Gen Virol* 1995; **76**: 3021-3029
- 25 **Shoji I**, Suzuki T, Sato M, Aizaki H, Chiba T, Matsuura Y, Miyamura T. Internal processing of hepatitis C virus NS3 protein. *Virology* 1999; **254**: 315-323
- 26 **Sali DL**, Ingram R, Wendel M, Gupta D, McNemar C, Tsarbopoulos A, Chen JW, Hong Z, Chase R, Risano C, Zhang R, Yao N, Kwong AD, Ramanathan L, Le HV, Weber PC. Serine protease of hepatitis C virus expressed in insect cells as the NS3/4A complex. *Biochemistry* 1998; **37**: 3392-3401
- 27 **Berdichevsky Y**, Zemel R, Bachmatov L, Abramovich A, Koren R, Sathiyamoorthy P, Golan-Goldhirsh A, Tur-Kaspa R, Benhar I. A novel high throughput screening assay for HCV NS3 serine protease inhibitors. *J Virol Methods* 2003; **107**: 245-255

Edited by Ma JY and Wang XL